
Size Effects on J-R Curves for A 302-B Plate

Prepared by A.L. Hiser, J.B. Terrell

Materials Engineering Associates, Inc.

Prepared for
U.S. Nuclear Regulatory
Commission

NOTICE

This report was prepared as an account of work sponsored by an agency of the United States Government. Neither the United States Government nor any agency thereof, or any of their employees, makes any warranty, expressed or implied, or assumes any legal liability of responsibility for any third party's use, or the results of such use, of any information, apparatus, product or process disclosed in this report, or represents that its use by such third party would not infringe privately owned rights.

NOTICE

Availability of Reference Materials Cited in NRC Publications

Most documents cited in NRC publications will be available from one of the following sources:

1. The NRC Public Document Room, 1717 H Street, N.W.
Washington, DC 20555
2. The Superintendent of Documents, U.S. Government Printing Office, Post Office Box 37082,
Washington, DC 20013-7082
3. The National Technical Information Service, Springfield, VA 22161

Although the listing that follows represents the majority of documents cited in NRC publications, it is not intended to be exhaustive.

Referenced documents available for inspection and copying for a fee from the NRC Public Document Room include NRC correspondence and internal NRC memoranda; NRC Office of Inspection and Enforcement bulletins, circulars, information notices, inspection and investigation notices; Licensee Event Reports; vendor reports and correspondence; Commission papers; and applicant and licensee documents and correspondence.

The following documents in the NUREG series are available for purchase from the GPO Sales Program: formal NRC staff and contractor reports, NRC-sponsored conference proceedings, and NRC booklets and brochures. Also available are Regulatory Guides, NRC regulations in the *Code of Federal Regulations*, and *Nuclear Regulatory Commission Issuances*.

Documents available from the National Technical Information Service include NUREG series reports and technical reports prepared by other federal agencies and reports prepared by the Atomic Energy Commission, forerunner agency to the Nuclear Regulatory Commission.

Documents available from public and special technical libraries include all open literature items, such as books, journal and periodical articles, and transactions. *Federal Register* notices, federal and state legislation, and congressional reports can usually be obtained from these libraries.

Documents such as theses, dissertations, foreign reports and translations, and non-NRC conference proceedings are available for purchase from the organization sponsoring the publication cited.

Single copies of NRC draft reports are available free, to the extent of supply, upon written request to the Division of Information Support Services, Distribution Section, U.S. Nuclear Regulatory Commission, Washington, DC 20555.

Copies of industry codes and standards used in a substantive manner in the NRC regulatory process are maintained at the NRC Library, 7920 Norfolk Avenue, Bethesda, Maryland, and are available there for reference use by the public. Codes and standards are usually copyrighted and may be purchased from the originating organization or, if they are American National Standards, from the American National Standards Institute, 1430 Broadway, New York, NY 10018.

Size Effects on J-R Curves for A 302-B Plate

Manuscript Completed: November 1988
Date Published: January 1989

Prepared by
A.L. Hiser, J.B. Terrell

Materials Engineering Associates, Inc.
9700-B Martin Luther King, Jr. Highway
Lanham, MD 20706-1837

Prepared for
Division of Engineering
Office of Nuclear Regulatory Research
U.S. Nuclear Regulatory Commission
Washington, DC 20555
NRC FIN B8900

ABSTRACT

This study was initially conceived to determine J-R curves from various sizes of specimens to investigate data extrapolation from small size specimens. Instead, this study resulted in the finding of a significant size effect or dependence for the low toughness A 302-B plate investigated. In particular the magnitude of this size dependence is unprecedented for reactor pressure vessel steels. The observed size dependence results in vastly reduced J-R curve toughness levels with increased specimen size, for compact specimens ranging in thickness from 12.7 to 152.4 mm, with all specimens proportional in terms of dimensions.

The plate used in this study was specially made to duplicate early production A 302-B plates, which typically exhibit low Charpy-V upper shelf energy levels. The minimal cross-rolling applied to the plate and the high sulfur content result in a high proportion of manganese-sulfide inclusions. The resultant microstructure is one possible explanation for the unexpected results for this plate. Other causes and ideas for future work are also described.

An additional observation is that initial crack length-to-width ratio (a/W) did have an influence on the J-R curves for this plate. Specifically, a long crack length ($a/W \sim 0.6$) can give somewhat higher J-R curve levels than a short crack length ($a/W \sim 0.5$), for large Δa levels. This finding has a direct impact on the applicability of J_D and J_M , and data extrapolation.

CONTENTS

	<u>Page</u>
ABSTRACT.....	iii
LIST OF FIGURES.....	vii
LIST OF TABLES.....	xii
FOREWORD.....	xiii
ACKNOWLEDGMENT.....	xvii
 1. INTRODUCTION.....	 1
2. PROGRAM PLAN.....	2
3. MATERIAL.....	3
4. CHARPY-V TESTS.....	6
4.1 Specimen Design/Test and Data Analysis Procedures.....	6
4.2 Test Results.....	6
5. TENSILE TESTS.....	19
5.1 Specimen Design and Test Procedures.....	19
5.2 Data Analysis Procedures.....	19
5.3 Test Results.....	21
6. J-R CURVE TESTS.....	27
6.1 Specimen Design and Preparation.....	27
6.2 Test Procedure.....	27
6.3 Data Analysis Procedures.....	30
6.4 Measurement of δ_5	35
6.5 Test Results.....	48
6.5.1 0.5T-CT Specimens.....	48
6.5.2 1T-CT Specimens.....	48
6.5.3 2T-CT Specimens.....	64
6.5.4 4T-CT Specimens.....	64
6.5.5 6T-CT Specimen.....	64
6.5.6 Size Comparisons.....	76
6.5.7 δ_5 Results.....	86
6.5.8 Additional Tests.....	93
6.5.9 Comparisons With Data From the U.S. Naval Academy.....	98
6.5.10 Crack Growth Prediction Errors.....	98
6.5.11 Comparison of Different J Equations.....	106
6.5.12 Normalization Method.....	109
6.6 Microstructural and Fractographic Evaluations.....	121
7. DISCUSSION.....	129
8. CONCLUSIONS.....	132

CONTENTS (con't)

	<u>Page</u>
REFERENCES.....	134
APPENDIX A Compilation of Results From Tensile Tests.....	A-1
APPENDIX B J-R Curve Data Analysis Procedures.....	B-1
APPENDIX C Compilation of Results From J-R Curve Tests.....	C-1
APPENDIX D Results From Normalization Method Analysis.....	D-1

LIST OF FIGURES

<u>Figure</u>		<u>Page</u>
1	C_V data for the A 302-B plate.....	12
2	Hyperbolic tangent curvefits to the C_V data.....	13
3	Previous C_V data for a different portion of this A302-B plate.....	14
4	Hyperbolic tangent curvefits to the previous C_V data.....	15
5	Average curvefits to the new and the previous C_V data.....	16
6	DT (5/8-in. thickness) data for the A 302-B plate.....	18
7	The tensile specimen design.....	20
8	Engineering stress-strain curves from the tensile tests.....	23
9	A typical true stress-strain curve and two sample fits to the Ramberg-Osgood equation.....	26
10	Schematic of the CT specimens.....	28
11	Displacement measurement locations.....	29
12	The J-R curve format used for these tests.....	34
13	Location of the δ_5 measurements.....	36
14	The specimens without holes demonstrate different R-curves than the specimen with holes.....	38
15	Load-displacement curves for the δ_5 check-out tests.....	39
16	Crack growth-plastic displacement curves for the δ_5 check-out tests.....	40
17	Key-curves for the δ_5 check-out tests.....	41
18	Fracture surfaces for the δ_5 check-out tests.....	42
19	Fracture surfaces for the δ_5 check-out tests using a Linde 80 weld.....	43
20	Data from specimens with holes demonstrate much greater variability than data from specimens without holes.....	44
21	Load-displacement curves for the δ_5 check-out tests (Linde 80 weld).....	45

LIST OF FIGURES

<u>Figure</u>		<u>Page</u>
22	Crack growth vs. load line displacement curves for the δ_5 check-out tests (Linde 80 weld).....	46
23	Key-curves for the δ_5 check-out tests (Linde 80 weld).....	47
24	The clip gage placements used in tests of the 0.5T-CT and 4T-CT specimens.....	51
25	J_{M*} -R curves from the tests of 0.5T-CT specimens.....	52
26	J_{D*} -R curves from the tests of 0.5T-CT specimens.....	53
27	Load-displacement curves for the 0.5T-CT specimens from the plate mid-thickness.....	54
28	Load-displacement curves for all of the 0.5T-CT specimens.....	55
29	Key-curves from the tests of 0.5T-CT specimens.....	56
30	Fracture surfaces of the 0.5T-CT specimens.....	57
31	Comparison of J_{M*} -R curves from 0.5T-CT specimens with those from the δ_5 check-out tests.....	58
32	Comparison of J_{D*} -R curves from 0.5T-CT specimens with those from the δ_5 check-out tests.....	59
33	Load-displacement curves from the main tests of 0.5T-CT specimens and the δ_5 check-out tests.....	60
34	J_{M*} - and J_{D*} -R curves from the tests of 1T-CT specimens.....	61
35	Load-displacement curves from the tests of 1T-CT specimens.....	62
36	Key-curves from the tests of 1T-CT specimens.....	63
37	Fracture surfaces of the 1T-CT specimens.....	65
38	J_{M*} - and J_{D*} -R curves from the tests of 2T-CT specimens.....	66
39	Load-displacement curves from the tests of 2T-CT specimens.....	67
40	Key-curves from the tests of 2T-CT specimens.....	68
41	Fracture surfaces of the 2T-CT specimens.....	69

LIST OF FIGURES

<u>Figure</u>		<u>Page</u>
42	J_{M^*} - and J_{D^*} -R curves from the tests of 4T-CT specimens.....	70
43	Load-displacement curves from the tests of 4T-CT specimens.....	71
44	Key-curves from the tests of 4T-CT specimens.....	72
45	Fracture surfaces of the 4T-CT specimens.....	73
46	J_{M^*} - and J_{D^*} -R curves from the test of a 6T-CT specimen.....	74
47	Load-displacement curve from the test of a 6T-CT specimen.....	75
48	Key-curve from the test of a 6T-CT specimen.....	77
49	Fracture surface of the 6T-CT specimen.....	78
50	J_{M-C} -R curves for all tests of this plate.....	79
51	J_D -R curves for all tests of this plate.....	80
52	J_M -R curves for all tests of this plate.....	81
53	J_{D^*} -R curves for all tests of this plate.....	82
54	J_{M^*} -R curves for all tests of this plate.....	83
55	Load-displacement curves for all tests of this plate.....	84
56	$\Delta a/W$ as a function of load-line displacement for the tests of this plate.....	85
57	$\Delta a/W$ as a function of δ_{P1}/W for the tests of this plate.....	87
58	δ_5 as a function of load-line displacement for the tests of the Linde 80 weld.....	88
59	δ_5 -R curves for the Linde 80 weld.....	89
60	Comparison of δ_5 to J for the tests of the Linde 80 weld.....	90
61	δ_5 as a function of load-line displacement for the tests of the A 302-B plate.....	91
62	δ_5 -R curves for the tests of the A 302-B plate.....	92
63	Comparison of δ_5 to J_{M-C} , J_{M^*} and J_{D^*} for the tests of A 302-B plate.....	94

LIST OF FIGURES

<u>Figure</u>		<u>Page</u>
64	J-R curves for the test at 24°C and those at 82°C.....	95
65	Fracture surfaces for the additional tests at 24°C and 82°C.....	96
66	Comparison of J-R curves for the additional test at 82°C with those for the previous tests at 82°C.....	97
67	Comparison of J-R curves from the additional tests at 24°C and 82°C.....	99
68	Comparison of USNA and MEA J_{M*} -R curves from 1T-CT specimens.....	100
69	Comparison of USNA and MEA J_{D*} -R curves from 1T-CT specimens.....	101
70	Comparison of USNA and MEA J_{M*} -R curves from 2T-CT specimens.....	102
71	Comparison of USNA and MEA J_{D*} -R curves from 2T-CT specimens.....	103
72	Load-displacement curves for the USNA tests.....	104
73	Key-curves for the USNA tests.....	105
74	J_D -R curves from large and small specimens of A 533-B plate and a Linde 80 weld.....	107
75	J_M -R curves for the same tests illustrated in Fig. 74.....	108
76	Comparison of the R-curves for the 0.5T-CT specimen (V50-118) using the various J formulations.....	110
77	Comparison of the R-curves for the 6T-CT specimen (V50-101) using the various J formulations.....	111
78	The initiation points used for the normalization evaluations.....	113
79	P_N vs. δ_{p1}/W (in a log-log format) for the 0.5T- and 6T-CT specimens.....	115
80	P_N vs. δ_{p1}/W (in a linear format) for the 0.5T- and 6T-CT specimens.....	116
81	J_{D*} -R curves for the 0.5T-CT, using compliance measurements and normalization evaluations.....	117
82	J_{M*} -R curves for the 0.5T-CT, using compliance measurements and normalization evaluations.....	118

LIST OF FIGURES

<u>Figure</u>		<u>Page</u>
83	J_{D^*} -R curves for the 6T-CT, using compliance measurements and normalization evaluations.....	119
84	J_{M^*} -R curves for the 6T-CT, using compliance measurements and normalization evaluations.....	120
85	Three-dimensional views showing microstructure and inclusion distribution of specimen V50-117.....	123
86	Three-dimensional views for specimen V50-102.....	124
87	Scanning electron fractograph of high toughness 0.5T-CT specimen V50-117 and low toughness 4T-CT specimen V50-102.....	125
88	Scanning electron fractograph of high toughness 0.5T-CT specimen V50-118 and low toughness 4T-CT specimen V50-103.....	126
89	Scanning electron fractograph of high toughness 0.5T-CT specimen V50-118 and low toughness 4T-CT specimen V50-103.....	127
90	Visual correlation of the L-LT surface showing the inclusion distribution microstructure with banding, and fracture surface with splits.....	128
91	Comparison of J_M -R curve data for the 0.5T-CT specimens with estimates using correlations.....	131

LIST OF TABLES

<u>Table</u>		<u>Page</u>
1	Summary of Procurement Specifications for A 302-B Steel Test Plate.....	4
2	Chemical Composition and Heat Treatment of A 302-B Plate.....	5
3	Charpy-V Data for A 302-B Plate (V50) (1/4-T Location, T-L Orientation).....	7
4	Charpy-V Data for A 302-B Plate (V50) (1/2-T Location, T-L Orientation).....	8
5	Charpy-V Data for A 302-B Plate (V50) (3/4-T Location, T-L Orientation).....	9
6	Average Charpy-V Data for A 302-B Plate (V50) (T-L Orientation).....	10
7	Results From Charpy-V Curve-Fitting.....	11
8	Comparison of New and Previous Charpy-V Data.....	11
9	Strength Data for A 302-B Plate (V50) at 82°C (180°F) (T-L Orientation).....	22
10	Ramberg-Osgood Curvefit Parameters.....	25
11	Summary of Test Results for A 302-B Plate (Code V50) at 82°C (180°F).....	49
12	Summary of J-R Curve Results for A 302-B Plate (Code V50) at 82°C (180°F).....	50

FOREWORD

The work reported here was performed at Materials Engineering Associates (MEA) under the program, Structural Integrity of Water Reactor Pressure Boundary Components, F. J. Loss, Program Manager. The program is sponsored by the Office of Nuclear Regulatory Research of the U. S. Nuclear Regulatory Commission (NRC). The technical monitor for the NRC is Alfred Taboada.

Prior reports under the current contract are listed below:

1. J. R. Hawthorne, "Significance of Nickel and Copper to Radiation Sensitivity and Postirradiation Heat Treatment Recovery of Reactor Vessel Steels," USNRC Report NUREG/CR-2948, Nov. 1982.
2. "Structural Integrity of Water Reactor Pressure Boundary Components, Annual Report for 1982," F. J. Loss, Ed., USNRC Report NUREG/CR-3228, Vol. 1, Apr. 1983.
3. J. R. Hawthorne, "Exploratory Assessment of Postirradiation Heat Treatment Variables in Notch Ductility Recovery of A 533-B Steel," USNRC Report NUREG/CR-3229, Apr. 1983.
4. W. H. Cullen, K. Torronen, and M. Kemppainen, "Effects of Temperature on Fatigue Crack Growth of A 508-2 Steel in LWR Environment," USNRC Report NUREG/CR-3230, Apr. 1983.
5. "Proceedings of the International Atomic Energy Agency Specialists' Meeting on Subcritical Crack Growth," Vols. 1 and 2, W. H. Cullen, Ed., USNRC Conference Proceeding NUREG/CP-0044, May 1983.
6. W. H. Cullen, "Fatigue Crack Growth Rates of A 508-2 Steel in Pressurized, High-Temperature Water," USNRC Report NUREG/CR-3294, June 1983.
7. J. R. Hawthorne, B. H. Menke, and A. L. Hiser, "Notch Ductility and Fracture Toughness Degradation of A 302-B and A 533-B Reference Plates from PSF Simulated Surveillance and Through-Wall Irradiation Capsules," USNRC Report NUREG/CR-3295, Vol. 1, Apr. 1984.
8. J. R. Hawthorne and B. H. Menke, "Postirradiation Notch Ductility and Tensile Strength Determinations for PSF Simulated Surveillance and Through-Wall Specimen Capsules," USNRC Report NUREG/CR-3295, Vol. 2, Apr. 1984.
9. A. L. Hiser and F. J. Loss, "Alternative Procedures for J-R Curve Determination," USNRC Report NUREG/CR-3402, July 1983.

10. A. L. Hiser, F. J. Loss, and B. H. Menke, "J-R Curve Characterization of Irradiated Low Upper Shelf Welds," USNRC Report NUREG/CR-3506, Apr. 1984.
11. W. H. Cullen, R. E. Taylor, K. Torronen, and M. Kemppainen, "The Temperature Dependence of Fatigue Crack Growth Rates of A 351 CF8A Cast Stainless Steel in LWR Environment," USNRC Report NUREG/CR-3546, Apr. 1984.
12. "Structural Integrity of Light Water Reactor Pressure Boundary Components -- Four-Year Plan 1984-1988," F. J. Loss, Ed., USNRC Report NUREG/CR-3788, Sep. 1984.
13. W. H. Cullen and A. L. Hiser, "Behavior of Subcritical and Slow-Stable Crack Growth Following a Postirradiation Thermal Anneal Cycle," USNRC Report NUREG/CR-3833, Aug. 1984.
14. "Structural Integrity of Water Reactor Pressure Boundary Components: Annual Report for 1983," F. J. Loss, Ed., USNRC Report NUREG/CR-3228, Vol. 2, Sept. 1984.
15. W. H. Cullen, "Fatigue Crack Growth Rates of Low-Carbon and Stainless Piping Steels in PWR Environment," USNRC Report NUREG/CR-3945, Feb. 1985.
16. W. H. Cullen, M. Kemppainen, H. Hanninen, and K. Torronen, "The Effects of Sulfur Chemistry and Flow Rate on Fatigue Crack Growth Rates in LWR Environments," USNRC Report NUREG/CR-4121, Feb. 1985.
17. "Structural Integrity of Water Reactor Pressure Boundary Components: Annual Report for 1984," F. J. Loss, Ed., USNRC Report NUREG/CR-3228, Vol. 3, June 1985.
18. A. L. Hiser, "Correlation of C_v and K_{Ic}/K_{Jc} Transition Temperature Increases Due to Irradiation," USNRC Report NUREG/CR-4395, Nov. 1985.
19. W. H. Cullen, G. Gabetta, and H. Hanninen, "A Review of the Models and Mechanisms For Environmentally-Assisted Crack Growth of Pressure Vessel and Piping Steels in PWR Environments," USNRC Report NUREG/CR-4422, Dec. 1985.
20. "Proceedings of the Second International Atomic Energy Agency Specialists' Meeting on Subcritical Crack Growth," W. H. Cullen, Ed., USNRC Conference Proceeding NUREG/CP-0067, Vols. 1 and 2, Apr. 1986.
21. J. R. Hawthorne, "Exploratory Studies of Element Interactions and Composition Dependencies in Radiation Sensitivity Development," USNRC Report NUREG/CR-4437, Nov. 1985.

22. R. B. Stonesifer and E. F. Rybicki, "Development of Models for Warm Prestressing," USNRC Report NUREG/CR-4491, Jan. 1987.
23. E. F. Rybicki and R. B. Stonesifer, "Computational Model for Residual Stresses in a Clad Plate and Clad Fracture Specimens," USNRC Report NUREG/CR-4635, Oct. 1986.
24. D. E. McCabe, "Plan for Experimental Characterization of Vessel Steel After Irradiation," USNRC Report NUREG/CR-4636, Oct. 1986.
25. E. F. Rybicki, J. R. Shadley, and A. S. Sandhu, "Experimental Evaluation of Residual Stresses in a Weld Clad Plate and Clad Test Specimens," USNRC Report NUREG/CR-4646, Oct. 1986.
26. "Structural Integrity of Water Reactor Pressure Boundary Components: Annual Report for 1985," F. J. Loss, Ed., USNRC Report NUREG/CR-3228, Vol. 4, June 1986.
27. G. Gabetta and W. H. Cullen, "Application of a Two-Mechanism Model for Environmentally-Assisted Crack Growth," USNRC Report NUREG/CR-4723, Oct. 1986.
28. W. H. Cullen, "Fatigue Crack Growth Rates in Pressure Vessel and Piping Steels in LWR Environments," USNRC Report NUREG/CR-4724, Mar. 1987.
29. W. H. Cullen and M. R. Jolles, "Fatigue Crack Growth of Part-Through Cracks in Pressure Vessel and Piping Steels: Air Environment Results, USNRC Report NUREG/CR-4828, Oct. 1988.
30. D. E. McCabe, "Evaluation of Surface Cracks Embedded in Reactor Vessel Cladding Unirradiated Bend Specimens," USNRC Report NUREG/CR-4841, May 1987.
31. H. Hanninen, M. Vulli, and W. H. Cullen, "Surface Spectroscopy of Pressure Vessel Steel Fatigue Fracture Surface Films Formed in PWR Environments," USNRC Report NUREG/CR-4863, July 1987.
32. A. L. Hiser and G. M. Callahan, "A User's Guide to the NRC's Piping Fracture Mechanics Data Base (PIFRAC)," USNRC Report NUREG/CR-4894, May 1987.
33. "Proceedings of the Second CSNI Workshop on Ductile Fracture Test Methods (Paris, France, April 17-19, 1985)," F. J. Loss, Ed., USNRC Conference Proceeding NUREG/CP-0064, Aug. 1988.
34. W. H. Cullen and D. Broek, "The Effects of Variable Amplitude Loading on A 533-B Steel in High-Temperature Air and Reactor Water Environments," USNRC Report NUREG/CR-4929 (in publication).

35. "Structural Integrity of Water Reactor Pressure Boundary Components: Annual Report for 1986," F. J. Loss, Ed., USNRC Report NUREG/CR-3228, Vol. 5, July 1987.
36. F. Ebrahimi et al., "Development of a Mechanistic Understanding of Radiation Embrittlement in Reactor Pressure Vessel Steels: Final Report," USNRC Report NUREG/CR-5063, Jan. 1988.
37. J. B. Terrell, "Fatigue Life Characterization of Smooth and Notched Piping Steel Specimens in 288°C Air Environments," USNRC Report NUREG/CR-5013, May 1988.
38. A. L. Hiser, "Tensile and J-R Curve Characterization of Thermally Aged Cast Stainless Steels," USNRC Report NUREG/CR-5024, Sept. 1988.
39. J. B. Terrell, "Fatigue Strength of Smooth and Notched Specimens of ASME SA 106-B Steel in PWR Environments," USNRC Report NUREG/CR-5136, Sept. 1988.
40. D. E. McCabe, "Fracture Evaluation of Surface Cracks Embedded in Reactor Vessel Cladding: Material Property Evaluations," USNRC Report NUREG/CR-5207, Sept. 1988.
41. J. R. Hawthorne and A. L. Hiser, "Experimental Assessments of Gundremmingen RPV Archive Material for Fluence Rate Effects Studies," USNRC Report NUREG/CR-5201, Oct, 1988.
42. J. B. Terrell, "Fatigue Strength of ASME SA 106-B Welded Steel Pipes in 288°C Air Environments," USNRC Report NUREG/CR-5195, Dec. 1988.

ACKNOWLEDGMENT

This work was sponsored by the Division of Engineering, with A. Taboada the technical monitor. M. Mayfield was key in conceiving and initiating this study.

The assistance of G. Wilkowski in sending copies of several references on the effects of splits and laminations on material toughness is appreciated.

The assistance of many people at MEA helped to give this study a successful conclusion. G. Lohr, H. Sanders and R. Taylor assisted in some of the experimental work. G. Baker assisted in the SEM work. Of particular assistance to this effort were E. D'Ambrosio, who conducted many of the tests, T. Ramey, who did much of the data processing, G. Carlson, who helped in graphics preparation, and L. Gelzer-Cargill, who prepared this manuscript.

1. INTRODUCTION

For structural integrity assessments concerning fully ductile upper shelf fracture, elastic-plastic fracture mechanics methodology, in particular the J integral, has received considerable attention. For upper shelf fracture, the J resistance or J-R curve is used to characterize the fracture resistance of structural steels, including those used in nuclear reactor pressure vessel (RPV) construction. For RPV steels in the unirradiated or preservice condition, evaluation of "valid" J-R curve trends to large crack growth levels is a straightforward manner, since test specimens up to the full thickness of the RPV can be tested using advanced test equipment and procedures. In contrast for the irradiated condition of RPV steels, evaluation of "valid" J-R curve trends is generally restricted to small crack growth increments, due to the limited size of the specimens available in reactor surveillance capsules or any other source of irradiated material. In fact, a 102-mm (4-in.) thick specimen is the largest RPV steel fracture toughness specimen tested in the irradiated condition (using J-R curve procedures) in the United States; RPVs range in thickness from 203 mm (8 in.) to 305 mm (12 in.), depending on the design, the vendor and the location on the RPV. Specimens in typical surveillance capsules range in thickness from 12.7 mm (0.5 in.) to 25.4 mm (1 in.).

Of the various concerns facing utilities with nuclear power plants, a requirement of Part 50 of Title 10 of the Code of Federal Regulations (10 CFR 50) specifies a minimum Charpy-V upper shelf level of 68 J (50 ft-lb) for the beltline materials of RPVs. Recent calculations by members of American Society of Mechanical Engineers (ASME) Section XI indicate that J-R curve data for crack growth increments ranging up to 15 mm or 20 mm may be required to demonstrate structural integrity for such low upper shelf materials, using procedures under consideration by ASME Section XI. From standards adopted by Committee E 24 of the American Society for Testing and Materials (ASTM), extremely large specimens, ranging in thickness up to 150 mm or 200 mm, are needed to give valid data for the large crack growth increments described above. Obviously, any use of such large specimens in irradiation programs such as surveillance capsules is generally impossible due to size constraint in the RPV. Therefore, procedures and methodology for taking the available valid data from small specimens (for crack growth intervals from ~ 1 mm to 2.5 mm), and extrapolating that data in a conservative manner up to the large crack growth intervals required, would fill the void needed to accurately and conservatively evaluate safety margins for cases in which low upper shelf material is a key concern.

2. PROGRAM PLAN

As initially conceived, the goal of this program was to develop J-R curve data, for a material exhibiting a low Charpy upper shelf energy level using small and large specimens. These data would form a reference data set for the development and validation of procedures to extrapolate small specimen data at small crack growth (Δa) levels to the large crack growth levels required to assess the structural stability of RPVs. The large test specimens would provide valid data to large crack growth intervals to validate or permit refinement of the extrapolation procedures.

Although most of the limiting low upper shelf toughness materials are in fact weld metals, a base plate was selected for this program. A weld metal was not chosen since RPV welds are typically fairly narrow, less than 51 mm (2 in.), and the large specimens, in particular, therefore would be composite or duplex specimens, composed primarily of base plate with the relatively narrow band of weld metal. In contrast, the small specimens would tend to be composed of all weld metal. In contrast, the use of base plate as the test material means that all specimens, both large and small, would be essentially homogeneous. Of particular concern in the use of weld metal is the difference in deformation characteristics among weld metal, base plate, and even the intermediate zones (such as heat affected zone and fusion line), and the effect that this would have on the apparent measured toughness.

Although some data from previous work looking at size effects for base plate are available (Ref. 1 and 2), these materials had high upper shelf energy levels and were thought not to be fully applicable to low upper shelf concerns.

To provide stepwise increases in the valid range of J-R curve data, several sizes of compact tension (CT) specimens were used. In particular, the smallest specimens (0.5T-CT size, with a thickness of 12.7 mm or 0.5 in.) were intended to simulate the smallest specimens available in RPV surveillance programs. A 6T-CT size with a thickness of 152.4 mm (6 in.), represented the largest specimen which could be removed from the plate. Intermediate size specimens were 1T-, 2T- and 4T-CT sizes, with full-thickness specimens used in each case. In all cases, the specimens were proportional.

As support information, Charpy-V notch (C_V) and tensile tests were also planned. The C_V specimens were sought to assess the toughness gradient through the plate thickness, to give an evaluation of the upper shelf energy level of this material and to guide selection of the test temperature for the fracture toughness specimens. The tensile tests likewise permitted an evaluation of through-thickness variability, but more importantly resulted in evaluation of the deformation (stress-strain) characteristics of the material at the temperature of the J-R curve tests.

3. MATERIAL

The material used in this program is an ASTM A 302-B plate, fabricated by Lukens Steel. The heat treatment applied to this plate was determined from a review of the metallurgical histories of many production A 302-B plates (including the ASTM A 302-B reference plate used in some RPV surveillance programs) used in early vessel construction. Appendix A of Ref. 3 gives additional information on the procurement of this heat.

Specifications for the plate are given in Table 1 (from Ref. 3). The sulfur content of the ingot used was 0.025%, in the range of those of early production A 302-B plates. In addition, a minimum of cross rolling was used, to maximize differences in properties for the high and the low toughness orientations.

Chemical composition and the actual heat treatment applied to the plate are given in Table 2.

As with most RPV base plates, the low toughness orientation for this plate is the T-L orientation, per ASTM E 399. From previous results (Ref. 3), this orientation was found to have a C_v upper shelf energy of 71 J (52 ft-lb); in contrast, the high toughness L-T orientation had a C_v upper shelf energy of 146 J (108 ft-lb).

Table 1 Summary of Procurement Specifications For
A 302-B Steel Test Plate

Specification	
ASTM type/grade	A 302-B (fire box quality)
Gage	6 in. (152 mm)
Pattern size (total)	113 in. x 110 in. (2.9 x 2.8 m) min (RD) ^a
Melt furnance	Electric
Melt treatment	VIP
Melt/slab number	C4076-1A
Ingot to plate cross rolling	Minimum - apply cross rolling only to reach pattern requirement
Heat treatment	1650° ±25°F, (899° ±14°C) 6 hr WQ ^b 1200° ±25°F, (649° ±14°C) 6 hr AC ^c stress relieve test specimens only 1150° ±25°F, (621 ±14°C) 24 hr, FC ^d to 600°F, AC
Testing	Ultrasonic to ASME Code Section III, Summer 1972, Addendum NB-2532.1 (ASME Code Case 1338, alt. 1, 100%)
Required properties	Plate (longitudinal orientation) shall meet C _v 30 ft-lb (41 J) at +10°F (-12°C). DW-NDT will be performed for information only. Longitudinal and transverse tensile tests shall confirm A 302-B plate properties for 1/4T location.
Marking	Patterns shall be marked to show primary rolling direction and orientation and position relative to prime plate and original.

^a (RD) Primary rolling direction.

^b Water quench

^c Air cool

^d Furnace cool

Table 2 Chemical Composition and Heat Treatment of A 302-B Plate

Element	B & W ^a	Lukens ^b
C	0.21	0.23
Mn	1.46	1.40
P	0.010	0.016
S	0.021	0.025
Si	0.24	0.24
Ni	0.23	-
Cr	0.06	-
Mo	0.54	0.57
Cu	0.059	-
V	0.012	-
Al ^c	0.034	-
Ti	0.008	-
Co	0.012	-
Cb	0.007	-
Ta	0.02	-
Sn	0.009	-
B	0.0006	-
Pb	0.004	-
As	0.004	-
Zn	0.00001	-

^a Courtesy Babcock and Wilcox Co.

^b Mill test report of Lukens Steel Co.

^c Total aluminum

Heat Treatment	
by Lukens:	Austenitized 1625°-1675°F (885°-913°C), held 1 h per in. minimum, water quenched; tempered 1220°F (660°C) held 1 h per in. min, water quenched.
by NRL:	Stress relief annealed 1150°F ±25°F (621°C ±14°C) for 32 h; furnace cooled to below 600°F (316°C) at 100°F (56°C) max per h.

4. CHARPY-V TESTS

4.1 Specimen Design/Test and Data Analysis Procedures

The C_v data were determined using the Type A specimen design given in ASTM Standard E 23. Test procedures were as outlined in that standard.

To simplify analysis of the test data, the energy results were curve-fit to a hyperbolic tangent (tanh) equation, as given by

$$C_v = A + B \tanh \left[\frac{T - T_o}{C} \right] \quad (1)$$

A, B, C and T_o are fitting parameters optimized for each data set.

In this case, the upper shelf is given as A+B, and the temperature at an arbitrary C_v level "E" is given by

$$T_E = T_o + C \tanh^{-1} \left(\frac{E-A}{B} \right) \quad (2)$$

4.2 Test Results

To assess through-thickness variability of this plate, specimens were machined from the 1/4T-, 1/2T- and 3/4T- thickness levels of the plate, with 12 specimens from each thickness level. Tabulated results for the individual C_v tests are given in Tables 3 to 5, with average values at each temperature given in Table 6. Results from curvefitting to Eq. 1 are given in Table 7. As indicated in Table 6 and illustrated in Fig. 1, the plate mid-thickness or 1/2T location demonstrates higher energy levels on the upper shelf than do the other thickness locations. As indicated in Table 7 and illustrated in Fig. 2 from tanh curve-fitting results, the 1/4T and 3/4T locations exhibit similar upper shelf levels, within 1%, whereas the 1/2T location has an upper shelf level which is 16% higher.

Previous C_v data for another portion of this plate (Ref. 3) likewise indicate higher upper shelf levels for the 1/2T location (Fig. 3). In this case, the tanh curves (Fig. 4) indicate that the 3/4T location has the lower overall upper shelf level.

Comparison of the upper shelf levels and transition temperatures for the new and the previous data (Table 8 and Fig. 5) illustrate the overall higher upper shelf energy levels (~ 10% higher) and lower transition temperatures for the portion of the plate used for the subject program. For both sets the 1/2T location has the highest upper shelf energy level, 10-15% higher than the average for all three locations.

Table 3 Charpy-V Data for A 302-B Plate (V50)
(1/4-T Location, T-L Orientation)

Temperature		Absorbed Energy		Lateral Expansion		Specimen Number
(°C)	(°F)	(J)	(ft-lb)	(mm)	(mils)	
-51	-60	9	7	0.10	4	206
-51	-60	7	5.5	0.08	3	209
-18	0	24	17.5	0.41	16	201
-18	0	27	20	0.46	18	210
27	80	54	40	1.09	43	205
27	80	68	50	1.22	48	208
82	180	75	55	1.32	52	203
82	180	65	48	1.19	47	212
177	350	66	49	1.22	48	202
177	350	73	54	1.32	52	211
288	550	64	47	1.24	49	204
288	550	69	51	1.27	50	207

Table 4 Charpy-V Data for A 302-B Plate (V50)
(1/2-T Location, T-L Orientation)

Temperature		Absorbed Energy		Lateral Expansion		Specimen Number
(°C)	(°F)	(J)	(ft-lb)	(mm)	(mils)	
-51	-60	15	11	0.18	7	218
-51	-60	11	8	0.13	5	221
-18	0	23	17	0.46	18	213
-18	0	26	19	0.48	19	222
27	80	64	47	1.24	49	217
27	80	77	57	1.32	52	220
82	180	76	56	1.37	54	215
82	180	71	52	1.40	55	224
177	350	79	58	1.50	59	214
177	350	89	66	1.47	58	223
288	550	83	61	1.52	60	216
288	550	81	60	1.47	58	219

Table 5 Charpy-V Data for A 302-B Plate (V50)
(3/4-T Location, T-L Orientation)

Temperature		Absorbed Energy		Lateral Expansion		Specimen Number
(°C)	(°F)	(J)	(ft-lb)	(mm)	(mils)	
-51	-60	11	8	0.13	5	230
-51	-60	7	5	0.08	3	233
-18	0	31	23	0.56	22	225
-18	0	28	21	0.53	21	234
27	80	60	44	1.14	45	229
27	80	64	47	1.22	48	232
82	180	60	44	1.24	49	227
82	180	64	47	1.22	48	236
177	350	72	53	1.42	56	226
177	350	72	53	1.37	54	235
288	550	70	52	1.40	55	228
288	550	75	55	1.35	53	231

Table 6 Average Charpy-V Data for A 302-B Plate (V50)
(T-L Orientation)

Test Temperature		Absorbed Energy (J)		
		1/4T	1/2T	3/4T
(°C)	(°F)			
-51	-60	8	13	9
-18	0	25	24	30
27	80	61	71	62
82	180	70	73	62
177	350	70	84	72
288	550	66	82	73

Table 7 Results From Charpy-V Curve-Fitting

Thickness Location	$C_v = A + B \tanh [(T - T_o)/C]$				Upper Shelf Energy ^e at 41J			
	A ^a	B ^b	C ^c	T _o ^d				
	(J)	(J)	(Δ°C)	(°C)	(J)	(ft-lb)	(°C)	(°F)
1/4T	36.8	31.9	32.3	-5.7	68.8	50.7	-2	29
1/2T	45.6	34.3	27.6	1.9	79.9	59.0	-2	28
3/4T	33.8	35.6	42.6	-13.7	69.4	51.2	-5	22
ALL	39.5	33.1	32.8	-4.4	72.6	53.6	-3	26

^a ft-lb = A x 0.74

^b ft-lb = B x 0.74

^c Δ°F = C x 0.56

^d °F = T_o x 1.8 + 32

^e Given by A + B

Table 8 Comparison of New and Previous Charpy-V Data

Thickness Location	Upper Shelf Energy		Temperature at 41J	
	(New/Previous)		(New/Previous)	
	(J)	(ft-lb)	(°C)	(°F)
1/4T	69/64	51/47	-2/2	29/35
1/2T	80/74	59/55	-2/5	28/42
3/4T	69/60	51/44	-5/12	22/54
ALL	73/65	53/48	-3/6	26/43

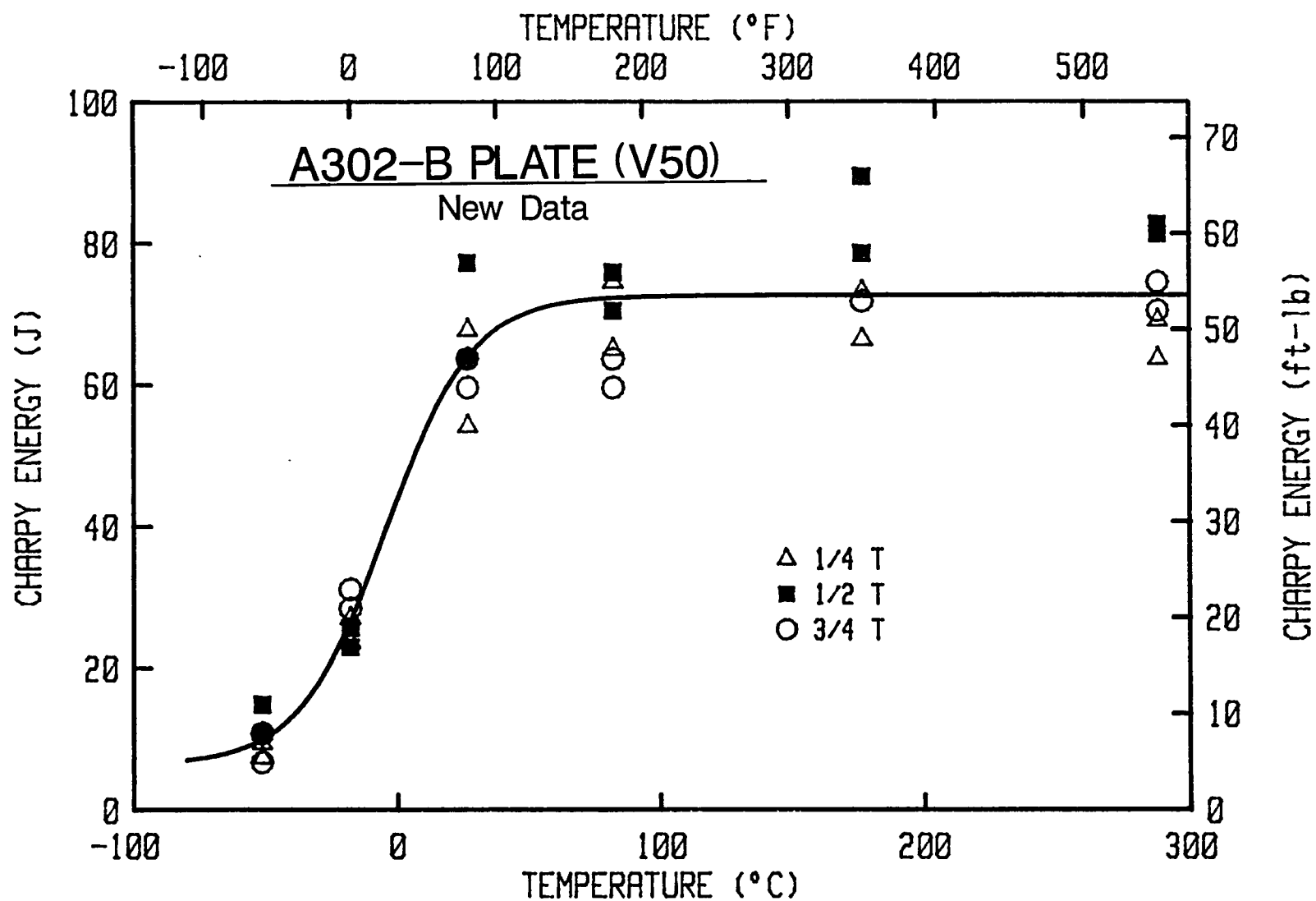


Fig. 1 C_v data for the A 302-B plate under study. On the upper shelf, the 1/2T location tends to exhibit higher energy levels than the 1/4T or 3/4T locations.

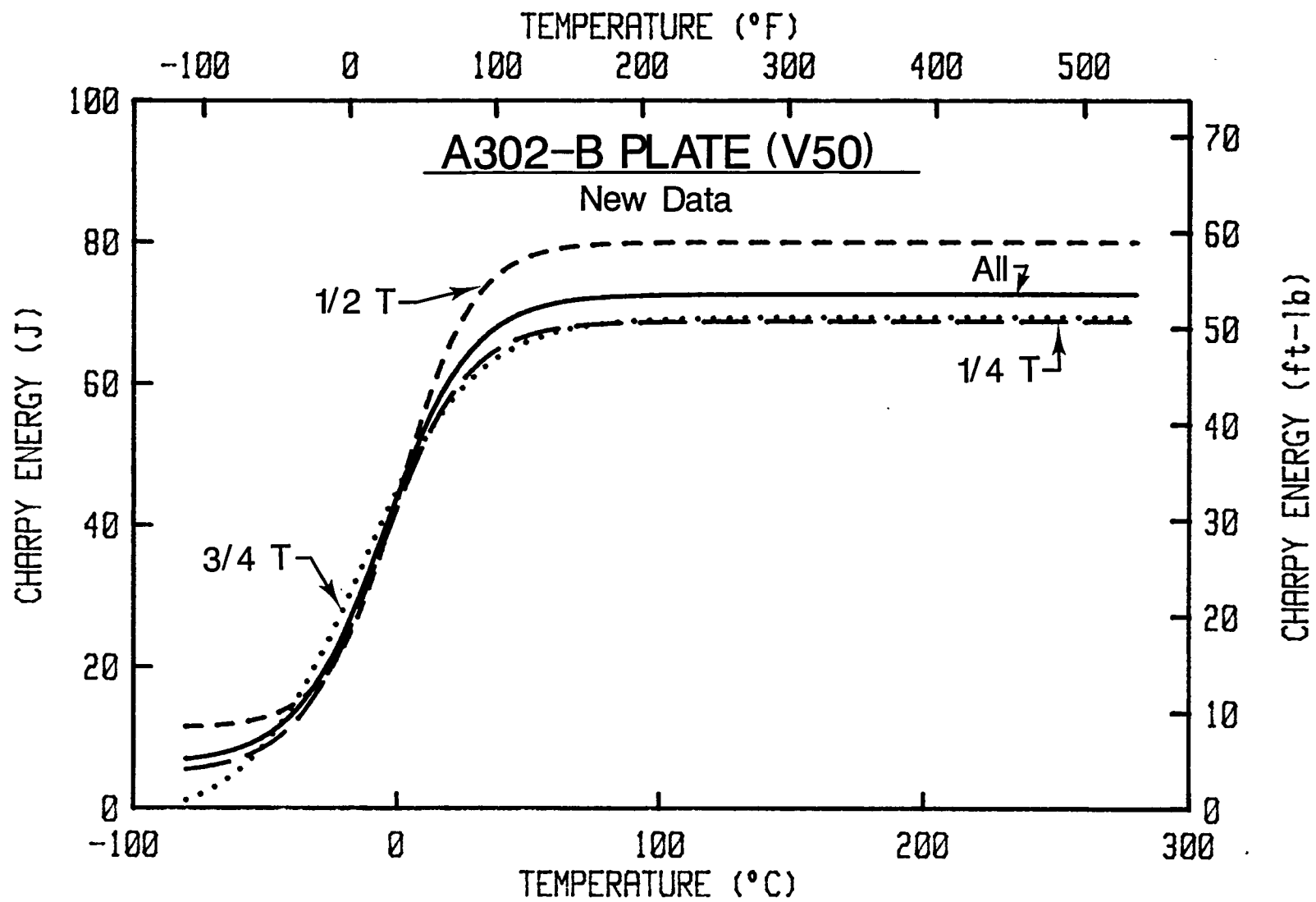


Fig. 2 Hyperbolic tangent curvefits to the C_v data illustrated in Fig. 1. On the upper shelf, the 1/2T location has the highest energy levels, whereas the 1/4T and 3/4T locations exhibit similar trends.

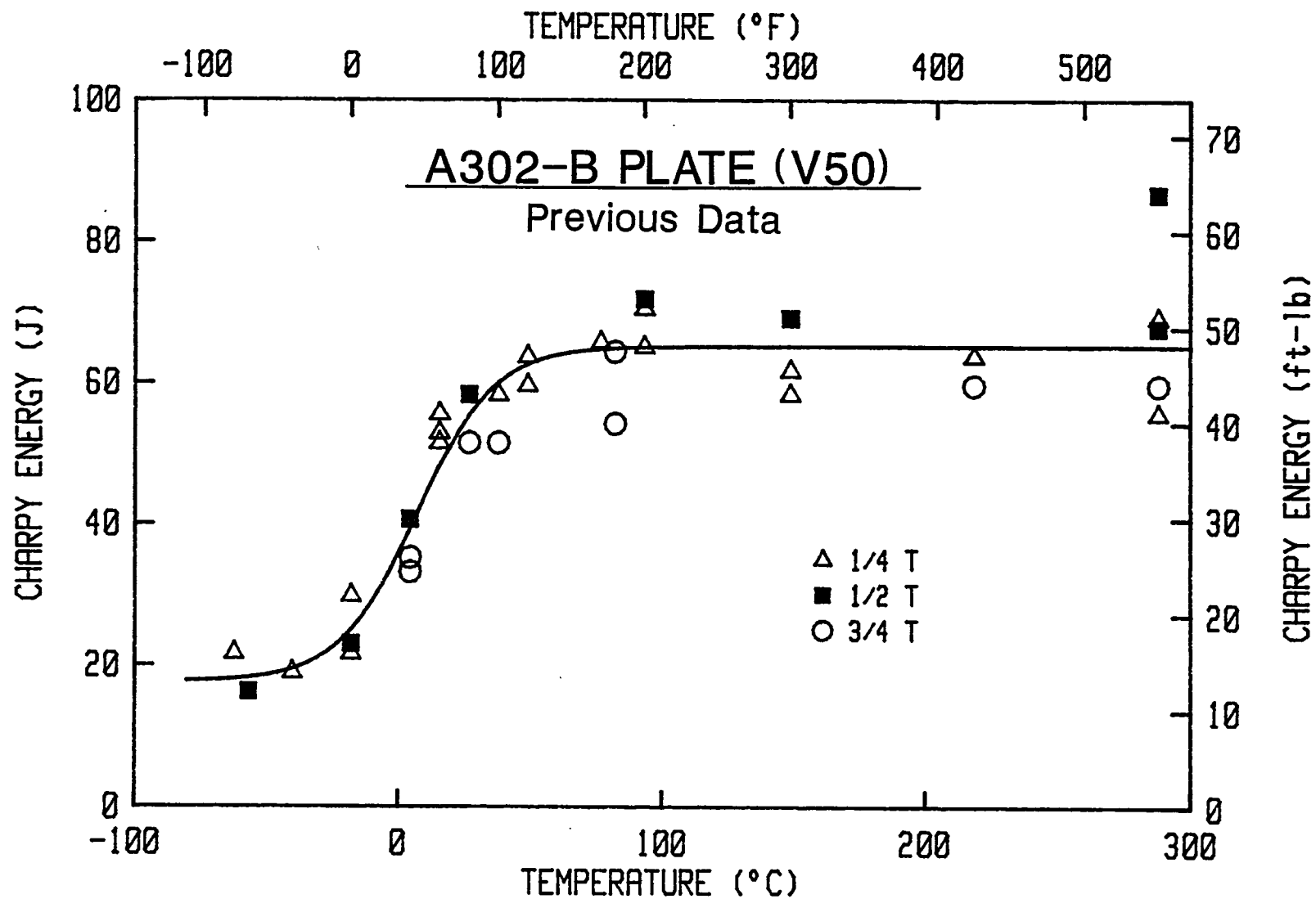


Fig. 3 Previous data for a different portion of this A 302-B plate also indicate higher upper shelf toughness for the 1/2T location.

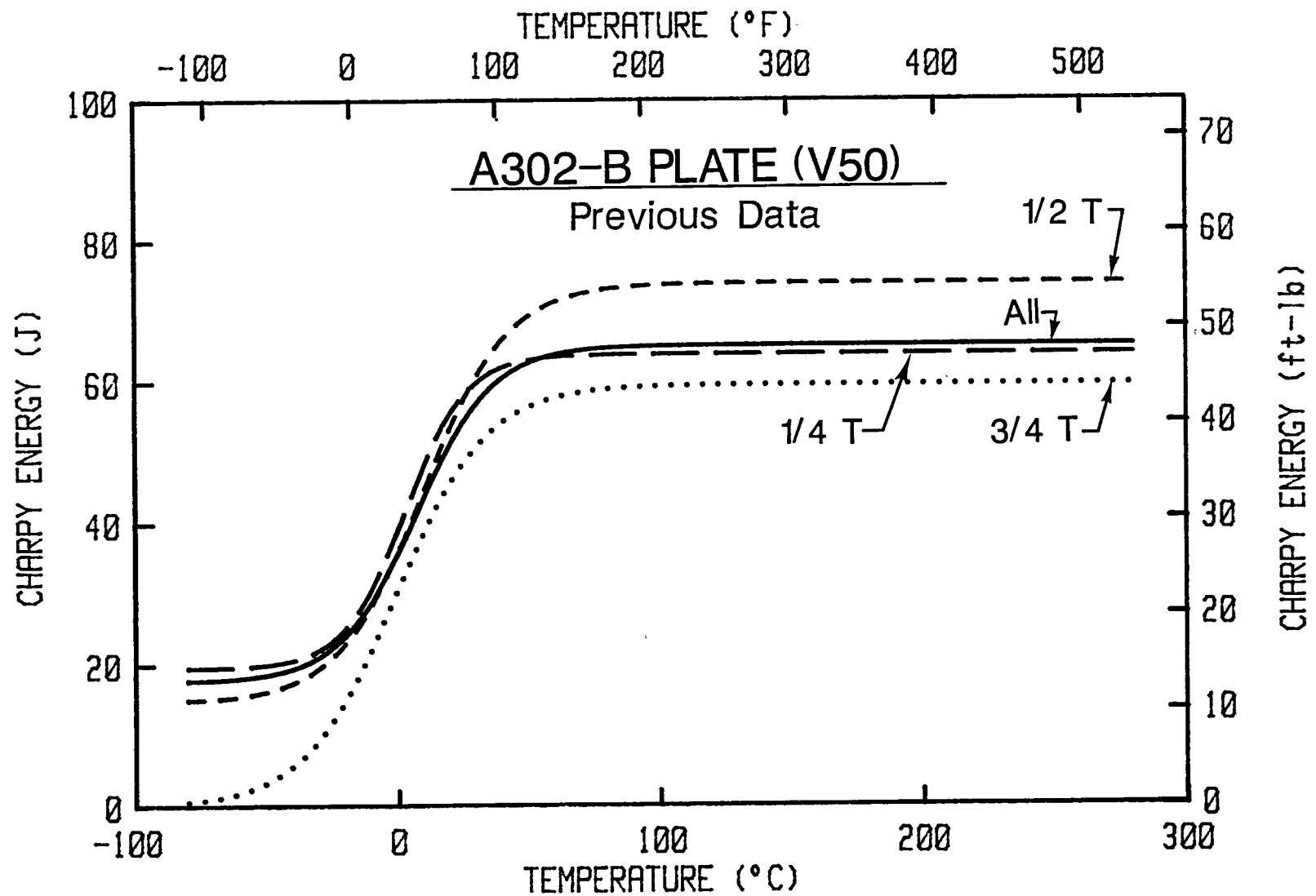


Fig. 4 Hyperbolic tangent curvefits to the C_v data illustrated in Fig. 3. In this case, the 3/4T location demonstrates the lowest upper shelf level.

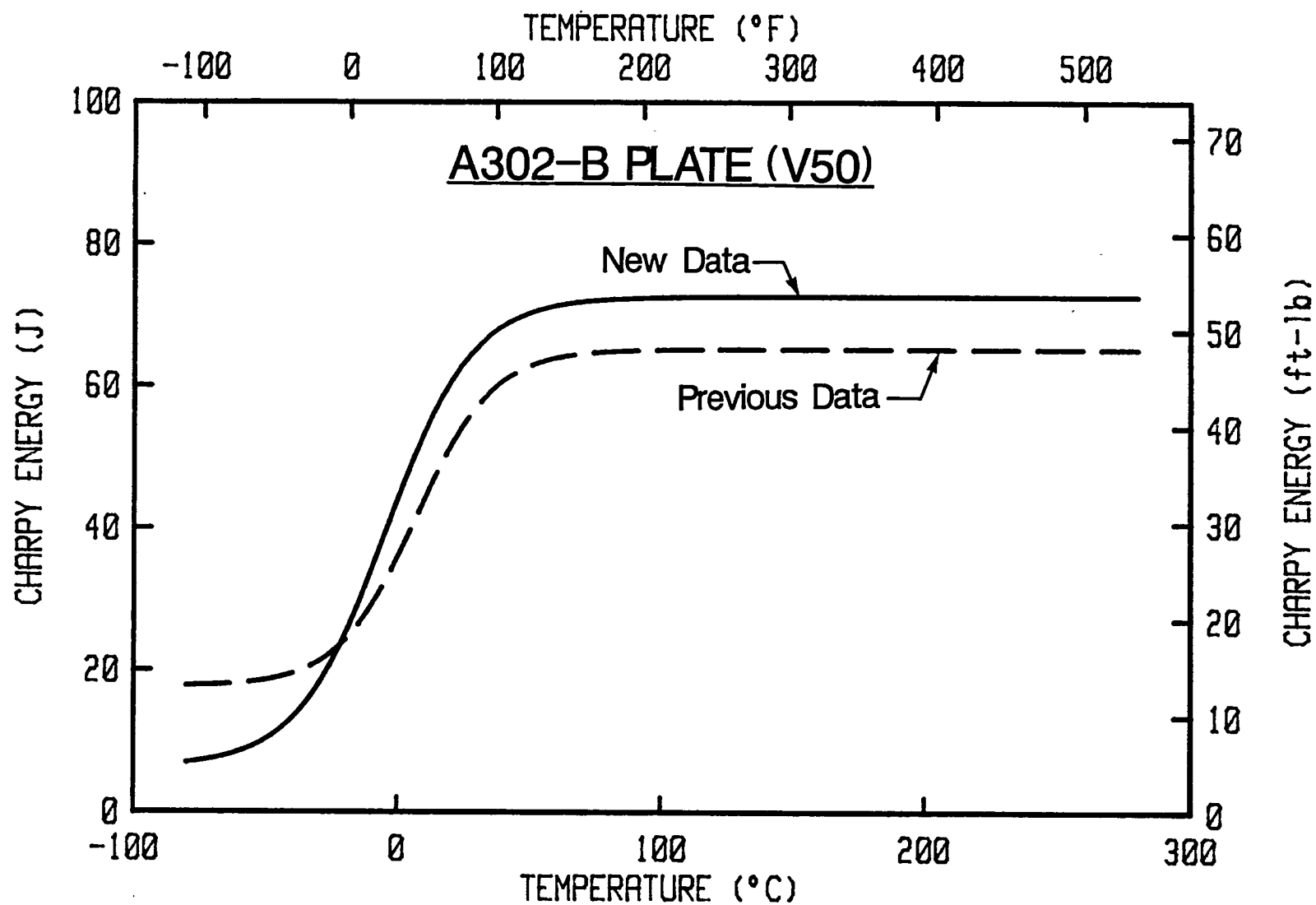


Fig. 5 Comparison of the average curvefits to the new and the previous C_v data for the A 302-B plate. The new data indicate higher overall toughness, with a higher upper shelf energy level and lower transition temperatures.

The differences between the new and the previous data are probably caused by variability along the plate. Since the new data are from the same portion of the plate as the fracture toughness (CT) specimens, the new results are more applicable to the fracture toughness data.

The selection of the test temperature for the fracture toughness tests was made based upon two requirements: (a) no brittle fracture of the 6T-CT specimen (in particular), and (b) the lowest possible temperature (above ambient) since some repositioning of transducers may be required during testing. For brittle fracture concern, dynamic brittle toughness must be considered, since portions of the fracture tests specimens could receive dynamic loading during the (nominal) static loading rate used in the fracture toughness testing.

Dynamic tear (DT) data are available for a portion of this plate tested previously. As illustrated in Fig. 6, the DT data indicate onset of the dynamic upper shelf at $\sim 40^{\circ}\text{C}$ (104°F) for a 5/8 in. thick section. This temperature will be higher for thicker sections because of the larger mechanical constraint associated with the latter. Research at the Naval Research Laboratory (NRL) with large DT specimens has indicated an elevation in the mid-transition DT energy region of $17\text{--}39^{\circ}\text{C}$ ($30\text{--}70^{\circ}\text{F}$) between 5/8-in. DT specimens and 3-in. to 12-in. thick DT specimens. The temperature at the onset of the upper shelf was similarly elevated but to a lesser degree. The upper shelf temperature for dynamic loading of thick sections was therefore conservatively estimated to be elevated by 39°C (70°F) over that for the 5/8-in. DT results, i.e., 79°C (174°F). Since the new C_v data have a lower transition temperature than the previous data, a temperature of 79°C (174°F) should adequately assure the absence of a cleavage mode of fracture for the CT tests. For convenience, the actual temperature was increased slightly to 82°C (180°F).

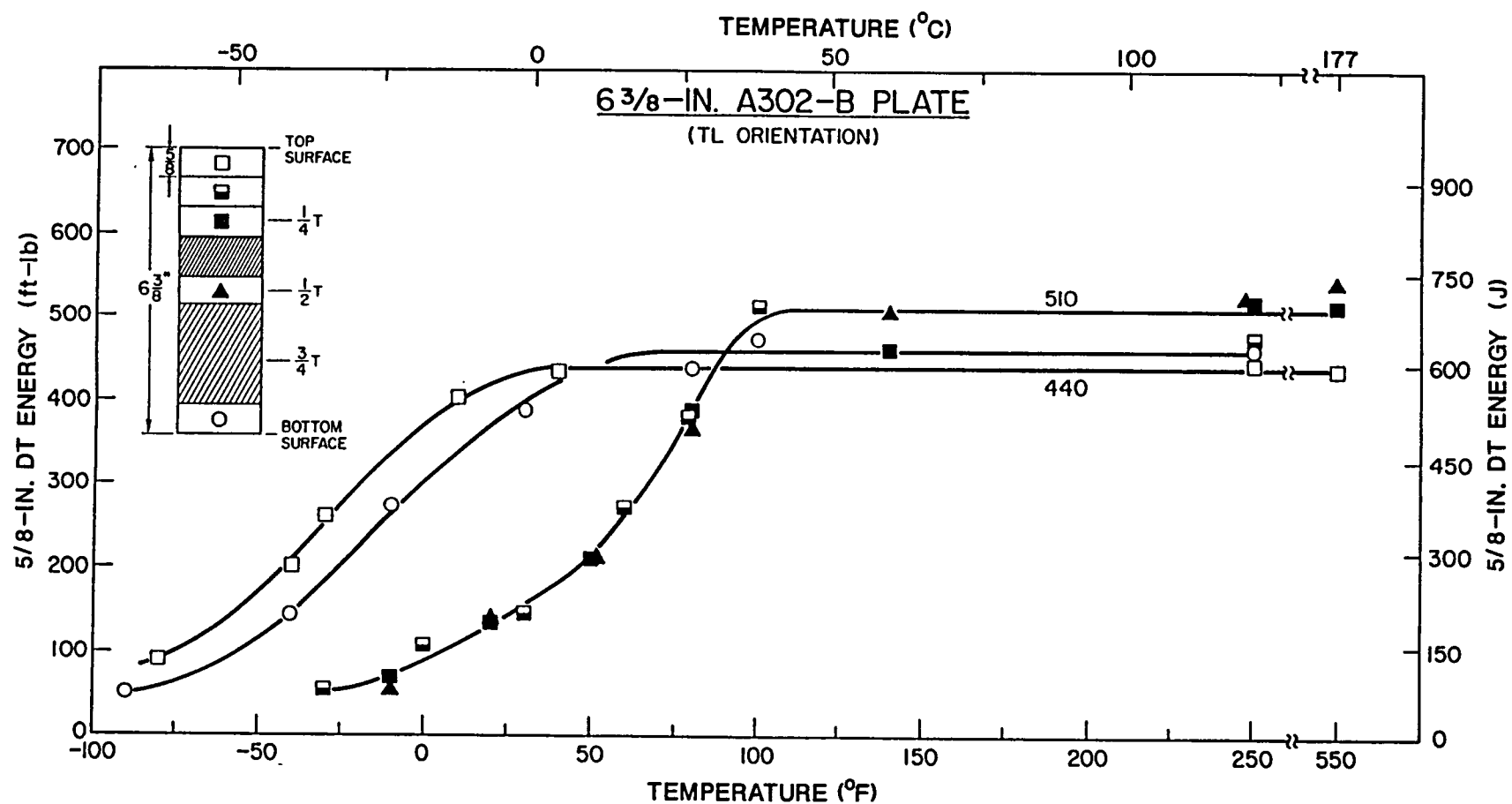


Fig. 6 DT (5/8-in. thickness) data for a different section of the A 302-B plate.

5. TENSILE TESTS

5.1 Specimen Design and Test Procedures

The tensile tests were performed using the standard round specimen design in ASTM Standard E 8 (Fig. 7). This specimen design has a gage diameter of 12.8 mm (0.505 in.), a gage length of 50.8 mm (2.0 in.) for evaluation of total elongation, with threaded ends for gripping purposes.

Testing was in accordance with ASTM Standards E 8 and E 21. The loading rate (on the elastic portion of the stress-strain curve) was ~ 500 MPa/min (72.5 ksi/min). Strain was evaluated from an axial transducer mounted across the center of the gage section, with a transducer gage length of 25.4 mm (1.0 in.).

Load and transducer displacement were stored on floppy disk for post-test processing of the test data.

5.2 Data Analysis Procedures

Engineering stress (σ_E) and strain (ϵ_E) were calculated from the initial gage diameter and length, respectively, as given by:

$$\sigma_E = \frac{P}{A_0} \quad (3)$$

$$\epsilon_E = \frac{\Delta L}{L_0} \quad (4)$$

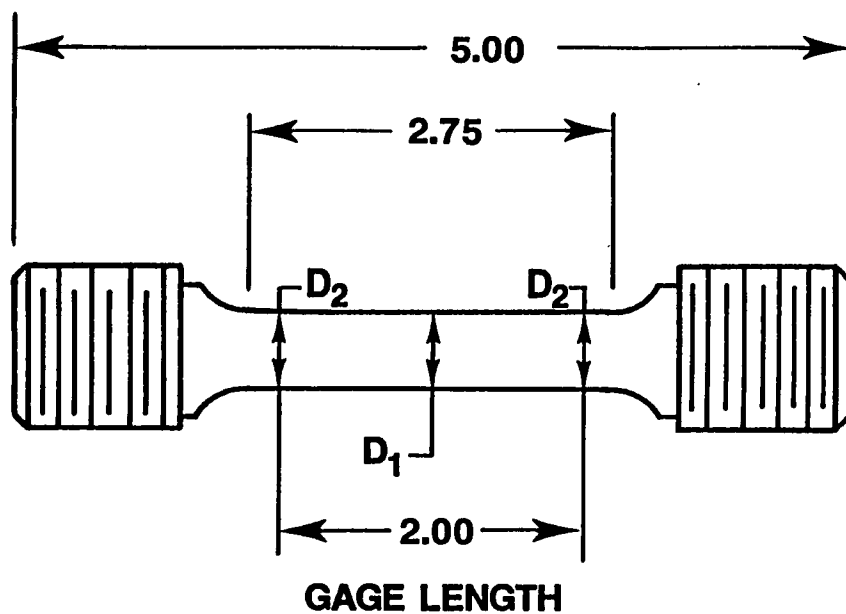
where, P is the applied load, A_0 is the gage section area given by πr_0^2 (where r_0 is the initial gage section radius), ΔL is the extensometer displacement and L_0 is the initial extensometer gage length.

Because of necking, true stress-strain values are calculated from measured load and extensometer displacement up to maximum load only; the final gage diameter and radius of curvature (of the necked region) are used to obtain values of true stress-strain at fracture. Up to maximum load, true strain (ϵ_T) is calculated from:

$$\epsilon_T = \log_e (\epsilon_E + 1) \quad (5)$$

whereas true stress (σ_T) is calculated from:

$$\sigma_T = \sigma_E (\epsilon_E + 1) \quad (6)$$



$$D_1 = .505 \pm .001$$

$$D_2 = \text{FROM } .001 \text{ TO } .002 > D_1$$

DIMENSIONS IN INCHES

1 in. = 25.4 mm

Fig. 7 The tensile specimen design has threaded ends and a gage diameter of 12.8 mm (0.505 in.).

based on assumptions of constant volume (i.e., incompressibility) and a homogeneous distribution of strain along the gage length (Ref. 4).

The true strain at fracture (ϵ_{Tf}) is calculated from:

$$\epsilon_{Tf} = \log_e (A_o/A_f) \quad (7)$$

where A_f , the final (measured) gage area, is given by πr_f^2 . Dimension r_f is the measured final gage section radius.

The true stress at fracture (σ_{Tf}) is calculated using a Bridgman correction (Ref. 5):

$$\sigma_{Tf} = P_f/[A_f (1 + 2 R/r_f) \log_e (1 + r_f/2R)] \quad (8)$$

where P_f is the load at fracture and R is the measured radius of curvature of the necked region. This correction, from a mathematical analysis, adjusts the average axial stress to account for the introduction of transverse stresses.

For use in structural analysis, the true stress-strain curve is approximated using a Ramberg-Osgood equation, as given by:

$$\frac{\epsilon_T}{\epsilon_o} = \frac{\sigma_T}{\sigma_o} + \alpha \left[\frac{\sigma_T}{\sigma_o} \right]^n \quad (9)$$

where σ_o and ϵ_o represent the true yield strength and the true yield strain, respectively. The parameters α and n are adjusted to optimize the fit to the measured data.

5.3 Test Results

Results from the tensile tests are summarized in Table 9. The 1/4T and 3/4T locations give nearly identical 0.2% offset yield and ultimate strengths; the 1/2T location exhibits somewhat lower strength by ~ 20 MPa (3 ksi) for both 0.2% offset yield and ultimate strength. For these six tests, the average elastic modulus was 205.5 GPa ($29.81 \cdot 10^6$ psi), within 2% of the value at this temperature using a correlation from a data base of RPV steel results (Ref. 6). Individual data sheets and tabulated listings of stress-strain are given in Appendix A for each specimen.

As illustrated in Fig. 8, the engineering stress-strain curves for the 1/4T and 3/4T tests are in excellent agreement, with the 1/2T tests also in good agreement with one another, albeit at slightly lower strength levels. No significant anomalies are apparent for any of the tests. (The fracture points are indicated by "x".)

Table 9 Strength Data for A 302-B Plate (V50) at 82°C (180°F)
(T-L Orientation)

Thickness Location	0.2% Offset Yield Strength		Ultimate Strength		Elongation in 50.8 mm	Reduction of Area	Specimen Number
	(MPa)	(ksi)	(MPa)	(ksi)	(%)	(%)	
1/4T	471	68.4	592	85.9	18.9	48.3	101
1/4T	463	67.2	591	85.7	18.3	51.9	102
1/2T	443	64.3	571	82.8	18.9	51.9	103
1/2T	448	65.0	571	82.8	21.5	54.3	104
3/4T	464	67.4	591	85.7	19.2	50.5	105
3/4T	464	67.4	591	85.7	18.6	50.0	106

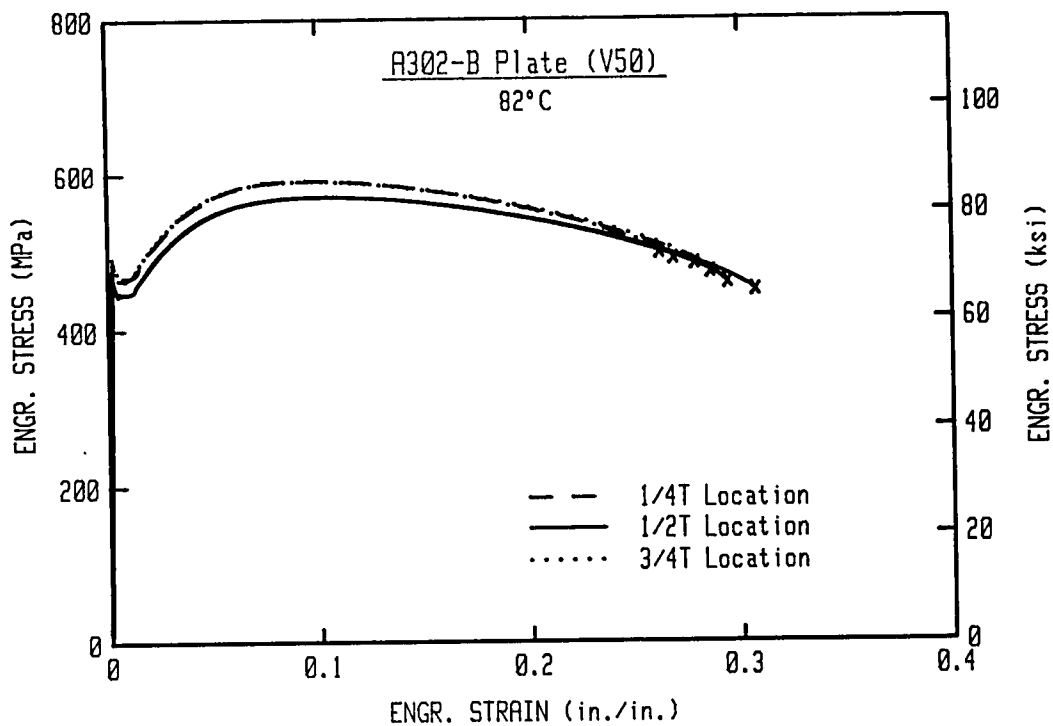
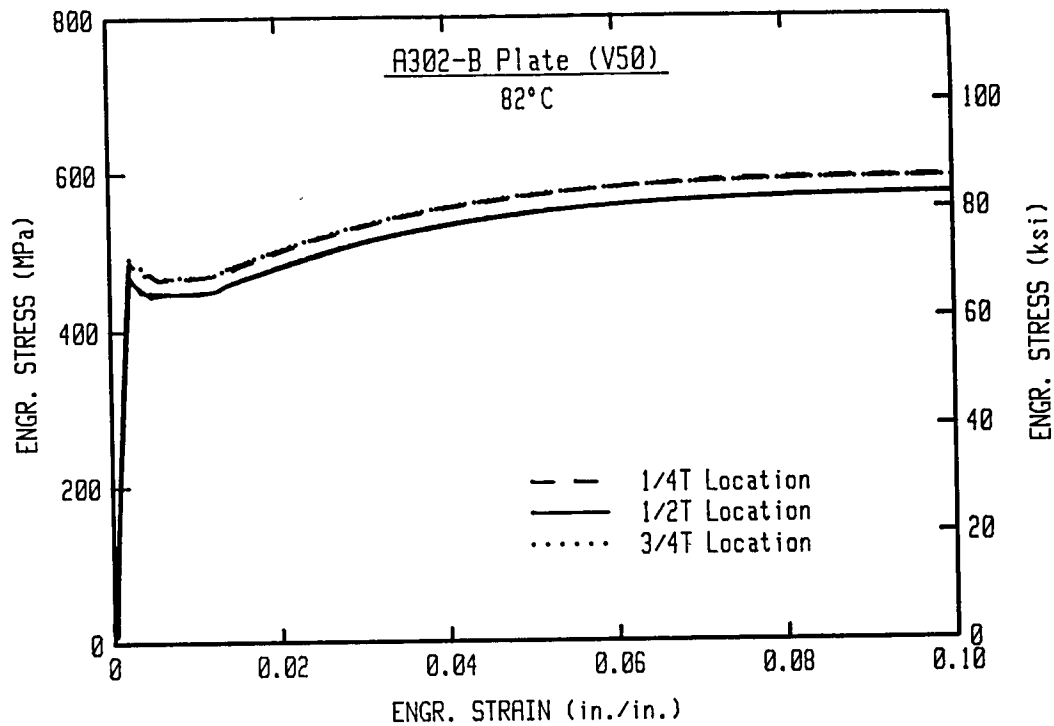


Fig. 8 Engineering stress-strain curves from the tensile tests of this plate. (Fracture points are indicated by "x".)

Results from fitting the true stress-strain data to the Ramberg-Osgood equation (Eq. 9) are summarized in Table 10. Due to the upper and lower yield behavior exhibited by these specimens and low alloy steels in general, the Ramberg-Osgood equation does not do an adequate job of fitting the entire stress-strain curve. Therefore, in Table 10, Case 1 represents the use of all data on the true stress-strain curve, and Case 2 represents the use of all data after the yield plateau. As illustrated in Fig. 9 for a typical case, these two methods give somewhat different results, with the resultant curves crossing between the yield plateau and the fracture point. One aspect of these true stress-strain curves is that they are evaluated only up to strain of ~ 0.1 (due to the occurrence of maximum load), with a straight line used to connect the fracture point of true σ - ϵ to those values at maximum load.

Table 10 Ramberg-Osgood Curvefit Parameters

$$\frac{\epsilon_T}{\epsilon_o} = \frac{\sigma_T}{\sigma_o} + \alpha \left[\frac{\sigma_T}{\sigma_o} \right]^n$$

Thickness Location	ϵ_o	σ_o (MPa)	Case 1 ^a		Case 2 ^b		Specimen Number
			α	n	α	n	
1/4T	0.00504	473.6	1.089	8.925	1.641	7.183	101
	0.00588	465.9	0.661	9.550	1.089	7.585	102
1/2T	0.00503	445.2	0.785	9.303	1.347	7.288	103
	0.00446	450.3	1.236	8.502	1.814	7.029	104
3/4T	0.00503	466.7	0.843	9.363	1.389	7.413	105
	0.00591	467.2	0.604	9.951	1.092	7.616	106

^a All true σ - ϵ data used.

^b Only true σ - ϵ data after yield are used.

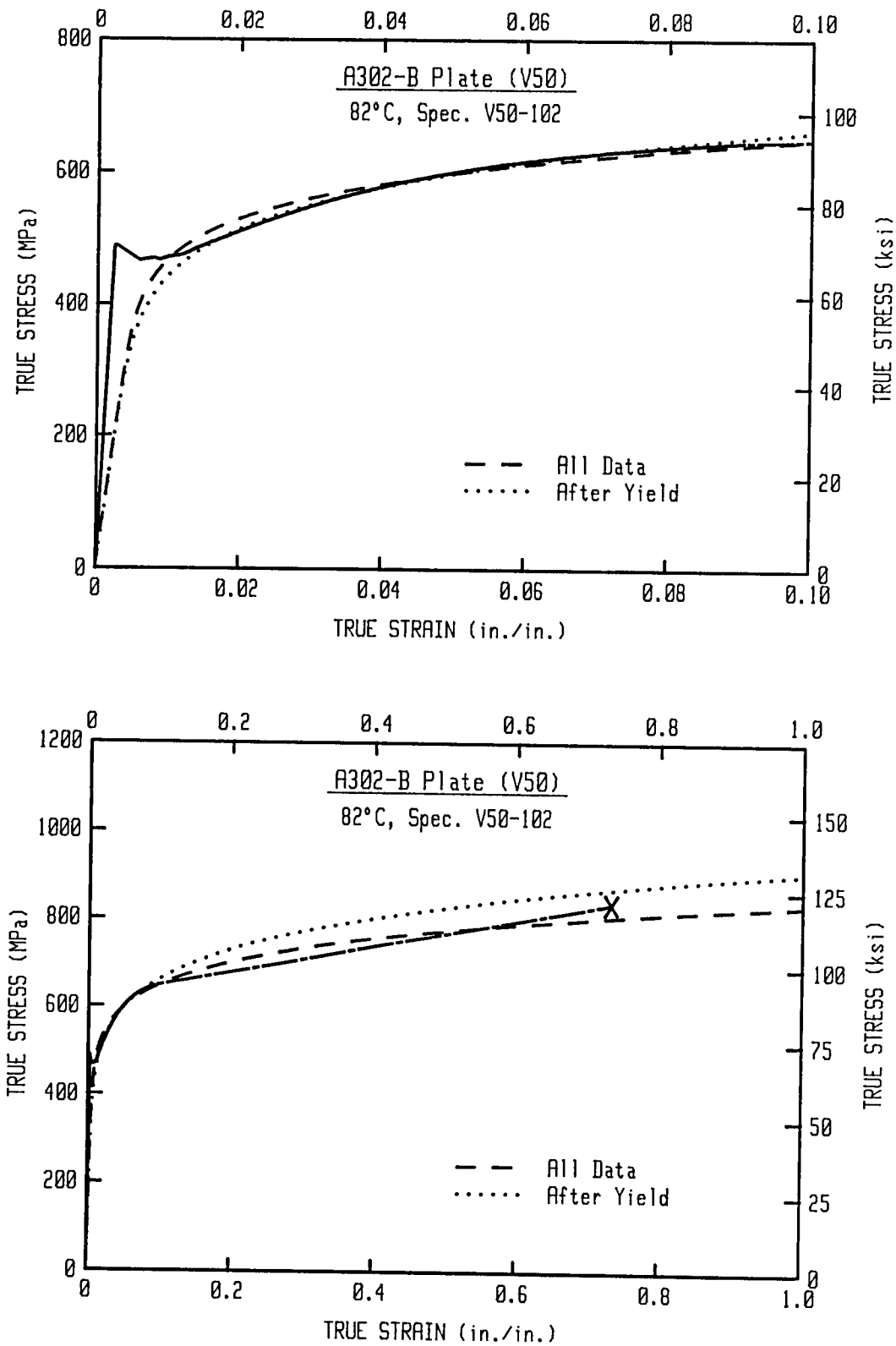


Fig. 9 A typical true stress-strain curve and two sample fits to the Ramberg-Osgood equation (Eq. 9). True stress-strain data after maximum load are approximated by linear interpolation to the fracture point (as indicated by the long dash-short dash line).

6. J-R CURVE TESTS

6.1 Specimen Design and Preparation

The J-R curve tests were conducted using CT specimens ranging in size from 0.5T- to 6T-CT, with intermediate sizes of 1T-, 2T- and 4T-CT also used. Dimensions for each size of specimen are given in Fig. 10. In general, the pin-hole sizes and specimens are consistent with those used in ASTM E 399, although for the small CT specimens (0.5T- and 1T-CT) the pin-holes spacing is increased, and the pin-hole size is reduced for the 0.5T-CT specimens. The latter modifications are in conformance with ASTM E 813 and E 1152 and are required to permit measurement of load-line displacements in the standard position (i.e., between the loading pinholes).

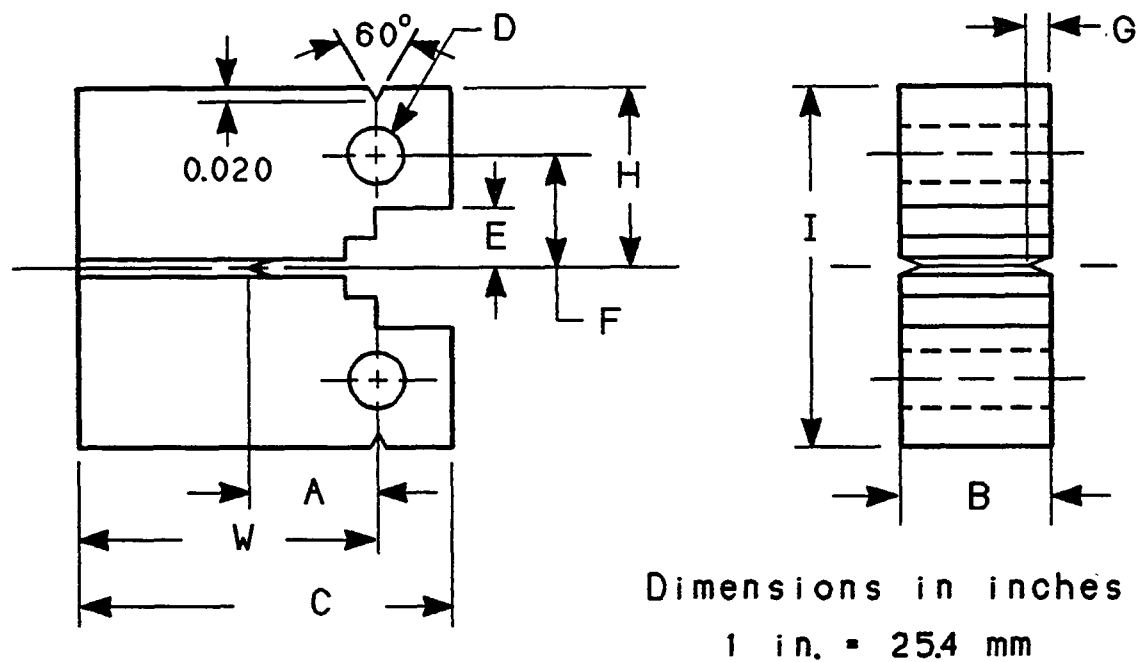
Displacements were measured at several locations on the specimens. For all specimens, loadline displacement was measured between the pinholes (V_{LL}) and at a location external to the pinholes (V_{LL}'), as illustrated in Fig. 11. Crack mouth or front-face displacement (V_M) was measured on the 2T-, 4T- and 6T-CT specimens. In addition, a crack-tip opening displacement (CTOD) was measured at the tip of the precrack on all specimens except the 0.5T-CT specimens, with a gage length of 5 mm (0.197 in.). The latter measurements, called δ_s , are described in Section 6.4.

After machining, fatigue precracks were introduced into the specimens via cycling at load levels within the linear elastic range. The target final (surface) crack-length to specimen width (a/W) ratio was 0.5. To facilitate crack initiation from the machined notches, the specimens were compressed to a load level not more than that required to give a stress intensity of 26 MPa \sqrt{m} (~ 24 ksi $\sqrt{in.}$), for a tensile load of the same magnitude. At the final stage of precracking, K_{max} was ~ 22 MPa \sqrt{m} (20 ksi $\sqrt{in.}$).

After precracking, all specimens were side grooved by 20% of the total specimen thickness (B), 10% per side, using a C_v notch cutter (45° included angle and 0.25 mm, 0.01 in., root radius). The resultant net specimen thickness (B_N) was then equal to 0.8 B . In general, side grooving is used to promote uniform (straight) crack growth during testing and to give lower bound J-R curve levels. The straight crack growth improves the performance of the unloading compliance method used for estimating crack growth during testing, and indicates a closer tendency towards generalized plane strain across the crack front.

6.2 Test Procedure

The procedures used for these tests are in accordance with ASTM Standards E 813 and E 1152. Specifically, the unloading compliance method was used to evaluate crack length during each test. Appropriate compliance expressions for the V_M , V_{LL} and V_{LL}' measurement positions were used in each case.



Specimen Size	A	B	C	D	E	F	G	H	I	W
0.5T-CT	0.43	0.50	1.25	0.188	0.200	0.375	0.050	0.60	1.20	1.00
1T-CT	0.90	1.00	2.50	0.500	0.320	0.654	0.100	1.20	2.40	2.00
2T-CT	1.85	2.00	5.00	1.000	0.360	1.100	0.200	2.40	4.80	4.00
4T-CT	3.75	4.00	10.00	2.000	0.734	2.200	0.400	4.80	9.60	8.00
6T-CT	5.65	6.00	15.00	3.000	0.734	3.300	0.600	7.20	14.40	12.00

Fig. 10 Schematic of the CT specimens used in these tests.

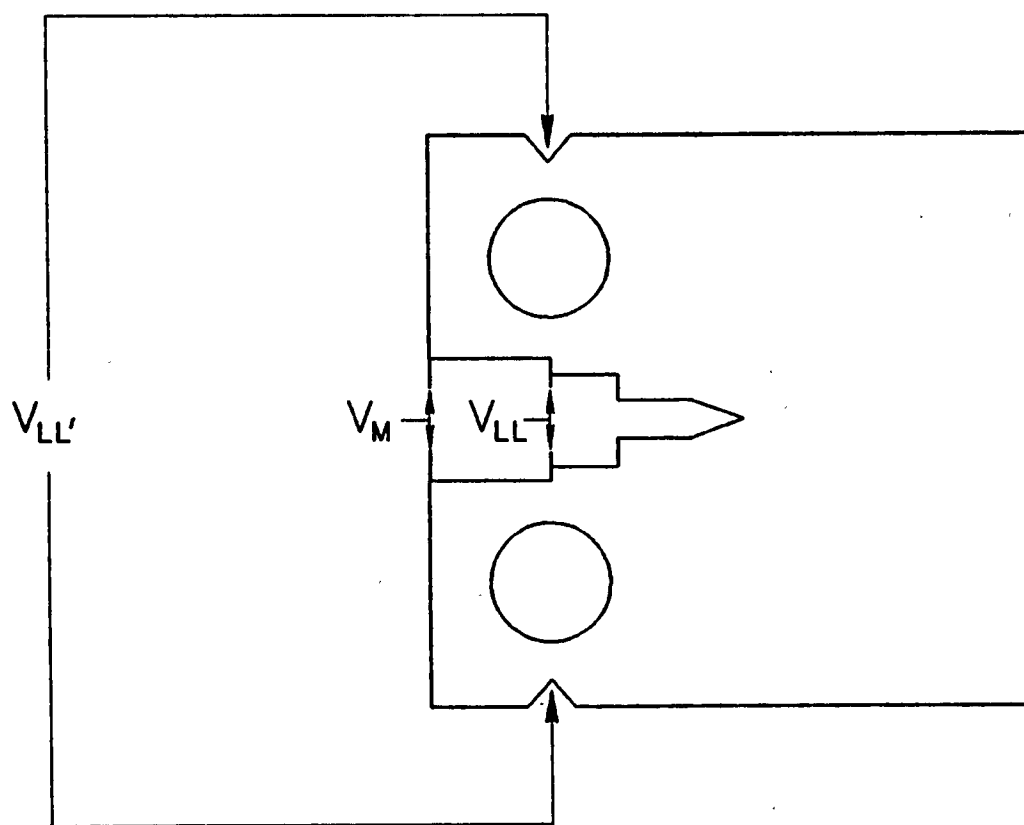


Fig. 11 Displacements were measured at several locations during these tests.

All tests were performed on a servohydraulic test frame, with the load capacity of the test frame and the load cell optimized for each specimen size. The 6T-CT specimen was tested in a frame with a load capacity of 2.4 MN (550 kips).

A forced-air recirculating environmental chamber (with resistance heaters) was used to achieve the desired test temperature, 82°C (180°F), in all cases. Multiple thermocouples were mounted on each specimen to check thermal gradients and drift during testing. All temperature measurements were within 1°C (2°F) of the desired test temperature throughout each test.

An analog trace of load vs. load-line displacement was made for each test. Load and displacement data (from the various displacement measurements) were digitized using digital voltmeters and stored on floppy disks using a desktop computer. This system simplified post-test analysis and correction of the test data.

After each test, the specimen was heated (using an acetylene torch) to promote oxidation of the exposed fracture surface, i.e., to heat tint the surface. Once the specimen had returned to near ambient temperature, the specimen was chilled to near liquid nitrogen temperature and then fractured, exposing the fracture surface. The specimen initial (precrack) and final (test) crack lengths were measured directly from the fracture surface using an optical measurement system. This system consists of an X-Y micrometer slide assembly and a magnifying eyepiece. In the case of the 6T-CT specimen, photographic measurements supplemented hand-held micrometer measurements. The crack lengths were evaluated using the 9/8 averaging technique, in which the two near surface measurements are averaged together, with the resultant value averaged with the other seven measurements.

6.3 Data Analysis Procedures

As mentioned previously, the unloading compliance method has been used to determine crack length during the testing of each specimen. The Hudak-Saxena calibration equation (Ref. 7) is used to relate the measurements of compliance on the specimen load line (V_{LL}) and crack mouth (V_M) to crack length. A modified Hudak-Saxena equation (Ref. 8) is used to relate compliance on the external load-line (V_{LL}') to crack length. Both rotation (Ref. 9) and modulus corrections are made to the compliance data; these are described in detail in Appendix B.

The J integral values have been evaluated using various forms of J. In terms of historical perspective, the initial form of the J integral proposed for use with compact specimens was based on an analysis of a deeply cracked beam in pure bending (Ref. 10), as given by

$$J = \frac{2}{b} \int_0^{\Delta} \left(\frac{P}{B} \right) d\Delta = \frac{2A}{Bb} \quad (10)$$

with A the area under the load-displacement record for the specimen and b the uncracked ligament, given by W-a. However, this form was found to give J values slightly less than G values for the case of failure in the linear range of the load-displacement curve. To correct this discrepancy, Merkle and Corten (Ref. 11) included the effect of axial force in their formulation of the J integral, termed here J_{M-C} . Clarke and Landes (Ref. 12) then simplified the equations to

$$J_{M-C} = \frac{2A}{Bb} \frac{(1 + \alpha)}{(1 + \alpha^2)} \quad (11)$$

with α a function of a_0/b ,

$$\alpha = [(2a/b)^2 + 2(2a/b) + 2]^{1/2} - (2a/b + 1).$$

While the J_{M-C} equation was satisfactory for evaluation of J values under conditions of little or no crack growth (such as J_{Ic}), use of the J integral for the case of a growing crack was needed for evaluation of safety margins in nuclear RPV and piping applications. For such applications, the use of only J_{Ic} values could be too conservative in providing meaningful assessments of structural integrity. To address the need to account for crack growth in the J integral, Ernst used a deformation theory of plasticity interpretation of J to develop a crack growth corrected form of the J integral, termed here J_D (Ref. 13). J_D is given by the following expression for CT specimens:

$$J_{D,i+1} = \left[J_{D,i} + \left(\frac{\eta}{b} \right)_i \frac{A_{i,i+1}}{B_N} \right] \left[1 - \left(\frac{\gamma}{b} \right)_i (a_{i+1} - a_i) \right] \quad (12)$$

where

$$\eta = 2 + 0.522 b/W$$

$$\gamma = 1 + 0.76 b/W$$

Deformation theory J, i.e., J_D , is the formulation of the J integral specified for use in ASTM Standards E 813 and E 1152. The validity criteria associated with J_D have restricted J_D -R curves to the point that they have been thought to be of little practical value for application to structural stability determinations, primarily due to the limits on crack extension. Evaluation of J_D -R curves for different sizes of CT specimens have demonstrated a specimen size dependence as well (Ref. 1, 2, and 14).

One negative characteristic of J_D is a tendency towards a size effect, whereby smaller specimens would give lower J-R curve levels than larger specimens, with negative J-R curve slopes resulting in many cases. To address these concerns, Ernst introduced a modified form of J, termed J_M (Ref. 1). Some of the attributes of J_M cited by Ernst

include a better description of the process of deformation and crack growth, specimen-size independence, and a large relaxation of the restrictions on the amount of crack extension and/or initial remaining ligament needed to produce valid data. The specimen size independent characteristic of J_M was initially demonstrated in Ref. 1 for an A 508 Class 2A steel using data from 0.5T- to 10T-CT specimens. Confirmation of this can also be found in Ref. 2 and 14.

J_M is given by (Ref. 1)

$$J_M = J_D - \int_{a_0}^a \frac{\partial [J_D - G]}{\partial a} \bigg|_{\delta_{pl}} da \quad (13)$$

where

J_D - deformation theory J

G - Griffith linear elastic energy release rate

$= K_I^2 (1-\nu^2)/E$

a_0, a - the initial and current crack lengths, respectively

$J_D - G = J_{pl}$, the plastic portion of the deformation theory J

δ_{pl} - the plastic portion of the displacement

ν - Poisson's ratio

and $K_I = P f\left(\frac{a}{W}\right) (WBB_N)^{-0.5}$

where P is the hold load at the unloading compliance measurement point, $f\left(\frac{a}{W}\right)$ is given in ASTM Standard E 399, and W , B , and B_N are the specimen width, thickness, and net thickness, respectively.

Reference 1 also provides an incremental form of Eq. 13:

$$J_{M \ i+1} = J_{D \ i+1} + \Delta J_{i+1} \quad (14)$$

where

$$\Delta J_{i+1} = \Delta J_i + \left(\frac{\gamma}{b} J_{pl}\right)_i (a_{i+1} - a_i) \quad (15)$$

The J_D and J_M equations described above represent "total area" forms of each whereby the area under the load-total displacement curve is used along with a single η term to evaluate J . Recent work indicates that the η term used tends to underestimate the elastic η , η_{el} , for the compact specimens. Therefore, a more appropriate way to evaluate J_D and J_M is to sum the elastic and plastic portions of each:

$$J = J_{el} + J_{pl} \quad (16)$$

In this case,

$$J_{el} = K^2 (1-\nu^2)/E \quad (17)$$

with K from ASTM E 399, ν is Poisson's ratio (0.3) and E is Young's modulus. The plastic part of the J integral is then evaluated by substituting A_{p1} (area under the load-plastic displacement curve) for A in Eq. 12 for evaluation of J_D . This same J_{p1} is used in Eq. 15 for evaluation of J_M . The forms of J and J_M which result from this separation of the elastic and plastic J are denoted by a subscript of "*", i.e., J_{D*} and J_{M*} for clarity sake.

The J integral does have certain validity criteria associated with it, generally to ensure that a region of "J dominance" exists. The primary criteria for "J dominance" include:

$$w = \frac{b}{J} \frac{dJ}{da} \gg 1 \quad (18)$$

$$\Delta a < (0.06 \text{ or } 0.1) b_0 \quad (19)$$

$$J < \min(b, B) \sigma_f / (15, 20 \text{ or } 25) \quad (20)$$

The w criteria (Eq. 18) is from Hutchison and Paris (Ref. 15), with a critical w value of 5 normally suggested. The Δa limit of 0.06 was suggested by Shih (Ref. 16), whereas ASTM E 1152 uses a limit of 0.1. The J limits can be found variously in ASTM E 813-81 and E 1152, with E 813-81 specifying the factor of 25 for J_{Ic} validity and 15 for data used to determine J_{Ic} , whereas ASTM E 1152 specifies 20 as an upper limit on J evaluation.

A typical J-R curve is illustrated in Fig. 12. The J-R curve format is in accordance with that of ASTM E 813-81. The line emanating from the origin, called the blunting line, is given by $J = 2\sigma_f \Delta a$, where σ_f is the flow strength (the average of the 0.2% offset yield strength and the ultimate strength). The exclusion lines are constructed parallel to the blunting line, but offset by 0.15 mm (0.006 in.) and 1.5 mm (0.060 in.).

By ASTM E 813-81 procedures, a straight line is fit to the test data between the 0.15 and 1.5 mm exclusion lines. This line is extrapolated back to the blunting line; the intersection is termed J_Q . J_{Ic} equals J_Q if various validity criteria are satisfied.

In the power-law evaluation of the J-R curve data, an equation of the form $J = C \Delta a^n$ is fit to the data between the exclusion lines. Power-law J_{Ic} values are defined as the intersection of the power-law curve with a line parallel to the blunting line but offset by 0.2 mm (according to ASTM E 813-87), or the 0.15-mm exclusion line. Previous experience has shown that the latter definition of J_{Ic} tends to give

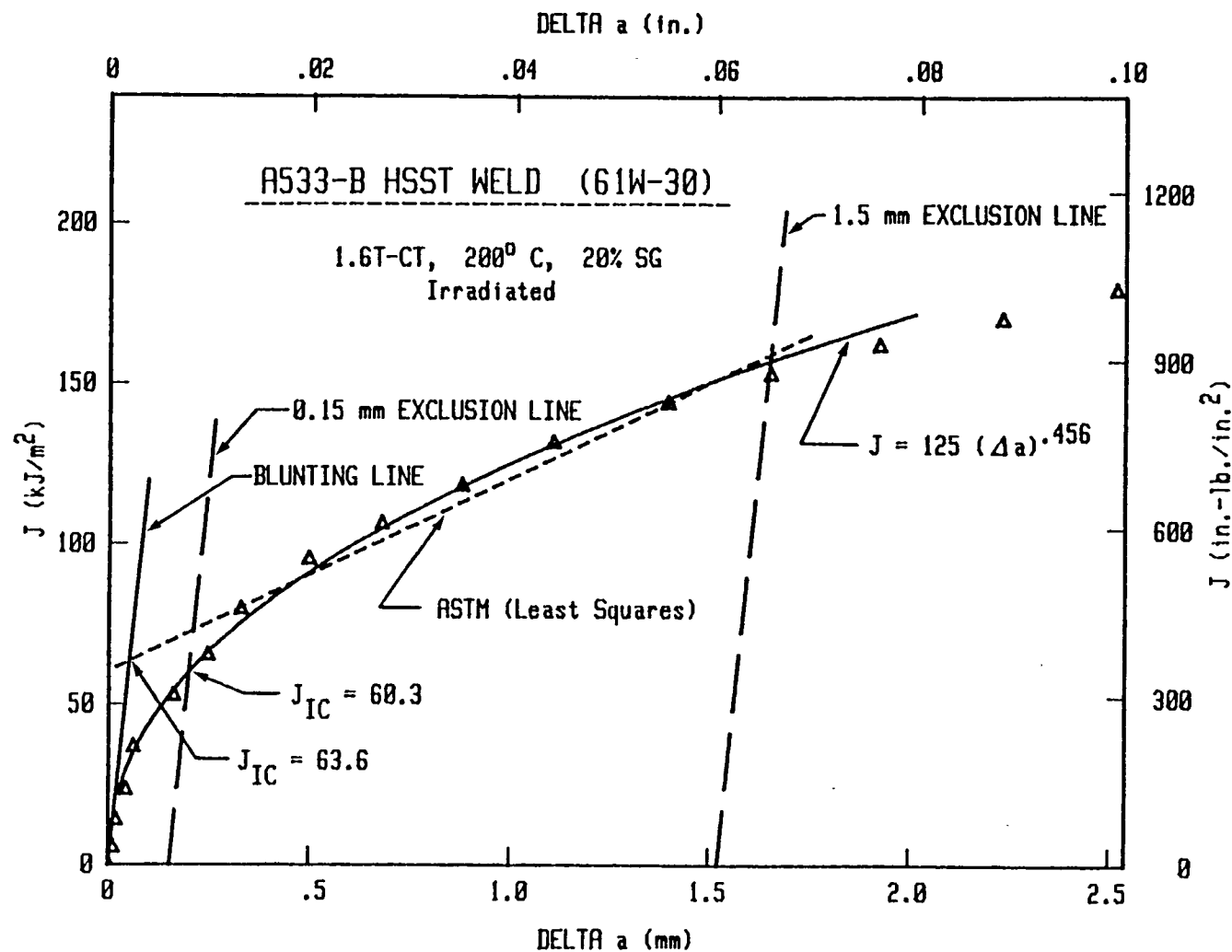


Fig. 12 The J-R curve format used for these tests is consistent with that of ASTM Standard E 813.

values nearly equivalent to those from ASTM E 813-81 for low alloy RPV steels.

Another parameter used to characterize the tearing resistance of structural materials is the tearing modulus, T_M , given by:

$$T_M = \frac{E}{\sigma_f^2} \frac{dJ}{da} \quad (21)$$

where dJ/da is the slope of the J-R curve. Since the J-R curve generally conforms to a power law with $0 < n < 1$, the value of T_M changes (decreases) with increasing crack growth. For comparison purposes, average values of T_M , termed T_{avg} , typically are used. The "ASTM" T_{avg} value (as defined here) uses the slope of the linear-fit curve as dJ/da ; the power-law T_{avg} value is determined from a fit of the power law to a straight line, defining dJ/da as an average slope evaluated in a closed-form manner (see Appendix H of Ref. 14).

An additional comparison which will be used with these tests is the "key-curves" from the tests. The key-curve for a test record compares normalized load (P_N , in units of stress) to normalized displacement, specifically the plastic displacement divided by specimen width (δ_{pl}/W). The normalized displacement is dimensionless. These quantities are defined as

$$P_N = \frac{PW}{Bb^2 g(a/W)} \quad (22)$$

$$\delta_{pl}/W = (\delta - P \cdot C)/W \quad (23)$$

with $g(a/W) = \exp[0.522(1-a/W)]$, P and δ are the measured load and load-line displacement, respectively, and C is the compliance (mm/kN or in./lb) required to give the current crack length. The key-curve tends to have a shape similar to that of a true stress-strain record, with P_N levels continually increasing as δ_{pl}/W increases. The important aspects of the key-curve are that crack growth is accounted for in the equations, and the deformation characteristics for different specimen sizes can be compared in this format.

6.4 Measurement of δ_s

Measurements of δ_s (Fig. 13) have been found to correlate well with those of (Ref. 17). In addition, δ_s has been found to correlate data from different sizes and geometries to greater crack growth increments than does the J integral (Ref. 17). Therefore, measuring δ_s on the tests was thought to be beneficial.

To make the measurements of δ_s on these specimens, a procedure was developed to mount an extensometer on small pins pressed into holes

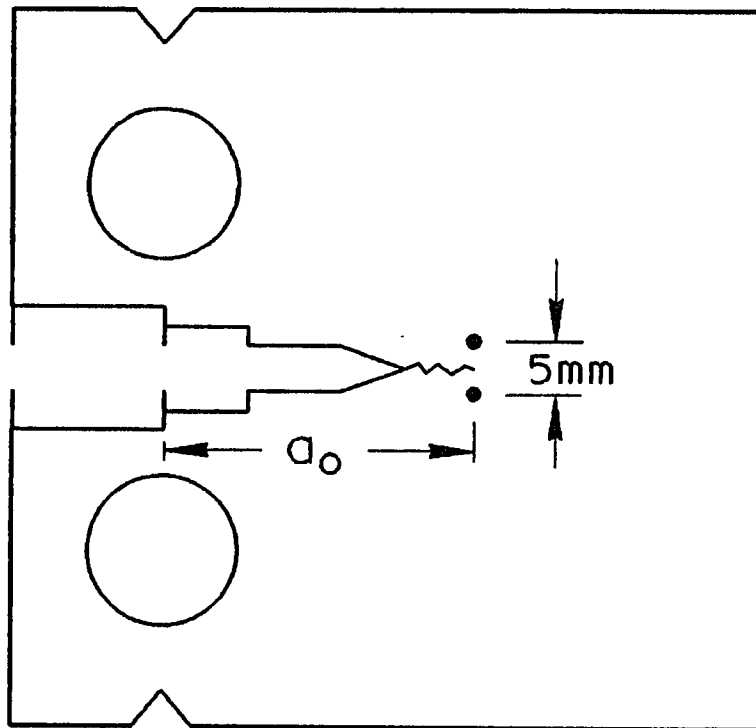


Fig. 13 Location of the δ_5 measurements made during these tests.

drilled into the side surfaces of the CT specimens. These holes were centered on the tip of the precrack, at a spacing of 5 mm (0.197 in.). Since these holes did enter into the specimen by a finite depth, ~ 0.3 mm (0.125 in.) for the 0.5T-CT and 1T-CT specimens, check tests were made to ensure that the presence of the holes would not cause a perturbation to the measured data (load-displacement or J-R curves). These check tests used 0.5T-CT specimens only since the holes would not exceed the side groove depth by a significant amount on the larger specimens. (For the 2T-, 4T-, and 6T-CT specimens, the δ_5 measurement points were located on the sloped surfaces of the side grooves. In these cases, the hole depths were the same as the side-groove depth.)

Initial check tests were made using remnants from the machining of the principal tests in this program. As illustrated in Fig. 14, some perturbation on the J_M - and J_D -R curves were apparent for these tests. Of note on these comparisons is the unusual and inconsistent behavior of the J-R curves from the specimens without holes, for $\Delta a > 4$ mm. Similar trends are obvious on the load-displacement curves (Fig. 15), the Δa displacement curves (Fig. 16) and the key-curves (Fig. 17). In all of these figures, the deviation point for the cases of with and without holes is indicated by an arrow; the arrow on each figure is at the same load, displacement and crack length triad.

In looking at the fracture surfaces for these specimens (Fig. 18), the lack of homogeneity was obvious, as the fracture surfaces demonstrated an extremely fibrous or "woody" appearance. These non-planar fracture surfaces were also thought to have caused a high error between the measured and the predicted crack length. The crack length errors, ranging from 0.49 mm to 0.79 mm or 8% to 12%, are not unusual for this heat, but are much higher than those from other RPV steels. One concern was whether these crack length errors may have skewed the results in some way. Since no obvious cause for the differences in the J-R curves could be found, it was hypothesized that material homogeneity could be the primary cause. To check this hypothesis, additional check-tests were made using a "clean" material (as assumed from the smooth fracture surfaces, Fig. 19). This material was a Linde 80 weld, which exhibits a C_v upper shelf energy of ~ 79 J (58 ft-lb). This heat was chosen due to the availability of prepared specimens and previous data.

Results for this heat of Linde 80 weld added further confusion to the situation (Fig. 20). For the condition of "without holes," the new and the previous data are in excellent agreement. However, the J-R curves for the specimens with holes indicate considerable variability, unexpected given the results for the other specimens. In terms of load-displacement (Fig. 21) and Δa -displacement curves (Fig. 22), data from the specimens with holes bracket those from specimens without holes. Similar good agreement is seen for the key-curves as well (Fig. 23).

On the basis of the results for these two heats, measurements of δ_5 were not made on the main tests of 0.5T-CT specimens.

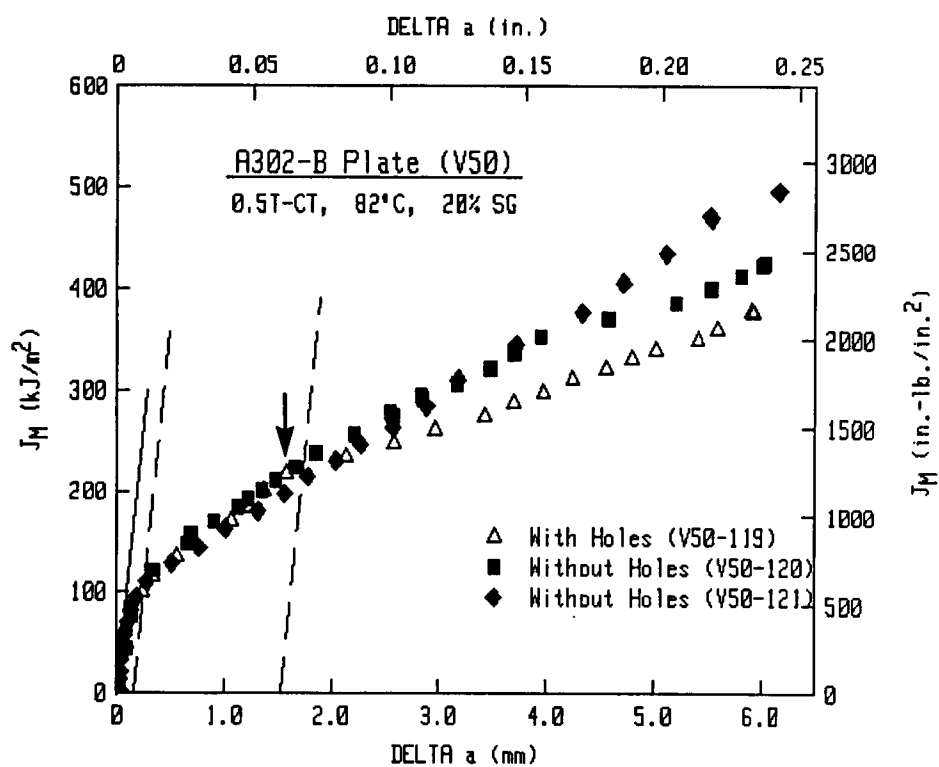
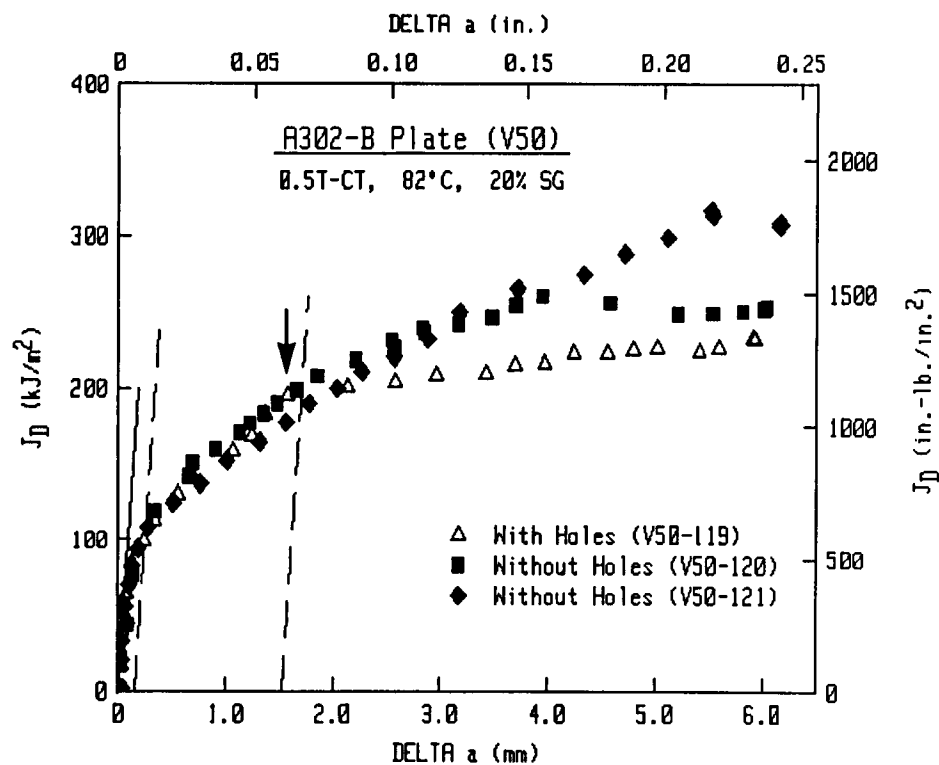


Fig. 14 Using both J_H and J_D , the specimens without holes demonstrate different R-curves than the specimen with holes. (The arrow indicates the approximate point of divergence.)

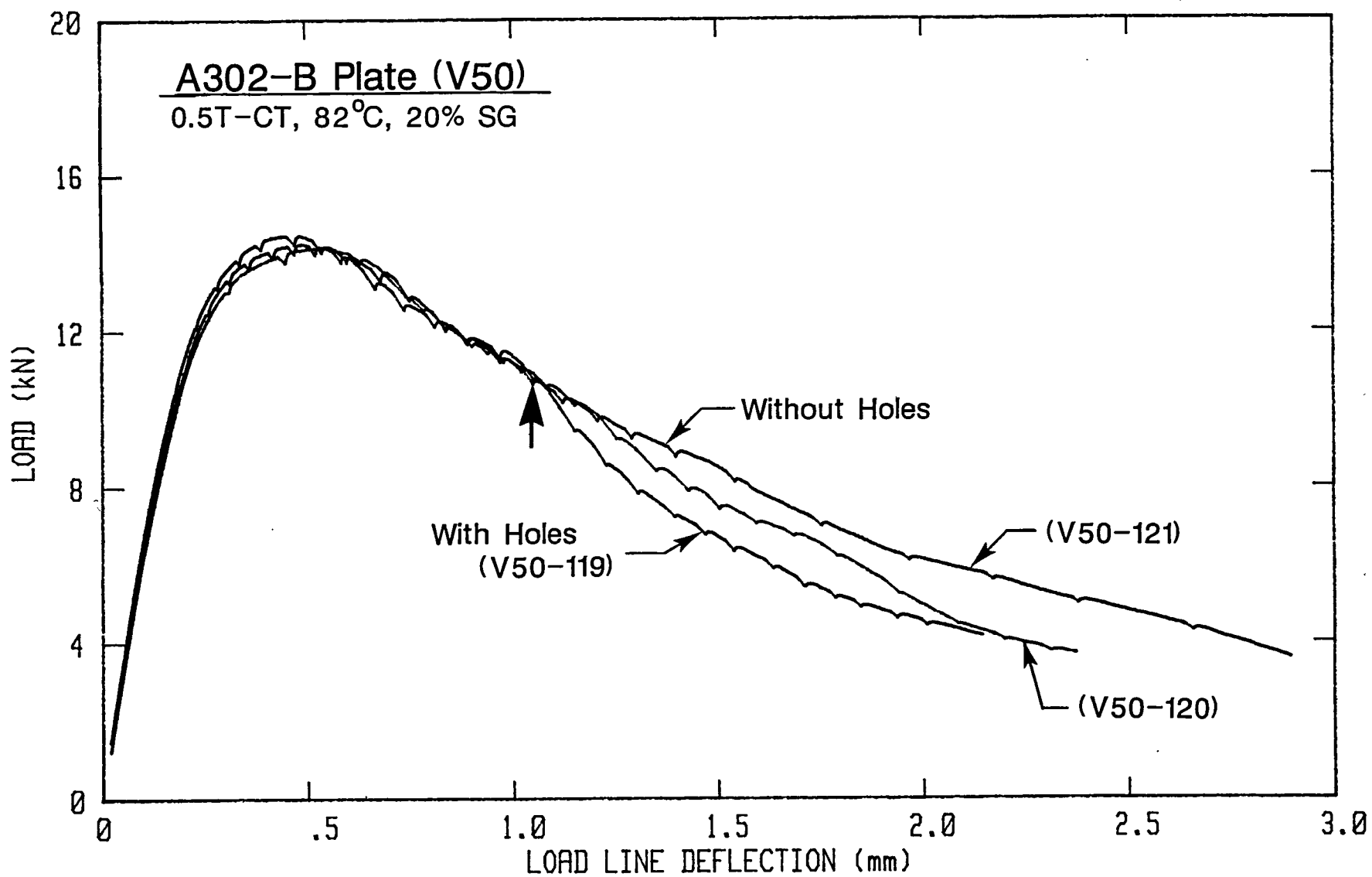


Fig. 15 Load-displacement curves for the δ_5 check-out tests illustrated in Fig. 14. The arrow on this figure is at the same point as that in Fig. 14, indicating the beginning of divergence.

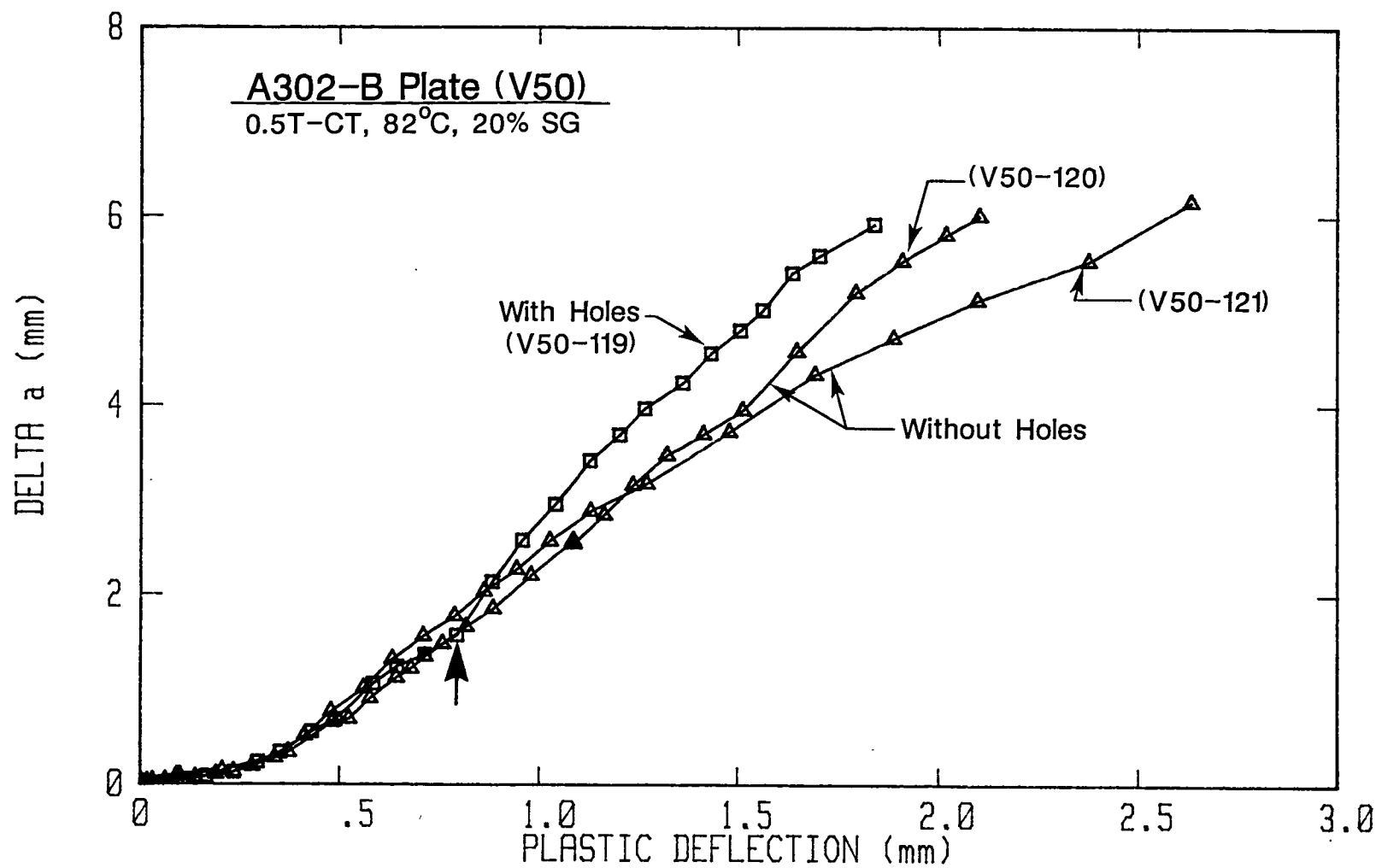


Fig. 16 Crack growth-plastic displacement curves for the δ_5 check-out tests, J-R curves are illustrated in Fig. 14. The arrow is consistent with those in Figs. 14 and 15.

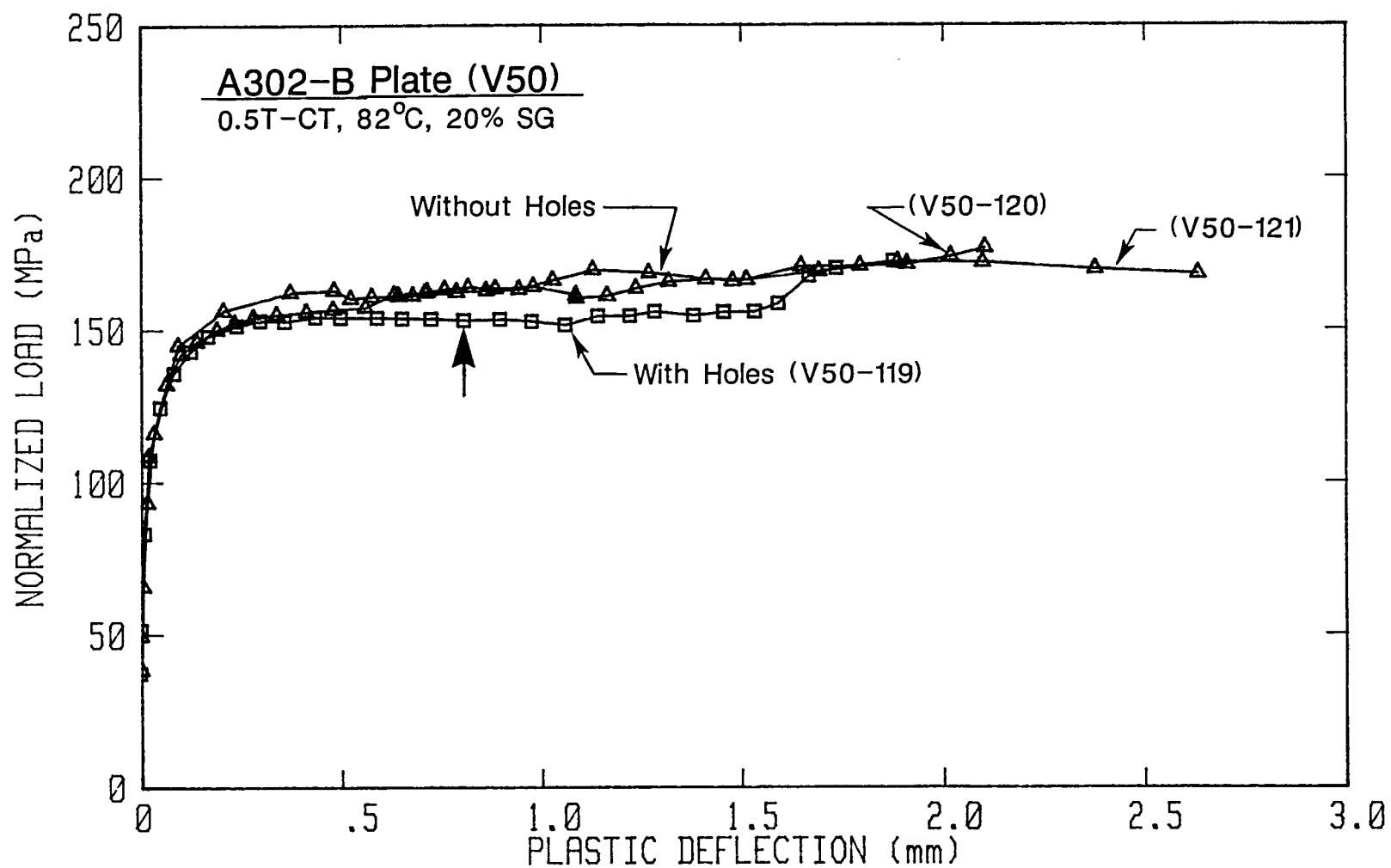


Fig. 17 Keycurves for the δ_5 check-out tests are not in as good of agreement before the arrow as in Figs 14 to 16.

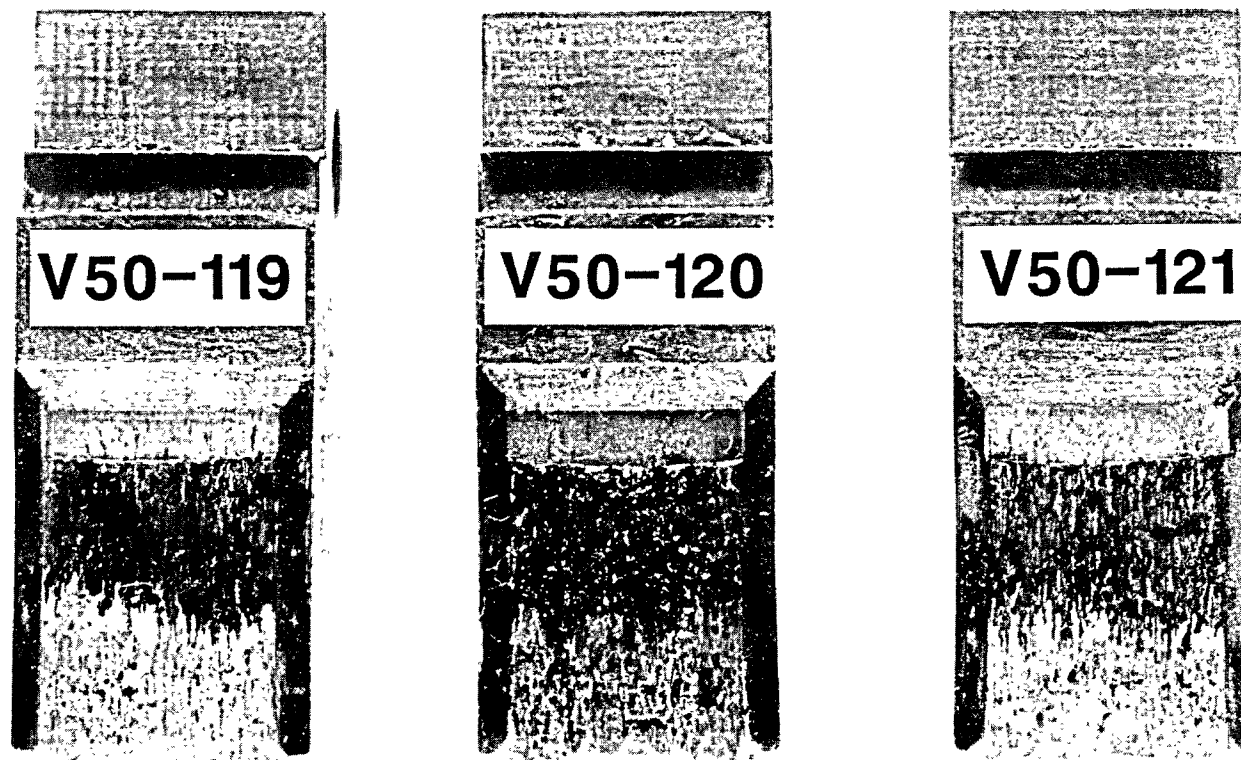


Fig. 18 Fracture surfaces for the δ_5 check-out tests. Specimen V50-119 (left) had δ_5 measurements (and holes).

Linde 80 Weld (0.5T-CT)

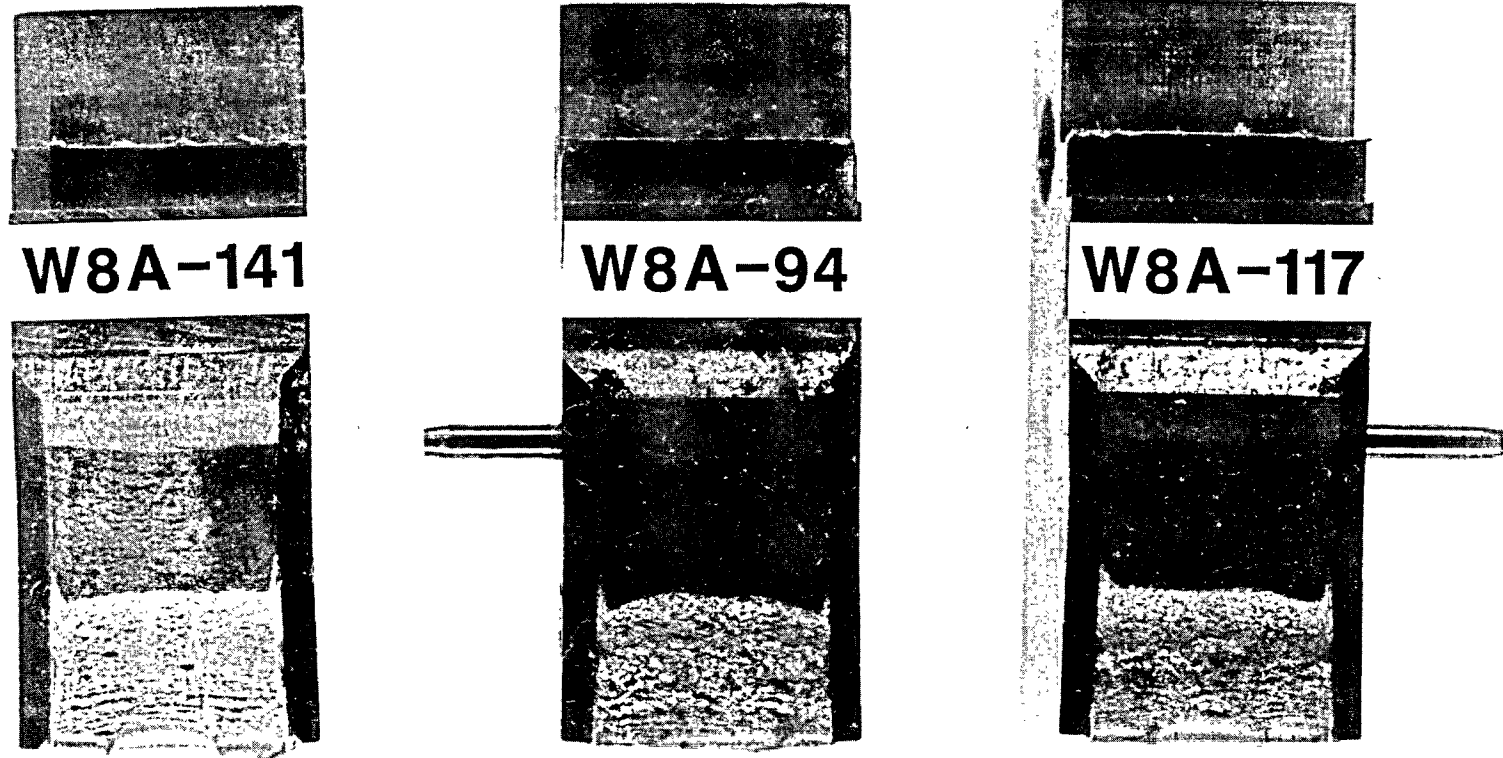


Fig. 19 Fracture surfaces for the δ_5 check-out tests using a Linde 80 weld. The smooth fracture surfaces are in contrast to those for the A 302-B plate in Fig. 18.

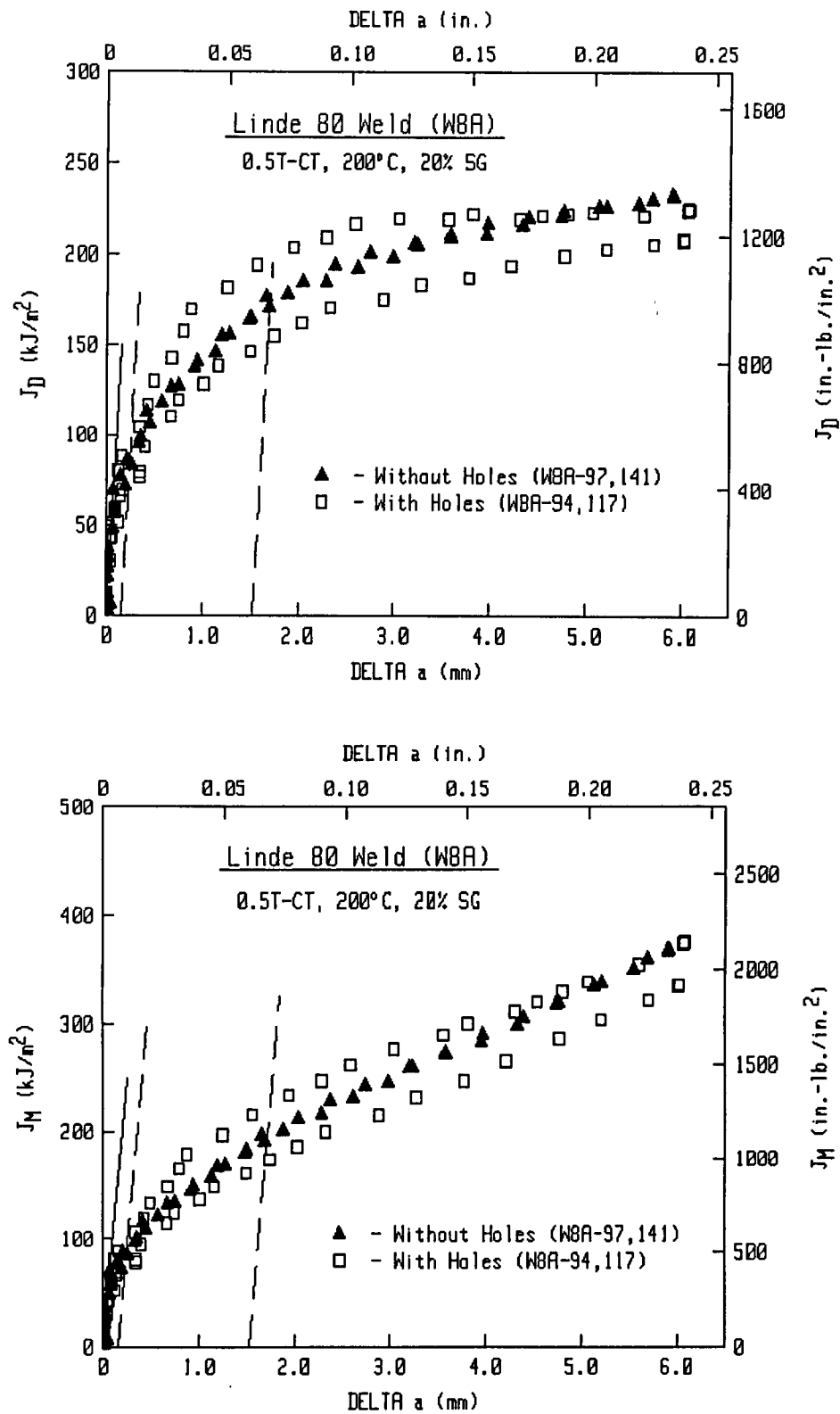


Fig. 20 Using J_M and J_D , data from specimens with holes demonstrate much greater variability than data from specimens without holes.

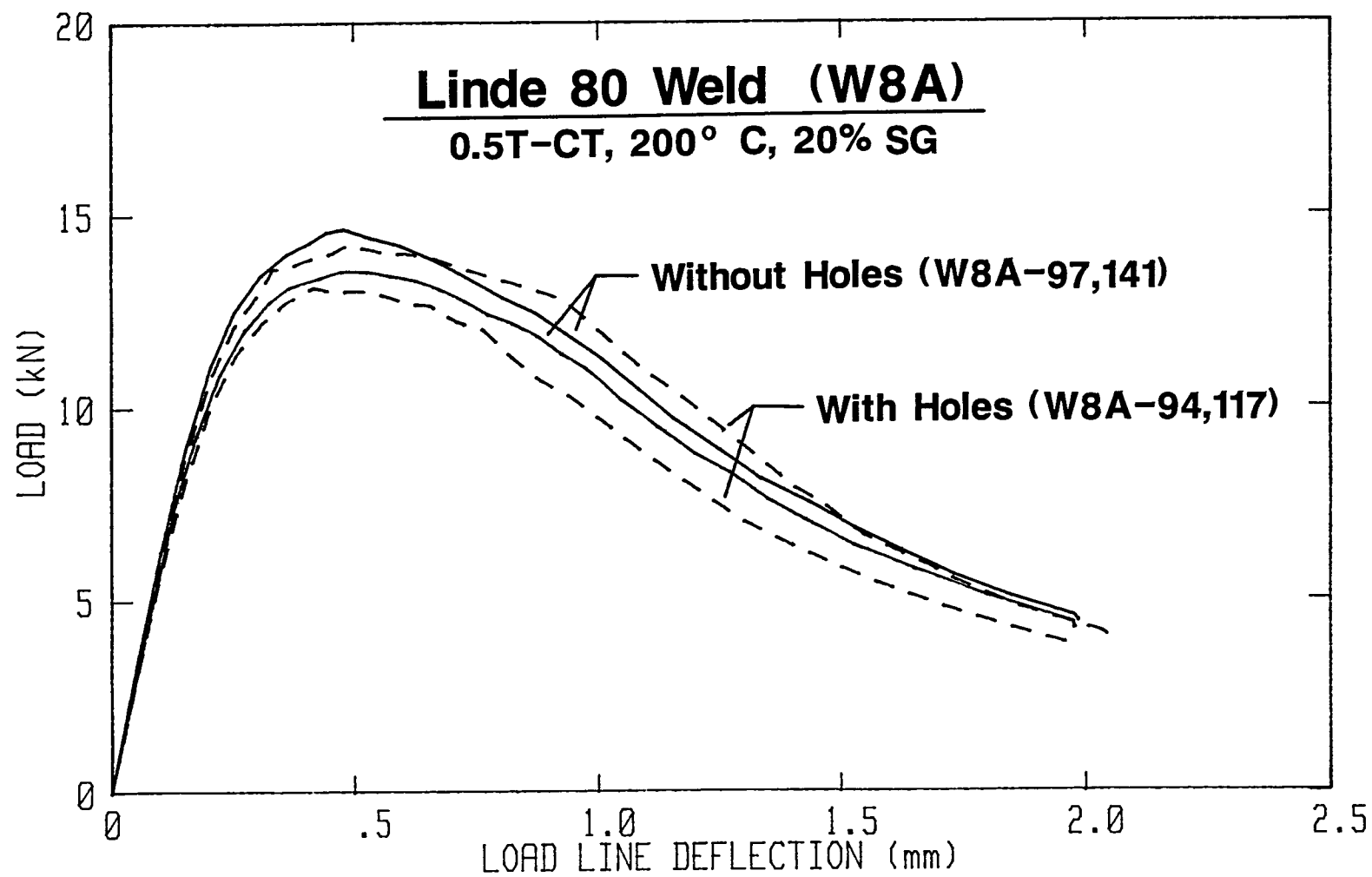


Fig. 21 Load-displacement curves for the δ_5 check-out tests illustrated in Fig. 20.

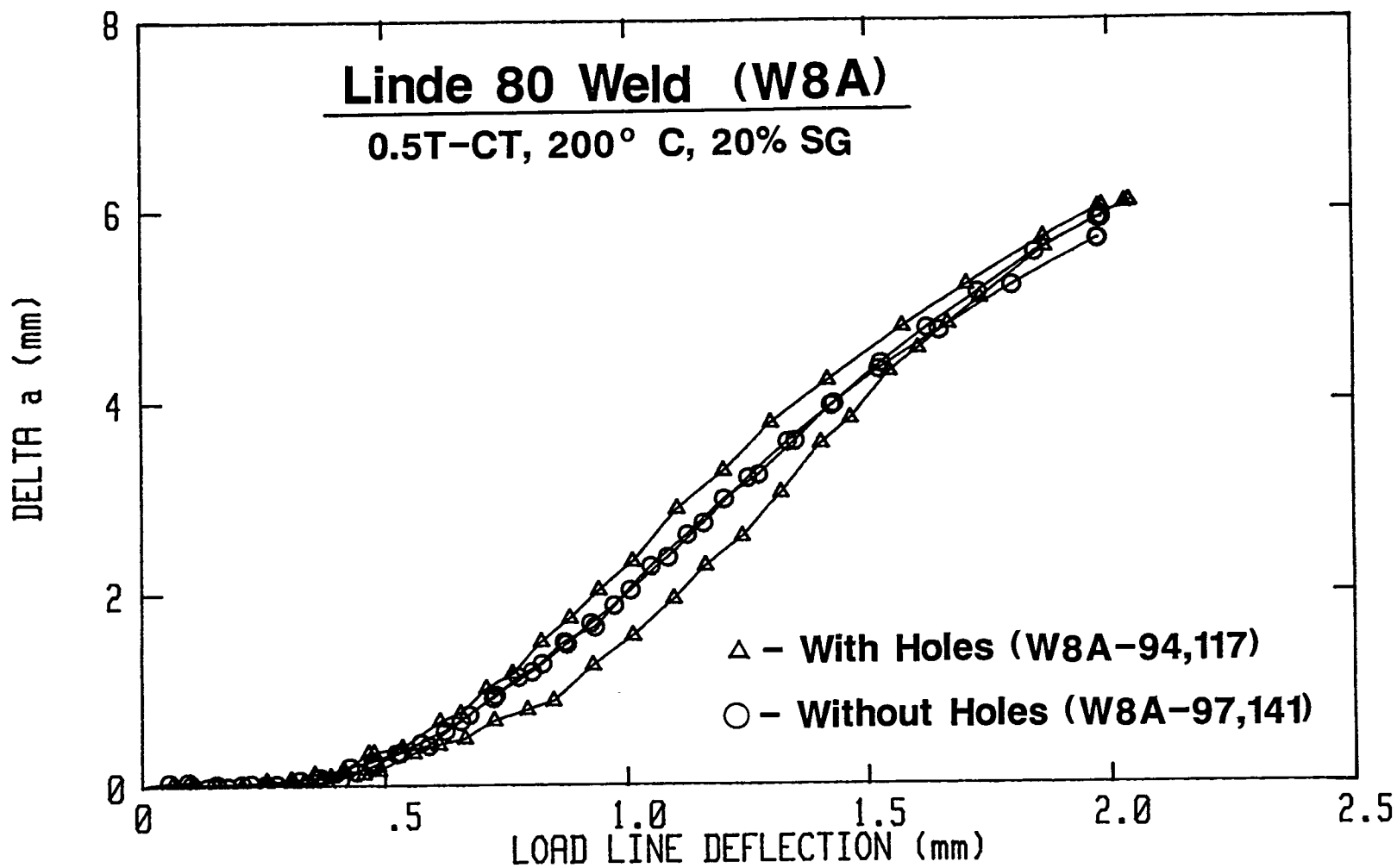


Fig. 22 Crack growth vs. load line displacement curves for the δ_5 check-out tests illustrated in Fig. 20.

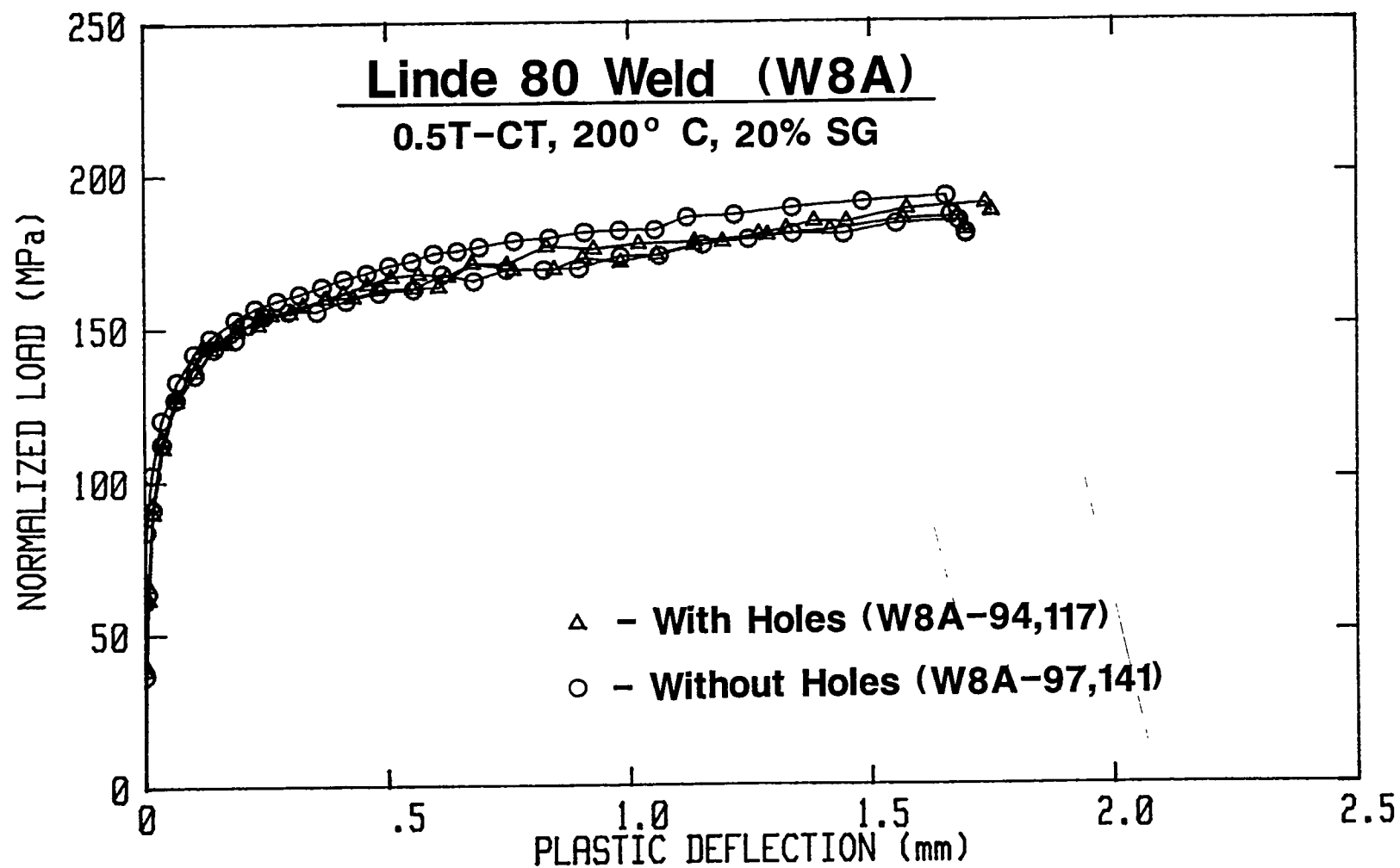


Fig. 23 Keycurves for the δ_5 check-out tests illustrated in Fig. 20.

6.5 Test Results

Detailed information on each test are given in Appendix C. A summary of the results for all tests are given in Tables 11 and 12.

Photographs of a 4T-CT specimen and a 0.5T-CT specimen with all of the clip gages attached are given in Fig. 24.

In general, the multiple clip gages gave similar Δa values throughout each test. For simplicity sake, all Δa evaluations are from V_{LL} measurements only.

6.5.1 0.5T-CT Specimens

J-R curve results for the 0.5T-CT specimens are summarized in Fig. 25 (J_{D*}) and Fig. 26 (J_{M*}). As indicated in each figure, data for the 1/4T and 3/4T thickness locations are within the same scatter band, with the two tests for the 1/2T locations yielding the highest and the lowest curves.

In contrast to the close agreement found for the 1/4T and 3/4T locations, the differences found with the 1/2T location is not easily explained. One difference between the test giving the lowest J-R curve and the other tests is that this test was interrupted several times, such that thickness measurements could be made (to check on lateral contraction during crack growth). After each such measurement, the specimen was allowed to return to the test temperature. These measurement points are obvious on the load-displacement curve as large decreases in load (Fig. 27). The low toughness of this specimen in comparison to the high toughness case is obvious from the narrower peak (in terms of displacement) at maximum load, the lower displacement at maximum load, and the overall lower displacements for this test. Comparing the load-displacement curves for all of these tests (Fig. 28) also demonstrates the good agreement of the 1/4T and 3/4T data, and the much lower displacements for the low J-R curve test. The key-curves from these tests are illustrated in Fig. 29.

The fracture surfaces for these specimens are illustrated in Fig. 30.

Comparison of these data with those for the reference tests (i.e., without holes) from the δ_s check-out tests indicate somewhat higher toughness for the δ_s check-out tests. As illustrated in Figs. 31 and 32, both J_{D*} and J_{M*} are higher for the δ_s check-out tests. Comparison of the load-displacement curves (Fig. 33) also illustrates the higher toughness of the previous tests. This variability may be due to through-thickness variability (i.e., the highest toughness is actually at the $\sim 0.4T$ location) or just variability at different locations in the plate.

6.5.2 1T-CT Specimens

J-R curve results for the 1T-CT specimens are summarized in Fig. 34, with the load-displacement curves for these two specimens compared in Fig. 35. The key-curves from these tests are illustrated in Fig. 36.

Table 11 Summary of Test Results for A 302-B Plate (Code V50) at 82°C (180°F)

Specimen I.D.	Specimen Designation	Thickness ^a Range (T)	Δa_m^b (mm)	$\Delta a_p^c - \Delta a_m$ (mm)	Error Percentage ^d (%)	Total Displacement (mm)	@ Maximum Load		(a/W) ₀
							Load (kN)	Displacement ^e (mm)	
V50-113	0.5T	0.20-0.27	6.93	-0.95	13.6	1.98	14.32	0.469	0.525
V50-116	0.5T	0.20-0.27	7.26	-1.13	15.5	2.23	14.05	0.436	0.521
V50-114	0.5T	0.46-0.54	6.97	-0.89	12.8	2.29	14.55	0.468	0.514
V50-117	0.5T	0.46-0.54	7.14	-0.89	12.4	2.01	14.97	0.341	0.509
V50-115	0.5T	0.73-0.80	7.00	-0.97	13.8	2.03	14.48	0.469	0.522
V50-118	0.5T	0.73-0.80	7.07	-0.91	12.8	1.96	14.74	0.416	0.507
V50-109 ^f	1T	0.26-0.42	13.17	-0.74	5.6	2.66	53.67	0.702	0.516
V50-112 ^f	1T	0.55-0.70	12.99	-0.93	7.2	2.64	52.29	0.659	0.531
V50-105 ^f	2T	0.18-0.49	26.78	-2.64	9.9	2.63	191.81	0.983	0.516
V50-108 ^f	2T	0.51-0.82	28.34	-4.13	14.6	2.44	194.26	0.981	0.513
V50-102 ^f	4T	0.19-0.81	58.91	-7.71	13.1	2.78	598.72	1.383	0.511
V50-103 ^f	4T	0.19-0.81	66.23	-15.26	23.0	2.95	563.67	1.318	0.513
V50-101 ^f	6T	0.03-0.97	86.49	-11.82	13.7	3.05	1091.20	1.649	0.518
V50-119 ^f	0.5T	0.38-0.46	6.41	-0.49	7.7	2.15	14.46	0.485	0.507
V50-120	0.5T	0.38-0.46	6.82	-0.66	9.6	2.38	14.17	0.554	0.512
V50-121	0.5T	0.38-0.46	6.81	-0.79	11.6	2.90	14.25	0.503	0.521
GPIB ^g	0.5T	0.42-0.50	6.25	-0.32	5.1	2.54	14.06	0.576	0.521
GPID	0.5T	0.42-0.50	2.17	-0.16	7.5	1.21	13.59	0.544	0.524

^a Thickness location with the top surface (OT) arbitrarily defined.

^b Optically-measured crack growth

^c Compliance-predicted crack growth

^d $(\Delta a_p - \Delta a_m) / \Delta a_m \cdot 100$

^e Load-line displacement (V_{LL})

^f Specimen had δ_5 measurement holes.

^g Tested at 24°C (75°F).

Table 12 Summary of J-R Curve Results for A 302-B Plate (Code V50) at 82°C (180°F)

Specimen I.D.	Specimen Designation	J Merkle-Corten (J_{M-C})			J Deformation (J_D)			J Modified (J_M)			J Deformation * (J_{D*})			J Modified * (J_{M*})		
		J_{Ic}^a (kJ/m ²)	T_{avg}	J_{50}^b (kJ/m ²)	J_{Ic}^a (kJ/m ²)	T_{avg}	J_{50}^b (kJ/m ²)	J_{Ic}^a (kJ/m ²)	T_{avg}	J_{50}^b (kJ/m ²)	J_{Ic}^a (kJ/m ²)	T_{avg}	J_{50}^b (kJ/m ²)	J_{Ic}^a (kJ/m ²)	T_{avg}	J_{50}^b (kJ/m ²)
V50-113	0.5T	117	42	184	116	32	162	117	42	183	117	31	161	118	42	183
V50-116	0.5T	99	42	198	98	33	159	98	42	204	98	32	158	98	42	203
V50-114	0.5T	118	51	272	116	41	181	117	52	309	117	41	180	118	51	309
V50-117	0.5T	72	37	192	71	31	141	71	37	213	70	31	142	70	37	215
V50-115	0.5T	110	38	181	110	28	152	110	38	185	111	27	152	111	37	185
V50-118	0.5T	94	54	225	92	46	173	92	55	223	92	45	173	92	55	222
V50-109 ^c	1T	118	33	182	118	28	166	117	32	180	117	27	164	117	31	178
V50-112 ^c	1T	112	39	189	111	34	170	111	38	189	114	34	170	114	38	190
V50-105 ^c	2T	105	26	138	104	24	136	104	25	139	110	22	137	110	23	141
V50-108 ^c	2T	115	20	139	114	17	132	114	18	138	117	17	133	117	18	139
V50-102 ^c	4T	106	18	125	105	17	122	105	18	123	103	17	119	103	17	120
V50-103 ^c	4T	103	10	111	103	9	109	103	10	109	99	9	105	99	9	105
V50-101 ^c	6T	92	14	109	92	14	106	92	14	108	91	13	106	91	14	106
V50-119 ^c	0.5T	109	55	230	107	45	191	108	56	233	106	45	191	107	56	233
V50-120	0.5T	116	54	293	115	43	221	115	55	310	113	44	219	113	55	307
V50-121	0.5T	111	45	335	109	36	238	110	45	394	108	36	240	109	45	402
GPIB ^d	0.5T	135	51	275	133	39	205	134	51	303	132	40	205	133	52	304
GPID	0.5T	136	45	^e	133	34	^e	135	45	^e	132	34	^e	134	45	^e

^a Using ASTM E 813-87 procedures.^b The J level where $J = 50 \text{ in.-lb/in.}^2 \times T_M$ (or $J = 8.75 \text{ kJ/m}^2 \times T_M$)^c Specimen had δ_5 measurement holes.^d Tested at 24°C (75°F).^e Cannot be determined.

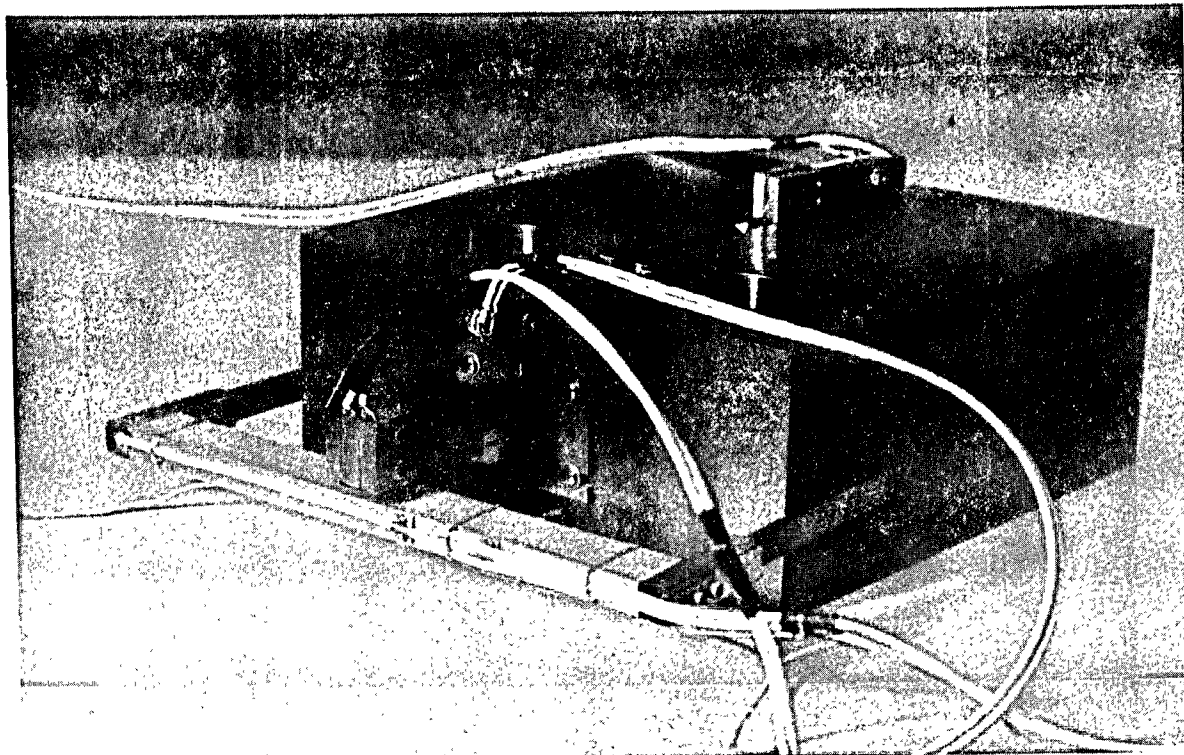
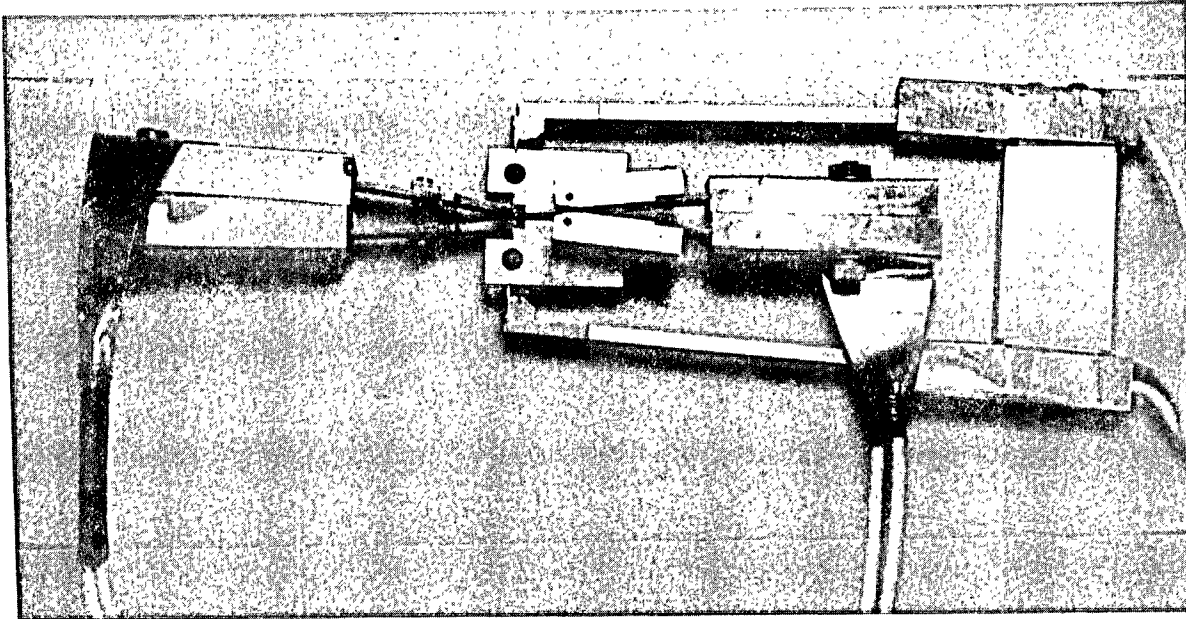


Fig. 24 Illustration of the clip gage placements used in tests of the 0.5T-CT and 4T-CT specimens. Only the load-line clip gages were used for the tests of 0.5T-CT specimens.

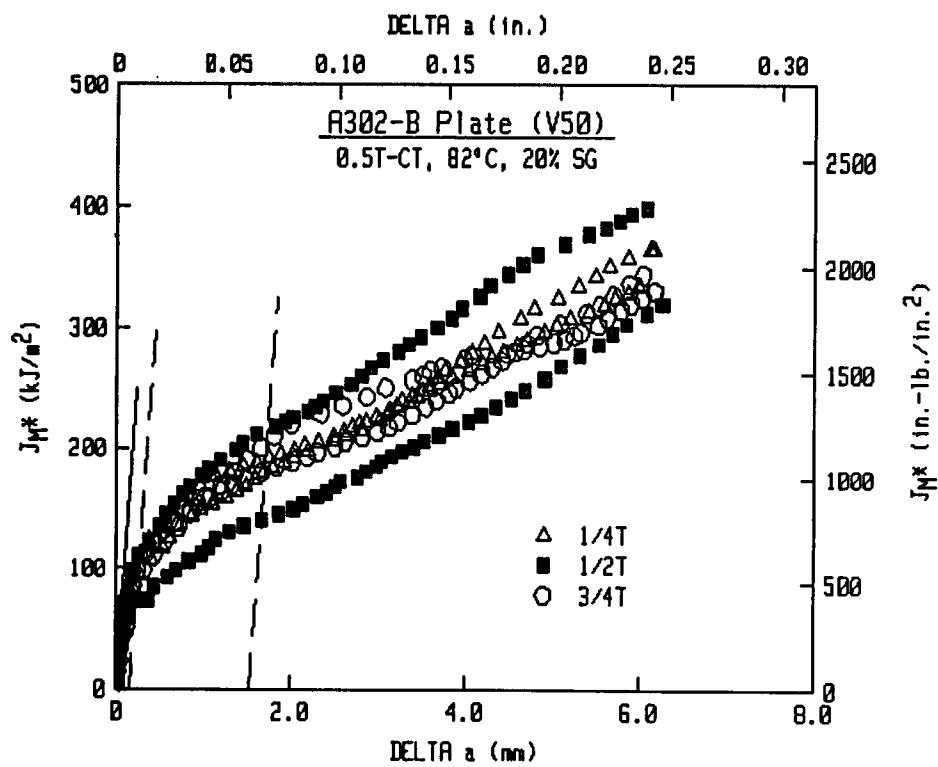
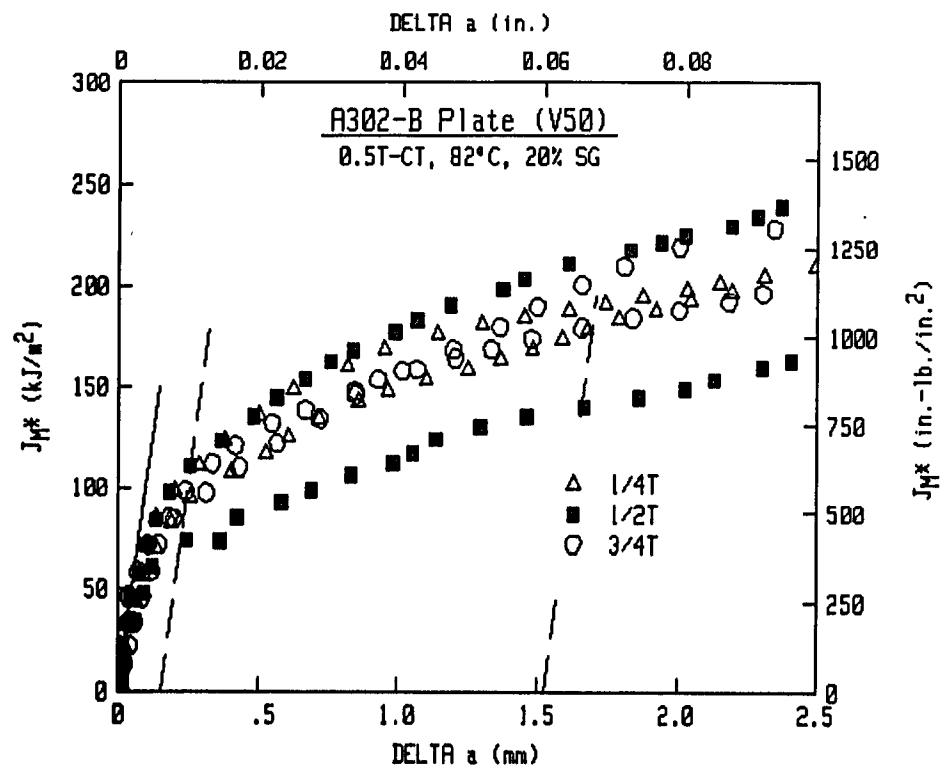


Fig. 25 J_{R^*} -R curves from the tests of 0.5T-CT specimens.

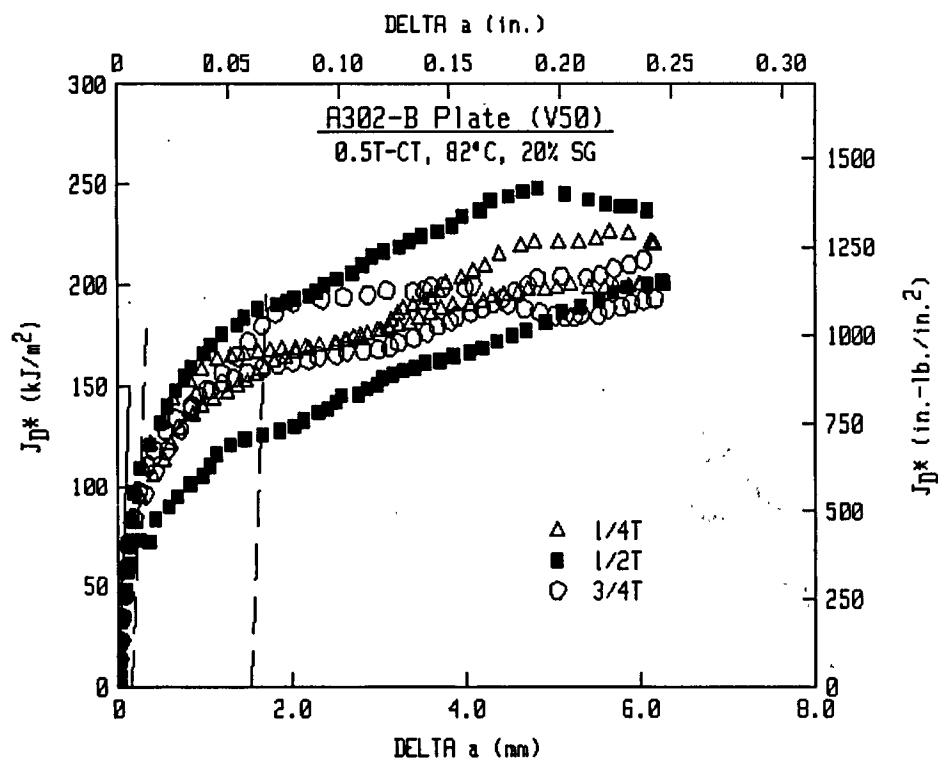
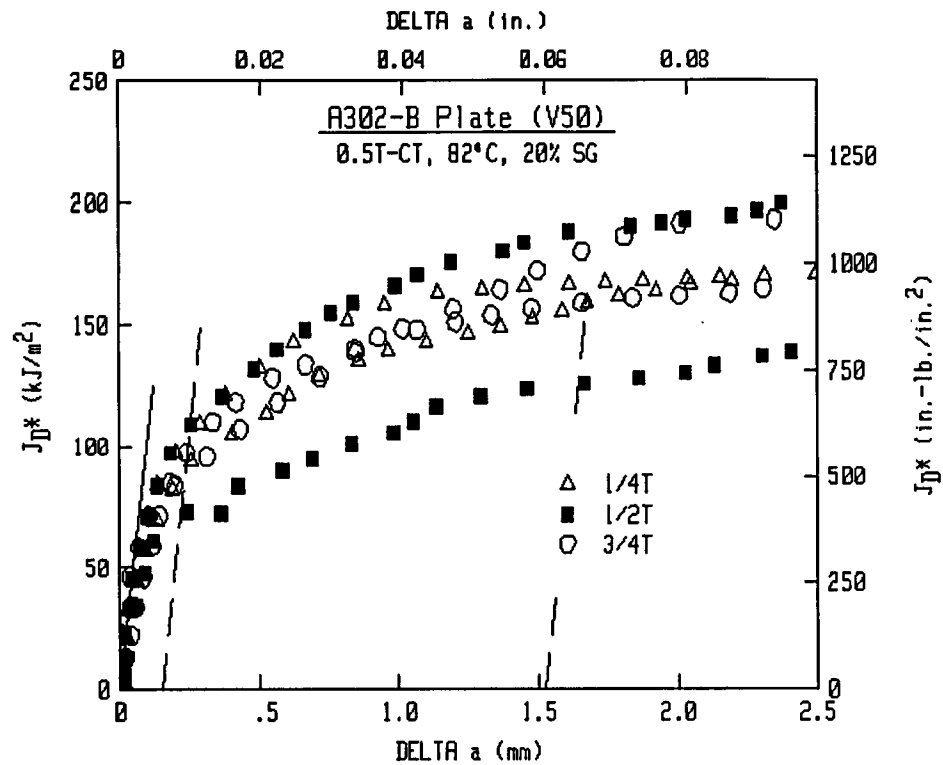


Fig. 26 J_{D^*} -R curves from the tests of 0.5T-CT specimens.

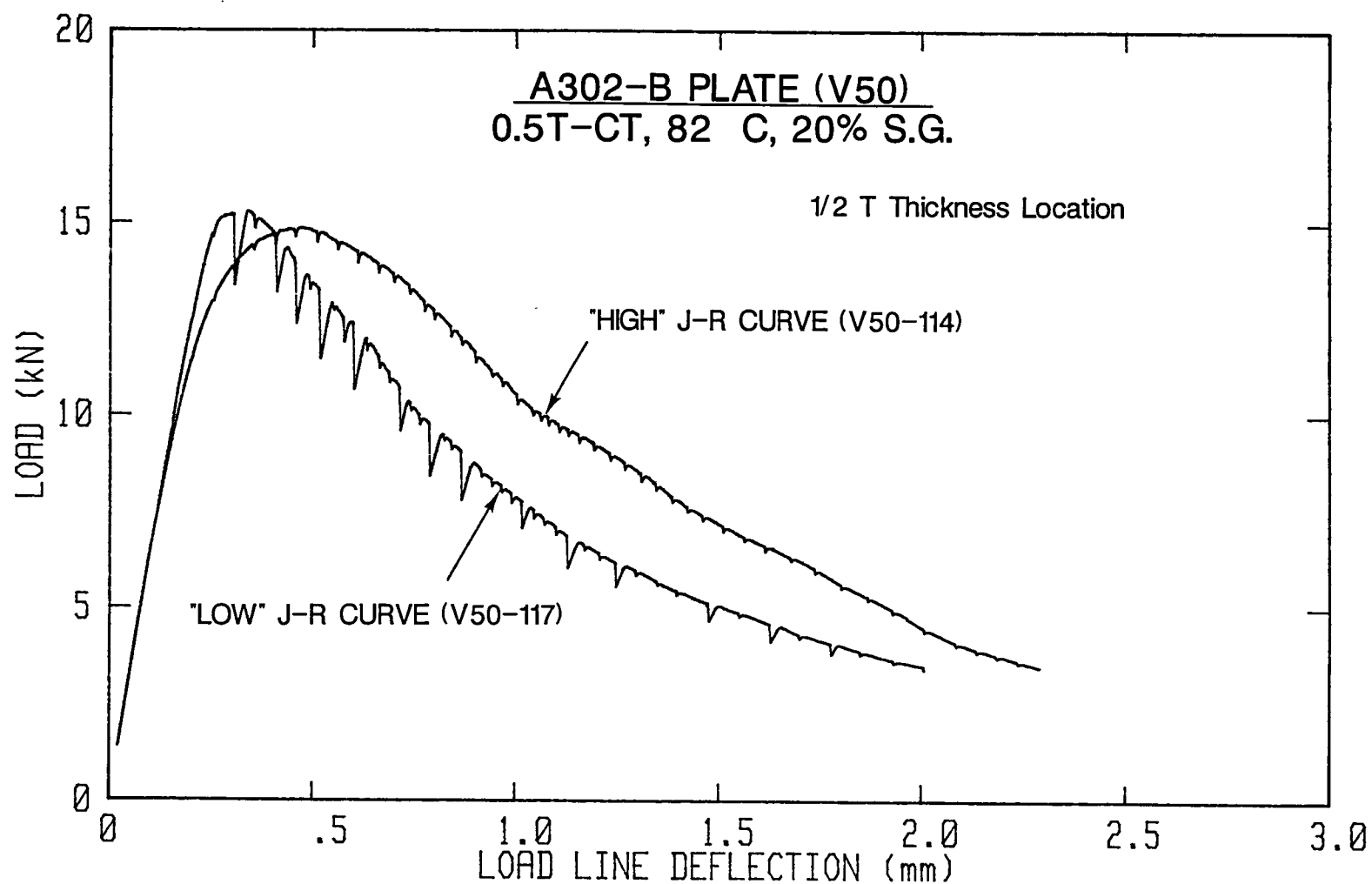


Fig. 27 Comparison of load-displacement curves for the 0.5T-CT specimens from the plate mid-thickness or 1/2T location.

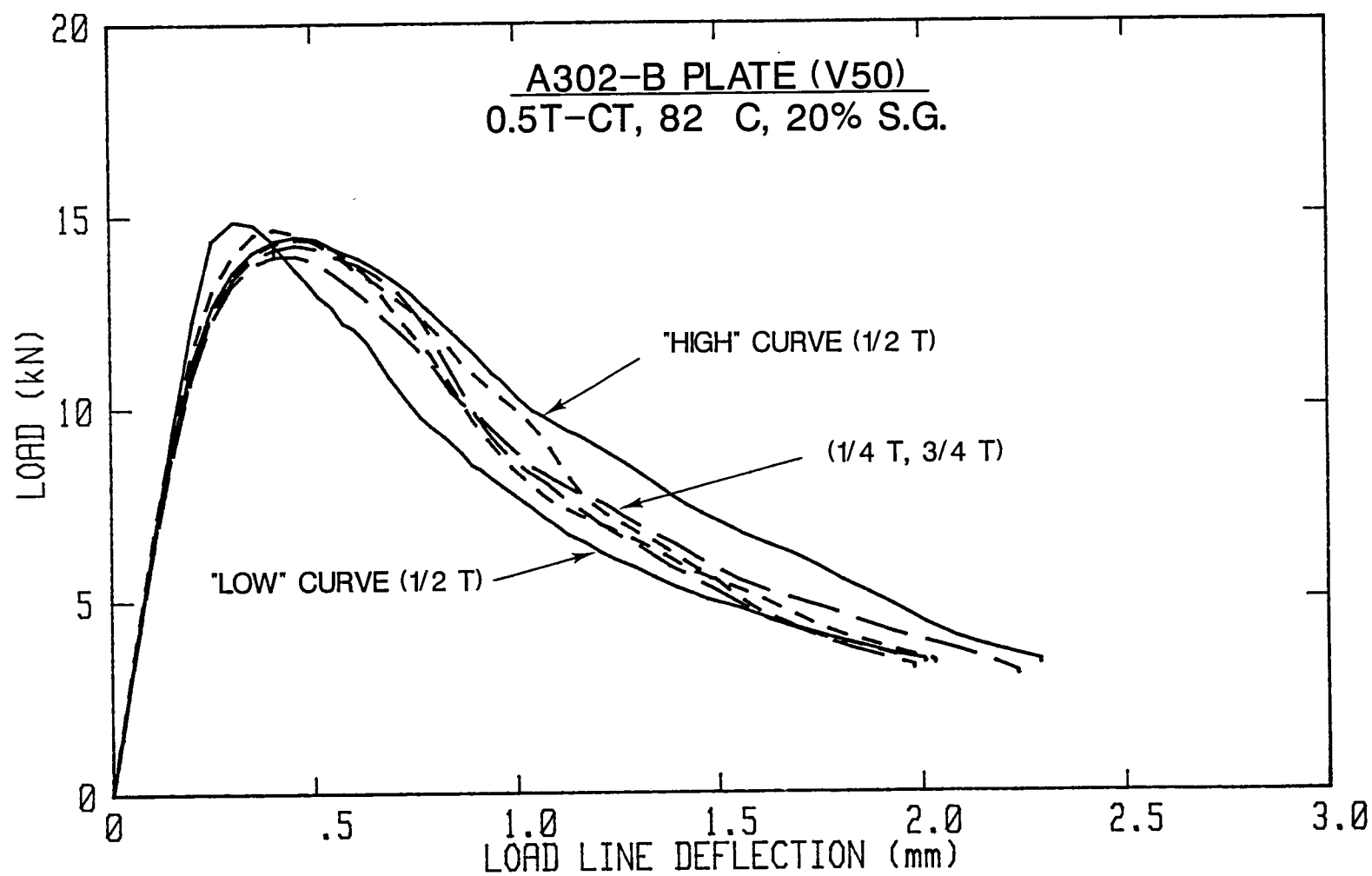


Fig. 28 Comparison of load-displacement curves for all of the 0.5T-CT specimens.

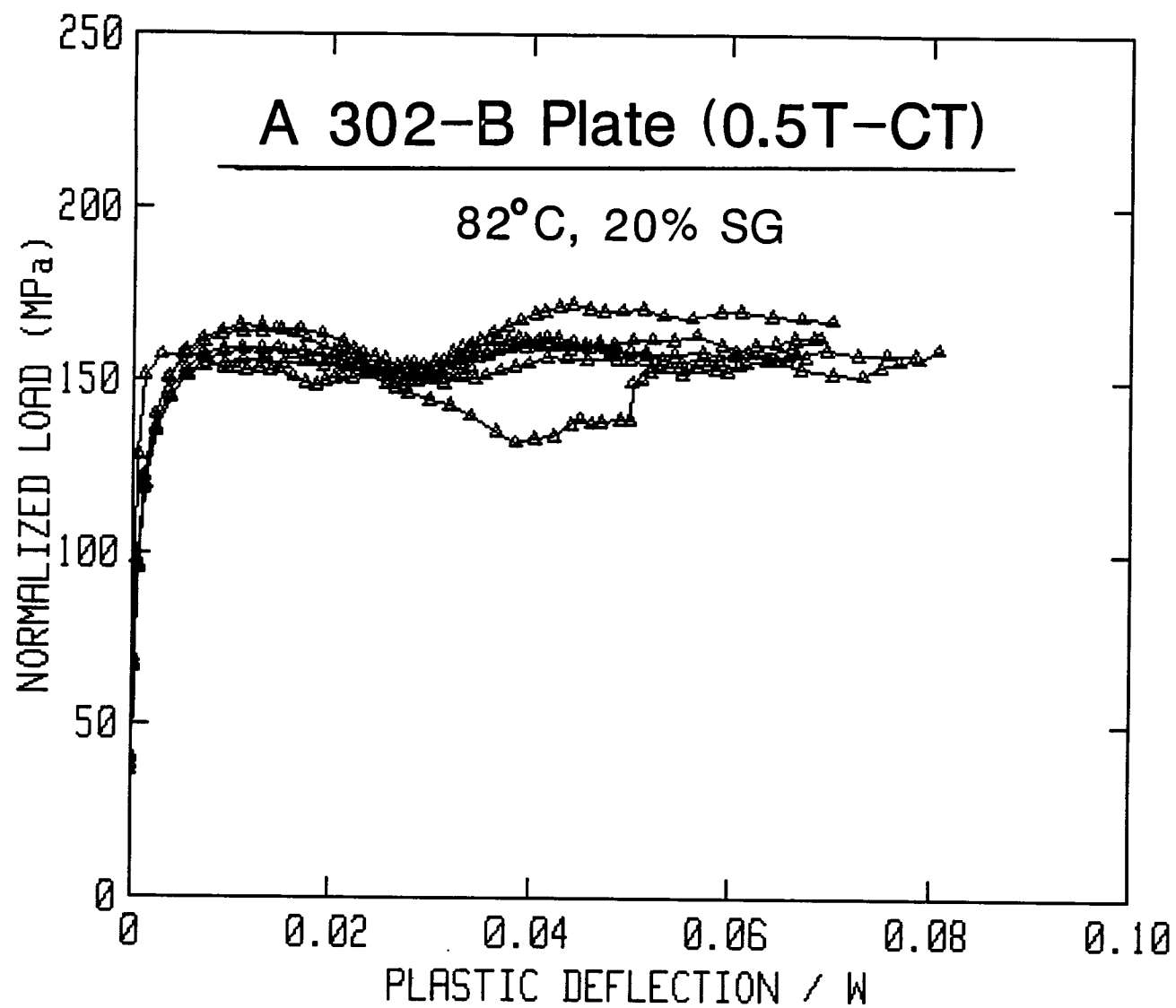
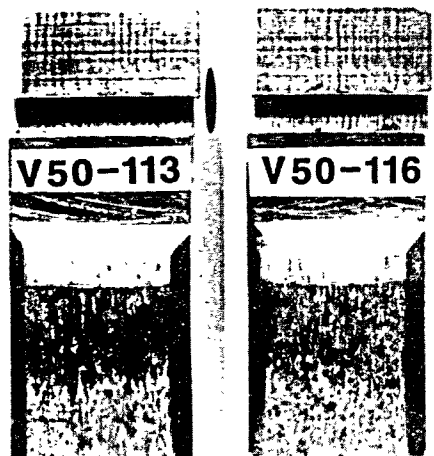


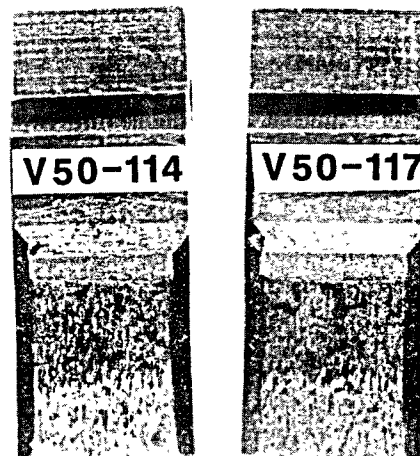
Fig. 29 Key-curves from the tests of 0.5T-CT specimens.

0.5T-CT Specimens

1/4T



1/2T



3/4T

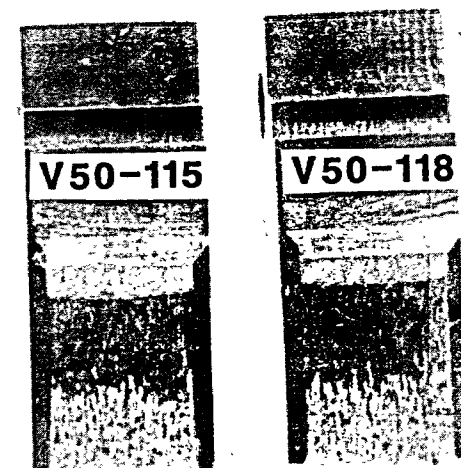


Fig. 30 Fracture surfaces of the 0.5T-CT specimens.

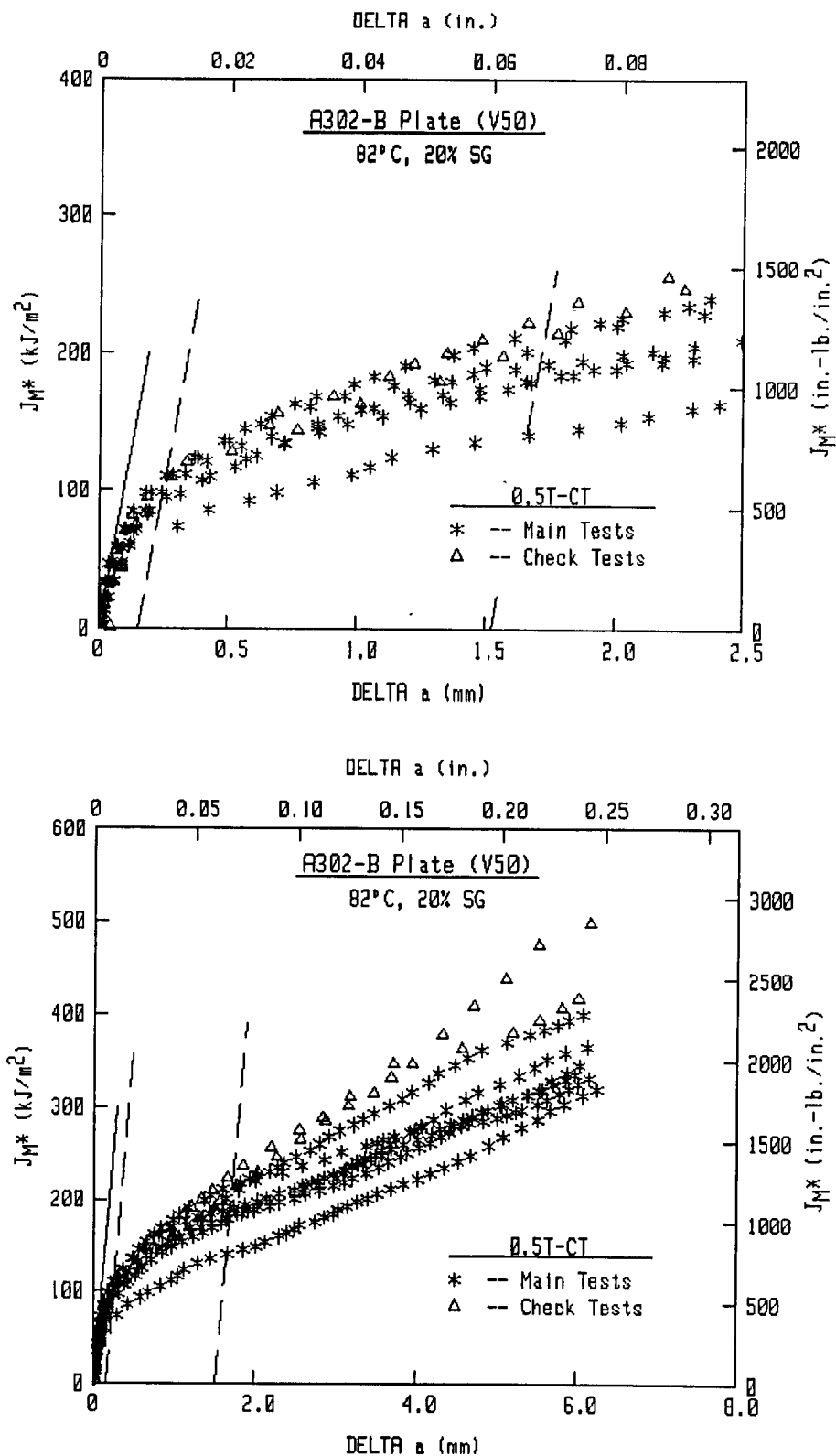


Fig. 31 Comparison of J_{R*} -R curves from 0.5T-CT specimens in Fig. 25 with those from the δ_5 check-out tests.

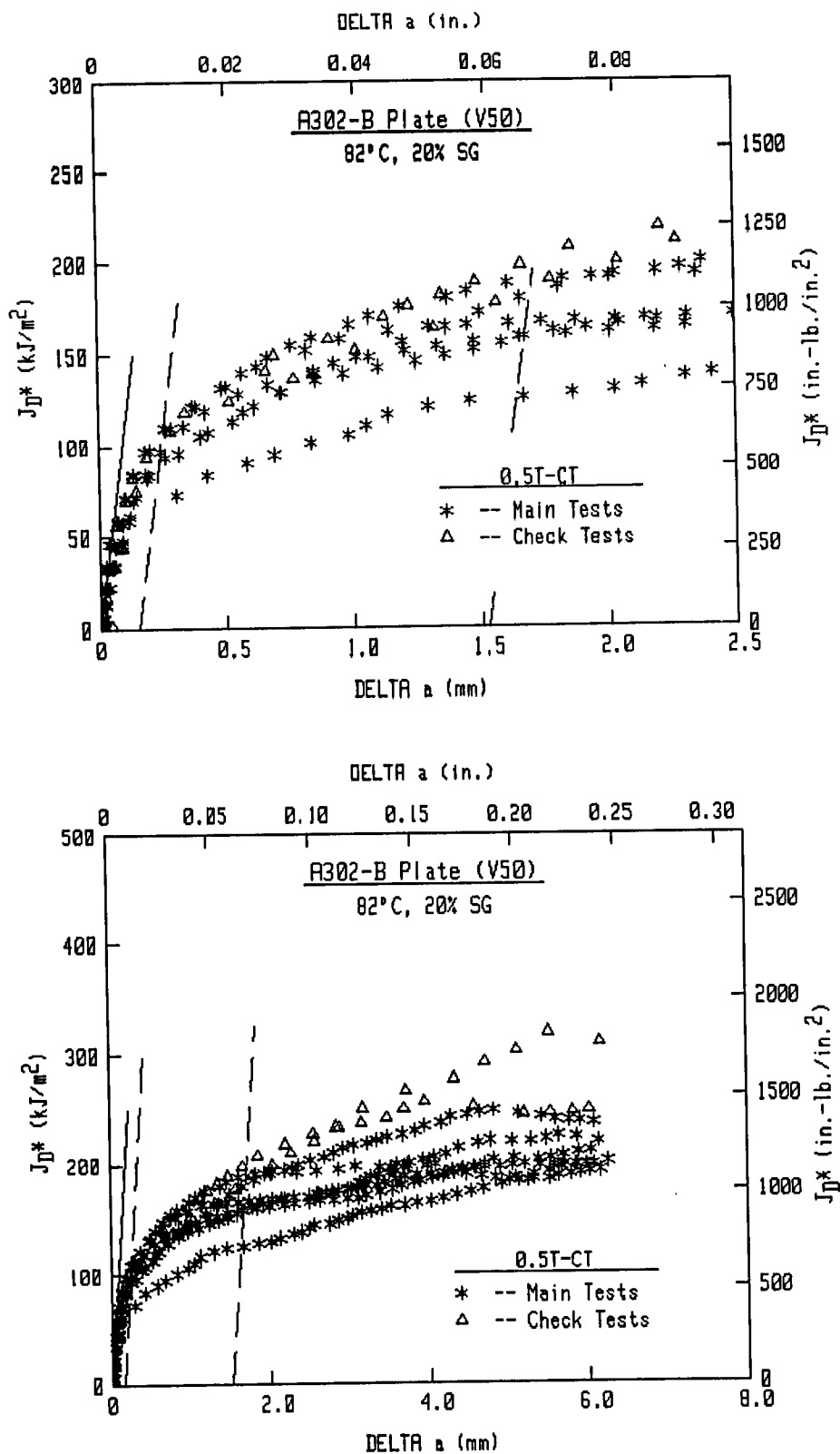


Fig. 32 Comparison of J_{D^*} -R curves from 0.5T-CT specimens in Fig. 26 with those from the $\delta 5$ check-out tests.

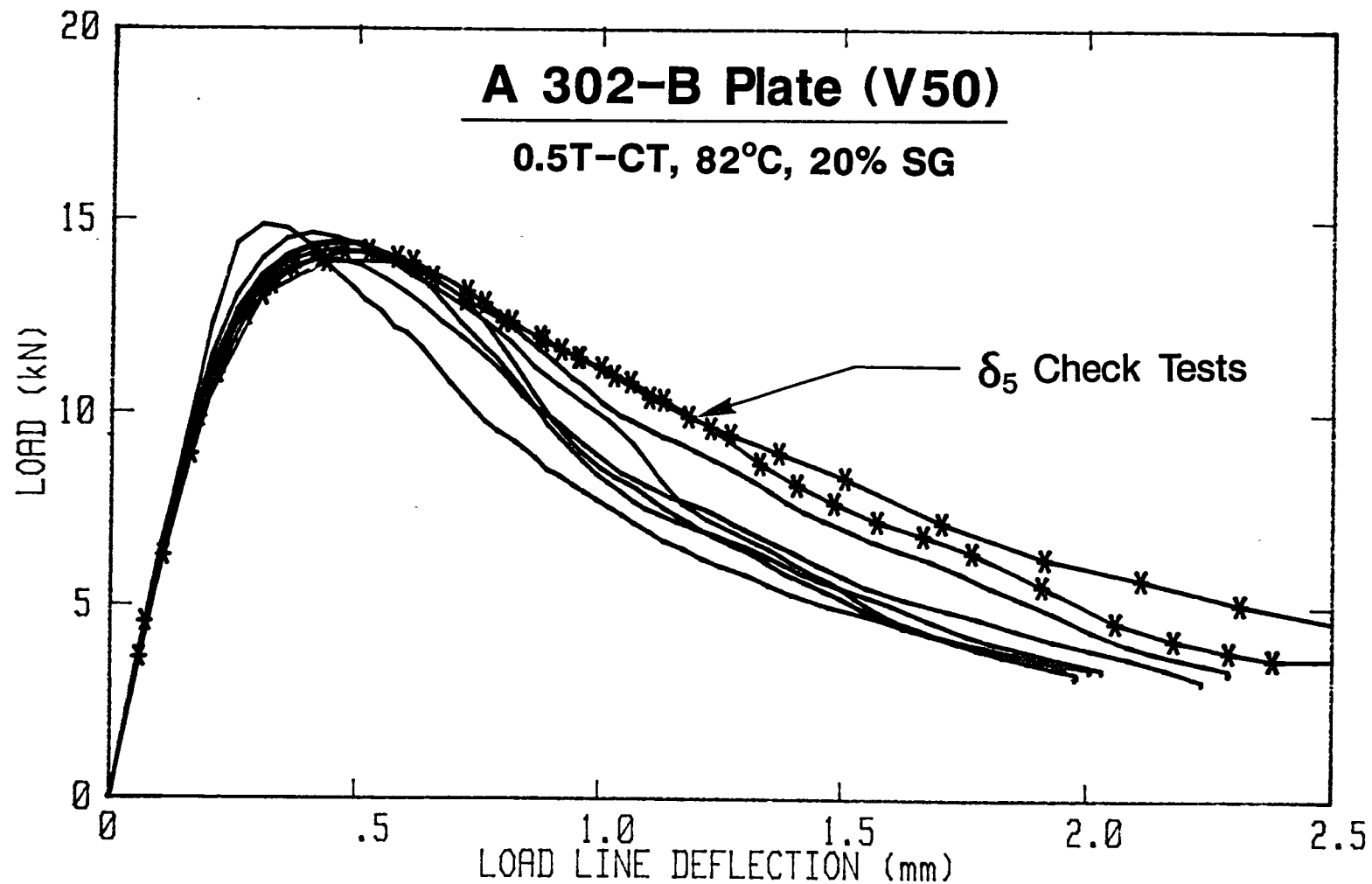


Fig. 33 Load-displacement curves from the main tests of 0.5T-CT specimens and the δ_5 check-out tests.

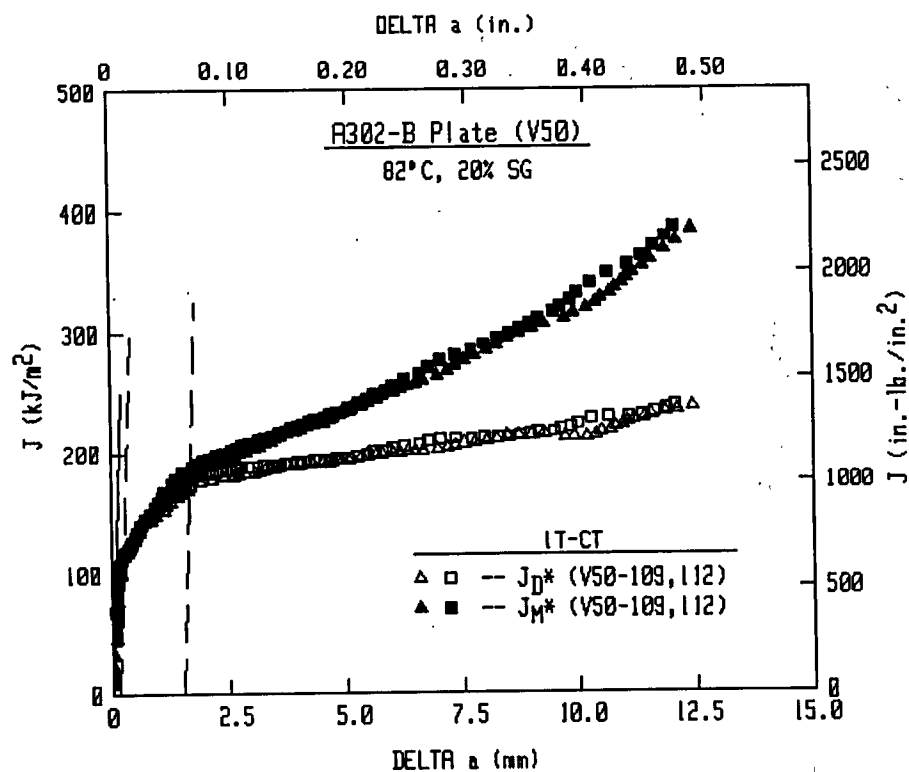
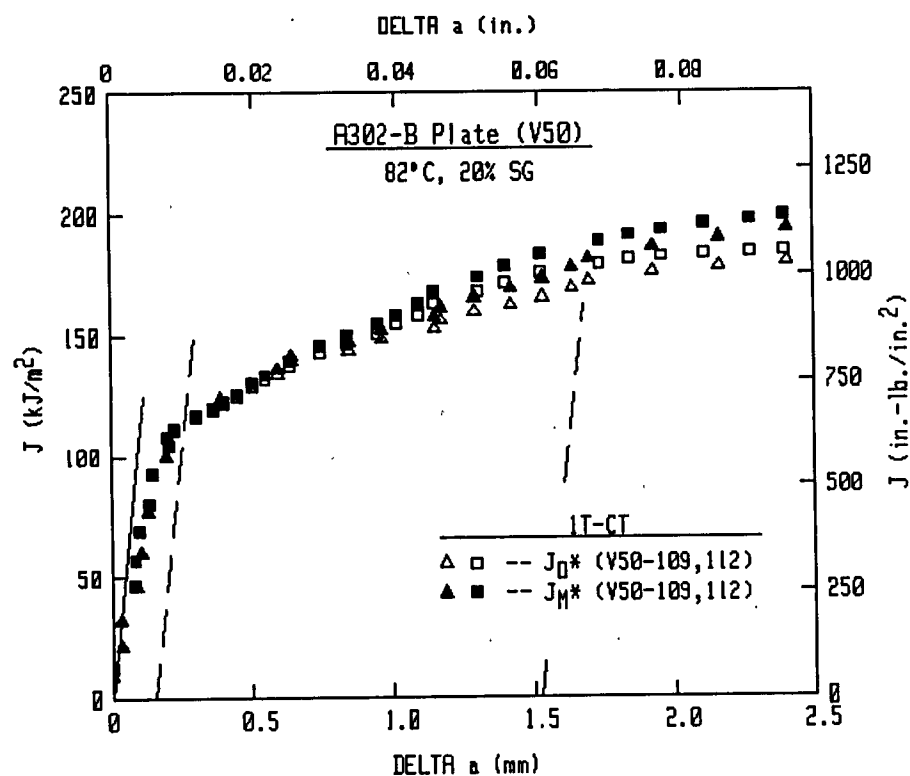


Fig. 34 J_{M^*} - and J_{D^*} -R curves from the tests of IT-CT specimens.

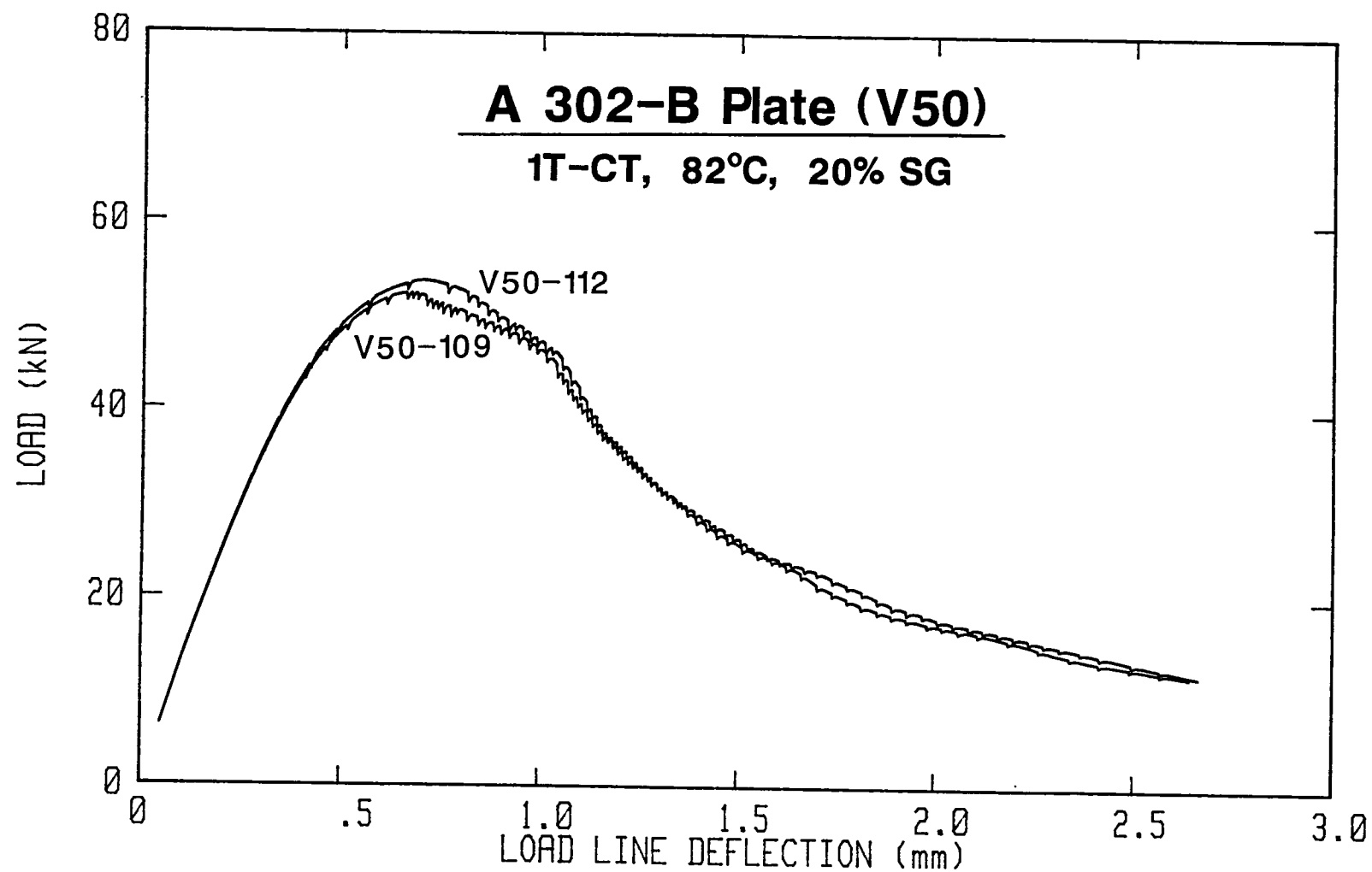


Fig. 35 Load-displacement curves from the tests of 1T-CT specimens.

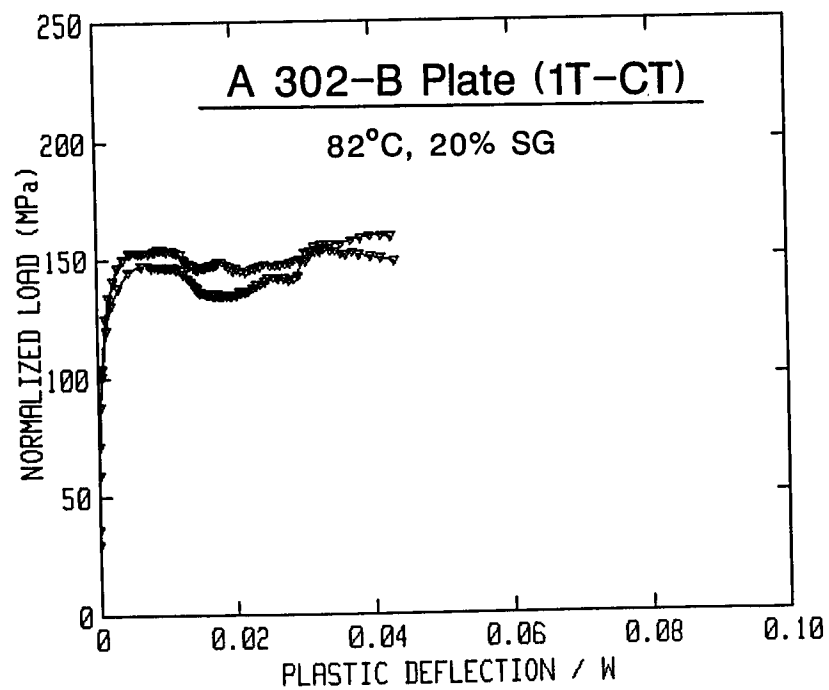
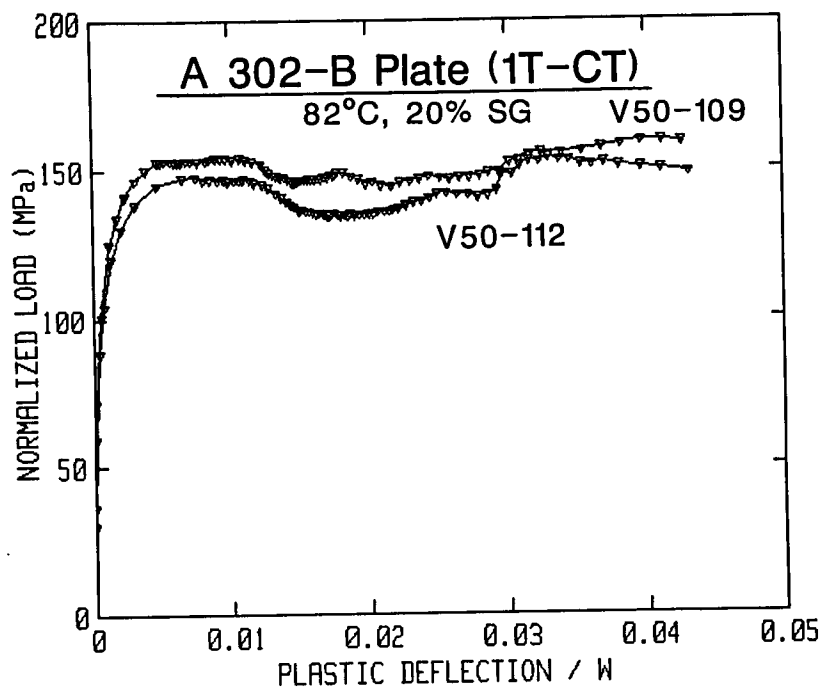


Fig. 36 Key-curves from the tests of 1T-CT specimens.

In all cases, the reproducibility of data is remarkable, in particular given the difference in the location of these two specimens.

The fracture surfaces of these two specimens are illustrated in Fig. 37.

6.5.3 2T-CT Specimens

J-R curves for the 2T-CT specimens are illustrated in Fig. 38, with the load-displacement curves illustrated in Fig. 39. Key-curves from these tests are illustrated in Fig. 40. As with results from the 1T-CT specimens, results for the 2T-CT specimens are in excellent agreement.

The fracture surfaces for these two specimens are illustrated in Fig. 41.

6.5.4 4T-CT Specimens

J-R curves for the 4T-CT specimens are illustrated in Fig. 42, with the load-displacement curves illustrated in Fig. 43. The key-curves from the tests are illustrated in Fig. 44. The load-displacement curves are similar in appearance at low displacements to near maximum load (i.e., below 1.3 mm) and at high displacements (i.e., above 2.15 mm) with no comparability of the results in between. In contrast, the J-R curves are comparable only to a J level of $\sim 100 \text{ kJ/m}^2$. At greater Δa and J levels, the shapes of the J-R curves from these two specimens are quite different. Whereas the J-R curve for specimen V50-102 is generally a smooth curve, that for specimen V50-103 has a steep slope for Δa up to $\sim 19 \text{ mm}$, with an abrupt reduction in slope at greater Δa levels. A possible explanation of this behavior is apparent in the fracture surface for this specimen (Fig. 45), where a large split area is obvious. As the crack progressed through this area, the toughness may have been quite variable in this area, causing the irregular J-R curve.

One unusual aspect in the J-R curves for these two specimens lies in the comparison of the J_{M^*} - and J_{D^*} -curves. For specimen V50-103, the J_{D^*} -R curve demonstrates a negative slope (i.e., the J level is decreasing) for Δa greater than $\sim 18 \text{ mm}$ (0.7 in.), whereas the J_{D^*} -R curve for specimen V50-102 demonstrates a very low but positive slope. In contrast, the J_{M^*} -R curves for both specimens demonstrate positive slopes, with the J_{M^*} -R curve of specimen V50-103 always exceeding that of specimen V50-102.

6.5.5 6T-CT Specimen

The J-R curves for the 6T-CT specimen are illustrated in Fig. 46. In this case, the J_{M^*} -R curve is essentially flat over the final few data points, and the J_{D^*} -R curve exhibits a negative slope with those same data points.

The load-displacement curve for this specimen (Fig. 47) is almost triangular in shape, indicative of low toughness and little

1T-CT

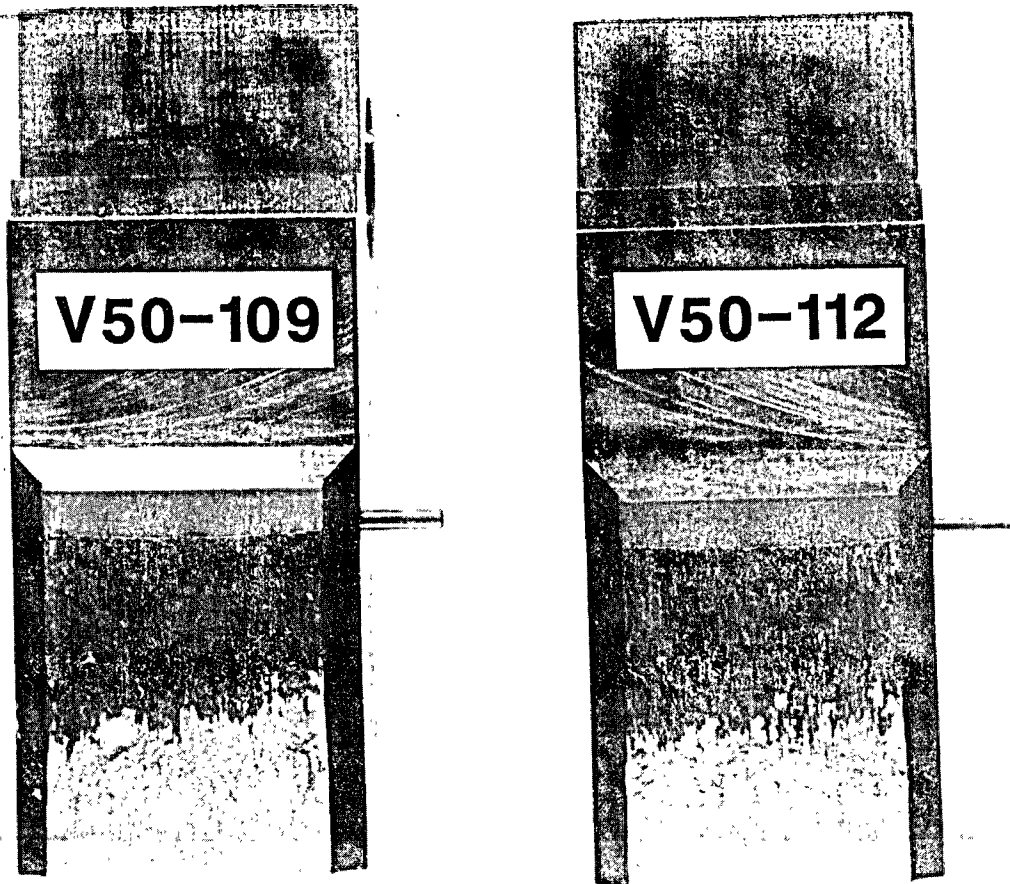


Fig. 37 Fracture surfaces of the 1T-CT specimens.

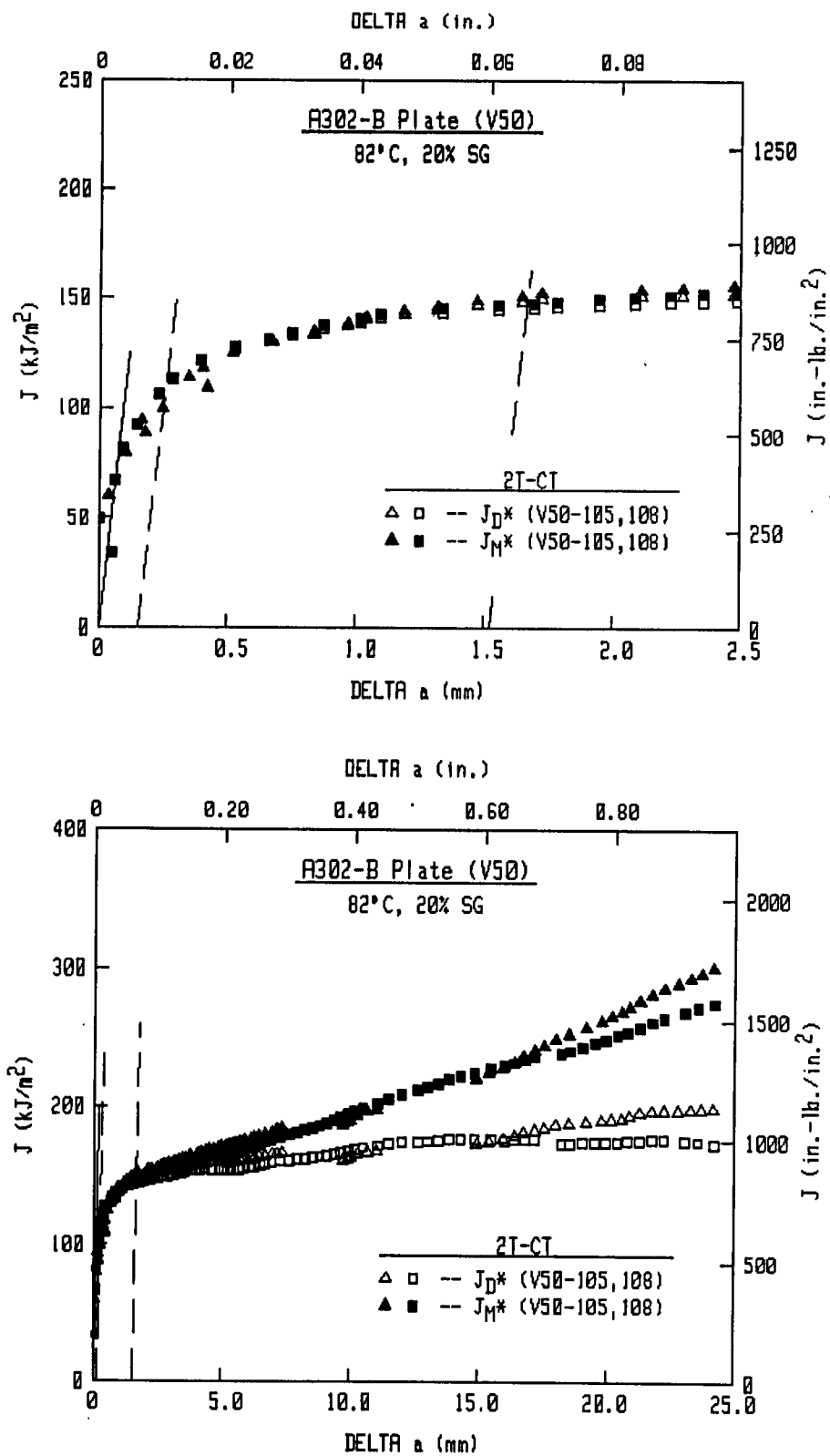


Fig. 38 J_{M^*} - and J_{D^*} -R curves from the tests of 2T-CT specimens.

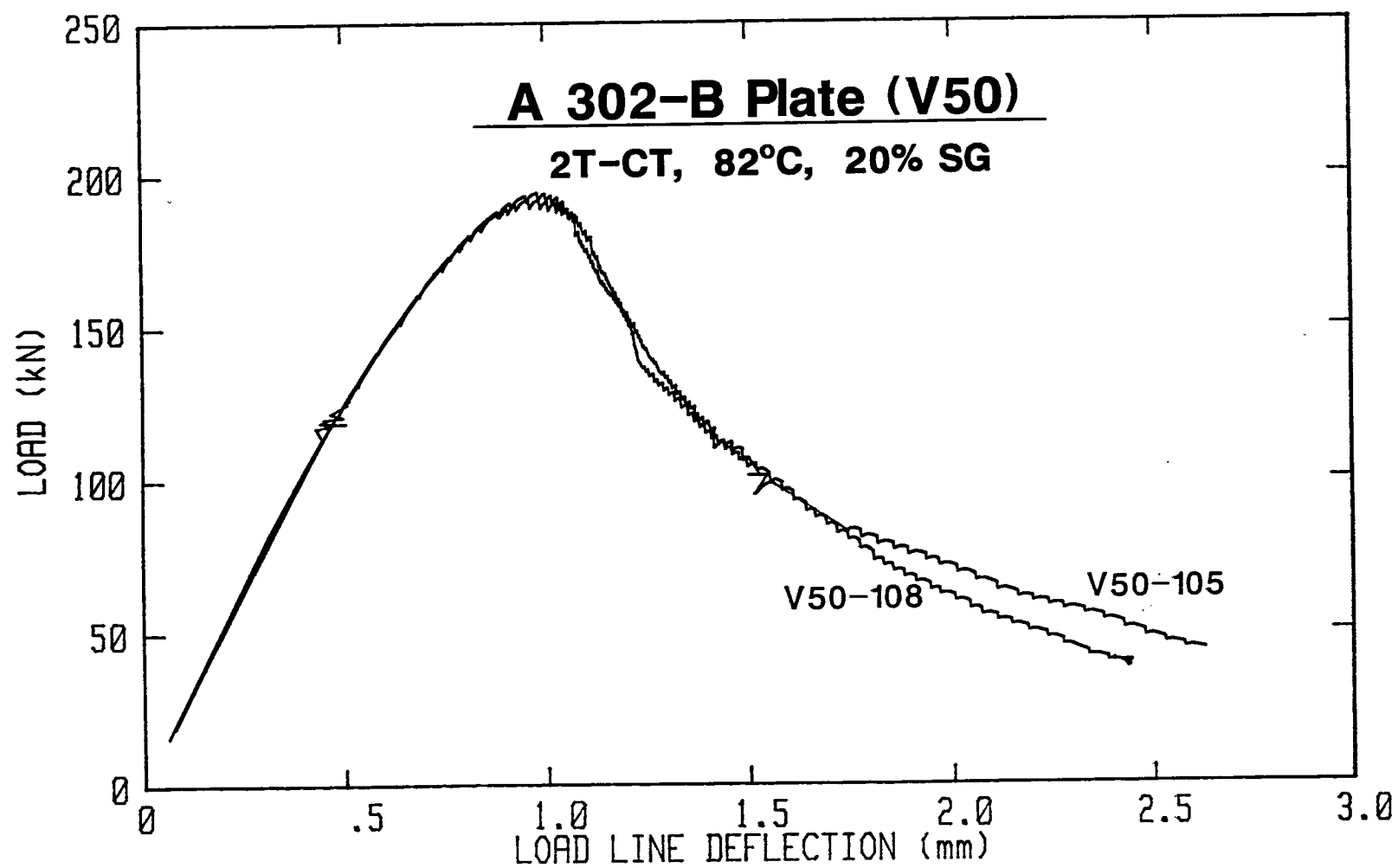


Fig. 39 Load-displacement curves from the tests of 2T-CT specimens.

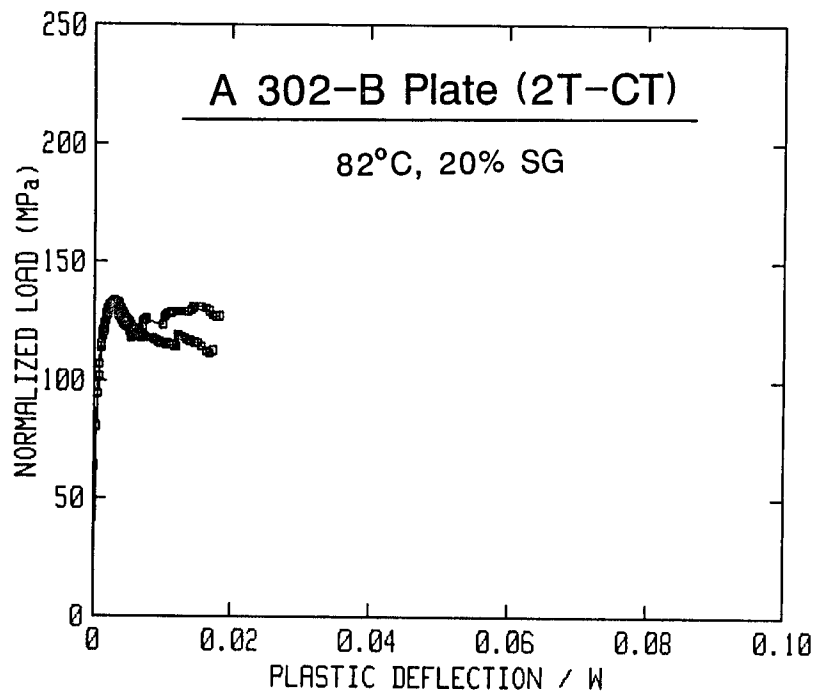
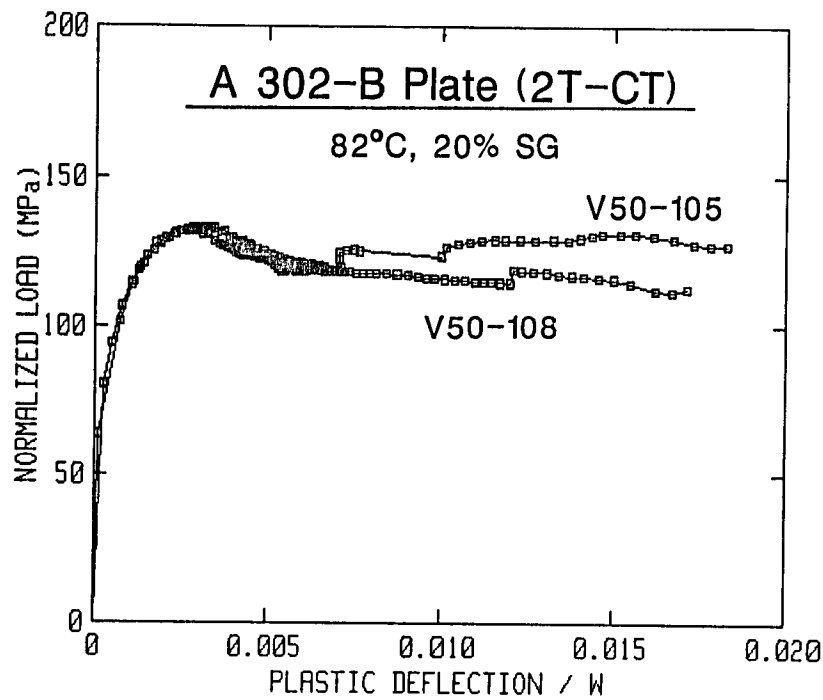


Fig. 40 Key-curves from the tests of 2T-CT specimens.

2T-CT

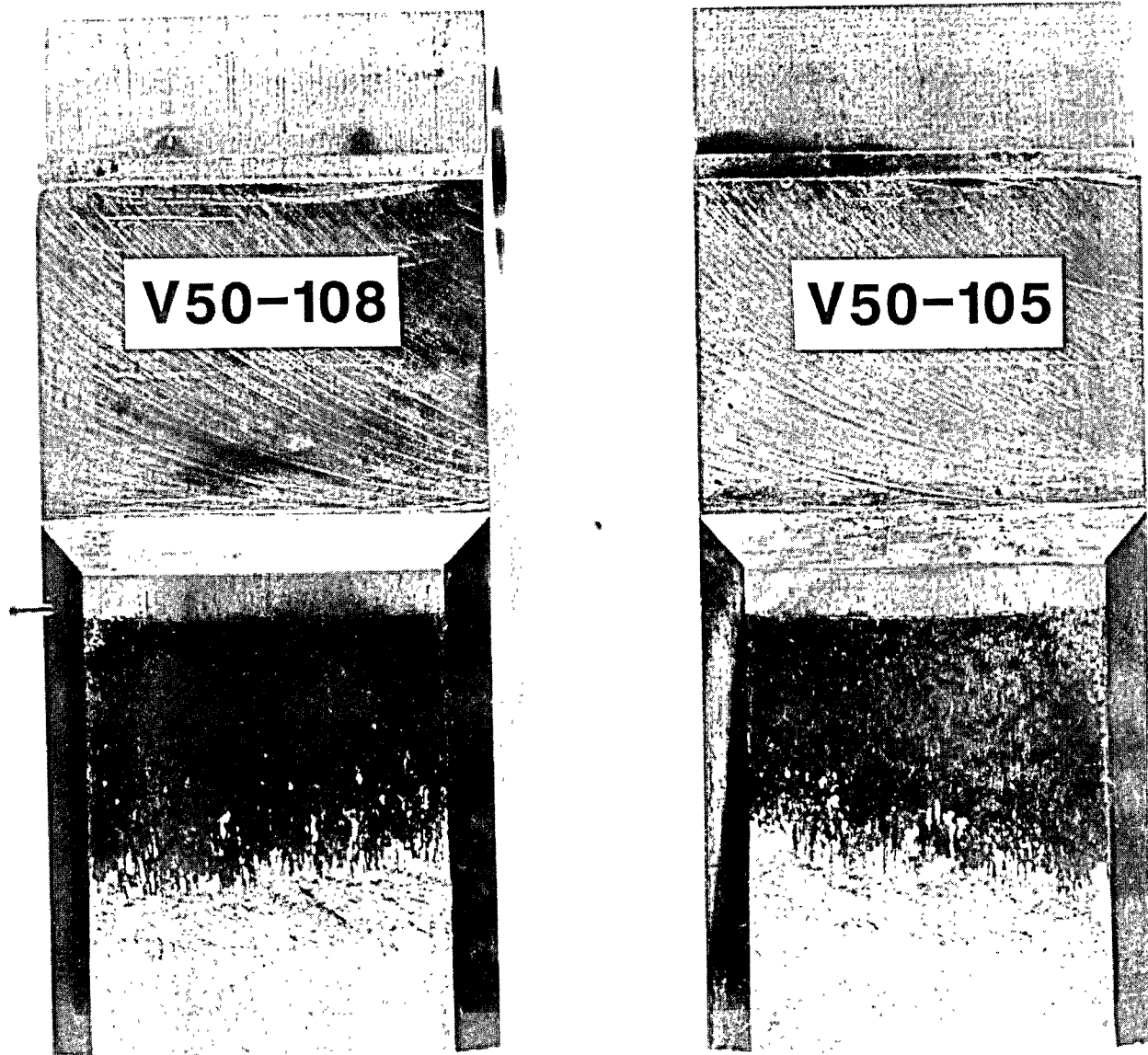


Fig. 41 Fracture surfaces of the 2T-CT specimens.

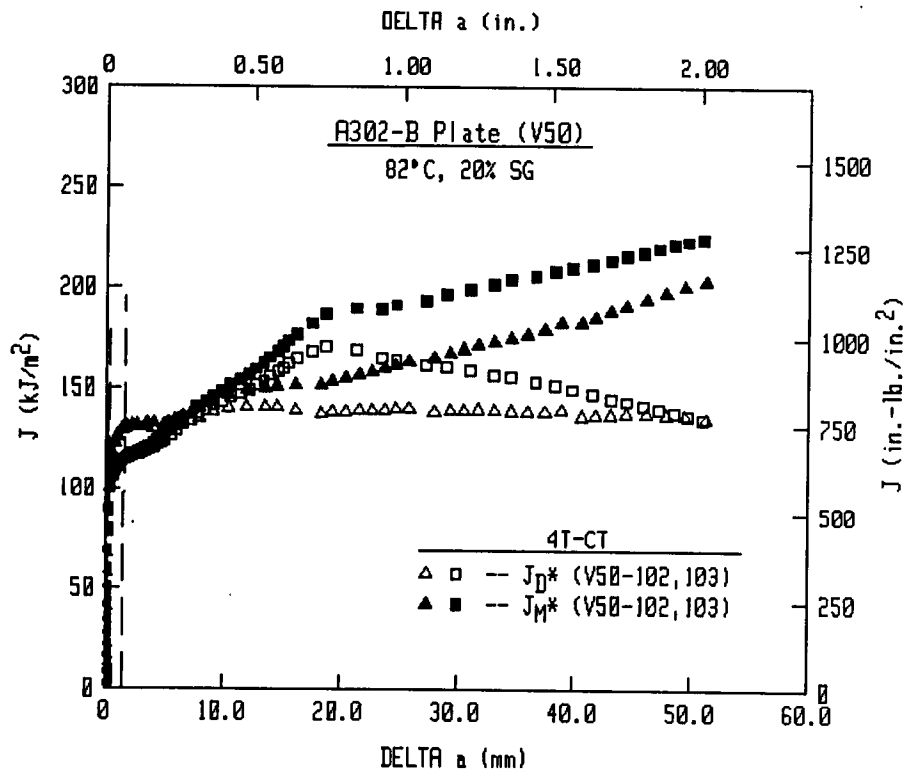
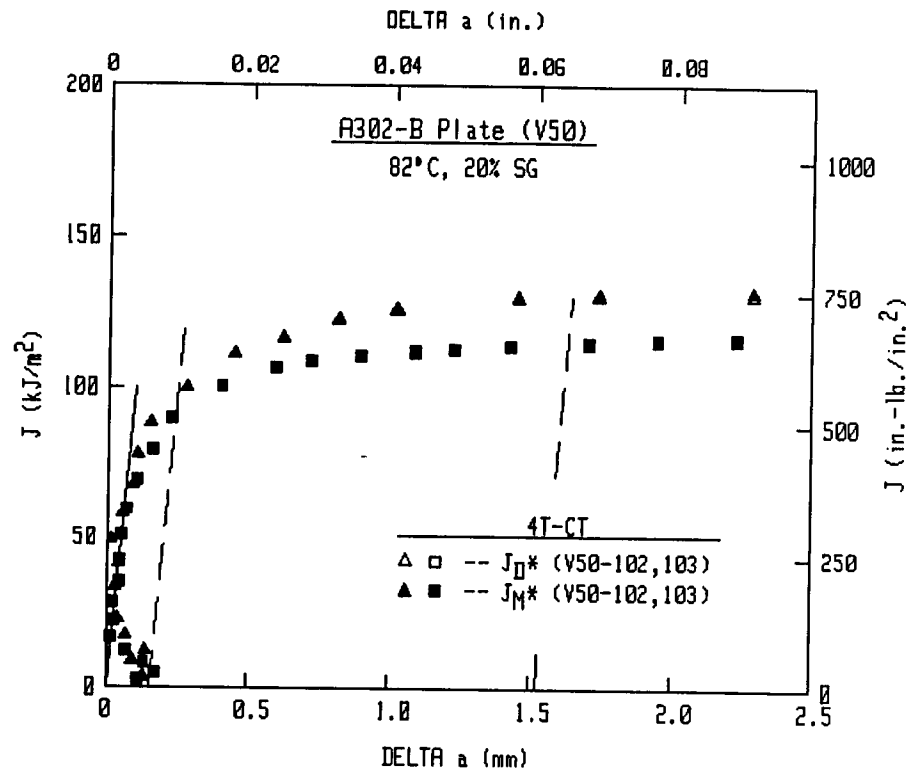


Fig. 42 J_M*- and J_D*-R curves from the tests of 4T-CT specimens.

A 302-B Plate (V50)

4T-CT, 82°C, 20% SG

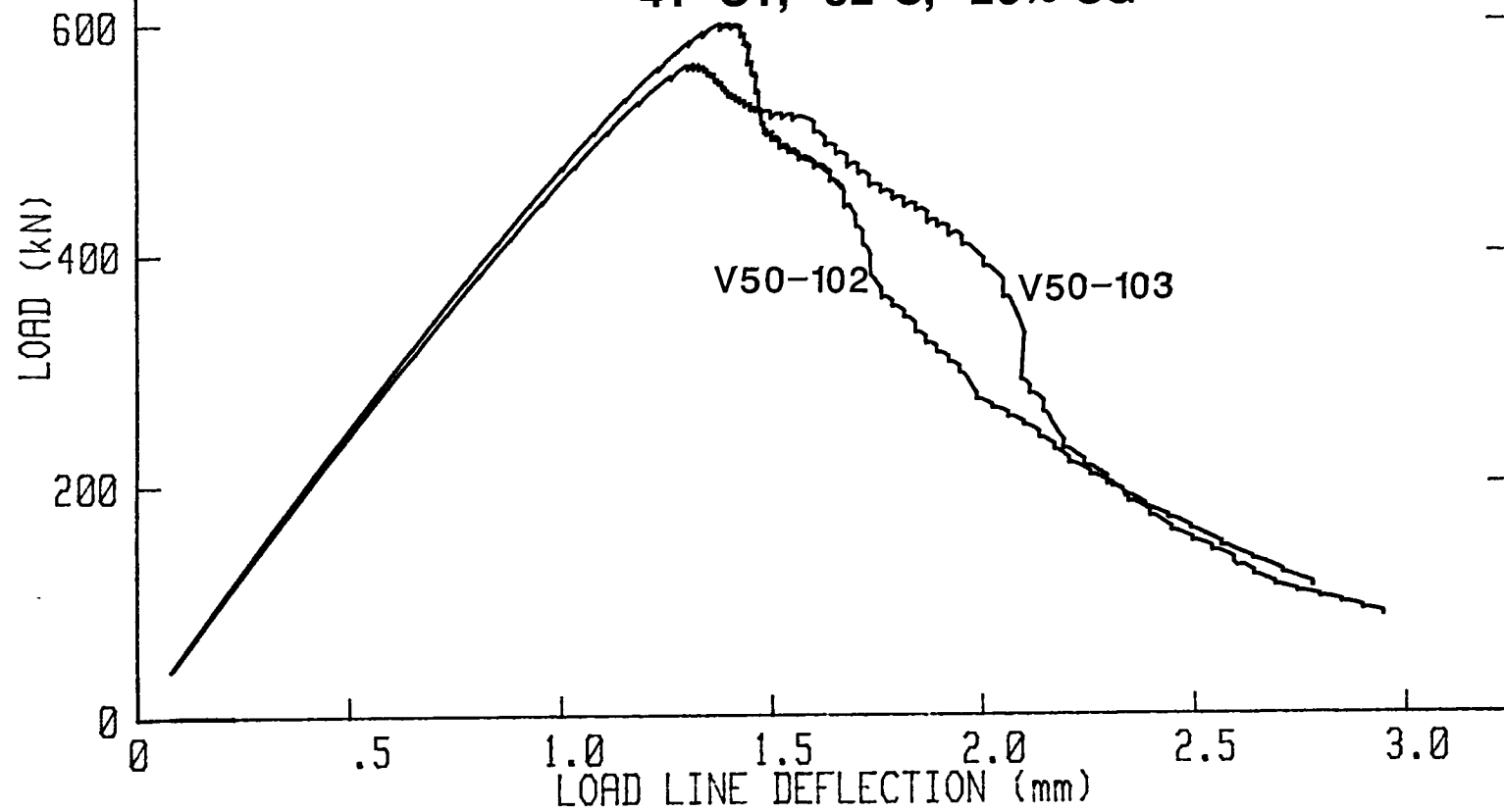


Fig. 43 Load-displacement curves from the tests of 4T-CT specimens.

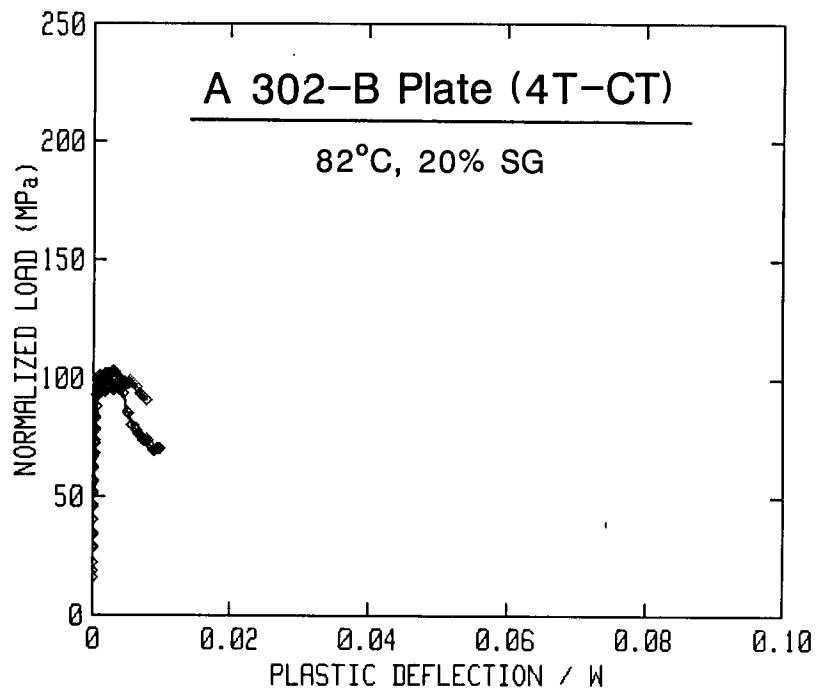
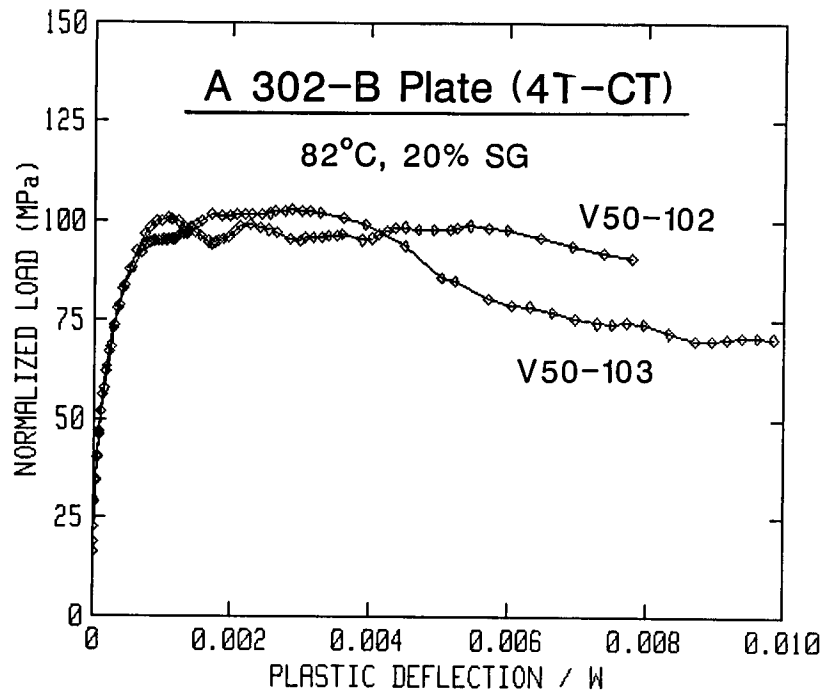


Fig. 44 Key-curves from the tests of 4T-CT specimens.

4T-CT

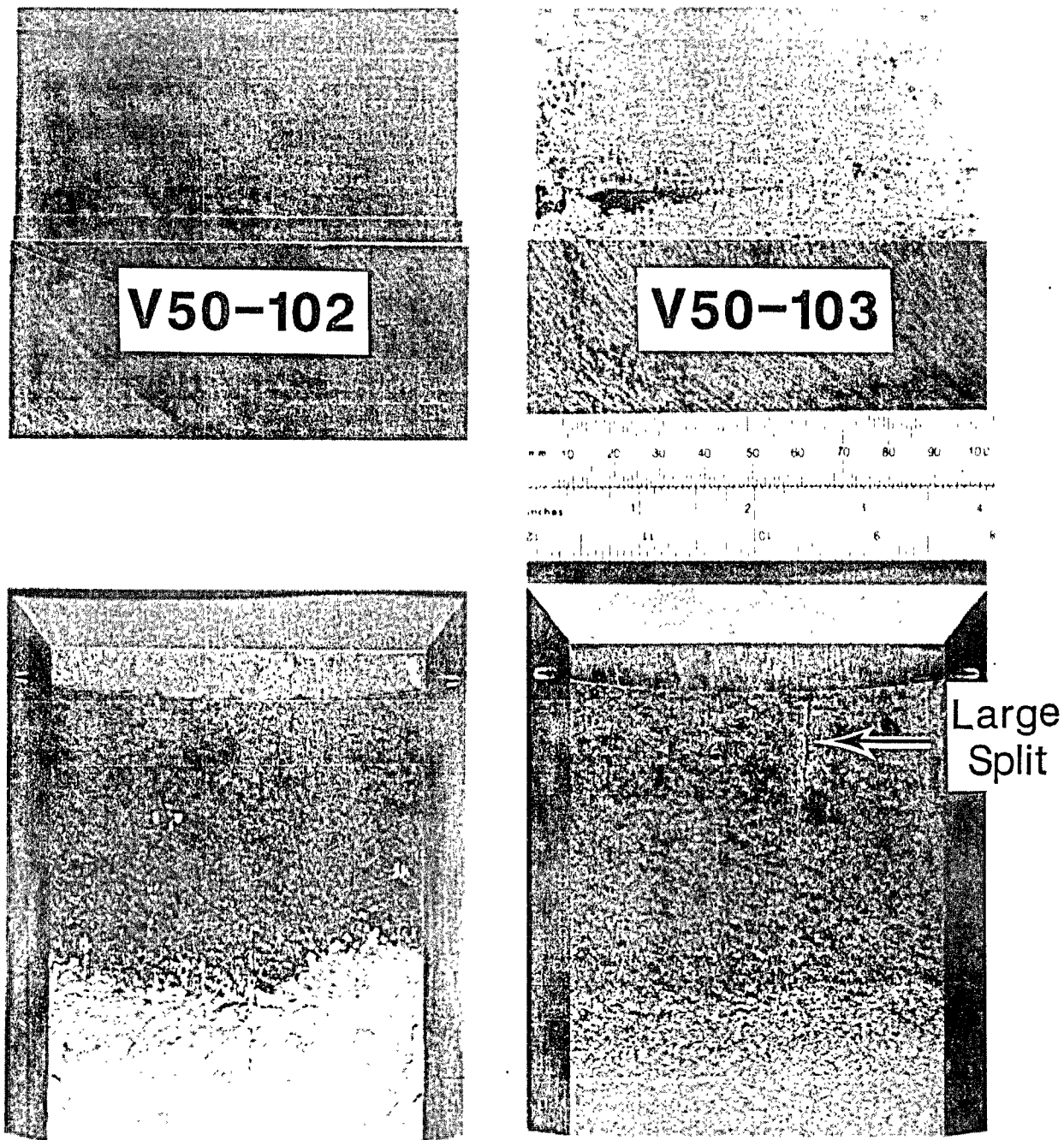


Fig. 45 Fracture surfaces of the 4T-CT specimens.

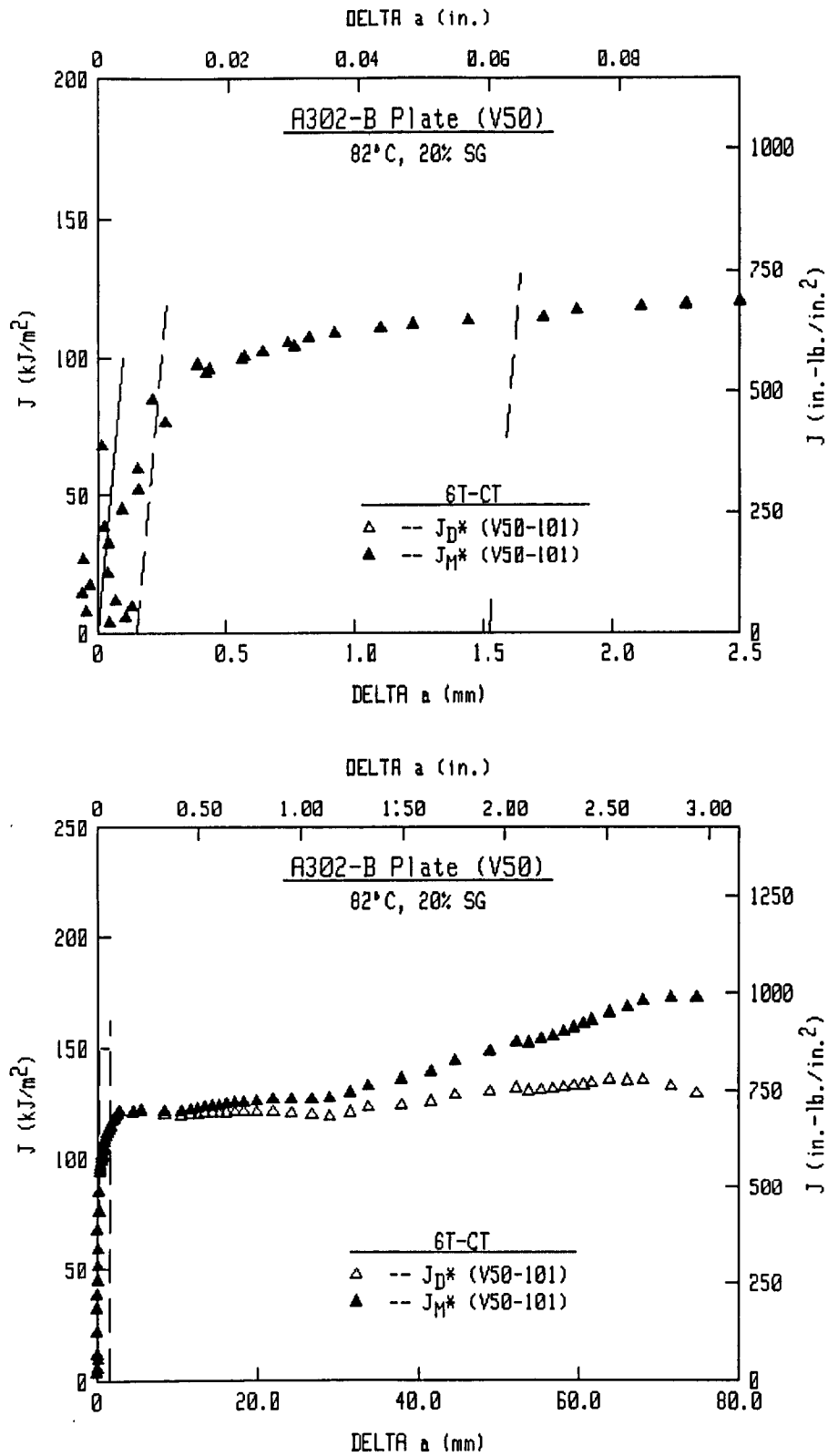


Fig. 46 J_M^* - and J_D^* -R curves from the test of a 6T-CT specimen.

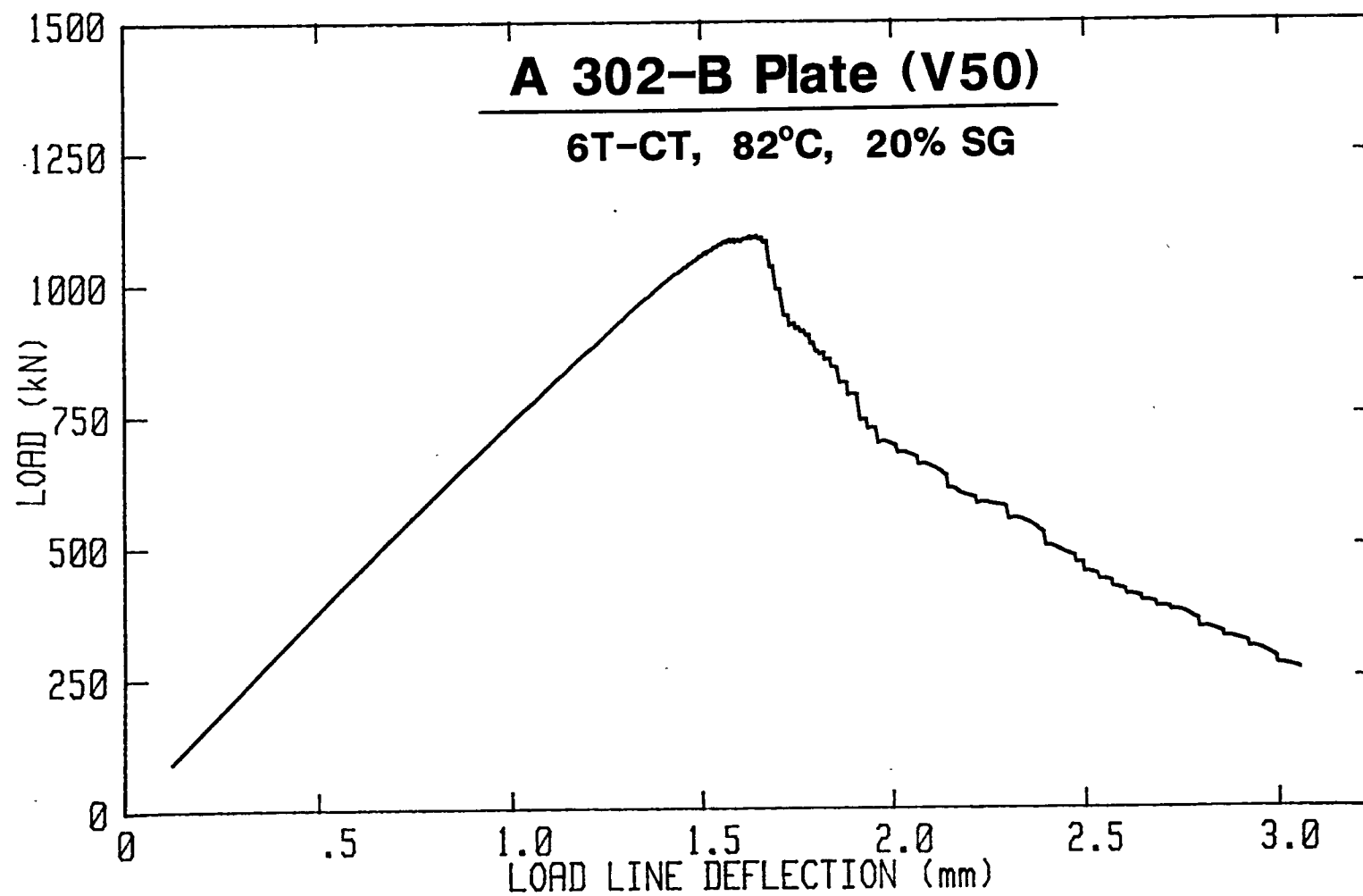


Fig. 47 The load-displacement curve from the test of a 6T-CT specimen.

plasticity. From an analysis using the procedures of ASTM E 399, a K_Q value of $134.1 \text{ MPa}\sqrt{\text{m}}$ ($122.0 \text{ ksi}\sqrt{\text{in.}}$) is determined. This value is just slightly above the validity limit for this material (given the specimen thickness and strength). The key-curve from this test (Fig. 48) is quite peculiar, although somewhat consistent with those from the other tests.

The fracture surface of this specimen is illustrated in Fig. 49.

6.5.6 Size Comparisons

Treated individually, the J-R curves are generally rather unremarkable. However, combining all of the curves gives a very surprising result. Such comparisons are given in Figs. 50 to 54 for each of the J equations. In all cases, the J-R curves are similar near J_{IC} , up to $\sim 0.25 \text{ mm}$ (0.01 in.) of Δa . Thereafter, larger specimen size results in reduced J-R curve levels. Although that result may not be very surprising, the extent of the reduction for each J equation is unprecedented. More specifically, the deformation J equations (J_D and J_{D*}) give the closest correspondence among data for the largest (6T-CT) and the smallest (0.5T-CT) specimens, yet at $\sim 6 \text{ mm}$ (0.24 in.) of Δa (the highest Δa levels for the 0.5T-CT specimens), the J levels for the 0.5T-CT specimens are a factor of two higher than those for the 6T-CT specimen. Extrapolating the 0.5T-CT J_D -R curves to 76 mm or 3 in. (the highest Δa level for the 6T-CT specimen) would give an overestimate in J of a factor of ten. Such a large size effect is without parallel in other work with reactor pressure vessel steels.

Comparison of the load-displacement curves for these tests yields several interesting points (Fig 55). The total displacement required to grow the crack by about one-half of the initial unbroken ligament does not increase significantly as the specimen size increases. This trend is most surprising given the magnitude of the differences in the crack growth levels. In particular, the 0.5T-CT specimens required $\sim 2.1 \text{ mm}$ (0.08 in.) of displacement for $\sim 6 \text{ mm}$ (0.24 in.) of predicted Δa or $\sim 7 \text{ mm}$ (0.28 in.) of measured Δa . In contrast, the 6T-CT specimen required $\sim 3 \text{ mm}$ (0.12 in.) of displacement for $\sim 74.5 \text{ mm}$ (2.93 in.) of predicted Δa or 86.5 mm (3.41 in.) of measured Δa . Therefore a 50% increase in displacement gives $\sim 1100\%$ increase in Δa , reflective of the much reduced toughness for the larger specimens.

The second point concerning the load-displacement curves is the gradual shape change which occurs with increasing specimen size. Specifically, as the specimen size increases, the load-displacement curve takes on a sharper appearance with a steeper slope after maximum load, implying a sharp increase in the crack growth rate (as a function of displacement). In contrast to the 6T-CT curve, the curves for the 0.5T-CT specimens are more rounded near maximum load, implying a gradual increase in the crack growth rate (as a function of displacement).

Comparison of $\Delta a/W$ as a function of load-line displacement is also quite interesting (Fig. 56). First, the displacement at which the rate of crack growth (as a function of displacement) begins to

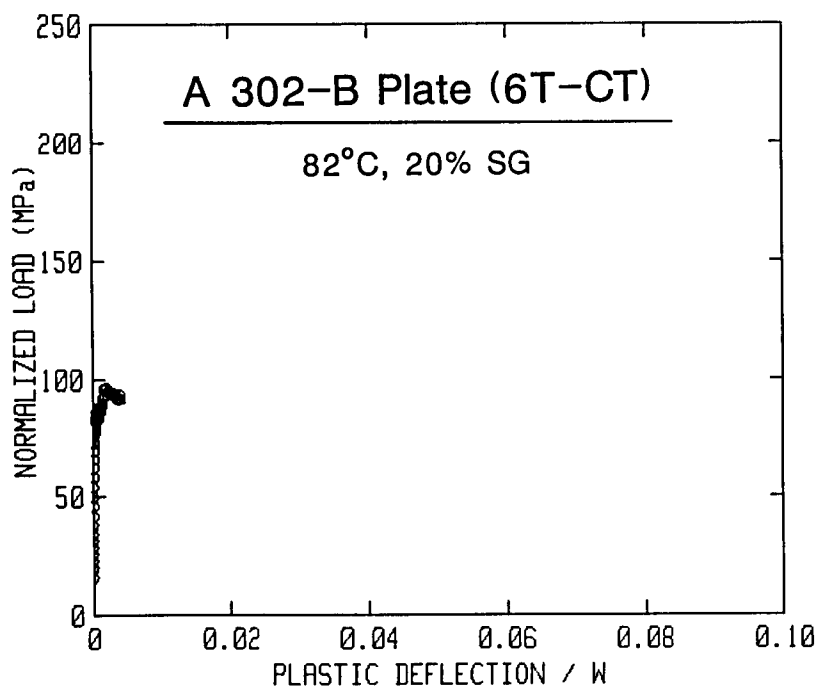
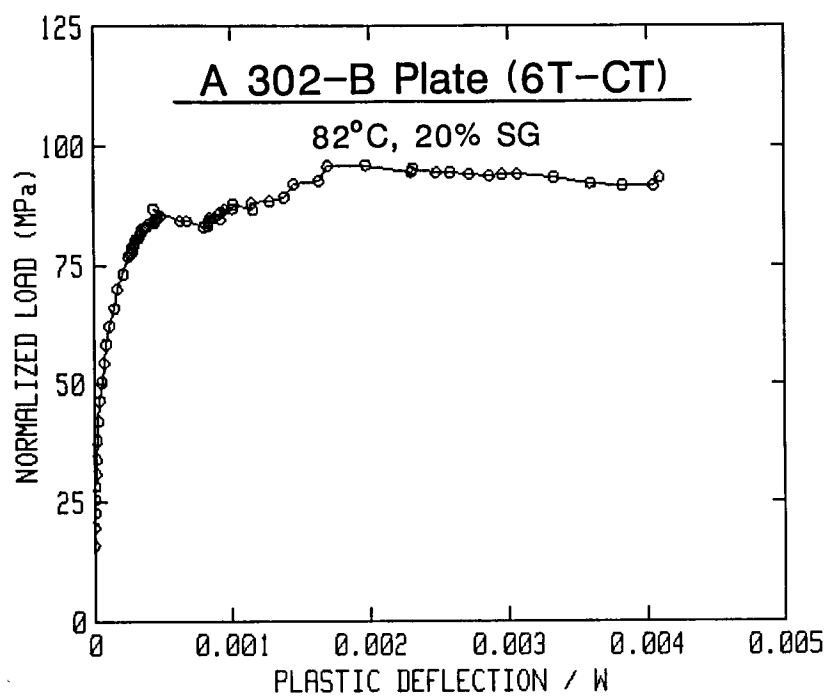


Fig. 48 The key-curve from the test of a 6T-CT specimen.

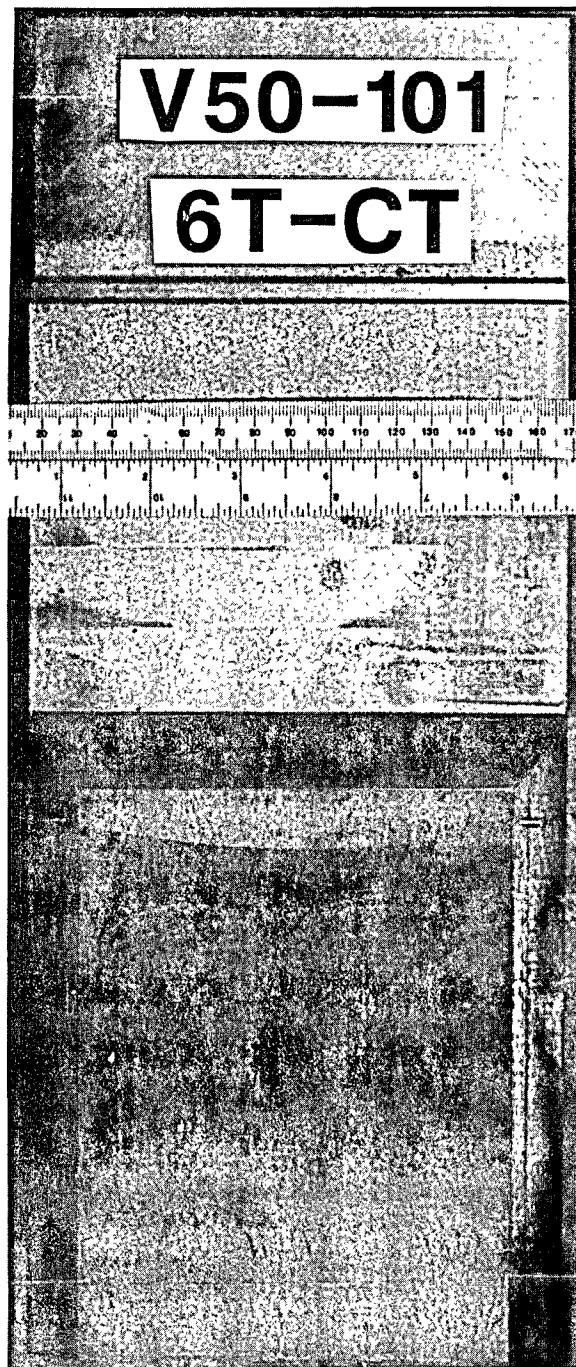


Fig. 49 Fracture surface of the
6T-CT specimen.

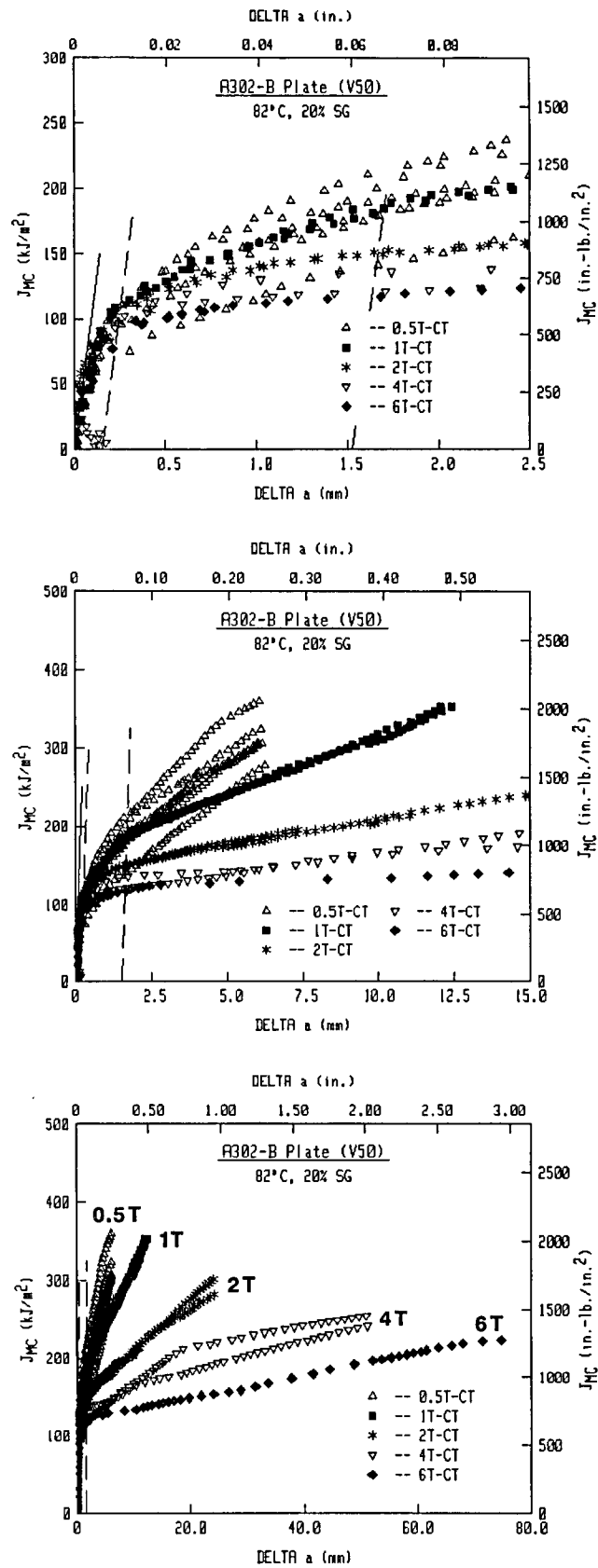


Fig. 50 Comparison of the J_{M-C} -R curves for all tests of this plate.

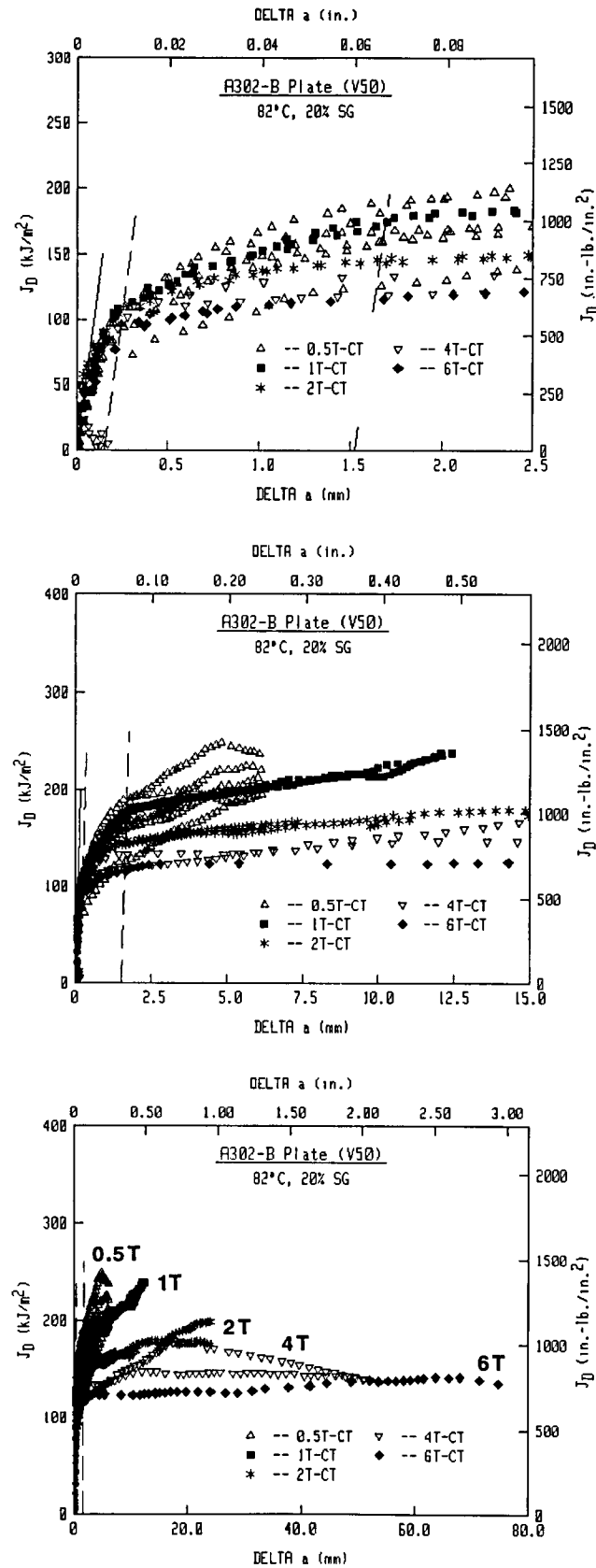


Fig. 51 Comparison of the J_D -R curves for all tests of this plate.

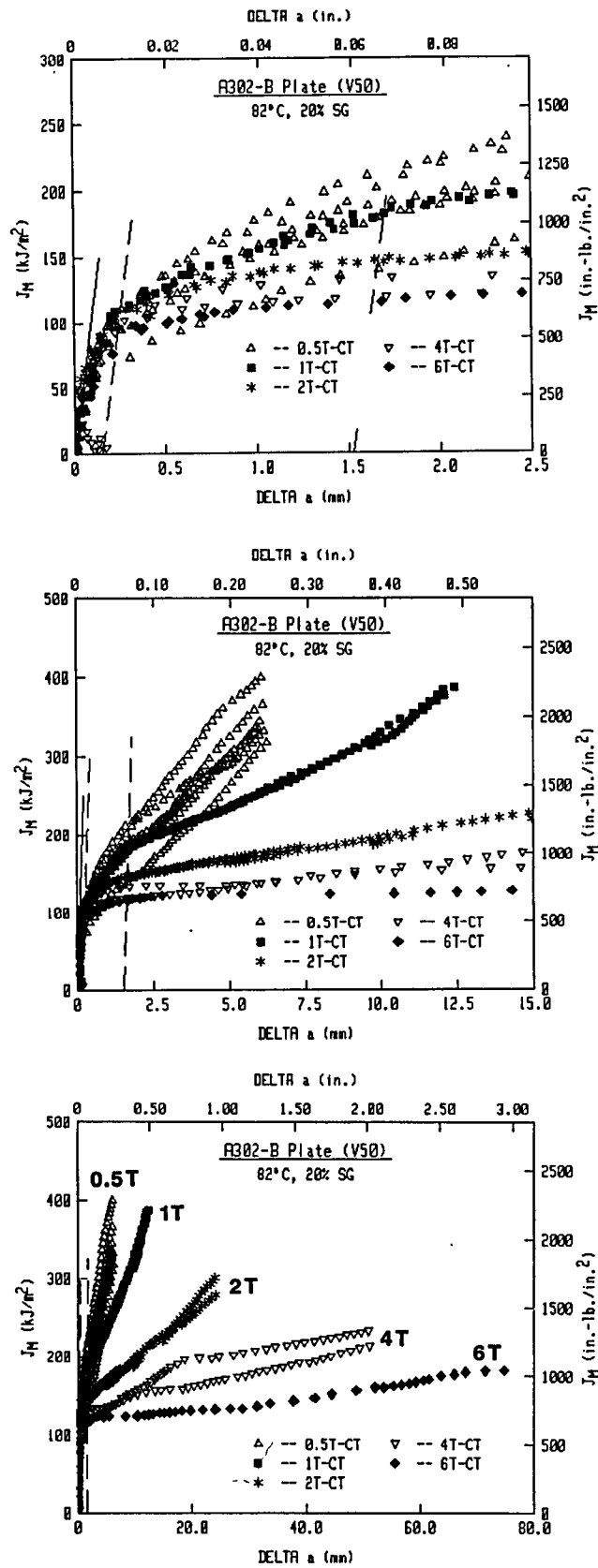


Fig. 52 Comparison of the J_M -R curves for all tests of this plate.

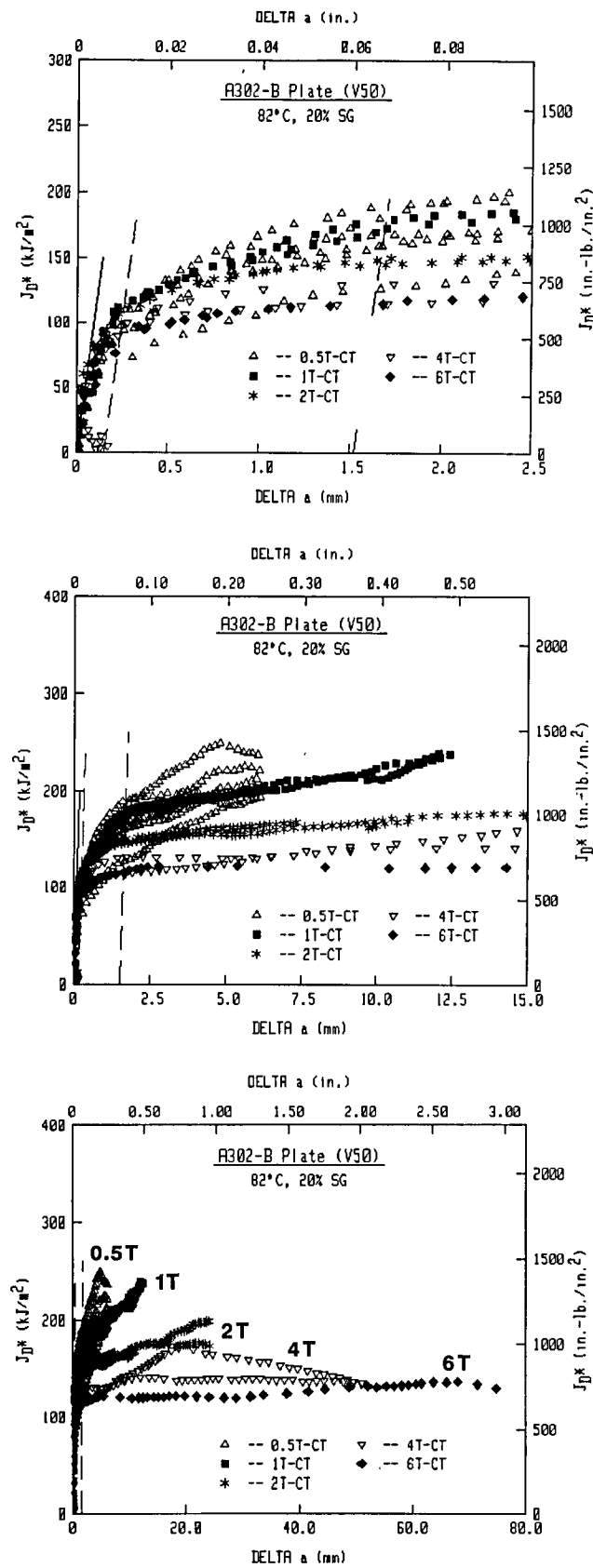


Fig. 53 Comparison of the J_{p*} -R curves for all tests of this plate.

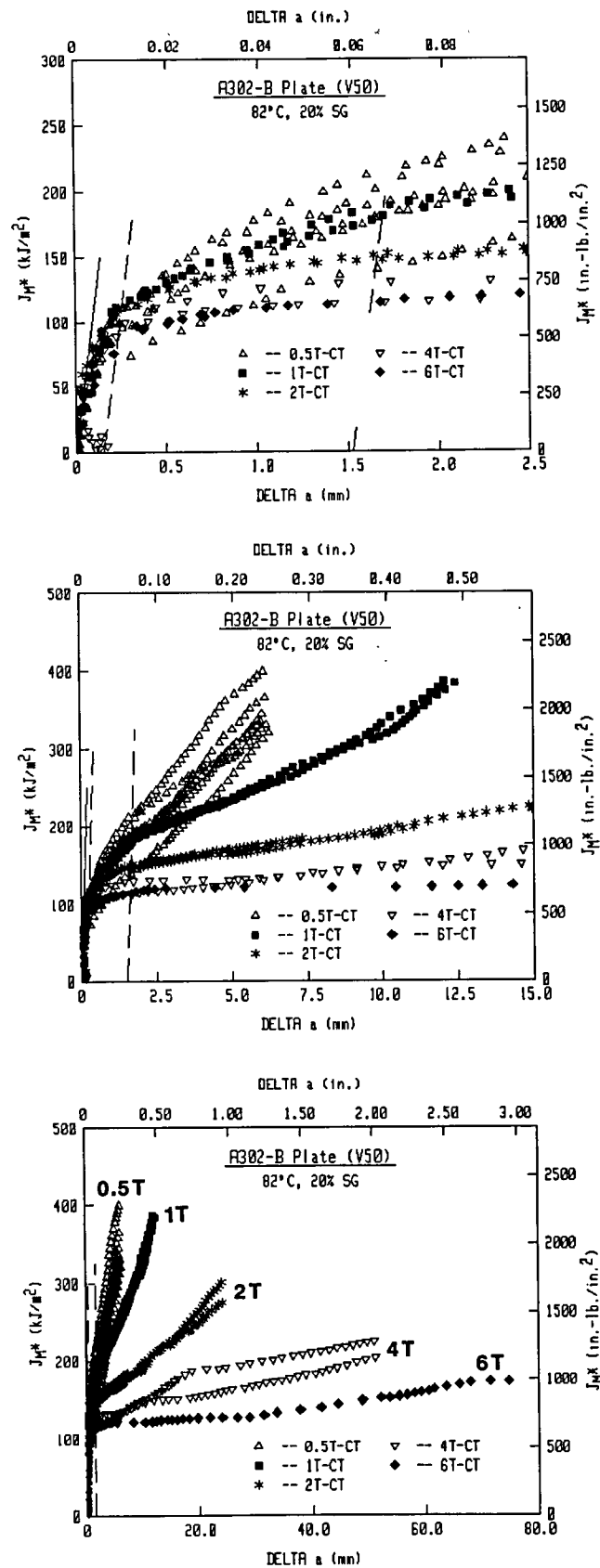


Fig. 54 Comparison of the J_{R^*} -R curves for all tests of this plate.

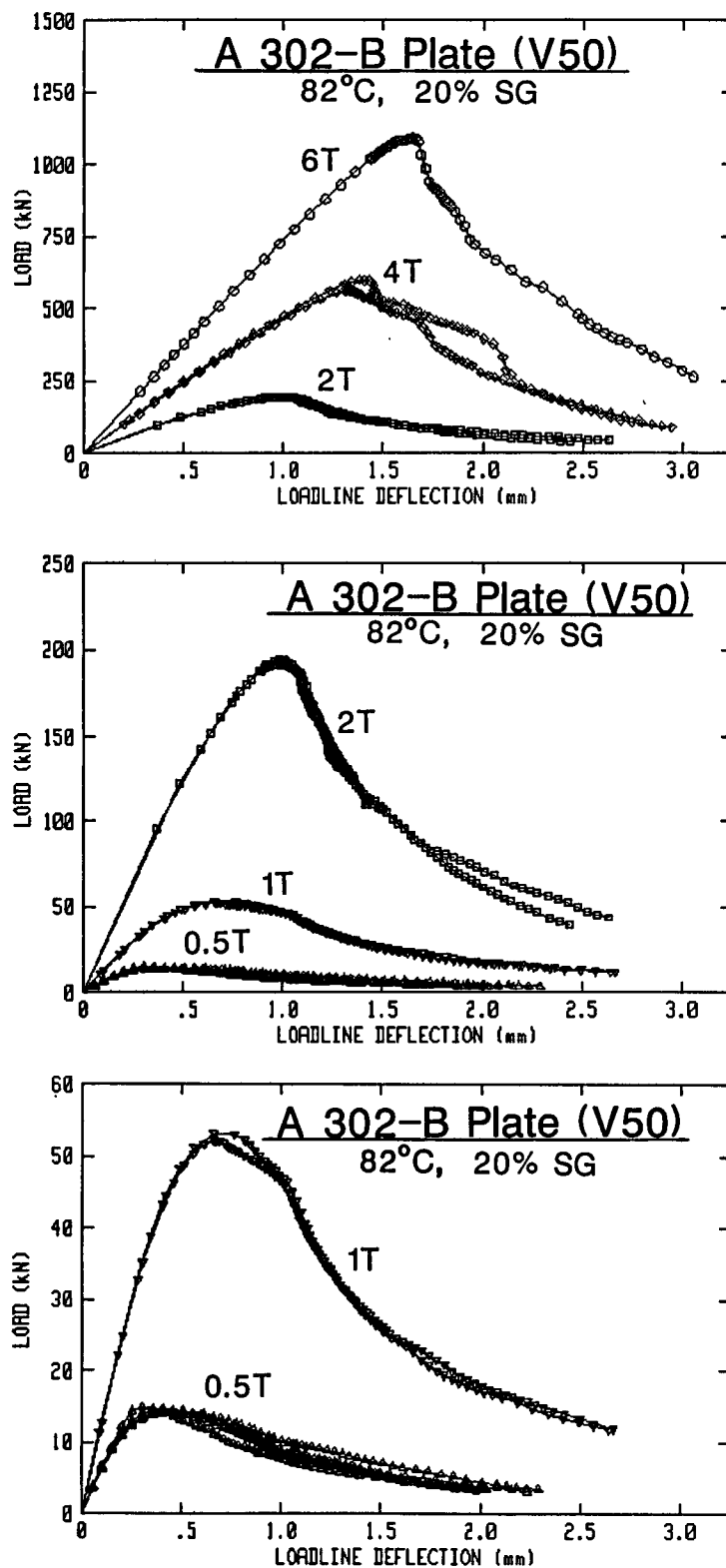


Fig. 55 Comparison of the load-displacement curves for all tests of this plate.

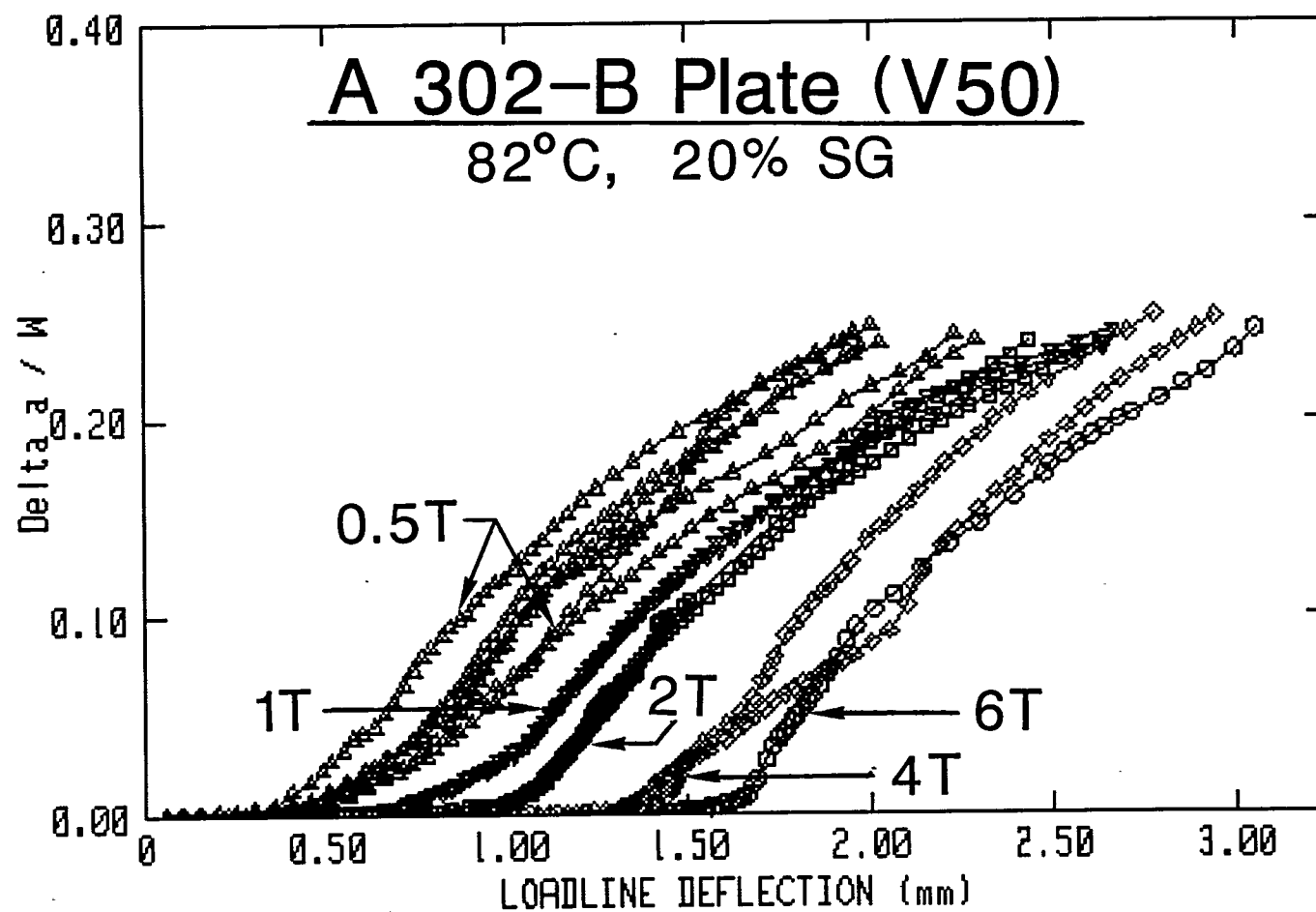


Fig. 56 Comparison of $\Delta a / W$ as a function of load-line displacement for the tests of this plate.

increase rapidly is greater for larger specimen sizes. Secondly, the overall shape (i.e., slope) of these curves is almost identical for all specimen sizes. By accounting for the difference in W for the various specimen sizes, the crack growth rate ($\Delta a/\text{displacement}$) for the 6T-CT specimen is therefore ~ 12 times that of the 0.5T-CT specimen.

Similar comparisons of $\Delta a/W$ as a function of δ_{pl}/W (plastic displacement divided by W) demonstrate the primarily elastic behavior of the 6T-CT specimen (Fig. 57). The last data point in each case represents the measured Δa and correction of the final plastic deflection by matching the compliance slope to the final Δa .

6.5.7 δ_5 Results

The δ_5 results are presented in three formats: δ_5 vs. load-line displacement, the δ_5 -R curve (δ_5 vs. Δa), and δ_5 vs. J . The first comparisons are for the Linde 80 weld specimens tested in the δ_5 check tests (Fig. 58 to 60), followed by comparisons for the A 302-B plate.

For the Linde 80 weld, δ_5 is virtually linear with load-line displacement for almost the entire range of data (Fig. 58). This linearity occurs after some nonlinearity at low displacement levels. The two specimens demonstrate some variability in behavior, as was found for the J-R curves and load-displacement curves as well.

The δ_5 -R curves (Fig. 59) have similar shape and overall appearance to the J-R curves. The magnitude and occurrence of differences between these two specimens is quite similar to those for the J-R curves.

In comparing δ_5 with J (Fig. 60), linearity between J and δ_5 is sought. After a parabolic-shaped region at low J and δ_5 levels, both J_{M*} and J_{D*} assume similar linear trends with δ_5 . However, J_{D*} deviates from linearity with δ_5 rather abruptly at lower levels of δ_5 than does J_{M*} . Since δ_5 has been found to correlate results to greater crack growth levels than does J (Ref. 17), the results in Fig. 60 imply that J_{M*} is applicable to greater crack growth levels than is J_{D*} .

For the A 302-B plate, comparison of δ_5 with load-line deflection are interesting (Fig. 61). (The data labeled "0.5T-CT" are from δ_5 check-test specimen V50-119.) The small specimens, specifically the 0.5T- and 1T-CT specimens, yield linear correspondence between these two quantities at almost all δ_5 levels. In contrast, the 2T-, 4T- and 6T-CT specimens follow the same general trend starting at low δ_5 levels, with the data for each specimen size "peeling-off" in order of increasing specimen size. After the "peel-off", each curve then pursues a linear behavior, such that each curve overall exhibits a bi-linear appearance. This "peel-off" occurs at maximum load for each specimen, with even the 0.5T- and 1T-CT specimens showing some slope change at maximum load.

The δ_5 -R curves (Fig. 62) look very much like the J-R curves. One difference with the J-R curve comparisons is that data for the 2T-CT

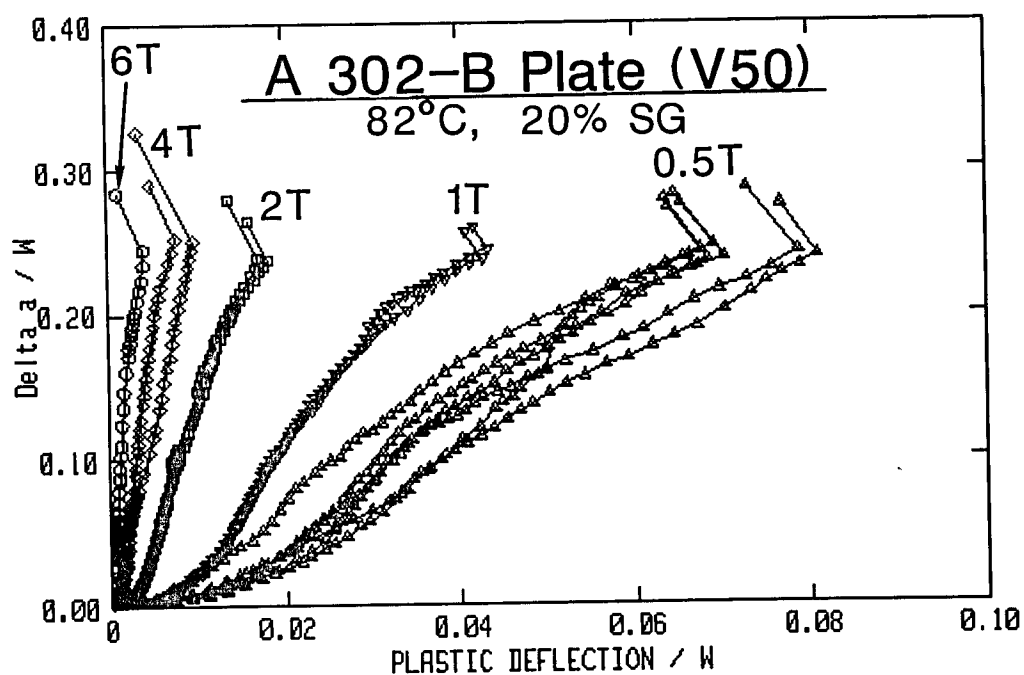
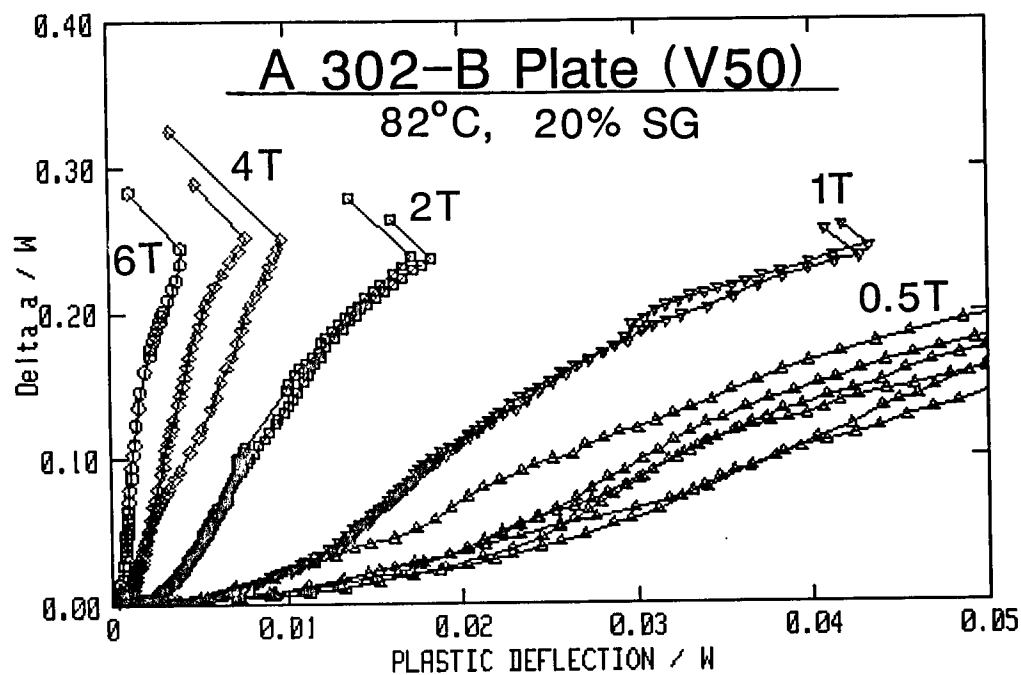


Fig. 57 Comparison of $\Delta a / W$ as a function of δ_{p1} / W for the tests of this plate.

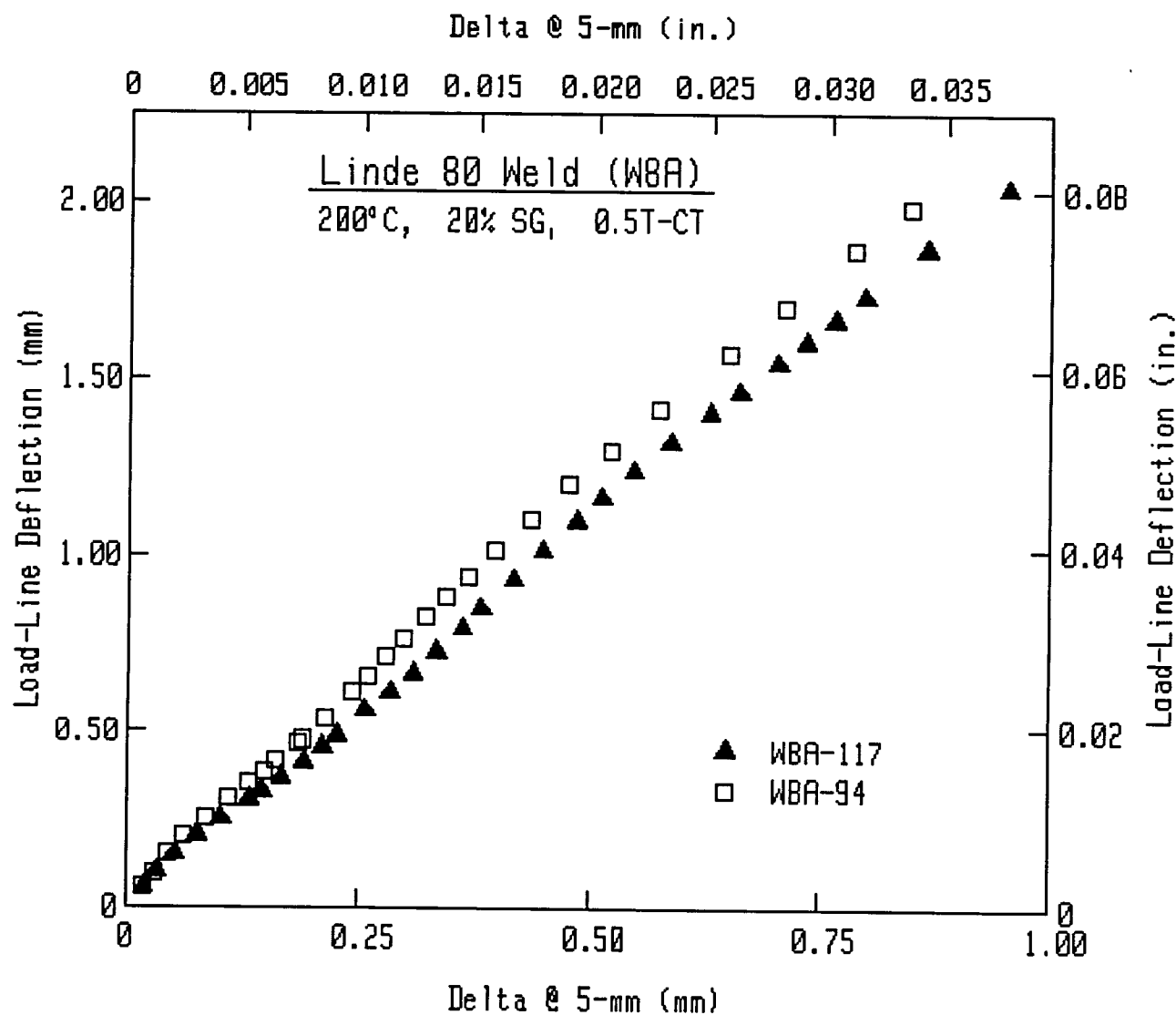


Fig. 58 Comparison of δ_5 as a function of load-line displacement for the tests of the Linde 80 weld.

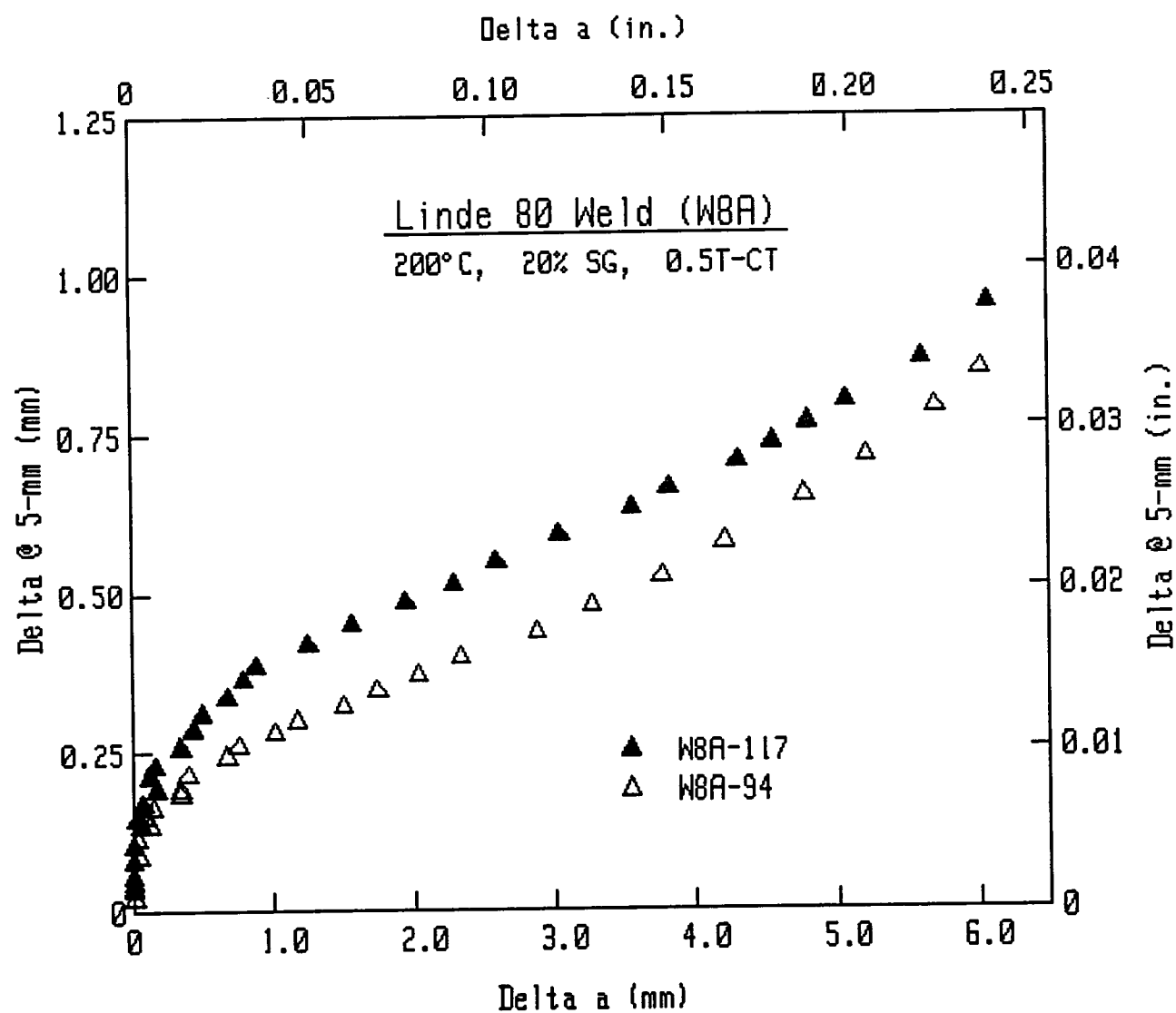


Fig. 59 The δ_5 -R curves for the Linde 80 weld look similar to the J-R curves.

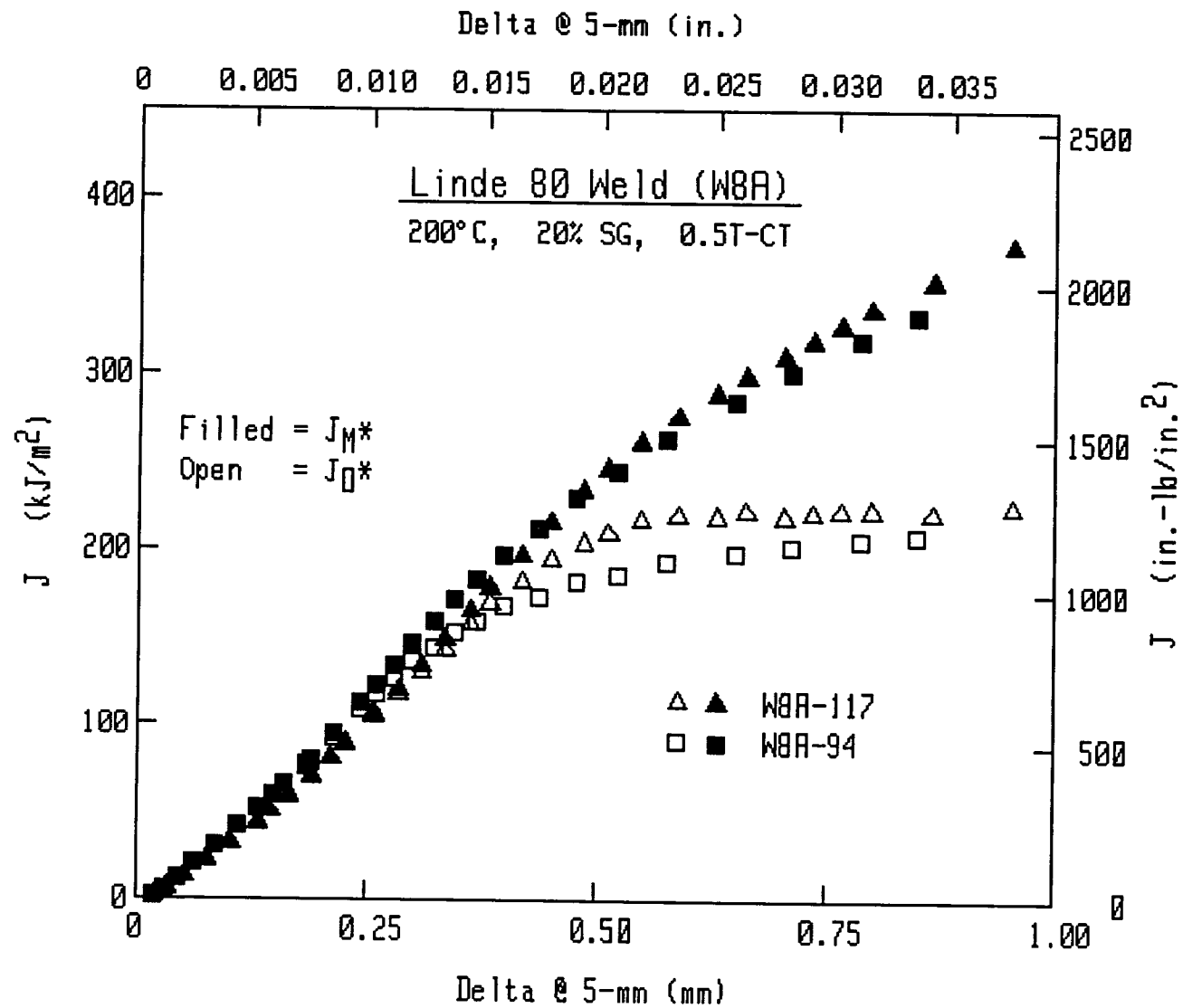


Fig. 60 Comparison of δ_5 to J for the tests of the Linde 80 weld.

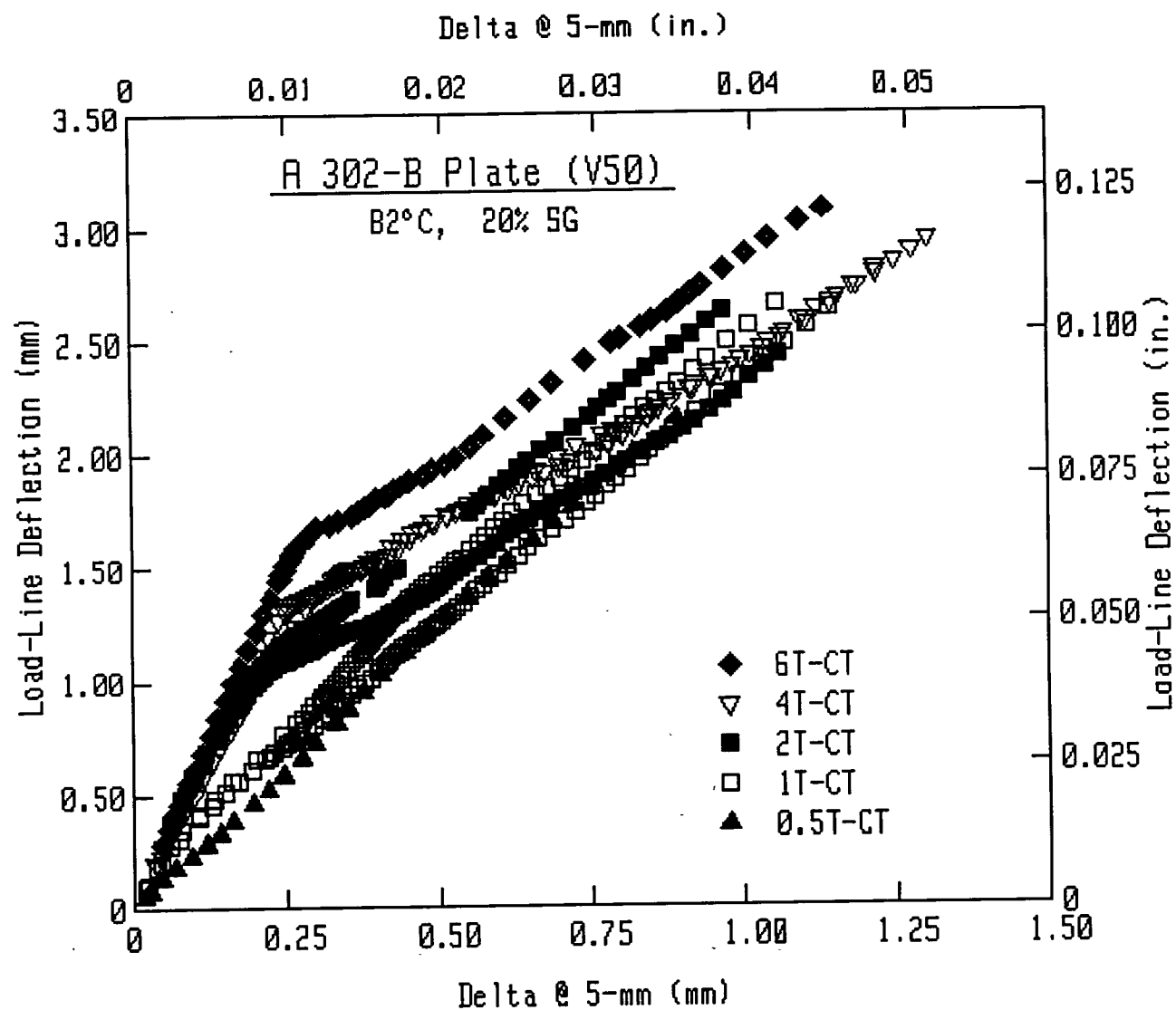


Fig. 61 Comparison of δ_5 as a function of load-line displacement for the tests of the A 302-B plate.

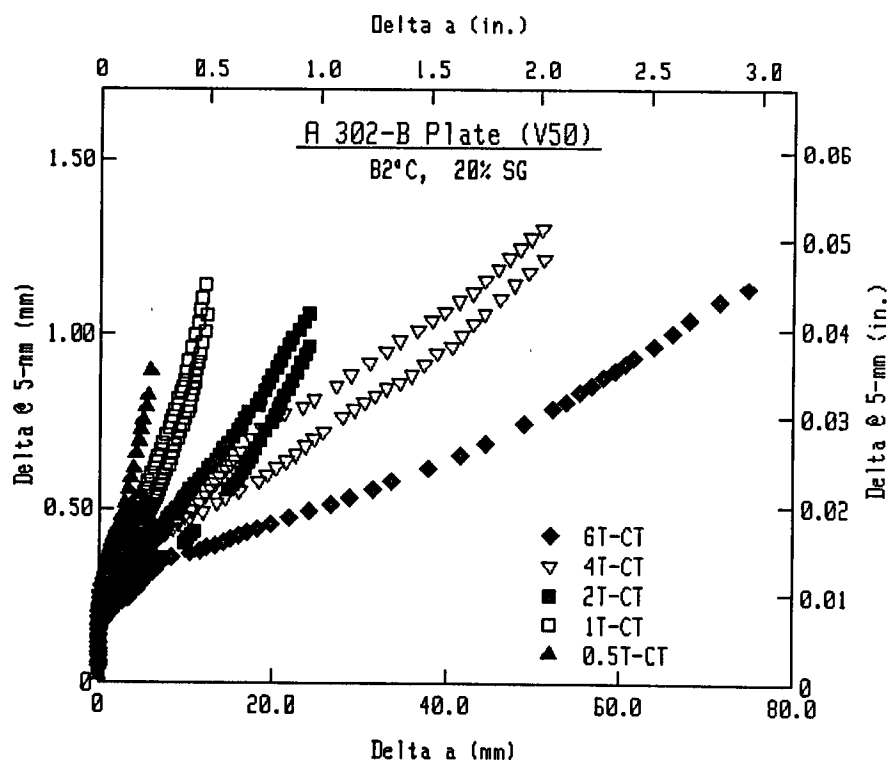
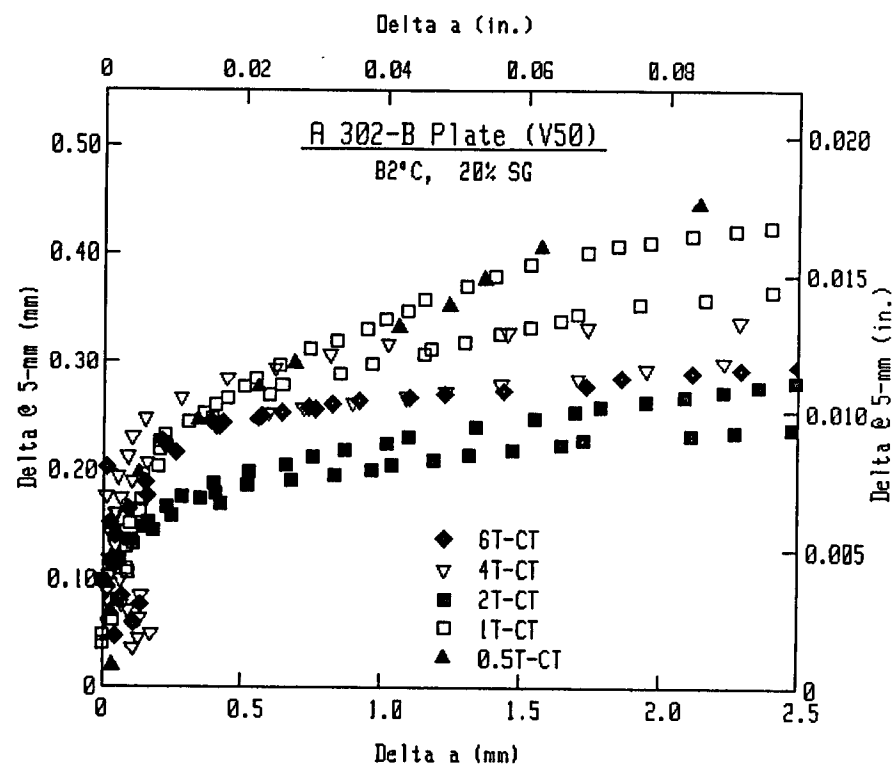


Fig. 62 The δ_5 -R curves for the tests of the A 302-B plate.

specimens are lower than those for the other specimens at small Δa levels. The other specimens demonstrate similar δ_s levels up to the point at which Δa increases rapidly in comparison to δ_s . The latter point is similar to the J_{IC} measurement point on the J-R curves.

Comparison of δ_s with J_{M-C} , J_{M*} and J_{D*} (Fig. 63) are as expected. Specifically δ_s is linear with J_{M*} to greater δ_s levels than for J_{M-C} or J_{D*} . Linearity between δ_s and J_{D*} applies only to smaller δ_s levels than for J_{M*} and J_{M-C} . The linear portions of these curves are similar in terms of J and δ_s levels, although the data for 2T-CT specimens exhibit somewhat lower δ_s levels in comparison to data for the other specimens.

In general, the δ_s results are consistent with the J results.

6.5.8 Additional Tests

Once the initial tests had been completed (0.5T-, 1T-, and 2T-CT specimens) and the size effect became apparent, two additional 0.5T-CT specimens were prepared and tested. These specimens were intended to help clarify some of the unusual and unexpected results found with the tests from the test program. These two specimens were machined from broken pieces of the 2T-CT specimens and were located on the specimen surface nearest to the plate mid-thickness. One of these additional specimens (GP1B) was subsequently tested at ambient temperature (24°C or 75°F) in a manner analogous to that used for the previous tests. The other specimen (GP1D) was tested at 82°C (180°F) to a limited crack growth range, to check on the crack-front morphology in the initial stages of crack growth.

The test at 24°C resulted in a higher J-R curve than those at 82°C (Fig. 64). This result is expected for RPV steels. One surprising aspect is that the crack for this specimen is somewhat straighter than for the previous tests (Fig. 65).

The other additional test, at 82°C (180°F), was also quite interesting. As indicated in Fig. 66, the J-R curve for this test is consistent with those from previous tests. The most surprising part of this test is the crack-front morphology. As illustrated in Fig. 65, this fracture surface exhibits severe lengthy splits in front of the bulk of the crack. These splits are identical to those found with most of the other A 302-B plate specimens, although these splits extend to a greater length. Presumably these splits are caused by separation of the manganese-sulfide (MnS) inclusions which permeate this plate. As well, the length of the split is presumably due to the stress field in front of the crack and possibly due to the strain history of the material prior to cracking. In particular, specimens tested to crack growth of around 50% of the unbroken ligament may have shorter splits due to the fact that the hinge point (i.e., separating regions of tension and compression) is much closer to the crack front than for shorter crack growth increments, limiting the length of the splits which can develop. In addition, this portion of the specimen, at $a/W \sim 0.75$, would have been under compression during the initial stages of the test. This prior loading may help to limit the splitting under subsequent tensile loading.

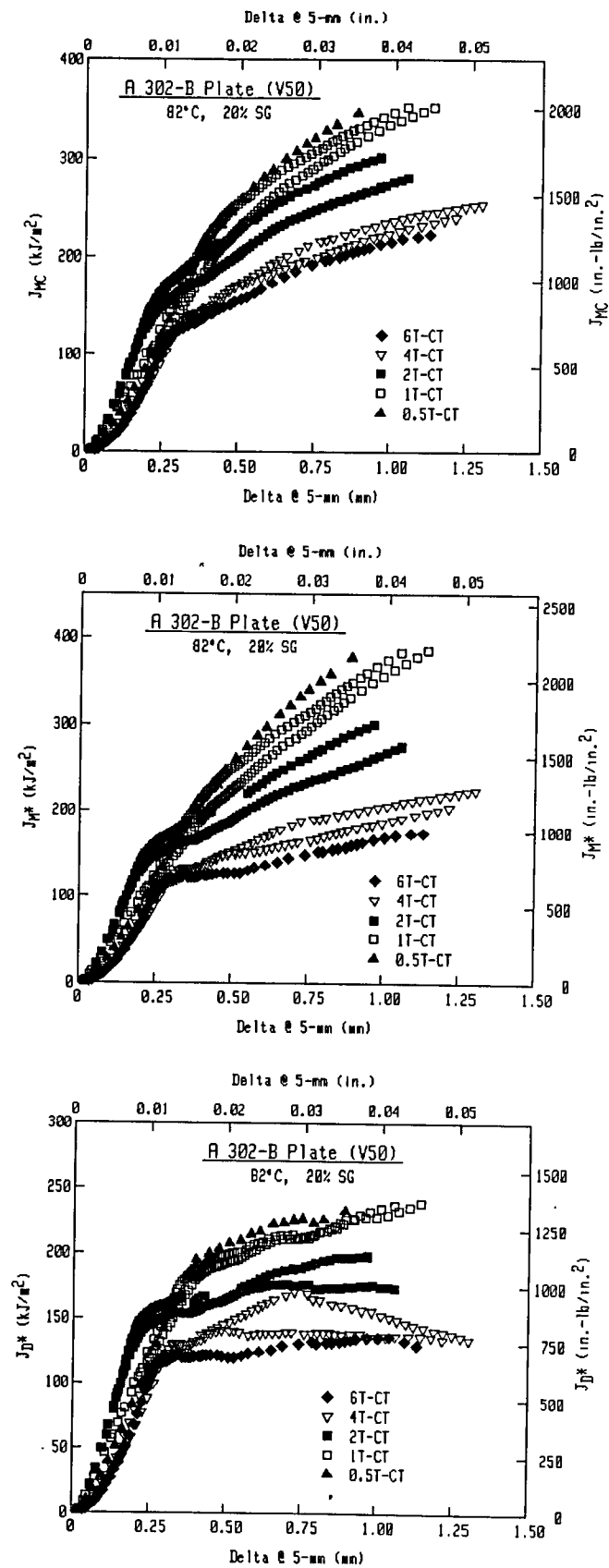


Fig. 63

Comparison of δ_5 to J_{M-C} ,
 J_{M*} and J_{D*} for the tests
of A 302-B plate.

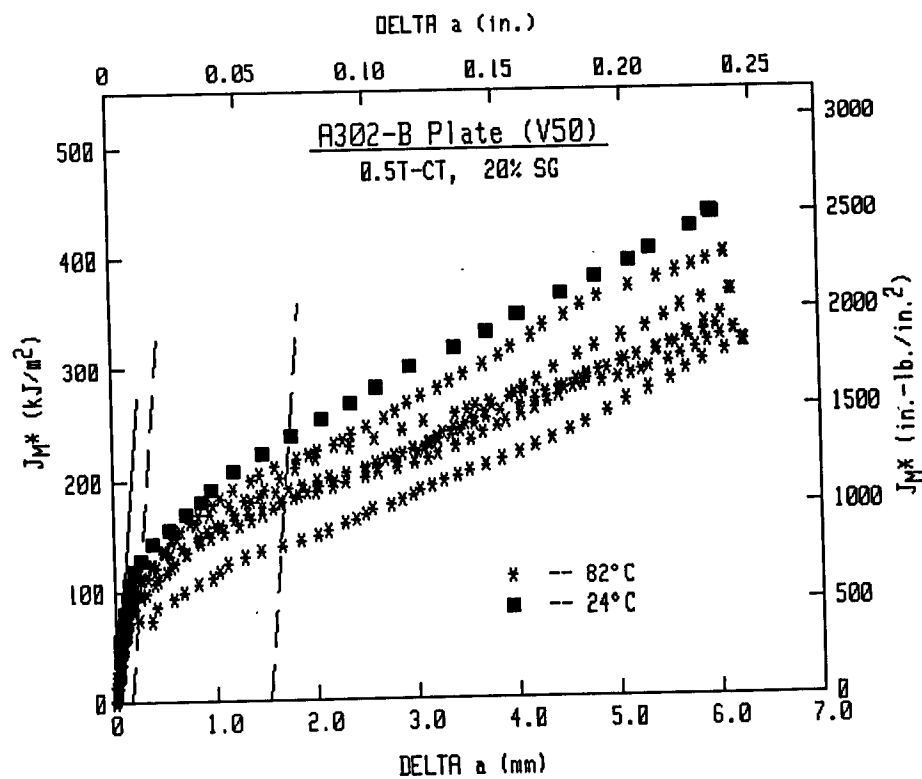
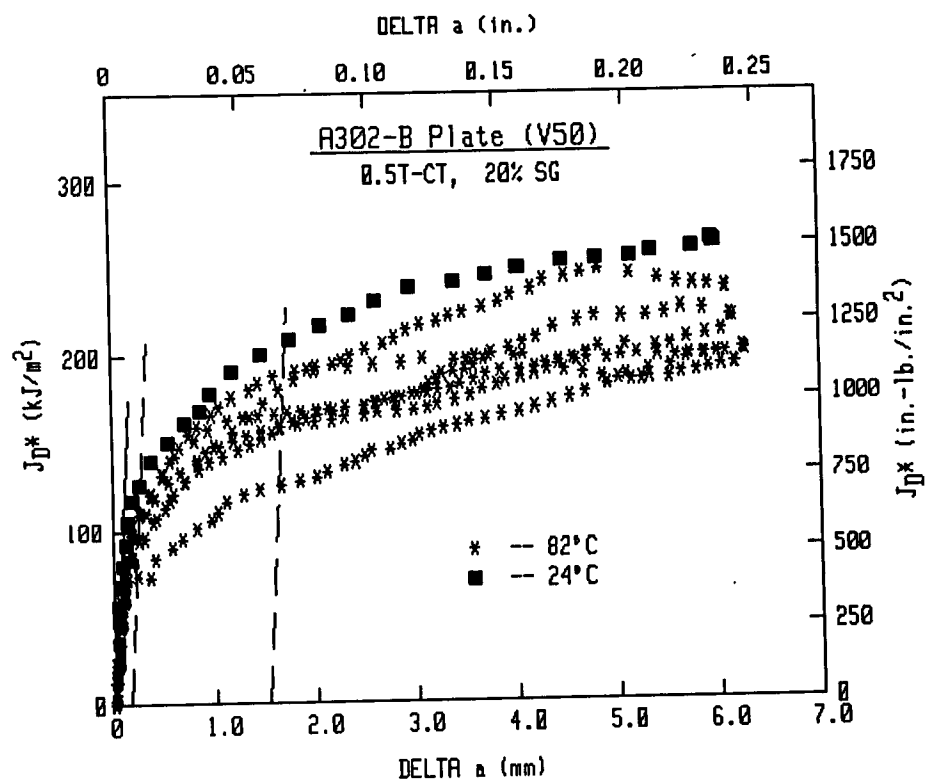


Fig. 64 Comparison of J-R curves for the test at 24°C with those at 82°C.

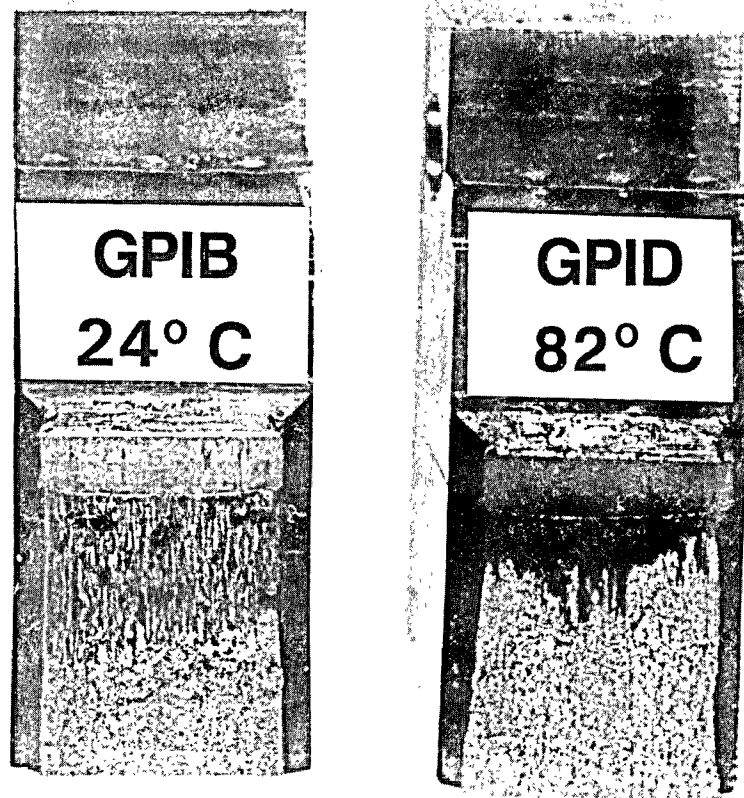


Fig. 65 The fracture surfaces for the additional tests at 24°C and 82°C.

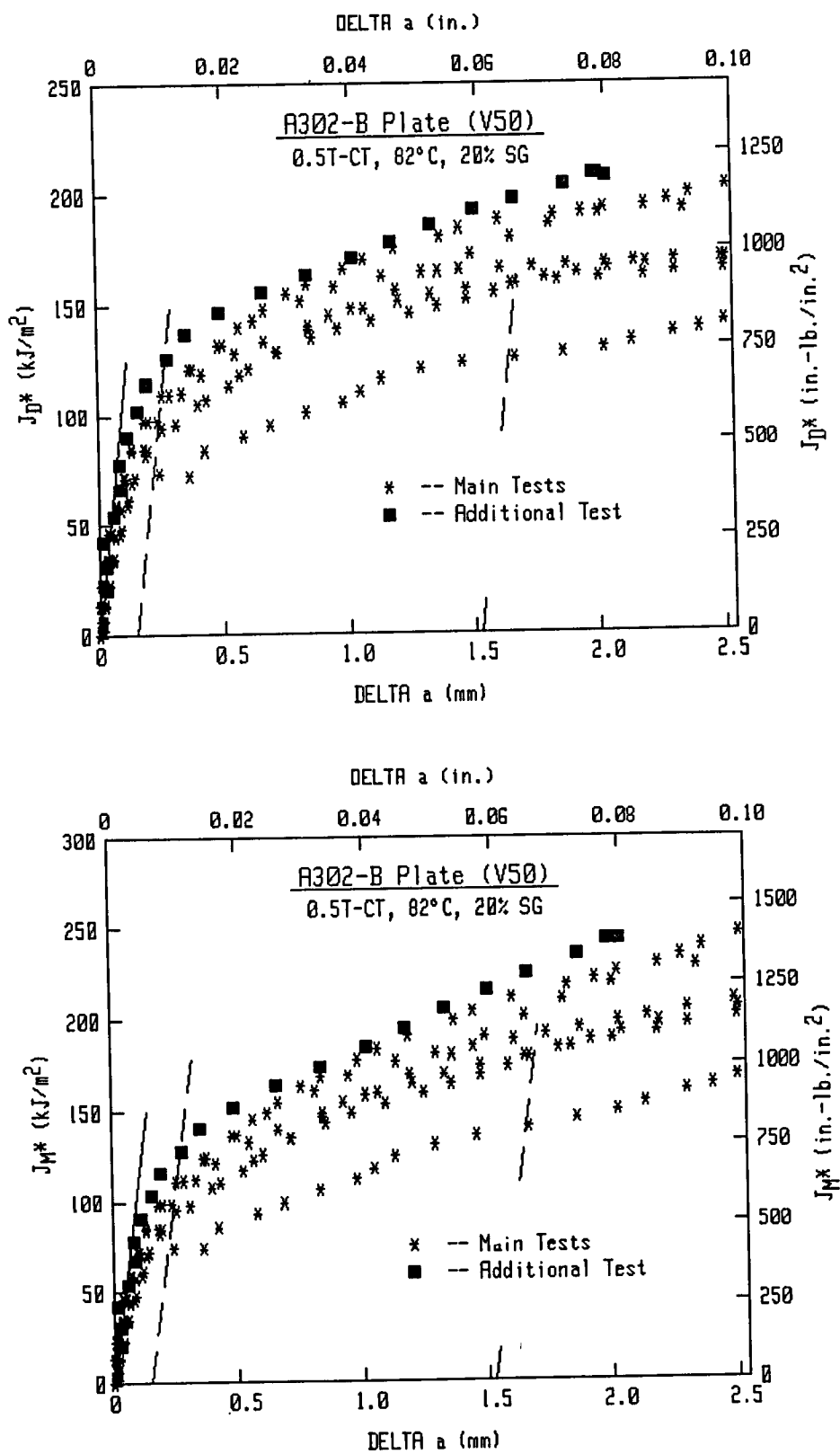


Fig. 66 Comparison of J-R curves for the additional test at 82°C (to a shorter Δa) with those for the previous tests at 82°C.

Comparison of the J-R curves for these additional tests indicates only small differences due to the different test temperatures (Fig. 67).

6.5.9 Comparisons With Data From the U.S. Naval Academy

Specimens blanks were provided to J. Joyce of the U.S Naval Academy (USNA) for machining of 1T- and 2T-CT specimens. One specimen of each size has been tested by USNA at 82°C (180°F) to confirm the results reported above. There are two differences in the test conditions at MEA and the USNA. Firstly, the initial crack lengths used at MEA represent a/W of ~ 0.5 , whereas the USNA uses a/W of ~ 0.6 . Secondly, the test system used at MEA is a servohydraulic system such that specimen displacement can be used for test control. In contrast, the USNA uses a screw-driven machine, such that cross-head displacement is used for test control. With the low toughness of this plate, test control by cross-head displacement is not a trivial challenge, given the high rate of crack growth as a function of specimen displacement, and the attendant load-shedding which occurs during crack growth. A very stiff system is required to ensure that any data can be acquired, since crack growth in this material can occur with a negative cross-head displacement rate for a less stiff system under specimen displacement control.

Comparisons between MEA results and those from the USNA are illustrated in Figs. 68 to 71 using J_{D*} and J_{M*} . Load-displacement curves for the USNA tests are illustrated in Fig. 72 (these are not comparable to the MEA curve due to a difference in the initial crack lengths). The J-R curves are in reasonable agreement to Δa levels up to ~ 5 mm for the data from 1T-CT specimens and ~ 7 to ~ 15 mm for the data from 2T-CT specimens. One consistent trend for both specimen sizes is that the USNA data are consistently above the MEA data (i.e., higher J levels) at large Δa levels. The cause for this could be the different initial crack lengths, whereby the data from the specimen with a longer initial crack could be violating J controlled crack growth at a lower Δa level than would data from the specimens with a shorter initial crack growth. The result of the somewhat higher J-R curves is that the J_{D*} (or J_D) curves tend to look "better" (i.e., less decrease in slope) than the lower J_{D*} (or J_D) curves, and the higher J_{M*} (or J_M) curves tend to look worse, since the inflection or "hook-up" is exacerbated. The end result is that the small specimen J-R curve data are elevated relative to that from larger specimens, when comparing results from an initial a/W of 0.5 to 0.6.

The key-curves for the USNA tests are in good agreement with those for the MEA tests (Fig. 73).

6.5.10 Crack Growth Prediction Errors

As indicated in Table 11, the crack growth prediction errors, as given by $\Delta a_p - \Delta a_m$, and the error percentages are quite large for these tests. This finding is not consistent with results from other RPV steels, where the errors tend to be 5% or lower. The high errors found for these tests are principally caused by the crack front and fracture surface morphologies. In the various fracture surface photo-

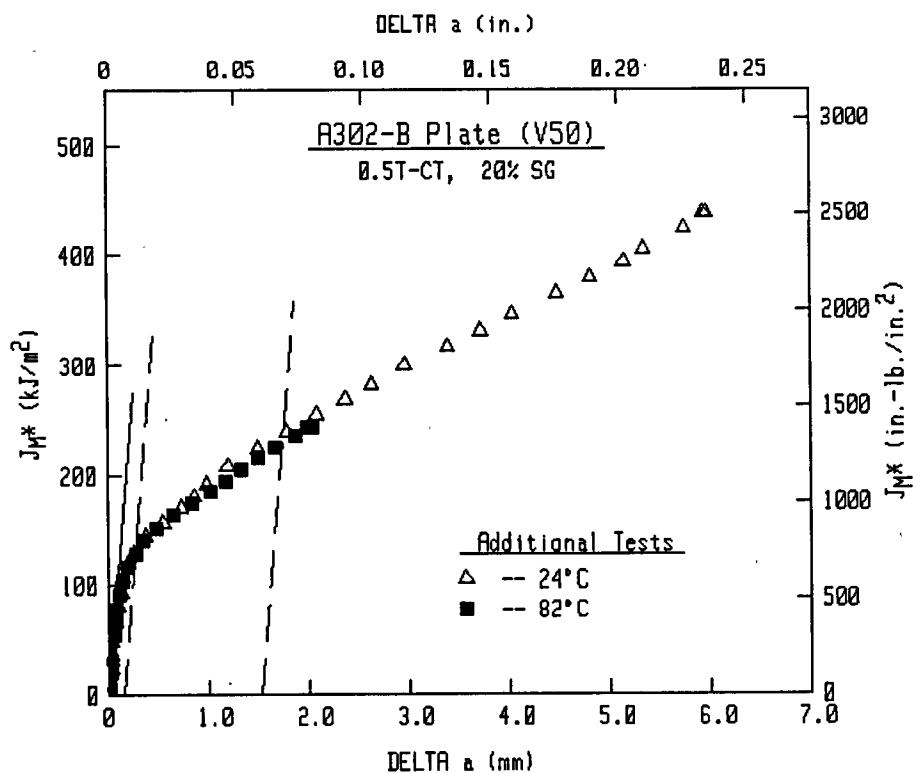
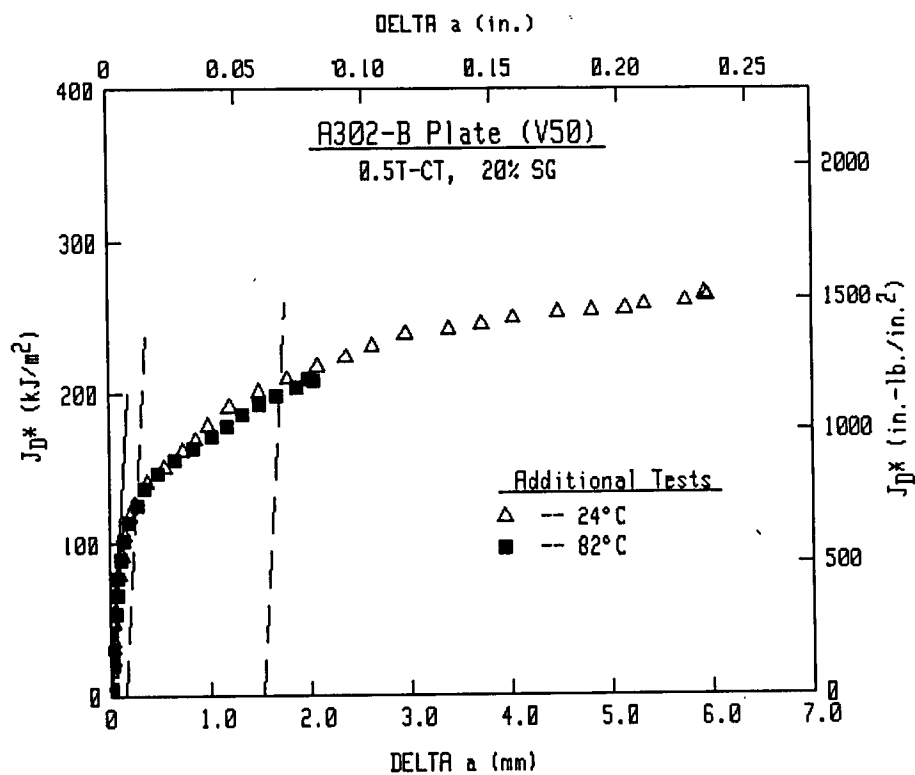


Fig. 67 Comparison of J-R curves from the additional tests at 24°C and 82°C.

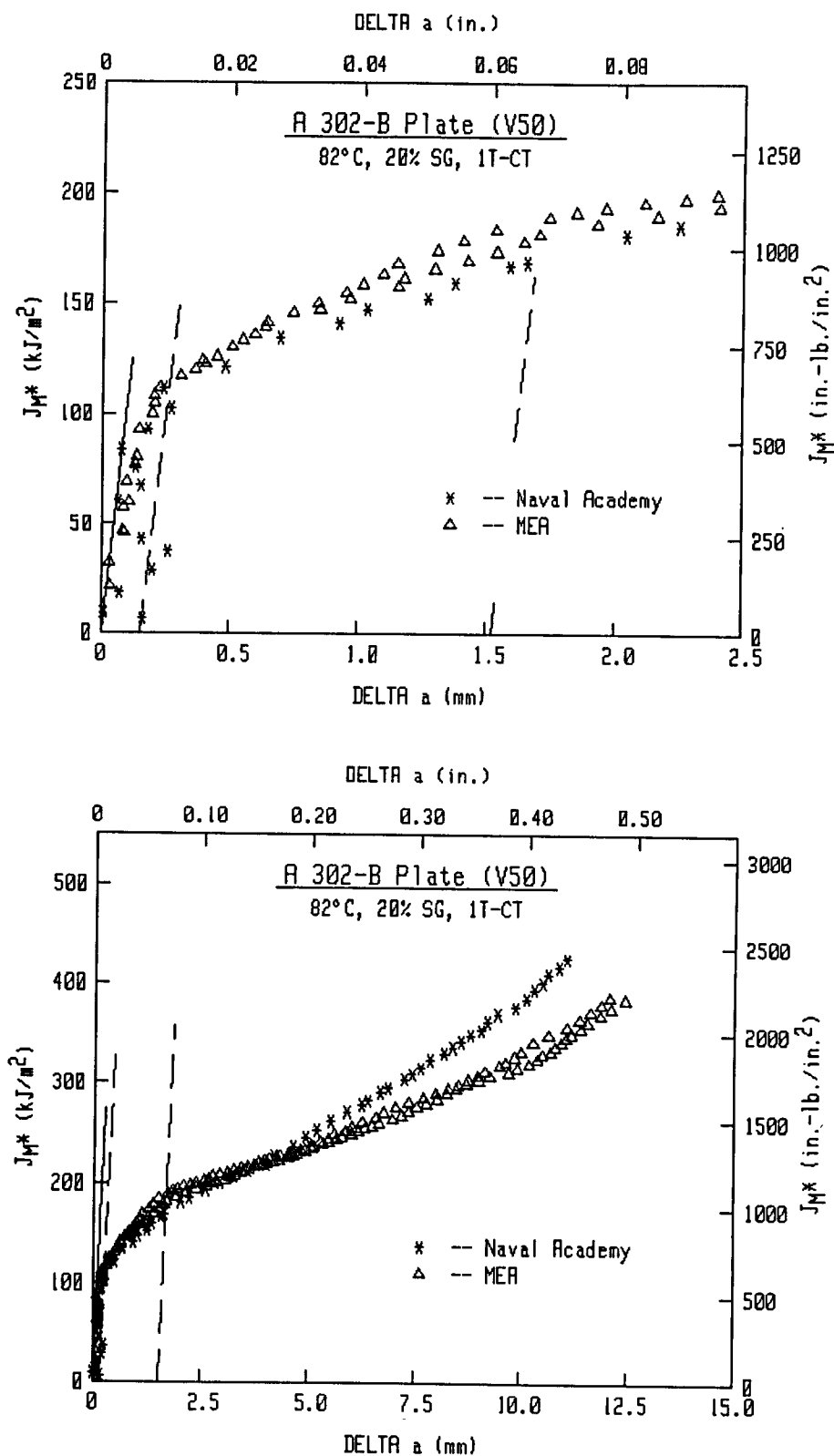


Fig. 68 Comparison of USNA and MEA J_{R^*} -R curves from 1T-CT specimens.

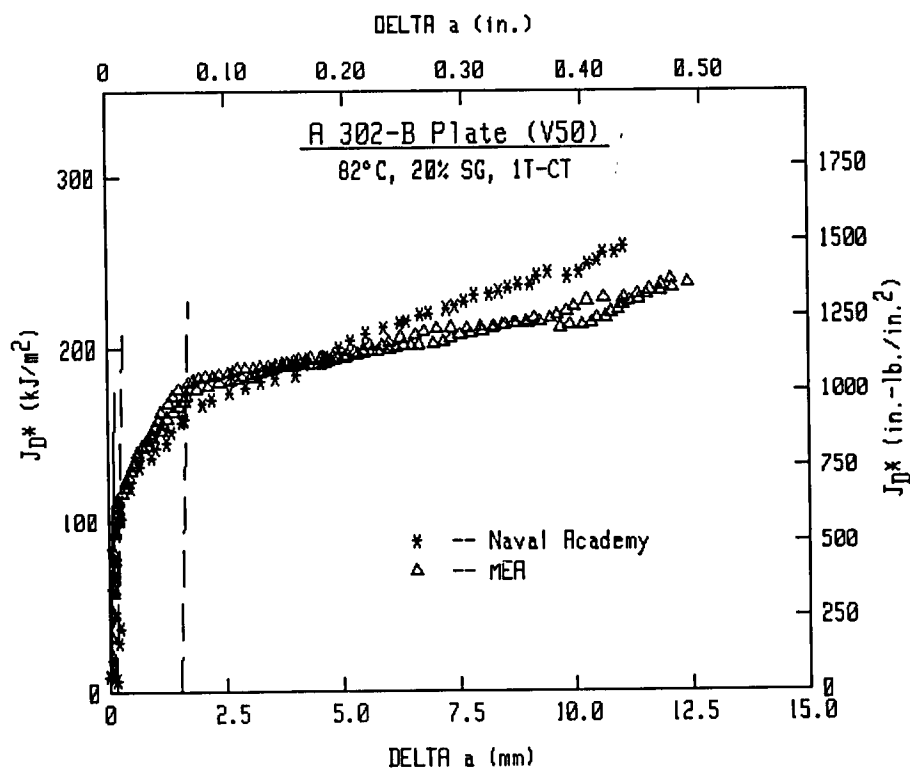
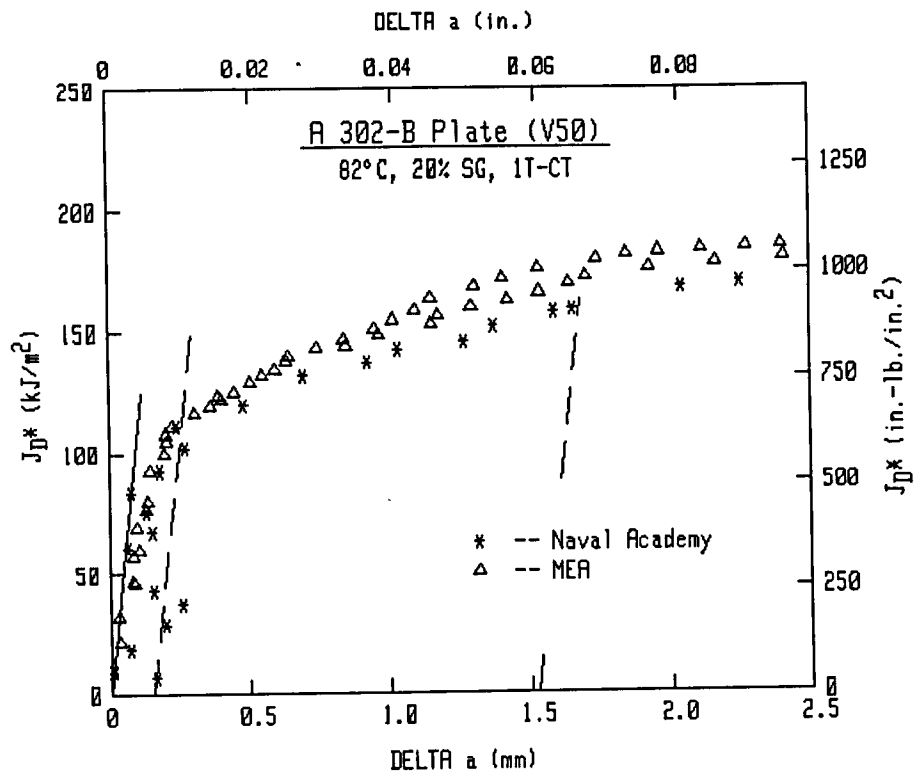


Fig. 69 Comparison of USNA and MEA J_{D^*} -R curves from 1T-CT specimens.

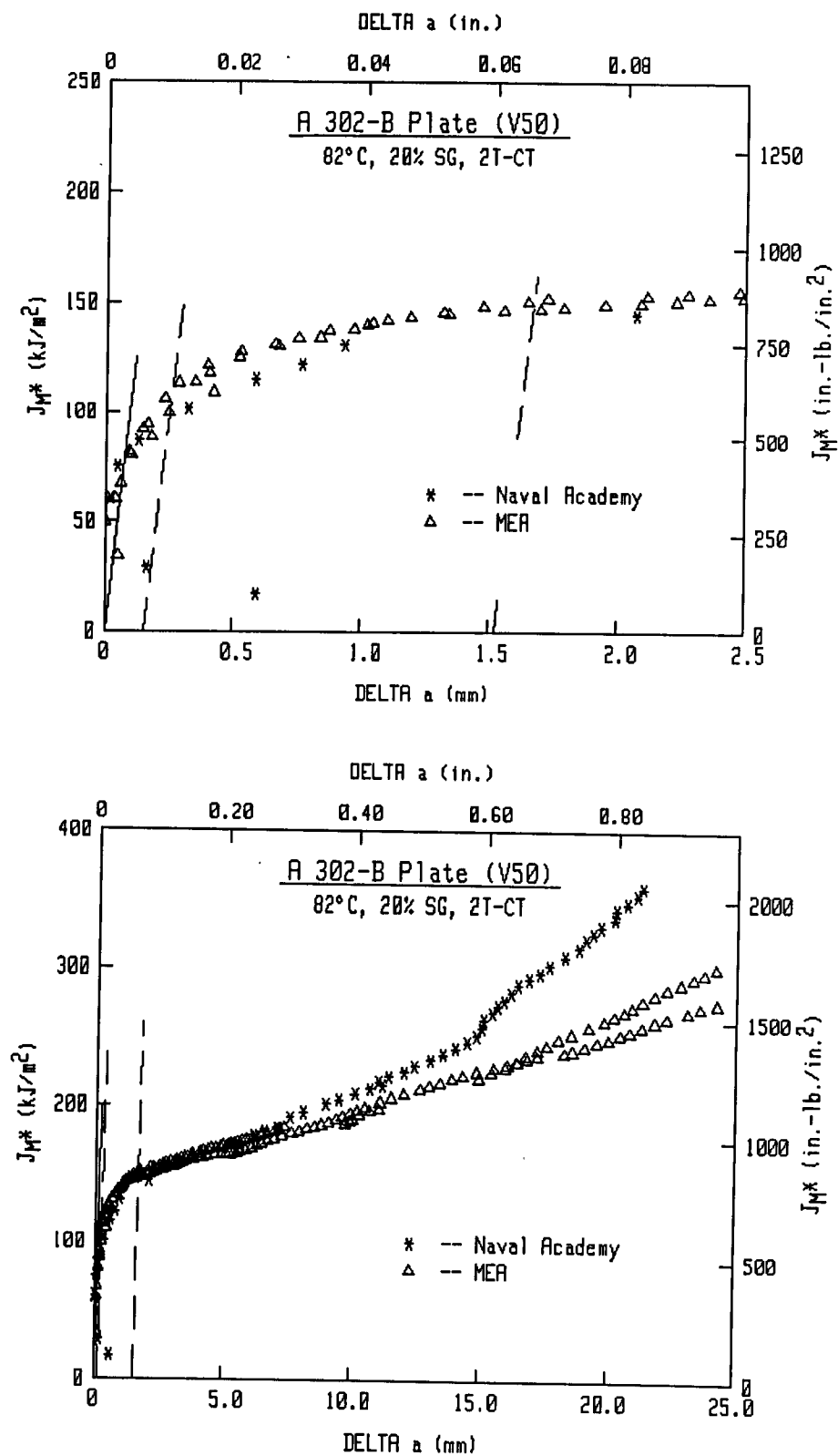


Fig. 70 Comparison of USNA and MEA J_R^* -R curves from 2T-CT specimens.

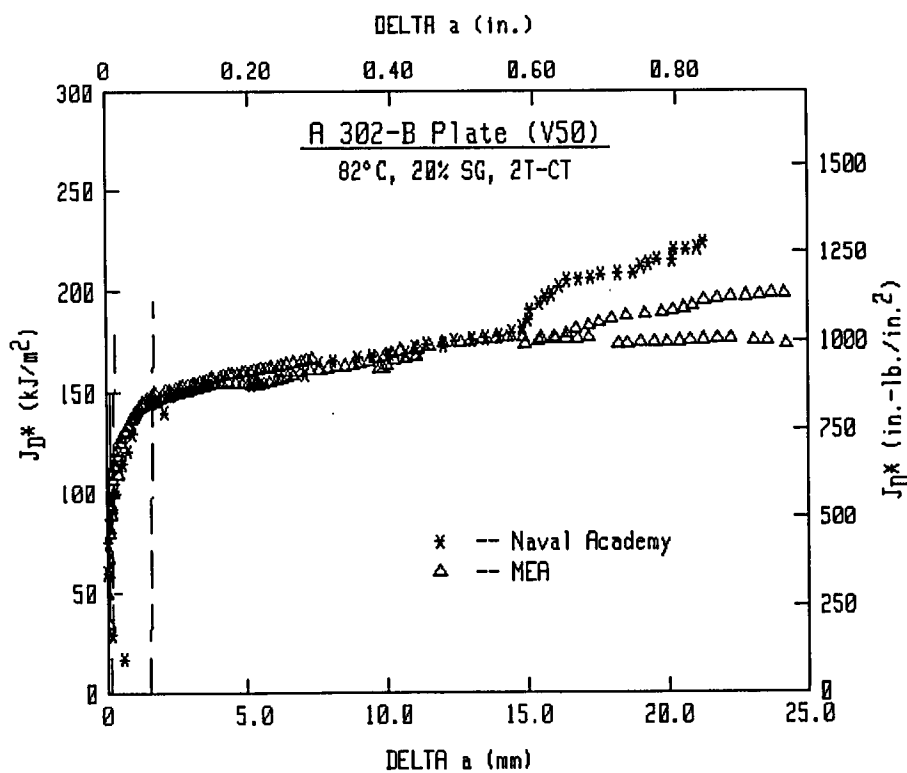
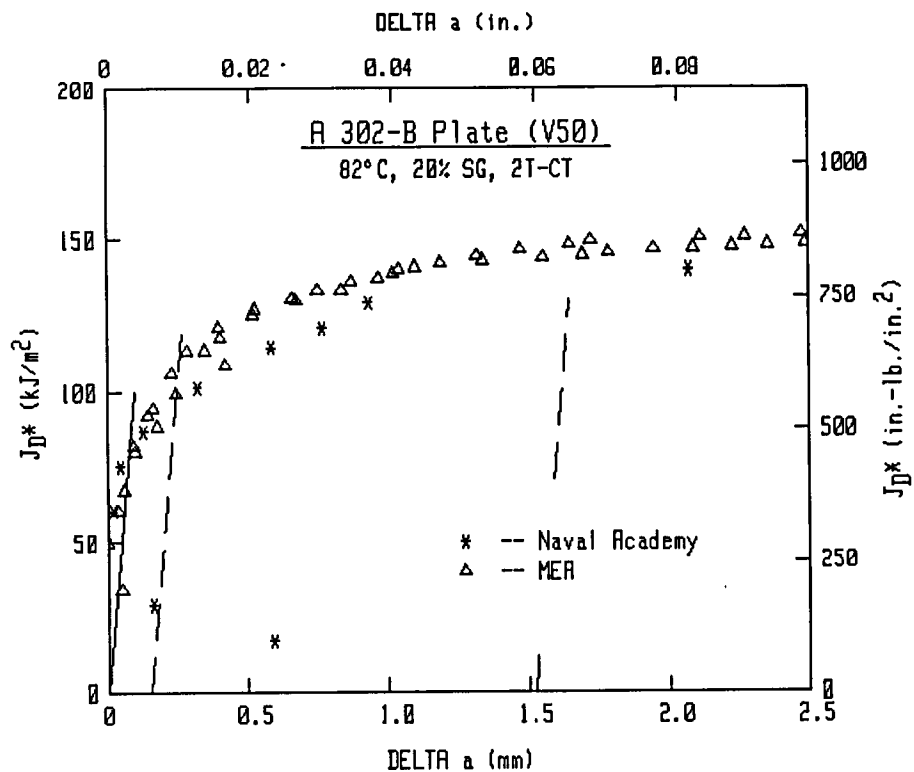


Fig. 71 Comparison of USNA and MEA J_{D^*} -R curves from 2T-CT specimens.

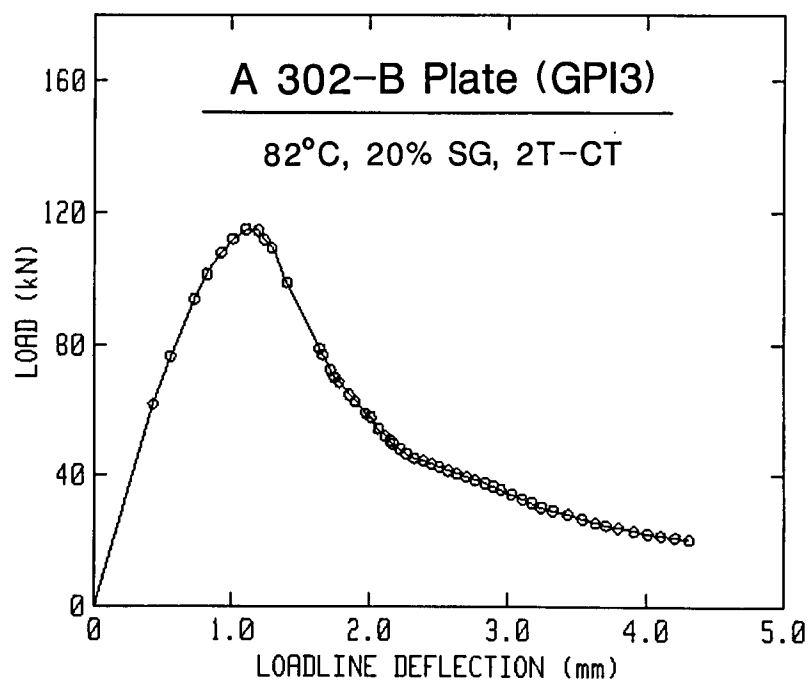
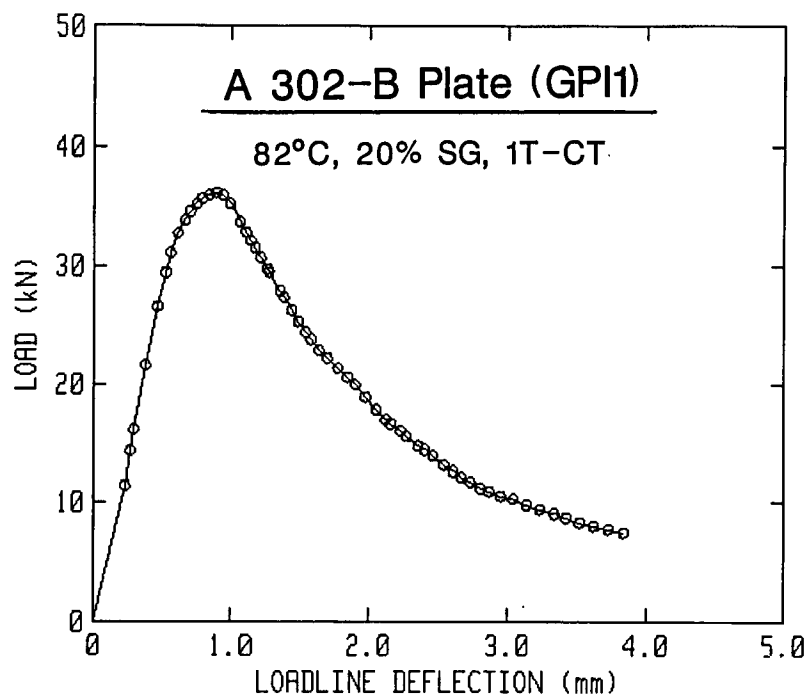


Fig. 72 Load-displacement curves for the USNA tests.

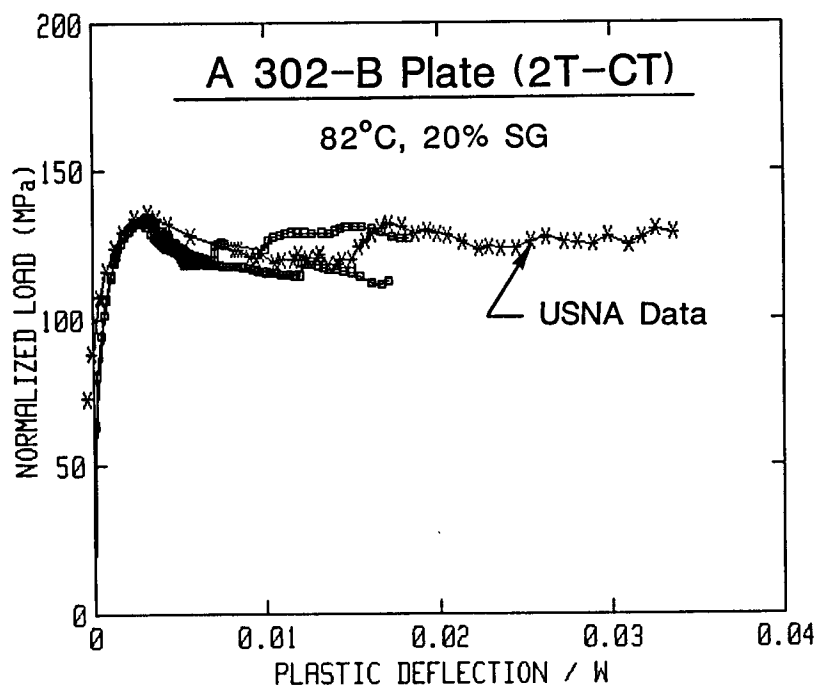
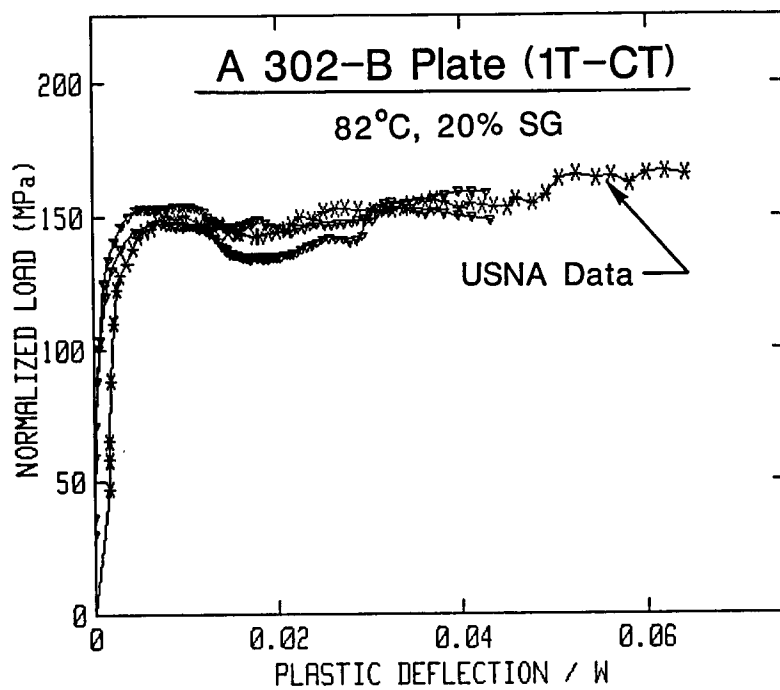


Fig. 73 Key-curves for the USNA tests.

graphs, the distinctly non-planar character of the fracture surfaces for this plate is obvious. In contrast, those for low toughness welds are generally flat, as illustrated in Fig. 19 for example. The Δa prediction errors for the welds are also quite low, at 0.18 mm (0.007 in.) or 2.9% on average, in comparison to those for the plate specimens.

The other characteristic which affects the crack growth predictions is the crack tip morphology. Again in comparing the fracture surfaces for the plate and those for the weld, the straight crack fronts for the weld yield good correspondence between measured and predicted crack growth. The distinctly irregular nature of the crack fronts for the plate specimens causes problems for the compliance measurements and also for the optical measurements of crack length. Overall, the compliance measurement problems result from a frictional interaction between features from the two fracture surfaces, and the cracking which occurs perpendicular to the crack plane at the crack tip. Such effects can be seen in hysteresis in some of the compliance unloadings, principally at the end of the tests. In addition, one must question the use of the standard compliance expressions for such irregularly shaped crack fronts; the "proper" compliance expression would give improved correspondence between Δa_p and Δa_m . The irregular crack fronts also make optical measurement of the crack length extremely difficult. To account for the irregularities, the measurements are made with subjective attempts at averaging the apparent crack length. However, this method is obviously not fool-proof.

6.5.11 Comparison of Different J Equations

With the various J equations available for evaluation of J-R curves, the selection of the proper equation for any specific application is not straight-forward. Although J_D was developed using a deformation theory of plasticity to account for crack growth, comparison of J_D -R curves from various sizes of specimens resulted in an apparent specimen size dependence, whereby the J_D -R curves for large specimens (in terms of planar dimensions and thickness) demonstrated higher J levels (at the same Δa level) than did smaller specimens (Ref. 2 and 14). Examples of this trend are illustrated in Fig. 74 from Ref. 2 and 14. As a consequence of the specimen size dependence found using J_D , Ernst later developed J_M , which was purported to include a better description of the process of deformation and crack growth. Confirmation of the improved performance of J_M as compared to that of J_D (in terms of minimizing specimen size dependence) can be seen in Fig. 75, whereby the different sizes of specimens give improved correspondence using J_M as opposed to J_D . One characteristic of the J_M -R curves found with the illustrated curves and in other cases is an inflection point in the J_M -R curve, whereby the J_M -R curve slope changes from decreasing in value to increasing. A general conclusion has been that this inflection or "hook" point is due to violation of the J_M -controlled crack growth region and data after that point are questionable.

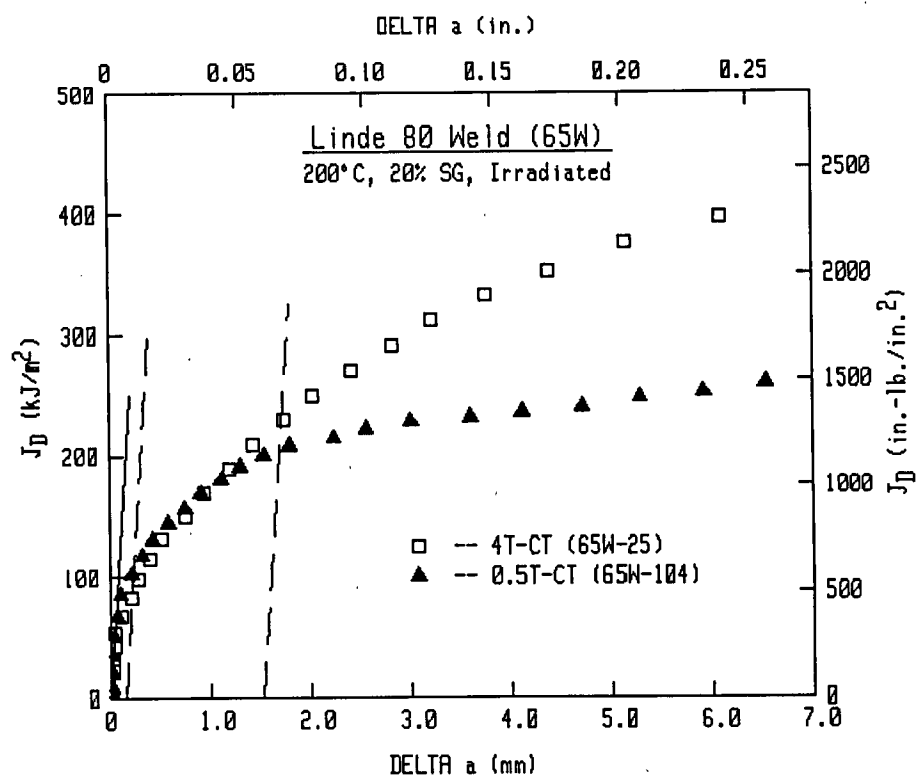
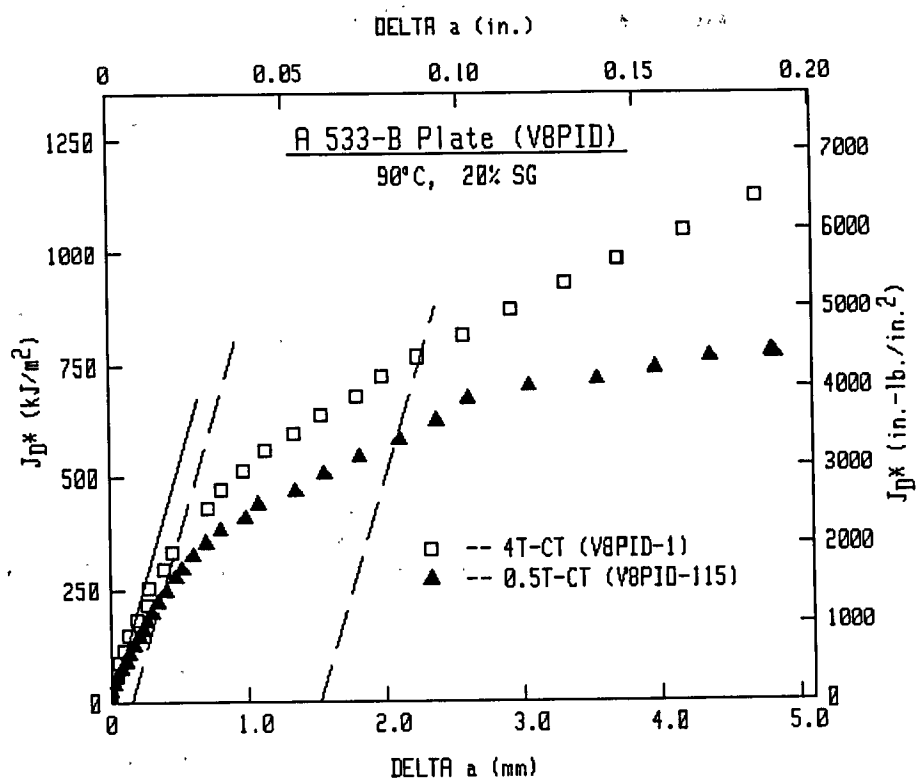


Fig. 74 J_d -R curves from large and small specimens of A 533-B plate and a Linde 80 weld.

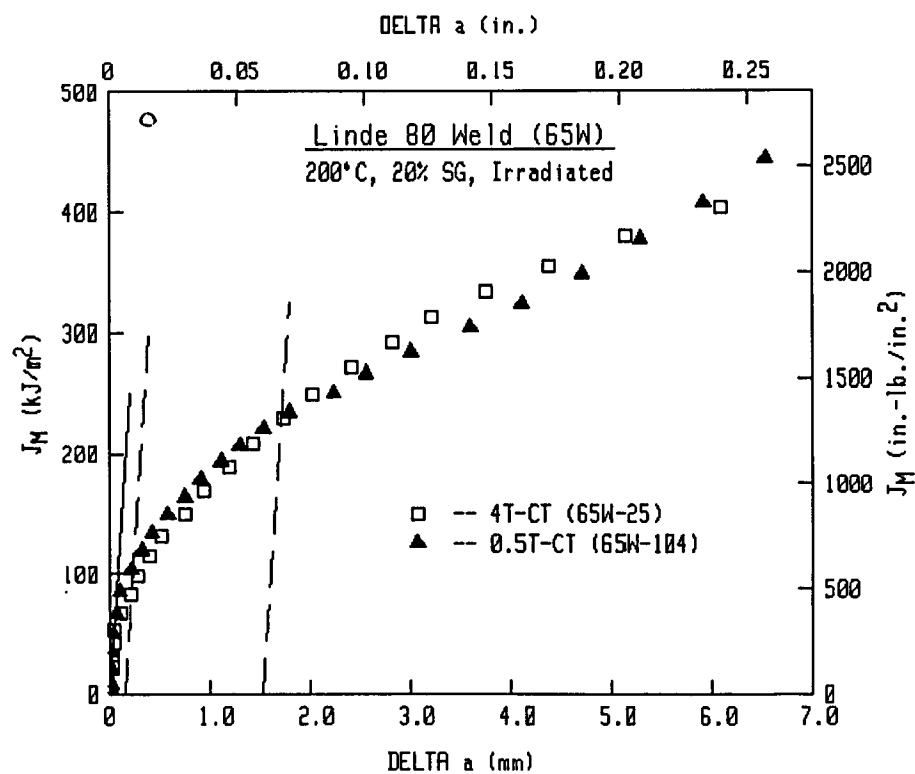
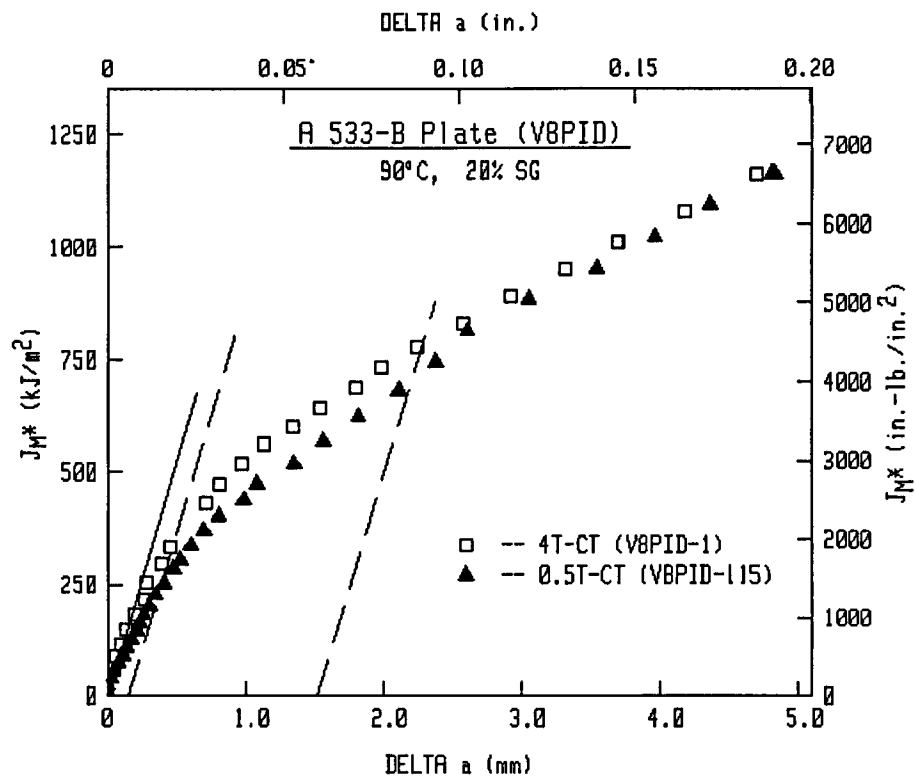


Fig. 75 J_M -R curves for the same tests illustrated in Fig. 74. The correspondence of data from different specimen sizes is much improved over that found with J_D .

All of the J-R curves illustrated in Fig. 74 and 75 were determined using an initial a/W of ~ 0.5 to 0.52 . If one were to postulate the relative positioning of the J-R curves for the large and small specimens with an initial a/W of ~ 0.6 , then the results illustrated in Figs. 68 to 71 indicate that all of the J-R curves would be elevated to a certain degree, but the J-R curves from the small specimens would be elevated more than those from the large specimens. Therefore, the J_D -R curves would probably indicate somewhat improved correspondence for the two specimen sizes, and the J_M -R curves would indicate somewhat higher toughness for the smaller specimens. Therefore, one would conclude that J_D gives the best correspondence of data from large and small specimens (or at least conservative data from small specimens), and J_M gives a somewhat poorer correspondence, with small specimens yielding non-conservative estimates of large specimen behavior.

As described in Section 6.3, J_D and J_M do not give J levels equivalent to those calculated from K for the case of the initial linear elastic portion of the test record. The quantities J_{D*} and J_{M*} are forms of J_D and J_M , respectively, representing the sum of elastic and plastic J levels, with elastic J calculated from K.

From the J-R curves illustrated in Fig. 50 to 54 none of the various J formulations resulted in any correspondence between the J-R curves from large and small specimens for Δa greater than ~ 0.25 mm (0.01 in.). To illustrate the significance of applying each formulation to this current study, data from the 6T-CT specimen (V50-101) and a 0.5T-CT specimen (V50-118) are evaluated using each of the J equations. As illustrated in Figs. 76 and 77 for each specimen, J_D and J_{D*} give the lowest J levels for each specimen size. In contrast, J_M and J_{M*} give the highest J levels of the 0.5T-CT specimen, whereas J_{M-C} gives the highest J levels for the 6T-CT specimen. For the 0.5T-CT specimen, J_M and J_{M*} give nearly identical J levels (as do J_D and J_{D*}); for the 6T-CT specimen, J_D and J_M give slightly higher J levels than their star (*) counterparts.

At the last data point on the J-R curves, $\Delta a/W$ and b/W are similar for both specimen sizes, at 0.24 and 0.245, respectively. For this data point, J_{M-C} divided by J_D or J_{D*} is 1.69 for the 6T-CT specimen and 1.58 for the 0.5T-CT. In contrast, the ratio of J_{M-C} to J_M or J_{M*} is 1.26 for the 6T-CT specimen and 0.92 for the 0.5T-CT. The good agreement in the relative levels of J_{M-C} and J_D or J_{D*} are expected since the crack growth correction incorporated by J_D and J_{D*} is a function of $\Delta a/W$ or b/W . Similar correspondence is expected with J_M and J_{M*} . The causes for the discontinuity between J_M and J_{M*} for the two specimen sizes is not known.

6.5.12 Normalization Method

With J-R curve testing, crack growth (Δa) prediction errors tend to be quite small, generally less than 5%. These errors tend to result in less crack growth predicted than that measured. For such cases, adjusting the data to account for the Δa error would result in fairly minor changes in the overall appearance of the J-R curve. In particular, the J level at the final data point is unchanged using J_{M-C}

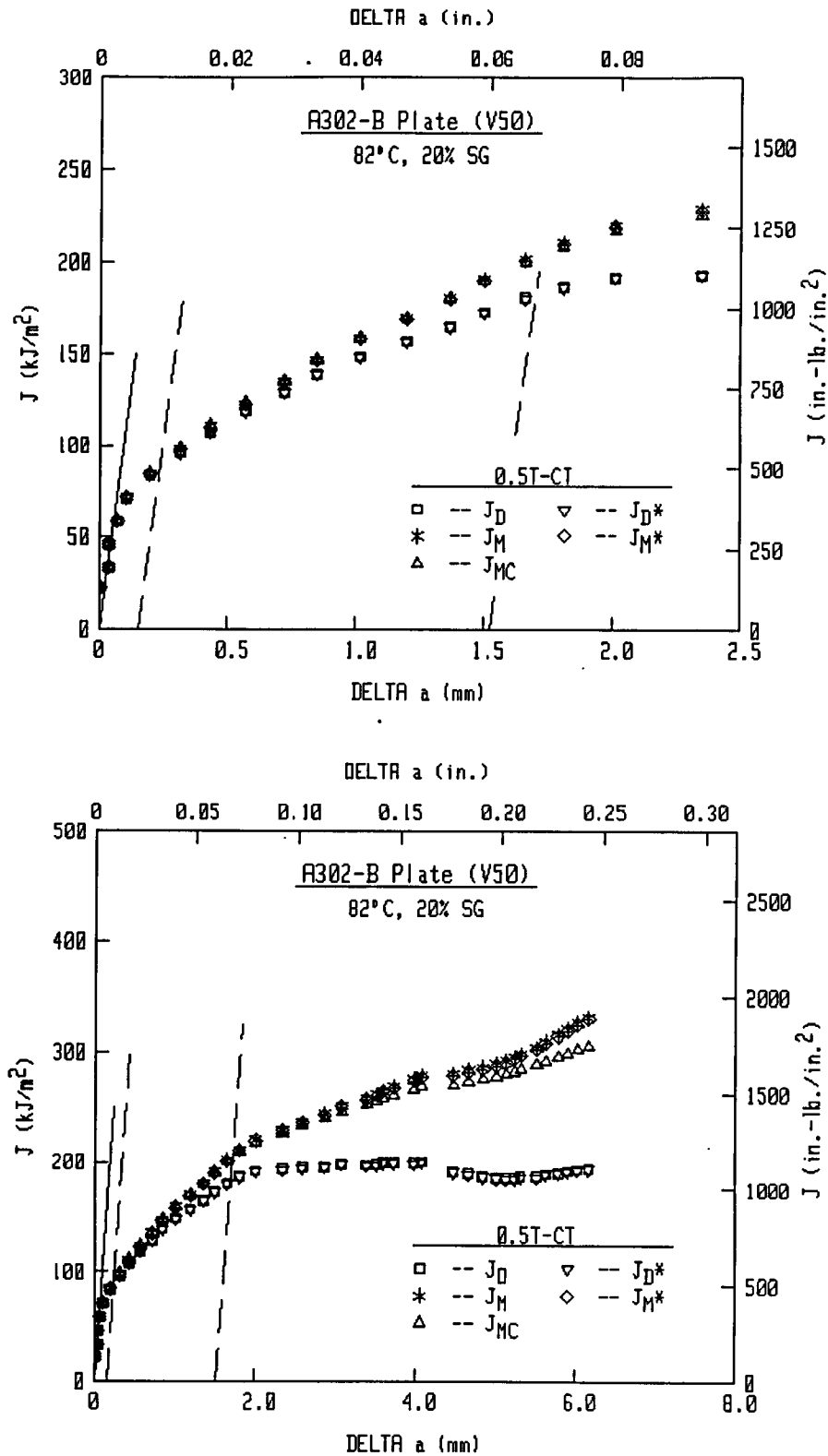


Fig. 76 Comparison of the R-curves for the 0.5T-CT specimen (V50-118) using the various J formulations.

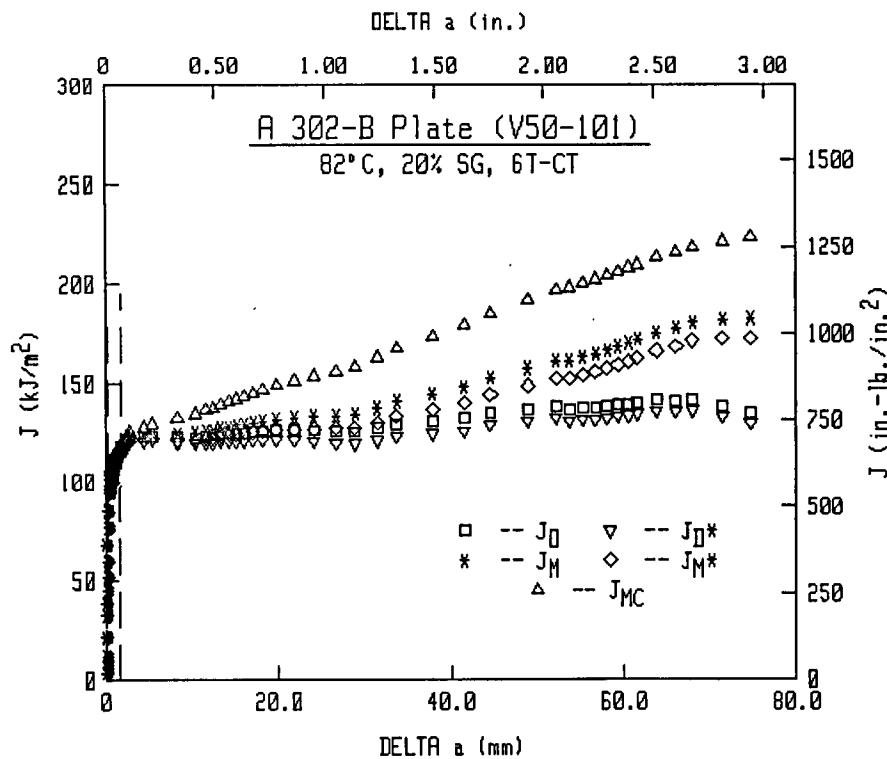
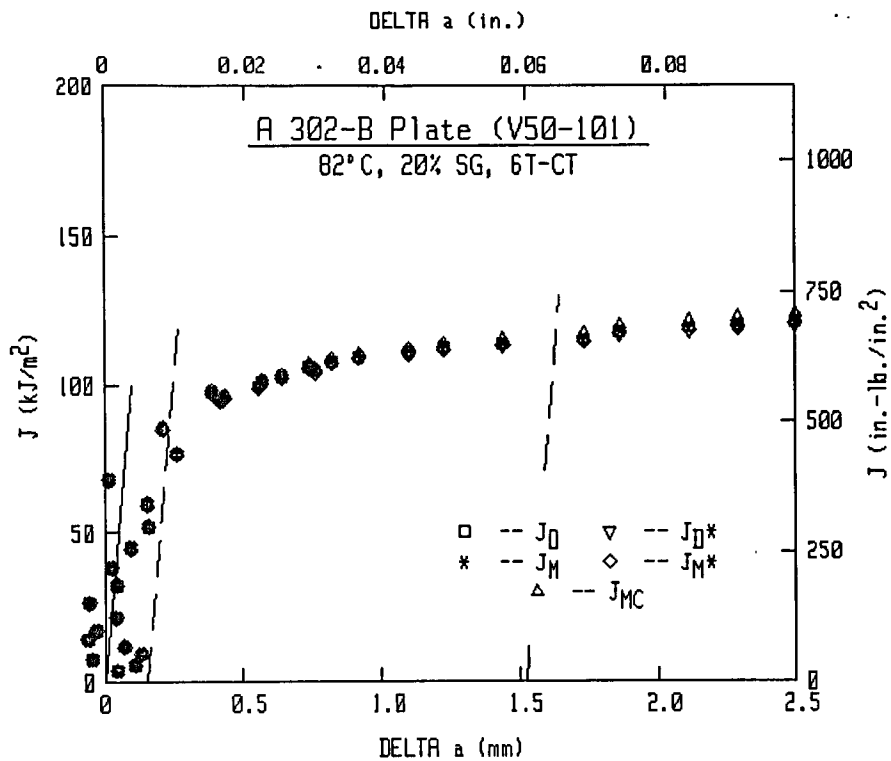


Fig. 77 Comparison of the R-curves for the 6T-CT specimen (V50-101) using the various J formulations.

(since this parameter is a function of initial crack length only), whereas J_M (J_{M*}) and J_D (J_{D*}) would change due to their Δa dependence. The problem in correcting the predicted Δa such that the final data point matches the measured Δa is that no intuitive procedure exists to make such a correction. In particular, one does not know when the error begins and what the propagation rate of the error is. As an example, does a 10% error mean that all compliance-predicted Δa values should be increased by 10%, or only those after initiation? Or is the error a non-linear function of predicted Δa ?

Herrera and Landes has made one attempt at establishing a procedure for matching predicted Δa to measured Δa . This "normalization" method (Ref. 18) uses a calibration curve approach analogous to the key-curve method. In this normalization method a unique calibration curve, derived in a manner similar to the key curve, is then used to calculate crack length at any point on the load-displacement record for the test.

This calibration curve is determined using Eq. 22 and 23. One assumption made is that the calibration curve (P_N vs. δ_{pl}/W) is well characterized by a power law equation of the form:

$$P_N = \beta (\delta_{pl}/W)^{1/n} \quad (24)$$

where n is thought to be well approximated by the exponent of the Ramberg-Osgood equation (Eq. 9). An alternative method would assume a linear trend between the initiation point and the final data point. In this format, the final data point (from the final load and displacement and the measured crack length) is used to evaluate a data pair of P_N and δ_{pl}/W . Additional data points can be determined up to crack growth initiation using the initial measured crack length, and several load and displacement pairs. For the analysis given in Ref. 18, one method for determining β and n is to plot the P_N vs. δ_{pl}/W data in a log-log format. A straight-line fit to the final data point and an initial portion of the data yields β and n . Another method used with this data from A 302-B plate was to use the load and displacement at initiation (to determine a data pair of P_N and δ_{pl}/W) along with the final data pair in a power-law fit to determine β and n . The initiation point was determined from the compliance data as the data point prior to the J-R curve data departing from the blunting line. Figure 78 indicates such initiation points for 0.5T and 6T-CT specimens.

To illustrate the effect of this normalization method, data from a 0.5T-CT specimen (V50-118) and a 6T-CT specimen (V50-101) will be used. Since this normalization method requires the user to define a calibration curve relating P_N to δ_{pl}/W , the following cases will be applied to the A 302-B plate data:

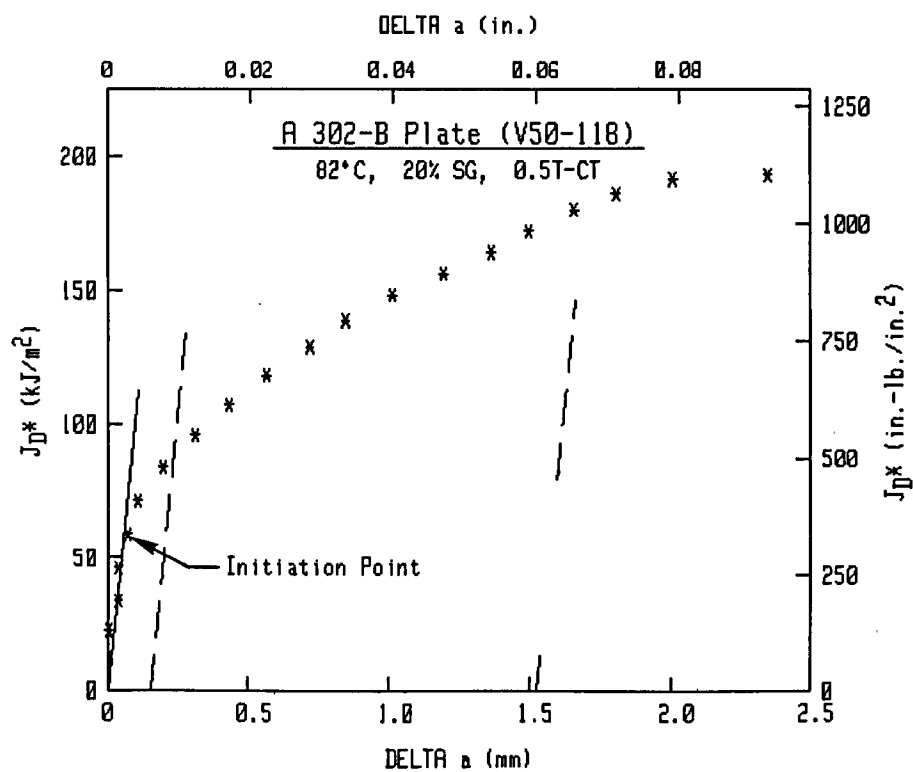
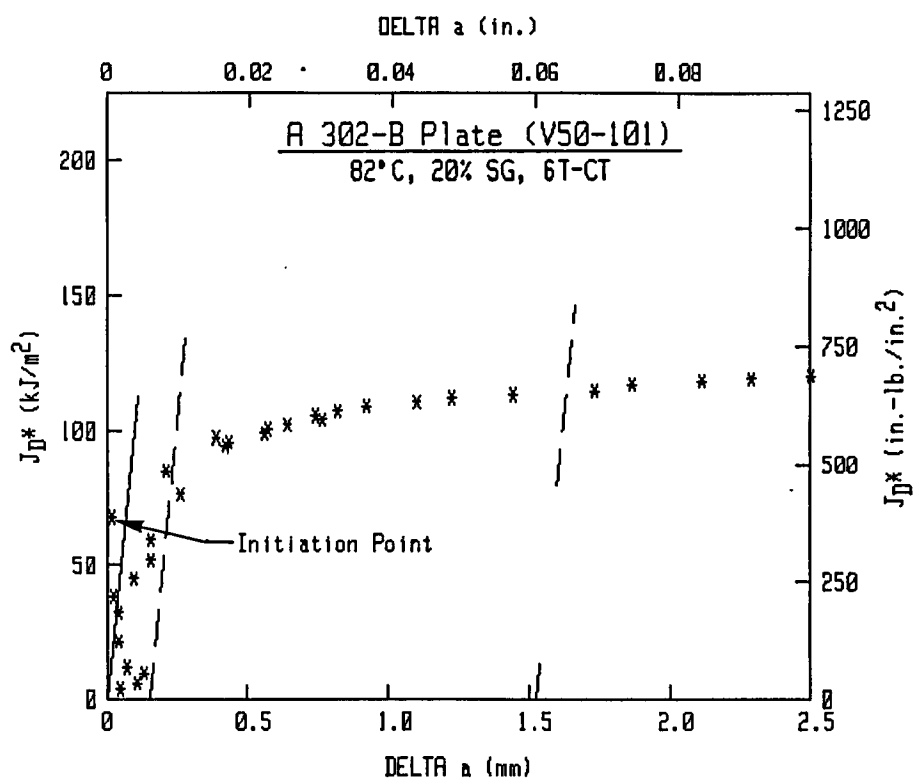


Fig. 78 The initiation point used for the normalization analyses.

- (1) β and n from the analysis method of Ref. 18.
- (2) β and n from only the initiation and the final data points.
- (3) a linear fit of P_N vs. δ_{pl}/W to the initiation and final data points (i.e., a linear relation is assumed instead of the power law relation in Eq. 24).
- (4) n from Ramberg-Osgood fits to the true stress-strain data, with β from the final data point (for this plate, the average n is 7.352 from Case 2 of Table 10).

An additional Case 5 was also applied to each specimen. For the 0.5T-CT specimen (V50-118), Case 5 used the same β and n values as Case 4, with Δa values determined from the beginning of the test instead of from the initiation point. For the 6T-CT specimen (V50-101), Case 5 used a linear portion of P_N vs. δ_{pl}/W (in a log-log plot) to define β and n , with the final crack length (a) not forced to match the measured final crack length. The rationale for Case 5 (6T-CT specimen) is that an accurate measurement of final crack length is not possible (or even defineable), given the irregularities in the crack front.

In Fig. 79, log-log plots of P_N vs. δ_{pl}/W for each specimen are illustrated. The initial crack lengths are used for all evaluations of P_N and δ_{pl}/W , with data points from the measured final crack length given as "X". The trend lines illustrated for each specimen represent Case 4 (i.e., n from true stress-strain data, 7.352). The β values for each specimen are reasonably close. Although the fit is a reasonable approximation to data from the 0.5T-CT specimen near the initiation point, the fit to the 6T-CT data do not come near the data at the initial portion of the test record. Therefore, Case 4 for the 6T-CT specimen gives large Δa values at the beginning of the test in order to match the P_N vs. δ_{pl}/W data with the assumed power-law curve. Comparison of P_N vs. δ_{pl}/W in a linear format (Fig. 80) demonstrates the good fit to data from the 0.5T-CT specimen and the poor correspondence for the 6T-CT specimen. In these plots the data points (*) are determined from the initial crack length, with the final data point (denoted by "x") evaluated from the final measured crack length. The irregular trend curve is the key-curve using actual compliance measurements and estimates of crack length. The highest curve, which intersects the final data point, represents the power-law fits illustrated in Fig. 79 for each specimen. In contrast to the good correspondence between the key-curve data and the power-law approximation for the 0.5T-CT specimen, the power law is much steeper than the key-curve data for the 6T-CT specimen.

Additional comparisons between the key-curve data and the various approximations (i.e., Cases 1 to 5) to the key-curve data are illustrated in Appendix D. The J-R curve data which result from the normalization method are illustrated in Figs. 81 to 84 using J_{D*} and J_{M*} . For the 0.5T-CT specimen, all of the normalization method applications give lower J-R curves than does the compliance method.

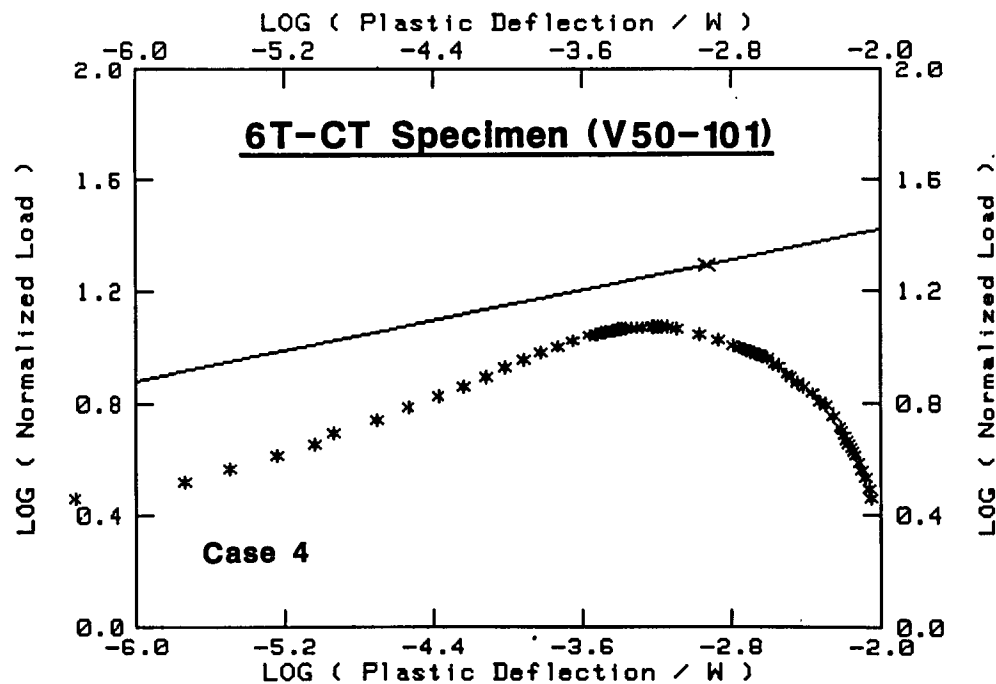
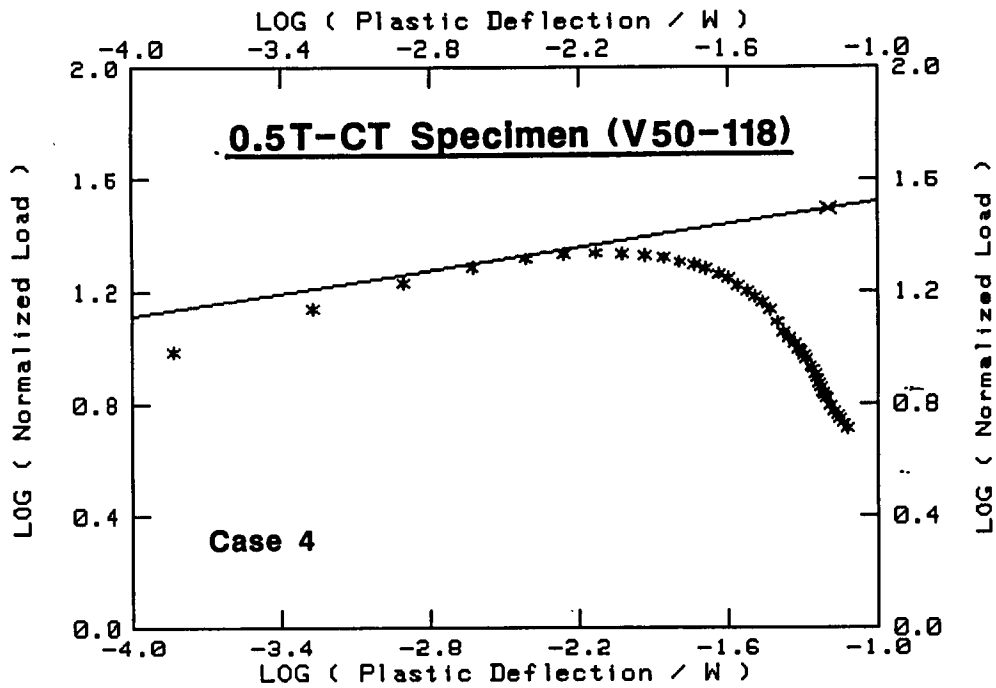


Fig. 79 P_N vs. δ_{p1}/W (in a log-log format) for the 0.5T- and 6T-CT specimens. The illustrated trend lines are from Case 4 normalizations.

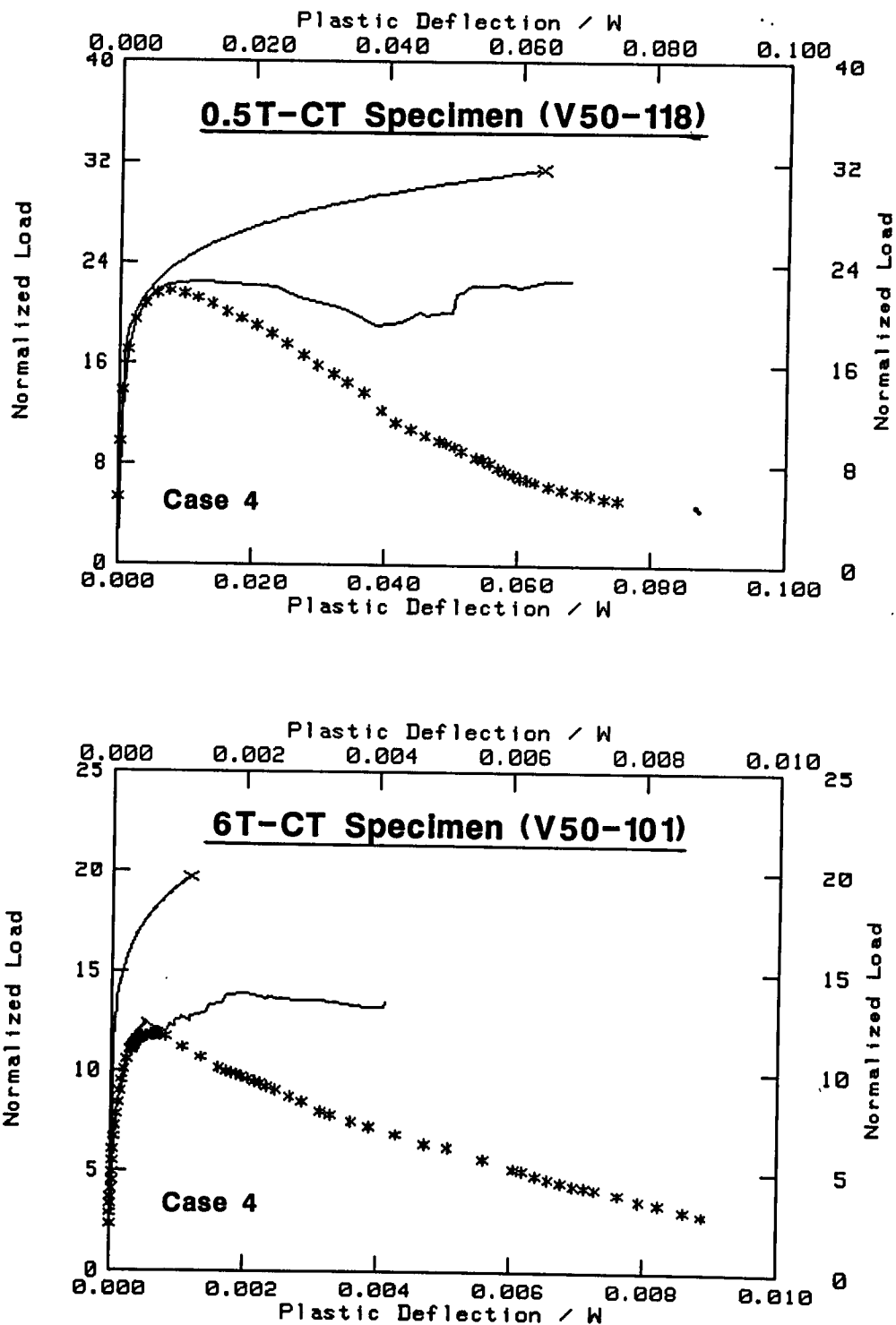


Fig. 80 P_N vs. δ_{p1}/W (in a linear format) for the 0.5T- and 6T-CT specimens. The irregular trend curve is from actual compliance measurements, whereas the highest curve is the power law determined from Case 4 normalization.

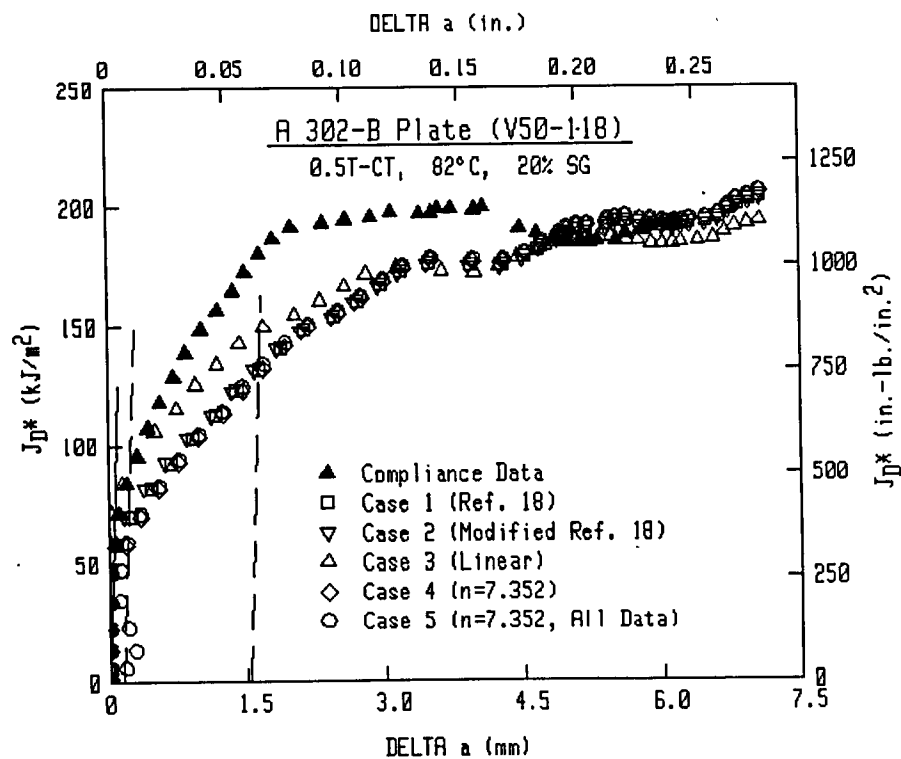
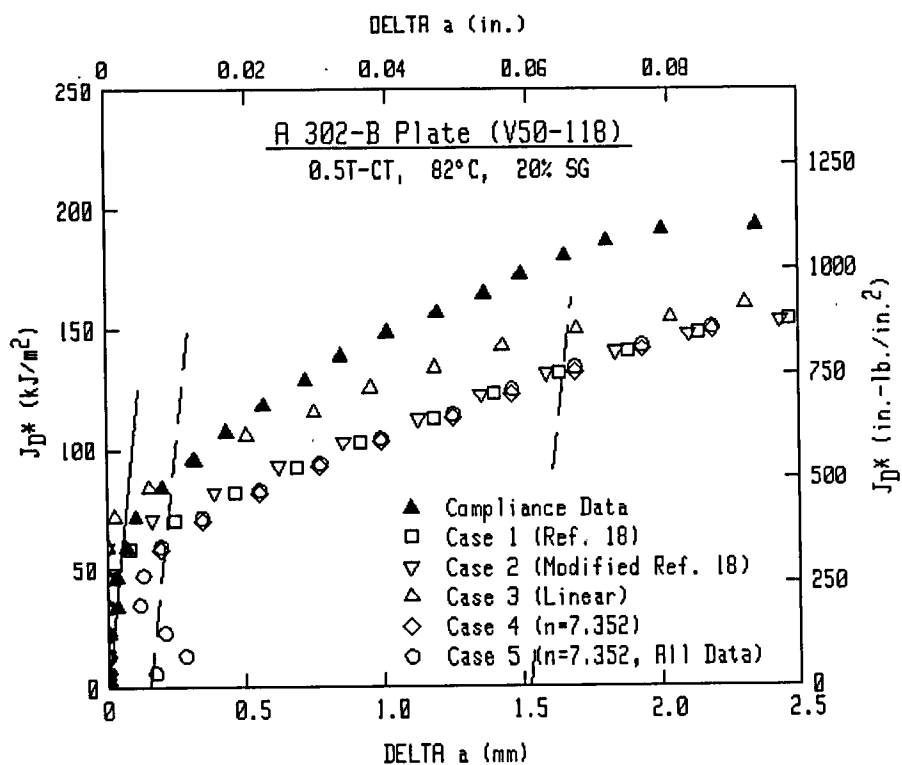


Fig. 81 Comparison of J_D^* -R curves for the 0.5T-CT, using compliance measurements and normalization evaluations.

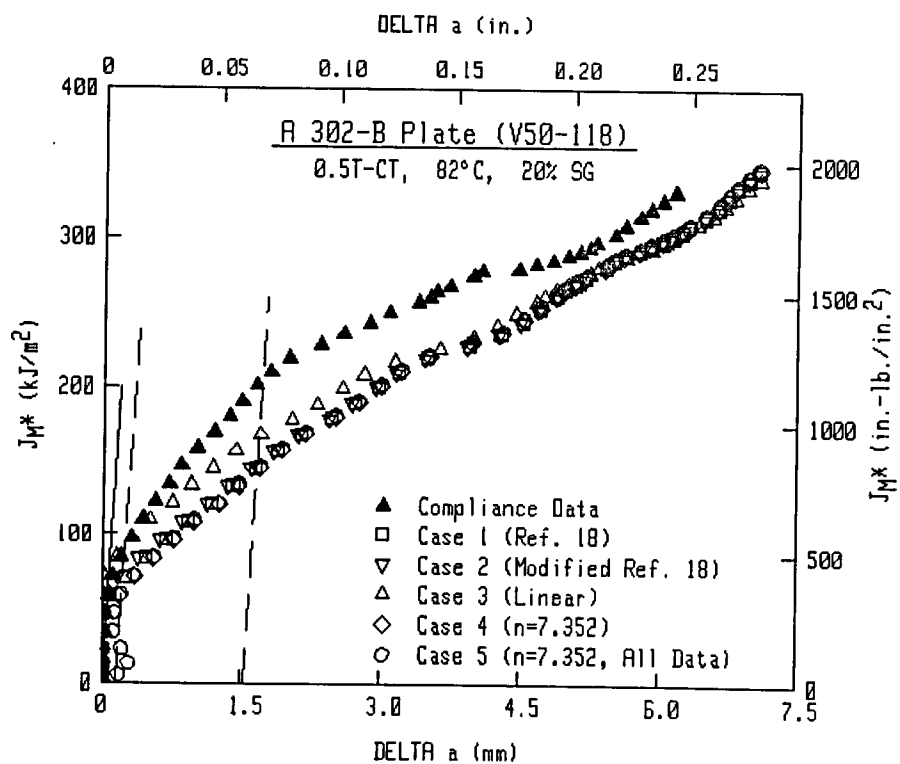
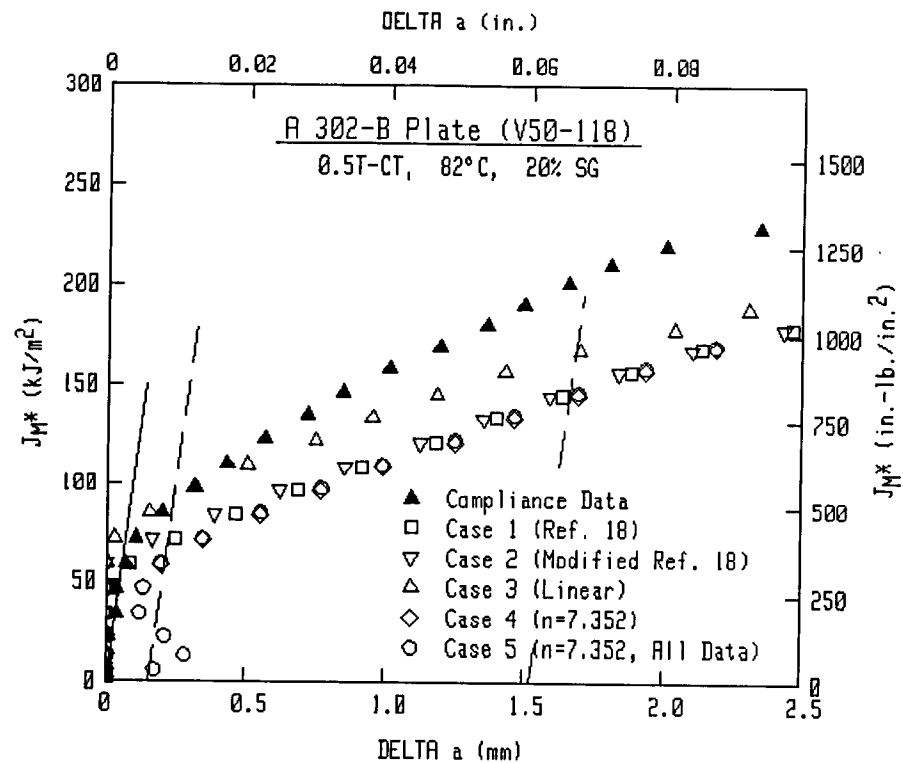


Fig. 82 Comparison of J_{M^*} -R curves for the 0.5T-CT, using compliance measurements and normalization evaluations.

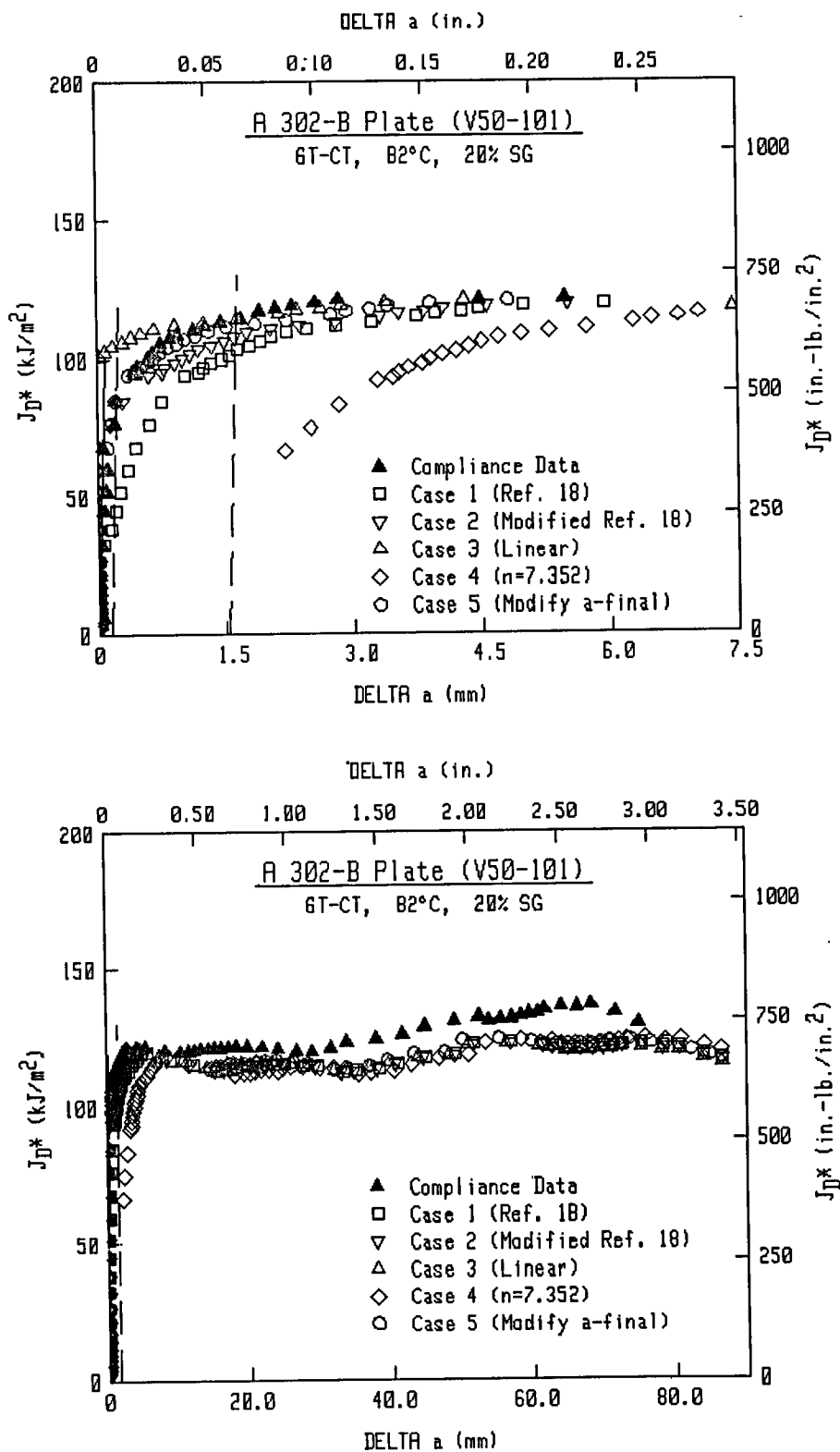


Fig. 83 Comparison of J_{p^*} -R curves for the 6T-CT, using compliance measurements and normalization evaluations.

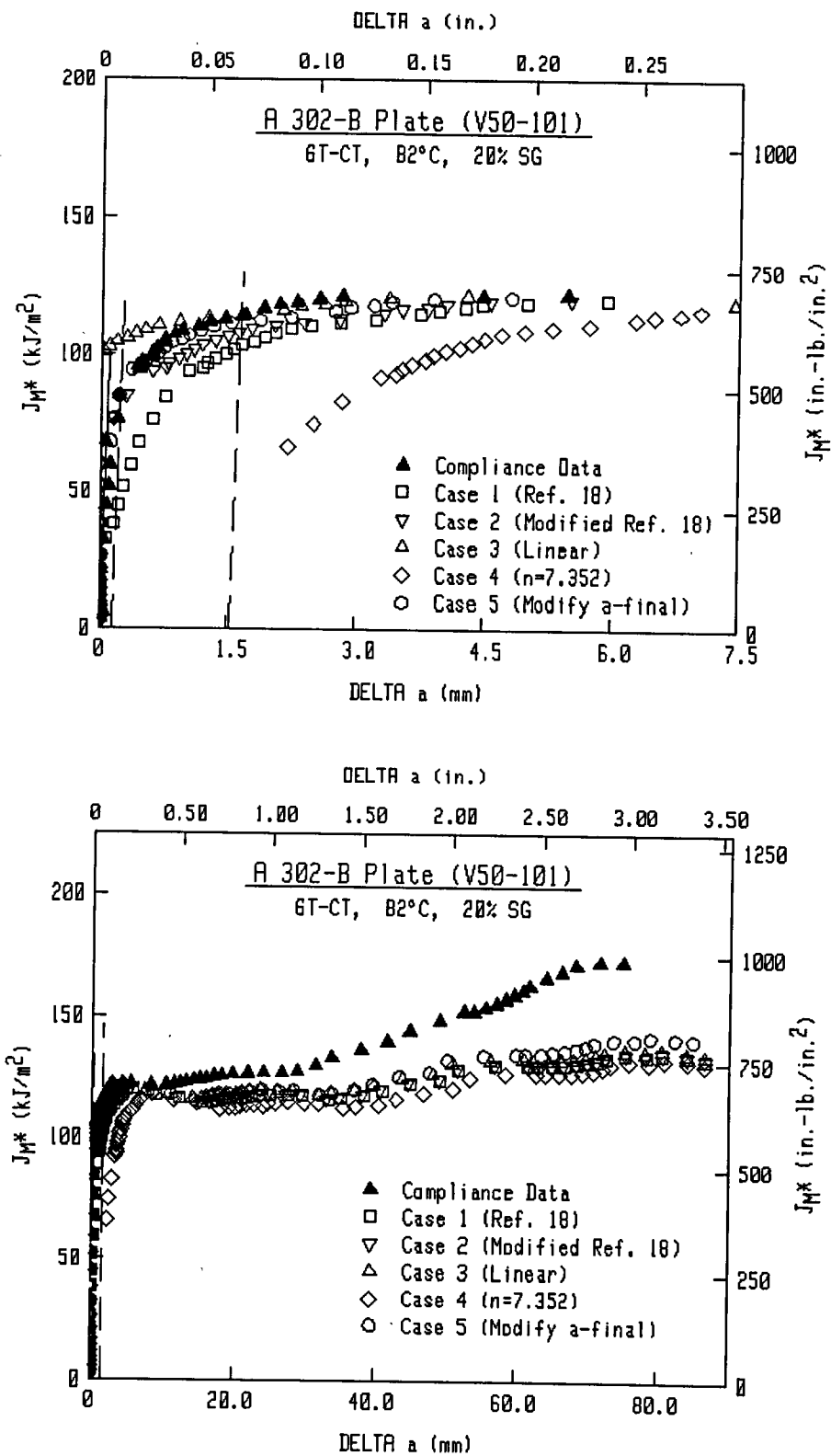


Fig. 84 Comparison of J_{M^*} -R curves for the 6T-CT, using compliance measurements and normalization evaluations.

With J_{D*} , compliance data indicate a decrease in J level at Δa of ~ 4 mm (0.16 in.), whereas the normalization data indicate increasing J at virtually all crack growth intervals. Each of the key-curve approximations give similar Δa and J levels at virtually all points on the J-R curves, except for Case 3, which involves a linear approximation to the key-curve between initiation and the measured final crack length. As Δa increases, data for Case 3 eventually merge with those for the other cases, although the J levels for Case 4 are below those for the other cases at the highest Δa levels. One troubling aspect of these normalization data is the elevation in Δa levels as a function of Δa . Although difficult to determine from these graphs of J_{D*} and J_{M*} data, the difference in Δa values from the compliance method and the normalization method increases rapidly from the initiation point to higher Δa levels. This difference increases to a maximum of 1.67 mm (0.066 in.) at Δa (compliance) of ~ 2.6 mm (0.102 in.); in contrast, the final crack lengths from optical measurements and compliance estimates differ by only 0.9 mm (0.035 in.).

For the 6T-CT specimen, each of the normalization method applications gives J-R levels which are lower than those from compliance data, principally at large Δa levels. As for the 0.5T-CT specimen, the normalization cases exhibit similar trends at large Δa levels. The major differences are evident at low Δa levels. In particular, Case 3 gives low initial Δa levels, and Case 4 gives a jump in Δa up to ~ 2 mm. The latter indicates that the initial crack length should be 2 mm longer than was measured. The reduction in the J_{M*} -R curve is much greater than that for the J_{D*} -R curve, when comparing normalization data with compliance data. In addition, differences between the J_{D*} - and J_{M*} -R curves are significantly reduced using the normalization method.

Overall, the normalization method does tend to bring the J-R curves from the large and small specimens somewhat closer together. However, the method does not significantly influence the size dependence observed for this plate.

6.6 Microstructural and Fractographic Evaluations

In an effort to explain the discrepancy in fracture toughness observed between the small and large specimens, microstructural and fractographic evaluations were performed on selected broken test specimens. In particular, fracture surfaces from 0.5T-CT specimens V50-117 (from the plate mid-thickness) and V50-118 (from the plate 3/4T thickness location) and 4T-CT specimens V50-102 and V50-103 were utilized. From the latter specimens, samples representing the plate mid-thickness and the plate 1/4T and 3/4T thickness locations were used. The selection of specific samples was intended to give comparison of characteristics through the plate thickness and also between regions which yielded high (0.5T-CT) and low (4T-CT) toughness.

Microstructural samples of one 0.5T-CT specimen (V50-117) and one 4T-CT specimen (V50-102) were prepared by grinding and polishing

selected surfaces to a 0.05 μ in. finish. The 0.5T-CT specimen was from the plate mid-thickness and yielded the lowest of the J-R curves from 0.5T-CT specimens. For the 4T-CT specimens, pieces representing the plate mid-thickness (piece 43) and the plate 1/4T thickness location (piece 22) were used. Inclusion counts were performed on polished specimens, whereas visual microstructural constituent identification and grain size assessments were performed on polished specimens which were etched with 2% Nital solution. The microstructures consisted primarily of ferrite and finely-spaced pearlite, interspersed with banding of material having a higher alloy content, possibly bainite (Figs. 85 and 86). The ASTM grain size ranged from 9 to 10; ASTM inclusion counts ranged from 1.5 to 2 for sulfides, and from 2 to 3 for aluminides (Figs. 85 and 86). No particular differences are found between the 1/4T and the plate mid-thickness, or between the low and high toughness specimens.

Scanning electron microscopy was performed on selected fracture surfaces as well. Some of the fracture surfaces were coated with oxide from the heat tinting operation. The oxide was removed using the ENDOX method (Ref. 19), followed by final surface cleaning with ethanol. The fracture surfaces of the 0.5T-CT specimens (V50-117 and 118) and the 4T-CT specimens (V50-102 and 103) are from the plate mid-thickness (Fig. 87) and from the plate 1/4T location (Figs. 88 and 89). Clearly, the most notable observation is that no noticeable differences in fracture surface appearance are apparent. All of the fracture surfaces exhibited extensive laminated tearing, or splits, oriented in the direction of crack growth. Brittle-like splits are the most prevalent feature, with small amounts of microvoid coalescence found in the areas between the splits. The width, length, relative number, and relative distribution of the splits are generally the same for every specimen examined. These splits resulted from either: (a) separation of interfaces between the material bulk (composed of ferrite and fine pearlite) and the prolific volume of inclusions, and/or (b) the splitting of a more brittle, alloy-rich banded structure (composed possibly of bainite). Figure 90 compares the fracture surface with the inclusion distribution and the banded microstructure. Clearly, the distribution of splitting correlates with both the alloy-rich bands and the inclusions. The role of microstructure in explaining the discrepancy in fracture toughness of these specimens is not clear, given in particular the similarities between fracture surfaces from low (4T-CT) and high (0.5T-CT) toughness specimens. For controlled-rolled steels, the transition temperature and upper shelf energy is usually lowered as the number of splits increases (Refs. 20-22). The 4T-CT specimens exhibited a higher number of splits than the 0.5T-CT specimens, but the relative density of splits was essentially constant for both specimen sizes. Thus, the decreased fracture toughness observed in the larger specimens may be influenced by the total number of splits as opposed to some relative parameter. No intuitive explanation for this influence is obvious. Additional work would be required to acquire a clearer understanding and, possibly, a mechanism which would explain the observed behavior.

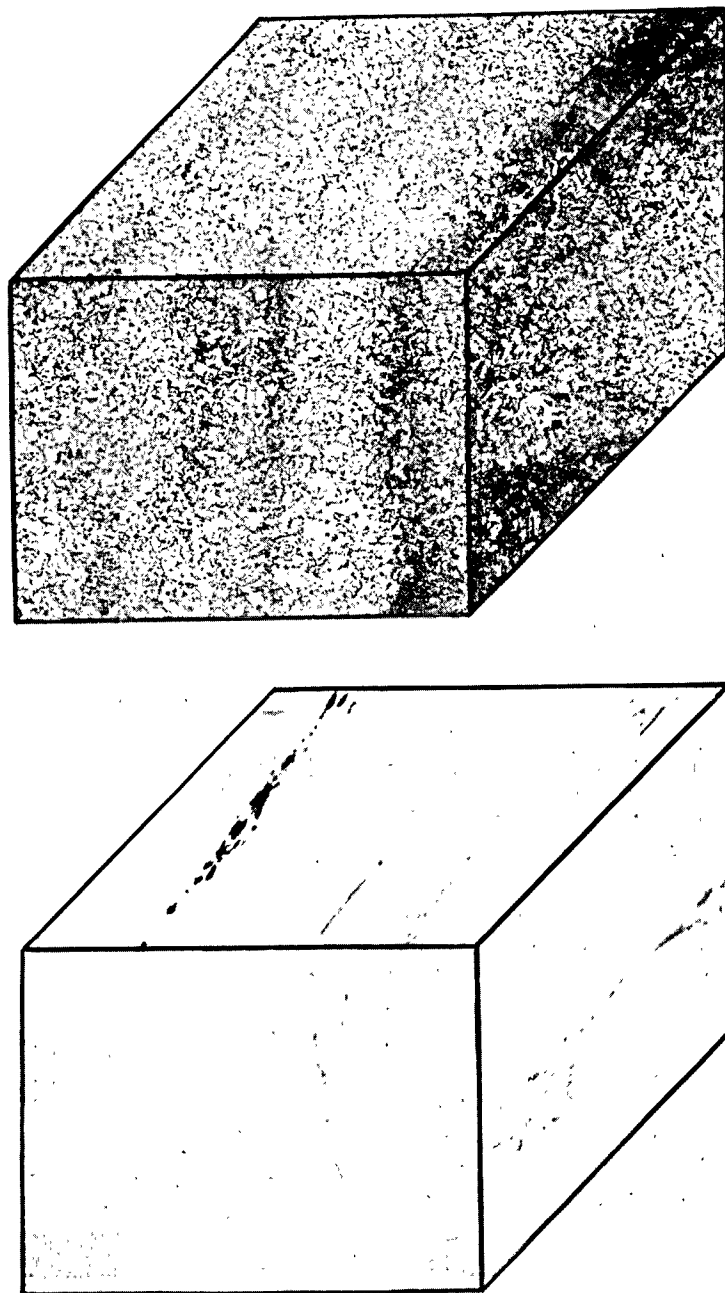


Fig. 85 Three-dimensional views showing microstructure (upper photo) and inclusion distribution (lower photo) of specimen V50-117 from the plate mid-thickness. Banding of the alloying elements can be observed as well as the sulfide (light grey) and aluminide (black) inclusions. The top plane is the L-LT surface (i.e., the fracture plane); the right plane is the L-ST surface; and the front plane is the LT-ST surface. 100X.

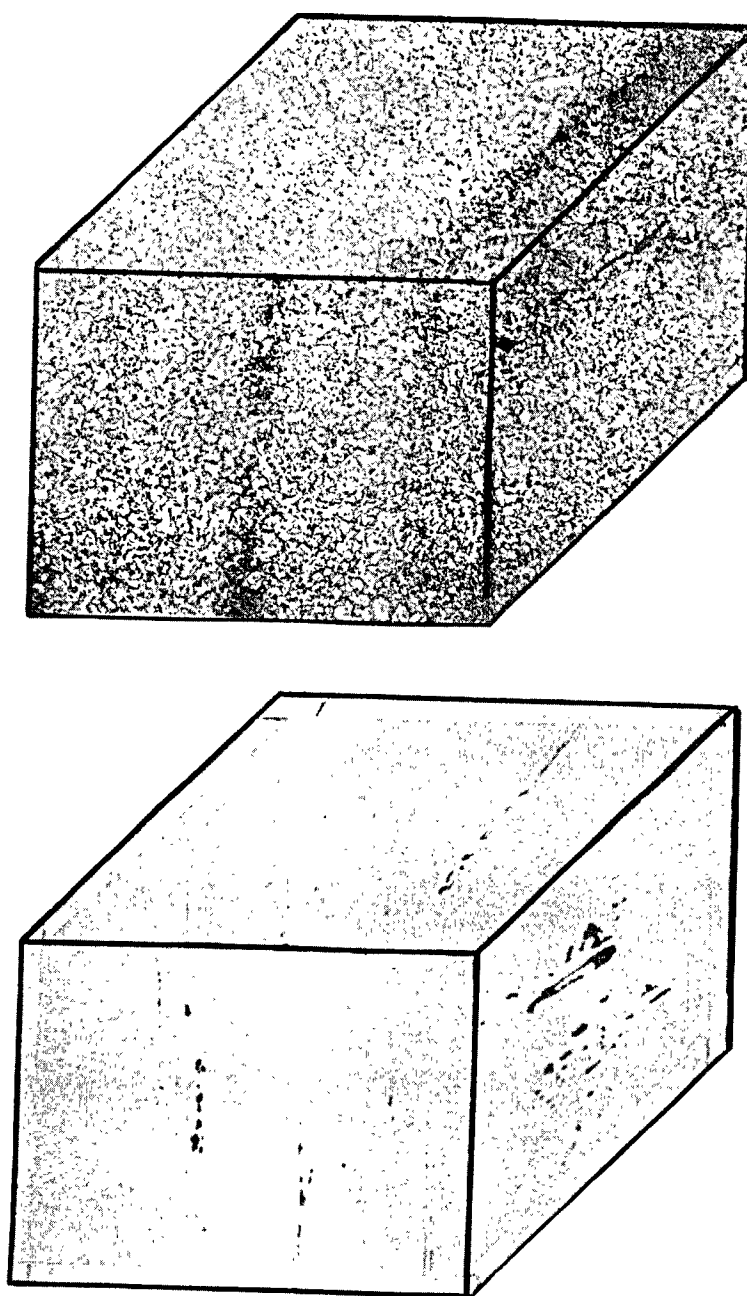


Fig. 86 Three-dimensional views as in Fig. 85, except that the specimen is V50-102 from the plate $1/4T$ thickness. 100X.

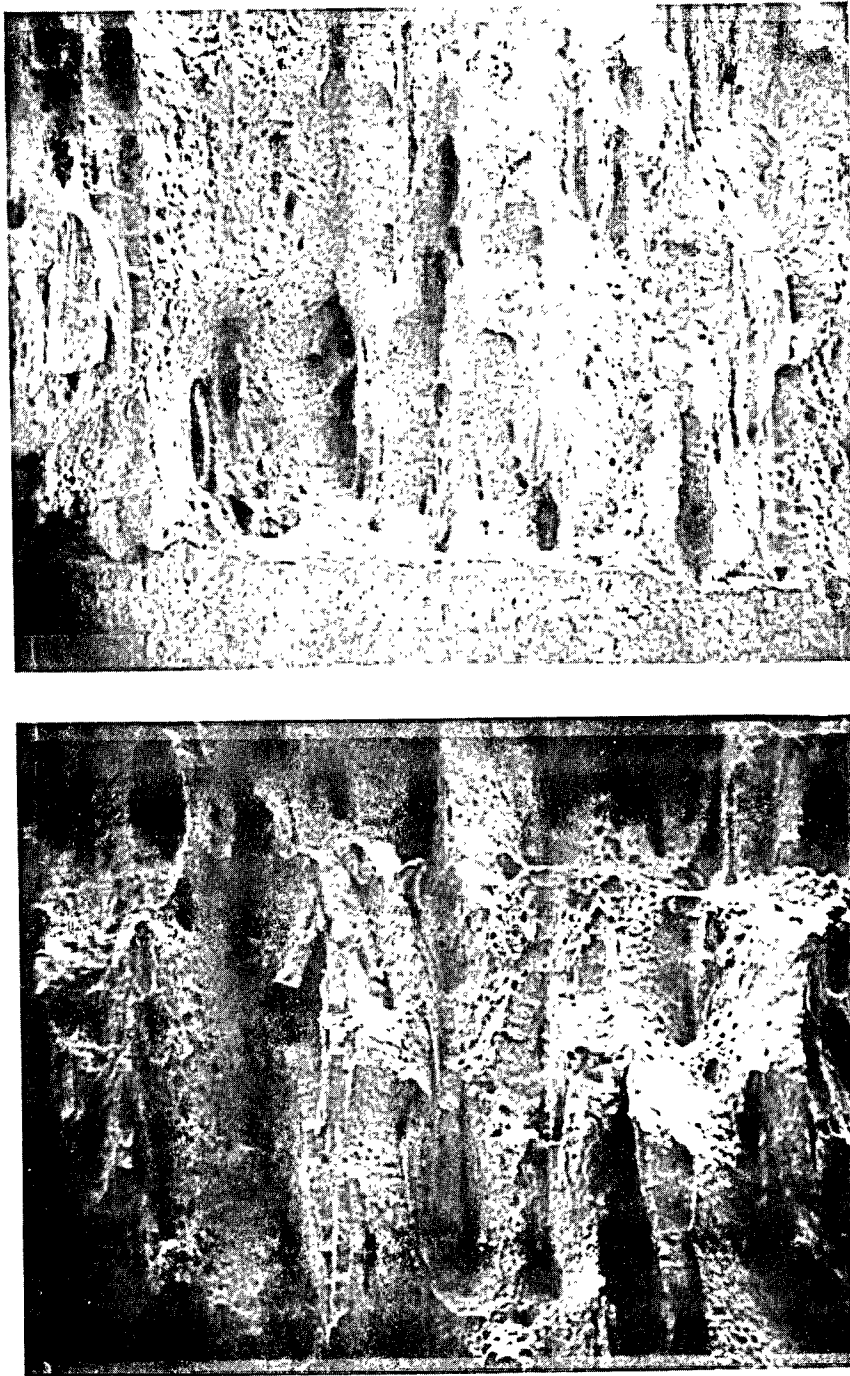


Fig. 87 Scanning electron fractograph of high toughness 0.5T-CT specimen V50-117 (upper photo) and low toughness 4T-CT specimen V50-102 (lower photo). Specimens were from the plate mid-thickness. 30X.

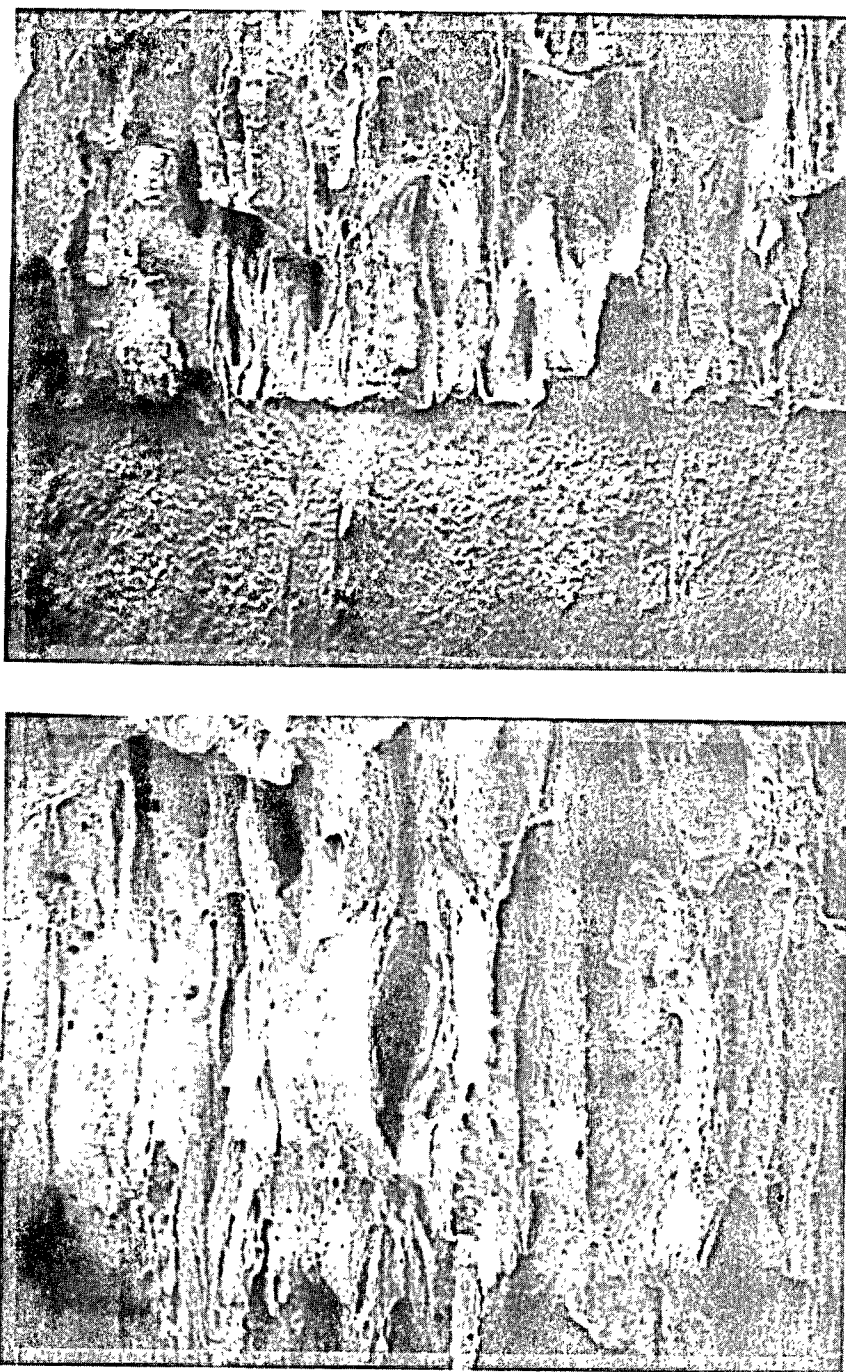


Fig. 88 Scanning electron fractograph of high toughness 0.5T-CT specimen V50-118 (upper photo) and low toughness 4T-CT specimen V50-103 (lower photo). Specimens were from the plate 1/4 thickness. 30X.

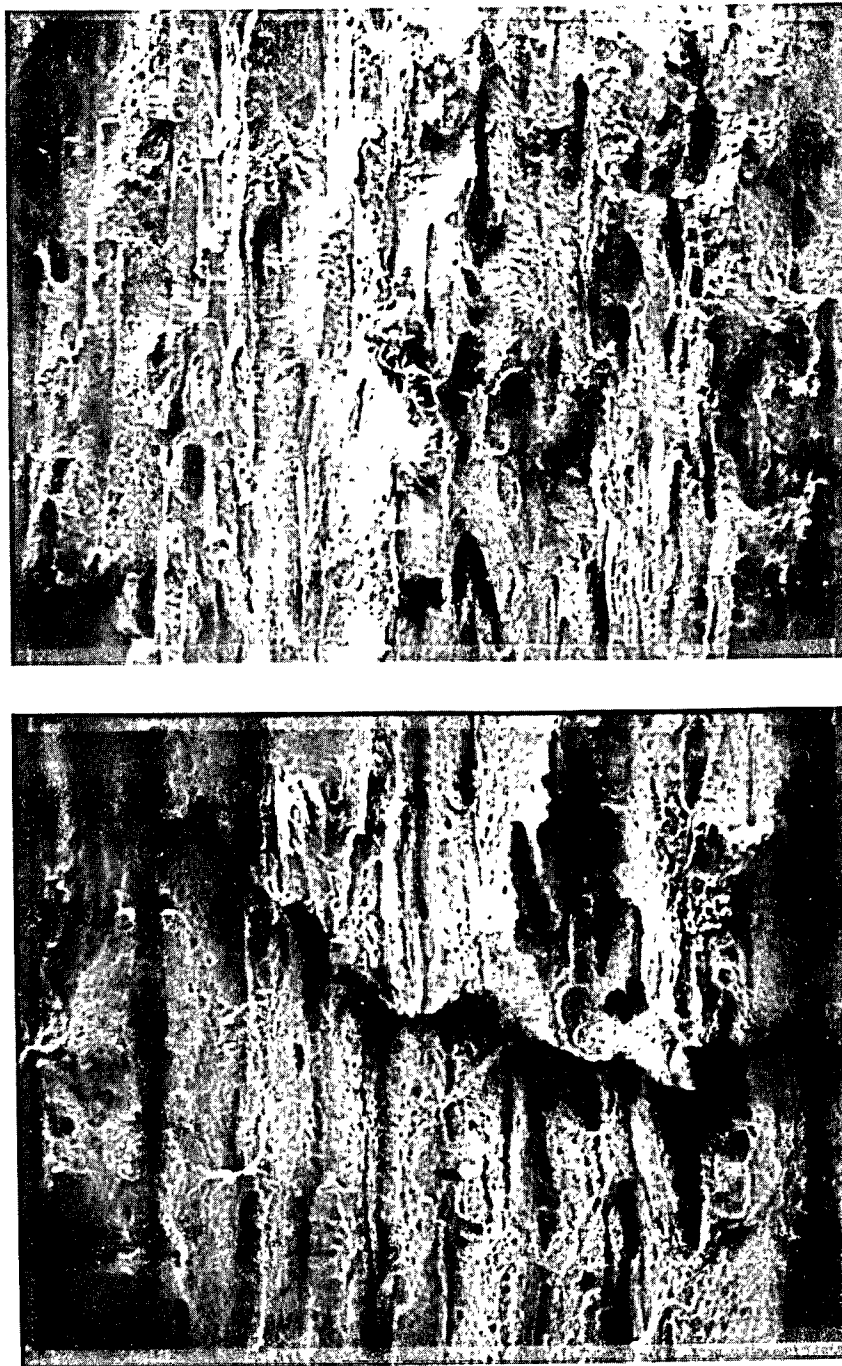


Fig. 89 Scanning electron fractograph of high toughness 0.5T-CT specimen V50-118 (upper photo) and low toughness 4T-CT specimen V50-103 (lower photo). Specimens were from the plate 1/4 thickness. 100X.

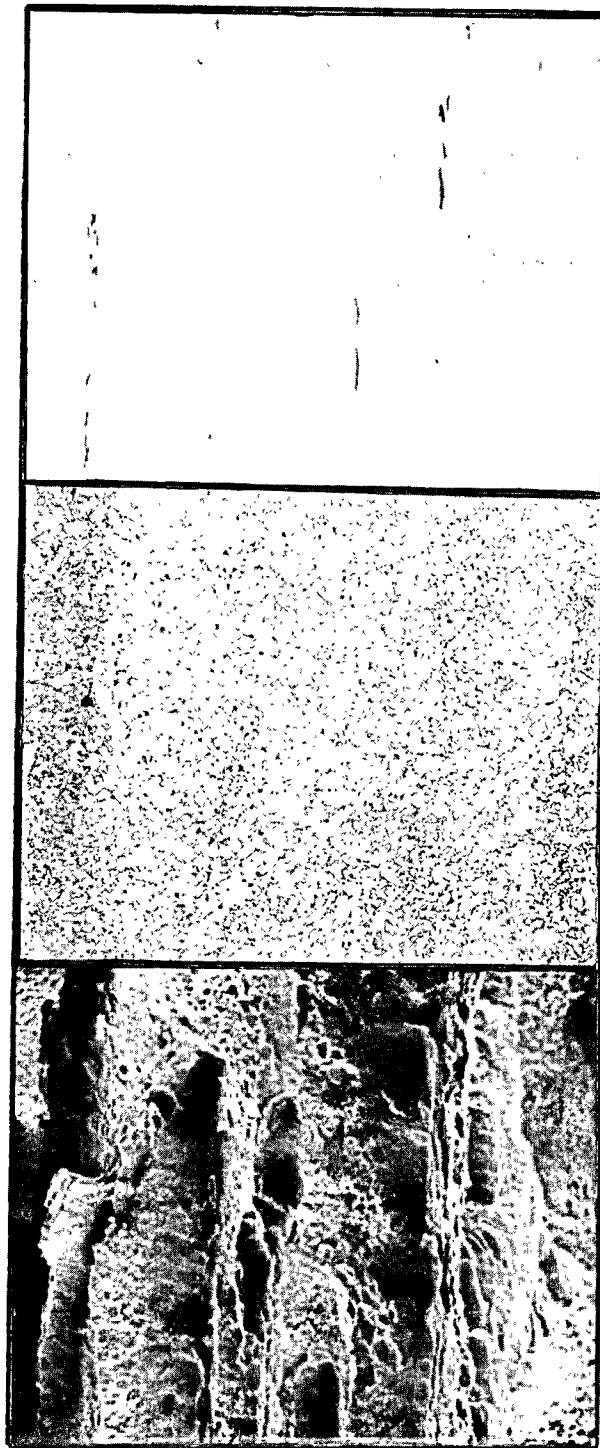


Fig. 90 Visual correlation of the L-LT surface showing the inclusion distribution (upper photo), microstructure with banding (middle photo), and fracture surface with splits (lower photo). Crack growth is from bottom to top. 100X.

7. DISCUSSION

The size dependence observed for the J-R curves of this A 302-B plate is quite unexpected, in particular given the magnitude of the differences between data from small (0.5T-CT) and large (4T- and 6T-CT) specimens. Although the microstructural and fractographic evaluation indicated no significant differences through the plate thickness or between the fracture surfaces for the high (0.5T-CT) and low (4T-CT) toughness specimens, the presence of the laminations or splits is undoubtedly the core cause for the size dependence. The mechanism(s) by which these laminations (probably) cause the size dependence is not identified or understood at this point (or within the scope of the present study), but clearly warrant investigation to assess the potential safety concerns for those commercial plants using such a material, or possibly other materials exhibiting similar characteristics.

In Ref. 20 to 22, the deleterious effect of this splitting behavior on the C_v impact toughness of controlled-rolled steels was generally tied to a relative measure of the splits, such as the number of splits per unit thickness, or a separation index giving the length of separations per unit area. In both cases, an increase in the lamination parameter was readily tied to reductions in toughness. Use of such a parameter would probably not indicate any difference in expected toughness for the specimens from this A 302-B plate, since the splits in this material tend to be fairly uniformly spaced, and each parameter would probably give the same value for both the low and the high toughness specimens. Possibly the total number of splits and not a relative parameter has the strongest influence on the specimen size dependency. The confounding part of these results, which defies explanation at this time, is how this laminated-type of microstructure results in such a marked reduction in toughness when increasing the specimen size.

Tests for three low strength structural steels (actually three grades of American Bureau of Shipping, ABS, steels), tested with 1T-CT specimens only, likewise resulted in some splits on the fracture surfaces (Ref. 23). In this case, the steel exhibiting a large single split had the highest J-R curve levels, whereas a heat with more numerous small (shorter) splits had the lowest toughness. In the latter case, the splits are quite small and very difficult to see without magnification. The third heat, which exhibited toughness levels intermediate to those of the other heats, had several splits which were of a size between those for the other heats. The ranking in toughness was found to coincide with that from C_v impact tests as well. These results would therefore appear to be in general agreement with those from Ref. 20 to 22. The (still) outstanding question is how these splits cause reduced toughness with increased specimen size.

One other postulated cause for the size dependence is the low test temperature, in particular with respect to the transition region. One suggestion is that a strain-aging type of mechanism is responsible for the low toughness in the large specimens, and use of a higher test temperature (more typical of RPV operating conditions) may give more

reasonable results. A second explanation relates to the closeness of the test temperature to the transition region and the possible influence of a cleavage micro-cracking mechanism, such as in the banded regions of the microstructure. Even with local cleavage resulting in the splits, the presence of ductile tearing between the splits and the similarity of fracture surfaces between large and small specimens make intuitive explanation of the size dependence impossible at this time.

Of particular bearing to the issue of J_M vs. J_D , the observed differences between J-R curves developed at MEA and the USNA are of interest. The postulated effect of using specimens with long initial crack length (a/W of ~ 0.6) as opposed to a short initial crack length (a/W of ~ 0.5) would help to explain discrepancies between results at USNA (and the David Taylor Research Center) and other investigators using similar materials. Although this initial crack length effect has not been reported in other work, a more careful evaluation of past results may indicate a similar effect. Separation of this variable from the J_M - J_D discussion should help to clarify the problems and advantages of using each formulation of J .

As an aside, correlations relating Charpy-V upper shelf energy level to J_M -R curve toughness have been developed. This work, while unpublished, was under consideration by ASME Section XI committee members. Applying these correlations to this plate (C_V energy of 73 J or 54 ft-lb) at the test temperature of 82°C (180°F), the power law for this plate is estimated to be:

$$J = 150.6 \Delta a^{0.3116} \quad \text{for } \Delta a < 2.5 \text{ mm}$$

$$J = 149.1 \Delta a^{0.3756} \quad \text{for } \Delta a > 5 \text{ mm}$$

As illustrated in Fig. 91, the estimated J-R curve is in good agreement with the measured data from the 0.5T-CT specimens.

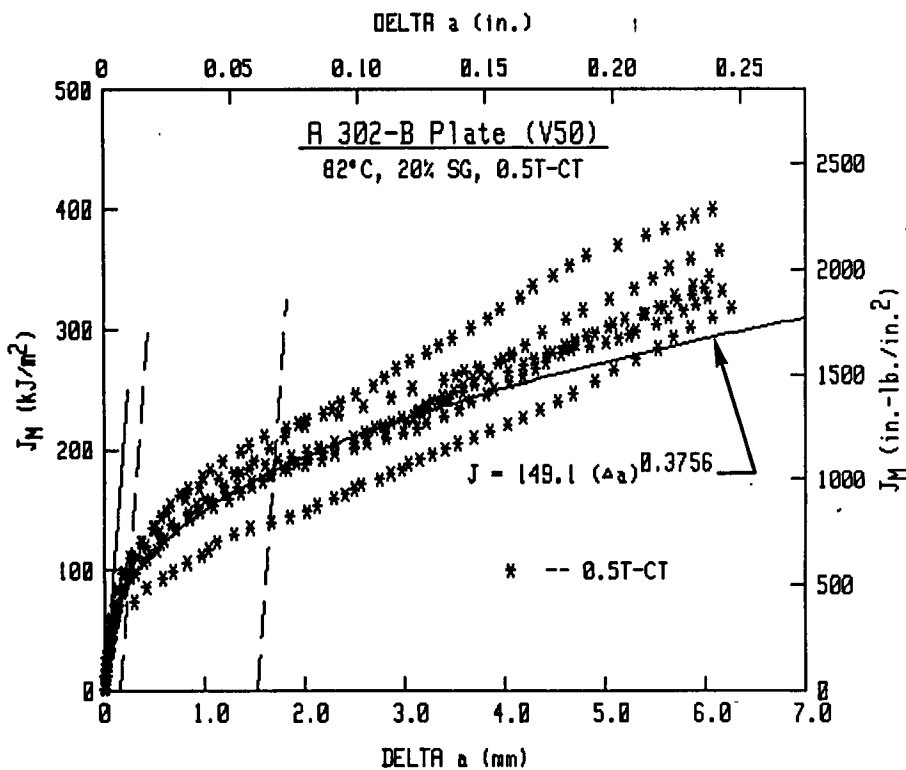
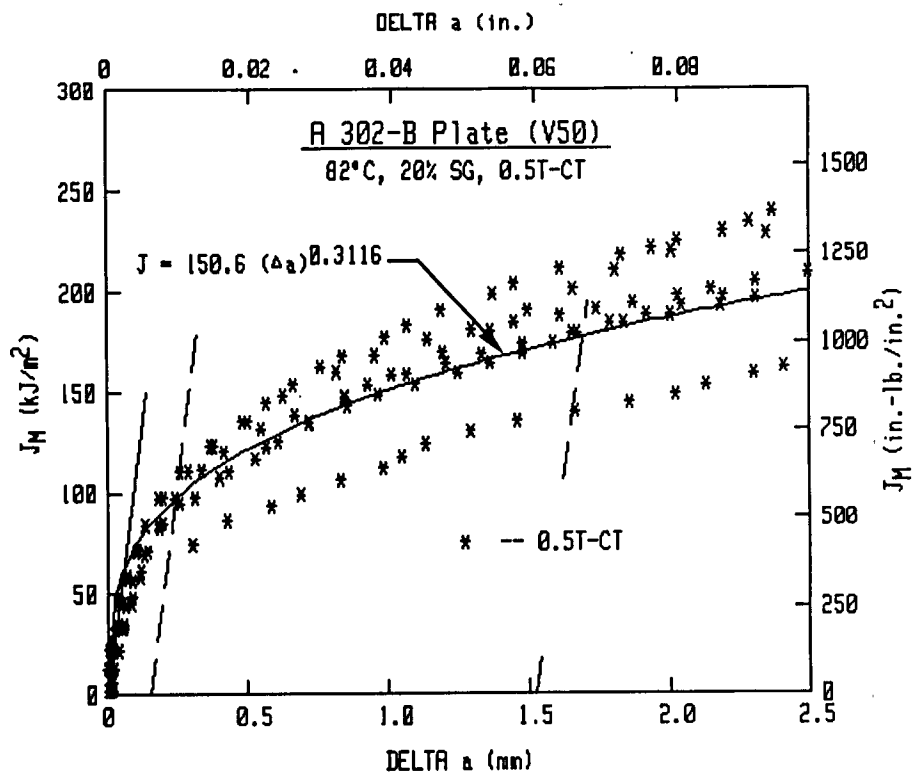


Fig. 91 Comparison of J_M -R curve data for the 0.5T-CT specimens with estimates using correlations.

8. CONCLUSIONS

This work was initially intended to provide guidance on data extrapolation procedures as would be required in the evaluation of RPVs for which low C_v upper shelf levels are measured or predicted. Instead, a significant size dependence was found for the A 302-B plate used in this study. This size dependence is without parallel from previous experience using elastic-plastic fracture mechanics techniques with RPV steels, and is evident regardless of the parameter (J , δ_5 , etc.) or the J formulation used. This size dependence could result in significant nonconservative estimates of thick section fracture behavior, if trends from small specimens are used as a benchmark. Of particular concern would be data from small surveillance specimens in a direct application to thick section RPV analyses.

The A 302-B plate used for this study is believed to be representative of steels used in early nuclear vessel construction. Consequently, the appearance of "splits" associated with either the MnS inclusions or the banded regions of the microstructure, and the resultant size effect, would be expected to occur in the A 302-B plates made according to the same practice. Consequently, an explanation of the size dependence observed for the A 302-B plate is required, in particular for potential application to those nuclear plants with similar materials, and to ensure that such an extreme behavior is not more widely applicable.

Conclusions from this work include:

- The A 302-B plate under study exhibited a significant size effect, with smaller specimens giving much higher J -R curve levels than large specimens. However, J_{IC} levels are similar for all specimen sizes.
- No significant through-thickness gradients or variability was seen from fracture toughness, tensile and Charpy-V tests.
- The high content of manganese-sulfide inclusions and/or the banded regions of the microstructure are probably the key causes of the size dependence observed, although the fracture appearance is similar for both large (low toughness) and small (high toughness) specimens.
- Although crack growth prediction errors were large (due to the "woody" appearance of the fracture surface and the extremely irregular crack front), the normalization method proposed by Herrera and Landes did not have a significant effect on the observed size dependence.
- Conclusions about the applicability of J_M and J_D may be geometry sensitive, with short initial a/W (~ 0.5) giving different indications than long initial a/W (~ 0.6).

In terms of extrapolation of the J-R curve data from small specimens to large crack growth levels, a need still exists to provide representative data from low C_v upper shelf weld metal to give guidance on such extrapolation. For this A 302-B plate, determination of the causes for the observed size dependence are needed. Specific recommendations on future work include:

- A similar data extrapolation study using a low C_v upper shelf weld metal; previous experience with such welds has generally yielded good correspondence between J-R curves from different size specimens. The recommended study is intended to give a broader range of specimen sizes (up to 6T-CT) under more closely controlled test conditions.
- A determination of the influence of MnS inclusions and/or the banded regions of the microstructure on the observed size dependence is needed to help determine the applicability of the size dependence to materials actually used in RPV construction. A first step in this determination is a limited study of either the "strong" orientation (L-T per ASTM) or possibly the T-S or L-S orientations in this A 302-B plate.
- Concerns about the relatively low test temperature, specifically the closeness to the transition region and the possibility of a strain-aging mechanism during these tests, could be settled by increasing the test temperature to between 200°C (392°F) and 300°C (572°F).
- Since the apparent size dependence has the appearance of a classic constraint effect, the use of reduced thickness specimens, such that $B < W/2$, would allow the separation of this variable from the list of possibilities.
- Some investigation into the geometry sensitivity of J_M and J_D , in particular initial a/W , could help to clarify the appropriateness of using each parameter in thick section applications, such as RPV safety analyses.

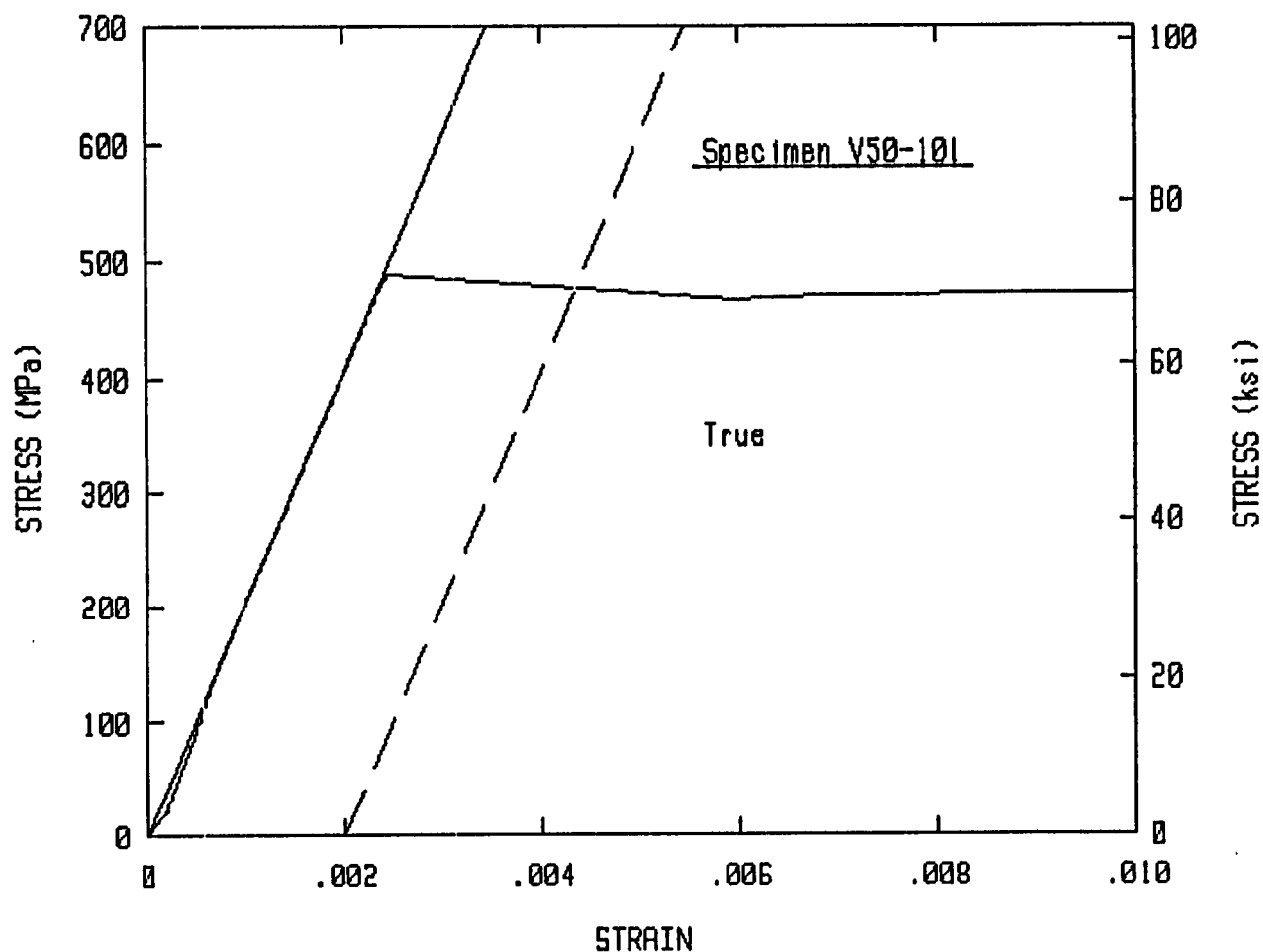
REFERENCES

1. H. A. Ernst, "Materials Resistance and Instability Beyond J-Controlled Crack Growth," Elastic-Plastic Fracture, ASTM STP 803 Vol. 1, American Society for Testing and Materials, Phila., PA, pp. 191-213.
2. F. J. Loss, Ed., "Structural Integrity of Water Reactor Pressure Boundary Components, Annual Report for 1983," USNRC Report NUREG/CR-3228, Vol. 2, Sep. 1984.
3. F. J. Loss, Ed., "Structural Integrity of Water Reactor Pressure Boundary Components, Progress Report Ending 29 Feb 1976," NRL Report 8006, Naval Research Laboratory, Wash., DC, Aug. 26, 1976.
4. G. E. Dieter, Mechanical Metallurgy, McGraw-Hill Book Company, New York, 1976.
5. P. W. Bridgman, Trans. Am. Soc. Met., Vol. 32, 1944, p. 553.
6. D. R. Ireland, W. L. Server, and R. A. Wullaert, "Procedures for Testing and Data Analysis, Task A - Topical Report," ETI Technical Report 75-43, Effects Technology, Inc., Santa Barbara, CA, Oct. 1975, pp. 5-46.
7. A. Saxena and S. J. Hudak, Jr., "Review and Extension of Compliance Information for Common Crack Growth Specimens," International Journal of Fracture, Vol. 14(5), Oct. 1978, pp. 453-468.
8. W. J. Mills, "Effect of Fast-Neutron Irradiation on Fracture Toughness of Alloy A-286," Fracture Mechanics: Fifteenth Symposium, ASTM STP 833, American Society for Testing and Materials, Phila., PA, 1984, pp. 499-515.
9. F. J. Loss, B. H. Menke, and R. A. Gray, Jr., "Development of J-R Curve Procedures," NRL Report 8327, Naval Research Laboratory, Washington, DC, Aug. 1979.
10. J. R. Rice, P. C. Paris, and J. G. Merkle, "Further Results on J Integral Analysis and Estimates," Progress in Flaw Growth and Fracture Toughness Testing, Proceedings of the 1972 National Symposium on Fracture Mechanics, ASTM STP 536, American Society for Testing and Materials, Phila., PA, 1973, pp. 231-245.
11. J. G. Merkle and H. T. Corten, "A J Integral Analysis for the Compact Specimen, Considering Axial Force as Well as Bending Effects," Trans. ASME, Journal of Pressure Vessel Technology, Nov. 1974, pp. 286-292.
12. G. A. Clarke and J. D. Landes, "Evaluation of J for the Compact Specimen," J. Testing and Evaluation, Vol. 7(5), Sep. 1979, pp. 264-269.

13. H. A. Ernst and P. C. Paris, "Techniques of Analysis of Load-Displacement Records by J-Integral Methods," USNRC Report NUREG/CR-1222, Jan. 1980.
14. A. L. Hiser, F. J. Loss, and B. H. Menke, "J-R Curve Characterization of Irradiated Low Upper Shelf Welds," USNRC Report NUREG/CR-3506, Apr. 1984.
15. J. R. Hutchinson and P. C. Paris, "The Theory of Stability Analysis of J-Controlled Crack Growth," Elastic-Plastic Fracture, ASTM STP 668, American Society for Testing and Materials, Phila., PA, Mar. 1979, pp. 37-64.
16. C. F. Shih, "An Engineering Approach for Examining Crack Growth and Stability in Flawed Structures," Proceedings of CSNI Specialists Meeting in Plastic Tearing Instability, USNRC Conference Proceeding NUREG/CP-0010, Jan. 1980.
17. K.-H. Schwalbe and D. Hellmann, "Correlation of Stable Crack Growth With the J-Integral and Crack Tip Opening Displacement, Effects of Geometry, Size, and Material," Progress Report on an Investigation of the Elastic-Plastic R-Curve Methodology, GKSS 84/E/37, Aug. 1984.
18. R. Herrera and J. D. Landes, "A Direct J-R Curve Analysis of Fracture Toughness Tests," Journal of Testing and Evaluation, JTEVA, Vol. 16, No. 5, Sept. 1988, pp. 427-449.
19. P. M. Yuzawich and C. W. Huges, "An Improved Technique For Removal of Oxide Scale From Fractured Surfaces of Ferrous Materials," Practical Metallography, Vol. 15, 1978, pp. 184-195.
20. J. D. Emburg, N. J. Petch, A. E. Wraith and E. S. Wright, "The Fracture of Mild Steel Laminates," Transactions of the Metallurgical Society of AIME, Vol. 239, Jan. 1967, pp. 114-118.
21. E. Miyoshi, M. Fukuda, H. Iwanaga and T. Okazawa, "The Effect of Separation on the Propagating Shear Fracture, Paper 4 Crack Propagation in Pipelines, The Institute of Gas Engineers, Mar. 1974, pp. 1-21.
22. W. A. Poynton and J. R. Christian, "An Experimental Study of Shear Fracture Propagation Using Small Scale Models," Paper 5, Crack Propagation in Pipelines, The Institute of Gas Engineers, Mar. 1974, pp. 1-26.
23. B. H. Menke, A. L. Hiser, J. R. Hawthorne and F. J. Loss, "R Curve Characterization of Low-Strength Structural Steels," EPRI NP-2715, Electric Power Research Institute, Palo Alto, CA, Oct. 1982.

APPENDIX A

COMPILATION OF RESULTS FROM TENSILE TESTS



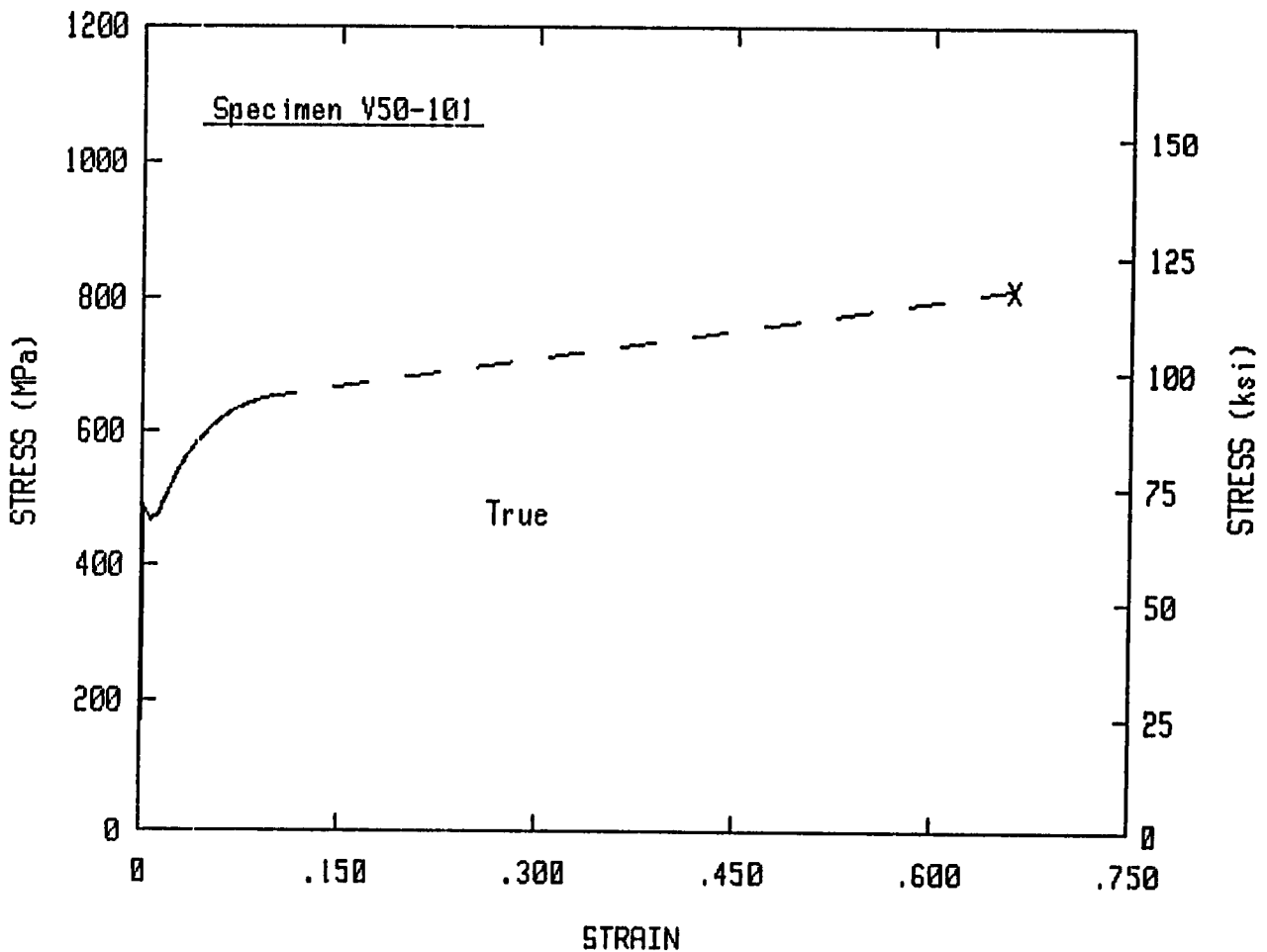
TEST SPECIMEN DATA

Date	= 04/12/88	Test Temperature	= 82.2 °C
Gage Length	= 25.4 mm	Gage Diameter	= 12.8 mm
Reduction in Area	= 48.3 %		
Elongation	= 18.9 % in 50.7 mm		

Material = A302-B
Material Form = Plate

True Stress/Strain Curve

Young's Modulus	= 20.33E+04 MPa	(used for Yield strength)
Elastic Testing Rate	= 499.1 MPa/min	(based on initial linear curve)
Yield Strength (0.2%)	= 473.6 MPa	
Fracture Stress	= 813 MPa	



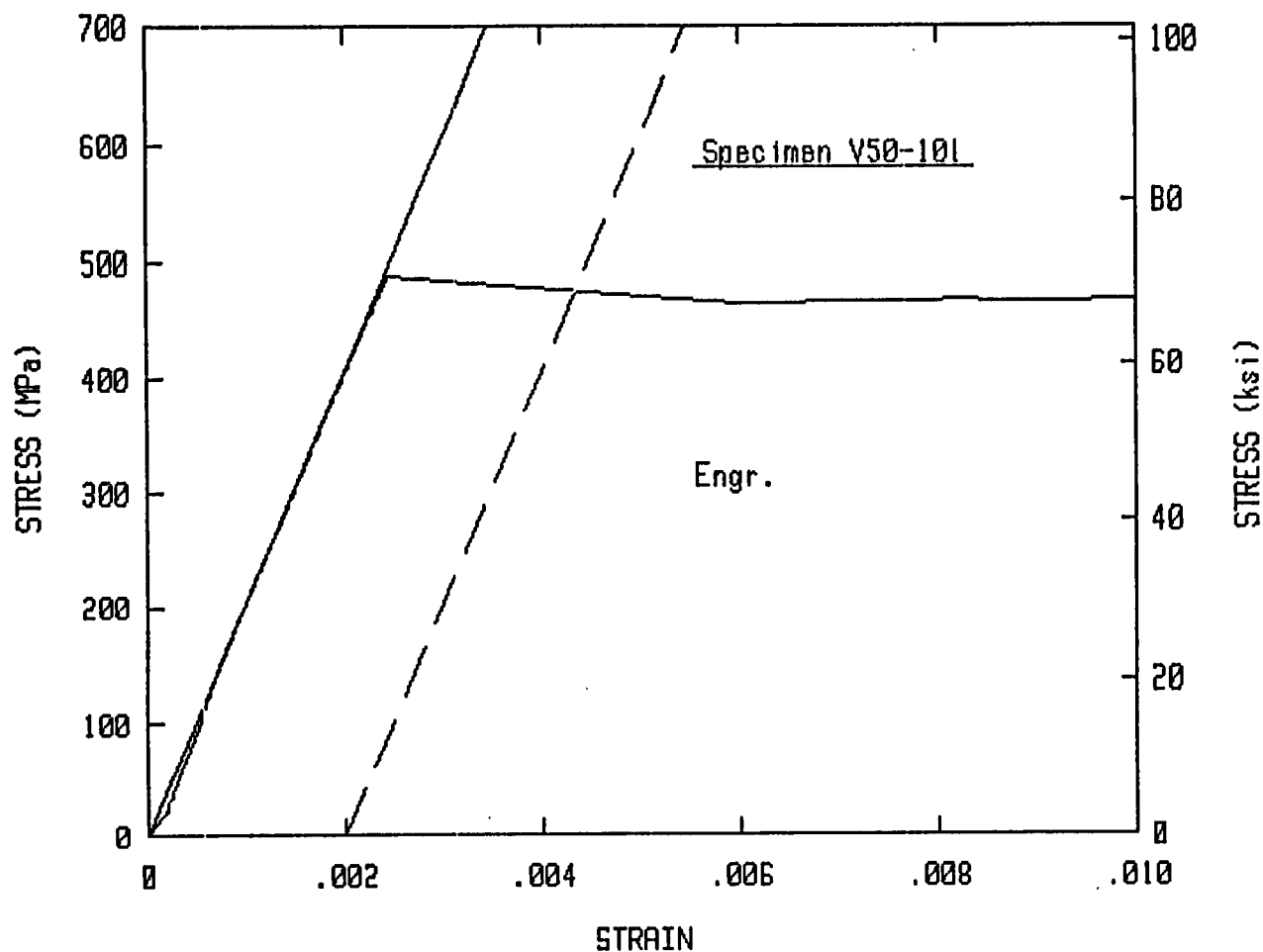
TEST SPECIMEN DATA

Date	= 04/12/88	Test Temperature	= 82.2 °C
Gage Length	= 25.4 mm	Gage Diameter	= 12.8 mm
Reduction in Area	= 48.3 %		
Elongation	= 18.9 % in 50.7 mm		

Material = A302-B
Material Form = Plate

True Stress/Strain Curve

Young's Modulus	= 20.33E+04 MPa	(used for Yield strength)
Elastic Testing Rate	= 499.1 MPa/min	(based on initial linear curve)
Yield Strength (0.2%)	= 473.6 MPa	
Fracture Stress	= 813 MPa	



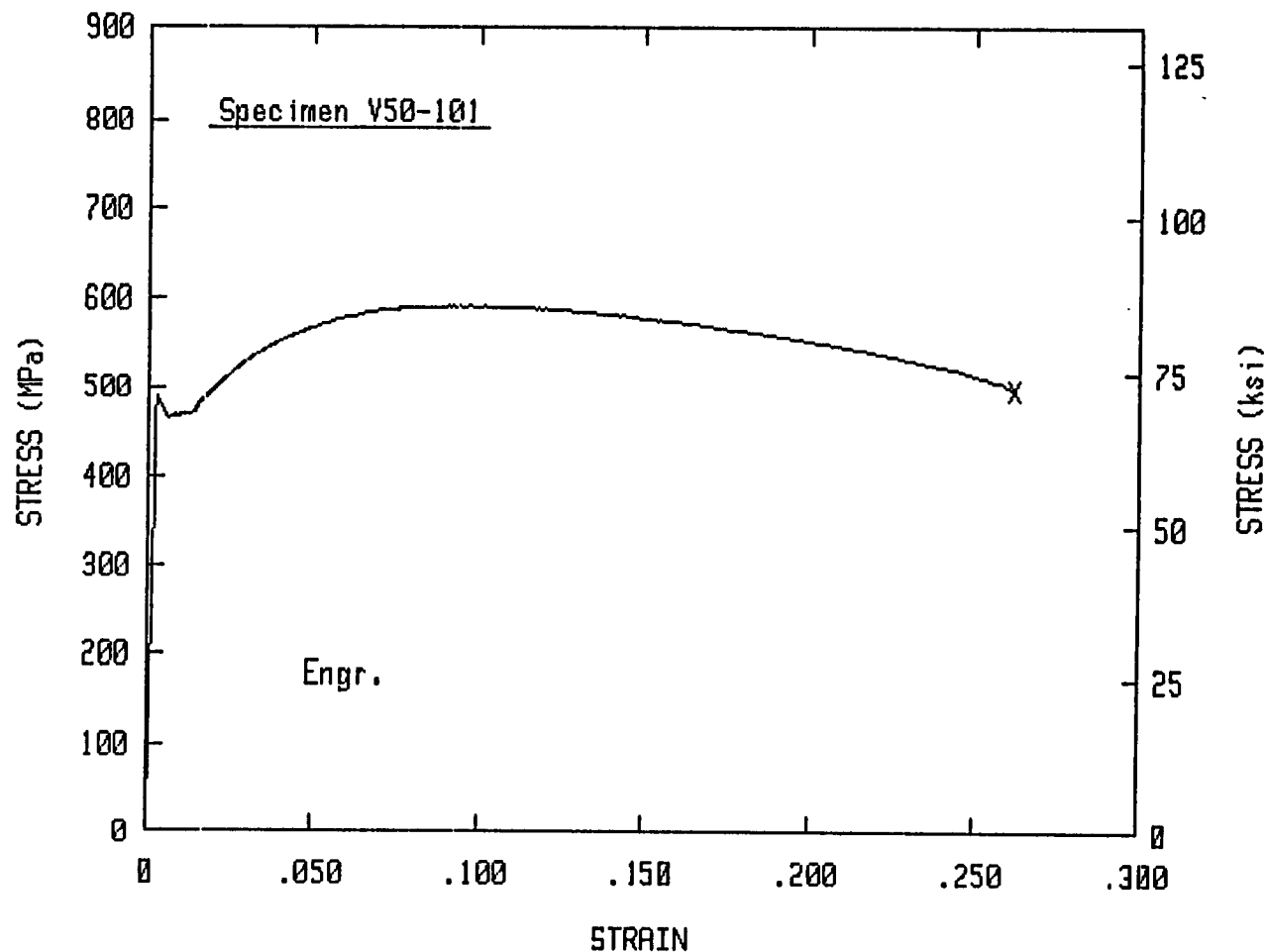
TEST SPECIMEN DATA

Date	= 04/12/88	Test Temperature	= 82.2 °C
Gage Length	= 25.4 mm	Gage Diameter	= 12.8 mm
Reduction in Area	= 48.3 %		
Elongation	= 18.9 % in 50.7 mm		

Material = A302-B
Material Form = Plate

Engineering Stress/Strain Curve

Young's Modulus	= 20.26E+04 MPa	(used for Yield strength)
Elastic Testing Rate	= 499.1 MPa/min	(based on initial linear curve)
Yield Strength (0.2%)	= 471.3 MPa	
Ultimate Strength	= 592.2 MPa	



TEST SPECIMEN DATA

Date	= 04/12/88	Test Temperature	= 82.2 °C
Gage Length	= 25.4 mm	Gage Diameter	= 12.8 mm
Reduction in Area	= 48.3 %		
Elongation	= 18.9 % in 50.7 mm		

Material = A302-B
Material Form = Plate

Engineering Stress/Strain Curve

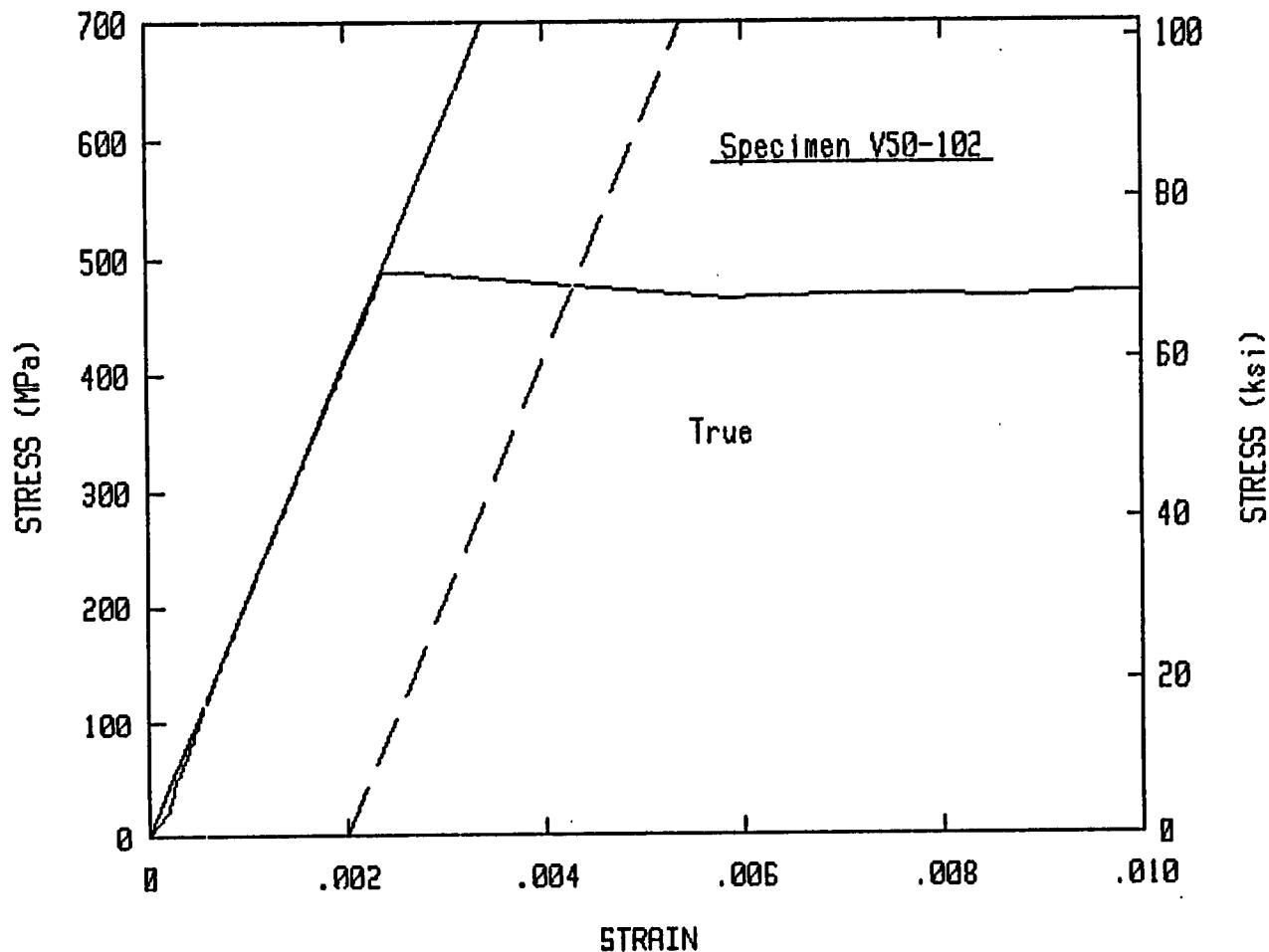
Young's Modulus	= 20.26E+04 MPa	(used for Yield strength)
Elastic Testing Rate	= 499.1 MPa/min	(based on initial linear curve)
Yield Strength (0.2%)	= 471.3 MPa	
Ultimate Strength	= 592.2 MPa	

Specimen : V50-101
Test Temp : 82°C

POINT #	ENGR. STRESS (MPa)	ENGR. STRAIN (mm/mm)	TRUE STRESS (MPa)	TRUE STRAIN (mm/mm)
1	22.89	0.0002	22.90	0.0002
2	25.78	0.0002	25.79	0.0002
3	54.87	0.0003	54.89	0.0003
4	86.28	0.0005	86.32	0.0005
5	119.40	0.0006	119.47	0.0006
6	153.20	0.0007	153.31	0.0007
7	187.83	0.0009	188.00	0.0009
8	223.27	0.0011	223.51	0.0011
9	259.13	0.0013	259.47	0.0013
10	294.38	0.0015	294.81	0.0015
11	329.98	0.0016	330.51	0.0016
12	365.71	0.0018	366.37	0.0018
13	401.03	0.0020	401.82	0.0020
14	435.72	0.0022	436.66	0.0022
15	469.32	0.0023	470.41	0.0023
16	465.74	0.0065	468.78	0.0065
17	468.22	0.0102	472.99	0.0101
18	470.42	0.0133	476.67	0.0132
19	474.14	0.0144	480.95	0.0143
20	479.58	0.0151	486.84	0.0150
21	486.74	0.0169	494.95	0.0167
22	500.58	0.0205	510.85	0.0203
23	513.66	0.0243	526.13	0.0240
24	525.50	0.0281	540.27	0.0277
25	536.17	0.0320	553.30	0.0315
26	545.46	0.0359	565.02	0.0352
27	553.31	0.0398	575.32	0.0390
28	559.51	0.0435	583.84	0.0426
29	564.47	0.0467	590.83	0.0456
30	570.36	0.0509	599.40	0.0496
31	577.73	0.0572	610.76	0.0556
32	585.81	0.0670	625.06	0.0649
33	588.84	0.0730	631.83	0.0705
34	590.76	0.0794	637.66	0.0764
35	591.18	0.0860	641.99	0.0825
36	591.59	0.0930	646.62	0.0889
37	591.93	0.1006		
38	591.04	0.1090		
39	589.53	0.1181		
40	587.05	0.1277		
41	583.74	0.1378		
42	580.16	0.1481		
43	575.41	0.1587		
44	570.11	0.1696		
45	565.29	0.1806		
46	558.48	0.1916		
47	551.80	0.2029		
48	543.67	0.2144		
49	535.55	0.2260		
50	497.68	0.2619	812.94	0.6599

Specimen : V50-101
Test Temp : 180°F

POINT #	ENGR. STRESS (ksi)	ENGR. STRAIN (in./in.)	TRUE STRESS (ksi)	TRUE STRAIN (in./in.)
1	3.32	0.0002	3.32	0.0002
2	3.74	0.0002	3.74	0.0002
3	7.96	0.0003	7.96	0.0003
4	12.51	0.0005	12.52	0.0005
5	17.32	0.0006	17.33	0.0006
6	22.22	0.0007	22.24	0.0007
7	27.24	0.0009	27.27	0.0009
8	32.38	0.0011	32.42	0.0011
9	37.58	0.0013	37.63	0.0013
10	42.70	0.0015	42.76	0.0015
11	47.86	0.0016	47.94	0.0016
12	53.04	0.0018	53.14	0.0018
13	58.16	0.0020	58.28	0.0020
14	63.20	0.0022	63.33	0.0022
15	68.07	0.0023	68.23	0.0023
16	67.55	0.0065	67.99	0.0065
17	67.91	0.0102	68.60	0.0101
18	68.23	0.0133	69.13	0.0132
19	68.77	0.0144	69.76	0.0143
20	69.56	0.0151	70.61	0.0150
21	70.60	0.0169	71.79	0.0167
22	72.60	0.0205	74.09	0.0203
23	74.50	0.0243	76.31	0.0240
24	76.22	0.0281	78.36	0.0277
25	77.76	0.0320	80.25	0.0315
26	79.11	0.0359	81.95	0.0352
27	80.25	0.0398	83.44	0.0390
28	81.15	0.0435	84.68	0.0426
29	81.87	0.0467	85.69	0.0456
30	82.72	0.0509	86.94	0.0496
31	83.79	0.0572	88.58	0.0556
32	84.96	0.0670	90.66	0.0649
33	85.40	0.0730	91.64	0.0705
34	85.68	0.0794	92.48	0.0764
35	85.74	0.0860	93.11	0.0825
36	85.80	0.0930	93.78	0.0889
37	85.85	0.1006		
38	85.72	0.1090		
39	85.50	0.1181		
40	85.14	0.1277		
41	84.66	0.1378		
42	84.15	0.1481		
43	83.46	0.1587		
44	82.69	0.1696		
45	81.99	0.1806		
46	81.00	0.1916		
47	80.03	0.2029		
48	78.85	0.2144		
49	77.67	0.2260		
50	72.18	0.2619	117.91	0.6599



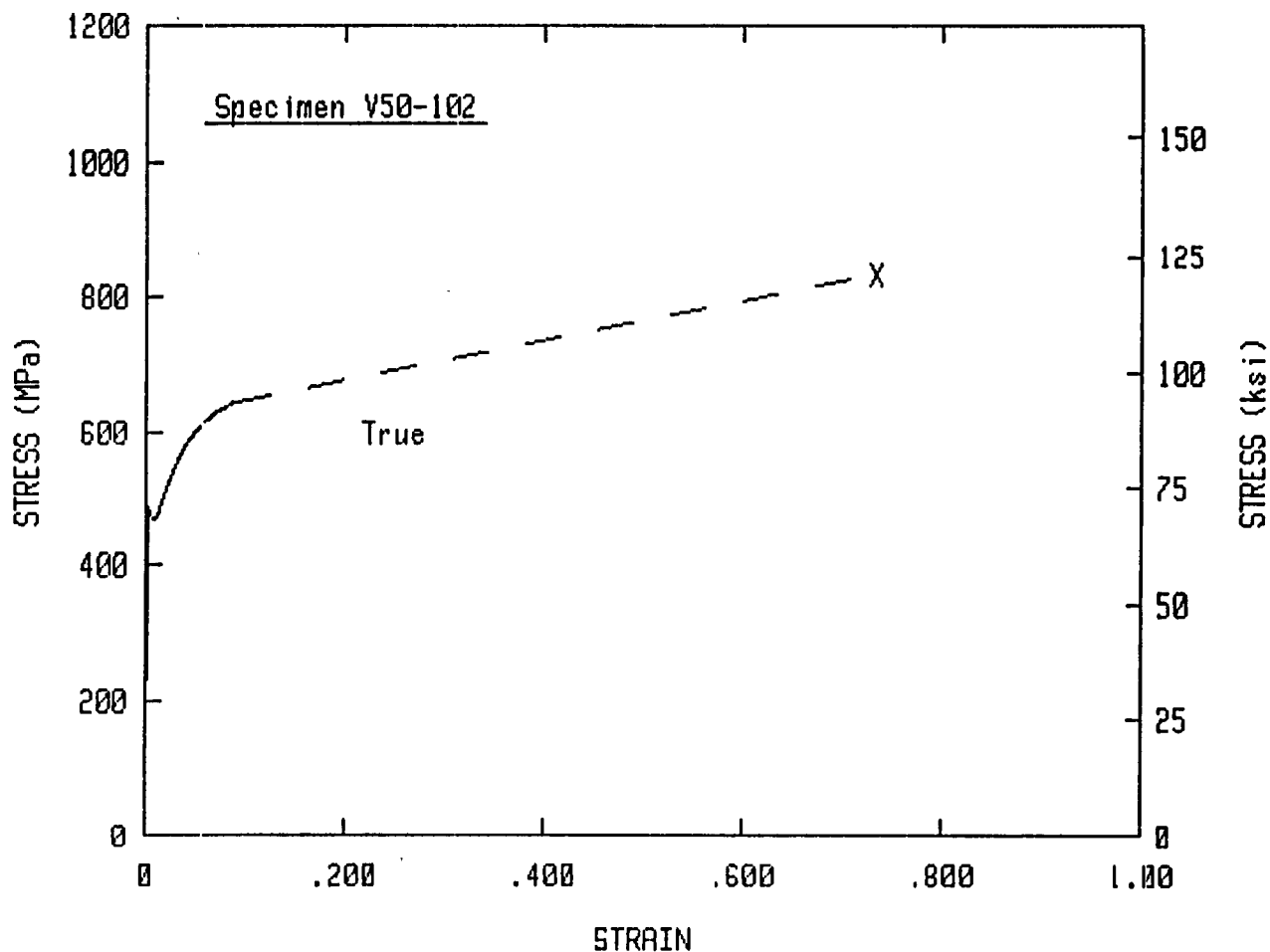
TEST SPECIMEN DATA

Date	= 04/12/88	Test Temperature	= 82.2 °C
Gage Length	= 25.4 mm	Gage Diameter	= 12.8 mm
Reduction in Area	= 51.9 %		
Elongation	= 18.3 % in 50.3 mm		

Material = A302-B
Material Form = Plate

True Stress/Strain Curve

Young's Modulus	= 20.70E+04 MPa	(used for Yield strength)
Elastic Testing Rate	= 485.6 MPa/min	(based on initial linear curve)
Yield Strength (0.2%)	= 465.8 MPa	
Fracture Stress	= 834.5 MPa	



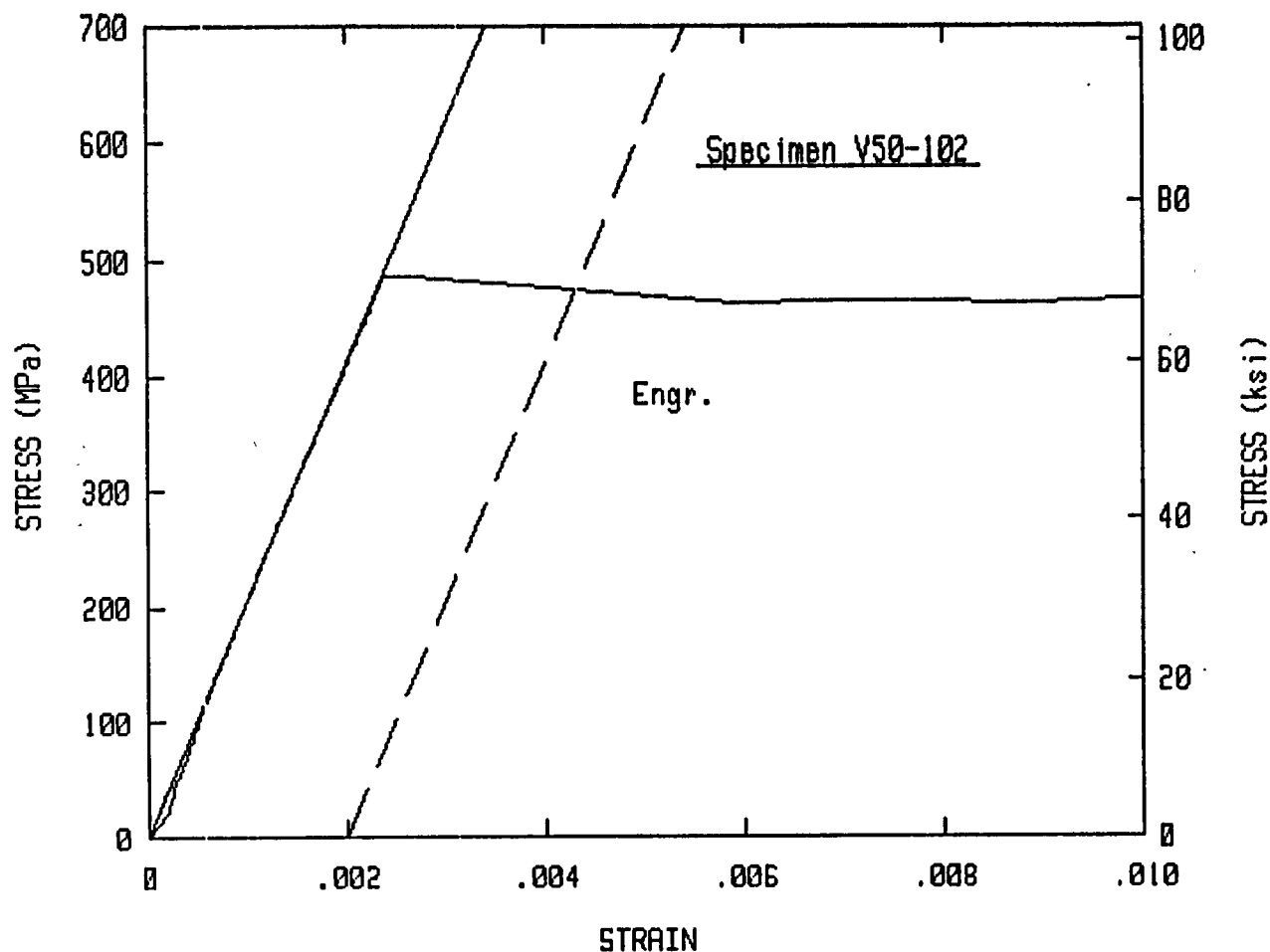
TEST SPECIMEN DATA

Date	= 04/12/88	Test Temperature	= 82.2 °C
Gage Length	= 25.4 mm	Gage Diameter	= 12.8 mm
Reduction in Area	= 51.9 %		
Elongation	= 18.3 % in 50.3 mm		

Material = A302-B
Material Form = Plate

True Stress/Strain Curve

Young's Modulus	= 20.70E+04 MPa	(used for Yield strength)
Elastic Testing Rate	= 485.6 MPa/min	(based on initial linear curve)
Yield Strength (0.2%)	= 465.8 MPa	
Fracture Stress	= 834.5 MPa	



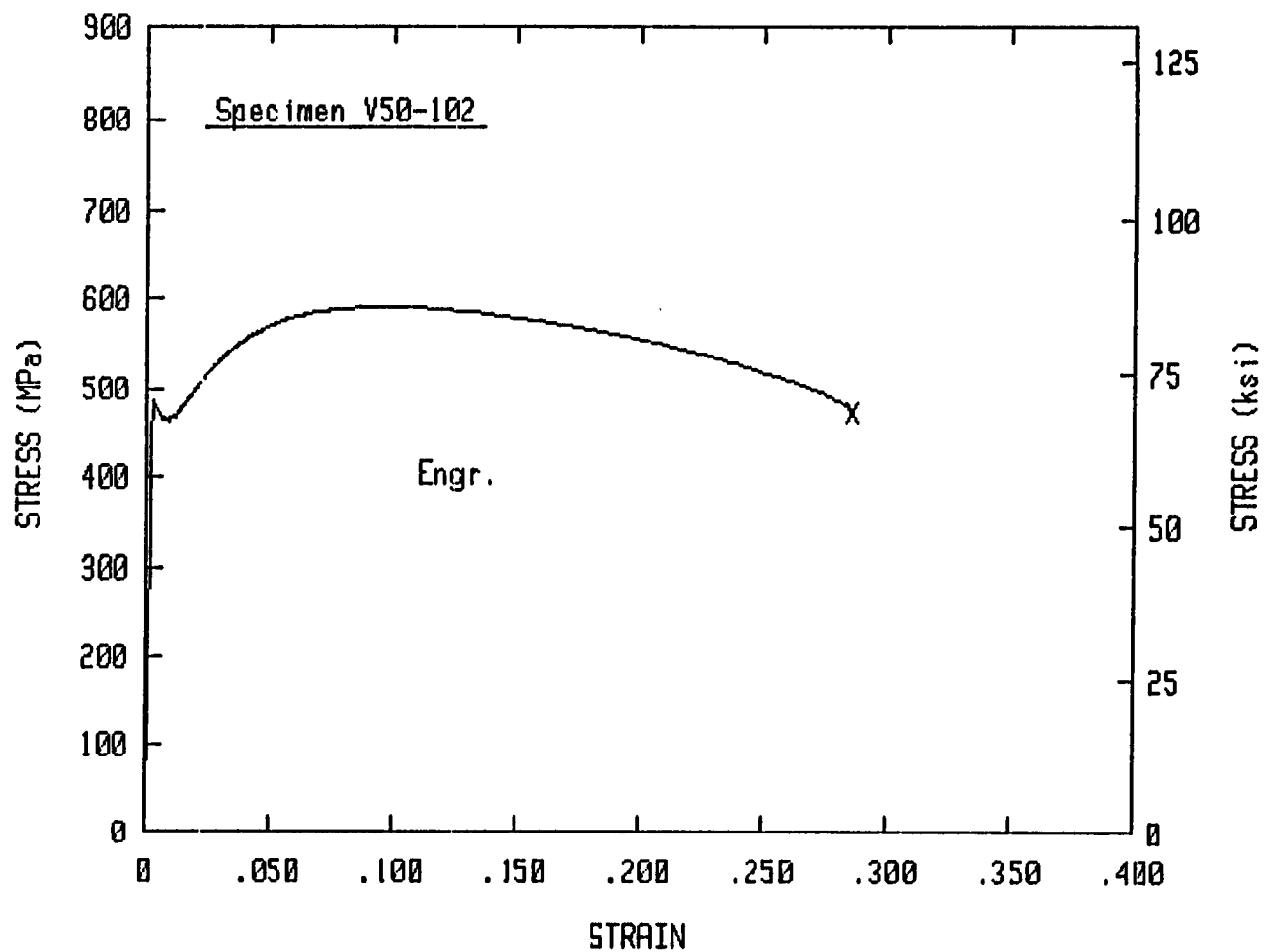
TEST SPECIMEN DATA

Date	= 04/12/88	Test Temperature	= 82.2 °C
Gage Length	= 25.4 mm	Gage Diameter	= 12.8 mm
Reduction in Area	= 51.9 %		
Elongation	= 18.3 % in 50.3 mm		

Material = A302-B
Material Form = Plate

Engineering Stress/Strain Curve

Young's Modulus	= 20.60E+04 MPa	(used for Yield strength)
Elastic Testing Rate	= 485.6 MPa/min	(based on initial linear curve)
Yield Strength (0.2%)	= 463.2 MPa	
Ultimate Strength	= 590.8 MPa	



TEST SPECIMEN DATA

Date	= 04/12/88	Test Temperature	= 82.2 °C
Gage Length	= 25.4 mm	Gage Diameter	= 12.8 mm
Reduction in Area	= 51.9 %		
Elongation	= 18.3 % in 50.3 mm		

Material = A302-B
Material Form = Plate

Engineering Stress/Strain Curve

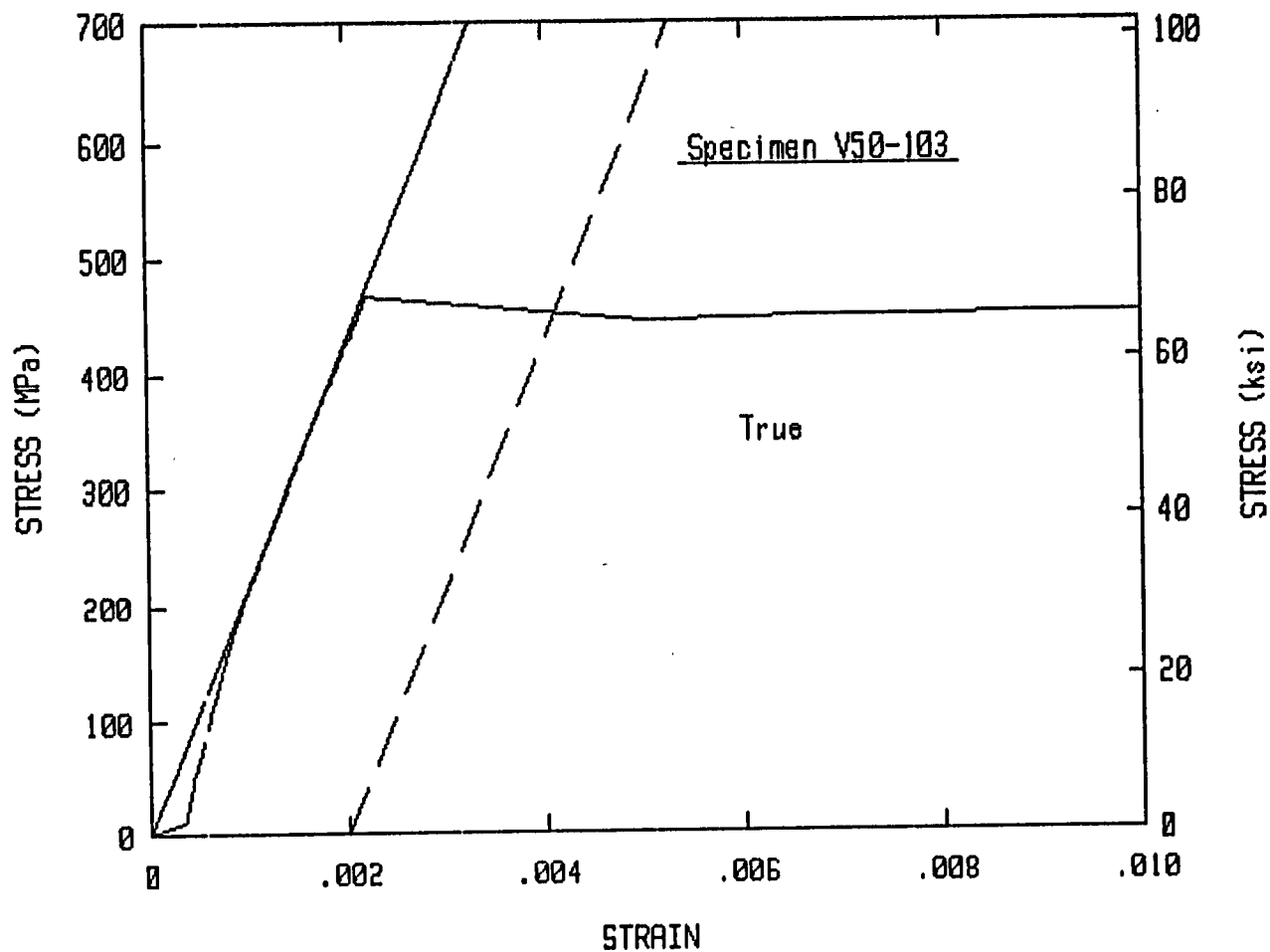
Young's Modulus	= 20.60E+04 MPa	(used for Yield strength)
Elastic Testing Rate	= 485.6 MPa/min	(based on initial linear curve)
Yield Strength (0.2%)	= 463.2 MPa	
Ultimate Strength	= 590.8 MPa	

Specimen : V50-102
Test Temp : 82°C

POINT #	ENGR. STRESS (MPa)	ENGR. STRAIN (mm/mm)	TRUE STRESS (MPa)	TRUE STRAIN (mm/mm)
1	20.43	0.0002	20.44	0.0002
2	28.52	0.0002	28.53	0.0002
3	57.07	0.0003	57.08	0.0003
4	87.19	0.0004	87.23	0.0004
5	119.66	0.0006	119.73	0.0006
6	152.61	0.0007	152.72	0.0007
7	186.50	0.0009	186.66	0.0009
8	221.13	0.0011	221.37	0.0011
9	255.76	0.0012	256.08	0.0012
10	290.60	0.0014	291.01	0.0014
11	326.05	0.0016	326.57	0.0016
12	360.96	0.0018	361.59	0.0018
13	396.00	0.0019	396.76	0.0019
14	430.22	0.0021	431.12	0.0021
15	464.43	0.0023	465.49	0.0023
16	463.74	0.0062	466.61	0.0062
17	465.81	0.0095	470.23	0.0094
18	469.46	0.0117	474.95	0.0116
19	472.90	0.0129	479.00	0.0128
20	479.03	0.0141	485.78	0.0140
21	487.43	0.0164	495.40	0.0162
22	502.50	0.0205	512.79	0.0203
23	516.41	0.0247	529.17	0.0244
24	529.70	0.0290	545.05	0.0286
25	541.13	0.0334	559.17	0.0328
26	550.76	0.0379	571.61	0.0372
27	559.51	0.0425	583.27	0.0416
28	566.39	0.0473	593.21	0.0463
29	572.45	0.0524	602.43	0.0510
30	577.89	0.0576	611.20	0.0560
31	581.95	0.0632	618.74	0.0613
32	585.53	0.0691	626.01	0.0668
33	587.74	0.0755	632.09	0.0728
34	589.18	0.0823	637.68	0.0791
35	590.08	0.0898	643.08	0.0860
36	590.56	0.0981		
37	589.87	0.1073		
38	588.63	0.1175		
39	585.95	0.1285		
40	582.43	0.1398		
41	577.96	0.1516		
42	572.86	0.1636		
43	567.56	0.1756		
44	561.50	0.1880		
45	554.62	0.2004		
46	546.29	0.2130		
47	537.48	0.2258		
48	527.77	0.2385		
49	516.69	0.2516		
50	472.97	0.2861	834.51	0.7321

Specimen : V50-102
Test Temp : 180°F

POINT #	ENGR. STRESS (ksi)	ENGR. STRAIN (in./in.)	TRUE STRESS (ksi)	TRUE STRAIN (in./in.)
1	2.96	0.0002	2.96	0.0002
2	4.14	0.0002	4.14	0.0002
3	8.28	0.0003	8.28	0.0003
4	12.65	0.0004	12.65	0.0004
5	17.36	0.0006	17.37	0.0006
6	22.13	0.0007	22.15	0.0007
7	27.05	0.0009	27.07	0.0009
8	32.07	0.0011	32.11	0.0011
9	37.10	0.0012	37.14	0.0012
10	42.15	0.0014	42.21	0.0014
11	47.29	0.0016	47.36	0.0016
12	52.35	0.0018	52.44	0.0018
13	57.43	0.0019	57.55	0.0019
14	62.40	0.0021	62.53	0.0021
15	67.36	0.0023	67.51	0.0023
16	67.26	0.0062	67.68	0.0062
17	67.56	0.0095	68.20	0.0094
18	68.09	0.0117	68.89	0.0116
19	68.59	0.0129	69.47	0.0128
20	69.48	0.0141	70.46	0.0140
21	70.70	0.0164	71.85	0.0162
22	72.88	0.0205	74.37	0.0203
23	74.90	0.0247	76.75	0.0244
24	76.83	0.0290	79.05	0.0286
25	78.48	0.0334	81.10	0.0328
26	79.88	0.0379	82.91	0.0372
27	81.15	0.0425	84.60	0.0416
28	82.15	0.0473	86.04	0.0463
29	83.03	0.0524	87.37	0.0510
30	83.82	0.0576	88.65	0.0560
31	84.41	0.0632	89.74	0.0613
32	84.92	0.0691	90.79	0.0668
33	85.24	0.0755	91.68	0.0728
34	85.45	0.0823	92.49	0.0791
35	85.58	0.0898	93.27	0.0860
36	85.65	0.0981		
37	85.55	0.1073		
38	85.37	0.1175		
39	84.98	0.1285		
40	84.47	0.1398		
41	83.83	0.1516		
42	83.09	0.1636		
43	82.32	0.1756		
44	81.44	0.1880		
45	80.44	0.2004		
46	79.23	0.2130		
47	77.95	0.2258		
48	76.55	0.2385		
49	74.94	0.2516		
50	68.60	0.2861	121.03	0.7321



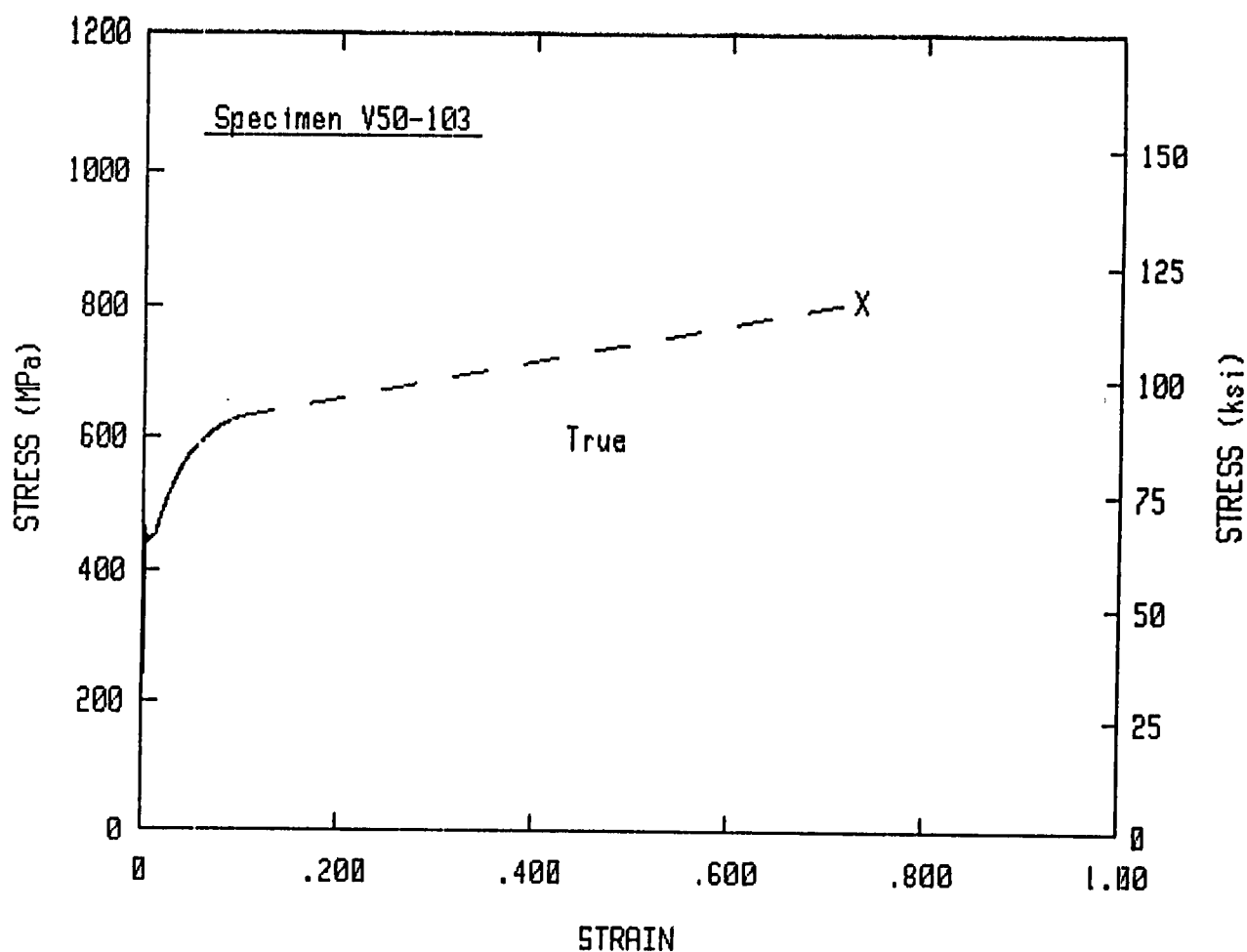
TEST SPECIMEN DATA

Date	= 04/12/88	Test Temperature	= 82.2 °C
Gage Length	= 25.4 mm	Gage Diameter	= 12.8 mm
Reduction in Area	= 51.9 %		
Elongation	= 18.9 % in 50.8 mm		

Material	= A302-B
Material Form	= Plate

True Stress/Strain Curve

Young's Modulus	= 21.38E+04 MPa	(used for Yield strength)
Elastic Testing Rate	= 478.7 MPa/min	(based on initial linear curve)
Yield Strength (0.2%)	= 445.2 MPa	
Fracture Stress	= 811 MPa	



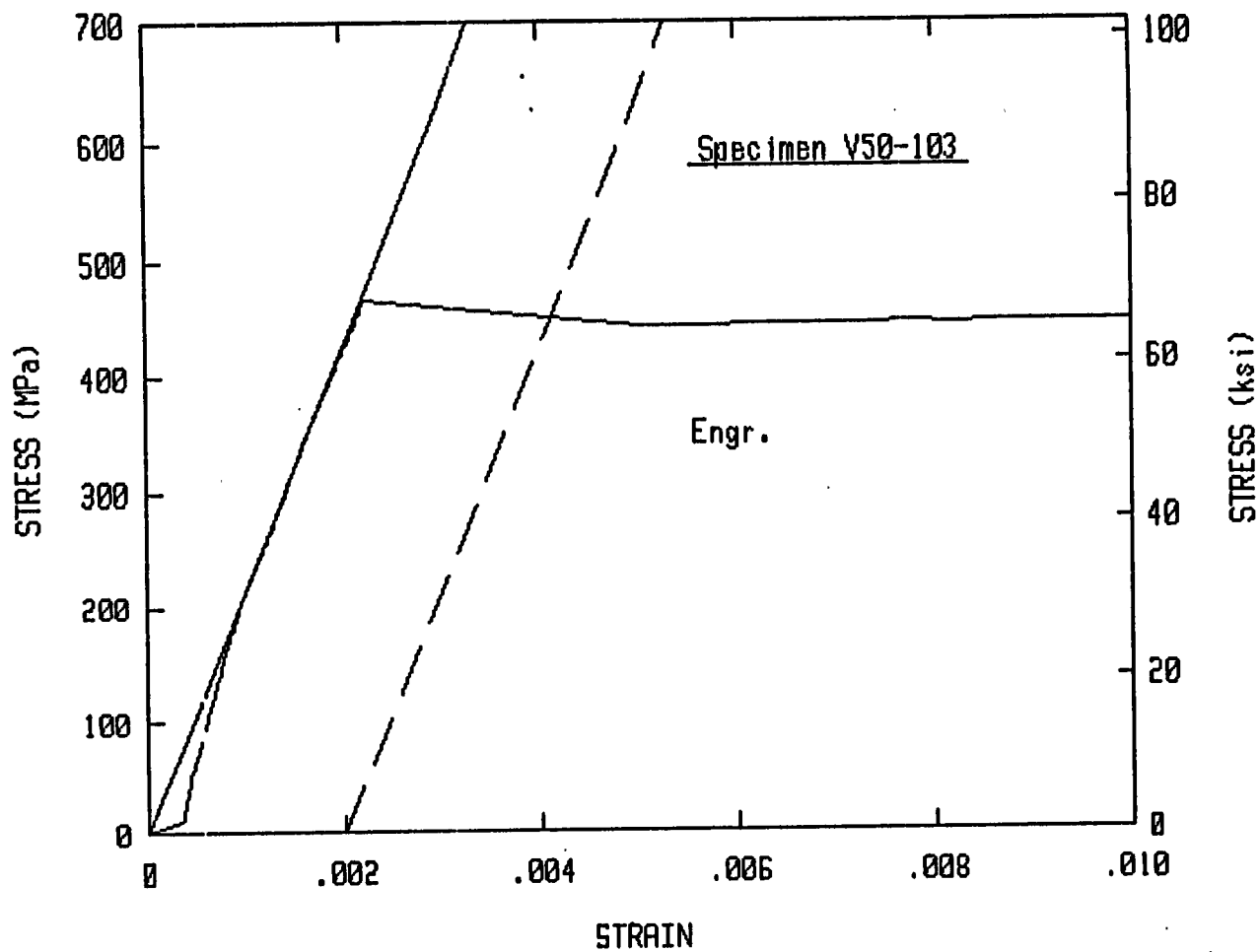
TEST SPECIMEN DATA

Date	= 04/12/88	Test Temperature	= 82.2 °C
Gage Length	= 25.4 mm	Gage Diameter	= 12.8 mm
Reduction in Area	= 51.9 %		
Elongation	= 18.9 % in 50.8 mm		

Material = A302-B
Material Form = Plate

True Stress/Strain Curve

Young's Modulus	= 21.38E+04 MPa	(used for Yield strength)
Elastic Testing Rate	= 478.7 MPa/min	(based on initial linear curve)
Yield Strength (0.2%)	= 445.2 MPa	
Fracture Stress	= 811 MPa	



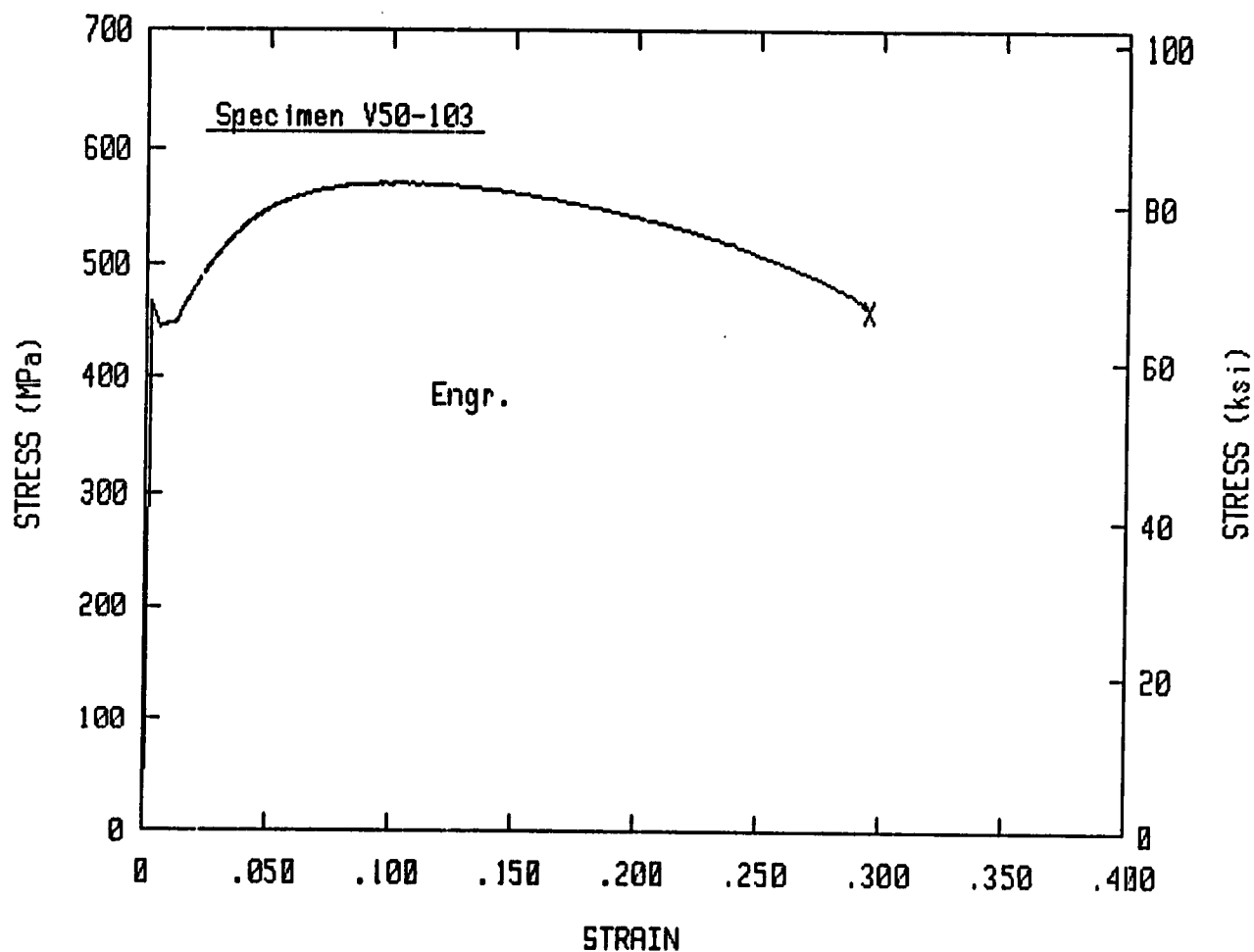
TEST SPECIMEN DATA

Date	= 04/12/88	Test Temperature	= 82.2 °C
Gage Length	= 25.4 mm	Gage Diameter	= 12.8 mm
Reduction in Area	= 51.9 %		
Elongation	= 18.9 % in 50.8 mm		

Material = A302-B
Material Form = Plate

Engineering Stress/Strain Curve

Young's Modulus	= 21.30E+04 MPa	(used for Yield strength)
Elastic Testing Rate	= 478.7 MPa/min	(based on initial linear curve)
Yield Strength (0.2%)	= 443.1 MPa	
Ultimate Strength	= 570.7 MPa	



TEST SPECIMEN DATA

Date	= 04/12/88	Test Temperature	= 82.2 °C
Gage Length	= 25.4 mm	Gage Diameter	= 12.8 mm
Reduction in Area	= 51.9 %		
Elongation	= 18.9 % in 50.8 mm		

Material = A302-B
Material Form = Plate

Engineering Stress/Strain Curve

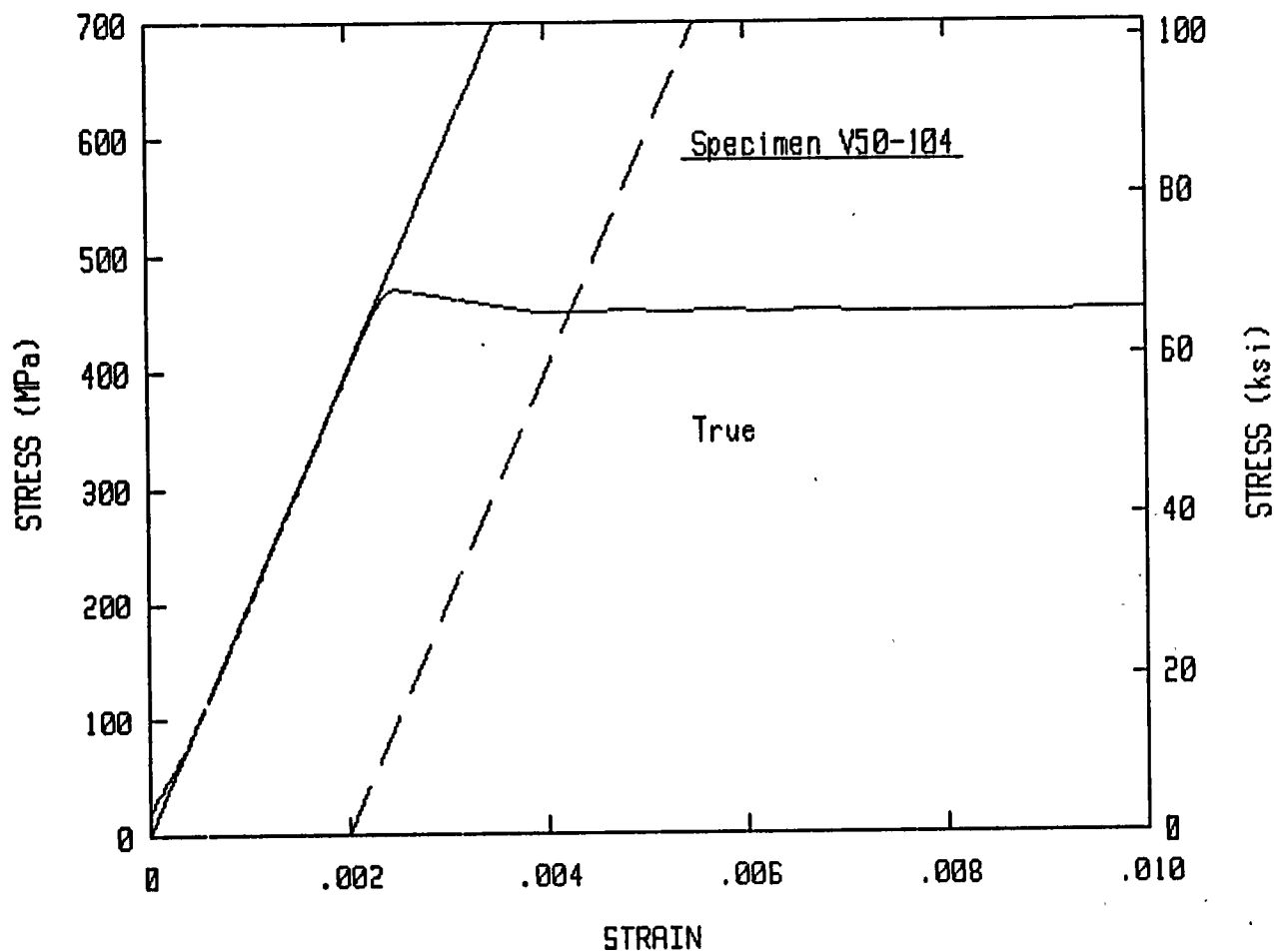
Young's Modulus	= 21.30E+04 MPa	(used for Yield strength)
Elastic Testing Rate	= 478.7 MPa/min	(based on initial linear curve)
Yield Strength (0.2%)	= 443.1 MPa	
Ultimate Strength	= 570.7 MPa	

Specimen : V50-103
Test Temp : 82°C

POINT #	ENGR. STRESS (MPa)	ENGR. STRAIN (mm/mm)	TRUE STRESS (MPa)	TRUE STRAIN (mm/mm)
1	9.71	0.0003	9.72	0.0003
2	19.32	0.0004	19.33	0.0004
3	48.98	0.0004	49.00	0.0004
4	80.49	0.0005	80.54	0.0005
5	111.50	0.0006	111.57	0.0006
6	143.11	0.0007	143.22	0.0007
7	175.88	0.0008	176.03	0.0008
8	208.31	0.0010	208.51	0.0010
9	242.61	0.0011	242.89	0.0011
10	276.42	0.0013	276.77	0.0013
11	310.84	0.0015	311.29	0.0015
12	345.33	0.0016	345.89	0.0016
13	379.41	0.0018	380.08	0.0018
14	414.24	0.0020	415.05	0.0020
15	448.39	0.0021	449.35	0.0021
16	445.64	0.0061	448.37	0.0061
17	448.05	0.0100	452.53	0.0100
18	449.42	0.0123	454.94	0.0122
19	453.14	0.0132	459.12	0.0131
20	459.06	0.0142	465.57	0.0141
21	468.91	0.0167	476.75	0.0166
22	484.88	0.0211	495.12	0.0209
23	499.27	0.0256	512.04	0.0253
24	512.00	0.0303	527.51	0.0298
25	523.30	0.0351	541.69	0.0345
26	533.55	0.0400	554.91	0.0393
27	542.09	0.0452	566.57	0.0442
28	549.18	0.0505	576.92	0.0493
29	554.41	0.0561	585.52	0.0546
30	559.10	0.0620	593.77	0.0602
31	563.16	0.0682	601.57	0.0660
32	566.19	0.0747	608.45	0.0720
33	568.87	0.0817	615.36	0.0785
34	569.77	0.0893	620.64	0.0855
35	570.32	0.0976	625.99	0.0931
36	570.39	0.1069		
37	569.49	0.1172		
38	568.11	0.1285		
39	565.08	0.1406		
40	561.23	0.1532		
41	556.89	0.1660		
42	551.45	0.1791		
43	545.19	0.1924		
44	537.96	0.2059		
45	530.04	0.2196		
46	521.30	0.2333		
47	511.04	0.2472		
48	499.61	0.2613		
49	486.74	0.2754		
50	459.61	0.2943	810.94	0.7322

Specimen : V50-103
Test Temp : 180°F

POINT #	ENGR. STRESS (ksi)	ENGR. STRAIN (in./in.)	TRUE STRESS (ksi)	TRUE STRAIN (in./in.)
1	1.41	0.0003	1.41	0.0003
2	2.80	0.0004	2.80	0.0004
3	7.10	0.0004	7.11	0.0004
4	11.67	0.0005	11.68	0.0005
5	16.17	0.0006	16.18	0.0006
6	20.76	0.0007	20.77	0.0007
7	25.51	0.0008	25.53	0.0008
8	30.21	0.0010	30.24	0.0010
9	35.19	0.0011	35.23	0.0011
10	40.09	0.0013	40.14	0.0013
11	45.08	0.0015	45.15	0.0015
12	50.09	0.0016	50.17	0.0016
13	55.03	0.0018	55.13	0.0018
14	60.08	0.0020	60.20	0.0020
15	65.03	0.0021	65.17	0.0021
16	64.63	0.0061	65.03	0.0061
17	64.98	0.0100	65.63	0.0100
18	65.18	0.0123	65.98	0.0122
19	65.72	0.0132	66.59	0.0131
20	66.58	0.0142	67.52	0.0141
21	68.01	0.0167	69.15	0.0166
22	70.33	0.0211	71.81	0.0209
23	72.41	0.0256	74.27	0.0253
24	74.26	0.0303	76.51	0.0298
25	75.90	0.0351	78.57	0.0345
26	77.39	0.0400	80.48	0.0393
27	78.62	0.0452	82.17	0.0442
28	79.65	0.0505	83.68	0.0493
29	80.41	0.0561	84.92	0.0546
30	81.09	0.0620	86.12	0.0602
31	81.68	0.0682	87.25	0.0660
32	82.12	0.0747	88.25	0.0720
33	82.51	0.0817	89.25	0.0785
34	82.64	0.0893	90.02	0.0855
35	82.72	0.0976	90.79	0.0931
36	82.73	0.1069		
37	82.60	0.1172		
38	82.40	0.1285		
39	81.96	0.1406		
40	81.40	0.1532		
41	80.77	0.1660		
42	79.98	0.1791		
43	79.07	0.1924		
44	78.02	0.2059		
45	76.88	0.2196		
46	75.61	0.2333		
47	74.12	0.2472		
48	72.46	0.2613		
49	70.60	0.2754		
50	66.66	0.2943	117.62	0.7322



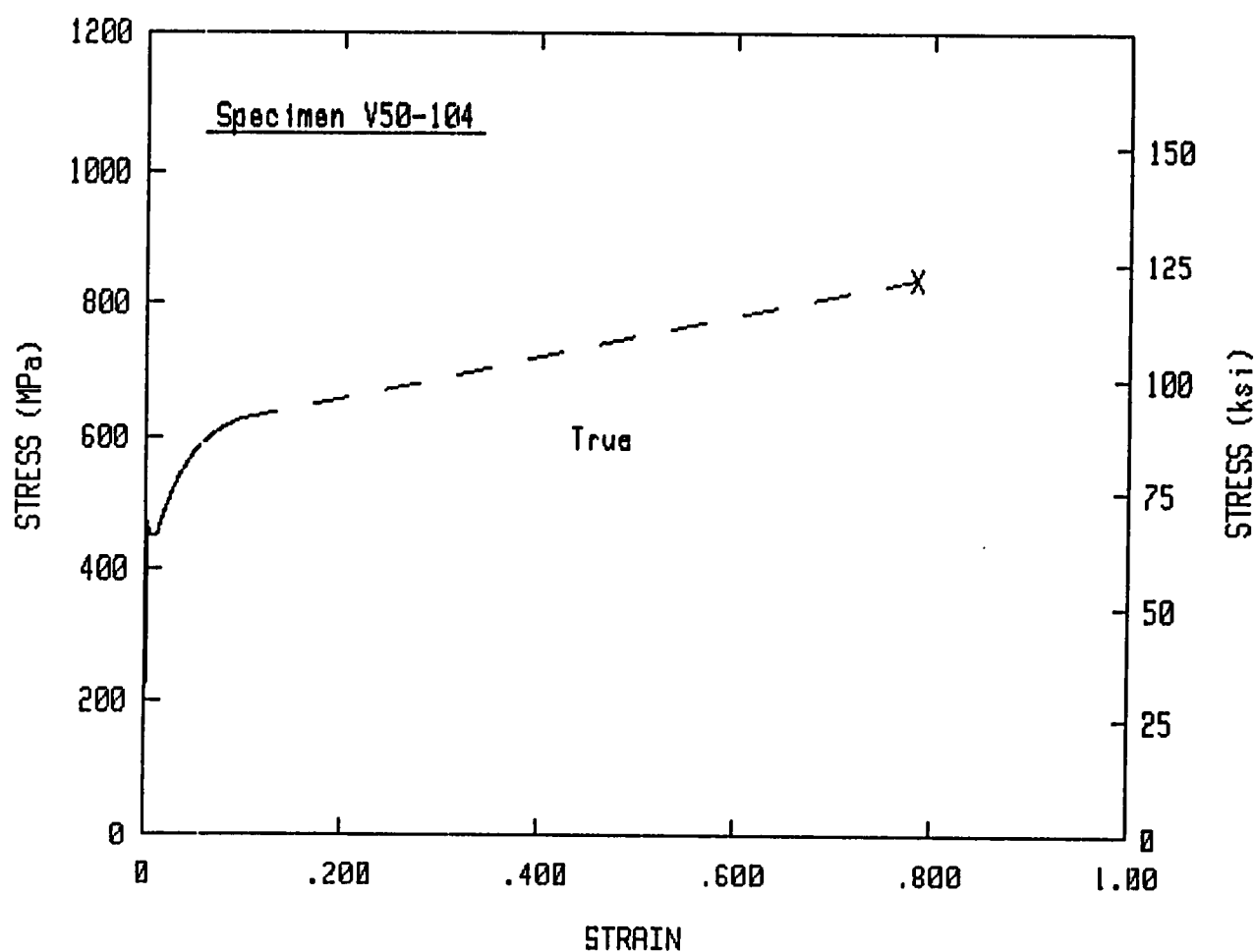
TEST SPECIMEN DATA

Date	= 04/12/88	Test Temperature	= 82.2 °C
Gage Length	= 25.4 mm	Gage Diameter	= 12.8 mm
Reduction in Area	= 54.3 %		
Elongation	= 21.5 % in 50.8 mm		

Material = A302-B
Material Form = Plate

True Stress/Strain Curve

Young's Modulus	= 20.03E+04 MPa	(used for Yield strength)
Elastic Testing Rate	= 485.1 MPa/min	(based on initial linear curve)
Yield Strength (0.2%)	= 450.3 MPa	
Fracture Stress	= 838 MPa	



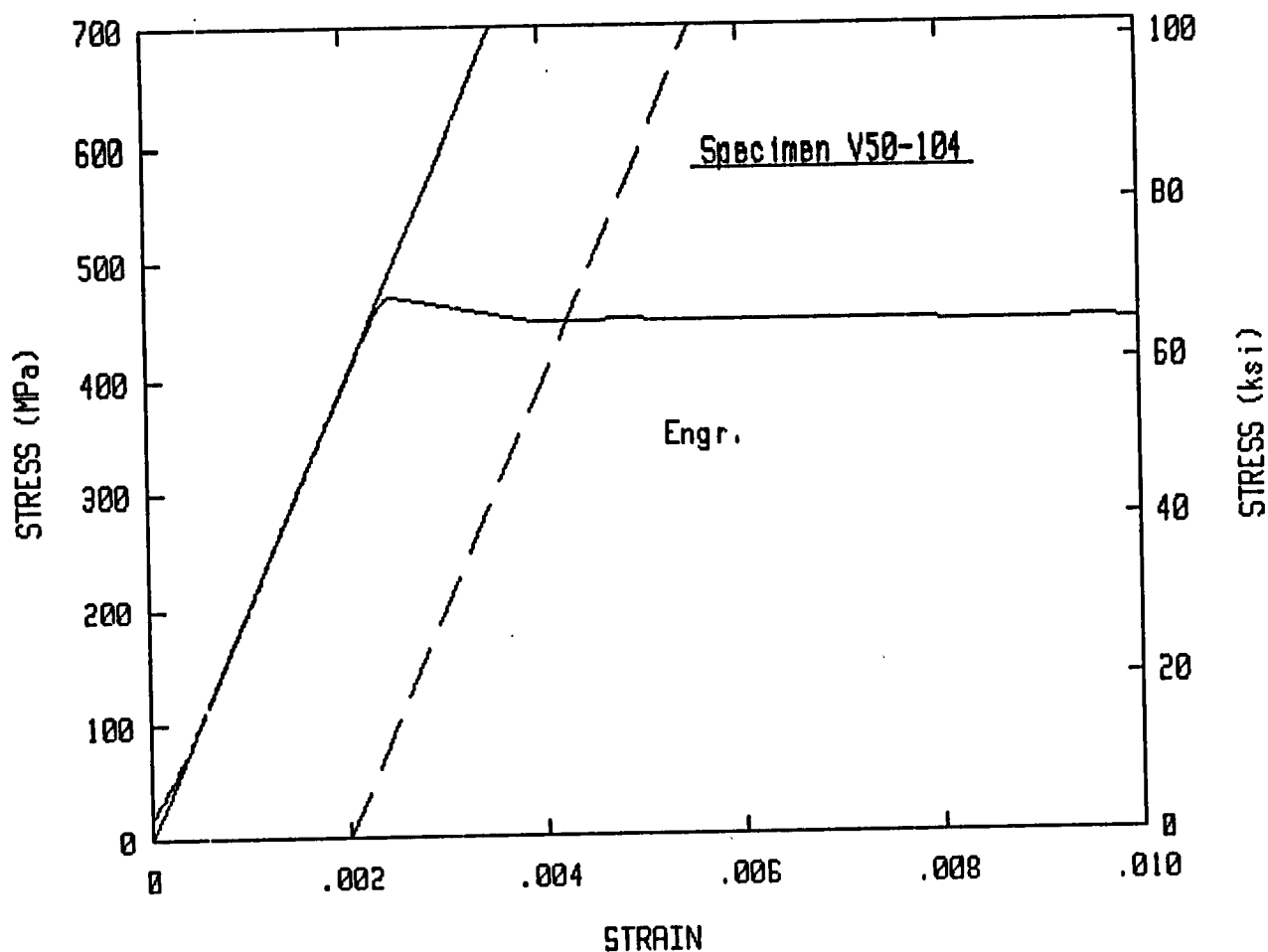
TEST SPECIMEN DATA

Date	= 04/12/88	Test Temperature	= 82.2 °C
Gage Length	= 25.4 mm	Gage Diameter	= 12.8 mm
Reduction in Area	= 54.3 %		
Elongation	= 21.5 % in 50.8 mm		

Material = A302-B
Material Form = Plate

True Stress/Strain Curve

Young's Modulus	= 20.03E+04 MPa	(used for Yield strength)
Elastic Testing Rate	= 485.1 MPa/min	(based on initial linear curve)
Yield Strength (0.2%)	= 450.3 MPa	
Fracture Stress	= 838 MPa	



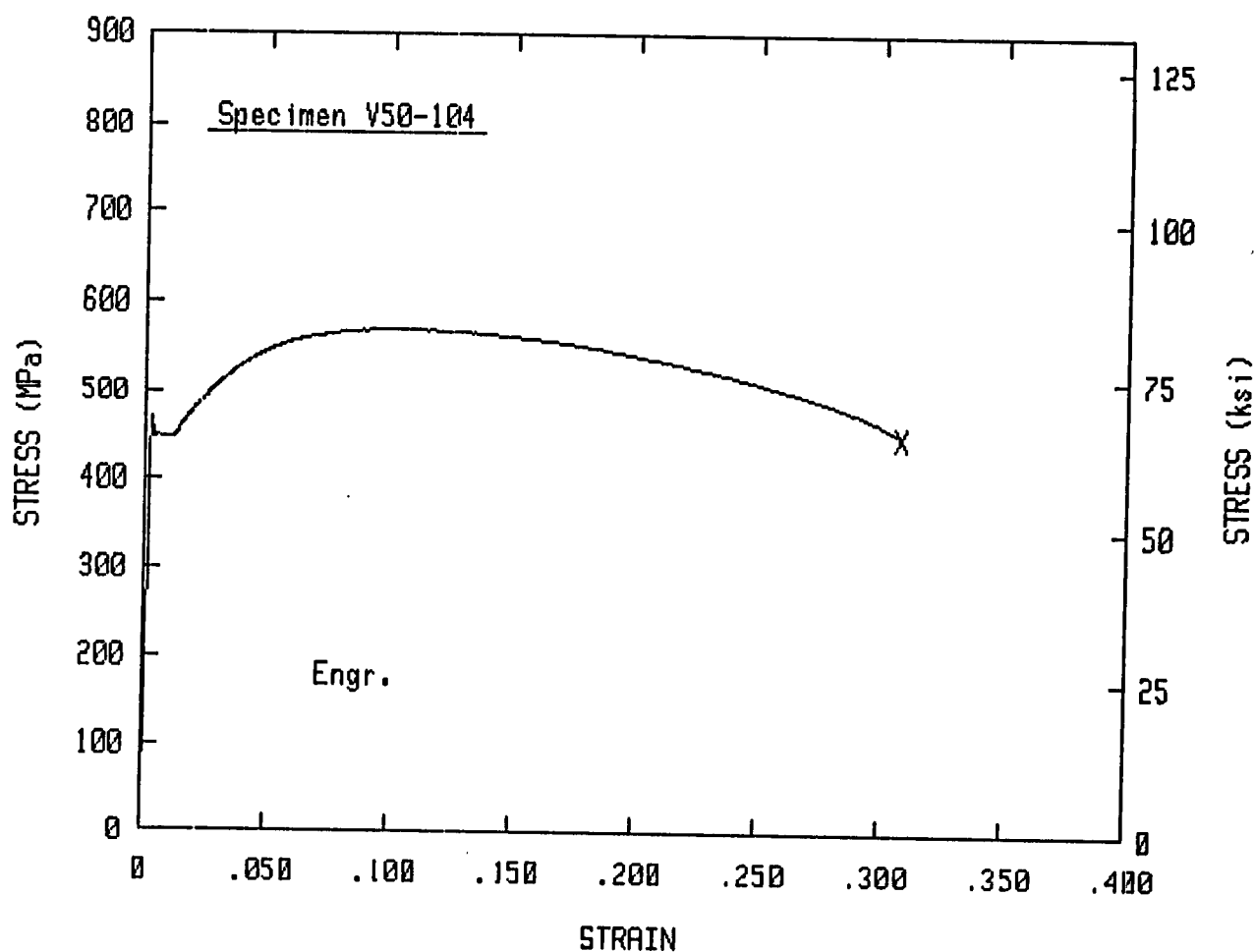
TEST SPECIMEN DATA

Date	= 04/12/88	Test Temperature	= 82.2 °C
Gage Length	= 25.4 mm	Gage Diameter	= 12.8 mm
Reduction in Area	= 54.3 %		
Elongation	= 21.5 % in 50.8 mm		

Material = A302-B
Material Form = Plate

Engineering Stress/Strain Curve

Young's Modulus	= 19.96E+04 MPa	(used for Yield strength)
Elastic Testing Rate	= 485.1 MPa/min	(based on initial linear curve)
Yield Strength (0.2%)	= 448.3 MPa	
Ultimate Strength	= 571 MPa	



TEST SPECIMEN DATA

Date	= 04/12/88	Test Temperature	= 82.2 °C
Gage Length	= 25.4 mm	Gage Diameter	= 12.8 mm
Reduction in Area	= 54.3 %		
Elongation	= 21.5 % in 50.8 mm		

Material = A302-B
Material Form = Plate

Engineering Stress/Strain Curve

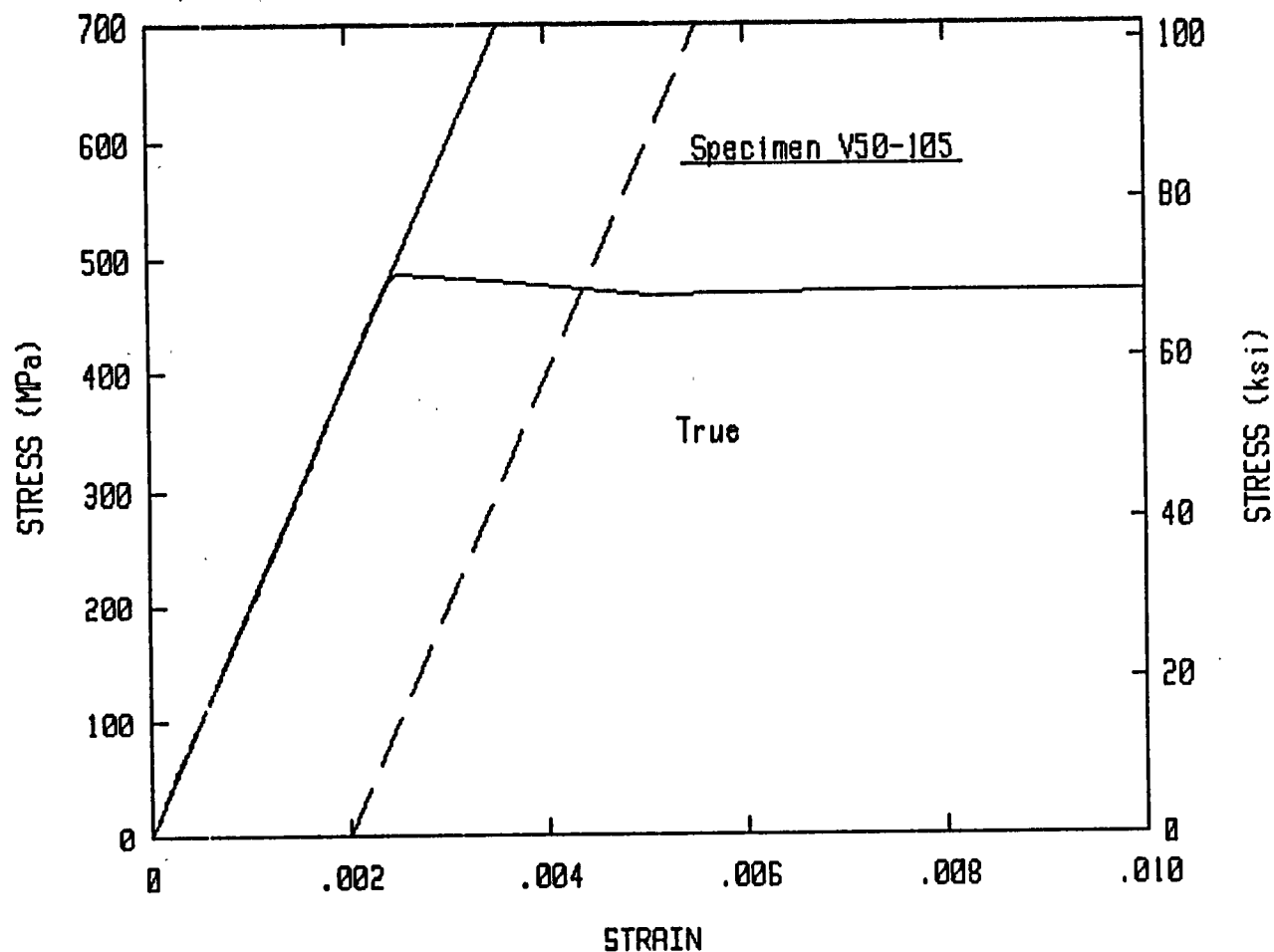
Young's Modulus	= 19.96E+04 MPa	(used for Yield strength)
Elastic Testing Rate	= 485.1 MPa/min	(based on initial linear curve)
Yield Strength (0.2%)	= 448.3 MPa	
Ultimate Strength	= 571 MPa	

Specimen : V50-104
Test Temp : 82°C

POINT #	ENGR. STRESS (MPa)	ENGR. STRAIN (mm/mm)	TRUE STRESS (MPa)	TRUE STRAIN (mm/mm)
1	18.99	0.0000	18.99	0.0000
2	22.07	0.0000	22.07	0.0000
3	50.44	0.0002	50.45	0.0002
4	81.82	0.0004	81.85	0.0004
5	114.13	0.0006	114.20	0.0006
6	148.59	0.0008	148.70	0.0008
7	182.94	0.0009	183.11	0.0009
8	217.35	0.0011	217.58	0.0011
9	251.42	0.0013	251.74	0.0013
10	286.54	0.0014	286.95	0.0014
11	321.30	0.0016	321.82	0.0016
12	356.83	0.0018	357.47	0.0018
13	391.18	0.0020	391.95	0.0020
14	425.74	0.0021	426.65	0.0021
15	459.41	0.0023	460.48	0.0023
16	447.43	0.0063	450.23	0.0062
17	446.60	0.0108	451.43	0.0108
18	450.18	0.0128	455.93	0.0127
19	455.14	0.0136	461.32	0.0135
20	461.20	0.0149	468.09	0.0148
21	470.70	0.0176	479.00	0.0175
22	486.33	0.0222	497.10	0.0219
23	501.20	0.0268	514.62	0.0264
24	514.00	0.0315	530.20	0.0310
25	524.88	0.0364	543.97	0.0357
26	534.66	0.0414	556.78	0.0405
27	542.71	0.0466	567.98	0.0455
28	549.94	0.0520	578.53	0.0507
29	555.58	0.0576	587.59	0.0560
30	560.40	0.0635	596.01	0.0616
31	563.43	0.0697	602.73	0.0674
32	566.46	0.0763	609.69	0.0735
33	568.60	0.0834	616.00	0.0801
34	569.97	0.0910	621.86	0.0871
35	570.80	0.0994	627.53	0.0948
36	570.52	0.1085		
37	569.28	0.1186		
38	567.77	0.1297		
39	565.15	0.1414		
40	561.92	0.1537		
41	557.31	0.1663		
42	552.55	0.1791		
43	546.15	0.1922		
44	539.47	0.2055		
45	531.97	0.2190		
46	523.64	0.2325		
47	514.48	0.2463		
48	503.40	0.2602		
49	491.28	0.2741		
50	449.70	0.3073	837.99	0.7831

Specimen : V50-104
Test Temp : 180°F

POINT #	ENGR. STRESS (ksi)	ENGR. STRAIN (in./in.)	TRUE STRESS (ksi)	TRUE STRAIN (in./in.)
1	2.75	0.0000	2.75	0.0000
2	3.20	0.0000	3.20	0.0000
3	7.32	0.0002	7.32	0.0002
4	11.87	0.0004	11.87	0.0004
5	16.55	0.0006	16.56	0.0006
6	21.55	0.0008	21.57	0.0008
7	26.53	0.0009	26.56	0.0009
8	31.52	0.0011	31.56	0.0011
9	36.47	0.0013	36.51	0.0013
10	41.56	0.0014	41.62	0.0014
11	46.60	0.0016	46.68	0.0016
12	51.75	0.0018	51.85	0.0018
13	56.74	0.0020	56.85	0.0020
14	61.75	0.0021	61.88	0.0021
15	66.63	0.0023	66.79	0.0023
16	64.89	0.0063	65.30	0.0062
17	64.77	0.0108	65.47	0.0108
18	65.29	0.0128	66.13	0.0127
19	66.01	0.0136	66.91	0.0135
20	66.89	0.0149	67.89	0.0148
21	68.27	0.0176	69.47	0.0175
22	70.54	0.0222	72.10	0.0219
23	72.69	0.0268	74.64	0.0264
24	74.55	0.0315	76.90	0.0310
25	76.13	0.0364	78.90	0.0357
26	77.55	0.0414	80.75	0.0405
27	78.71	0.0466	82.38	0.0455
28	79.76	0.0520	83.91	0.0507
29	80.58	0.0576	85.22	0.0560
30	81.28	0.0635	86.44	0.0616
31	81.72	0.0697	87.42	0.0674
32	82.16	0.0763	88.43	0.0735
33	82.47	0.0834	89.34	0.0801
34	82.67	0.0910	90.19	0.0871
35	82.79	0.0994	91.02	0.0948
36	82.75	0.1085		
37	82.57	0.1186		
38	82.35	0.1297		
39	81.97	0.1414		
40	81.50	0.1537		
41	80.83	0.1663		
42	80.14	0.1791		
43	79.21	0.1922		
44	78.24	0.2055		
45	77.16	0.2190		
46	75.95	0.2325		
47	74.62	0.2463		
48	73.01	0.2602		
49	71.25	0.2741		
50	65.22	0.3073	121.54	0.7831



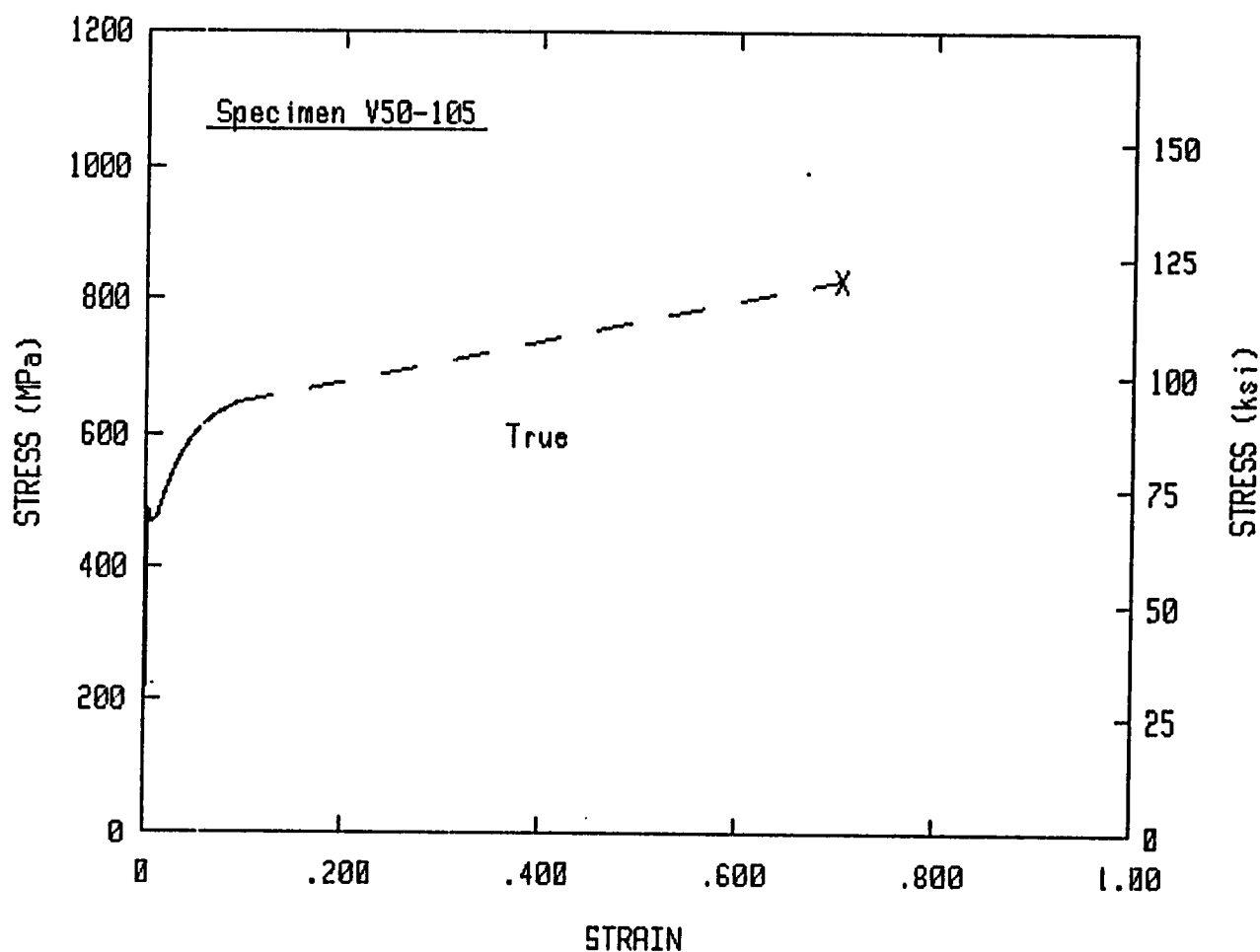
TEST SPECIMEN DATA

Date	= 04/12/88	Test Temperature	= 82.2 °C
Gage Length	= 25.4 mm	Gage Diameter	= 12.8 mm
Reduction in Area	= 50.5 %		
Elongation	= 19.2 % in 50.8 mm		

Material = A302-B
Material Form = Plate

True Stress/Strain Curve

Young's Modulus	= 19.92E+04 MPa	(used for Yield strength)
Elastic Testing Rate	= 496.9 MPa/min	(based on initial linear curve)
Yield Strength (0.2%)	= 466.7 MPa	
Fracture Stress	= 828 MPa	



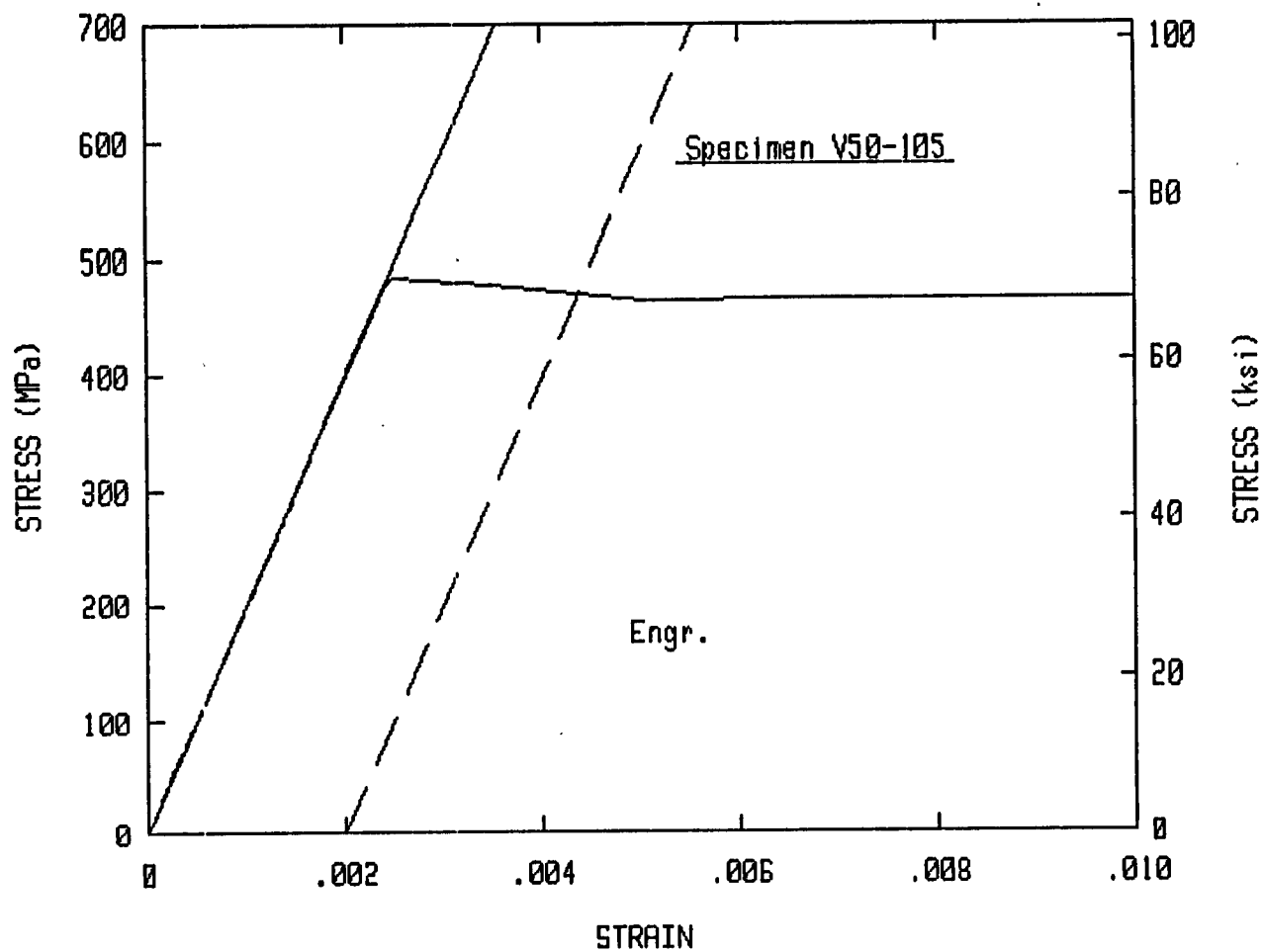
TEST SPECIMEN DATA

Date	= 04/12/88	Test Temperature	= 82.2 °C
Gage Length	= 25.4 mm	Gage Diameter	= 12.8 mm
Reduction in Area	= 50.5 %		
Elongation	= 19.2 % in 50.8 mm		

Material = A302-B
Material Form = Plate

True Stress/Strain Curve

Young's Modulus	= 19.92E+04 MPa	(used for Yield strength)
Elastic Testing Rate	= 496.9 MPa/min	(based on initial linear curve)
Yield Strength (0.2%)	= 466.7 MPa	
Fracture Stress	= 828 MPa	



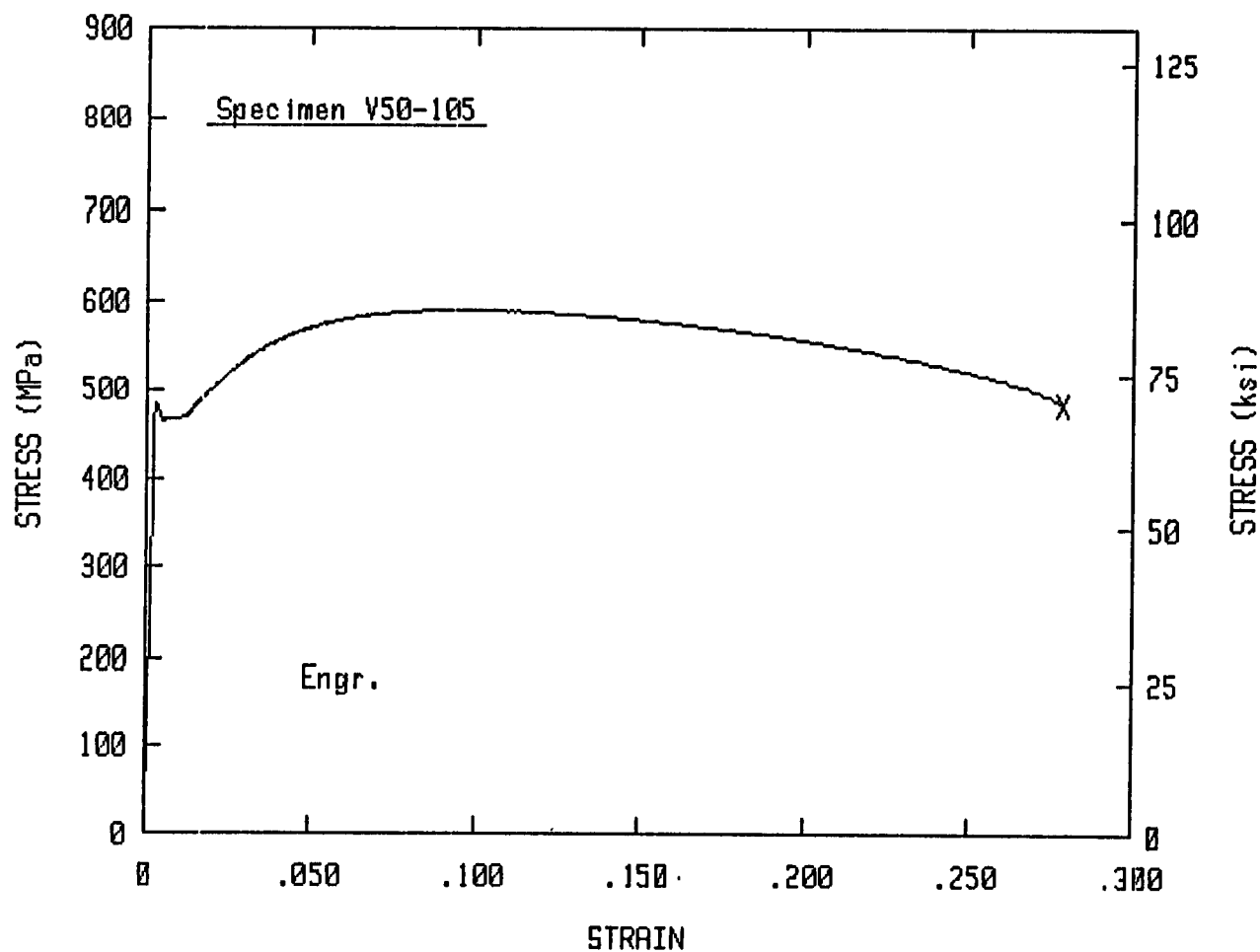
TEST SPECIMEN DATA

Date	= 04/12/88	Test Temperature	= 82.2 °C
Gage Length	= 25.4 mm	Gage Diameter	= 12.8 mm
Reduction in Area	= 50.5 %		
Elongation	= 19.2 % in 50.8 mm		

Material = A302-B
Material Form = Plate

Engineering Stress/Strain Curve

Young's Modulus	= 19.85E+04 MPa	(used for Yield strength)
Elastic Testing Rate	= 496.9 MPa/min	(based on initial linear curve)
Yield Strength (0.2%)	= 464.4 MPa	
Ultimate Strength	= 590.9 MPa	



TEST SPECIMEN DATA

Date	= 04/12/88	Test Temperature	= 82.2 °C
Gage Length	= 25.4 mm	Gage Diameter	= 12.8 mm
Reduction in Area	= 50.5 %		
Elongation	= 19.2 % in 50.8 mm		

Material = A302-B
Material Form = Plate

Engineering Stress/Strain Curve

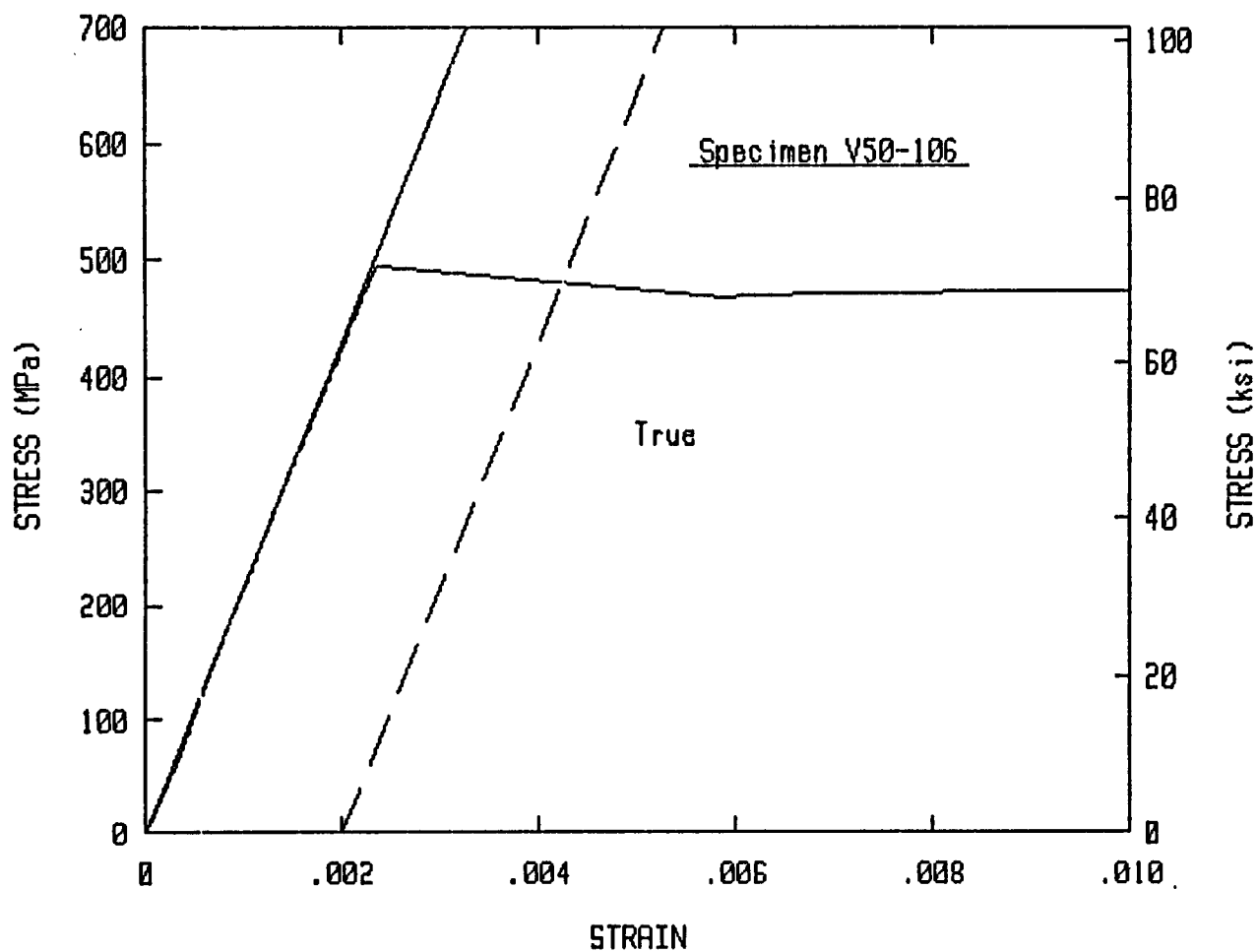
Young's Modulus	= 19.85E+04 MPa	(used for Yield strength)
Elastic Testing Rate	= 496.9 MPa/min	(based on initial linear curve)
Yield Strength (0.2%)	= 464.4 MPa	
Ultimate Strength	= 590.9 MPa	

Specimen : V50-105
Test Temp : 82°C

POINT #	ENGR. STRESS (MPa)	ENGR. STRAIN (mm/mm)	TRUE STRESS (MPa)	TRUE STRAIN (mm/mm)
1	15.12	0.0001	15.12	0.0001
2	14.60	0.0001	14.61	0.0001
3	14.78	0.0001	14.79	0.0001
4	32.30	0.0001	32.30	0.0001
5	61.62	0.0003	61.64	0.0003
6	93.69	0.0005	93.74	0.0005
7	128.10	0.0006	128.18	0.0006
8	162.96	0.0008	163.09	0.0008
9	198.12	0.0010	198.32	0.0010
10	233.39	0.0012	233.66	0.0012
11	269.46	0.0014	269.83	0.0014
12	304.30	0.0015	304.76	0.0015
13	340.79	0.0017	341.37	0.0017
14	375.83	0.0019	376.54	0.0019
15	412.39	0.0021	413.24	0.0021
16	447.50	0.0022	448.50	0.0022
17	481.30	0.0024	482.48	0.0024
18	466.77	0.0077	470.36	0.0076
19	468.15	0.0114	473.47	0.0113
20	471.59	0.0127	477.58	0.0126
21	478.68	0.0140	485.38	0.0139
22	494.31	0.0180	503.22	0.0179
23	508.63	0.0222	519.94	0.0220
24	522.54	0.0266	536.41	0.0262
25	535.55	0.0310	552.14	0.0305
26	546.22	0.0355	565.63	0.0349
27	554.90	0.0402	577.19	0.0394
28	563.36	0.0450	588.71	0.0440
29	570.11	0.0500	598.63	0.0488
30	575.96	0.0553	607.79	0.0538
31	580.30	0.0607	615.55	0.0590
32	584.02	0.0666	622.89	0.0644
33	586.29	0.0727	628.90	0.0702
34	588.15	0.0793	634.82	0.0764
35	589.94	0.0865	640.99	0.0830
36	590.42	0.0944	646.17	0.0902
37	590.14	0.1032		
38	589.53	0.1128		
39	587.39	0.1234		
40	584.22	0.1347		
41	580.71	0.1463		
42	576.31	0.1582		
43	570.94	0.1702		
44	565.22	0.1823		
45	558.82	0.1948		
46	551.25	0.2073		
47	543.19	0.2199		
48	534.10	0.2327		
49	524.05	0.2455		
50	483.85	0.2786	827.94	0.7033

Specimen : V50-105
Test Temp : 180°F

POINT #	ENGR. STRESS (ksi)	ENGR. STRAIN (in./in.)	TRUE STRESS (ksi)	TRUE STRAIN (in./in.)
1	2.19	0.0001	2.19	0.0001
2	2.12	0.0001	2.12	0.0001
3	2.14	0.0001	2.14	0.0001
4	4.68	0.0001	4.68	0.0001
5	8.94	0.0003	8.94	0.0003
6	13.59	0.0005	13.60	0.0005
7	18.58	0.0006	18.59	0.0006
8	23.64	0.0008	23.65	0.0008
9	28.74	0.0010	28.76	0.0010
10	33.85	0.0012	33.89	0.0012
11	39.08	0.0014	39.14	0.0014
12	44.13	0.0015	44.20	0.0015
13	49.43	0.0017	49.51	0.0017
14	54.51	0.0019	54.61	0.0019
15	59.81	0.0021	59.94	0.0021
16	64.90	0.0022	65.05	0.0022
17	69.81	0.0024	69.98	0.0024
18	67.70	0.0077	68.22	0.0076
19	67.90	0.0114	68.67	0.0113
20	68.40	0.0127	69.27	0.0126
21	69.43	0.0140	70.40	0.0139
22	71.69	0.0180	72.99	0.0179
23	73.77	0.0222	75.41	0.0220
24	75.79	0.0266	77.80	0.0262
25	77.67	0.0310	80.08	0.0305
26	79.22	0.0355	82.04	0.0349
27	80.48	0.0402	83.71	0.0394
28	81.71	0.0450	85.38	0.0440
29	82.69	0.0500	86.82	0.0488
30	83.54	0.0553	88.15	0.0538
31	84.17	0.0607	89.28	0.0590
32	84.70	0.0666	90.34	0.0644
33	85.03	0.0727	91.21	0.0702
34	85.30	0.0793	92.07	0.0764
35	85.56	0.0865	92.97	0.0830
36	85.63	0.0944	93.72	0.0902
37	85.59	0.1032		
38	85.50	0.1128		
39	85.19	0.1234		
40	84.73	0.1347		
41	84.23	0.1463		
42	83.59	0.1582		
43	82.81	0.1702		
44	81.98	0.1823		
45	81.05	0.1948		
46	79.95	0.2073		
47	78.78	0.2199		
48	77.47	0.2327		
49	76.01	0.2455		
50	70.18	0.2786	120.08	0.7033



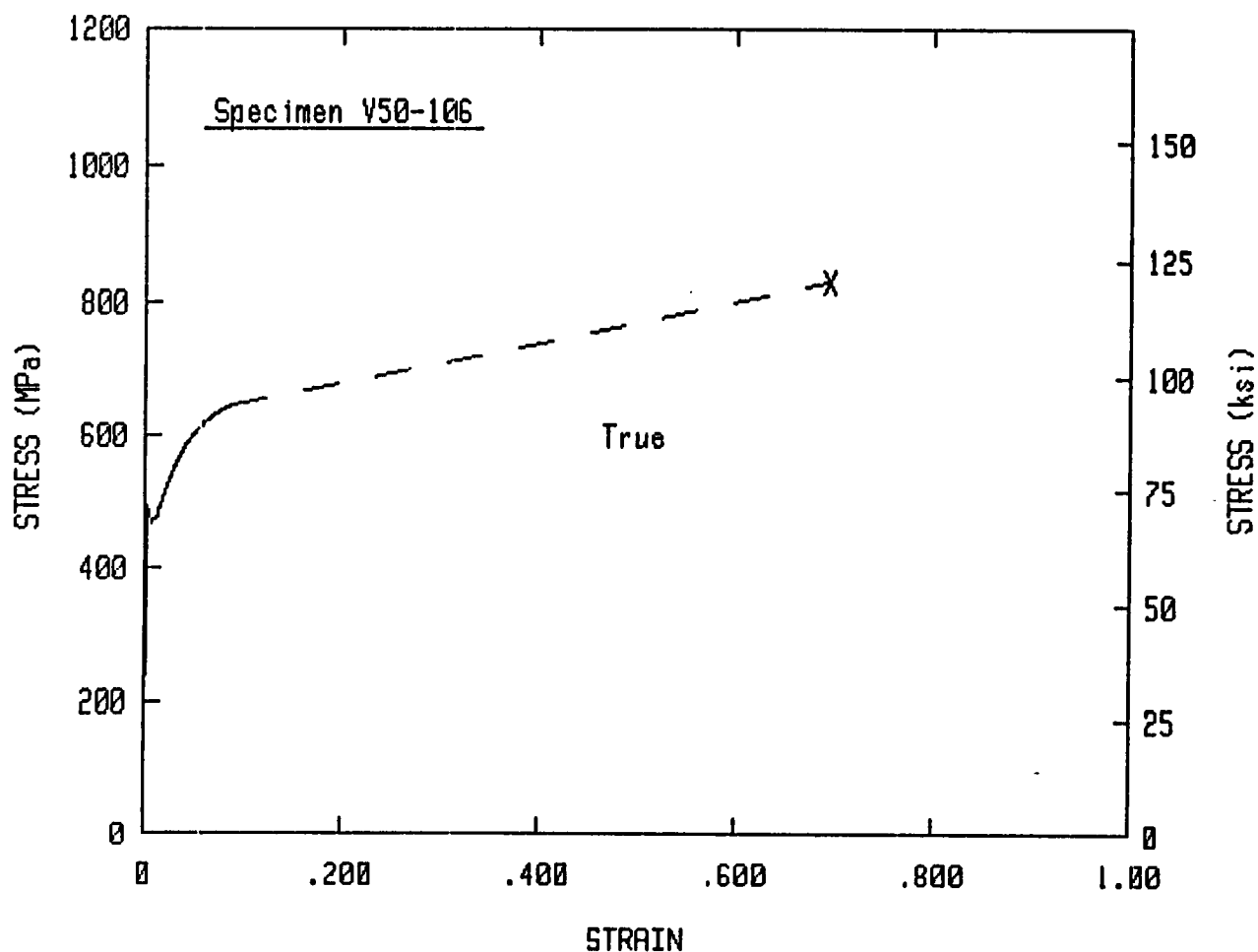
TEST SPECIMEN DATA

Date	= 04/12/88	Test Temperature	= 82.2 °C
Gage Length	= 25.4 mm	Gage Diameter	= 12.8 mm
Reduction in Area	= 50 %		
Elongation	= 18.6 % in 50.8 mm		

Material = A302-B
Material Form = Plate

True Stress/Strain Curve

Young's Modulus	= 21.42E+04 MPa	(used for Yield strength)
Elastic Testing Rate	= 485.5 MPa/min	(based on initial linear curve)
Yield Strength (0.2%)	= 467.2 MPa	
Fracture Stress	= 829.7 MPa	



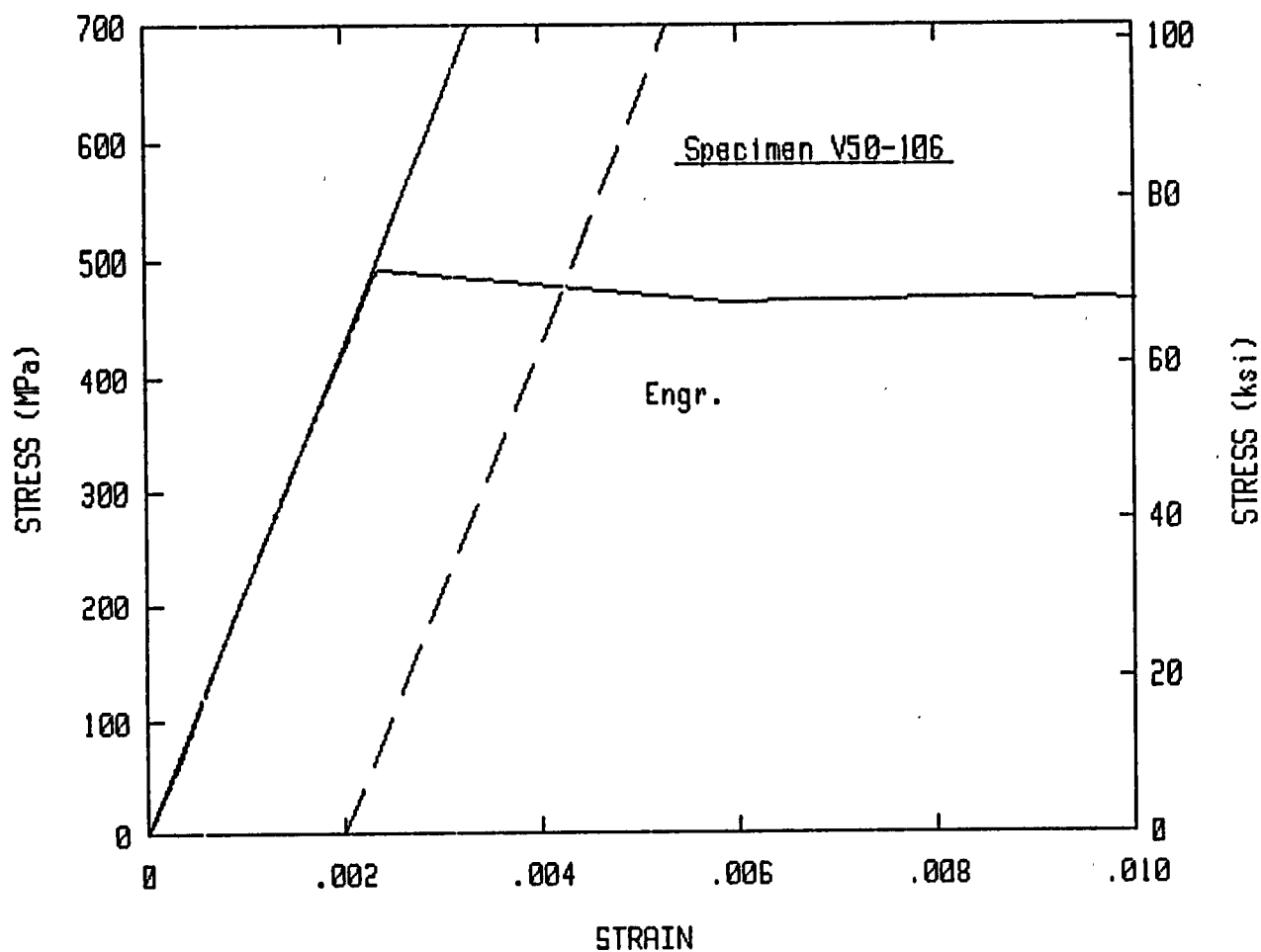
TEST SPECIMEN DATA

Date	= 04/12/88	Test Temperature	= 82.2 °C
Gage Length	= 25.4 mm	Gage Diameter	= 12.8 mm
Reduction in Area	= 50 %		
Elongation	= 18.6 % in 50.8 mm		

Material = A302-B
Material Form = Plate

True Stress/Strain Curve

Young's Modulus	= 21.42E+04 MPa	(used for Yield strength)
Elastic Testing Rate	= 485.5 MPa/min	(based on initial linear curve)
Yield Strength (0.2%)	= 467.2 MPa	
Fracture Stress	= 829.7 MPa	



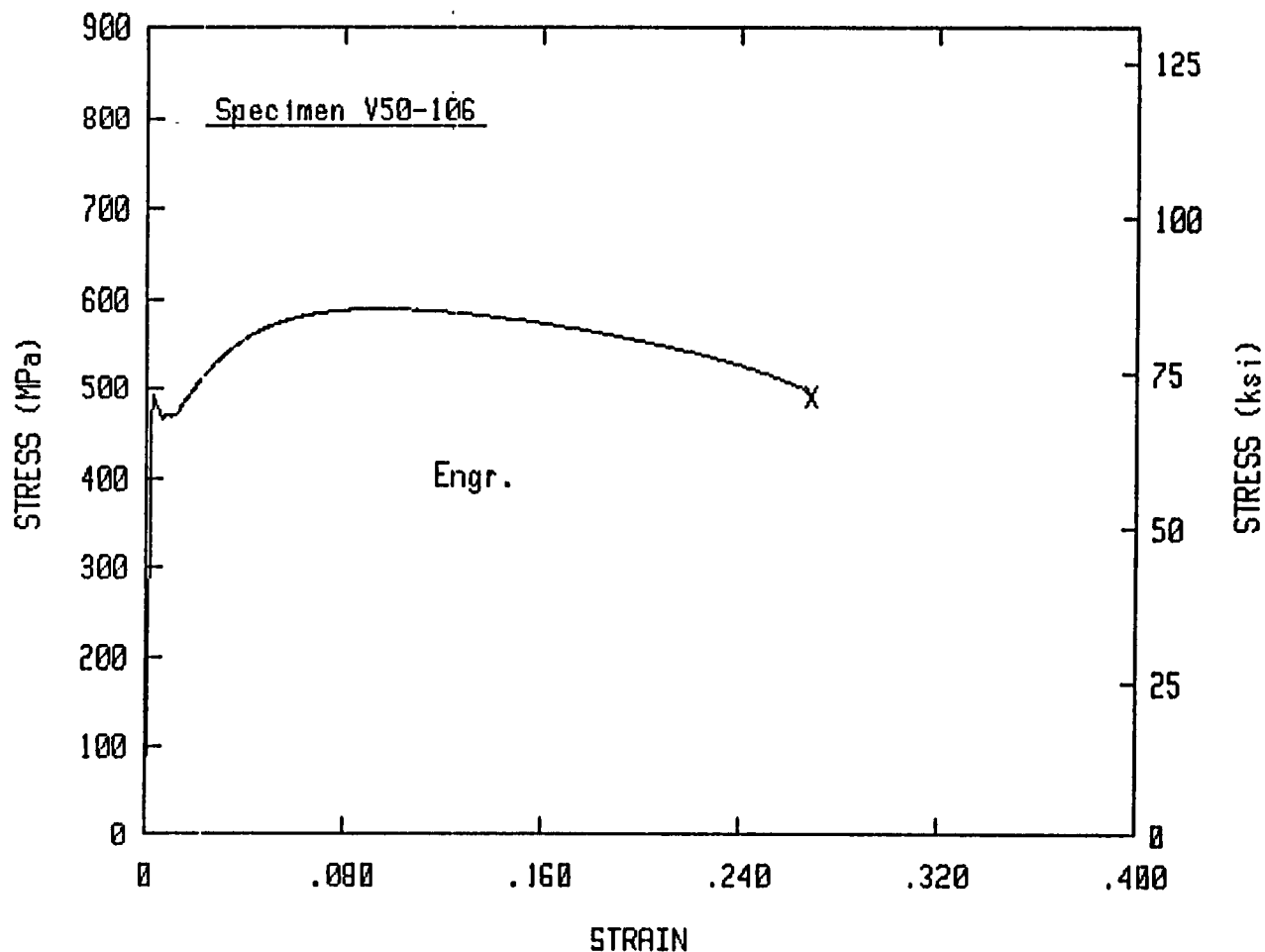
TEST SPECIMEN DATA

Date	= 04/12/88	Test Temperature	= 82.2 °C
Gage Length	= 25.4 mm	Gage Diameter	= 12.8 mm
Reduction in Area	= 50 %		
Elongation	= 18.6 % in 50.8 mm		

Material = A302-B
Material Form = Plate

Engineering Stress/Strain Curve

Young's Modulus	= 21.34E+04 MPa	(used for Yield strength)
Elastic Testing Rate	= 485.5 MPa/min	(based on initial linear curve)
Yield Strength (0.2%)	= 464.5 MPa	
Ultimate Strength	= 590.7 MPa	



TEST SPECIMEN DATA

Date	= 04/12/88	Test Temperature	= 82.2 °C
Gage Length	= 25.4 mm	Gage Diameter	= 12.8 mm
Reduction in Area	= 50 %		
Elongation	= 18.6 % in 50.8 mm		

Material = A302-B
Material Form = Plate

Engineering Stress/Strain Curve

Young's Modulus	= 21.34E+04 MPa	(used for Yield strength)
Elastic Testing Rate	= 485.5 MPa/min	(based on initial linear curve)
Yield Strength (0.2%)	= 464.5 MPa	
Ultimate Strength	= 590.7 MPa	

Specimen : V50-106
Test Temp : 82°C

POINT #	ENGR. STRESS (MPa)	ENGR. STRAIN (mm/mm)	TRUE STRESS (MPa)	TRUE STRAIN (mm/mm)
1	15.88	0.0001	15.88	0.0001
2	15.82	0.0001	15.82	0.0001
3	18.24	0.0001	18.24	0.0001
4	21.49	0.0001	21.50	0.0001
5	27.55	0.0001	27.55	0.0001
6	55.61	0.0003	55.62	0.0003
7	85.69	0.0004	85.72	0.0004
8	116.78	0.0006	116.84	0.0006
9	148.73	0.0007	148.84	0.0007
10	181.10	0.0008	181.25	0.0008
11	214.59	0.0010	214.81	0.0010
12	248.95	0.0012	249.23	0.0012
13	283.09	0.0013	283.47	0.0013
14	317.52	0.0015	317.99	0.0015
15	351.59	0.0017	352.18	0.0017
16	385.67	0.0018	386.37	0.0018
17	419.96	0.0020	420.79	0.0020
18	454.04	0.0022	455.01	0.0022
19	486.95	0.0023	488.08	0.0023
20	468.29	0.0083	472.19	0.0083
21	471.11	0.0123	476.93	0.0123
22	482.26	0.0148	489.39	0.0147
23	497.41	0.0189	506.79	0.0187
24	512.07	0.0231	523.88	0.0228
25	525.71	0.0273	540.05	0.0269
26	537.20	0.0317	554.22	0.0312
27	547.53	0.0362	567.33	0.0355
28	556.82	0.0408	579.56	0.0400
29	564.88	0.0457	590.67	0.0446
30	571.76	0.0507	600.74	0.0494
31	576.79	0.0559	609.06	0.0544
32	581.13	0.0615	616.85	0.0597
33	584.57	0.0673	623.91	0.0651
34	587.53	0.0735	630.74	0.0710
35	589.39	0.0803	636.71	0.0772
36	590.56	0.0876	642.30	0.0840
37	590.63	0.0957		
38	590.14	0.1046		
39	588.56	0.1144		
40	586.01	0.1251		
41	582.92	0.1362		
42	578.99	0.1477		
43	574.38	0.1594		
44	568.46	0.1714		
45	562.54	0.1837		
46	555.45	0.1961		
47	547.67	0.2088		
48	539.06	0.2215		
49	529.77	0.2343		
50	490.11	0.2684	829.70	0.6932

Specimen : V50-106
Test Temp : 180°F

POINT #	ENGR. STRESS (ksi)	ENGR. STRAIN (in./in.)	TRUE STRESS (ksi)	TRUE STRAIN (in./in.)
1	2.30	0.0001	2.30	0.0001
2	2.29	0.0001	2.29	0.0001
3	2.65	0.0001	2.65	0.0001
4	3.12	0.0001	3.12	0.0001
5	4.00	0.0001	4.00	0.0001
6	8.07	0.0003	8.07	0.0003
7	12.43	0.0004	12.43	0.0004
8	16.94	0.0006	16.95	0.0006
9	21.57	0.0007	21.59	0.0007
10	26.27	0.0008	26.29	0.0008
11	31.12	0.0010	31.16	0.0010
12	36.11	0.0012	36.15	0.0012
13	41.06	0.0013	41.11	0.0013
14	46.05	0.0015	46.12	0.0015
15	50.99	0.0017	51.08	0.0017
16	55.94	0.0018	56.04	0.0018
17	60.91	0.0020	61.03	0.0020
18	65.85	0.0022	65.99	0.0022
19	70.63	0.0023	70.79	0.0023
20	67.92	0.0083	68.49	0.0083
21	68.33	0.0123	69.17	0.0123
22	69.95	0.0148	70.98	0.0147
23	72.14	0.0189	73.50	0.0187
24	74.27	0.0231	75.98	0.0228
25	76.25	0.0273	78.33	0.0269
26	77.91	0.0317	80.38	0.0312
27	79.41	0.0362	82.28	0.0355
28	80.76	0.0408	84.06	0.0400
29	81.93	0.0457	85.67	0.0446
30	82.93	0.0507	87.13	0.0494
31	83.66	0.0559	88.34	0.0544
32	84.29	0.0615	89.47	0.0597
33	84.78	0.0673	90.49	0.0651
34	85.21	0.0735	91.48	0.0710
35	85.48	0.0803	92.35	0.0772
36	85.65	0.0876	93.16	0.0840
37	85.66	0.0957		
38	85.59	0.1046		
39	85.36	0.1144		
40	84.99	0.1251		
41	84.54	0.1362		
42	83.98	0.1477		
43	83.31	0.1594		
44	82.45	0.1714		
45	81.59	0.1837		
46	80.56	0.1961		
47	79.43	0.2088		
48	78.18	0.2215		
49	76.84	0.2343		
50	71.08	0.2684	120.34	0.6932

APPENDIX B

J-R CURVE DATA ANALYSIS PROCEDURES

Appendix B

J-R CURVE DATA ANALYSIS PROCEDURES

1. OVERVIEW

J-R curve evaluation requires measurements of applied load, load-line displacement and crack length for the subject test specimen. Load and displacement are readily determined using a load cell and a clip gage, respectively. Instantaneous crack length generally is not directly measureable. Typically, it is inferred by evaluations of some other parameter in collaboration with equations relating that parameter (or changes in it) to the crack length (or changes in it). For static loading conditions, the single specimen compliance (SSC) method, also called the unloading compliance method, normally is used for evaluating crack length throughout a J-R curve test as the crack grows; hence, the J-R curve can be obtained from a single test specimen.

2. CRACK LENGTH EVALUATION - COMPLIANCE METHOD

The compliance method uses the spring-like nature of the CT specimen (as given by the slope of the elastic load-displacement record) to establish crack length. As illustrated in Fig. B-1, the load-displacement record for a J-R curve test has a linear elastic portion at the beginning of the record, followed by plasticity formation up to maximum load, with decreasing load accompanying increased displacement thereafter. The sloped lines at various points on the record in Figure B-1 represent compliance measurements made during the test. These compliance unloadings represent a decrease in load of ~ 10% of the maximum load (actually a fixed "unload" of displacement), and then a reloading to the previous load level. A linear record of load (ΔP) versus displacement ($\Delta \delta$) results (Fig. B-2). This figure also demonstrates the significant compliance (slope) changes from the initial crack length conditions at the right ($a/W \sim 0.52$) to the final crack length conditions at the left ($a/W \sim 0.78$). The $\Delta \delta / \Delta P$, is combined with other terms to give (Ref. B-1):

$$U_{LL} = \frac{1}{\left[\frac{B_e E \Delta \delta}{\Delta P} \right]^{1/2} + 1} \quad (B-1)$$

where $B_e = B - (B - B_N)^2 / B$
 B = gross specimen thickness
 B_N = net specimen thickness
 E = modulus of elasticity

The crack length for a load-line mounted clip gage is given by the calibration equation of Hudak-Saxena (Ref. B-1):

$$a/W = 1.000196 - 4.06319 U_{LL} + 11.242 U_{LL}^2 - 106.043 U_{LL}^3 + 464.355 U_{LL}^4 - 650.677 U_{LL}^5 \quad (B-2)$$

Two corrections to the compliance crack lengths are made: a rotation correction and a modulus correction.

The calibration equation (Eq. B-2) was determined from elastic specimens which had not been plastically deformed. Since these J-R curve tests can result in significant plastic deformation, a "rotation" correction must be applied to the measured slope values.

The rotation-corrected compliance, C_c , is then evaluated from (Ref. B-2):

$$C_c = \frac{C_m}{\left[\frac{H^*}{R} \sin \theta - \cos \theta \right] \left[\frac{D}{R} \sin \theta - \cos \theta \right]} \quad (B-3)$$

where (Fig. B-3),

- C_c - compliance corrected for rotation of the specimen
- C_m - measured compliance = $\frac{\Delta \delta}{\Delta P}$
- H^* - initial half span of the load points (center of pin holes)
- R - radius of rotation of the crack centerline, $(W+a)/2$ where a is the last crack length
- D - one-half of the initial distance between the displacement measurement points
- θ - angle of rotation of a rigid body element about the unbroken midsection line, or
- $\theta = \sin^{-1} \left[(d_m/2 + D)/(D^2 + R^2)^{1/2} \right] - \tan^{-1}(D/R)$
- d_m - total measured load line displacement
- P_c - corrected load
- d_c - one-half of the corrected displacement

The modulus correction is used to provide a consistent starting point (initial crack length) between the compliance "measurements" of

crack length and the optically-measured initial crack length. A "match modulus" (which matches the compliance and optical initial crack lengths) is evaluated from Eq. B-1 and B-2 in an iterative manner, by first determining the proper U_{LL} to give the optically-measured initial (pre-test) crack length. Using an initial (pre-test) compliance value (C_0), the match modulus, E_M , is determined by inverting Eq. B-1:

$$E_M = \left[\frac{1}{U_{LL}} - 1 \right]^2 / (B_e C_0) \quad (B-4)$$

Combining these two corrections, a corrected definition of Eq. B-1 results:

$$U_{LL,C} = \frac{1}{[B_e E_M C]^{1/2} + 1} \quad (B-5)$$

This corrected value of U_{LL} is then used with Eq. B-2 to determine the crack length and, after subtracting the initial crack length, the crack growth for the specimen. These crack growth values are typically referred to as "predicted" crack growth values, or Δa_p .

3. J INTEGRAL EVALUATION - J_D and J_M

Both the deformation theory (J_D) and modified (J_m) forms of the J-integral are used here. The values of J_M and J_D are calculated using the following equations (Ref. B-3):

$$J_{D \ i+1} = \left[J_{D \ i} + \left(\frac{\eta}{b} \right)_i \frac{A_{i,i+1}}{B_N} \right] \left[1 - \left(\frac{\gamma}{b} \right)_i (a_{i+1} - a_i) \right] \quad (B-6)$$

η = $2 + 0.522 \ b/W$ for compacts

γ = $1 + 0.76 \ b/W$ for compacts

b = unbroken ligament = $W - a$

W = specimen width

A = area under load-loadline displacement record

a = crack length

$$J_M = J_D - \int_{a_0}^a \frac{\partial [J_D - G]}{\partial a} \bigg|_{\delta_{pl}} da \quad (B-7)$$

where

- J_D - deformation theory J
- G - Griffith linear elastic energy release rate
 $- K^2 (1-\nu^2)/E$
- a_0, a - the initial and current crack lengths
- $J_{D-G} = J_{pl}$, the plastic portion of the deformation theory J
- δ_{pl} - the plastic portion of the displacement
- ν - Poisson's ratio

$$\text{and } K = P f\left(\frac{a}{w}\right) (WBB_N)^{-1/2}$$

where P is the hold load at a partial unloading, $f(\frac{a}{w})$ is given in ASTM standard E 399, and W , B , and B_N are the specimen width, thickness, and net thickness, respectively.

Reference B-3 also provides an incremental form of Eq. B-7:

$$J_{M \ i+1} = J_{D \ i+1} + \Delta J_{i+1} \quad (B-8)$$

where

$$\Delta J_{i+1} = \Delta J_i + \left(\frac{\gamma}{b} J_{pl}\right)_i (a_{i+1} - a_i) \quad (B-9)$$

Deformation theory J, i.e., J_D , is the formulation of the J integral specified for use in the ASTM standards E 813-81 and E 1152. The validity criteria associated with J_D have restricted J_D -R curve evaluations to the point that they have been thought to be of little value for application to structural stability determinations, primarily due to the limits on crack extension. Evaluation of J_D -R curves for different sizes of CT specimens have demonstrated a specimen size dependence as well.

4. J-R CURVE EVALUATION

A typical J-R curve is illustrated in Fig. B-4. The J-R curve format is in accordance with that of ASTM E 813-81. The line emanating from the origin, called the blunting line, is given by $J = 2\sigma_f \Delta a$, where σ_f is the flow strength (the average of the 0.2% offset yield strength and the ultimate strength). The exclusion lines are constructed parallel to the blunting line, but offset by 0.15 mm (0.006 in.) and 1.5 mm (0.006 in.).

By ASTM E 813-81 procedures, a straight line is fit to the test data between the 0.15 and 1.5 mm exclusion lines. This line is extrapolated back to the blunting line; the intersection is termed J_Q . J_{Ic} equals J_Q if various validity criteria are satisfied.

In the power law evaluation of the J-R curve data, an equation of the form $J = C\Delta a^n$ is fit to the data between the exclusion lines. The power law J_{Ic} is then evaluated as the intersection of the power law curve with the 0.15 mm exclusion line. Previous experience has shown that the power law definition of J_{Ic} tends to give values nearly equivalent to the ASTM E 813-81 values for low alloy (ferritic) steels.

The tearing modulus, T_M , is used to characterize the tearing resistance of structural materials. T_M is given by

$$T_M = \frac{E}{\sigma_f} \frac{1}{2} \frac{dJ}{da} \quad (B-10)$$

where dJ/da is the slope of the J-R curve. Since the J-R curve conforms to a power law, T_M changes (decreases) with increasing crack growth. For comparison purposes, average values of T_M , termed T_{avg} , have been defined. The ASTM T_{avg} value (as defined by MEA) uses the slope of the linear fit curve as dJ/da ; the power law T_{avg} value is determined from a fit of the power law curve to a straight line, defining dJ/da as an average slope evaluated in a closed-form manner (see Appendix B of Ref. B-4).

REFERENCES

- B-1. A. Saxena, S. J. Hudak, Jr., "Review and Extension of Compliance Information for Common Crack Growth Specimens," International Journal of Fracture, Vol. 14, No. 5, Oct. 1978, pp. 453-468.
- B-2. F. J. Loss, B. H. Menke, and R. A. Gray, Jr., "Development of J-R Curve Procedures," NRL-EPRI Research Program (RP 886-2), Evaluation and Prediction of Neutron Embrittlement in Reactor Pressure Vessel Materials Annual Progress Report for CY 1978, J. R. Hawthorne, Ed., NRL Report 8327, Naval Research Laboratory, Washington, DC, Aug. 1979.
- B-3. H. A. Ernst, "Material Resistance and Instability Beyond J-Controlled Crack Growth," Elastic-Plastic Fracture: Second Symposium, Vol. I: Inelastic Crack Analysis, ASTM STP 803, American Society for Testing and Materials, Philadelphia, PA 1983.
- B-4. A. L. Hiser, F. J. Loss, and B. H. Menke, "J-R Curve Characterization of Irradiated Low Upper Shelf Welds," USNRC Report NUREG/CR-3506, Apr. 1984.

1.6T-CT (62W-32)
UNIRRADIATED, 200°C, 20%

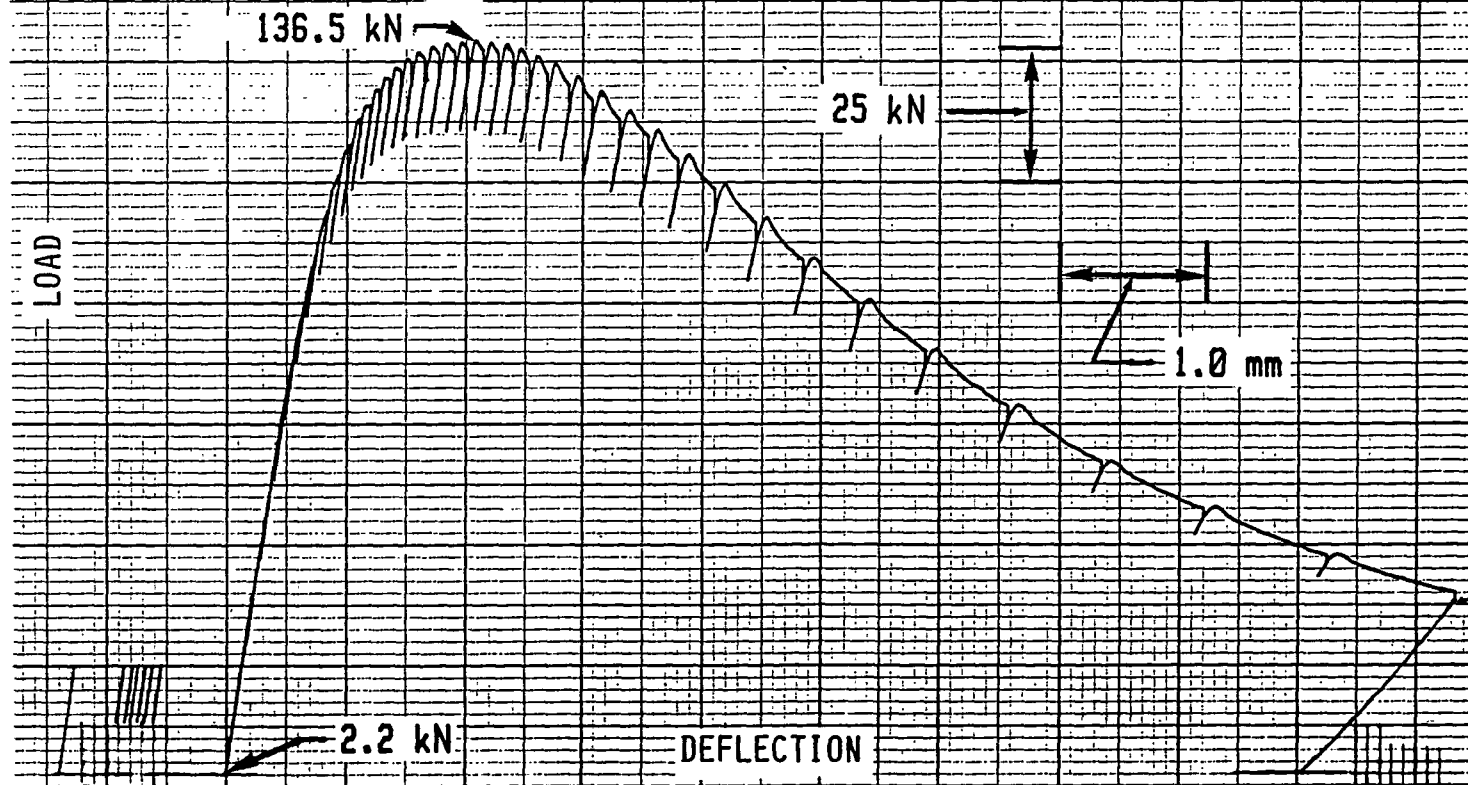


Fig. B-1 Typical load-displacement record for a J-R curve test. The test record is for a low-alloy steel specimen.

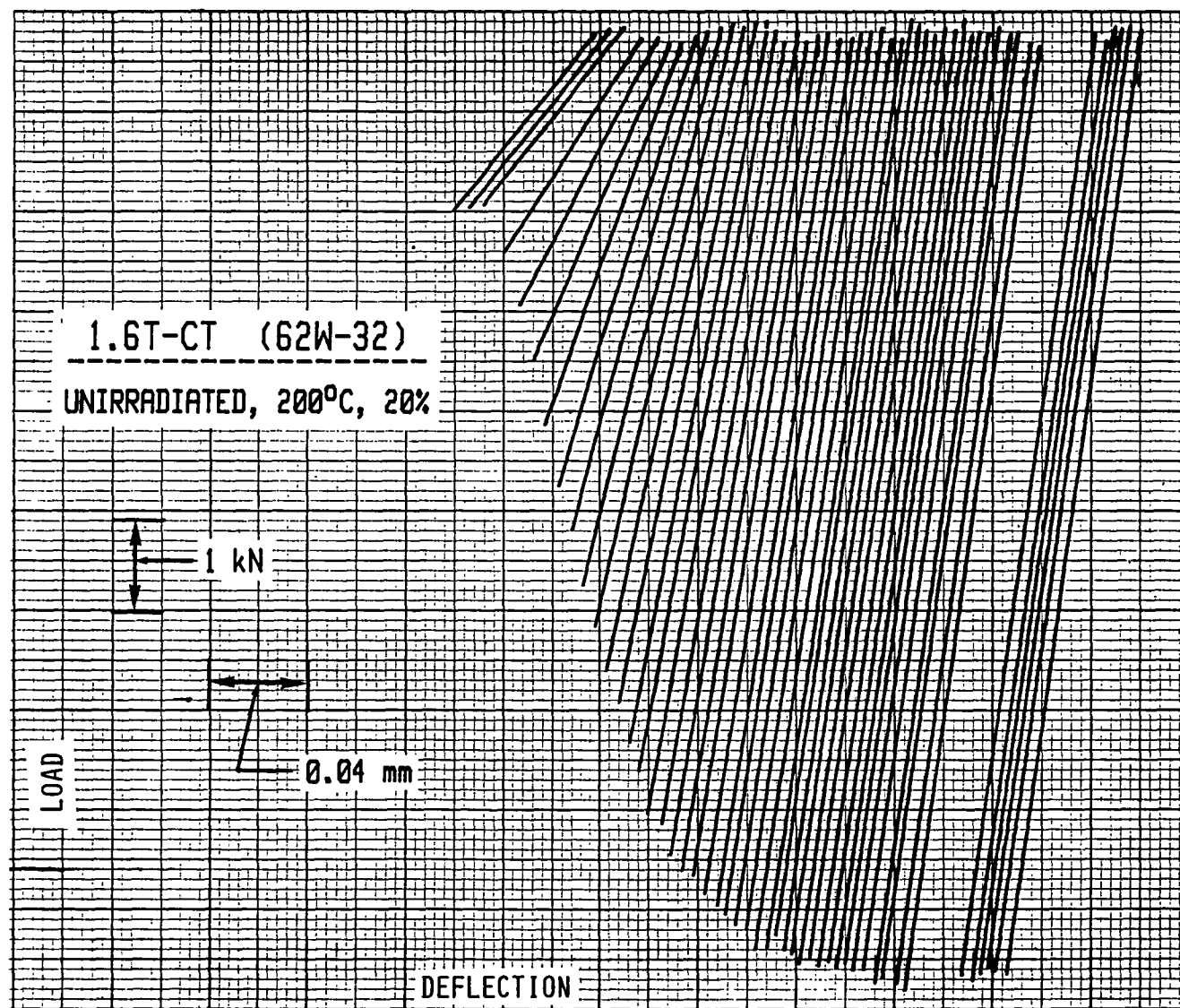


Fig. B-2 Unloading compliance traces for the J-R curve test in Fig. B-1. In this case, the test data progress from right to left chronologically. Significant slope changes are apparent.

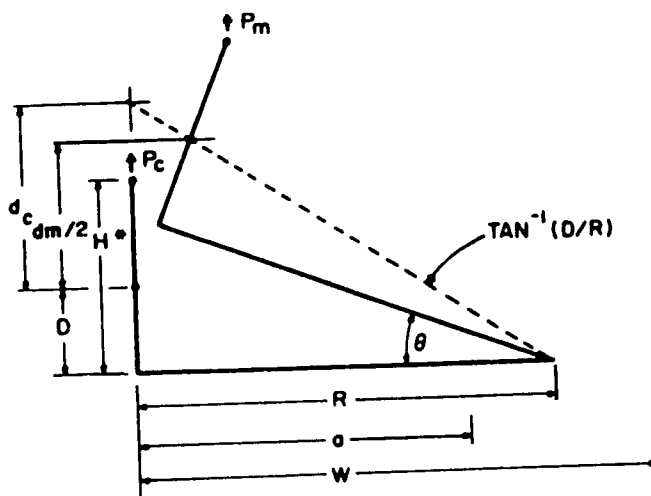
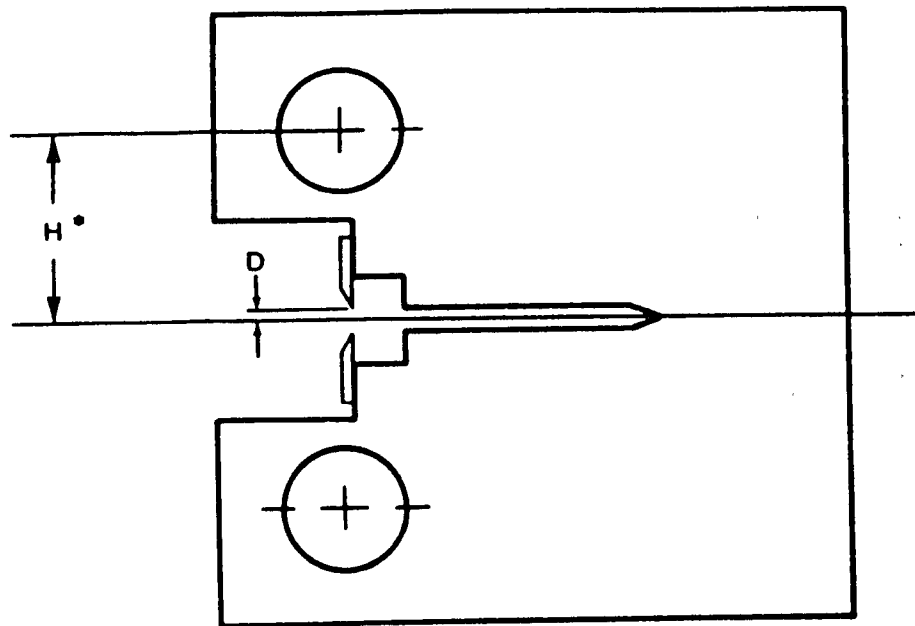


Fig. B-3 Elastic compliance correction for specimen rotation.

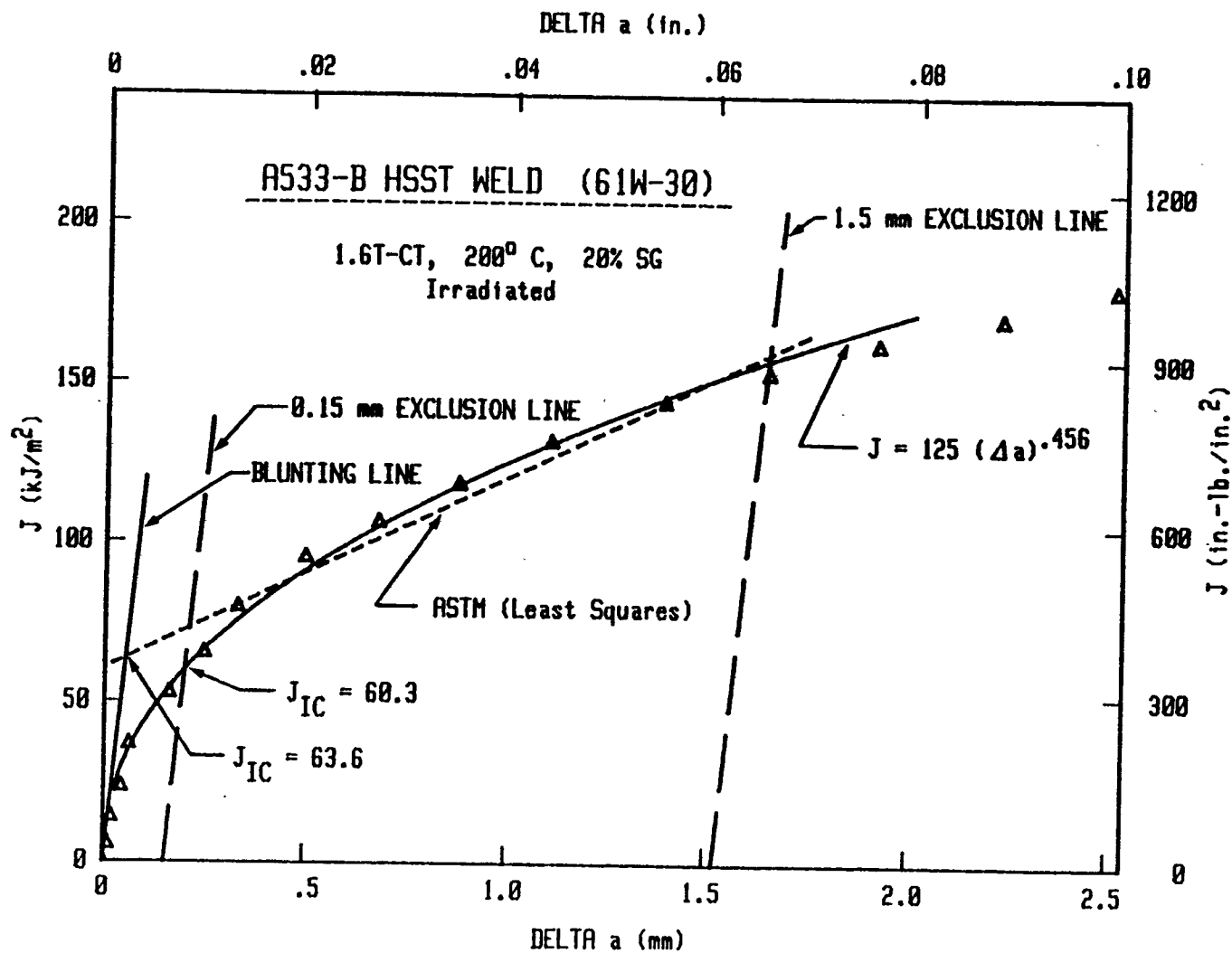


Fig. B-4 Example of a typical J-R curve. The ASTM E 813-81 format is used in these cases.

APPENDIX C

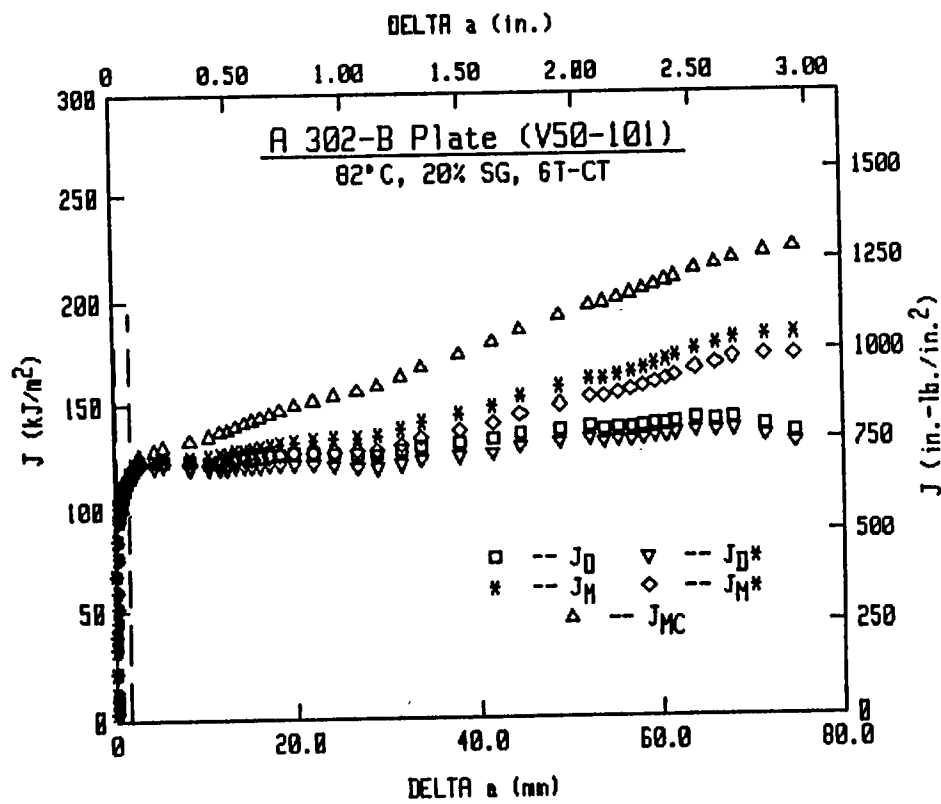
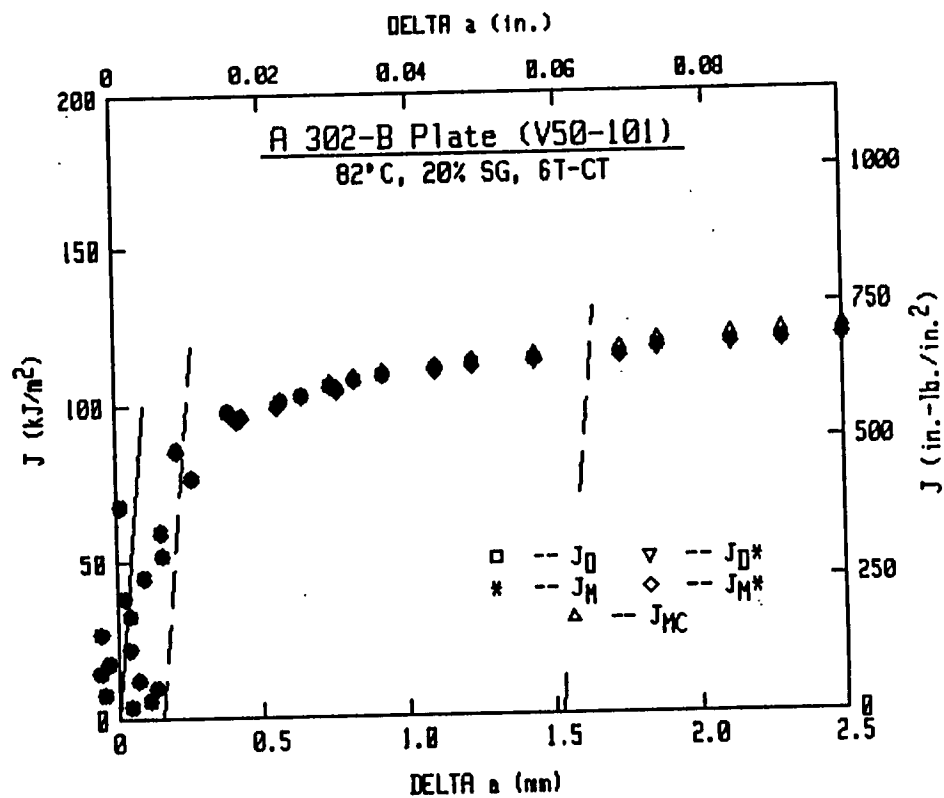
COMPILATION OF RESULTS FROM J-R CURVE TESTS

APPENDIX C

Overview

The results from the J-R curve tests are given in tabular and graphical formats. For each specimen, a table gives load, load-line deflection, total area (under the load-deflection curve), the elastic slope, crack length, Δa , and J values for each data point. The J values under a heading of "Je" are total J evaluated using Eq. 15 from ASTM Standard E 1152-87. The load-displacement curve, key-curve, and J-R curves are illustrated for each specimen.

V50-101 (6T-CT)



Specimen V50-101

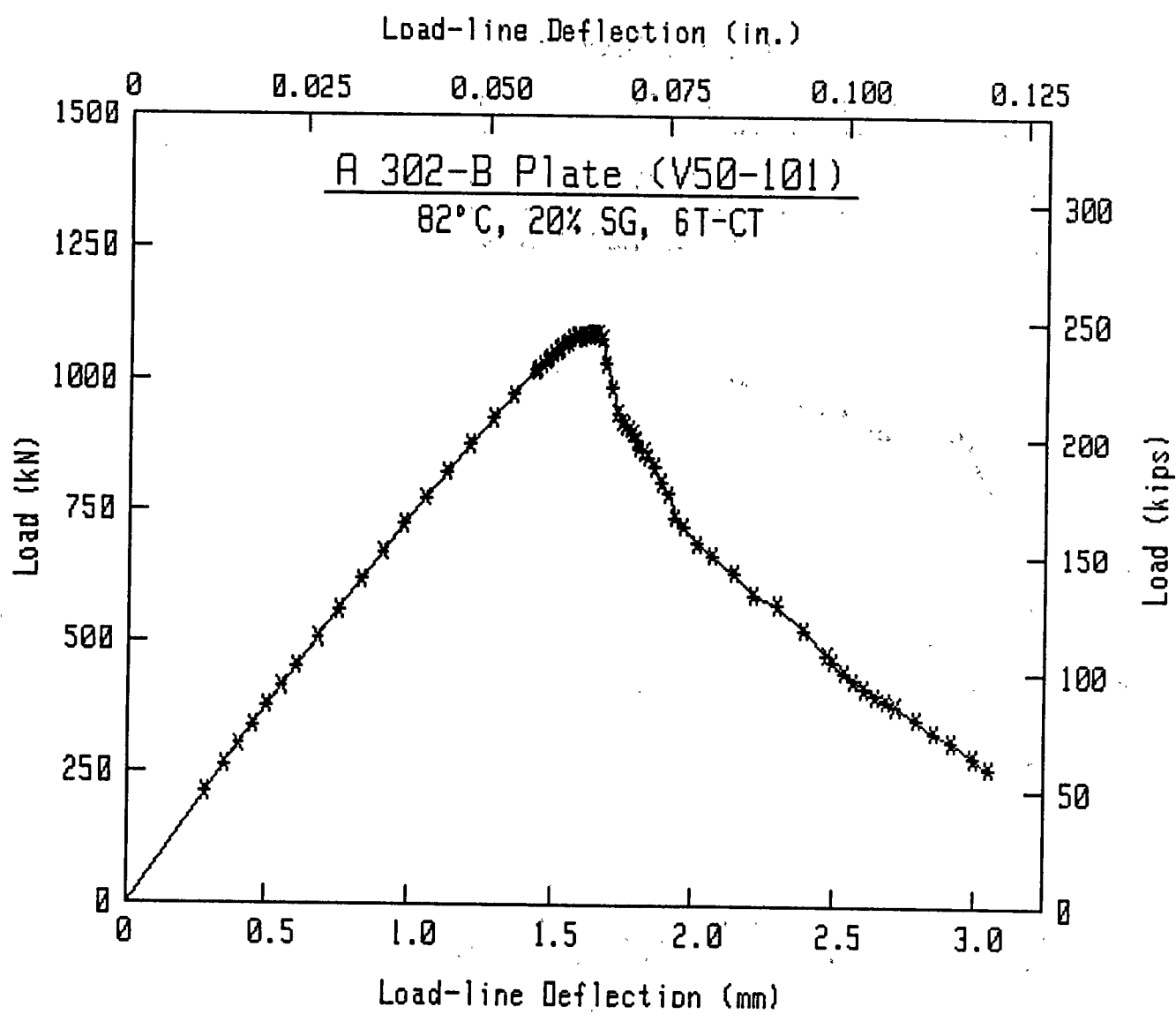
Material Type : A 302-B Plate
Side Groove : 20%
Thickness : 6 in.
Temperature : 180°F
Width : 12 in.
Ao : 6.2149 in.
Af : 9.6202 in.
Flow Stress : 75700 psi.
Young's Mod : 29336000 psi.
Initial Slope : 2.32293E-7 in./lbs.
Razor Spacing : .1 in.
Hold-Load Dis : 3.3 in.
Razor-LL Dis : 0 in.

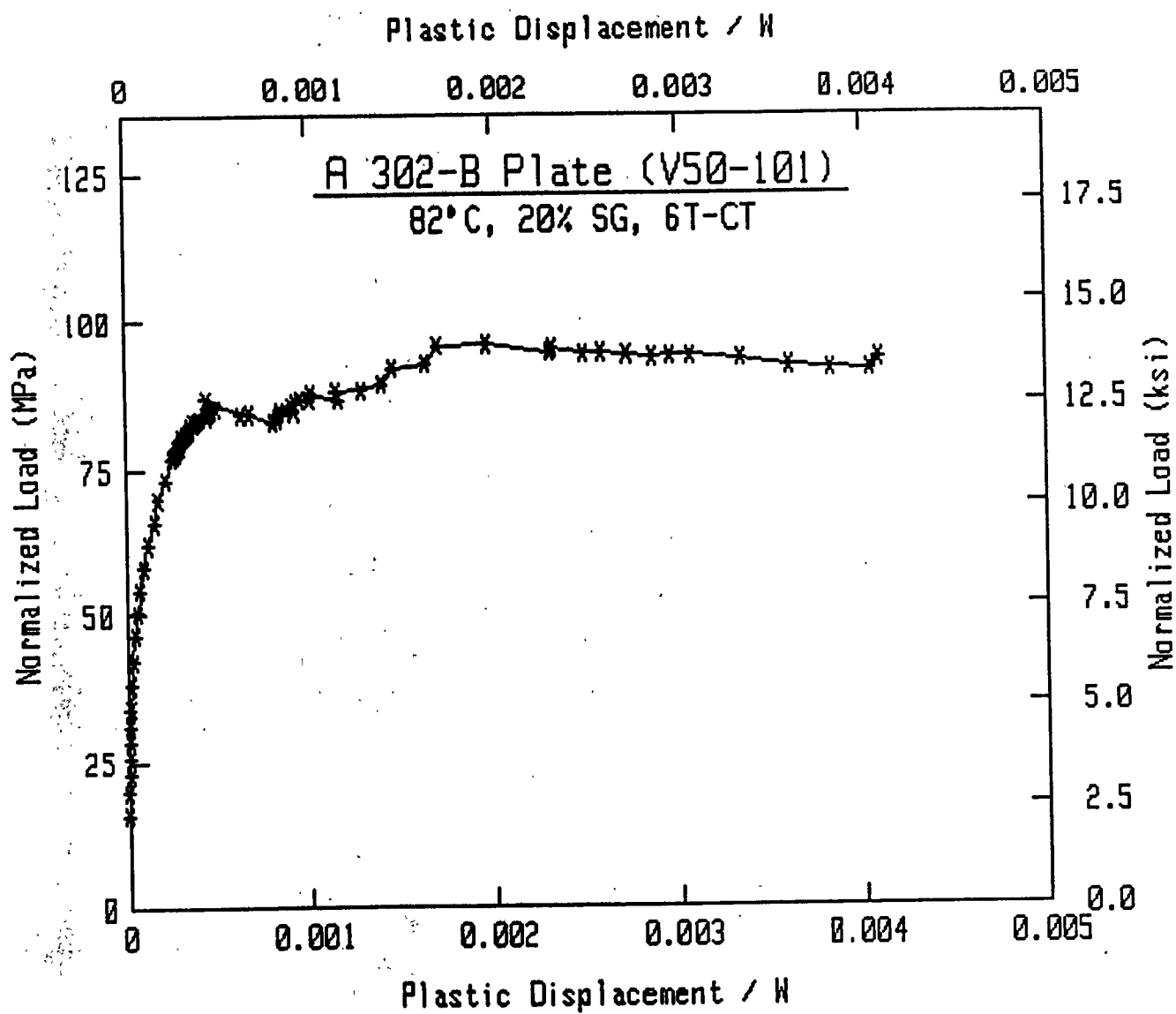
Load (lbs)	Defl. (in.)	Area (in.-lbs)	Slope (in./lbs)	Post-a (in.)	Delta-a (in.)	Jmc	Jd	Jm (in.-lbs/in. ²)	Jd*	Jm*	Je
47928.4	0.0111	266.2	2.31544E-07	6.2167	0.0018	21.6	21.6	21.6	21.5	21.5	21.5
59527.6	0.0138	411.3	2.31716E-07	6.2192	0.0043	33.4	33.4	33.4	33.1	33.1	33.1
68412.0	0.0159	544.3	2.31288E-07	6.2131	-0.0018	44.2	44.2	44.2	43.9	43.9	43.9
76564.0	0.0178	682.7	2.31615E-07	6.2201	0.0052	55.5	55.3	55.3	55.0	55.0	55.0
85083.0	0.0198	845.2	2.31523E-07	6.2177	0.0028	68.7	68.5	68.5	68.1	68.1	68.1
93223.0	0.0217	1016.9	2.31431E-07	6.2125	-0.0024	82.6	82.4	82.4	82.0	82.0	82.0
102008.0	0.0238	1219.6	2.31678E-07	6.2137	-0.0012	99.1	98.8	98.8	98.3	98.3	98.3
113941.5	0.0267	1529.0	2.31759E-07	6.2165	0.0016	124.2	123.8	123.8	123.2	123.2	123.2
126118.5	0.0296	1882.2	2.31734E-07	6.2127	-0.0022	152.9	152.5	152.5	151.7	151.7	151.7
138914.5	0.0328	2296.7	2.32113E-07	6.2166	0.0017	186.6	185.9	185.9	184.9	184.9	184.9
150669.0	0.0357	2717.6	2.32026E-07	6.2159	0.0010	220.8	220.0	220.0	218.9	218.9	218.9
162624.5	0.0387	3187.2	2.32278E-07	6.2186	0.0037	258.9	258.0	258.0	256.6	256.6	256.6
174147.0	0.0416	3678.8	2.32517E-07	6.2211	0.0062	298.8	297.6	297.6	296.1	296.1	296.1
185759.5	0.0446	4217.4	2.32487E-07	6.2210	0.0061	342.6	341.4	341.4	339.6	339.6	339.6
197404.5	0.0476	4802.2	2.31924E-07	6.2155	0.0006	390.1	389.3	389.3	387.5	387.5	387.5
208740.5	0.0507	5422.7	2.32872E-07	6.2252	0.0103	440.5	438.6	438.7	436.3	436.3	436.3
218773.0	0.0535	6020.1	2.32657E-07	6.2232	0.0083	489.0	487.3	487.4	484.9	484.9	484.9
229180.5	0.0565	6703.4	2.33464E-07	6.2315	0.0166	544.6	541.7	541.9	538.8	538.9	538.8
230081.0	0.0569	6797.2	2.33512E-07	6.2320	0.0171	552.2	549.3	549.4	546.3	546.5	546.3
231655.0	0.0574	6906.4	2.33333E-07	6.2302	0.0153	561.0	558.4	558.5	555.5	555.6	555.5
233474.0	0.0580	7046.8	2.34000E-07	6.2369	0.0220	572.5	568.9	569.1	565.7	565.8	565.7
234667.5	0.0585	7148.5	2.34041E-07	6.2374	0.0225	580.7	577.1	577.3	573.8	574.0	573.8
236278.5	0.0590	7274.3	2.34323E-07	6.2402	0.0253	590.9	587.0	587.2	583.5	583.7	583.5
238069.5	0.0596	7417.5	2.34808E-07	6.2450	0.0301	602.6	597.9	598.2	594.2	594.5	594.2
238999.0	0.0600	7516.2	2.34711E-07	6.2441	0.0292	610.6	606.1	606.4	602.4	602.7	602.4
240407.5	0.0605	7645.9	2.35027E-07	6.2473	0.0324	621.1	616.2	616.5	612.4	612.7	612.4
241567.0	0.0610	7758.8	2.35421E-07	6.2512	0.0363	630.3	624.8	625.2	620.8	621.1	620.8
242827.0	0.0616	7888.5	2.36132E-07	6.2583	0.0434	640.8	634.3	634.8	629.9	630.4	629.9
243487.5	0.0620	8003.8	2.36624E-07	6.2632	0.0483	650.2	643.0	643.6	638.3	638.9	638.3
243664.0	0.0625	8112.3	2.37486E-07	6.2717	0.0568	659.0	650.5	651.3	645.5	646.2	645.5
243702.5	0.0630	8231.2	2.38658E-07	6.2832	0.0683	668.7	658.4	659.4	652.9	653.8	652.9
244272.0	0.0638	8423.6	2.39176E-07	6.2883	0.0734	684.3	673.4	674.5	667.6	668.6	667.6
244948.0	0.0642	8534.2	2.40198E-07	6.2982	0.0833	693.3	680.8	682.1	674.6	675.8	674.6
244854.0	0.0645	8611.5	2.40911E-07	6.3051	0.0902	699.6	686.1	687.5	679.5	680.8	679.5
245301.5	0.0649	8713.3	2.41765E-07	6.3133	0.0984	707.8	693.1	694.7	686.1	687.6	686.1
244661.0	0.0654	8822.6	2.43219E-07	6.3272	0.1123	716.7	699.7	701.7	692.1	694.0	692.1
242896.5	0.0660	8973.8	2.50115E-07	6.3918	0.1769	729.0	701.2	704.6	690.7	693.8	690.6
231876.5	0.0665	9094.0	2.54295E-07	6.4299	0.2150	738.8	704.7	709.4	693.2	697.5	693.3
221653.0	0.0674	9294.1	2.67455E-07	6.5446	0.3297	755.0	701.3	710.3	686.1	694.2	686.3
210823.0	0.0681	9448.2	2.77447E-07	6.6269	0.4120	767.5	700.0	712.5	682.6	694.0	683.0
207602.0	0.0688	9581.5	2.83359E-07	6.6739	0.4590	778.4	703.2	717.9	684.4	697.7	684.8
205868.0	0.0692	9674.6	2.87764E-07	6.7080	0.4931	785.9	705.2	721.4	685.3	700.0	685.7
204466.5	0.0698	9783.8	2.91885E-07	6.7394	0.5245	794.8	709.2	726.8	688.2	704.2	688.6
202414.5	0.0703	9888.9	2.97236E-07	6.7792	0.5643	803.3	711.2	730.7	689.0	706.6	689.4
199326.0	0.0708	9982.3	3.02122E-07	6.8148	0.5999	810.9	713.0	734.2	689.9	709.0	690.3
195957.0	0.0712	10067.0	3.06866E-07	6.8486	0.6337	817.8	714.3	737.3	690.5	711.1	690.9
194749.0	0.0718	10192.1	3.12745E-07	6.8896	0.6747	828.0	717.9	743.0	692.7	715.2	693.2

Specimen V50-101

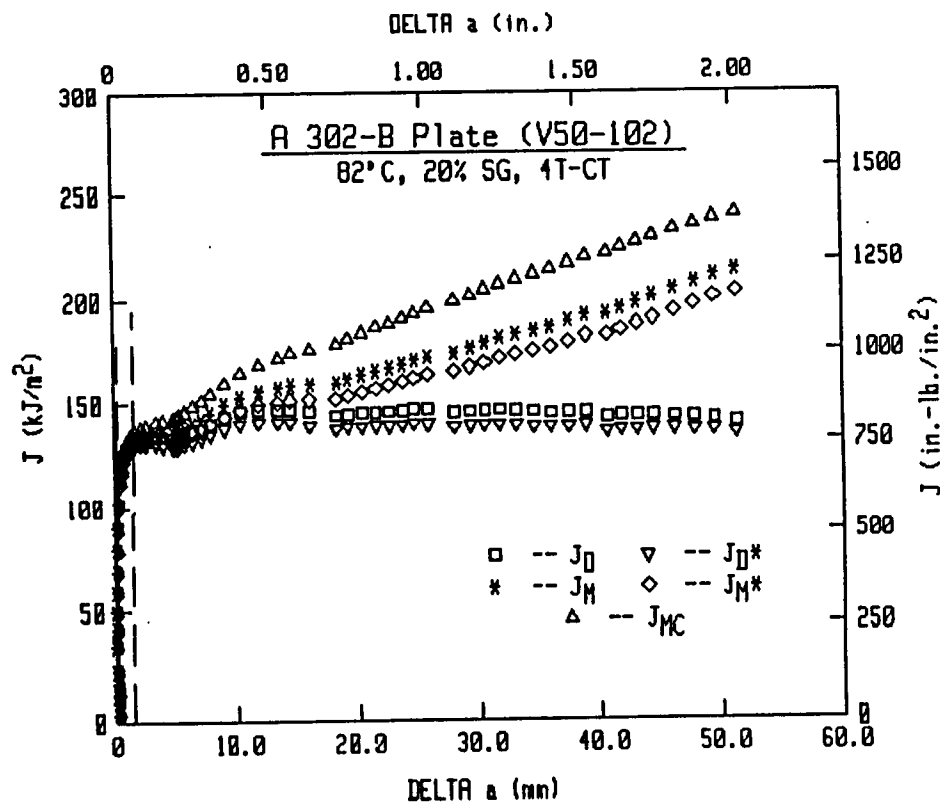
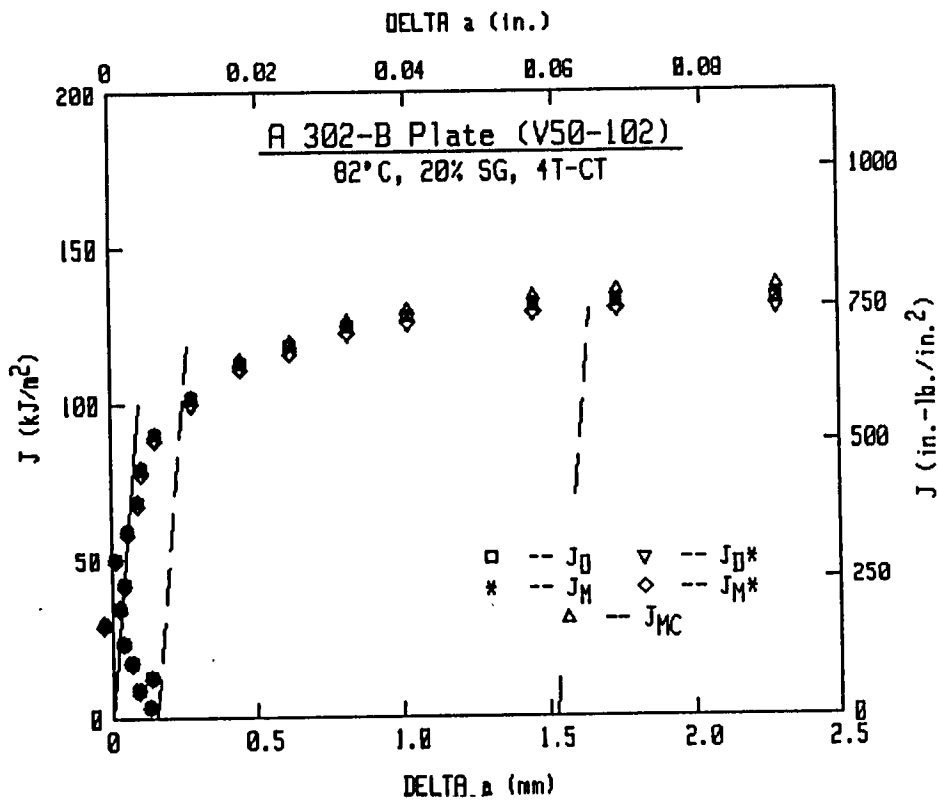
Material Type : A 302-B Plate
Side Groove : 20%
Thickness : 6 in.
Temperature : 180°F
Width : 12 in.
Ao : 6.2149 in.
Af : 9.6202 in.
Flow Stress : 75700 psi.
Young's Mod : 29336000 psi.
Initial Slope : 2.32293E-7 in./lbs.
Razor Spacing : .1 in.
Hold-Load Dis : 3.3 in.
Razor-LL Dis : 0 in.

Load (lbs)	Defl. (in.)	Area (in.-lbs)	Slope (in./lbs)	Post-a (in.)	Delta-a (in.)	Jmc <-	Jd - - - - -	Jm - - - - - (in.-lbs/in.²)	Jd* - - - - -	Jm* - - - - -	Je - - - - ->
192104.0	0.0724	10306.7	3.19238E-07	6.9336	0.7187	837.3	720.0	747.3	693.6	718.0	694.1
188125.0	0.0732	10454.4	3.28581E-07	6.9949	0.7800	849.3	721.7	752.3	693.9	721.1	694.4
181651.5	0.0742	10626.6	3.41727E-07	7.0775	0.8626	863.3	721.6	756.8	692.3	723.5	692.9
176379.0	0.0751	10796.7	3.56768E-07	7.1668	0.9519	877.1	720.0	760.2	688.9	724.4	689.6
166019.5	0.0761	10966.7	3.74910E-07	7.2681	1.0532	890.9	716.0	762.6	684.3	725.3	685.2
162158.0	0.0772	11135.9	3.91133E-07	7.3532	1.1383	904.6	715.3	767.3	682.1	727.6	683.0
154924.5	0.0792	11449.1	4.11993E-07	7.4558	1.2409	930.1	724.9	784.0	691.1	742.8	692.3
149920.5	0.0813	11765.9	4.31178E-07	7.5442	1.3293	955.8	737.9	803.5	703.3	760.7	704.6
142255.5	0.0843	12204.2	4.69965E-07	7.7072	1.4923	991.4	746.1	824.2	710.1	778.3	711.9
132891.5	0.0872	12603.4	5.08896E-07	7.8532	1.6383	1023.8	754.4	844.8	718.7	797.7	721.0
128923.0	0.0905	13027.0	5.43965E-07	7.9721	1.7572	1058.3	771.8	872.6	735.2	823.3	737.7
117775.5	0.0943	13494.9	5.99925E-07	8.1411	1.9262	1096.3	781.0	898.6	745.5	848.5	748.9
107696.0	0.0975	13845.7	6.48599E-07	8.2711	2.0562	1124.8	787.6	920.1	754.2	870.7	758.2
104641.5	0.0982	13921.2	6.73318E-07	8.3319	2.1170	1130.9	780.6	920.3	746.9	869.8	750.9
99945.5	0.0998	14075.7	6.99925E-07	8.3940	2.1791	1143.4	782.9	930.2	749.8	879.7	754.0
96660.5	0.1012	14214.5	7.25953E-07	8.4517	2.2368	1154.7	784.5	939.2	751.5	888.2	755.7
93244.0	0.1027	14354.8	7.50707E-07	8.5038	2.2889	1166.1	787.8	949.6	755.2	898.3	759.5
90177.0	0.1042	14495.7	7.74349E-07	8.5514	2.3365	1177.6	792.5	960.9	760.3	909.6	764.6
87687.5	0.1057	14623.5	8.00172E-07	8.6011	2.3862	1187.9	794.9	970.5	762.7	918.6	767.1
85555.0	0.1071	14747.4	8.21196E-07	8.6399	2.4250	1198.0	799.9	981.4	768.0	929.3	772.4
80406.0	0.1101	14992.2	8.71317E-07	8.7270	2.5121	1217.9	806.3	1001.7	775.0	949.2	779.7
74713.5	0.1125	15178.4	9.27660E-07	8.8168	2.6019	1233.0	804.2	1014.7	774.0	962.4	779.1
70593.0	0.1151	15366.8	9.79361E-07	8.8926	2.6777	1248.3	806.8	1030.9	777.2	978.4	782.6
64102.0	0.1180	15561.4	1.08249E-06	9.0280	2.8131	1264.1	791.1	1040.0	762.0	986.4	768.3
59489.0	0.1202	15696.3	1.19520E-06	9.1565	2.9416	1275.1	769.6	1041.9	740.3	986.6	747.4





V50-102 (4T-CT)



Specimen V50-102

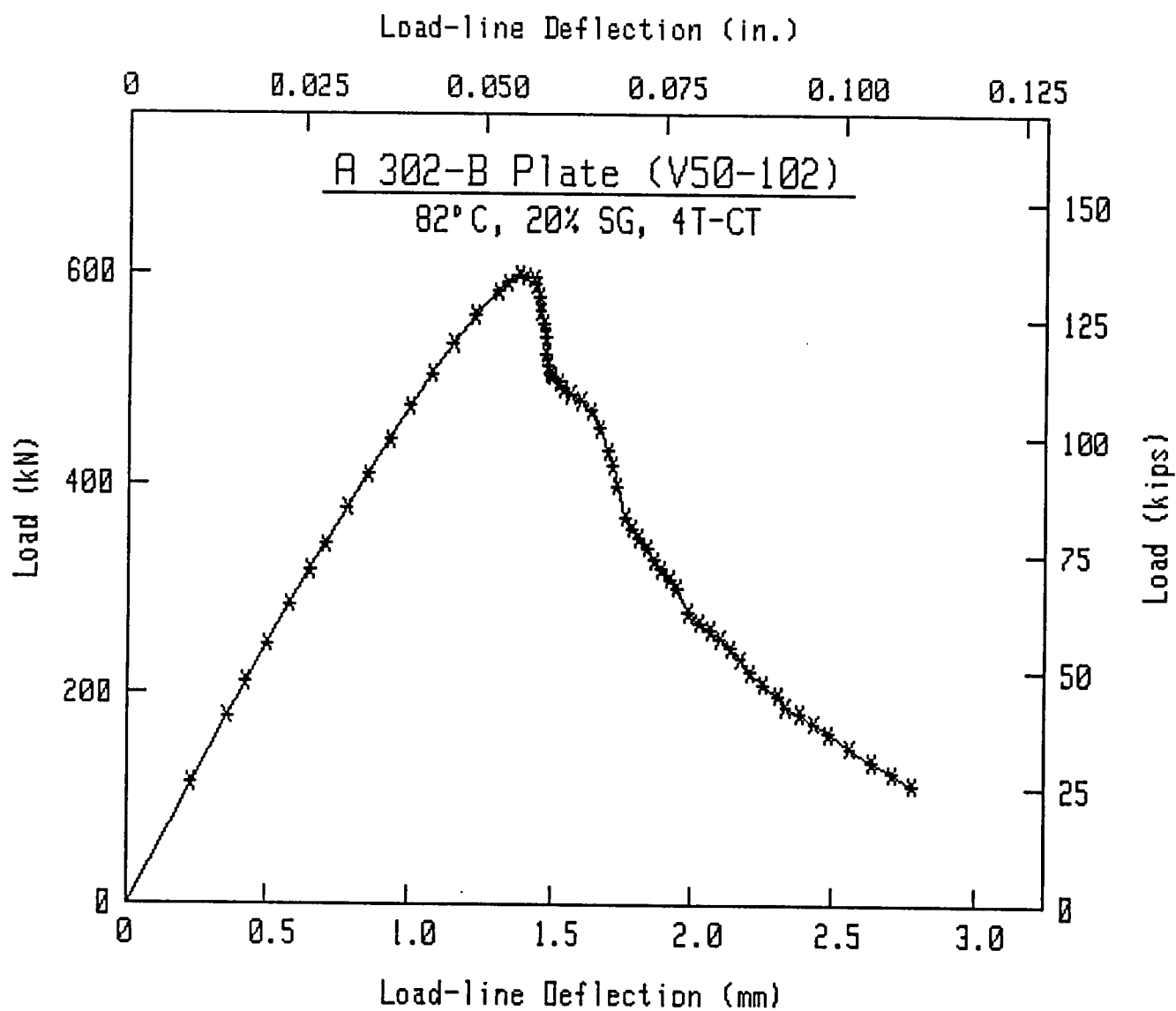
Material Type : STEEL
Side Groove : 20%
Thickness : 4 in.
Temperature : 180°F
Width : 8 in.
Ao : 4.0918 in.
Af : 6.4109 in.
Flow Stress : 75700 psi.
Young's Mod : 29336000 psi.
Initial Slope : 3.44945E-7 in./lbs.
Razor Spacing : .1 in.
Hold-Load Dis : 2.2 in.
Razor-LL Dis : 0 in.

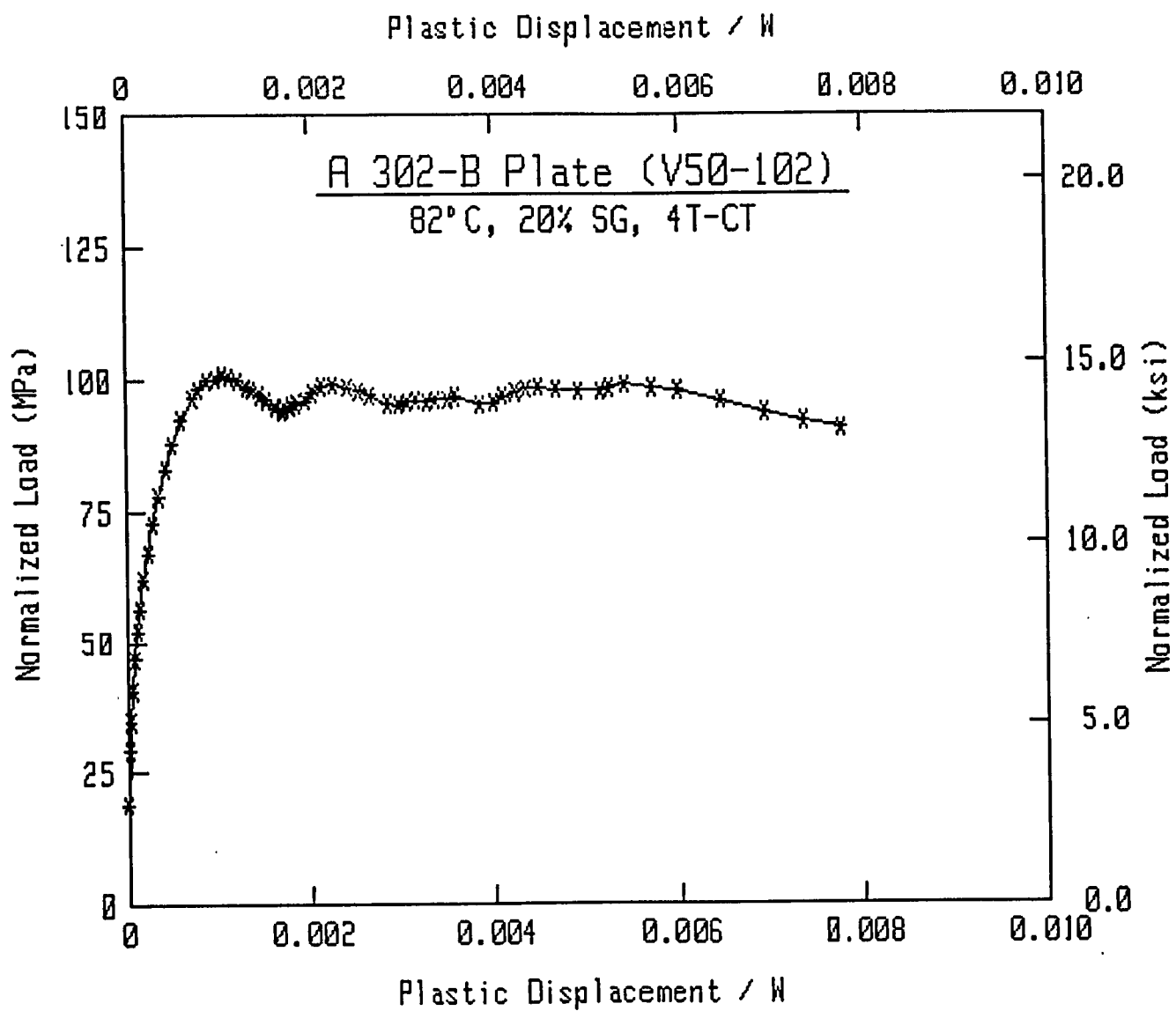
Load (lbs)	Defl. (in.)	Area (in.-lbs)	Slope (in./lbs)	Post-a (in.)	Delta-a (in.)	Jmc	Jd	Jm	Jd*	Jm*	Je
						<- - - - -	- - - - -	(in.-lbs/in.)	- - - - -	- - - - -	- - - - -
25917.8	0.0090	116.4	3.45994E-07	4.0969	0.0051	21.0	20.9	20.9	20.5	20.5	20.5
40180.0	0.0141	283.5	3.45614E-07	4.0954	0.0036	51.2	51.1	51.1	50.0	50.0	50.0
47575.0	0.0167	400.3	3.45964E-07	4.0972	0.0054	72.3	72.2	72.2	70.5	70.5	70.5
55705.0	0.0197	554.2	3.45301E-07	4.0944	0.0026	100.1	100.1	100.1	97.8	97.8	97.8
64105.0	0.0228	739.1	3.45022E-07	4.0933	0.0015	133.5	133.5	133.5	130.5	130.5	130.5
71487.5	0.0256	927.2	3.44448E-07	4.0908	-0.0010	167.5	167.5	167.5	163.8	163.8	163.8
77055.0	0.0277	1084.5	3.44893E-07	4.0929	0.0011	195.9	195.8	195.7	191.4	191.4	191.4
84847.5	0.0307	1329.8	3.44981E-07	4.0935	0.0017	240.2	240.0	239.9	234.6	234.6	234.6
92082.5	0.0336	1584.2	3.44683E-07	4.0923	0.0005	286.2	286.0	286.0	279.7	279.7	279.7
99612.5	0.0366	1877.6	3.45025E-07	4.0940	0.0022	339.2	338.7	338.7	331.3	331.3	331.3
106635.0	0.0396	2184.4	3.45295E-07	4.0954	0.0036	394.6	393.8	393.9	385.3	385.4	385.3
113515.0	0.0426	2514.5	3.45397E-07	4.0960	0.0042	454.2	453.3	453.3	443.6	443.7	443.6
119915.0	0.0455	2856.7	3.45765E-07	4.0978	0.0060	516.0	514.7	514.8	503.8	503.9	503.8
126070.0	0.0486	3230.3	3.46825E-07	4.1028	0.0110	583.5	581.2	581.4	568.9	569.1	568.9
131085.0	0.0515	3607.2	3.48243E-07	4.1094	0.0176	651.6	647.8	648.3	634.2	634.6	634.2
132907.5	0.0529	3784.5	3.49733E-07	4.1162	0.0244	683.6	678.3	679.1	663.8	664.6	663.8
134592.5	0.0544	3996.2	3.51458E-07	4.1239	0.0321	721.9	714.7	715.9	699.3	700.4	699.3
134207.5	0.0553	4112.6	3.53287E-07	4.1321	0.0403	742.9	733.7	735.4	717.8	719.3	717.8
133955.0	0.0564	4253.9	3.57123E-07	4.1491	0.0573	768.4	754.9	757.7	737.7	740.2	737.7
132510.0	0.0567	4300.7	3.59700E-07	4.1603	0.0685	776.9	760.4	764.0	742.6	745.9	742.7
129955.0	0.0572	4358.1	3.64744E-07	4.1819	0.0901	787.2	764.9	770.2	746.1	750.9	746.2
126882.5	0.0574	4382.5	3.68854E-07	4.1993	0.1075	791.6	764.6	771.4	745.3	751.4	745.4
124335.0	0.0578	4437.9	3.76117E-07	4.2295	0.1377	801.6	766.5	775.9	745.7	754.2	745.9
121337.5	0.0580	4460.6	3.81402E-07	4.2509	0.1591	805.7	764.8	776.1	743.3	753.6	743.5
117670.0	0.0582	4487.7	3.89983E-07	4.2850	0.1932	810.6	760.4	775.0	737.6	750.9	737.8
115165.0	0.0584	4513.9	3.93054E-07	4.2970	0.2052	815.4	762.0	777.9	739.2	753.7	739.4
113665.0	0.0587	4539.6	3.95689E-07	4.3071	0.2153	820.0	764.0	781.0	741.0	756.5	741.3
113022.5	0.0591	4592.8	4.00223E-07	4.3244	0.2326	829.6	769.2	788.1	745.3	762.5	745.6
111785.0	0.0599	4678.8	4.07028E-07	4.3499	0.2581	845.2	778.2	800.0	753.1	773.1	753.5
110415.0	0.0607	4761.4	4.14669E-07	4.3780	0.2862	860.1	785.8	810.9	759.5	782.5	759.9
109065.0	0.0617	4875.6	4.22705E-07	4.4067	0.3149	880.7	799.3	827.9	771.7	797.9	772.1
107720.0	0.0632	5037.5	4.35731E-07	4.4518	0.3600	910.0	816.7	851.1	787.1	818.5	787.6
105602.5	0.0646	5189.8	4.51350E-07	4.5036	0.4118	937.5	830.1	871.4	798.4	836.1	799.0
101940.0	0.0659	5326.6	4.70322E-07	4.5634	0.4716	962.2	837.8	887.5	804.3	849.6	805.2
97190.0	0.0670	5430.2	4.91513E-07	4.6266	0.5348	980.9	837.8	896.9	803.2	857.0	804.3
94000.0	0.0677	5495.9	5.05265E-07	4.6656	0.5738	992.8	838.3	903.5	803.2	862.6	804.4
89427.5	0.0684	5562.0	5.28411E-07	4.7283	0.6365	1004.7	831.0	906.3	795.0	863.7	796.4
82990.0	0.0694	5647.9	5.62695E-07	4.8147	0.7229	1020.2	819.8	909.8	783.4	865.6	785.3
80555.0	0.0704	5726.9	5.78577E-07	4.8523	0.7605	1034.5	824.0	920.7	787.5	875.8	789.5
78575.0	0.0715	5811.5	5.98146E-07	4.8969	0.8051	1049.8	827.0	931.9	789.8	885.6	791.9
76275.0	0.0725	5892.7	6.18974E-07	4.9421	0.8503	1064.4	829.1	942.5	791.3	894.9	793.6
73697.5	0.0735	5965.2	6.40286E-07	4.9864	0.8946	1077.5	829.6	951.5	791.8	903.2	794.1
71757.5	0.0745	6039.1	6.61491E-07	5.0285	0.9367	1090.9	831.2	961.5	793.0	912.1	795.5
69725.0	0.0756	6117.2	6.81685E-07	5.0668	0.9750	1105.0	835.2	973.3	796.9	923.2	799.5
67842.5	0.0766	6185.4	7.05501E-07	5.1101	1.0183	1117.3	835.0	982.2	796.4	931.0	799.1
62562.5	0.0783	6293.3	7.56326E-07	5.1961	1.1043	1136.8	827.9	993.8	790.0	941.8	793.3
60320.0	0.0797	6381.1	7.89510E-07	5.2480	1.1562	1152.7	829.4	1006.9	791.5	954.1	795.0

Specimen V50-102

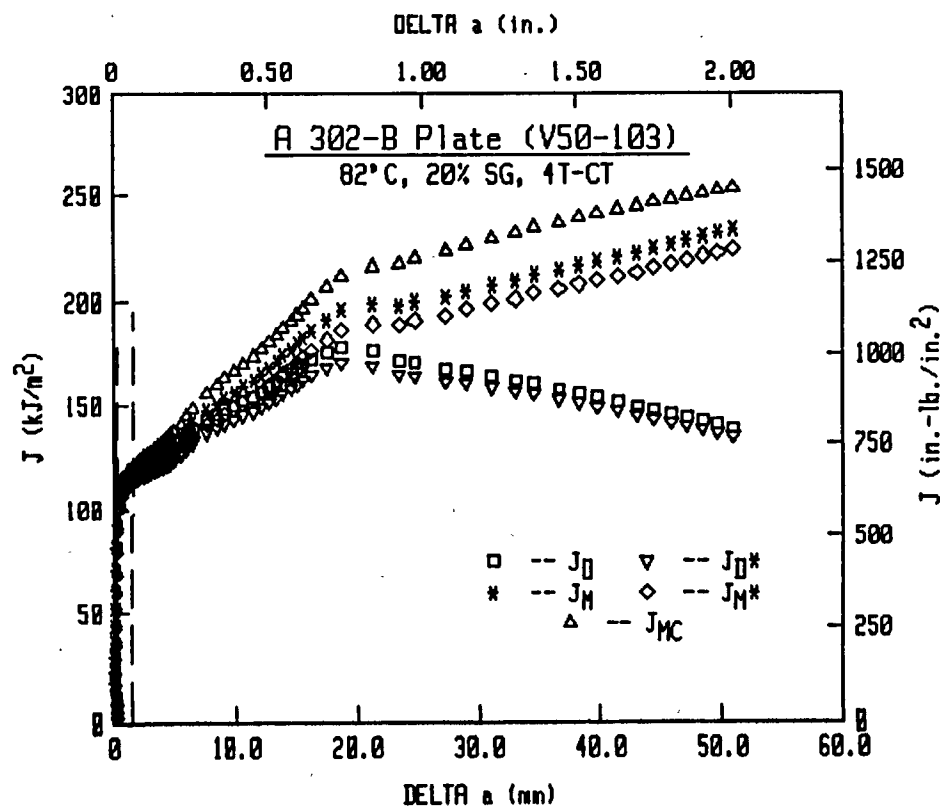
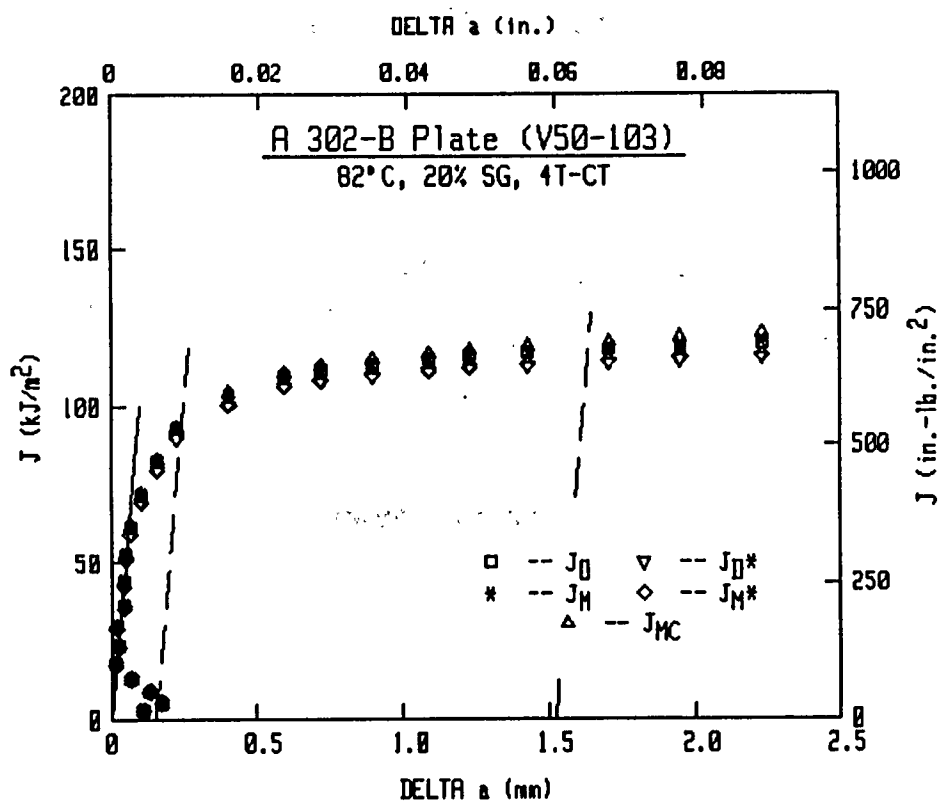
Material Type : STEEL
Side Groove : 20%
Thickness : 4 in.
Temperature : 180°F
Width : 8 in.
Ao : 4.0918 in.
Af : 6.4109 in.
Flow Stress : 75700 psi.
Young's Mod : 29336000 psi.
Initial Slope : 3.44945E-7 in./lbs.
Razor Spacing : .1 in.
Hold-Load Dis : 2.2 in.
Razor-LL Dis : 0 in.

Load (lbs)	Defl. (in.)	Area (in.-lbs)	Slope (in./lbs)	Post-a (in.)	Delta-a (in.)	Jmc < - - - - -	Jd - - - - -	Jm (in.-lbs/in. ²)	Jd*	Jm*	Je - - - - ->
58812.5	0.0812	6469.3	8.21628E-07	5.2954	1.2036	1168.6	832.7	1021.1	794.4	967.0	798.0
56942.5	0.0827	6552.1	8.56285E-07	5.3438	1.2520	1183.5	834.3	1034.0	795.9	979.0	799.7
54912.5	0.0841	6631.3	8.96216E-07	5.3963	1.3045	1197.8	833.4	1045.7	794.9	989.6	798.8
52487.5	0.0855	6706.6	9.43241E-07	5.4540	1.3622	1211.5	829.5	1055.8	791.1	998.8	795.3
49787.5	0.0869	6776.1	9.91443E-07	5.5091	1.4173	1224.0	825.2	1065.3	787.4	1007.9	791.9
47255.0	0.0888	6870.7	1.04549E-06	5.5666	1.4748	1241.1	826.6	1081.7	789.5	1023.9	794.2
44922.5	0.0908	6963.5	1.10221E-06	5.6226	1.5308	1257.9	828.1	1098.5	791.6	1040.2	796.7
42390.0	0.0920	7013.9	1.17802E-06	5.6914	1.5996	1267.0	812.5	1101.5	776.0	1042.0	781.4
40940.0	0.0939	7093.3	1.23117E-06	5.7360	1.6442	1281.3	815.9	1117.5	779.3	1057.0	785.0
38725.0	0.0960	7175.9	1.29706E-06	5.7877	1.6959	1296.2	817.1	1133.7	781.5	1073.2	787.3
36632.5	0.0980	7253.1	1.36769E-06	5.8391	1.7473	1310.2	816.9	1149.0	782.0	1088.3	788.1
33490.8	0.1009	7354.7	1.47144E-06	5.9081	1.8163	1328.5	815.7	1169.8	782.5	1109.4	789.2
30564.3	0.1038	7445.7	1.58201E-06	5.9744	1.8826	1345.0	812.6	1189.0	781.1	1129.1	788.5
28034.3	0.1067	7529.0	1.69904E-06	6.0378	1.9460	1360.0	808.7	1207.4	778.4	1147.6	786.3
25585.3	0.1094	7603.1	1.84263E-06	6.1075	2.0157	1373.4	798.6	1222.7	769.4	1162.7	778.0





V50-103 (4T-CT)



Specimen V50-103

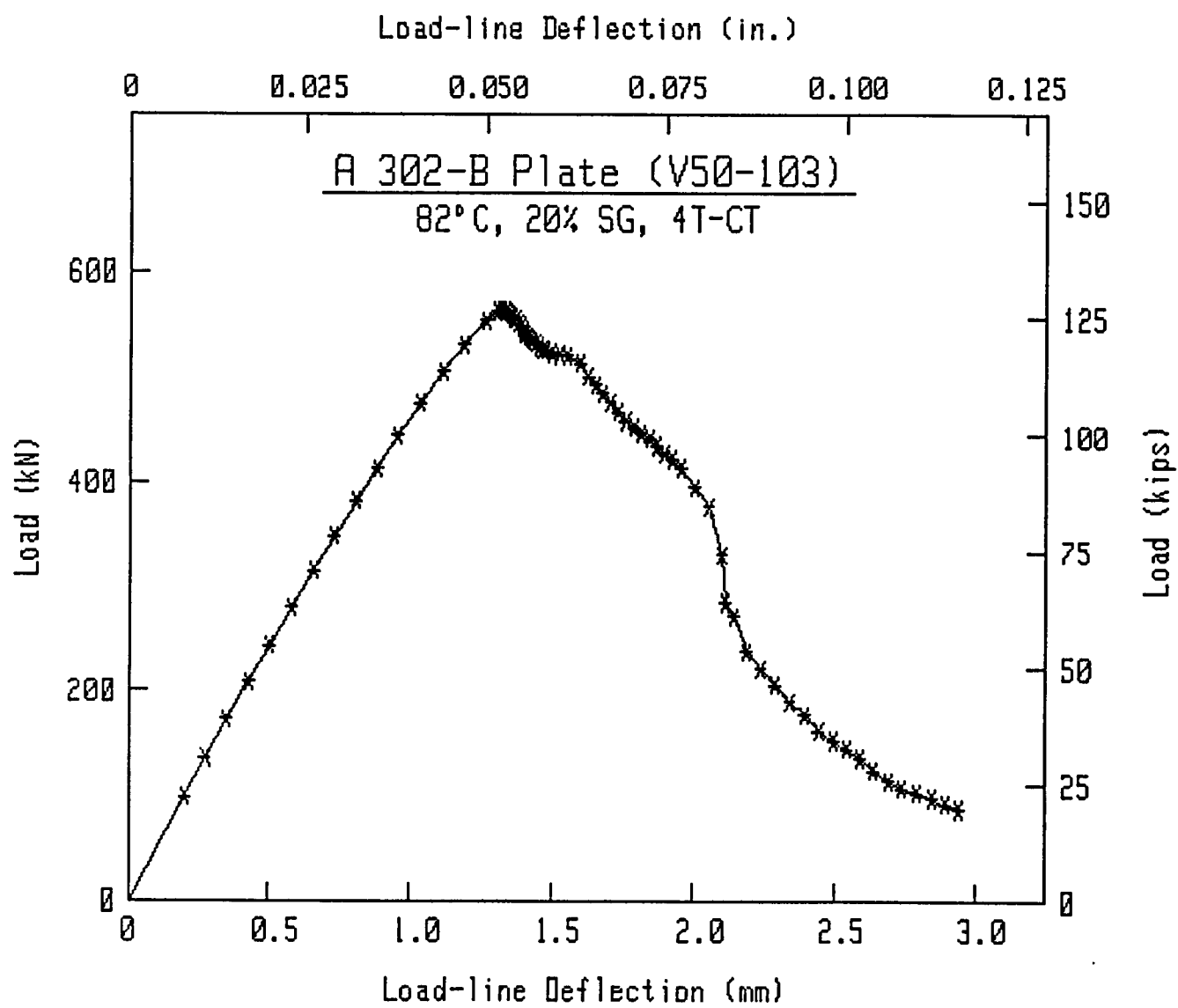
Material Type : STEEL
Side Groove : 20%
Thickness : 4 in.
Temperature : 180°F
Width : 8 in.
Ao : 4.1058 in.
Af : 6.7132 in.
Flow Stress : 75700 psi.
Young's Mod : 29336000 psi.
Initial Slope : 3.5325E-7 in./lbs.
Razor Spacing : .1 in.
Hold-Load Dis : 2.2 in.
Razor-LL Dis : 0 in.

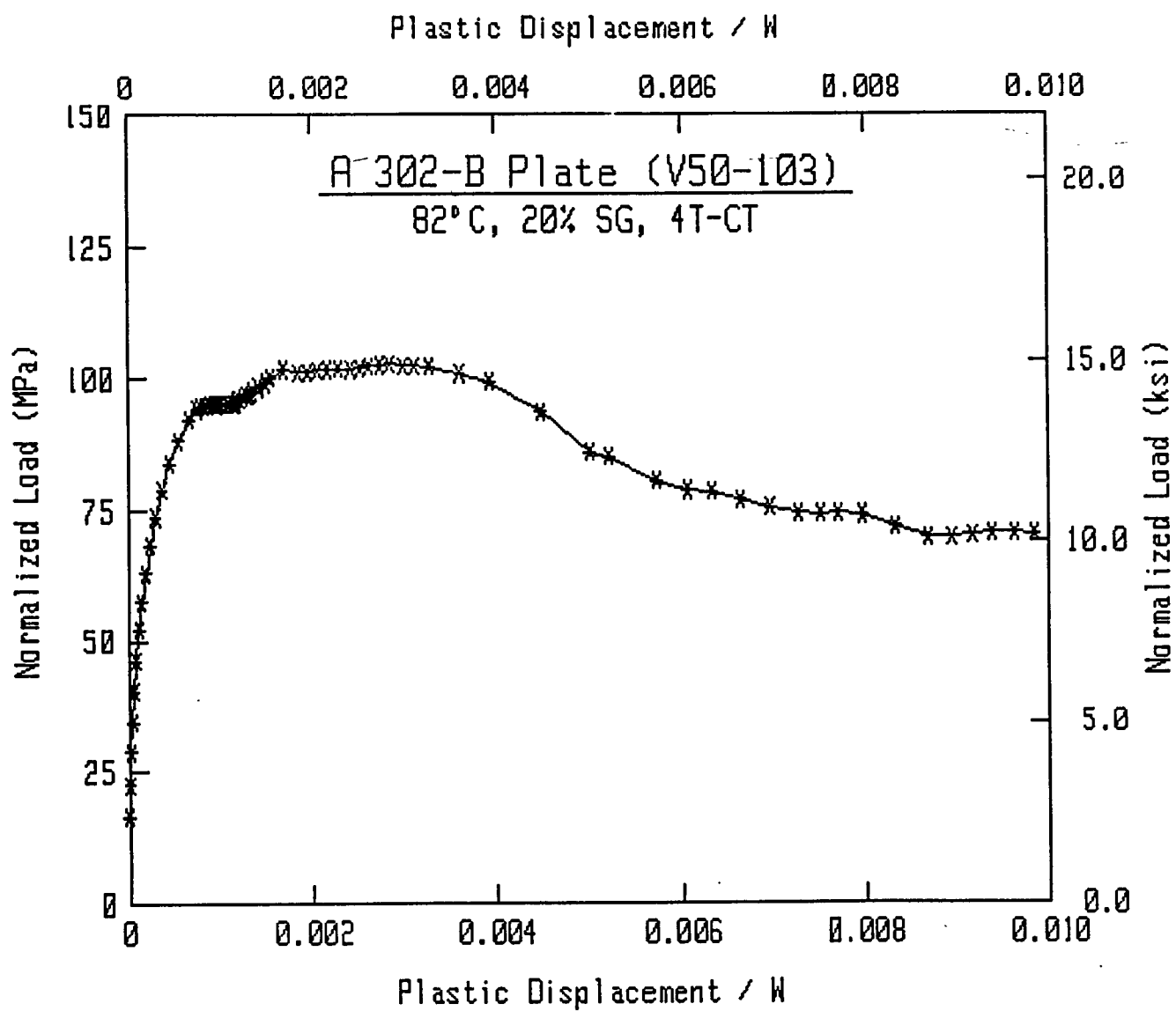
Load (lbs)	Defl. (in.)	Area (in.-lbs)	Slope (in./lbs)	Post-a (in.)	Delta-a (in.)	Jmc !<- - - - -	Jd - - - - -	Jm (in.-lbs/in. ²)	Jd* - - - - -	Jm* - - - - -	Je - - - - -!
22269.8	0.0079	88.1	3.54163E-07	4.1101	0.0043	16.0	15.9	15.9	15.3	15.3	15.3
30543.0	0.0109	166.8	3.54699E-07	4.1126	0.0068	30.2	30.1	30.1	29.0	29.0	29.0
38972.5	0.0140	273.2	3.54279E-07	4.1110	0.0052	49.5	49.4	49.4	47.6	47.6	47.6
46832.5	0.0169	397.1	3.53685E-07	4.1085	0.0027	72.0	71.9	71.9	69.2	69.2	69.2
54785.0	0.0198	547.3	3.53173E-07	4.1064	0.0006	99.2	99.2	99.2	95.5	95.5	95.5
62832.5	0.0228	725.8	3.53212E-07	4.1068	0.0010	131.5	131.5	131.5	126.6	126.6	126.6
70712.5	0.0259	927.9	3.53131E-07	4.1065	0.0007	168.2	168.1	168.1	161.8	161.8	161.8
78252.5	0.0288	1147.7	3.53335E-07	4.1076	0.0018	208.0	207.7	207.7	200.1	200.1	200.1
85775.0	0.0318	1394.7	3.53274E-07	4.1075	0.0017	252.7	252.4	252.4	243.2	243.2	243.2
93012.5	0.0348	1659.1	3.53315E-07	4.1078	0.0020	300.6	300.3	300.3	289.4	289.4	289.4
100032.5	0.0378	1945.4	3.53402E-07	4.1084	0.0026	352.5	352.0	352.0	339.4	339.4	339.4
106982.5	0.0408	2260.4	3.53712E-07	4.1099	0.0041	409.6	408.8	408.8	394.3	394.4	394.3
113607.5	0.0439	2597.2	3.54177E-07	4.1121	0.0063	470.7	469.4	469.5	453.0	453.1	453.0
119350.0	0.0468	2936.5	3.54730E-07	4.1147	0.0089	532.1	530.4	530.6	512.1	512.2	512.1
124402.5	0.0497	3299.0	3.56285E-07	4.1217	0.0159	597.8	594.6	595.1	574.3	574.7	574.3
126485.0	0.0514	3501.3	3.57966E-07	4.1292	0.0234	634.5	629.7	630.5	608.2	608.8	608.2
126712.5	0.0519	3571.7	3.59092E-07	4.1341	0.0283	647.2	641.4	642.4	619.4	620.3	619.5
126572.5	0.0524	3635.8	3.60693E-07	4.1411	0.0353	658.9	651.4	652.8	629.0	630.2	629.1
126307.5	0.0529	3695.3	3.62444E-07	4.1487	0.0429	669.6	660.5	662.3	637.6	639.1	637.6
125762.5	0.0532	3735.3	3.63723E-07	4.1542	0.0484	676.9	666.5	668.6	643.4	645.2	643.4
125082.5	0.0535	3774.8	3.65553E-07	4.1621	0.0563	684.0	671.8	674.4	648.4	650.6	648.4
124767.5	0.0539	3819.9	3.68116E-07	4.1730	0.0672	692.2	677.5	680.7	653.3	656.0	653.3
123742.5	0.0542	3861.2	3.70406E-07	4.1826	0.0768	699.7	682.7	686.6	658.1	661.5	658.2
123200.0	0.0546	3906.6	3.73025E-07	4.1936	0.0878	707.9	688.4	693.0	663.2	667.1	663.2
122235.0	0.0549	3946.7	3.76227E-07	4.2069	0.1011	715.2	692.5	698.0	666.6	671.4	666.7
121530.0	0.0552	3979.4	3.78738E-07	4.2172	0.1114	721.1	695.9	702.2	669.6	675.0	669.7
120962.5	0.0555	4018.8	3.81006E-07	4.2264	0.1206	728.3	700.9	707.9	674.1	680.1	674.2
120642.5	0.0559	4062.5	3.84416E-07	4.2401	0.1343	736.2	705.5	713.5	677.8	684.7	677.9
120122.5	0.0563	4110.1	3.87236E-07	4.2514	0.1456	744.8	711.5	720.4	683.2	690.8	683.2
119635.0	0.0567	4163.2	3.90777E-07	4.2654	0.1596	754.4	717.8	727.8	688.6	697.2	688.7
119002.5	0.0572	4225.3	3.94241E-07	4.2789	0.1731	765.7	725.9	737.0	696.0	705.5	696.1
118337.5	0.0576	4270.2	3.96857E-07	4.2890	0.1832	773.8	731.6	743.6	701.2	711.5	701.4
118105.0	0.0581	4324.5	4.00150E-07	4.3016	0.1958	783.7	738.5	751.5	707.3	718.5	707.4
117517.5	0.0591	4439.7	4.06408E-07	4.3252	0.2194	804.5	753.7	768.9	721.1	734.2	721.2
117137.5	0.0601	4561.7	4.11622E-07	4.3445	0.2387	826.6	771.5	788.5	737.6	752.3	737.8
116977.5	0.0611	4679.9	4.16569E-07	4.3625	0.2567	848.1	788.8	807.6	753.7	770.0	753.9
115422.5	0.0631	4912.9	4.29601E-07	4.4088	0.3030	890.3	819.4	843.2	781.8	802.4	782.1
112500.0	0.0642	5029.3	4.39253E-07	4.4418	0.3360	911.4	831.6	859.3	793.3	817.4	793.7
110777.5	0.0651	5138.0	4.46470E-07	4.4659	0.3601	931.1	845.2	876.0	806.1	832.9	806.6
108937.5	0.0662	5255.2	4.56219E-07	4.4977	0.3919	952.3	857.9	892.9	817.7	848.2	818.2
107137.5	0.0672	5365.8	4.65064E-07	4.5257	0.4199	972.4	870.5	909.4	829.5	863.5	830.1
104975.0	0.0683	5476.6	4.76167E-07	4.5599	0.4541	992.4	881.0	925.0	839.0	877.5	839.7
102995.0	0.0694	5587.5	4.85095E-07	4.5867	0.4809	1012.5	894.1	942.2	851.7	893.9	852.4
101657.5	0.0704	5696.5	4.93259E-07	4.6106	0.5048	1032.3	907.7	959.8	864.7	910.4	865.4
100352.5	0.0715	5800.5	5.01995E-07	4.6356	0.5298	1051.1	920.0	976.2	876.0	925.5	876.8
99362.5	0.0726	5911.0	5.08889E-07	4.6550	0.5492	1071.1	935.6	995.3	891.3	943.9	892.1
97845.0	0.0737	6018.4	5.18846E-07	4.6823	0.5765	1090.6	947.5	1012.2	902.5	959.6	903.4

Specimen V50-103

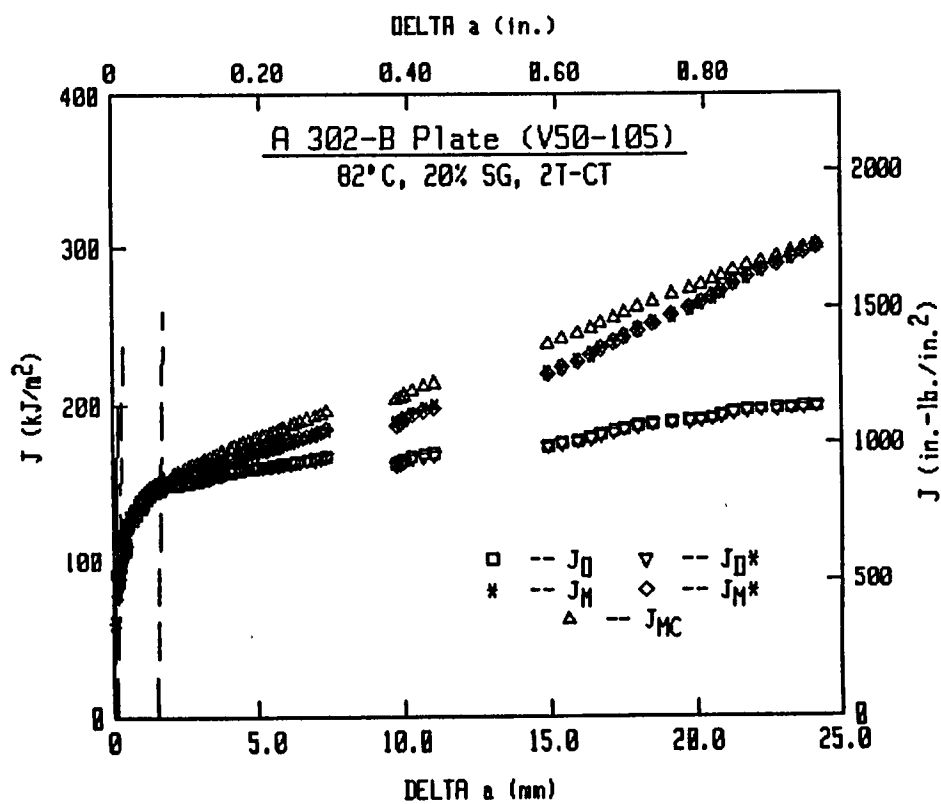
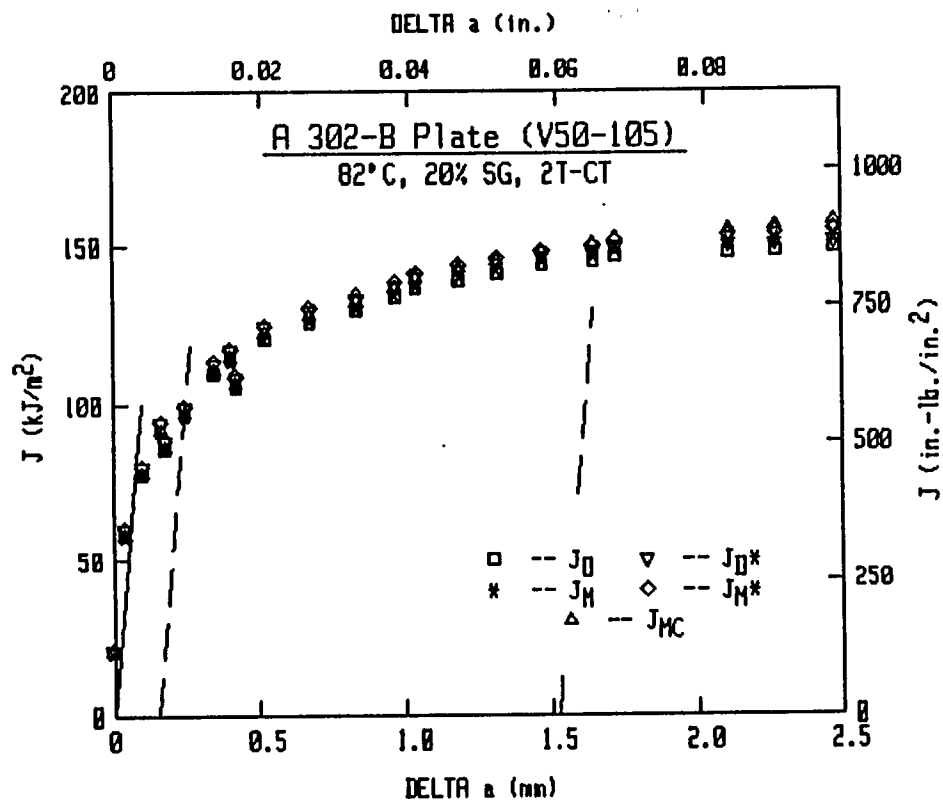
Material Type : STEEL
 Side Groove : 20%
 Thickness : 4 in.
 Temperature : 180°F
 Width : 8 in.
 Ao : 4.1058 in.
 Af : 6.7132 in.
 Flow Stress : 75700 psi.
 Young's Mod : 29336000 psi.
 Initial Slope : 3.5325E-7 in./lbs.
 Razor Spacing : .1 in.
 Hold-Load Dis : 2.2 in.
 Razor-LL Dis : 0 in.

Load (lbs)	Defl. (in.)	Area (in.-lbs)	Slope (in./lbs)	Post-a (in.)	Delta-a (in.)	Jmc !<- - - - -	Jd - - - - -	Jm (in.-lbs/in. ²)	Jd* - - - - -	Jm* - - - - -	Je - - - - -
96182.5	0.0746	6109.7	5.25914E-07	4.7013	0.5955	1107.2	959.3	1027.7	914.4	974.8	915.3
95052.5	0.0757	6207.9	5.32703E-07	4.7192	0.6134	1124.9	972.9	1044.9	927.7	991.4	928.7
93165.0	0.0769	6322.0	5.43394E-07	4.7468	0.6410	1145.6	986.0	1063.7	940.5	1009.5	941.6
88802.5	0.0789	6509.4	5.63577E-07	4.7969	0.6911	1179.6	1005.1	1094.1	960.2	1039.6	961.6
84535.0	0.0808	6671.3	5.83614E-07	4.8444	0.7386	1208.9	1019.9	1120.5	975.8	1065.8	977.4
74245.0	0.0827	6819.5	6.29748E-07	4.9456	0.8398	1235.8	1008.4	1136.0	967.1	1082.5	970.0
63942.5	0.0832	6851.4	6.72656E-07	5.0311	0.9253	1241.6	978.9	1131.2	942.2	1081.0	946.0
61025.0	0.0845	6929.3	6.99840E-07	5.0815	0.9757	1255.7	975.2	1142.6	939.0	1092.1	943.0
53487.5	0.0863	7034.5	7.58701E-07	5.1819	1.0761	1274.8	955.9	1154.8	922.4	1105.5	927.7
49640.0	0.0883	7132.3	8.01458E-07	5.2483	1.1425	1292.5	950.3	1170.8	918.2	1122.0	924.0
46322.5	0.0904	7232.2	8.59139E-07	5.3305	1.2247	1310.6	938.3	1186.1	906.7	1136.5	913.2
42622.5	0.0923	7316.7	9.18382E-07	5.4073	1.3015	1325.9	925.2	1199.1	894.7	1149.6	901.9
39762.5	0.0943	7399.2	9.69003E-07	5.4676	1.3618	1340.8	919.3	1214.5	890.0	1165.3	897.6
36445.0	0.0963	7473.3	1.04413E-06	5.5494	1.4436	1354.3	901.5	1225.8	873.1	1176.4	881.5
34389.8	0.0982	7541.8	1.10838E-06	5.6130	1.5072	1366.7	890.9	1238.3	863.0	1188.4	871.8
32672.3	0.1001	7602.8	1.17353E-06	5.6724	1.5666	1377.7	880.4	1249.6	852.8	1199.2	861.9
30536.8	0.1021	7665.8	1.25339E-06	5.7392	1.6334	1389.2	867.2	1261.1	840.1	1210.3	849.7
27886.3	0.1039	7719.0	1.33480E-06	5.8013	1.6955	1398.8	853.5	1271.1	827.8	1220.9	837.9
25693.3	0.1059	7772.4	1.41185E-06	5.8554	1.7496	1408.5	843.9	1282.6	819.4	1232.9	829.8
24235.0	0.1080	7823.7	1.50043E-06	5.9125	1.8067	1417.8	832.3	1293.6	808.2	1243.5	819.0
23169.0	0.1101	7872.7	1.58458E-06	5.9626	1.8568	1426.6	823.6	1304.9	799.7	1254.3	810.7
22076.5	0.1121	7918.8	1.67893E-06	6.0144	1.9086	1435.0	813.3	1315.4	789.5	1264.2	800.8
20926.5	0.1141	7960.3	1.77496E-06	6.0630	1.9572	1442.5	803.1	1325.1	779.7	1273.5	791.1
19781.5	0.1160	7998.5	1.88081E-06	6.1124	2.0066	1449.4	791.5	1333.8	768.5	1281.9	780.1





V50-105 (2T-CT)



Specimen V50-105

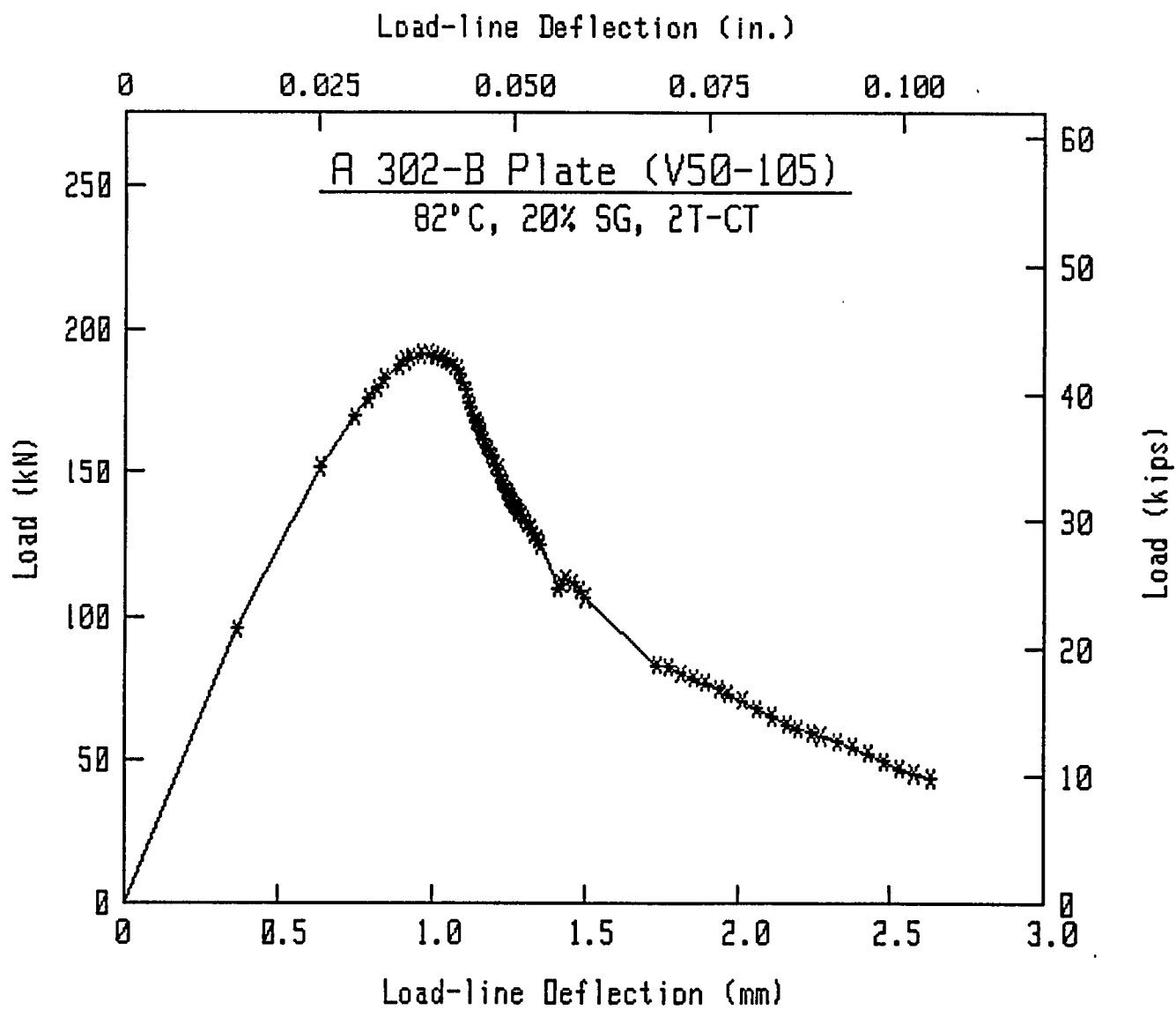
Material Type : A302-B PLATE
Side Groove : 20%
Thickness : 2 in.
Temperature : 180°F
Width : 4 in.
Ao : 2.0624 in.
Af : 3.1166 in.
Flow Stress : 75700 psi.
Young's Mod : 29372000 psi.
Initial Slope : 6.5065E-7 in./lbs.
Razor Spacing : .115 in.
Hold-Load Dis : 1.1 in.
Razor-LL Dis : 0 in.

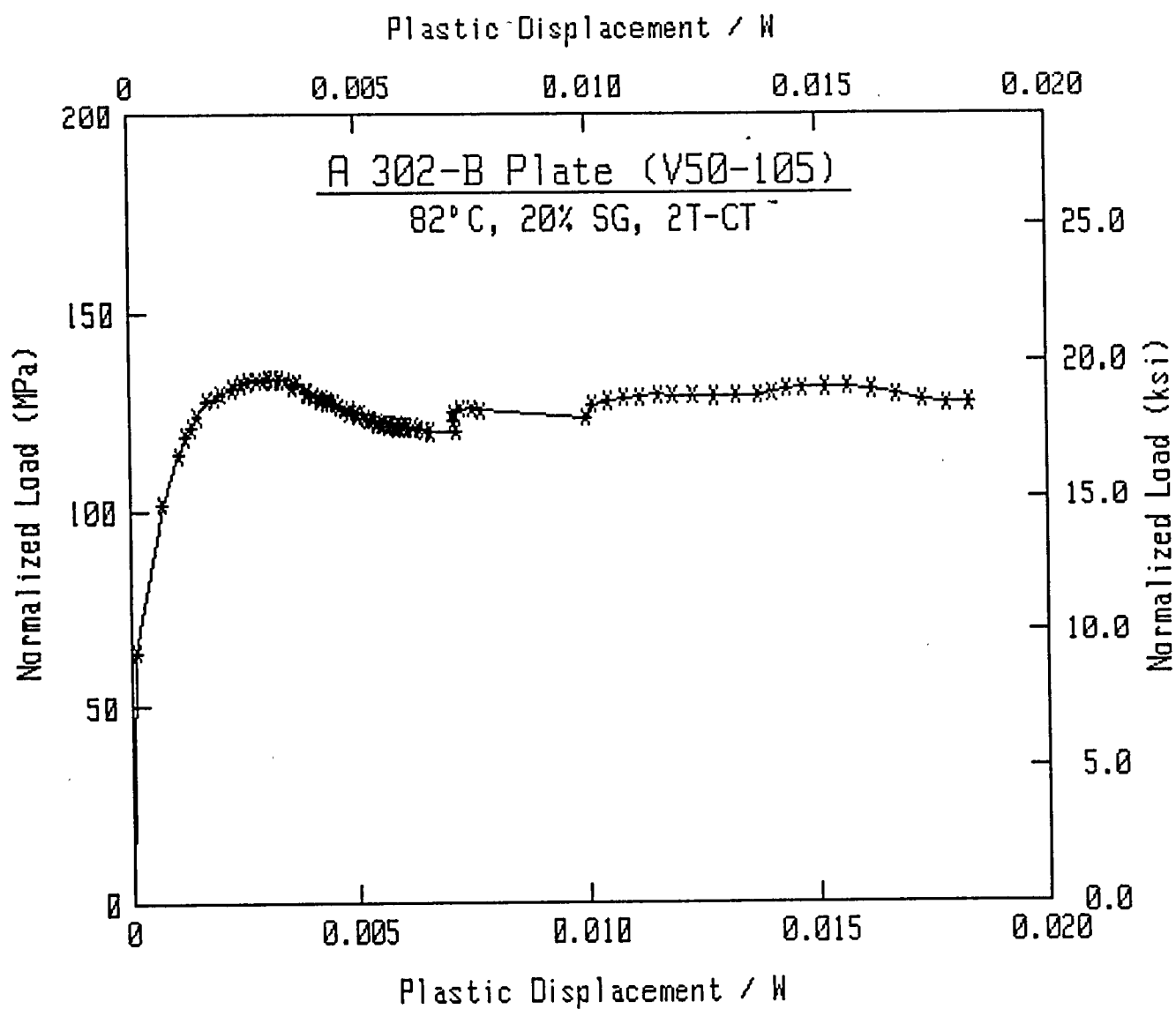
Load (lbs)	Defl. (in.)	Area (in.-lbs)	Slope (in./lbs)	Post-a (in.)	Delta-a (in.)	Jmc [< - - - - -]	Jd - - - - -]	Jm (in.-lbs/in. ²)	Jd* - - - - -]	Jm* - - - - -]	Je - - - - -]
21499.0	0.0145	157.1	6.49839E-07	2.0622	-0.0002	114.4	114.2	114.2	118.8	118.8	118.8
34166.0	0.0251	456.4	6.50814E-07	2.0639	0.0015	332.3	331.3	331.3	343.0	343.0	343.0
38230.0	0.0293	608.4	6.52634E-07	2.0663	0.0039	442.9	441.0	441.2	456.3	456.5	456.3
39651.0	0.0310	674.6	6.55112E-07	2.0694	0.0070	491.1	488.2	488.6	504.8	505.2	504.8
40454.0	0.0321	718.1	6.54609E-07	2.0688	0.0064	522.7	520.0	520.4	537.5	537.9	537.5
41194.0	0.0332	760.6	6.57326E-07	2.0721	0.0097	553.7	549.8	550.4	567.9	568.6	568.0
42256.0	0.0350	837.0	6.63076E-07	2.0790	0.0166	609.3	602.6	603.9	621.6	623.1	621.6
42571.0	0.0358	870.4	6.60534E-07	2.0761	0.0137	633.6	628.3	629.3	647.9	649.1	648.0
42830.0	0.0366	904.5	6.62407E-07	2.0783	0.0159	658.5	652.2	653.5	672.1	673.5	672.1
43096.0	0.0379	962.6	6.66236E-07	2.0829	0.0205	700.8	692.5	694.5	712.5	714.7	712.5
43114.0	0.0390	1006.5	6.71430E-07	2.0890	0.0266	732.7	721.5	724.5	741.3	744.6	741.4
42981.0	0.0397	1039.4	6.76919E-07	2.0953	0.0329	756.7	742.4	746.6	761.7	766.3	761.8
42833.0	0.0405	1073.4	6.81440E-07	2.1005	0.0381	781.5	764.6	769.9	783.6	789.3	783.8
42647.0	0.0411	1096.2	6.83874E-07	2.1033	0.0409	798.1	779.9	785.7	798.7	805.0	798.8
42508.0	0.0416	1121.2	6.89097E-07	2.1092	0.0468	816.3	795.1	802.2	813.4	821.1	813.5
42211.0	0.0421	1140.9	6.93593E-07	2.1143	0.0519	830.6	806.8	815.1	824.6	833.6	824.8
41908.0	0.0427	1164.3	6.99062E-07	2.1204	0.0580	847.6	820.6	830.4	837.8	848.4	838.0
41492.0	0.0431	1181.9	7.05438E-07	2.1273	0.0649	860.5	829.5	841.1	846.0	858.4	846.2
40894.0	0.0435	1196.4	7.08183E-07	2.1303	0.0679	871.0	838.6	850.9	854.4	867.6	854.6
40304.0	0.0440	1218.1	7.22459E-07	2.1456	0.0832	886.8	845.3	861.9	859.3	876.9	859.6
39352.0	0.0442	1227.2	7.28471E-07	2.1519	0.0895	893.5	848.3	866.7	861.6	881.1	861.9
38970.0	0.0446	1240.2	7.36069E-07	2.1598	0.0974	902.9	853.2	874.0	865.4	887.4	865.7
38347.0	0.0448	1248.9	7.42678E-07	2.1666	0.1042	909.2	855.5	878.4	867.1	891.2	867.4
37901.0	0.0450	1257.7	7.45592E-07	2.1696	0.1072	915.7	860.4	884.2	871.5	896.6	871.8
37767.0	0.0453	1267.1	7.53332E-07	2.1774	0.1150	922.5	862.6	888.9	873.2	900.8	873.5
37447.0	0.0455	1277.1	7.59547E-07	2.1836	0.1212	929.8	866.3	894.6	876.3	906.0	876.7
37000.0	0.0458	1284.9	7.64168E-07	2.1881	0.1257	935.4	869.3	899.2	878.8	910.0	879.2
36687.0	0.0460	1294.0	7.69056E-07	2.1929	0.1305	942.0	873.2	904.7	882.2	915.1	882.6
36323.0	0.0463	1304.1	7.76194E-07	2.1998	0.1374	949.4	876.5	910.3	884.9	920.2	885.3
35842.0	0.0466	1313.9	7.80209E-07	2.2037	0.1413	956.5	881.5	916.8	889.5	926.2	889.8
35552.0	0.0468	1322.8	7.85445E-07	2.2087	0.1463	963.0	885.2	922.2	892.7	931.2	893.1
35041.0	0.0470	1330.5	7.88057E-07	2.2112	0.1488	968.6	889.5	927.5	896.6	936.1	897.0
34849.0	0.0474	1343.8	7.99678E-07	2.2220	0.1596	978.3	892.5	934.5	899.0	942.6	899.4
34319.0	0.0477	1352.5	8.05229E-07	2.2272	0.1648	984.6	895.9	939.9	901.8	947.4	902.3
34018.0	0.0481	1366.2	8.13551E-07	2.2348	0.1724	994.6	901.5	948.5	907.0	955.6	907.4
33508.0	0.0483	1374.2	8.19766E-07	2.2404	0.1780	1000.5	904.0	953.2	908.9	959.8	909.4
33111.0	0.0485	1382.0	8.27714E-07	2.2474	0.1850	1006.1	905.3	957.3	909.6	963.4	910.1
32791.0	0.0488	1389.6	8.35036E-07	2.2539	0.1915	1011.6	906.8	961.5	910.8	967.1	911.3
32373.0	0.0490	1397.1	8.39194E-07	2.2575	0.1951	1017.1	910.3	966.5	913.8	971.7	914.3
32209.0	0.0493	1405.2	8.48380E-07	2.2655	0.2031	1023.0	911.2	970.7	914.4	975.6	914.9
31856.0	0.0495	1412.0	8.52875E-07	2.2693	0.2069	1028.0	914.0	975.1	916.8	979.7	917.3
31591.0	0.0497	1418.5	8.60019E-07	2.2754	0.2130	1032.7	914.9	978.6	917.3	982.8	917.8
31381.0	0.0499	1426.2	8.65248E-07	2.2797	0.2173	1038.3	918.0	983.7	920.2	987.6	920.7
31144.0	0.0502	1434.5	8.72564E-07	2.2858	0.2234	1044.3	920.4	988.7	922.2	992.2	922.7
30854.0	0.0504	1441.1	8.78330E-07	2.2906	0.2282	1049.1	922.3	992.7	923.8	996.0	924.4
30564.0	0.0506	1447.0	8.82592E-07	2.2941	0.2317	1053.5	924.7	996.6	925.9	999.6	926.5
30404.0	0.0510	1458.8	8.94930E-07	2.3040	0.2416	1062.1	927.1	1003.5	927.9	1006.1	928.5

Specimen V50-105

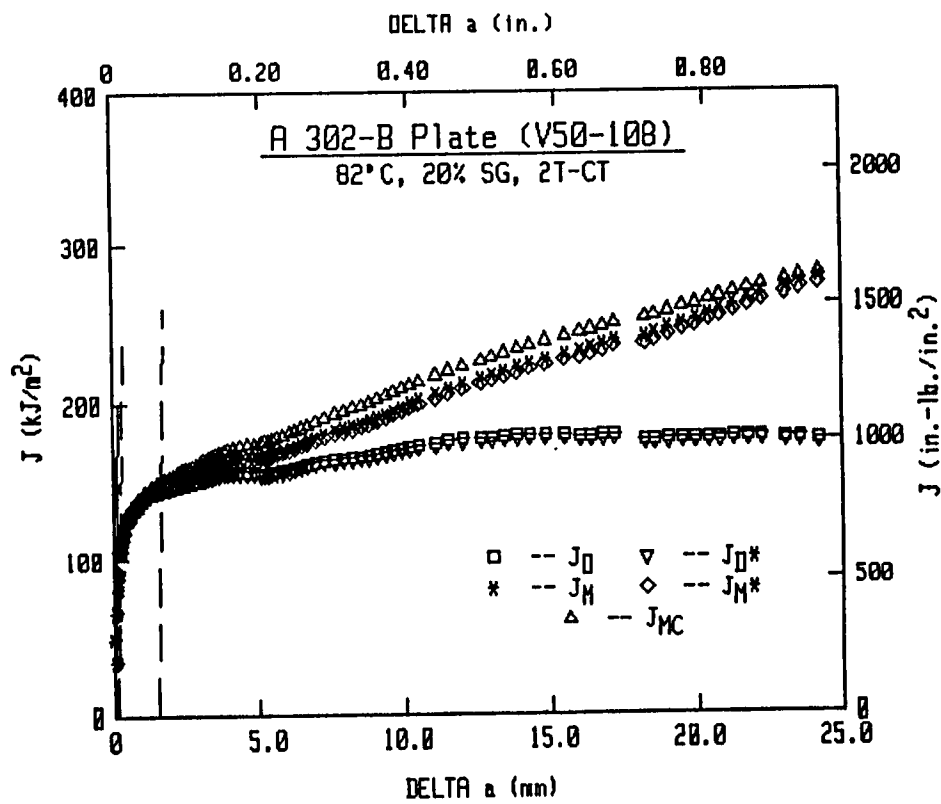
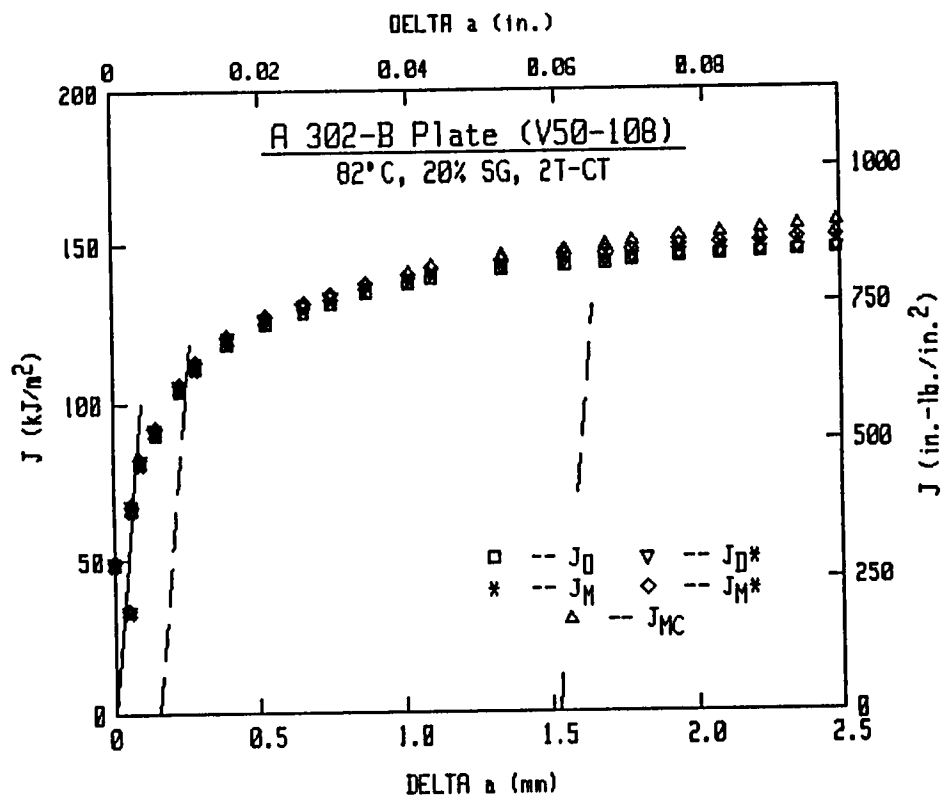
Material Type : A302-B PLATE
Side Groove : 20%
Thickness : 2 in.
Temperature : 180°F
Width : 4 in.
Ao : 2.0624 in.
Af : 3.1166 in.
Flow Stress : 75700 psi.
Young's Mod : 29372000 psi.
Initial Slope : 6.5065E-7 in./lbs.
Razor Spacing : .115 in.
Hold-Load Dis : 1.1 in.
Razor-LL Dis : 0 in.

Load (lbs)	Defl. (in.)	Area (in.-lbs)	Slope (in./lbs)	Post-a (in.)	Delta-a (in.)	Jac !<--	Jd --	Jm --	Jd* (in.-lbs/in. ²)	Jm* --	Je -->!
30080.0	0.0513	1468.3	9.01716E-07	2.3094	0.2470	1068.9	930.8	1009.8	931.4	1012.1	932.0
29771.0	0.0517	1478.6	9.10748E-07	2.3165	0.2541	1076.5	934.1	1016.3	934.3	1018.3	934.9
29392.0	0.0521	1493.0	9.23018E-07	2.3260	0.2636	1086.9	938.9	1025.6	938.7	1027.2	939.4
28898.0	0.0526	1505.3	9.36375E-07	2.3362	0.2738	1095.9	941.5	1033.1	940.9	1034.2	941.6
28524.0	0.0530	1517.1	9.46710E-07	2.3439	0.2815	1104.5	945.6	1040.9	944.5	1041.6	945.3
28123.0	0.0534	1530.0	9.57523E-07	2.3518	0.2894	1113.9	950.3	1049.6	948.9	1050.0	949.7
24724.0	0.0537	1590.9	1.09907E-06	2.4459	0.3835	1158.2	926.4	1072.4	920.2	1067.6	924.5
25031.0	0.0561	1600.5	1.10791E-06	2.4513	0.3889	1165.2	930.7	1079.5	924.6	1074.7	928.8
25340.0	0.0566	1614.8	1.11603E-06	2.4561	0.3937	1175.6	939.6	1090.8	933.4	1085.9	937.6
25123.0	0.0575	1636.5	1.13365E-06	2.4665	0.4041	1191.4	950.6	1107.3	944.3	1102.2	948.5
24572.0	0.0585	1661.3	1.16264E-06	2.4831	0.4207	1209.5	959.3	1124.9	952.6	1119.4	957.0
23992.0	0.0592	1677.5	1.18710E-06	2.4966	0.4342	1221.2	962.7	1135.8	955.8	1129.9	960.2
18672.0	0.0684	1871.3	1.52241E-06	2.6506	0.5882	1362.4	989.6	1257.5	988.8	1257.6	1007.6
18594.0	0.0699	1897.9	1.57189E-06	2.6694	0.6070	1381.7	998.6	1279.1	997.5	1278.8	1016.2
18083.0	0.0715	1927.1	1.63038E-06	2.6905	0.6281	1403.0	1008.0	1302.9	1006.8	1302.6	1025.4
17649.0	0.0730	1955.0	1.68278E-06	2.7085	0.6461	1423.3	1019.1	1326.8	1017.8	1326.4	1036.4
17296.0	0.0745	1979.8	1.72317E-06	2.7219	0.6595	1441.3	1031.6	1349.1	1030.4	1348.7	1048.9
16823.0	0.0762	2008.3	1.78002E-06	2.7401	0.6777	1462.1	1043.1	1374.2	1041.9	1373.7	1060.3
16431.0	0.0774	2029.5	1.82458E-06	2.7537	0.6913	1477.5	1051.6	1393.1	1050.3	1392.6	1068.6
15904.0	0.0792	2057.9	1.88677E-06	2.7720	0.7096	1498.2	1062.8	1418.8	1061.5	1418.3	1079.8
15330.0	0.0810	2085.9	1.95941E-06	2.7922	0.7298	1518.6	1071.3	1443.9	1069.9	1443.2	1088.2
14649.0	0.0831	2117.2	2.05703E-06	2.8179	0.7555	1541.4	1077.3	1471.4	1075.9	1470.8	1094.3
14018.1	0.0851	2145.4	2.15416E-06	2.8418	0.7794	1561.9	1082.0	1496.7	1080.6	1496.0	1099.0
13692.0	0.0866	2165.7	2.22018E-06	2.8571	0.7947	1576.7	1087.6	1516.0	1086.3	1515.3	1104.7
13388.0	0.0881	2186.5	2.29157E-06	2.8730	0.8106	1591.8	1093.2	1535.9	1091.8	1535.2	1110.1
13120.9	0.0895	2204.8	2.34444E-06	2.8844	0.8220	1605.1	1101.4	1554.6	1100.0	1553.8	1118.3
12737.1	0.0916	2232.0	2.42354E-06	2.9007	0.8383	1624.9	1114.0	1582.6	1112.7	1582.0	1130.9
12300.8	0.0935	2255.7	2.51653E-06	2.9189	0.8565	1642.2	1120.0	1606.3	1118.7	1605.6	1137.0
11772.0	0.0955	2279.7	2.61871E-06	2.9379	0.8755	1659.7	1125.4	1630.7	1124.1	1629.9	1142.3
11167.9	0.0975	2302.6	2.74164E-06	2.9593	0.8969	1676.3	1126.2	1653.5	1124.9	1652.6	1143.3
10608.2	0.0995	2324.3	2.85912E-06	2.9786	0.9162	1692.1	1128.5	1676.0	1127.1	1675.2	1145.6
10187.6	0.1015	2344.3	2.96479E-06	2.9950	0.9326	1706.7	1132.4	1697.7	1131.1	1696.9	1149.6
9817.7	0.1035	2364.4	3.08613E-06	3.0128	0.9504	1721.3	1134.6	1719.7	1133.3	1718.8	1151.7





V50-108 (2T-CT)



Specimen V50-108

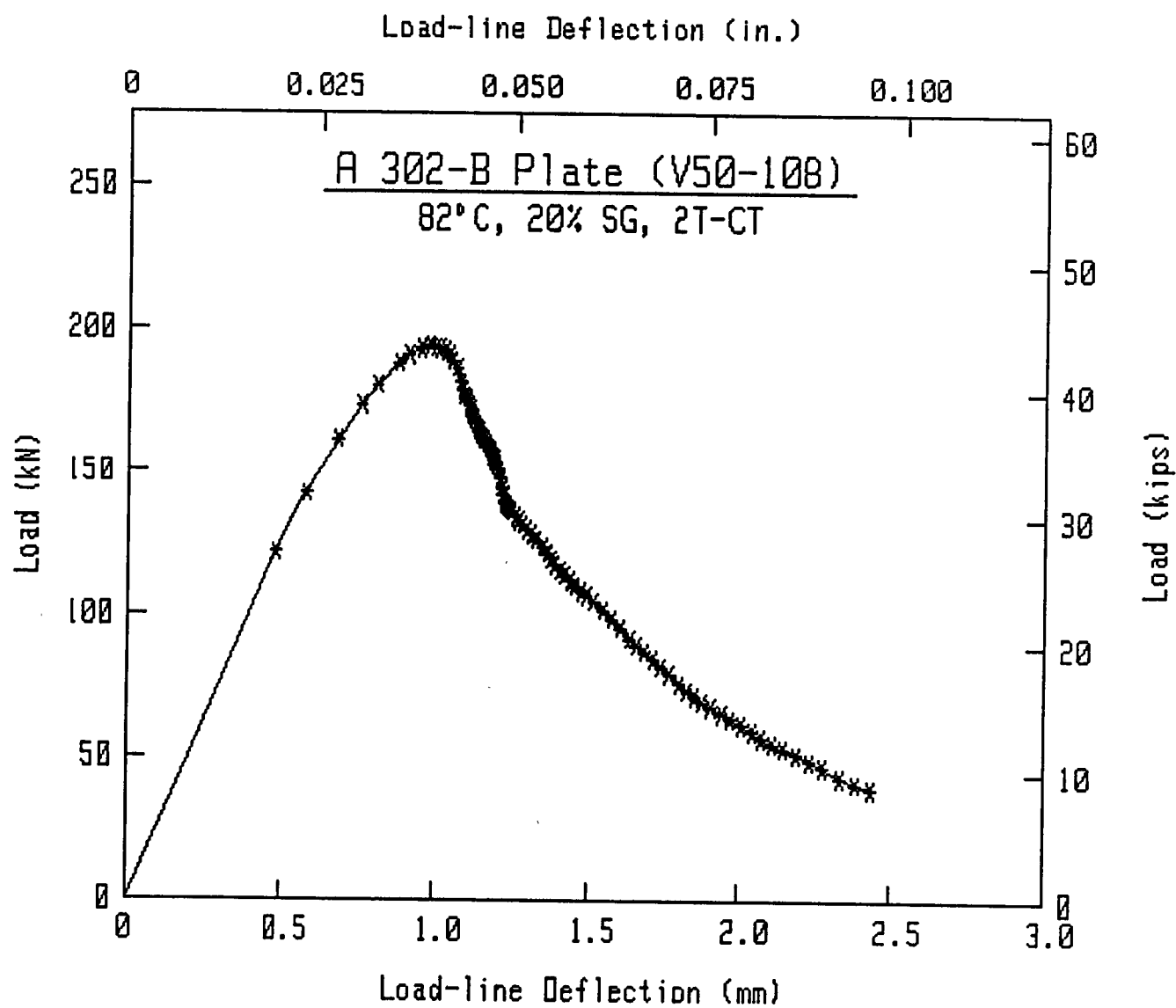
Material Type : A302-B Plate
Side Groove : 20%
Thickness : 2 in.
Temperature : 180°F
Width : 4 in.
Ao : 2.0532 in.
Af : 3.1691 in.
Flow Stress : 75700 psi.
Young's Mod : 29372000 psi.
Initial Slope : 6.5665E-7 in./lbs.
Razor Spacing : .115 in.
Hold-Load Dis : 1.1 in.
Razor-LL Dis : 0 in.

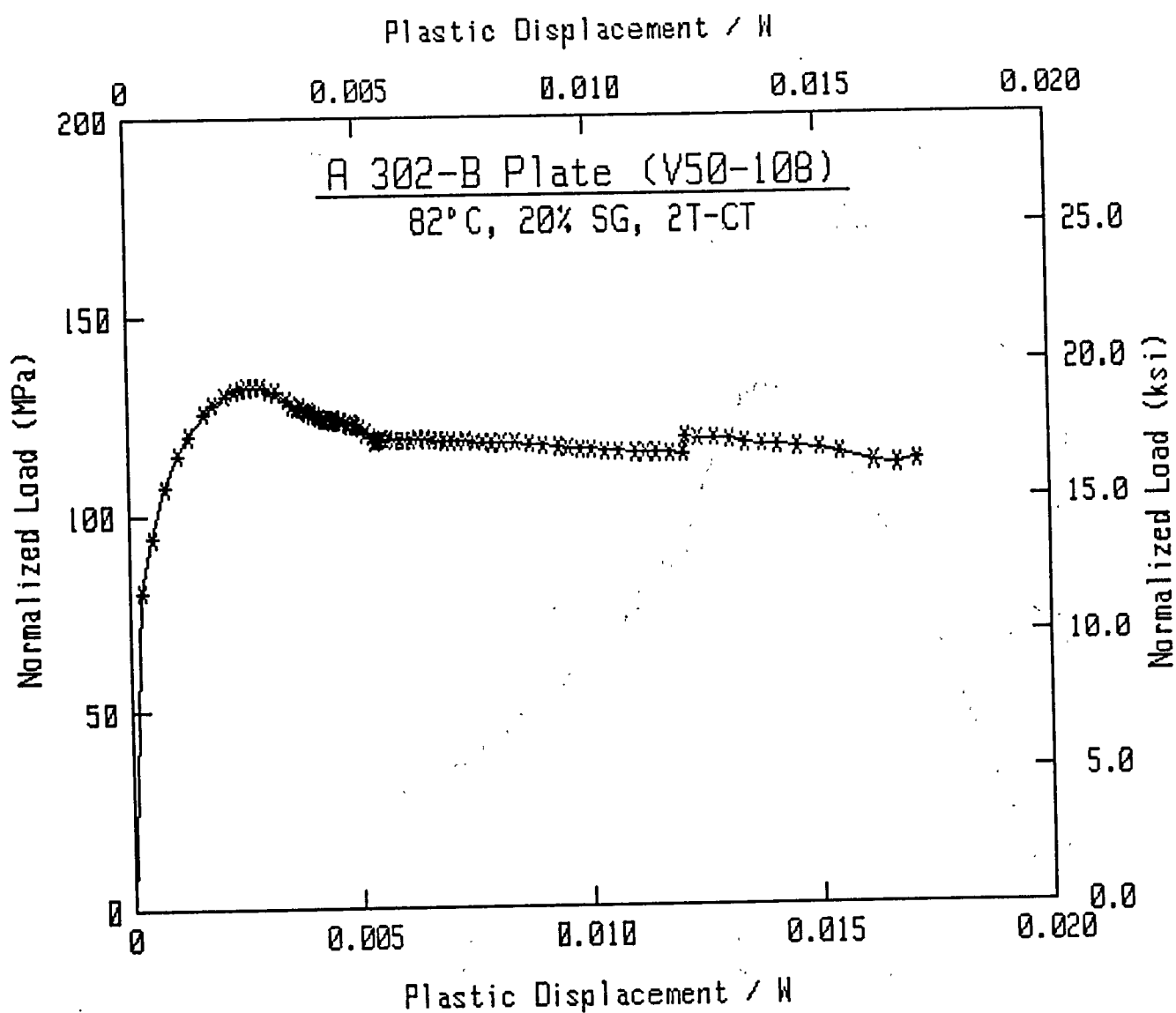
Load (lbs)	Defl. (in.)	Area (in.-lbs)	Slope (in./lbs)	Post-a (in.)	Delta-a (in.)	Jmc (in.)	Jd (in.)	Jm (in.-lbs/in. ²)	Jd* (in.-lbs/in. ²)	Jm* (in.-lbs/in. ²)	Je (in.-lbs/in. ²)
27348.0	0.0190	263.6	6.57452E-07	2.0552	0.0020	191.1	190.5	190.5	194.4	194.4	194.4
32025.0	0.0231	382.5	6.55622E-07	2.0532	0.0000	277.3	277.0	276.9	283.0	283.0	283.0
36251.0	0.0271	520.2	6.57483E-07	2.0556	0.0024	377.1	376.0	376.0	384.1	384.2	384.1
38987.0	0.0301	633.3	6.58425E-07	2.0569	0.0037	459.1	457.5	457.6	467.2	467.4	467.2
40548.0	0.0321	713.1	6.59977E-07	2.0589	0.0057	517.0	514.6	514.9	525.2	525.6	525.3
42277.0	0.0348	824.4	6.62792E-07	2.0623	0.0091	597.7	594.0	594.6	605.5	606.2	605.6
42928.0	0.0361	880.3	6.64447E-07	2.0644	0.0112	638.2	633.7	634.6	645.6	646.6	645.6
43456.0	0.0376	945.3	6.68107E-07	2.0688	0.0156	685.3	678.8	680.3	690.8	692.5	690.9
43652.0	0.0388	995.8	6.72462E-07	2.0739	0.0207	721.9	713.0	715.4	724.9	727.4	725.0
43599.0	0.0395	1028.0	6.76914E-07	2.0791	0.0259	745.3	733.9	737.1	745.4	748.9	745.5
43460.0	0.0401	1052.4	6.80087E-07	2.0828	0.0296	763.0	749.8	753.7	761.0	765.2	761.1
43290.0	0.0407	1079.4	6.84235E-07	2.0875	0.0343	782.5	766.9	771.8	777.7	782.9	777.9
42978.0	0.0413	1105.5	6.89337E-07	2.0933	0.0401	801.4	782.8	789.0	793.1	799.6	793.3
42463.0	0.0417	1123.9	6.92078E-07	2.0964	0.0432	814.7	794.6	801.5	804.5	811.7	804.6
41926.0	0.0424	1150.0	7.00581E-07	2.1059	0.0527	833.7	808.4	817.6	817.0	826.6	817.2
40835.0	0.0428	1166.1	7.08273E-07	2.1144	0.0612	845.4	815.4	826.7	822.9	834.7	823.1
40164.0	0.0430	1175.8	7.13508E-07	2.1200	0.0668	852.4	819.2	832.2	826.2	839.6	826.4
39797.0	0.0432	1185.3	7.16741E-07	2.1235	0.0703	859.3	824.2	838.1	830.7	845.1	830.9
39526.0	0.0436	1199.1	7.22726E-07	2.1299	0.0767	869.3	830.7	846.5	836.7	852.9	836.9
39042.0	0.0438	1208.0	7.27887E-07	2.1354	0.0822	875.8	834.1	851.4	839.5	857.3	839.7
38672.0	0.0441	1217.4	7.33151E-07	2.1409	0.0877	882.5	837.7	856.7	842.6	862.1	842.8
38273.0	0.0443	1226.3	7.37922E-07	2.1459	0.0927	889.0	841.4	862.0	845.8	866.9	846.1
37918.0	0.0445	1235.2	7.42998E-07	2.1511	0.0979	895.5	844.9	867.1	848.8	871.6	849.1
37520.0	0.0447	1242.5	7.47295E-07	2.1555	0.1023	900.7	847.7	871.3	851.2	875.3	851.4
37152.0	0.0450	1251.2	7.52203E-07	2.1604	0.1072	907.0	851.2	876.4	854.2	880.0	854.4
36943.0	0.0452	1259.7	7.58105E-07	2.1664	0.1132	913.2	854.0	881.1	856.5	884.3	856.8
36640.0	0.0454	1267.9	7.63142E-07	2.1714	0.1182	919.2	857.0	885.9	859.2	888.7	859.5
36371.0	0.0457	1279.8	7.67309E-07	2.1755	0.1223	927.8	863.5	893.8	862.9	893.8	863.2
36261.0	0.0460	1291.0	7.74057E-07	2.1821	0.1289	935.9	867.8	900.4	866.8	900.0	867.1
35903.0	0.0462	1298.9	7.79099E-07	2.1870	0.1338	941.6	870.7	905.0	869.3	904.2	869.6
35629.0	0.0464	1307.1	7.83863E-07	2.1916	0.1384	947.6	874.1	910.0	872.3	908.8	872.6
35410.0	0.0467	1318.0	7.90301E-07	2.1977	0.1445	955.5	878.5	916.7	876.3	915.0	876.6
34975.0	0.0469	1325.3	7.95869E-07	2.2030	0.1498	960.7	880.7	920.8	878.1	918.7	878.4
34669.0	0.0472	1333.6	8.01749E-07	2.2084	0.1552	966.8	883.5	925.7	880.5	923.3	880.9
34298.0	0.0474	1341.8	8.10228E-07	2.2163	0.1631	972.7	884.7	929.8	881.1	926.8	881.5
33914.0	0.0477	1352.3	8.18929E-07	2.2242	0.1710	980.3	887.6	935.8	883.6	932.3	884.0
33250.0	0.0480	1359.7	8.31390E-07	2.2353	0.1821	985.7	885.9	938.4	881.1	934.1	881.6
32465.0	0.0481	1365.8	8.42824E-07	2.2454	0.1922	990.1	883.9	940.5	878.5	935.5	878.9
31895.0	0.0483	1371.5	8.51281E-07	2.2527	0.1995	994.3	883.6	943.1	877.6	937.6	878.1
31326.0	0.0484	1375.5	8.58340E-07	2.2587	0.2055	997.2	882.7	944.7	876.4	938.8	876.9
31180.0	0.0486	1380.9	8.64794E-07	2.2642	0.2110	1001.1	883.3	947.6	876.7	941.3	877.2
30989.0	0.0488	1386.9	8.70055E-07	2.2686	0.2154	1005.4	885.1	951.2	878.2	944.7	878.8
30824.0	0.0491	1395.2	8.76895E-07	2.2743	0.2211	1011.4	887.8	956.3	880.7	949.5	881.3
30564.0	0.0495	1406.5	8.87792E-07	2.2832	0.2300	1019.6	890.8	963.1	883.3	955.8	883.8
30200.0	0.0500	1421.4	8.99347E-07	2.2925	0.2393	1030.5	896.4	972.8	888.5	965.1	889.1
29814.0	0.0503	1433.2	9.08056E-07	2.2994	0.2462	1039.0	901.1	980.5	892.9	972.5	893.5
29514.0	0.0508	1447.4	9.18963E-07	2.3080	0.2548	1049.3	906.6	989.8	898.1	981.4	898.7

Specimen V50-108

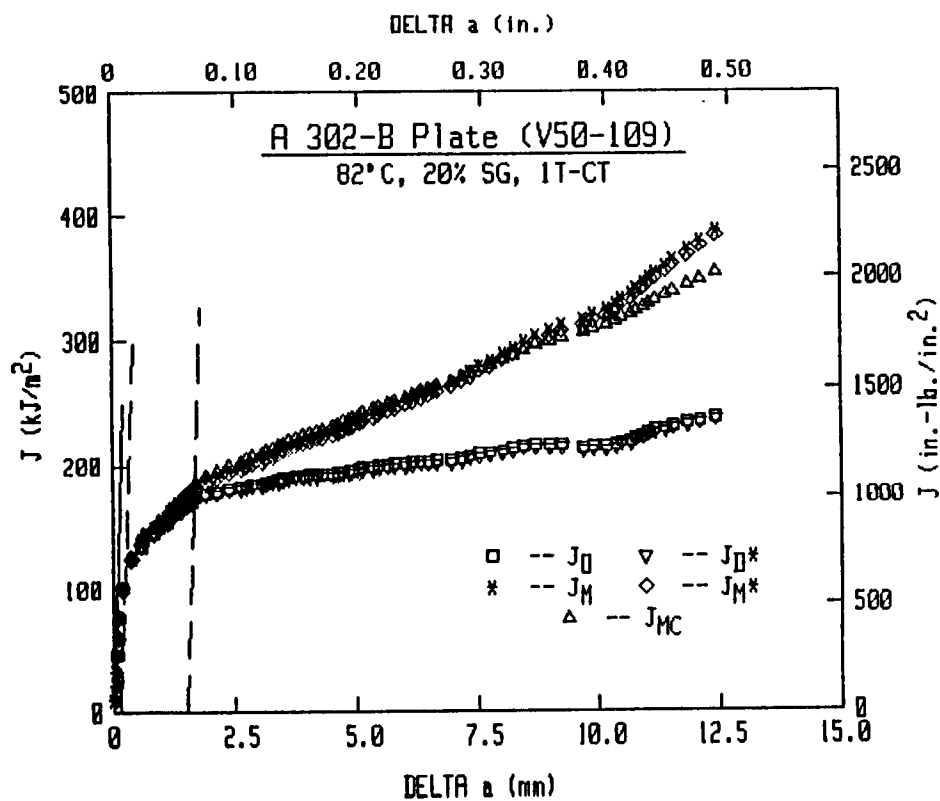
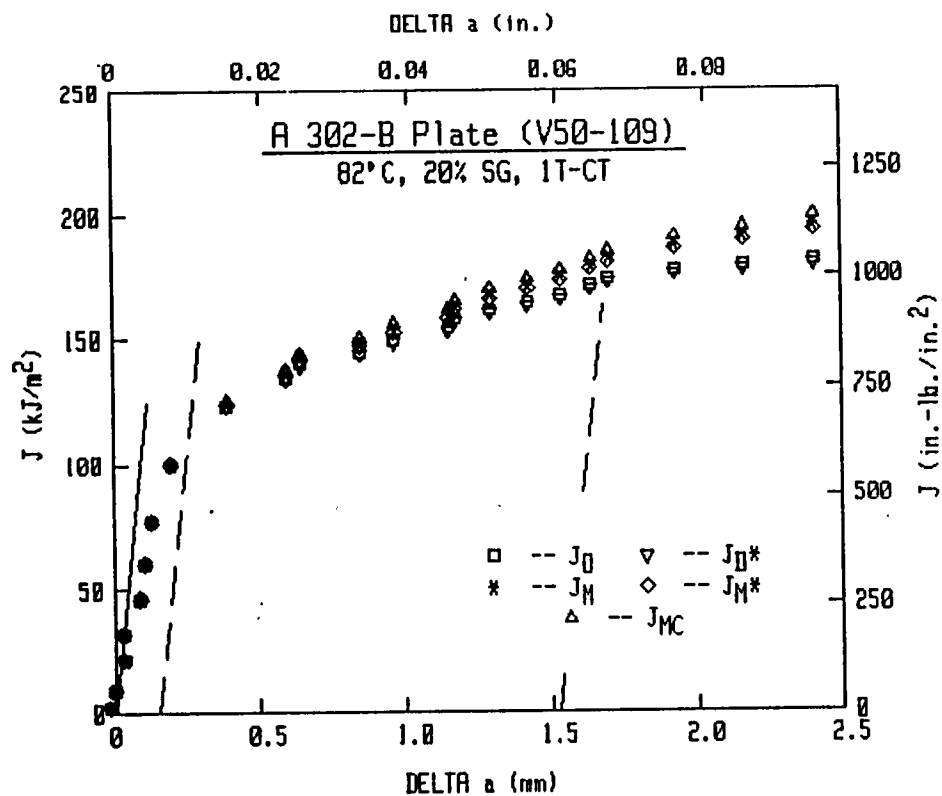
Material Type : A302-B Plate
Side Groove : 20%
Thickness : 2 in.
Temperature : 180°F
Width : 4 in.
Ao : 2.0532 in.
Af : 3.1691 in.
Flow Stress : 75700 psi.
Young's Mod : 29372000 psi.
Initial Slope : 6.5665E-7 in./lbs.
Razor Spacing : .115 in.
Hold-Load Dis : 1.1 in.
Razor-LL Dis : 0 in.

Load (lbs)	Defl. (in.)	Area (in.-lbs)	Slope (in./lbs)	Post-a (in.)	Delta-a (in.)	Jmc <- - - - -	Jd - - - - -	Jm (in.-lbs/in. ²)	Jd* - - - - -	Jm* - - - - -	Jσ - - - - -
29167.0	0.0514	1462.8	9.29383E-07	2.3160	0.2628	1060.5	913.5	1000.4	904.7	991.7	905.4
28800.0	0.0520	1480.1	9.43299E-07	2.3266	0.2734	1073.0	920.1	1011.9	910.9	1002.7	911.6
28337.0	0.0526	1498.2	9.60151E-07	2.3391	0.2859	1086.1	925.8	1023.6	916.3	1013.9	917.0
27818.0	0.0532	1516.3	9.80374E-07	2.3537	0.3005	1099.3	930.1	1034.9	920.0	1024.7	920.9
27292.0	0.0538	1531.7	9.96661E-07	2.3652	0.3120	1110.4	934.4	1044.9	924.0	1034.2	924.9
26830.0	0.0543	1545.3	1.01349E-06	2.3768	0.3236	1120.3	937.1	1053.5	926.4	1042.3	927.4
26383.0	0.0549	1559.8	1.03144E-06	2.3889	0.3357	1130.8	940.1	1062.7	929.1	1051.1	930.1
25966.0	0.0555	1575.2	1.04843E-06	2.4001	0.3469	1141.9	944.7	1073.1	933.5	1061.1	934.5
25586.0	0.0560	1589.8	1.06408E-06	2.4102	0.3570	1152.6	949.5	1083.2	938.0	1070.9	939.1
25176.0	0.0567	1607.6	1.08279E-06	2.4220	0.3688	1165.5	955.6	1095.6	943.8	1083.0	945.0
24734.0	0.0574	1624.3	1.09948E-06	2.4323	0.3791	1177.5	961.9	1107.6	950.0	1094.7	951.2
24340.0	0.0582	1642.3	1.11844E-06	2.4438	0.3906	1190.6	968.4	1120.6	956.4	1107.4	957.6
23952.0	0.0589	1660.9	1.13688E-06	2.4547	0.4015	1204.1	976.0	1134.4	963.8	1120.9	965.1
23533.0	0.0598	1681.3	1.15790E-06	2.4668	0.4136	1218.9	984.1	1149.5	971.8	1135.9	973.1
22806.0	0.0611	1710.4	1.19834E-06	2.4893	0.4361	1239.9	991.0	1169.9	978.3	1155.6	979.9
22142.0	0.0622	1736.6	1.23122E-06	2.5068	0.4536	1259.0	999.7	1189.4	986.9	1174.9	988.7
21452.0	0.0634	1761.3	1.26896E-06	2.5262	0.4730	1276.9	1005.4	1207.3	992.4	1192.4	994.4
20600.0	0.0646	1786.8	1.31823E-06	2.5503	0.4971	1295.4	1007.5	1225.1	994.4	1209.8	996.7
20070.0	0.0655	1804.1	1.35033E-06	2.5653	0.5121	1307.9	1010.3	1237.8	997.1	1222.3	999.5
19536.0	0.0665	1824.7	1.38656E-06	2.5817	0.5285	1322.8	1014.9	1253.6	1001.7	1237.8	1004.3
18981.0	0.0676	1844.8	1.42740E-06	2.5995	0.5463	1337.4	1017.8	1268.7	1004.5	1252.7	1007.2
18414.0	0.0686	1864.6	1.46836E-06	2.6167	0.5635	1351.8	1021.0	1284.1	1007.9	1267.9	1010.7
17788.0	0.0698	1885.6	1.52171E-06	2.6381	0.5849	1367.0	1021.4	1299.7	1008.1	1283.2	1011.2
17011.0	0.0711	1907.6	1.58884E-06	2.6635	0.6103	1382.9	1018.8	1315.6	1005.5	1298.7	1008.9
16446.0	0.0720	1923.7	1.64704E-06	2.6844	0.6312	1394.6	1014.9	1327.2	1001.7	1310.1	1005.3
16049.0	0.0730	1939.1	1.68947E-06	2.6989	0.6457	1405.7	1016.5	1339.8	1003.3	1322.5	1007.1
15607.0	0.0740	1955.4	1.73630E-06	2.7145	0.6613	1417.6	1018.2	1353.3	1005.0	1335.9	1008.9
15181.0	0.0752	1973.0	1.78541E-06	2.7301	0.6769	1430.3	1021.0	1368.3	1007.9	1350.8	1011.9
14671.1	0.0766	1994.0	1.92512E-06	2.7715	0.7183	1445.5	1001.2	1379.9	987.5	1361.2	992.5
14276.1	0.0775	2007.4	1.97259E-06	2.7846	0.7314	1455.3	1002.6	1391.6	989.0	1372.9	994.0
13812.0	0.0790	2027.4	2.04219E-06	2.8030	0.7498	1469.8	1005.6	1409.4	992.2	1390.6	997.4
13293.6	0.0804	2046.7	2.11820E-06	2.8222	0.7690	1483.8	1007.2	1426.6	994.0	1407.7	999.4
12784.9	0.0816	2062.4	2.19069E-06	2.8396	0.7864	1495.1	1006.6	1440.5	993.5	1421.5	999.1
12333.4	0.0831	2080.8	2.26758E-06	2.8571	0.8039	1508.5	1008.9	1457.8	996.1	1438.8	1001.9
11955.2	0.0844	2096.7	2.33815E-06	2.8726	0.8194	1520.0	1010.7	1472.9	998.1	1454.0	1004.0
11482.9	0.0861	2116.4	2.42797E-06	2.8912	0.8380	1534.3	1013.4	1492.2	1001.0	1473.2	1007.2
11020.8	0.0880	2137.0	2.52671E-06	2.9107	0.8575	1549.2	1016.3	1512.7	1004.1	1493.6	1010.4
10523.7	0.0895	2153.7	2.62263E-06	2.9285	0.8753	1561.4	1016.3	1529.3	1004.3	1510.2	1010.9
9658.2	0.0920	2178.7	2.80983E-06	2.9609	0.9077	1579.4	1009.3	1552.9	997.7	1533.8	1005.2
9223.0	0.0939	2196.6	2.93342E-06	2.9806	0.9274	1592.4	1008.9	1571.8	997.5	1552.6	1005.3
8811.6	0.0959	2214.7	3.10719E-06	3.0064	0.9532	1605.6	1001.5	1590.1	990.3	1570.8	998.4





V50-109 (1T-CT)



Specimen V50-109

Material Type : A302-B PLATE

Side Groove : 20%

Thickness : 1 in.

Temperature : 180°F

Width : 2 in.

As : 1.0316 in.

Af : 1.5503 in.

Flow Stress : 75700 psi.

Young's Mod : 29372000 psi.

Initial Slope : 1.37109E-6 in./lbs.

Razor Spacing : .1 in.

Hold-Load Dis : .655 in.

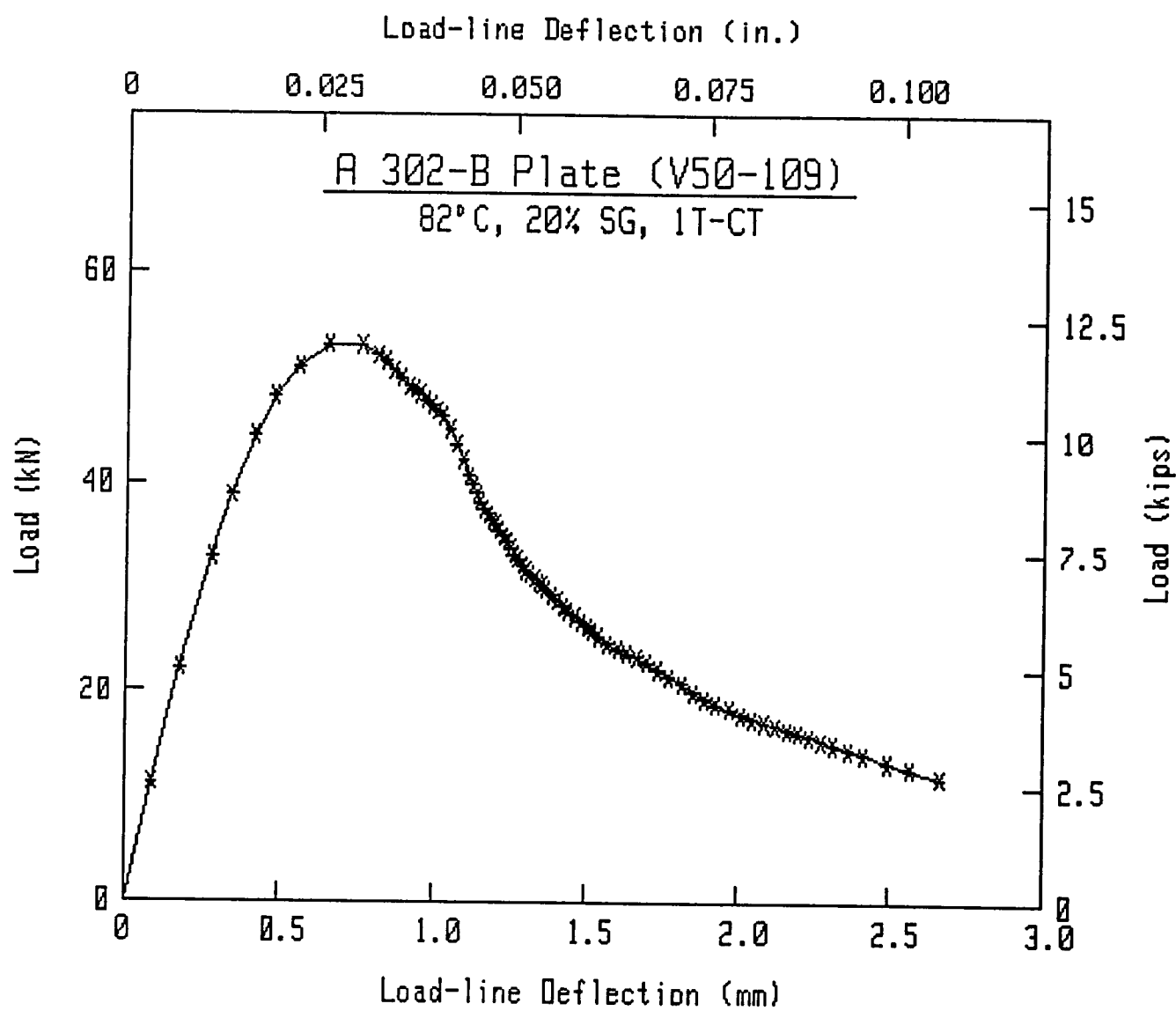
Razor-LL Dis : 0 in.

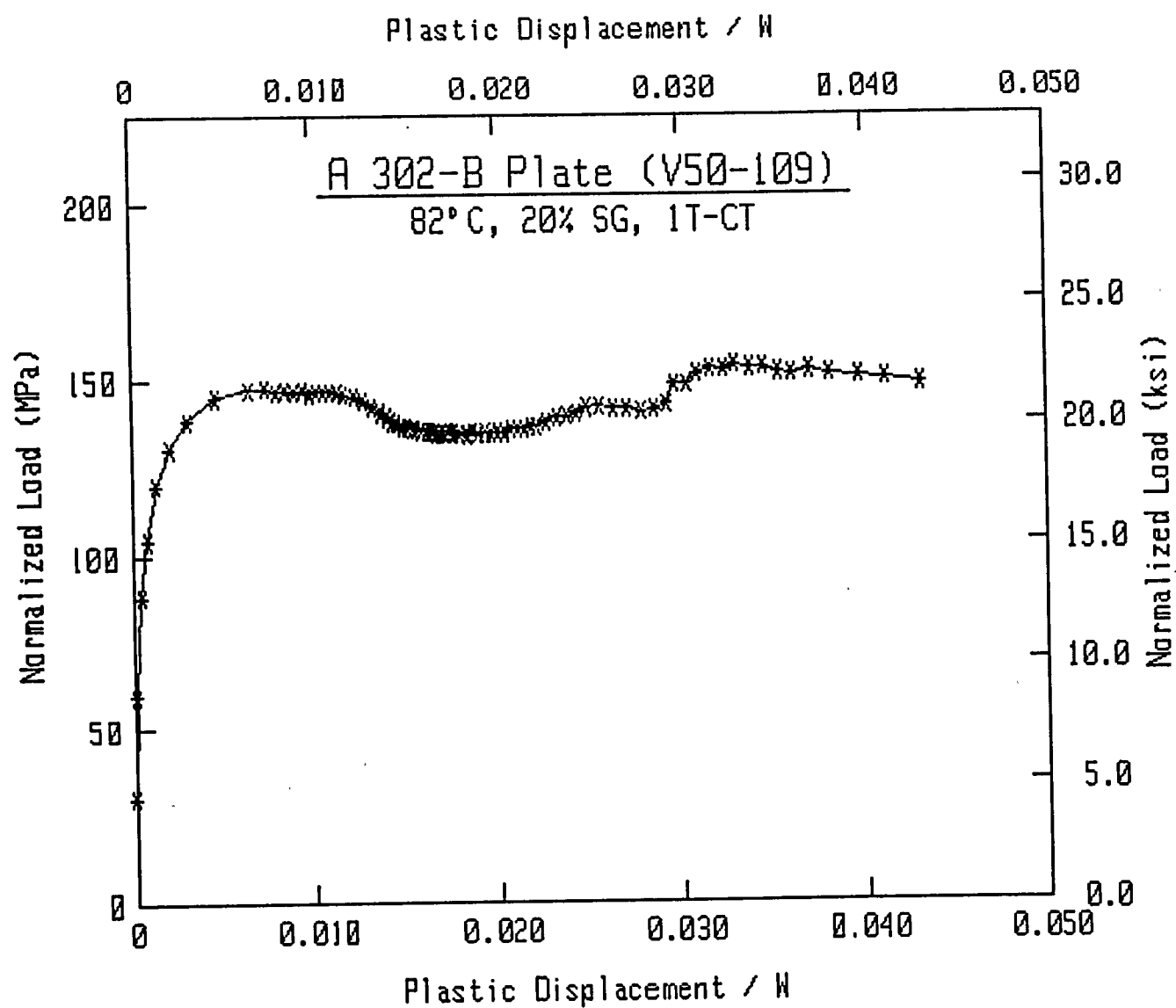
Load (lbs)	Defl. (in.)	Area (in.-lbs)	Slope (in./lbs)	Post-a (in.)	Delta-a (in.)	Jmc	Jd	Jm (in.-lbs/in. ²)	Jd*	Jm*	Jc
2555.4	0.0035	4.5	1.36804E-06	1.0310	-0.0006	13.0	13.0	13.0	13.0	13.0	13.0
5003.0	0.0071	10.0	1.36948E-06	1.0316	0.0000	52.5	52.4	52.4	52.1	52.1	52.1
7390.0	0.0110	42.5	1.37320E-06	1.0329	0.0013	123.7	123.2	123.2	122.7	122.7	122.7
8730.0	0.0135	63.1	1.37206E-06	1.0328	0.0012	183.7	183.2	183.2	182.5	182.5	182.5
10018.0	0.0165	91.3	1.37974E-06	1.0351	0.0035	265.8	264.4	264.6	263.5	263.7	263.5
10862.0	0.0192	118.9	1.38152E-06	1.0358	0.0042	346.2	344.5	344.9	343.4	343.8	343.5
11498.0	0.0221	152.0	1.38382E-06	1.0367	0.0051	442.7	440.7	441.2	439.3	439.9	439.4
11964.0	0.0260	197.4	1.39274E-06	1.0394	0.0078	575.2	571.3	572.9	569.4	571.0	569.6
11942.0	0.0301	246.3	1.41900E-06	1.0470	0.0154	717.6	706.8	712.8	704.2	710.1	704.6
11744.0	0.0321	269.8	1.44840E-06	1.0550	0.0234	786.0	767.1	778.5	763.9	775.2	764.5
11612.0	0.0330	281.8	1.45535E-06	1.0569	0.0253	820.9	800.6	813.4	795.3	808.1	795.9
11420.0	0.0341	293.6	1.48617E-06	1.0650	0.0334	855.3	826.0	845.0	820.0	838.9	820.7
11256.0	0.0350	304.6	1.50390E-06	1.0696	0.0380	887.4	853.3	876.2	847.0	867.9	847.8
11092.0	0.0361	316.3	1.53303E-06	1.0770	0.0454	921.3	878.8	908.0	872.0	900.9	872.8
11016.0	0.0367	323.2	1.53670E-06	1.0779	0.0463	941.5	898.6	928.7	891.9	921.7	892.7
10914.0	0.0375	331.9	1.55552E-06	1.0826	0.0510	966.8	918.6	953.1	911.5	945.6	912.5
10784.0	0.0383	340.1	1.57664E-06	1.0877	0.0561	990.8	936.7	976.1	929.2	968.2	930.2
10672.0	0.0390	347.6	1.59489E-06	1.0921	0.0605	1012.7	953.6	997.3	945.8	989.2	946.9
10546.0	0.0398	356.6	1.61213E-06	1.0962	0.0646	1038.9	975.4	1023.4	967.4	1014.9	968.5
10440.0	0.0404	363.1	1.62252E-06	1.0986	0.0670	1057.9	991.9	1042.5	983.9	1034.0	985.0
10162.0	0.0415	374.2	1.66139E-06	1.1075	0.0759	1090.1	1012.6	1073.1	1004.0	1063.9	1005.2
9848.0	0.0423	382.3	1.70363E-06	1.1168	0.0852	1113.5	1023.3	1094.4	1014.2	1084.6	1015.6
9494.0	0.0432	390.9	1.74829E-06	1.1263	0.0947	1138.6	1035.3	1117.9	1025.9	1107.5	1027.5
9162.0	0.0440	397.6	1.79435E-06	1.1358	0.1042	1158.4	1041.6	1135.8	1031.9	1125.0	1033.6
8966.0	0.0445	402.1	1.81719E-06	1.1404	0.1088	1171.4	1048.5	1148.5	1038.7	1137.5	1040.5
8784.0	0.0450	406.7	1.84101E-06	1.1451	0.1135	1184.7	1055.6	1161.6	1045.7	1150.5	1047.6
8580.0	0.0454	410.7	1.88197E-06	1.1530	0.1214	1196.4	1055.6	1171.8	1045.4	1160.2	1047.3
8414.0	0.0459	414.9	1.90086E-06	1.1566	0.1250	1208.8	1063.5	1184.4	1053.3	1172.9	1055.3
8310.0	0.0464	419.1	1.92891E-06	1.1618	0.1302	1220.9	1068.4	1196.3	1058.0	1184.5	1060.1
8172.0	0.0470	423.4	1.95416E-06	1.1665	0.1349	1233.5	1074.9	1209.0	1064.4	1197.1	1066.5
8098.0	0.0475	427.4	1.97407E-06	1.1700	0.1384	1245.1	1081.9	1221.0	1071.4	1208.9	1073.5
7968.0	0.0479	431.2	2.00024E-06	1.1747	0.1431	1256.0	1086.4	1231.9	1075.8	1219.7	1077.9
7840.0	0.0485	435.7	2.03195E-06	1.1802	0.1486	1269.2	1092.0	1245.3	1081.2	1232.8	1083.4
7722.0	0.0490	439.5	2.06816E-06	1.1863	0.1547	1280.2	1093.8	1255.9	1082.9	1243.1	1085.1
7592.0	0.0495	443.4	2.09775E-06	1.1913	0.1597	1291.5	1098.3	1267.4	1087.3	1254.5	1089.6
7448.0	0.0500	446.9	2.13344E-06	1.1971	0.1655	1301.9	1100.0	1277.7	1089.0	1264.5	1091.3
7346.0	0.0504	449.7	2.16497E-06	1.2021	0.1705	1310.0	1100.5	1285.5	1089.3	1272.2	1091.7
7216.0	0.0510	454.3	2.21908E-06	1.2105	0.1789	1323.4	1101.1	1298.5	1089.6	1284.7	1092.2
7108.0	0.0515	457.7	2.24706E-06	1.2147	0.1831	1333.3	1105.2	1309.0	1093.8	1295.1	1096.3
7020.0	0.0520	461.2	2.27357E-06	1.2187	0.1871	1343.6	1110.3	1320.1	1098.9	1306.2	1101.4
6922.0	0.0526	465.5	2.31020E-06	1.2240	0.1924	1356.1	1115.5	1333.5	1104.0	1319.4	1106.6
6838.0	0.0530	468.0	2.33059E-06	1.2269	0.1953	1363.3	1118.8	1341.3	1107.3	1327.2	1109.9
6786.0	0.0535	471.4	2.36622E-06	1.2320	0.2004	1373.2	1121.4	1351.8	1109.7	1337.4	1112.4
6696.0	0.0540	474.9	2.38468E-06	1.2346	0.2030	1383.5	1129.0	1363.5	1117.4	1349.2	1120.1
6564.0	0.0548	480.2	2.44557E-06	1.2428	0.2112	1398.8	1131.9	1379.6	1120.1	1364.9	1122.9
6464.0	0.0555	484.5	2.48222E-06	1.2477	0.2161	1411.5	1138.2	1393.8	1126.4	1379.0	1129.3
6336.0	0.0563	489.6	2.53922E-06	1.2550	0.2234	1426.3	1142.3	1410.0	1130.5	1395.0	1133.5

Specimen V50-109

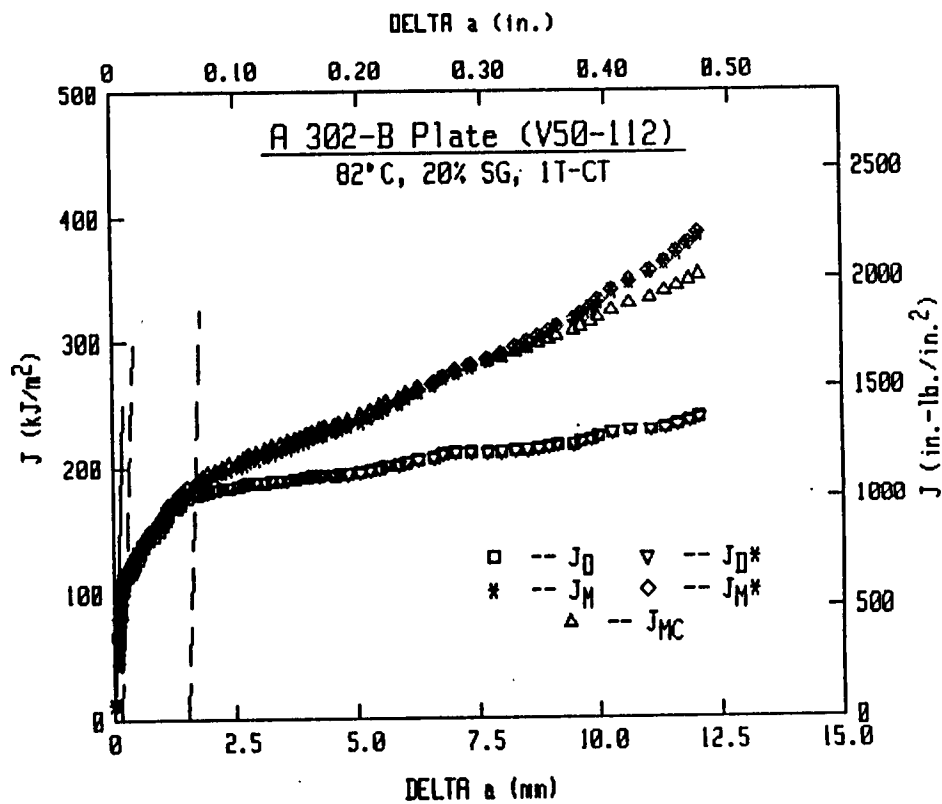
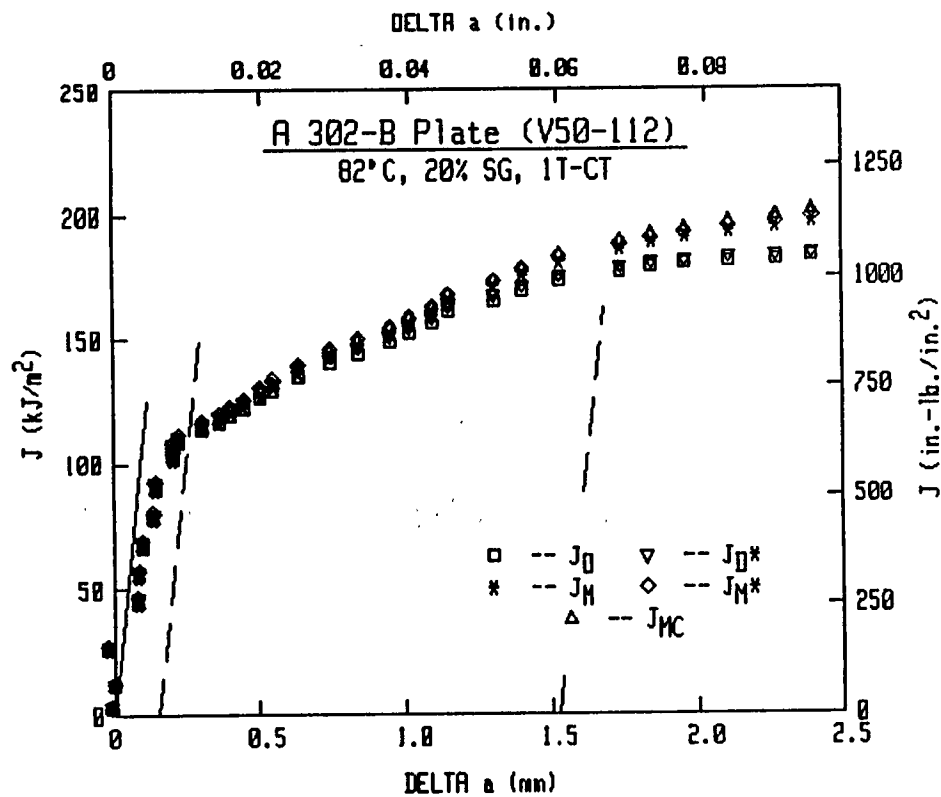
Material Type : A302-B PLATE
Side Groove : 20%
Thickness : 1 in.
Temperature : 180°F
Width : 2 in.
Ao : 1.0316 in.
Af : 1.5503 in.
Flow Stress : 75700 psi.
Young's Mod : 29372000 psi.
Initial Slope : 1.37109E-6 in./lbs.
Razor Spacing : .1 in.
Hold-Load Dis : .655 in.
Razor-LL Dis : 0 in.

Load (lbs)	Defl. (in.)	Area (in.-lbs)	Slope (in./lbs)	Post-a (in.)	Delta-a (in.)	Jac < - - - - -	Jd - - - - -	Jm (in.-lbs/in. ²)	Jd*	Jm*	Je - - - - ->
6232.0	0.0569	493.3	2.58136E-06	1.2603	0.2287	1437.1	1145.3	1421.8	1133.5	1406.7	1136.6
6118.0	0.0578	498.9	2.65530E-06	1.2693	0.2377	1453.2	1147.7	1439.3	1135.7	1423.8	1138.9
6012.0	0.0585	503.5	2.70485E-06	1.2752	0.2436	1466.8	1153.3	1454.8	1141.2	1439.2	1144.5
5904.8	0.0593	508.2	2.75715E-06	1.2812	0.2496	1480.4	1158.5	1470.4	1146.5	1454.7	1149.9
5796.2	0.0600	512.0	2.82052E-06	1.2883	0.2567	1491.4	1158.2	1482.4	1146.1	1466.5	1149.6
5692.8	0.0607	516.2	2.87828E-06	1.2945	0.2629	1503.8	1161.3	1496.6	1149.3	1480.6	1152.9
5535.4	0.0620	523.4	2.99341E-06	1.3065	0.2749	1524.9	1163.8	1520.3	1151.6	1503.9	1155.5
5428.2	0.0633	530.4	3.08127E-06	1.3152	0.2836	1545.2	1172.3	1544.8	1160.1	1528.1	1164.2
5338.4	0.0645	536.8	3.14493E-06	1.3213	0.2897	1563.7	1184.0	1567.8	1171.8	1551.0	1176.1
5247.2	0.0657	543.5	3.22639E-06	1.3289	0.2973	1583.3	1194.0	1592.2	1181.8	1575.2	1186.2
5145.2	0.0670	550.0	3.32596E-06	1.3378	0.3062	1602.1	1199.9	1615.1	1187.6	1597.9	1192.2
4985.0	0.0685	557.7	3.44812E-06	1.3482	0.3166	1624.6	1207.3	1642.9	1195.1	1625.4	1200.0
4827.6	0.0700	564.9	3.55254E-06	1.3567	0.3251	1645.6	1217.2	1669.9	1205.1	1652.4	1210.3
4692.4	0.0716	572.4	3.65650E-06	1.3649	0.3333	1667.4	1229.1	1698.5	1217.2	1681.0	1222.5
4509.0	0.0730	579.0	3.78812E-06	1.3747	0.3431	1686.6	1233.0	1723.0	1221.3	1705.5	1227.0
4356.2	0.0745	585.6	3.94936E-06	1.3861	0.3545	1706.1	1233.4	1747.7	1221.8	1730.0	1227.8
4248.4	0.0760	592.0	4.09960E-06	1.3961	0.3645	1724.6	1236.0	1772.0	1224.4	1754.0	1230.7
4149.6	0.0775	598.3	4.37843E-06	1.4134	0.3818	1743.0	1219.8	1792.8	1207.3	1773.7	1214.7
4026.0	0.0790	604.3	4.52003E-06	1.4216	0.3900	1760.4	1225.7	1817.0	1213.5	1797.8	1221.0
3938.8	0.0805	610.3	4.71370E-06	1.4323	0.4007	1777.9	1225.4	1840.5	1213.0	1820.9	1220.9
3859.4	0.0821	616.4	4.86491E-06	1.4402	0.4086	1795.6	1232.9	1866.0	1220.5	1846.2	1228.6
3795.4	0.0835	621.8	4.94649E-06	1.4444	0.4128	1811.5	1247.8	1890.7	1235.7	1871.0	1243.7
3709.8	0.0850	627.4	5.10953E-06	1.4523	0.4207	1827.7	1252.5	1914.2	1240.4	1894.4	1248.7
3634.8	0.0865	632.9	5.19226E-06	1.4562	0.4246	1843.8	1268.5	1939.8	1256.7	1920.1	1264.9
3554.0	0.0880	638.4	5.32083E-06	1.4621	0.4305	1859.6	1278.2	1964.1	1266.5	1944.4	1274.9
3461.4	0.0895	643.6	5.41264E-06	1.4663	0.4347	1874.7	1292.0	1988.4	1280.7	1969.0	1289.1
3388.4	0.0910	648.8	5.52358E-06	1.4711	0.4395	1890.0	1304.0	2012.9	1292.9	1993.5	1301.3
3287.8	0.0930	655.5	5.73655E-06	1.4799	0.4483	1909.6	1311.0	2043.2	1300.0	2023.7	1308.8
3182.2	0.0951	662.0	5.89084E-06	1.4861	0.4545	1928.6	1325.4	2074.3	1314.7	2054.9	1323.6
3016.0	0.0982	671.8	6.20745E-06	1.4980	0.4664	1957.1	1338.0	2119.9	1327.7	2100.6	1337.3
2877.4	0.1011	680.2	6.49580E-06	1.5081	0.4765	1981.5	1349.3	2160.2	1339.3	2141.1	1349.4
2693.2	0.1049	690.9	6.88812E-06	1.5209	0.4893	2012.8	1364.0	2212.7	1354.7	2194.0	1365.9





V50-112 (1T-CT)



Specimen V50-112

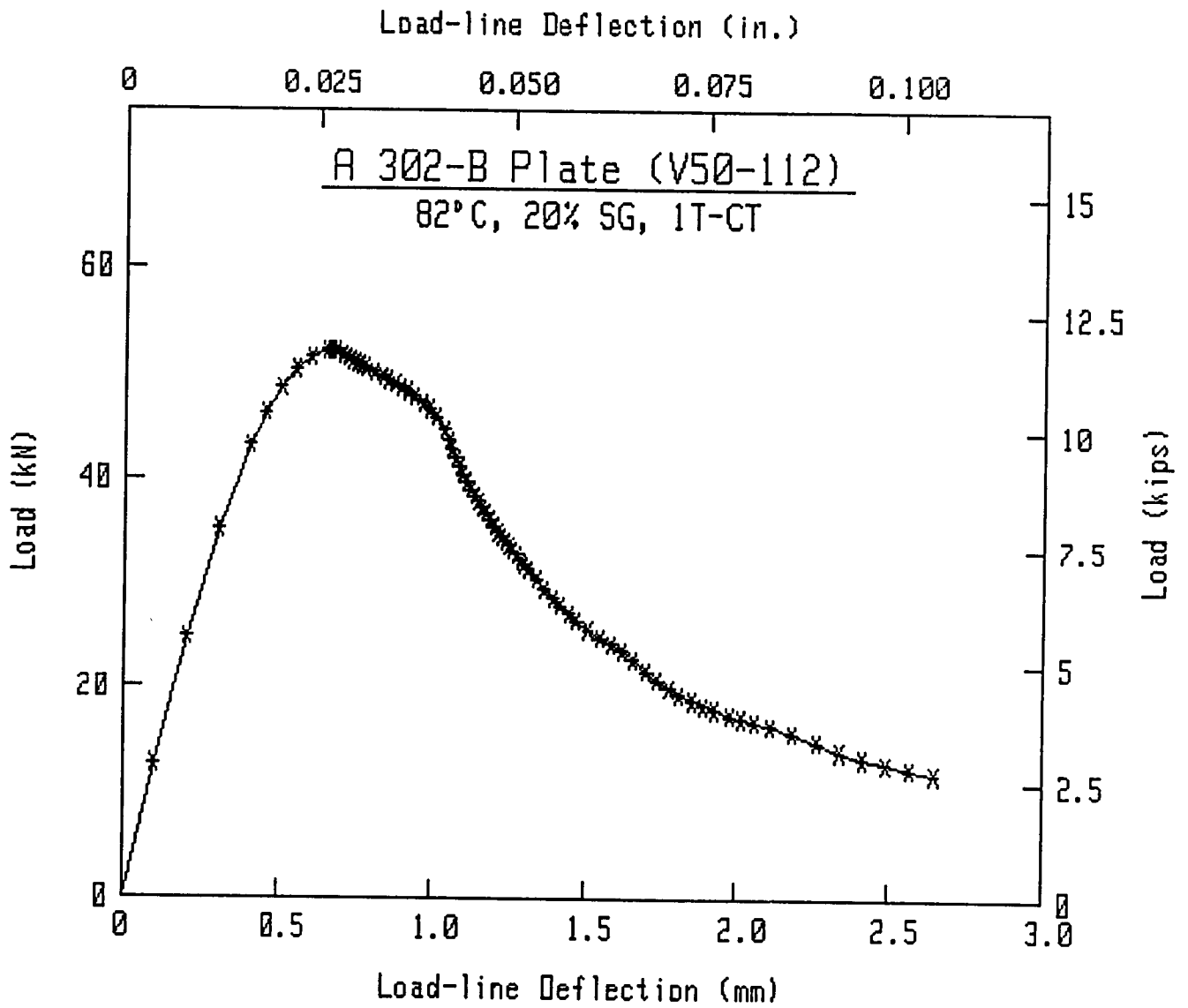
Material Type : A302-B PLATE
Side Groove : 20%
Thickness : 1 in.
Temperature : 180°F
Width : 2 in.
Ao : 1.062 in.
Af : 1.5736 in.
Flow Stress : 75700 psi.
Young's Mod : 29372000 psi.
Initial Slope : 1.38544E-6 in./lbs.
Razor Spacing : .1 in.
Hold-Load Dis : .655 in.
Razor-LL Dis : 0 in.

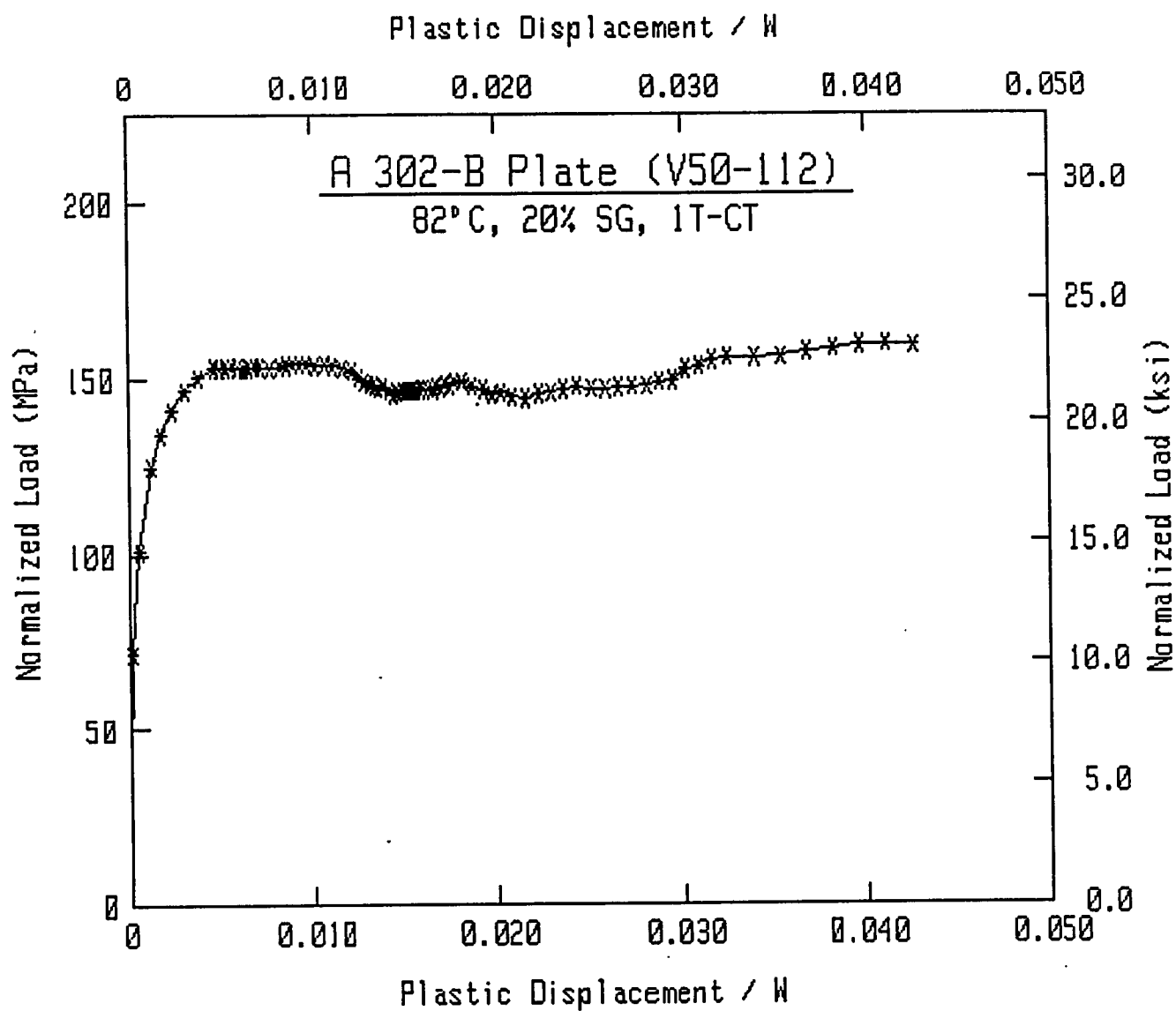
Load (lbs)	Defl. (in.)	Area (in.-lbs)	Slope (in./lbs)	Post-a (in.)	Delta-a (in.)	Jmc !<- - - - -	Jd - - - - -	Jm (in.-lbs/in.²)	Jd* - - - - -	Jm* - - - - -	Je - - - - ->!
2872.0	0.0040	5.7	1.38295E-06	1.0616	-0.0004	17.1	17.1	17.1	18.0	18.0	18.0
5590.8	0.0080	23.1	1.38359E-06	1.0620	0.0000	69.2	69.0	69.0	72.7	72.7	72.7
7902.0	0.0121	50.3	1.37986E-06	1.0612	-0.0008	150.7	150.5	150.5	157.7	157.7	157.7
9722.0	0.0160	85.5	1.39325E-06	1.0652	0.0032	256.4	254.5	254.7	265.4	265.7	265.4
10408.0	0.0180	105.7	1.39349E-06	1.0653	0.0033	316.8	314.8	315.1	327.4	327.8	327.5
10942.0	0.0201	127.3	1.39469E-06	1.0658	0.0038	381.6	379.5	379.8	393.5	393.9	393.5
11330.0	0.0220	149.3	1.40010E-06	1.0674	0.0054	447.4	444.4	445.1	459.4	460.2	459.5
11602.0	0.0240	172.2	1.40060E-06	1.0677	0.0057	515.9	512.9	513.7	528.7	529.6	528.8
11746.0	0.0260	195.3	1.40907E-06	1.0701	0.0081	585.3	580.5	582.2	596.7	598.6	596.8
11738.0	0.0265	201.5	1.40860E-06	1.0700	0.0080	603.9	599.3	601.0	615.5	617.4	615.6
11736.0	0.0271	207.9	1.41126E-06	1.0708	0.0088	623.0	617.8	619.8	634.1	636.3	634.2
11656.0	0.0280	218.8	1.42309E-06	1.0740	0.0120	655.6	647.6	651.2	663.5	667.4	663.7
11576.0	0.0285	224.8	1.43156E-06	1.0763	0.0143	673.8	663.7	668.5	679.4	684.6	679.6
11524.0	0.0291	230.9	1.43751E-06	1.0779	0.0159	692.0	680.5	686.2	696.1	702.2	696.3
11478.0	0.0296	236.6	1.44402E-06	1.0796	0.0176	709.1	696.1	702.8	711.6	718.6	711.7
11430.0	0.0303	245.4	1.45232E-06	1.0819	0.0199	735.4	720.4	728.4	735.7	744.2	735.9
11382.0	0.0309	251.7	1.45888E-06	1.0836	0.0216	754.5	738.0	747.1	753.3	762.8	753.5
11270.0	0.0319	263.2	1.47200E-06	1.0870	0.0250	788.8	769.1	780.5	783.9	796.0	784.2
11168.0	0.0330	275.8	1.48865E-06	1.0913	0.0293	826.6	802.5	817.2	817.1	832.4	817.4
11098.0	0.0337	283.7	1.50340E-06	1.0951	0.0331	850.3	822.3	839.8	836.6	854.8	836.9
11014.0	0.0346	293.4	1.52076E-06	1.0994	0.0374	879.2	846.6	867.6	860.6	882.5	861.0
10948.0	0.0354	301.4	1.53109E-06	1.1020	0.0400	903.2	868.1	891.3	881.9	906.0	882.3
10864.0	0.0361	309.9	1.54378E-06	1.1051	0.0431	928.8	890.5	916.4	904.0	930.9	904.5
10752.0	0.0371	319.7	1.55268E-06	1.1073	0.0453	958.3	918.2	946.2	931.5	960.4	931.9
10622.0	0.0381	331.2	1.57803E-06	1.1134	0.0514	992.6	945.3	979.2	958.2	993.2	958.8
10492.0	0.0390	340.0	1.59494E-06	1.1173	0.0553	1019.1	967.3	1005.2	979.9	1019.0	980.4
10310.0	0.0399	350.2	1.61633E-06	1.1223	0.0603	1049.5	991.9	1035.1	1003.9	1048.3	1004.5
10042.0	0.0410	360.8	1.65301E-06	1.1305	0.0685	1081.4	1012.7	1065.1	1023.9	1077.6	1024.7
9818.0	0.0415	366.2	1.67177E-06	1.1347	0.0727	1097.5	1023.5	1080.6	1034.1	1092.7	1035.0
9636.0	0.0420	370.8	1.69288E-06	1.1392	0.0772	1111.3	1031.0	1093.5	1041.1	1105.1	1042.0
9432.0	0.0425	375.6	1.72088E-06	1.1452	0.0832	1125.8	1037.0	1106.6	1046.6	1117.8	1047.5
9260.0	0.0430	379.9	1.75148E-06	1.1515	0.0895	1138.7	1040.7	1118.0	1049.8	1128.7	1050.8
9098.0	0.0435	384.2	1.77558E-06	1.1564	0.0944	1151.4	1046.5	1129.8	1055.2	1140.2	1056.2
8930.0	0.0440	389.2	1.81613E-06	1.1644	0.1024	1166.3	1049.6	1142.9	1057.7	1152.9	1058.9
8766.0	0.0445	393.5	1.83828E-06	1.1687	0.1067	1179.4	1056.8	1155.6	1064.5	1165.3	1065.8
8622.0	0.0450	397.8	1.85428E-06	1.1718	0.1098	1192.3	1066.0	1168.8	1073.5	1178.3	1074.7
8496.0	0.0455	402.0	1.88946E-06	1.1784	0.1164	1204.8	1068.6	1180.1	1075.8	1189.3	1077.1
8352.0	0.0460	406.2	1.93097E-06	1.1859	0.1239	1217.4	1069.7	1191.3	1076.5	1200.2	1078.0
8242.0	0.0466	410.6	1.96197E-06	1.1914	0.1294	1230.6	1075.1	1204.0	1081.6	1212.7	1083.1
8104.0	0.0470	414.4	1.99683E-06	1.1975	0.1355	1241.9	1077.3	1214.5	1083.4	1222.9	1085.0
7966.0	0.0475	418.6	2.03545E-06	1.2040	0.1420	1254.6	1080.2	1226.5	1086.0	1234.6	1087.7
7840.0	0.0481	422.7	2.07122E-06	1.2100	0.1480	1266.8	1083.8	1238.3	1089.3	1246.2	1091.0
7750.0	0.0485	426.2	2.09793E-06	1.2143	0.1523	1277.3	1088.1	1248.8	1093.5	1256.5	1095.2
7660.0	0.0490	429.9	2.12797E-06	1.2191	0.1571	1288.5	1092.6	1260.1	1097.8	1267.7	1099.6
7560.0	0.0495	433.3	2.15364E-06	1.2231	0.1611	1298.8	1097.3	1270.6	1102.3	1278.0	1104.1
7454.0	0.0500	437.2	2.19769E-06	1.2298	0.1678	1310.3	1098.5	1281.6	1103.3	1288.9	1105.2
7364.0	0.0504	440.5	2.22178E-06	1.2334	0.1714	1320.1	1103.5	1291.9	1108.0	1299.0	1110.0

Specimen V50-112

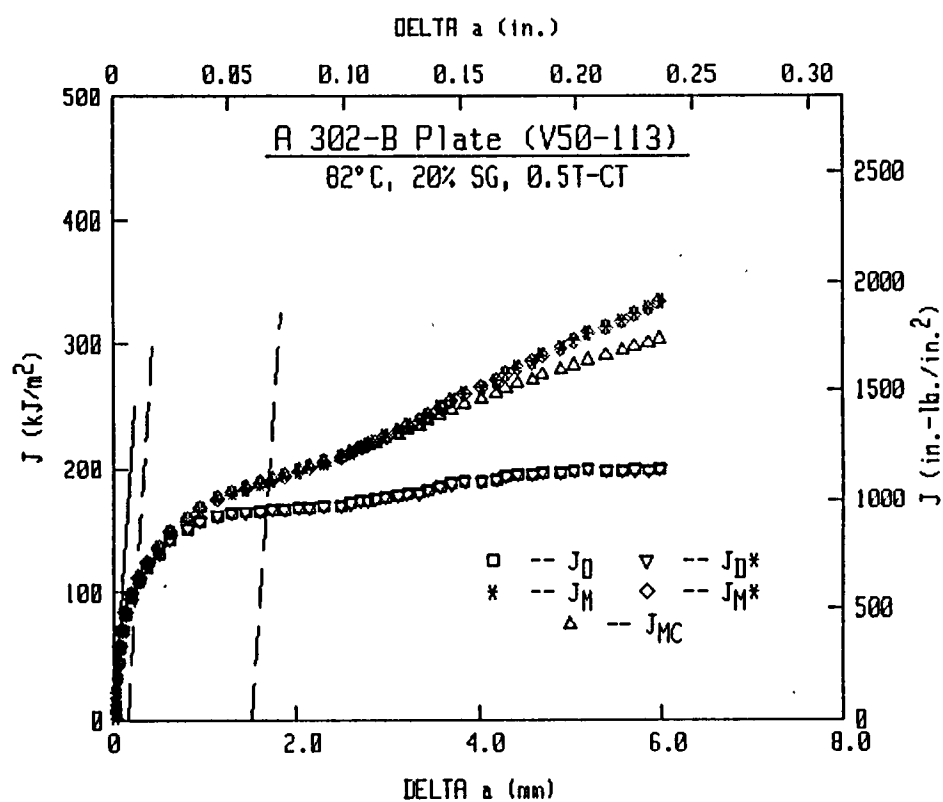
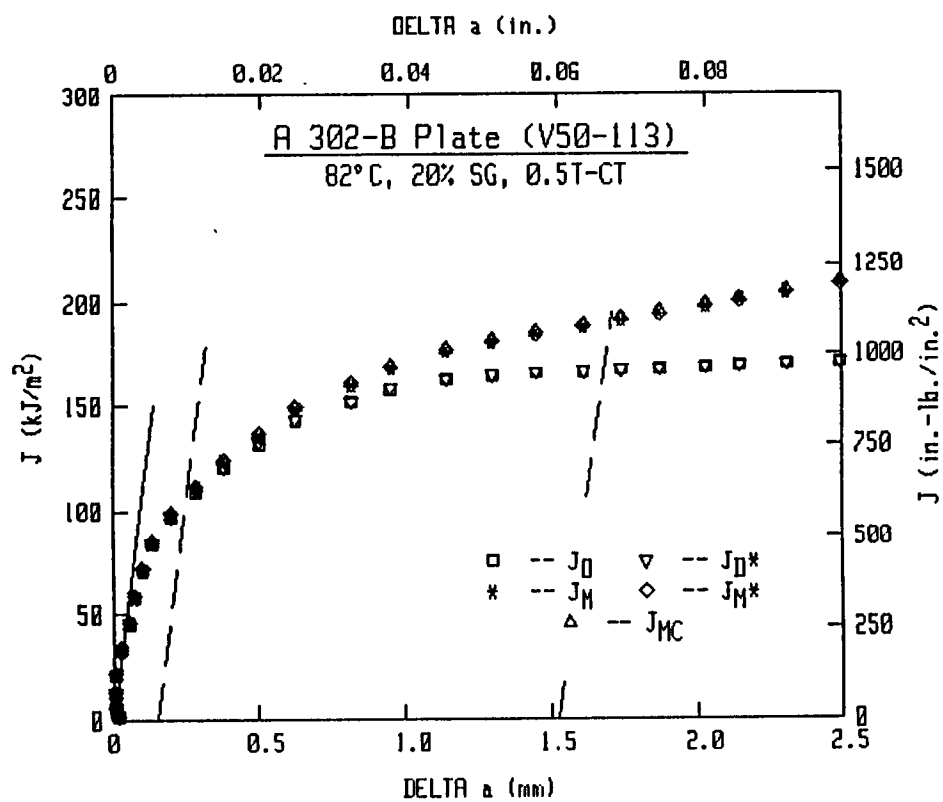
Material Type : A302-B PLATE
Side Groove : 20%
Thickness : 1 in.
Temperature : 180°F
Width : 2 in.
Ao : 1.062 in.
Af : 1.5736 in.
Flow Stress : 75700 psi.
Young's Mod : 29372000 psi.
Initial Slope : 1.38544E-6 in./lbs.
Razor Spacing : .1 in.
Hold-Load Dis : .655 in.
Razor-LL Dis : 0 in.

Load (lbs)	Defl. (in.)	Area (in.-lbs)	Slope (in./lbs)	Post-a (in.)	Delta-a (in.)	Jmc {< - - - - -	Jd - - - - -	Jm (in.-lbs/in. ²)	Jd* - - - - -	Jm* - - - - -	Je - - - - ->!
7230.0	0.0510	444.6	2.27921E-06	1.2418	0.1798	1332.5	1102.5	1303.3	1106.7	1310.1	1108.8
7128.0	0.0514	447.7	2.30761E-06	1.2459	0.1839	1341.9	1106.1	1313.0	1110.2	1319.7	1112.3
7040.0	0.0520	451.9	2.35780E-06	1.2528	0.1908	1354.3	1107.9	1325.3	1111.8	1331.9	1114.0
6842.0	0.0530	458.7	2.43182E-06	1.2628	0.2008	1374.6	1113.5	1346.2	1117.0	1352.5	1119.5
6618.0	0.0540	465.5	2.49341E-06	1.2707	0.2087	1395.1	1123.2	1368.5	1126.4	1374.5	1129.0
6426.0	0.0550	471.7	2.55370E-06	1.2783	0.2163	1413.7	1131.3	1388.8	1134.3	1394.6	1137.1
6264.0	0.0559	477.8	2.59560E-06	1.2834	0.2214	1432.0	1144.0	1410.0	1146.8	1415.7	1149.7
6096.0	0.0570	484.1	2.68637E-06	1.2940	0.2320	1450.9	1146.0	1430.0	1148.6	1435.5	1151.8
5935.0	0.0580	490.4	2.73609E-06	1.2997	0.2377	1469.8	1158.6	1452.3	1161.0	1457.7	1164.3
5736.2	0.0595	499.0	2.82544E-06	1.3094	0.2474	1495.6	1171.0	1482.0	1173.3	1487.3	1176.8
5569.8	0.0611	507.9	2.94332E-06	1.3217	0.2597	1522.1	1179.0	1512.2	1181.2	1517.4	1185.1
5445.0	0.0625	515.5	3.02065E-06	1.3293	0.2673	1545.1	1192.4	1540.0	1194.7	1545.2	1198.7
5296.4	0.0640	523.6	3.12824E-06	1.3396	0.2776	1569.4	1201.9	1568.9	1204.1	1574.2	1208.5
5119.2	0.0654	531.2	3.26338E-06	1.3517	0.2897	1592.0	1204.6	1595.0	1206.5	1600.1	1211.4
4858.2	0.0670	539.1	3.43098E-06	1.3658	0.3038	1615.8	1204.2	1622.5	1205.9	1627.4	1211.3
4667.4	0.0685	546.0	3.57281E-06	1.3771	0.3151	1636.4	1206.4	1647.4	1207.9	1652.1	1213.8
4509.8	0.0700	553.0	3.72217E-06	1.3882	0.3262	1657.5	1209.6	1673.6	1211.1	1678.3	1217.3
4361.4	0.0714	559.3	3.85576E-06	1.3977	0.3357	1676.3	1213.7	1697.6	1215.1	1702.2	1221.6
4230.0	0.0731	566.2	3.99181E-06	1.4069	0.3449	1697.0	1221.2	1724.9	1222.6	1729.5	1229.3
4127.6	0.0745	572.2	4.12697E-06	1.4156	0.3536	1714.9	1226.0	1748.6	1227.3	1753.3	1234.3
4040.4	0.0760	578.3	4.23115E-06	1.4220	0.3600	1733.4	1237.4	1774.5	1238.8	1779.3	1245.9
3920.2	0.0780	586.2	4.46140E-06	1.4354	0.3734	1756.8	1237.7	1805.1	1239.0	1809.8	1246.8
3857.4	0.0794	591.7	4.56632E-06	1.4412	0.3792	1773.5	1248.4	1829.3	1249.8	1834.1	1257.6
3778.2	0.0811	598.1	4.72063E-06	1.4494	0.3874	1792.5	1256.0	1856.3	1257.5	1861.2	1265.5
3705.2	0.0830	605.1	4.84002E-06	1.4556	0.3936	1813.7	1273.1	1888.2	1274.6	1893.2	1282.8
3541.8	0.0860	616.0	5.06770E-06	1.4666	0.4046	1846.2	1294.0	1936.8	1295.7	1942.0	1304.4
3353.8	0.0890	626.4	5.38385E-06	1.4808	0.4188	1877.5	1303.2	1982.6	1304.8	1987.8	1314.4
3158.6	0.0920	636.4	5.78582E-06	1.4973	0.4353	1907.2	1302.8	2025.6	1304.4	2030.8	1315.3
3017.4	0.0950	645.4	6.10565E-06	1.5092	0.4472	1934.5	1312.7	2068.3	1314.3	2073.6	1325.9
2906.8	0.0980	654.4	6.39392E-06	1.5193	0.4573	1961.3	1328.1	2112.3	1329.9	2117.7	1341.9
2791.4	0.1011	663.1	6.68026E-06	1.5287	0.4667	1987.3	1344.4	2156.0	1346.2	2161.6	1358.7
2685.4	0.1040	671.2	6.94129E-06	1.5367	0.4747	2011.8	1362.2	2198.3	1364.1	2204.0	1376.9





V50-113 (0.5T-CT)



Specimen V50-113

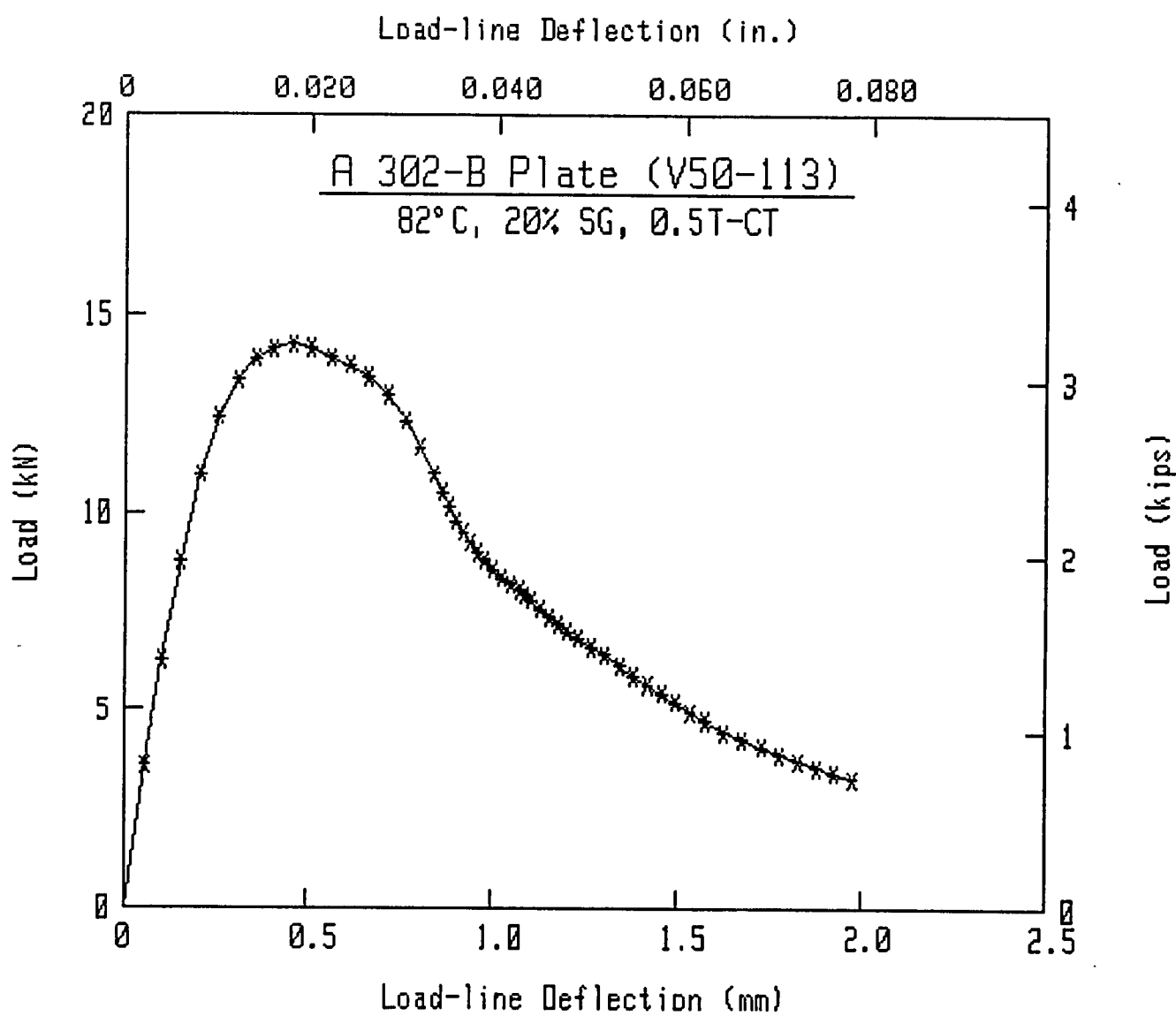
Material Type : A302-B PLATE
Side Groove : 20%
Thickness : .5 in.
Temperature : 180°F
Width : 1 in.
Ao : .5245 in.
Af : .7974 in.
Flow Stress : 75700 psi.
Young's Mod : 29372000 psi.
Initial Slope : 2.7486E-6 in./lbs.
Razor Spacing : .058 in.
Hold-Load Dis : .375 in.
Razor-LL Dis : 0 in.

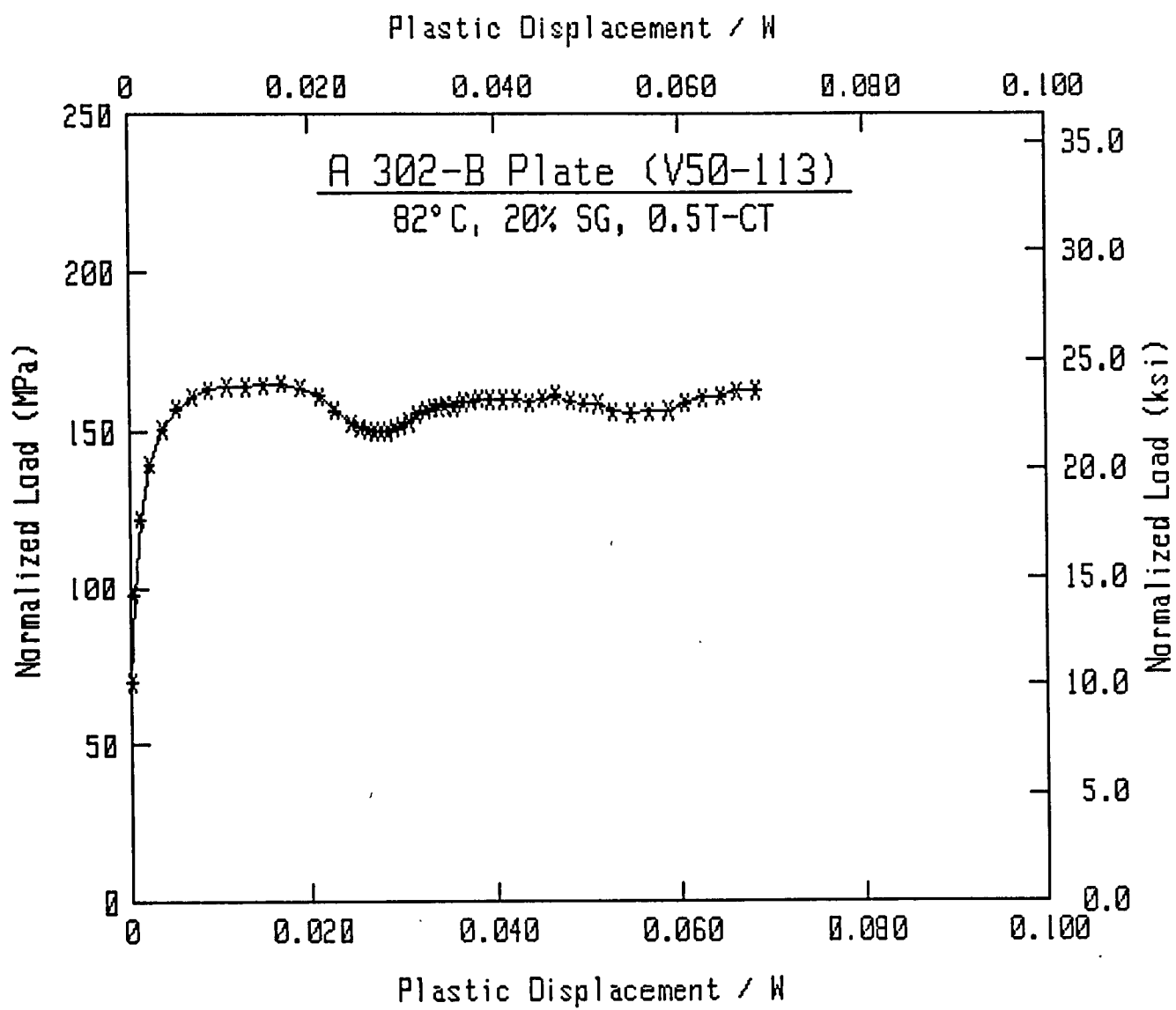
Load (lbs)	Defl. (in.)	Area (in.-lbs)	Slope (in./lbs)	Post-a (in.)	Delta-a (in.)	Jmc : < - - - - -	Jd - - - - -	Jm (in.-lbs/in.²)	Jd* - - - - -	Jm* - - - - -	Je - - - - -
810.5	0.0022	.9	2.75655E-06	0.5252	0.0007	10.7	10.7	10.7	11.1	11.1	11.1
1404.4	0.0040	2.9	2.74969E-06	0.5249	0.0004	34.2	34.2	34.2	35.2	35.2	35.2
1970.8	0.0059	6.2	2.74741E-06	0.5248	0.0003	73.0	73.0	73.0	75.0	75.0	75.0
2461.6	0.0080	10.7	2.74590E-06	0.5249	0.0004	126.7	126.5	126.5	129.7	129.7	129.7
2802.0	0.0100	16.1	2.75402E-06	0.5256	0.0011	190.2	189.6	189.7	193.5	193.7	193.6
3008.0	0.0120	22.0	2.76743E-06	0.5267	0.0022	260.3	258.9	259.3	263.4	263.9	263.4
3126.8	0.0140	28.0	2.77564E-06	0.5274	0.0029	331.1	329.2	330.0	333.9	334.7	334.0
3180.4	0.0160	34.3	2.78980E-06	0.5285	0.0040	406.1	403.2	404.7	408.0	409.5	408.1
3204.8	0.0180	40.7	2.80588E-06	0.5298	0.0053	482.0	477.7	480.3	482.5	485.2	482.7
3184.4	0.0200	47.3	2.84116E-06	0.5324	0.0079	560.1	552.4	557.7	557.0	562.4	557.3
3132.4	0.0220	53.6	2.89074E-06	0.5358	0.0113	634.3	621.3	631.0	625.7	635.6	626.1
3087.2	0.0240	59.7	2.94475E-06	0.5395	0.0150	706.4	687.4	702.6	691.7	707.1	692.3
3021.2	0.0260	65.7	3.01976E-06	0.5443	0.0198	777.9	750.0	773.4	754.0	777.7	754.8
2922.8	0.0280	71.8	3.09585E-06	0.5492	0.0247	858.0	813.0	845.5	816.5	849.4	817.6
2774.0	0.0300	77.5	3.22163E-06	0.5567	0.0322	918.0	864.3	912.6	867.4	916.1	869.0
2625.6	0.0315	81.5	3.31389E-06	0.5620	0.0375	965.1	899.8	960.1	902.2	962.9	904.1
2465.2	0.0330	85.4	3.45156E-06	0.5695	0.0450	1011.0	927.4	1005.6	929.3	1008.0	931.7
2363.2	0.0339	87.7	3.57340E-06	0.5757	0.0512	1037.9	938.3	1032.1	939.7	1034.0	942.4
2282.0	0.0347	89.5	3.69327E-06	0.5816	0.0571	1059.4	944.4	1053.2	945.4	1054.6	948.3
2196.8	0.0355	91.2	3.82806E-06	0.5880	0.0635	1080.3	948.5	1073.6	949.1	1074.7	952.3
2137.2	0.0363	92.8	3.94175E-06	0.5931	0.0686	1099.3	954.2	1092.9	954.5	1093.7	957.9
2076.4	0.0370	94.3	4.06325E-06	0.5983	0.0738	1117.0	958.0	1110.8	958.1	1111.4	961.6
2018.4	0.0378	96.0	4.21197E-06	0.6045	0.0800	1137.3	962.0	1131.6	961.8	1131.9	965.6
1975.6	0.0385	97.5	4.32800E-06	0.6091	0.0846	1154.1	966.9	1149.3	966.5	1149.4	970.5
1923.2	0.0394	99.3	4.49500E-06	0.6154	0.0909	1175.5	971.5	1171.8	970.9	1171.7	975.2
1874.4	0.0405	101.3	4.69905E-06	0.6227	0.0982	1199.1	975.5	1196.7	974.7	1196.3	979.3
1840.0	0.0414	103.0	4.82687E-06	0.6271	0.1026	1220.0	986.3	1220.4	985.4	1220.0	990.2
1806.0	0.0423	104.6	4.94301E-06	0.6310	0.1065	1238.5	995.9	1241.6	994.9	1241.0	999.8
1775.6	0.0429	105.6	5.04538E-06	0.6342	0.1097	1250.8	999.7	1255.4	998.7	1254.8	1003.7
1747.2	0.0434	106.6	5.15005E-06	0.6375	0.1130	1262.5	1003.0	1268.8	1001.9	1268.1	1007.0
1698.8	0.0444	108.3	5.28967E-06	0.6417	0.1172	1282.4	1013.1	1292.1	1011.9	1291.3	1017.1
1652.8	0.0455	110.1	5.49000E-06	0.6475	0.1230	1303.6	1019.1	1316.6	1017.8	1315.7	1023.3
1615.2	0.0464	111.6	5.63463E-06	0.6515	0.1270	1321.7	1027.8	1338.4	1026.4	1337.4	1032.0
1570.0	0.0474	113.2	5.83201E-06	0.6567	0.1322	1340.0	1032.1	1360.1	1030.6	1358.9	1036.4
1532.4	0.0485	114.9	5.96918E-06	0.6602	0.1357	1360.1	1045.3	1385.3	1043.8	1384.1	1049.7
1481.6	0.0499	117.1	6.18590E-06	0.6655	0.1410	1386.1	1059.3	1417.9	1057.9	1416.8	1064.1
1437.2	0.0514	119.2	6.39228E-06	0.6703	0.1458	1411.7	1074.7	1450.8	1073.2	1449.6	1079.7
1374.8	0.0529	121.4	6.64345E-06	0.6759	0.1514	1437.1	1086.4	1483.2	1085.0	1482.0	1091.8
1315.6	0.0544	123.4	7.00989E-06	0.6835	0.1590	1460.9	1087.4	1512.9	1085.9	1511.6	1093.3
1268.4	0.0560	125.4	7.33382E-06	0.6898	0.1653	1484.8	1094.3	1544.1	1092.8	1542.7	1100.6
1218.8	0.0575	127.2	7.55022E-06	0.6938	0.1693	1506.6	1108.4	1574.3	1107.0	1573.0	1115.0
1171.6	0.0590	129.0	7.84469E-06	0.6989	0.1744	1527.5	1115.9	1603.0	1114.5	1601.7	1122.8
1114.8	0.0605	130.8	8.23762E-06	0.7054	0.1809	1548.6	1117.5	1631.6	1116.1	1630.2	1124.8
1066.5	0.0620	132.4	8.50426E-06	0.7096	0.1851	1567.5	1126.8	1658.8	1125.4	1657.4	1134.3
1000.0	0.0640	134.4	9.05489E-06	0.7176	0.1931	1592.0	1126.0	1692.9	1124.5	1691.4	1134.3
962.0	0.0659	136.3	9.45984E-06	0.7231	0.1986	1614.4	1134.5	1726.2	1133.2	1724.8	1143.4
918.2	0.0680	138.3	9.94679E-06	0.7292	0.2047	1637.4	1140.6	1760.6	1139.3	1759.2	1150.0

Specimen V50-113

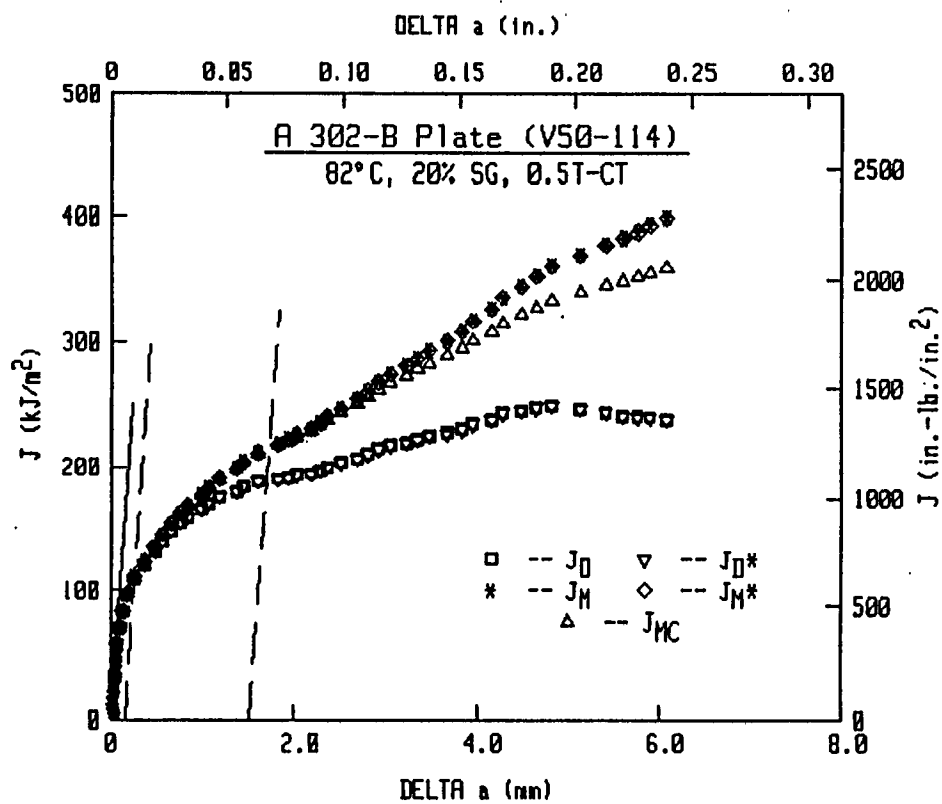
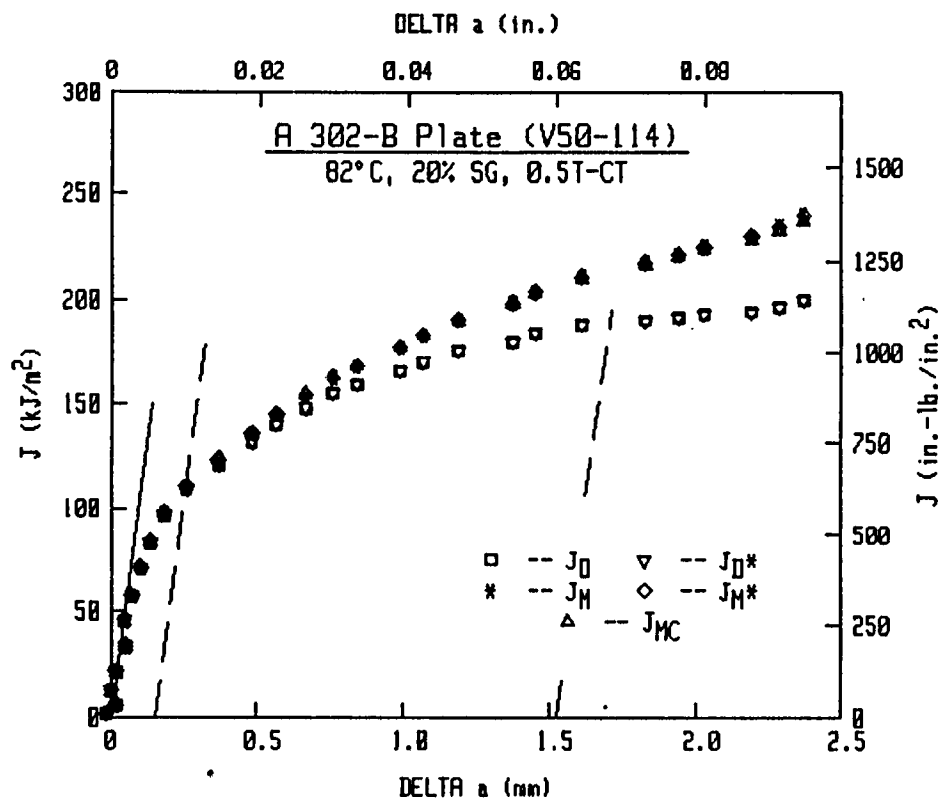
Material Type : A302-B PLATE
Side Groove : 20%
Thickness : .5 in.
Temperature : 180°F
Width : 1 in.
Ao : .5245 in.
Af : .7974 in.
Flow Stress : 75700 psi.
Young's Mod : 29372000 psi.
Initial Slope : 2.7486E-6 in./lbs.
Razor Spacing : .058 in.
Hold-Load Dis : .375 in.
Razor-LL Dis : 0 in.

Load (lbs)	Defl. (in.)	Area (in.-lbs)	Slope (in./lbs)	Post-a (in.)	Delta-a (in.)	Jmc :-	Jd :-	Jm (in.-lbs/in. ²)	Jd* :-	Jm* :-	Je :->!
874.4	0.0699	140.0	1.06389E-05	0.7372	0.2127	1658.0	1133.1	1790.6	1131.6	1789.0	1143.2
834.7	0.0719	141.7	1.12893E-05	0.7441	0.2196	1678.3	1131.2	1821.6	1129.6	1819.9	1141.9
800.9	0.0740	143.4	1.18204E-05	0.7494	0.2249	1698.1	1137.5	1853.8	1136.0	1852.1	1148.7
768.4	0.0759	144.9	1.24831E-05	0.7554	0.2309	1716.2	1136.3	1883.0	1134.7	1881.1	1147.8
736.8	0.0779	146.4	1.30388E-05	0.7602	0.2357	1733.9	1141.8	1912.9	1140.2	1911.0	1153.6





V50-114 (0.5T-CT)



Specimen V50-114

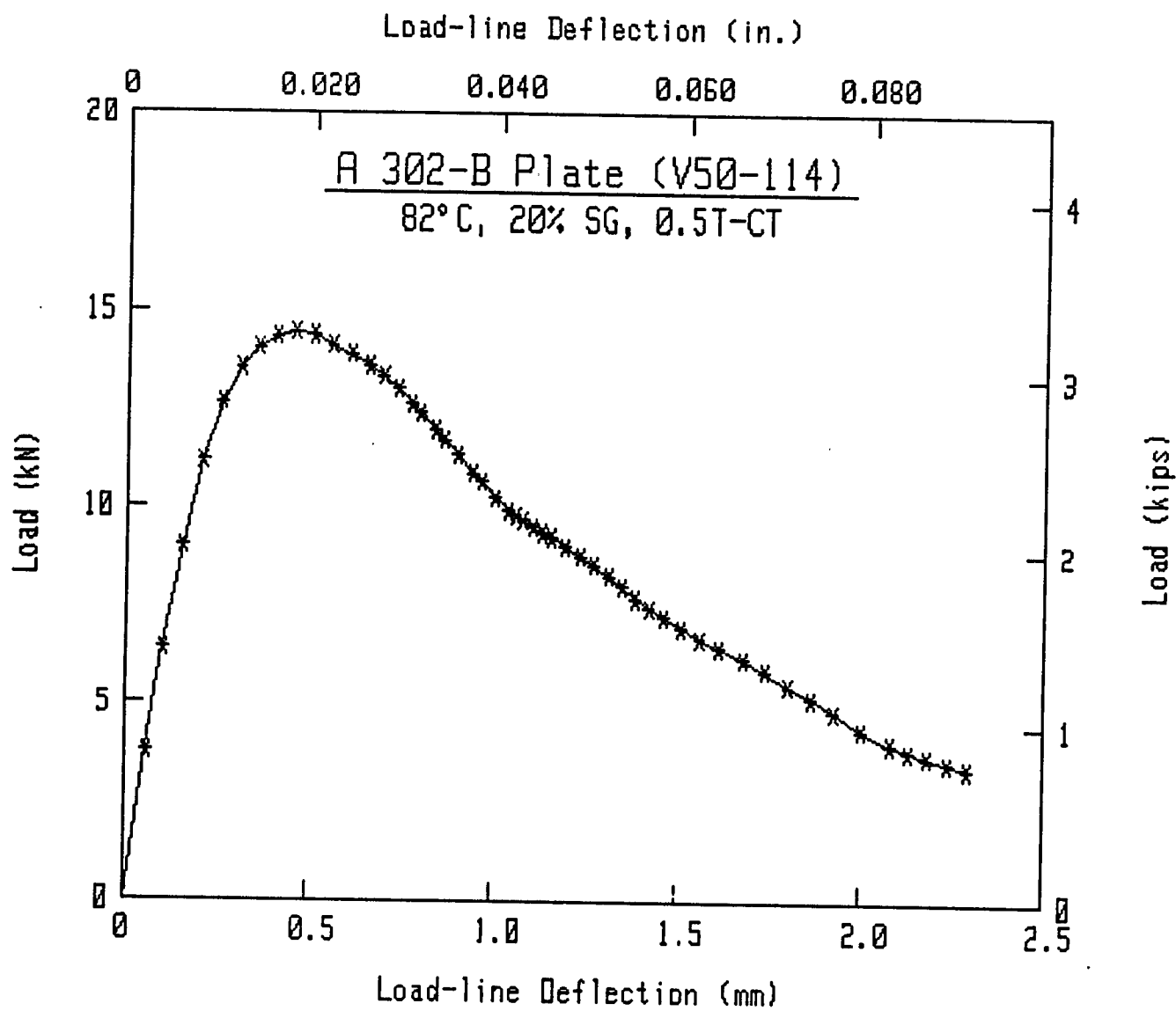
Material Type : A302-B PLATE
Side Groove : 20%
Thickness : .5 in.
Temperature : 180°F
Width : 1 in.
Ao : .5145 in.
Af : .7889 in.
Flow Stress : 75700 psi.
Young's Mod : 29372000 psi.
Initial Slope : 2.64E-6 in./lbs.
Razor Spacing : .058 in.
Hold-Load Dis : .375 in.
Razor-LL Dis : 0 in.

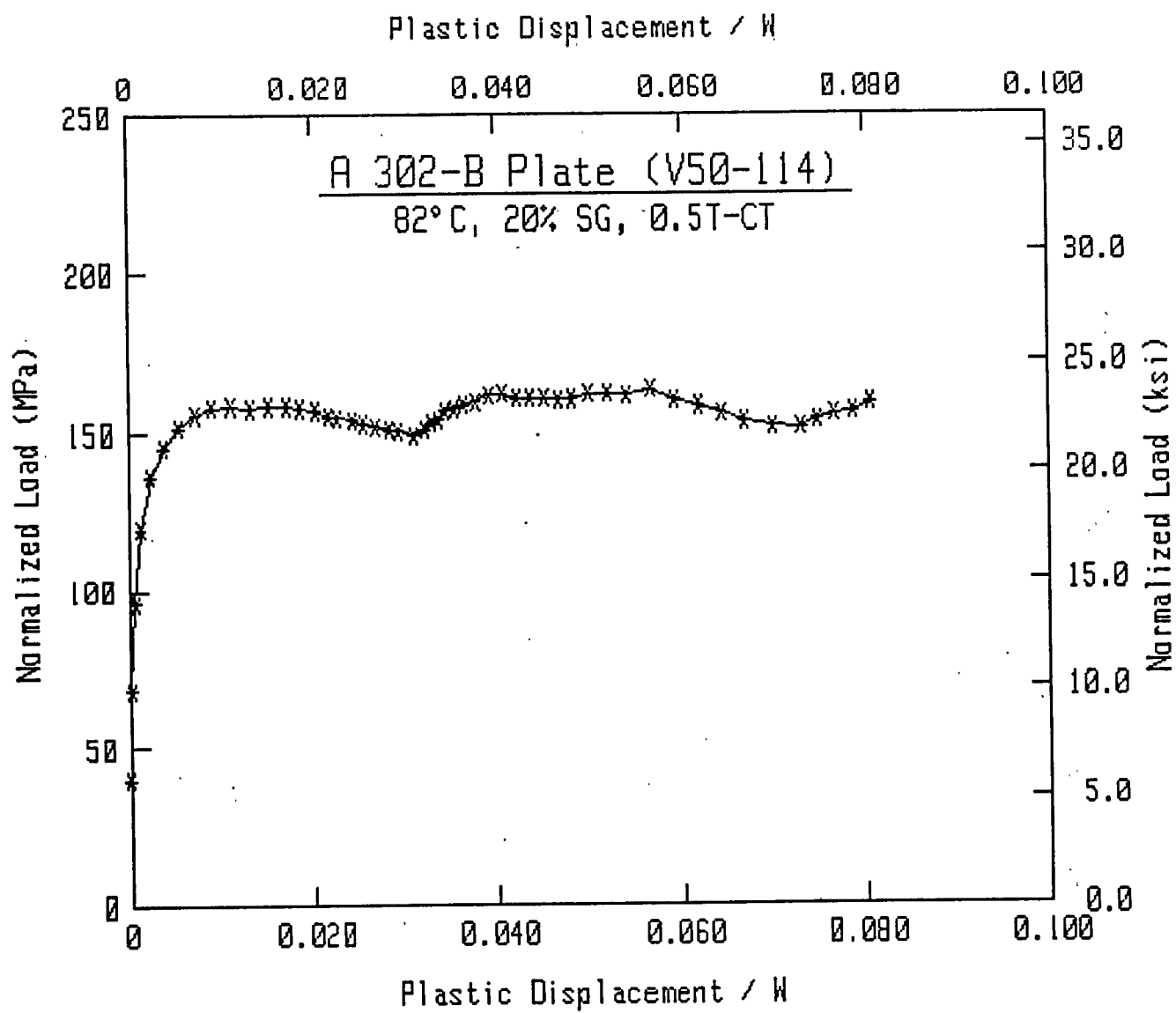
Load (lbs)	Defl. (in.)	Area (in.-lbs)	Slope (in./lbs)	Post-a (in.)	Delta-a (in.)	Jmc !< - - -	Jd - - -	Jm (in.-lbs/in. ²)	Jd* - - -	Jm* - - -	Je - - ->!
849.8	0.0023	1.0	2.62968E-06	0.5139	-0.0006	11.1	11.1	11.1	11.6	11.6	11.6
1436.4	0.0040	2.9	2.64516E-06	0.5152	0.0007	33.9	33.7	33.7	34.8	34.8	34.8
2029.6	0.0059	6.3	2.63462E-06	0.5145	0.0000	73.6	73.5	73.5	75.4	75.3	75.4
2518.8	0.0080	10.9	2.64181E-06	0.5152	0.0007	126.9	126.5	126.5	129.2	129.2	129.2
2852.8	0.0100	16.5	2.65624E-06	0.5165	0.0020	191.3	190.2	190.5	193.5	193.8	193.6
3047.2	0.0120	22.3	2.65188E-06	0.5163	0.0018	258.8	257.9	258.1	261.6	261.8	261.6
3164.0	0.0139	28.3	2.66395E-06	0.5173	0.0028	328.9	327.2	327.9	331.0	331.7	331.1
3228.4	0.0160	34.9	2.67764E-06	0.5185	0.0040	405.8	403.0	404.5	406.9	408.4	407.0
3253.2	0.0179	41.2	2.69389E-06	0.5198	0.0053	479.1	474.9	477.5	478.8	481.4	478.9
3236.8	0.0200	48.0	2.71860E-06	0.5217	0.0072	558.2	551.6	556.3	555.3	560.0	555.5
3176.4	0.0220	54.4	2.75802E-06	0.5247	0.0102	632.0	621.0	629.5	624.3	632.8	624.7
3127.2	0.0240	60.7	2.81784E-06	0.5290	0.0145	705.7	687.4	702.2	690.4	705.3	691.0
3059.2	0.0259	66.8	2.88330E-06	0.5335	0.0190	776.0	749.6	772.0	752.3	774.9	753.1
2999.6	0.0274	71.3	2.93212E-06	0.5368	0.0223	828.7	796.3	824.8	798.8	827.5	799.7
2930.0	0.0290	75.9	2.99132E-06	0.5407	0.0262	882.2	842.3	878.6	844.5	881.0	845.6
2841.2	0.0304	80.1	3.04878E-06	0.5444	0.0299	930.9	883.7	927.9	885.6	930.0	886.9
2790.8	0.0314	82.8	3.09909E-06	0.5476	0.0331	962.0	908.0	959.2	909.6	961.0	911.0
2696.4	0.0330	87.3	3.19598E-06	0.5534	0.0389	1014.4	947.0	1012.0	948.3	1013.6	949.9
2636.0	0.0341	90.0	3.24940E-06	0.5565	0.0420	1046.5	972.3	1045.1	973.4	1046.5	975.2
2555.2	0.0354	93.6	3.33284E-06	0.5613	0.0468	1088.0	1002.7	1087.8	1003.5	1089.0	1005.5
2449.6	0.0370	97.5	3.46764E-06	0.5686	0.0541	1133.9	1029.4	1134.4	1030.0	1135.3	1032.5
2402.0	0.0380	99.9	3.52544E-06	0.5716	0.0571	1161.7	1050.3	1163.9	1050.8	1164.7	1053.4
2303.6	0.0395	103.5	3.64845E-06	0.5779	0.0634	1202.6	1074.9	1206.6	1075.1	1207.1	1078.0
2229.2	0.0409	106.7	3.83045E-06	0.5865	0.0720	1240.6	1087.6	1245.3	1087.4	1245.4	1091.0
2205.2	0.0417	108.4	3.92740E-06	0.5909	0.0764	1260.6	1095.1	1266.3	1094.7	1266.3	1098.5
2178.0	0.0425	110.1	4.00508E-06	0.5944	0.0799	1279.5	1104.7	1286.6	1104.2	1286.4	1108.0
2140.4	0.0435	112.3	4.15715E-06	0.6008	0.0863	1305.3	1111.5	1313.7	1110.7	1313.2	1114.9
2108.4	0.0444	114.2	4.24708E-06	0.6045	0.0900	1327.9	1124.7	1338.8	1123.8	1338.1	1128.1
2081.6	0.0455	116.4	4.33133E-06	0.6078	0.0933	1353.5	1142.7	1367.9	1141.6	1367.1	1146.0
2029.2	0.0469	119.4	4.48236E-06	0.6136	0.0991	1388.0	1161.6	1406.6	1160.4	1405.6	1165.2
1974.4	0.0485	122.6	4.67615E-06	0.6206	0.1061	1425.2	1178.8	1448.4	1177.4	1447.2	1182.7
1925.2	0.0499	125.4	4.80678E-06	0.6252	0.1107	1457.8	1200.7	1486.8	1199.3	1485.6	1204.7
1861.6	0.0515	128.4	4.93983E-06	0.6297	0.1152	1492.6	1225.4	1528.3	1224.0	1527.1	1229.7
1803.6	0.0529	131.0	5.10375E-06	0.6349	0.1204	1522.9	1241.1	1564.2	1239.6	1562.9	1245.5
1732.0	0.0545	133.8	5.32396E-06	0.6416	0.1271	1555.4	1252.9	1602.5	1251.3	1601.0	1257.8
1674.8	0.0560	136.3	5.49466E-06	0.6465	0.1320	1584.3	1268.2	1638.0	1266.7	1636.5	1273.4
1626.0	0.0575	138.7	5.67977E-06	0.6516	0.1371	1612.6	1282.0	1673.1	1280.4	1671.6	1287.4
1565.6	0.0595	142.0	5.97065E-06	0.6592	0.1447	1650.2	1296.0	1719.5	1294.4	1717.9	1302.2
1502.4	0.0615	145.0	6.23205E-06	0.6656	0.1511	1685.7	1312.9	1764.7	1311.4	1763.2	1319.7
1451.6	0.0635	148.0	6.43736E-06	0.6704	0.1559	1720.5	1337.1	1810.9	1335.8	1809.6	1344.4
1389.6	0.0661	151.7	6.80950E-06	0.6785	0.1640	1763.6	1355.2	1867.3	1354.0	1866.1	1363.6
1321.2	0.0685	154.9	7.03508E-06	0.6832	0.1687	1800.8	1383.7	1918.9	1382.8	1917.8	1392.6
1234.4	0.0710	158.2	7.45493E-06	0.6912	0.1767	1838.7	1394.0	1970.0	1393.2	1969.1	1404.1
1162.0	0.0735	161.2	7.82487E-06	0.6978	0.1833	1873.4	1408.1	2018.8	1407.5	2018.0	1419.0
1089.1	0.0760	164.0	8.21708E-06	0.7044	0.1899	1905.9	1419.1	2065.2	1418.6	2064.5	1430.8
983.4	0.0790	167.1	9.03337E-06	0.7166	0.2021	1942.8	1402.3	2115.0	1401.1	2113.5	1416.0
902.4	0.0820	170.0	9.87585E-06	0.7276	0.2131	1975.6	1386.9	2161.5	1385.1	2159.5	1402.3

Specimen V50-114

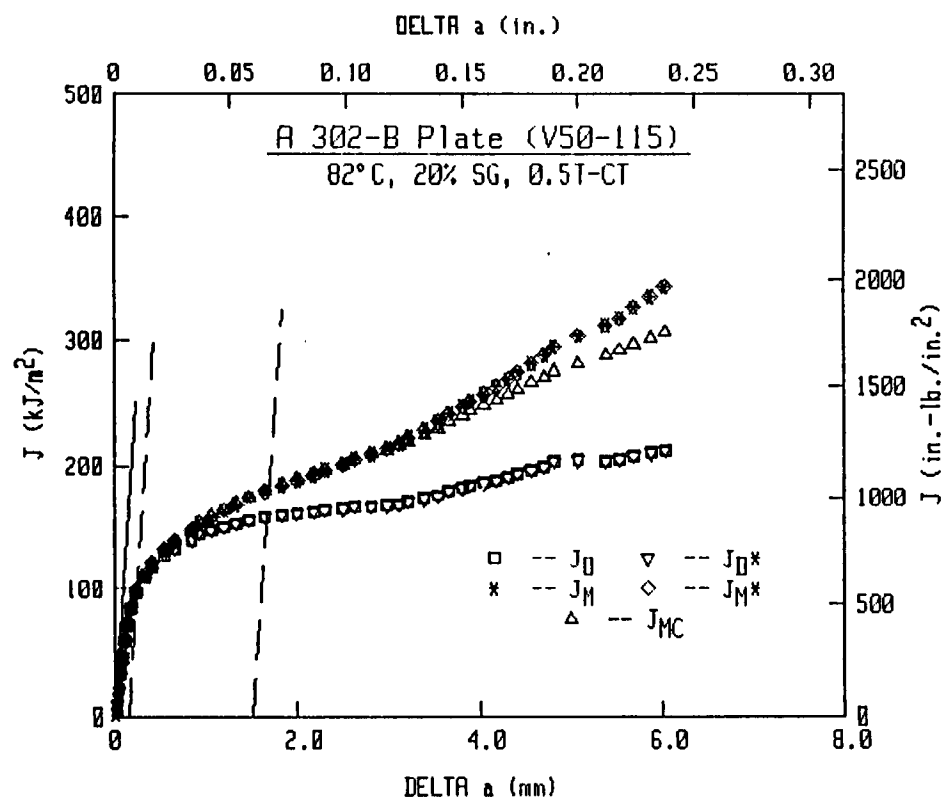
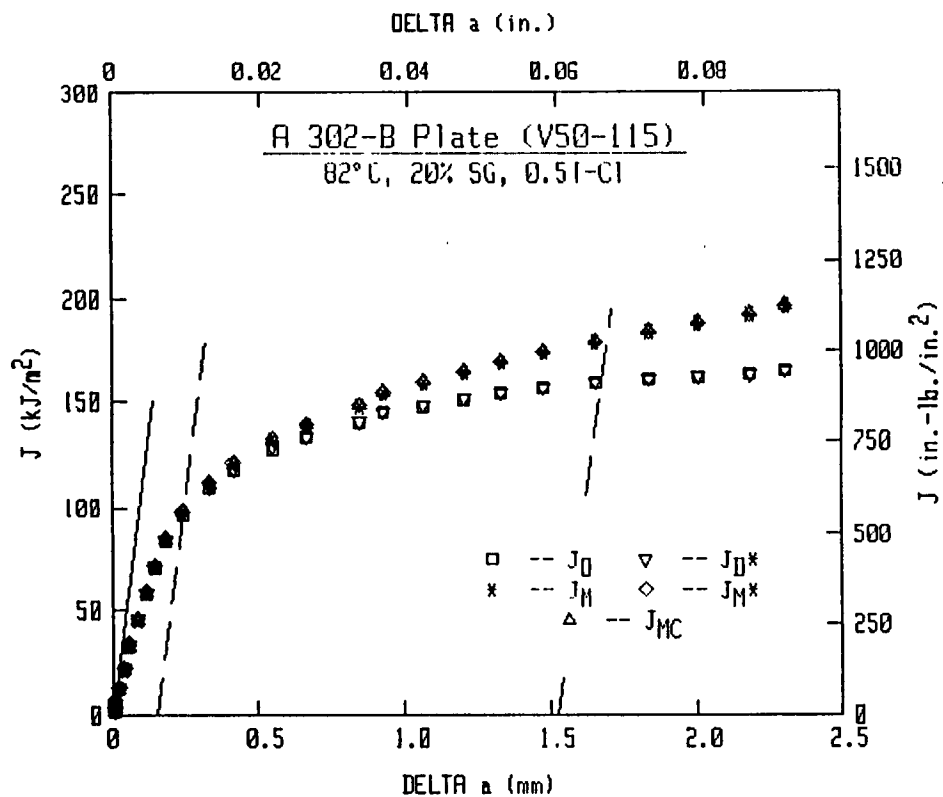
Material Type : A302-B PLATE
Side Groove : 20%
Thickness : .5 in.
Temperature : 180°F
Width : 1 in.
Ao : .5145 in.
Af : .7889 in.
Flow Stress : 75700 psi.
Young's Mod : 29372000 psi.
Initial Slope : 2.64E-6 in./lbs.
Razor Spacing : .058 in.
Hold-Load Dis : .375 in.
Razor-LL Dis : 0 in.

Load (lbs)	Defl. (in.)	Area (in.-lbs)	Slope (in./lbs)	Post-a (in.)	Delta-a (in.)	Jmc !<- - - - -	Jd - - - - -	Jm (in.-lbs/in. ²)	Jd*	Jm*	Je - - - - ->!
863.2	0.0840	171.7	1.05145E-05	0.7351	0.2206	1995.8	1373.6	2191.4	1371.5	2188.9	1389.5
830.3	0.0859	173.3	1.10772E-05	0.7413	0.2268	2015.0	1367.9	2221.4	1365.6	2218.7	1384.1
797.5	0.0880	175.0	1.16068E-05	0.7466	0.2321	2034.4	1367.4	2253.0	1365.0	2250.1	1383.8
764.1	0.0902	176.7	1.23691E-05	0.7538	0.2393	2054.2	1356.1	2284.5	1353.5	2281.2	1373.1





V50-115 (0.5T-CT)



Specimen V50-115

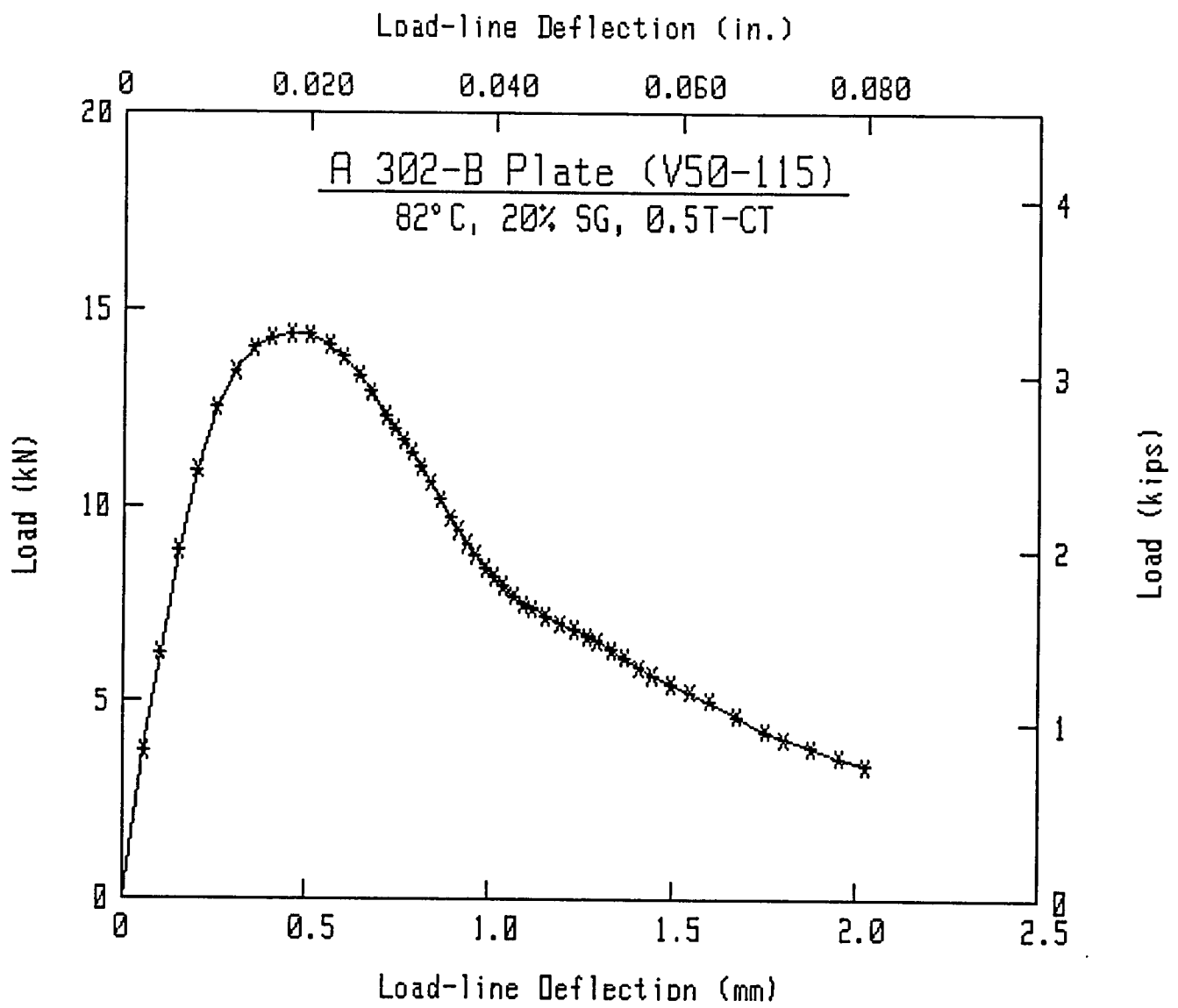
Material Type : A302-B PLATE
Side Groove : 20%
Thickness : .5 in.
Temperature : 180°F
Width : 1 in.
Ao : .5222 in.
Af : .7978 in.
Flow Stress : 75700 psi.
Young's Mod : 29372000 psi.
Initial Slope : 2.7096E-6 in./lbs.
Razor Spacing : .06 in.
Hold-Load Dis : .375 in.
Razor-LL Dis : 0 in.

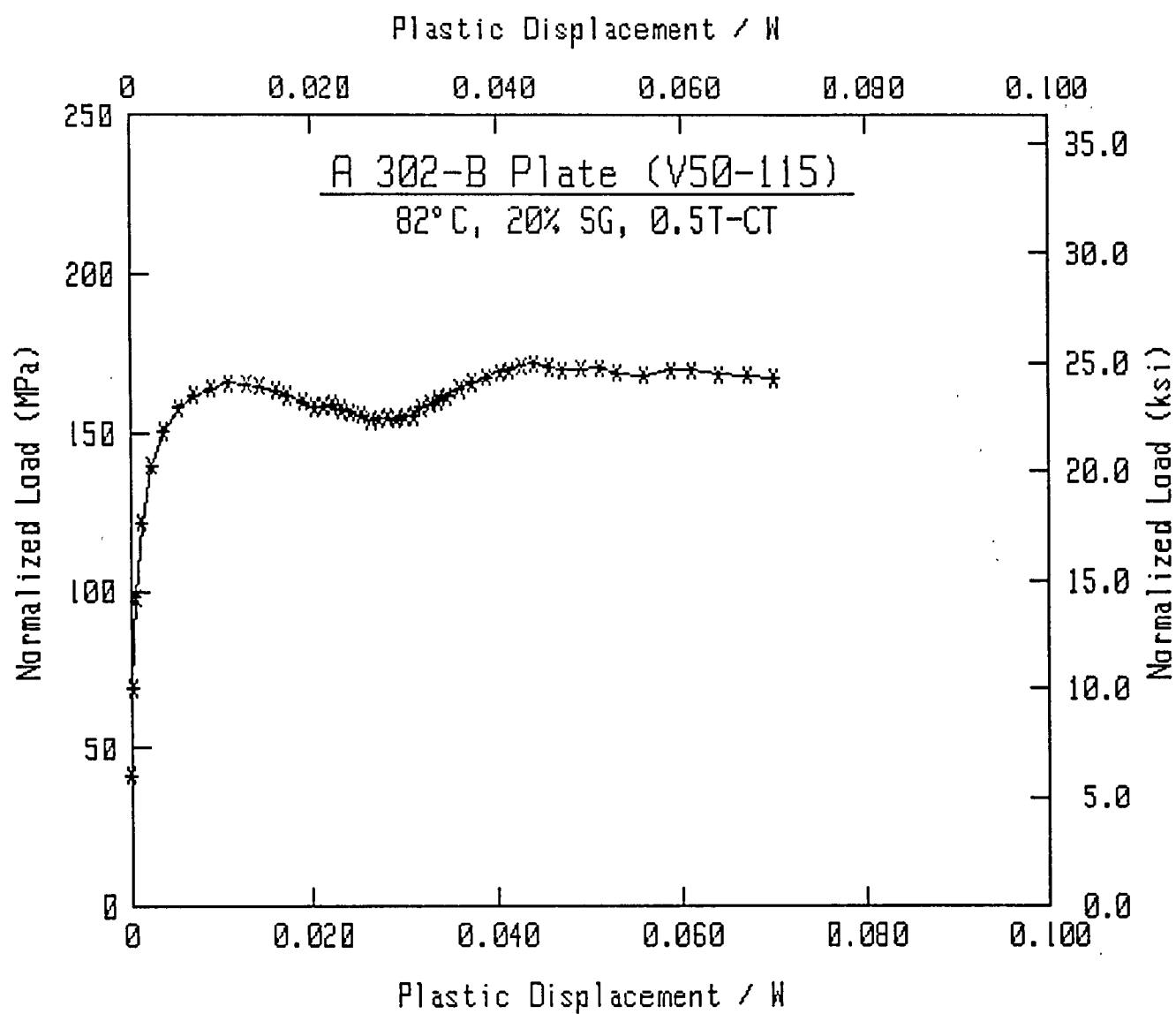
Load (lbs)	Defl. (in.)	Area (in.-lbs)	Slope (in./lbs)	Post-a (in.)	Delta-a (in.)	Jmc < - - - - -	Jd - - - - -	Jm (in.-lbs/in. ²)	Jd* - - - - -	Jm* - - - - -	Je - - - - -
841.1	0.0023	1.0	2.71075E-06	0.5225	0.0003	11.4	11.3	11.3	11.9	11.9	11.9
1407.6	0.0040	2.9	2.70915E-06	0.5225	0.0003	33.9	33.8	33.8	35.2	35.2	35.2
1994.4	0.0060	6.3	2.71565E-06	0.5231	0.0009	73.7	73.5	73.5	76.1	76.1	76.1
2462.0	0.0079	10.6	2.72360E-06	0.5238	0.0016	124.7	124.2	124.2	128.0	128.0	128.0
2817.6	0.0100	16.1	2.73085E-06	0.5245	0.0023	189.2	188.4	188.6	193.2	193.3	193.2
3022.8	0.0120	21.9	2.74483E-06	0.5256	0.0034	258.0	258.5	257.0	261.8	262.4	261.9
3154.0	0.0140	28.3	2.76020E-06	0.5268	0.0046	333.6	331.3	332.3	337.0	338.1	337.1
3216.0	0.0160	34.5	2.77317E-06	0.5279	0.0057	406.8	403.7	405.5	409.5	411.3	409.6
3236.0	0.0180	40.9	2.79367E-06	0.5294	0.0072	482.3	477.8	480.9	483.5	486.7	483.7
3231.6	0.0199	47.3	2.82390E-06	0.5317	0.0095	558.0	550.8	556.2	556.4	562.0	556.7
3171.6	0.0220	54.0	2.87777E-06	0.5354	0.0132	636.8	624.0	634.3	629.3	639.7	629.8
3108.4	0.0235	58.5	2.92531E-06	0.5386	0.0164	689.8	671.9	686.8	676.8	691.9	677.4
3002.4	0.0253	64.0	3.00519E-06	0.5439	0.0217	754.9	727.7	751.0	732.0	755.6	732.8
2907.6	0.0264	67.4	3.07957E-06	0.5485	0.0263	794.7	758.4	789.9	762.2	794.1	763.3
2772.8	0.0280	71.9	3.19650E-06	0.5556	0.0334	848.1	797.4	842.2	800.7	845.9	802.1
2700.8	0.0290	74.8	3.25148E-06	0.5588	0.0366	881.8	825.3	876.6	828.3	880.0	829.8
2630.0	0.0300	77.3	3.34883E-06	0.5642	0.0420	911.9	843.4	906.1	845.9	909.1	847.6
2564.4	0.0310	79.9	3.44940E-06	0.5697	0.0475	942.3	861.8	936.2	863.9	938.9	865.9
2479.2	0.0319	82.2	3.54705E-06	0.5747	0.0525	969.7	877.9	963.8	879.7	966.2	881.8
2392.0	0.0329	84.7	3.66049E-06	0.5804	0.0582	998.6	893.8	993.0	895.3	995.0	897.6
2290.4	0.0340	87.2	3.80916E-06	0.5874	0.0652	1028.7	907.1	1023.3	908.0	1024.8	910.8
2178.0	0.0351	89.7	3.96856E-06	0.5946	0.0724	1057.2	918.1	1052.2	918.6	1053.4	921.8
2106.4	0.0360	91.6	4.12258E-06	0.6012	0.0790	1080.2	924.7	1075.7	925.0	1076.6	928.4
2032.8	0.0370	93.6	4.29716E-06	0.6082	0.0860	1104.0	930.6	1100.1	930.6	1100.8	934.4
1968.4	0.0379	95.5	4.42001E-06	0.6130	0.0908	1125.5	941.3	1123.6	941.2	1124.1	945.1
1893.6	0.0390	97.6	4.63547E-06	0.6208	0.0986	1150.7	946.1	1150.2	945.7	1150.4	950.2
1844.4	0.0399	99.3	4.77483E-06	0.6257	0.1035	1171.3	955.4	1173.2	954.9	1173.3	959.5
1793.2	0.0409	101.2	5.00321E-06	0.6332	0.1110	1193.0	957.1	1196.4	956.3	1196.2	961.4
1734.8	0.0420	103.0	5.22249E-06	0.6400	0.1178	1214.8	961.4	1220.6	960.5	1220.3	965.9
1691.2	0.0430	104.7	5.40215E-06	0.6453	0.1231	1234.5	968.3	1243.3	967.3	1242.9	972.9
1664.0	0.0440	106.4	5.53503E-06	0.6490	0.1268	1254.5	981.0	1267.6	980.0	1267.2	985.7
1618.4	0.0455	108.8	5.78759E-06	0.6558	0.1336	1283.1	993.7	1301.8	992.7	1301.3	998.9
1576.8	0.0469	111.2	6.02161E-06	0.6618	0.1396	1311.0	1008.7	1336.1	1007.7	1335.6	1014.1
1543.6	0.0485	113.6	6.22159E-06	0.6666	0.1444	1339.3	1028.4	1372.1	1027.5	1371.7	1034.2
1499.2	0.0500	115.8	6.47145E-06	0.6724	0.1502	1365.9	1042.1	1405.7	1041.2	1405.3	1048.2
1474.4	0.0510	117.4	6.61912E-06	0.6757	0.1535	1383.9	1054.2	1429.4	1053.3	1429.0	1060.4
1428.0	0.0525	119.5	6.90354E-06	0.6816	0.1594	1409.6	1065.6	1462.5	1064.7	1462.0	1072.1
1381.6	0.0540	121.6	7.17203E-06	0.6870	0.1648	1433.8	1077.5	1494.4	1076.7	1494.0	1084.4
1324.4	0.0555	123.7	7.43929E-06	0.6920	0.1698	1458.7	1091.8	1528.1	1090.9	1527.7	1098.9
1280.4	0.0570	125.6	7.67226E-06	0.6962	0.1740	1481.1	1106.2	1559.3	1105.4	1558.8	1113.5
1228.8	0.0590	128.2	8.01279E-06	0.7021	0.1799	1511.1	1124.1	1601.2	1123.5	1600.9	1132.0
1183.2	0.0610	130.6	8.35296E-06	0.7076	0.1854	1539.6	1141.5	1641.9	1141.0	1641.7	1150.0
1134.4	0.0630	132.9	8.63398E-06	0.7119	0.1897	1566.6	1162.2	1681.6	1161.8	1681.6	1171.0
1044.7	0.0659	136.1	9.38104E-06	0.7223	0.2001	1604.7	1168.4	1735.1	1167.9	1735.0	1178.8
959.8	0.0689	139.1	1.03469E-05	0.7342	0.2120	1640.3	1163.0	1785.0	1162.2	1784.4	1175.4
914.2	0.0710	141.0	1.08810E-05	0.7402	0.2180	1663.1	1169.7	1820.5	1168.9	1819.9	1182.6
862.6	0.0740	143.7	1.14758E-05	0.7463	0.2241	1694.1	1189.0	1871.0	1188.4	1870.7	1202.7

Specimen V50-115

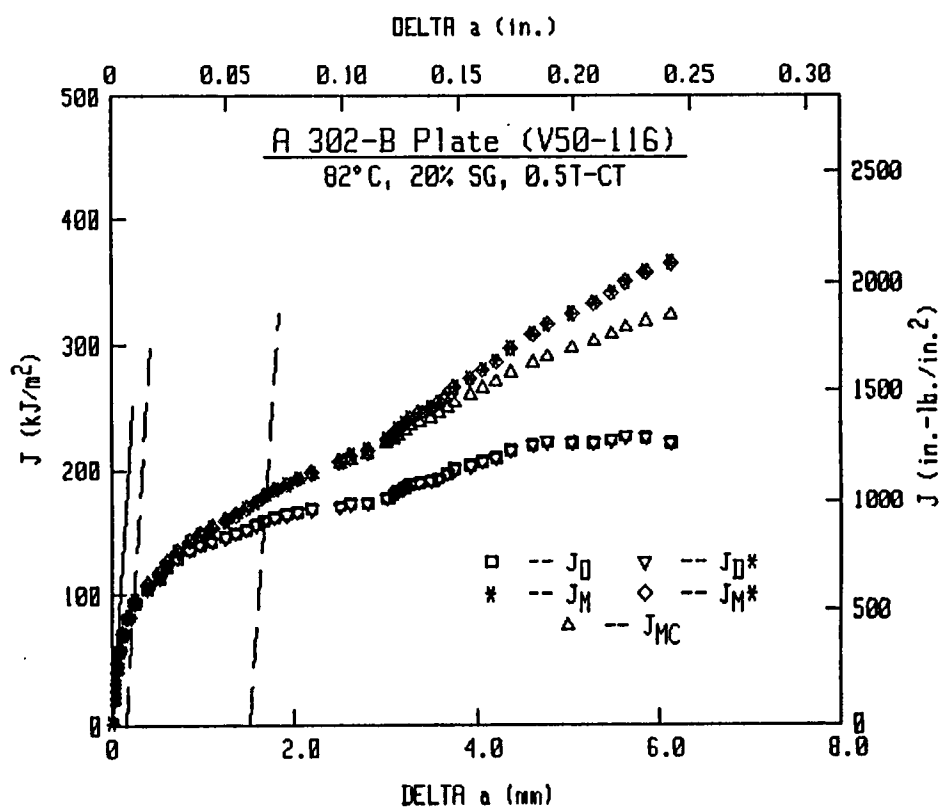
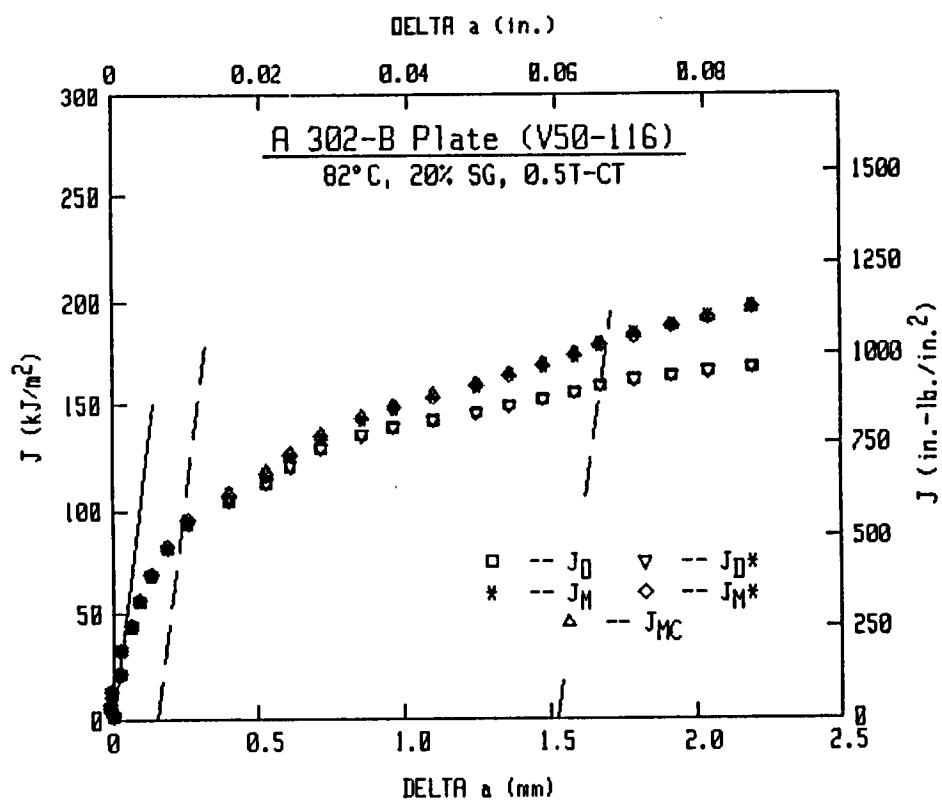
Material Type : A302-B PLATE
Side Groove : 20%
Thickness : .5 in.
Temperature : 180°F
Width : 1 in.
Ao : .5222 in.
Af : .7978 in.
Flow Stress : 75700 psi.
Young's Mod : 29372000 psi.
Initial Slope : 2.7096E-6 in./lbs.
Razor Spacing : .06 in.
Hold-Load Dis : .375 in.
Razor-LL Dis : 0 in.

Load (lbs)	Defl. (in.)	Area (in.-lbs)	Slope (in./lbs)	Post-a (in.)	Delta-a (in.)	Jmc !< - - - - -	Jd - - - - -	Jm (in.-lbs/in. ²)	Jd* - - - - -	Jm* - - - - -	Je - - - - ->!
808.3	0.0770	146.3	1.22392E-05	0.7536	0.2314	1724.4	1200.6	1920.6	1200.2	1920.5	1215.4
763.1	0.0800	148.6	1.29396E-05	0.7597	0.2375	1751.7	1213.6	1966.9	1213.5	1967.0	1229.2





V50-116 (0.5T-CT)



Specimen V50-116

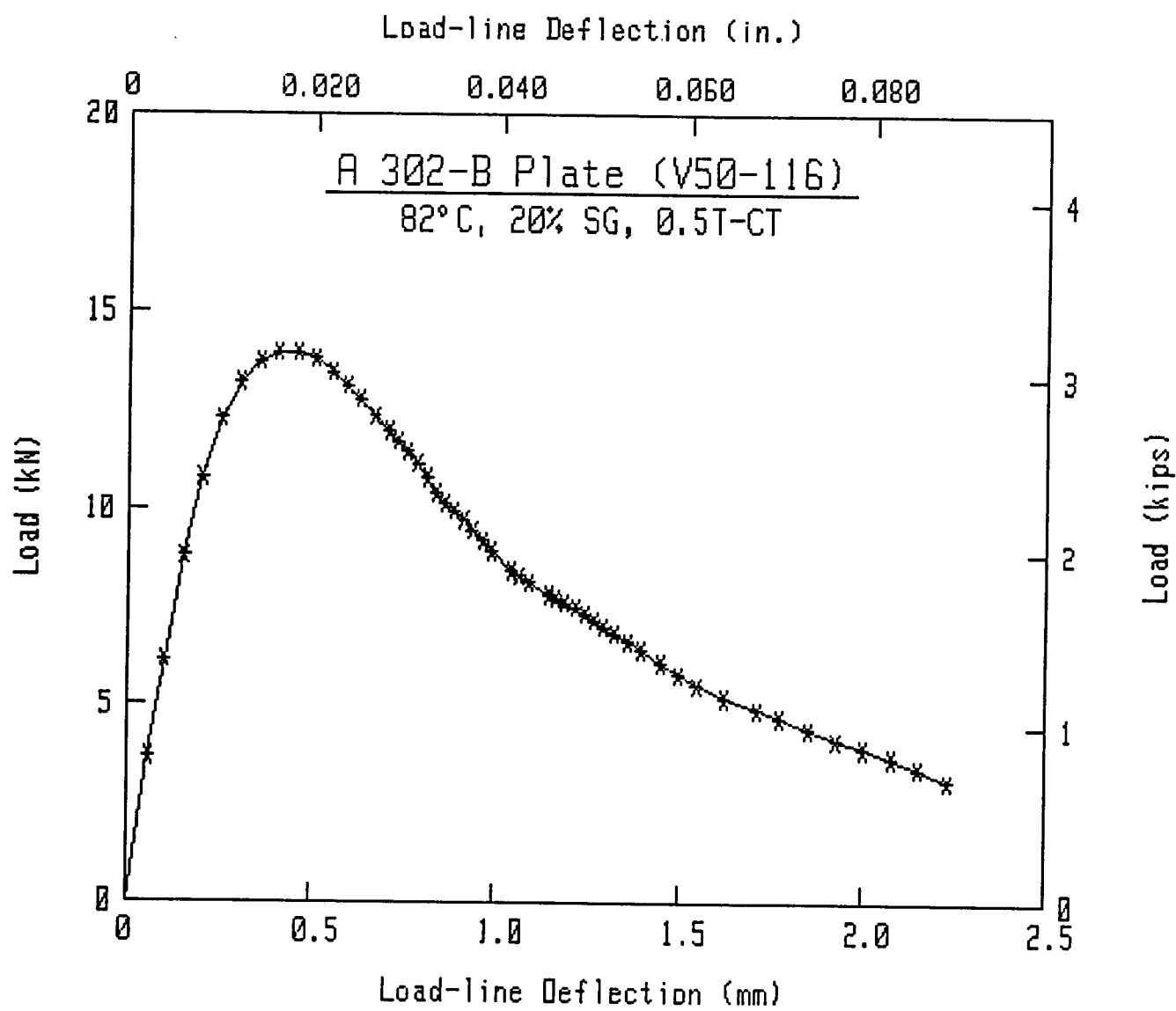
Material Type : A302-B PLATE
Side Groove : 20%
Thickness : .5 in.
Temperature : 180°F
Width : 1 in.
Ao : .5211 in.
Af : .8069 in.
Flow Stress : 75700 psi.
Young's Mod : 29372000 psi.
Initial Slope : 2.752E-6 in./lbs.
Razor Spacing : .06 in.
Hold-Load Dis : .375 in.
Razor-LL Dis : 0 in.

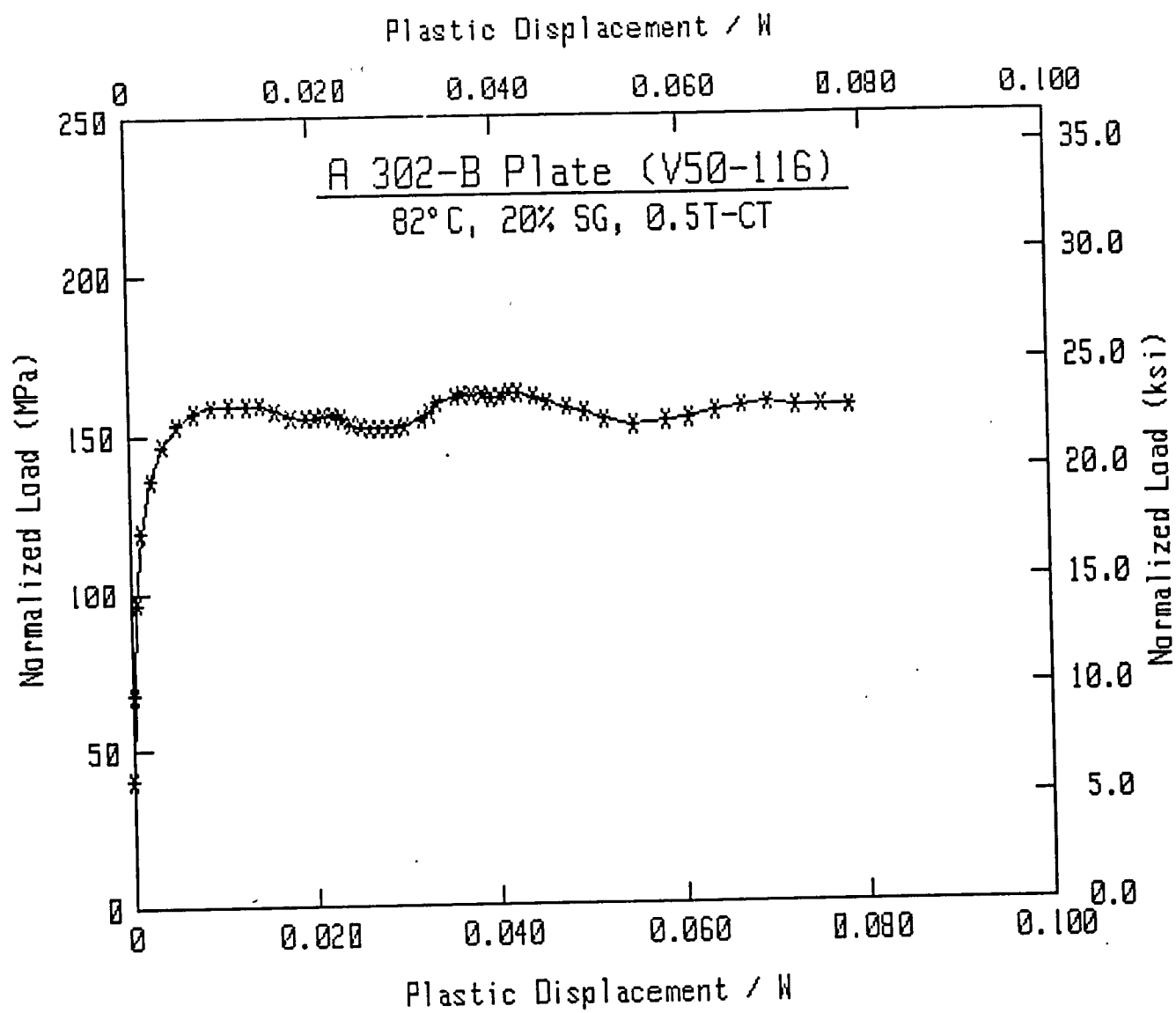
Load (lbs)	Defl. (in.)	Area (in.-lbs)	Slope (in./lbs)	Post-a (in.)	Delta-a (in.)	Jmc !<- - - -	Jd - - -	Jm (in.-lbs/in.²)	Jd* - - -	Jm* - - -	Je - - ->!
828.4	0.0023	1.0	2.75066E-06	0.5212	0.0001	11.2	11.2	11.2	11.6	11.6	11.6
1383.6	0.0040	2.8	2.74286E-06	0.5207	-0.0004	33.1	33.1	33.1	33.8	33.8	33.8
1977.2	0.0061	6.3	2.74286E-06	0.5209	-0.0002	73.7	73.6	73.6	74.8	74.8	74.8
2433.2	0.0080	10.5	2.75720E-06	0.5221	0.0010	123.2	122.5	122.6	124.3	124.3	124.3
2769.6	0.0100	15.8	2.75758E-06	0.5222	0.0011	185.6	184.8	184.9	186.8	186.9	186.8
2971.2	0.0119	21.4	2.77535E-06	0.5236	0.0025	251.8	250.1	250.6	252.3	252.8	252.3
3088.8	0.0140	27.6	2.78819E-06	0.5247	0.0036	325.1	322.6	323.6	324.8	325.8	324.9
3138.0	0.0160	33.9	2.81024E-06	0.5263	0.0052	398.3	394.3	396.4	396.5	398.6	396.6
3140.8	0.0180	40.2	2.83911E-06	0.5285	0.0074	472.8	466.5	470.4	468.5	472.4	468.7
3106.8	0.0200	46.3	2.87860E-06	0.5313	0.0102	545.2	535.4	542.2	537.2	544.1	537.6
3024.4	0.0219	52.4	2.96251E-06	0.5369	0.0158	617.0	598.5	612.3	600.0	613.9	600.6
2952.4	0.0235	57.1	3.03965E-06	0.5419	0.0208	671.7	645.2	666.1	646.4	667.3	647.2
2876.0	0.0249	61.3	3.08985E-06	0.5451	0.0240	721.5	690.4	716.2	691.2	717.2	692.2
2778.0	0.0265	65.7	3.15808E-06	0.5493	0.0282	772.6	734.6	767.7	735.2	768.4	736.4
2696.8	0.0280	69.8	3.25222E-06	0.5548	0.0337	820.9	772.5	815.8	772.9	816.3	774.2
2639.6	0.0290	72.4	3.32663E-06	0.5591	0.0380	852.1	795.4	847.0	795.5	847.2	797.0
2578.8	0.0300	75.0	3.42363E-06	0.5644	0.0433	882.4	814.7	877.0	814.4	876.9	816.1
2510.8	0.0310	77.7	3.53623E-06	0.5703	0.0492	914.7	834.3	909.1	833.7	908.6	835.7
2431.6	0.0320	80.1	3.62394E-06	0.5748	0.0537	942.8	853.4	938.0	852.5	937.2	854.6
2346.8	0.0330	82.4	3.71665E-06	0.5793	0.0582	969.9	871.0	966.0	869.9	965.0	872.1
2282.8	0.0340	84.8	3.80685E-06	0.5836	0.0625	997.5	889.7	994.9	888.4	993.7	890.8
2235.2	0.0350	87.1	3.88050E-06	0.5870	0.0659	1024.5	910.3	1023.9	908.9	1022.6	911.4
2182.8	0.0360	89.3	3.98152E-06	0.5916	0.0705	1050.6	926.5	1051.7	925.0	1050.2	927.7
2122.8	0.0369	91.3	4.10056E-06	0.5967	0.0756	1074.4	938.2	1076.7	936.5	1075.0	939.4
2066.4	0.0379	93.4	4.21727E-06	0.6016	0.0805	1098.9	951.6	1103.1	949.7	1101.2	952.8
2007.2	0.0390	95.5	4.36611E-06	0.6075	0.0864	1124.3	962.5	1130.2	960.5	1128.1	963.8
1895.6	0.0411	99.6	4.70389E-06	0.6199	0.0988	1171.6	977.1	1179.9	974.9	1177.6	979.6
1865.6	0.0420	101.3	4.83569E-06	0.6244	0.1033	1191.8	986.5	1202.6	984.2	1200.2	989.1
1826.0	0.0430	103.2	5.05225E-06	0.6315	0.1104	1214.2	989.7	1226.8	987.2	1224.0	992.4
1757.6	0.0451	106.9	5.33051E-06	0.6400	0.1189	1258.2	1014.3	1277.8	1011.9	1275.1	1017.8
1735.6	0.0459	108.4	5.42626E-06	0.6428	0.1217	1274.9	1025.7	1298.1	1023.2	1295.3	1029.2
1710.8	0.0469	110.1	5.48871E-06	0.6447	0.1236	1295.5	1045.6	1324.0	1043.1	1321.2	1049.2
1682.8	0.0480	111.9	5.60006E-06	0.6478	0.1267	1316.9	1061.5	1350.4	1059.0	1347.6	1065.1
1649.2	0.0490	113.5	5.67826E-06	0.6500	0.1289	1336.0	1078.2	1374.6	1075.7	1371.7	1081.9
1609.2	0.0499	115.1	5.83908E-06	0.6542	0.1331	1354.6	1085.8	1397.2	1083.4	1394.3	1089.6
1573.6	0.0510	116.7	6.02686E-06	0.6590	0.1379	1373.5	1091.8	1420.1	1089.3	1417.1	1095.7
1536.4	0.0520	118.4	6.16780E-06	0.6625	0.1414	1392.8	1103.6	1444.6	1101.1	1441.5	1107.6
1487.6	0.0536	120.7	6.32909E-06	0.6663	0.1452	1420.5	1125.2	1480.7	1122.8	1477.7	1129.5
1442.4	0.0550	122.8	6.45723E-06	0.6693	0.1482	1445.3	1146.6	1513.7	1144.4	1510.8	1151.2
1366.8	0.0570	125.6	6.76447E-06	0.6760	0.1549	1478.2	1162.2	1556.1	1160.0	1553.3	1167.4
1302.0	0.0590	128.3	7.02636E-06	0.6815	0.1604	1509.4	1181.3	1597.8	1179.4	1595.3	1187.1
1236.0	0.0610	130.8	7.31277E-06	0.6871	0.1660	1539.3	1197.7	1638.3	1196.1	1636.0	1204.2
1166.4	0.0640	134.4	7.65802E-06	0.6935	0.1724	1581.9	1228.4	1697.9	1227.4	1696.1	1236.1
1099.7	0.0676	138.5	8.21715E-06	0.7030	0.1819	1629.5	1249.9	1763.7	1249.4	1762.4	1259.5
1055.4	0.0700	141.1	8.62310E-06	0.7093	0.1882	1660.3	1263.5	1808.0	1262.8	1806.5	1273.5
987.7	0.0730	144.1	9.37198E-06	0.7199	0.1988	1696.1	1261.1	1857.9	1260.2	1856.1	1272.8
926.3	0.0760	147.1	1.01296E-05	0.7295	0.2084	1730.6	1262.5	1908.1	1261.6	1906.3	1275.8

Specimen V50-116

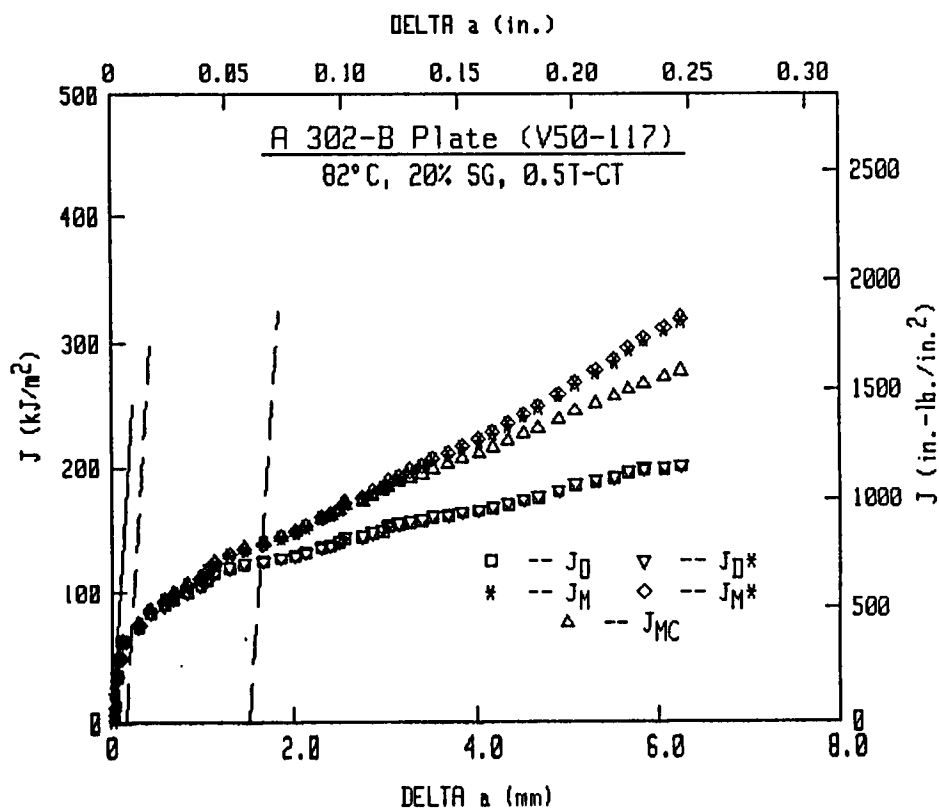
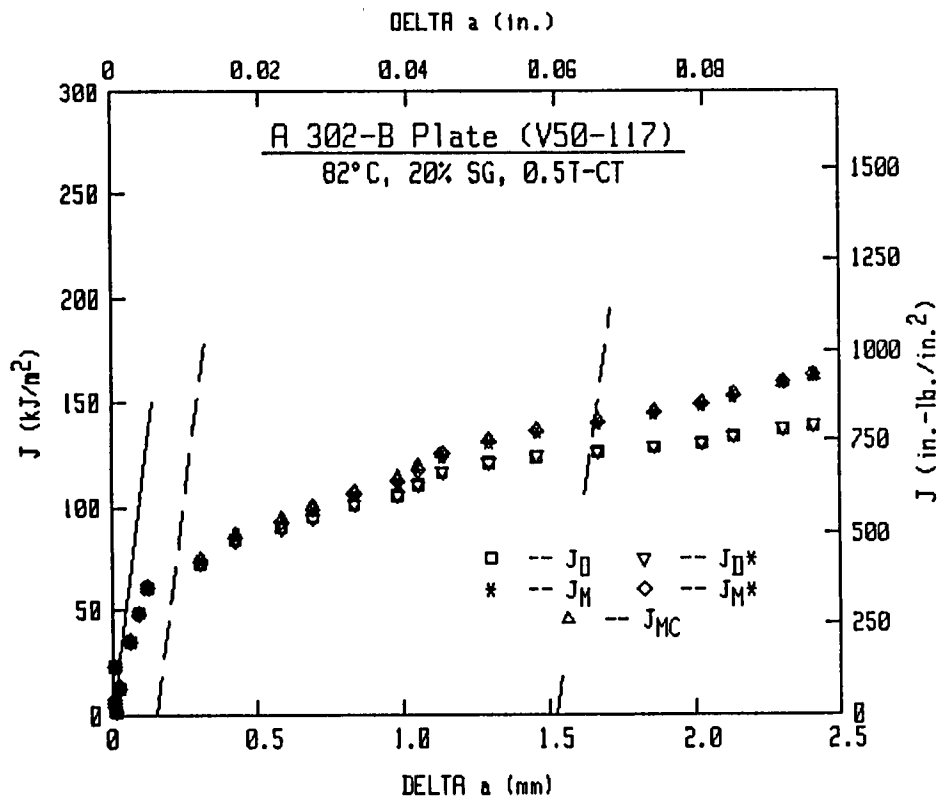
Material Type : A302-B PLATE
 Side Groove : 20%
 Thickness : .5 in.
 Temperature : 180°F
 Width : 1 in.
 Ao : .5211 in.
 Af : .8069 in.
 Flow Stress : 75700 psi.
 Young's Mod : 29372000 psi.
 Initial Slope : 2.752E-6 in./lbs.
 Razor Spacing : .06 in.
 Hold-Load Dis : .375 in.
 Razor-LL Dis : 0 in.

Load (lbs)	Defl. (in.)	Area (in.-lbs)	Slope (in./lbs)	Post-a (in.)	Delta-a (in.)	Jmc	Jd	Jm	Jd*	Jm*	Je
!<- - - - - (in.-lbs/in. ²) - - - - ->!											
877.6	0.0790	149.7	1.07801E-05	0.7370	0.2159	1762.0	1271.7	1956.8	1270.8	1955.0	1285.9
828.0	0.0820	152.4	1.13614E-05	0.7431	0.2220	1792.9	1287.5	2006.8	1287.2	2005.3	1302.8
771.4	0.0850	154.7	1.22478E-05	0.7517	0.2306	1820.7	1283.7	2050.5	1282.8	2048.7	1299.7
698.9	0.0880	156.9	1.35365E-05	0.7626	0.2415	1846.6	1261.5	2089.9	1259.5	2086.9	1279.2





V50-117 (0.5T-CT)



Specimen V50-117

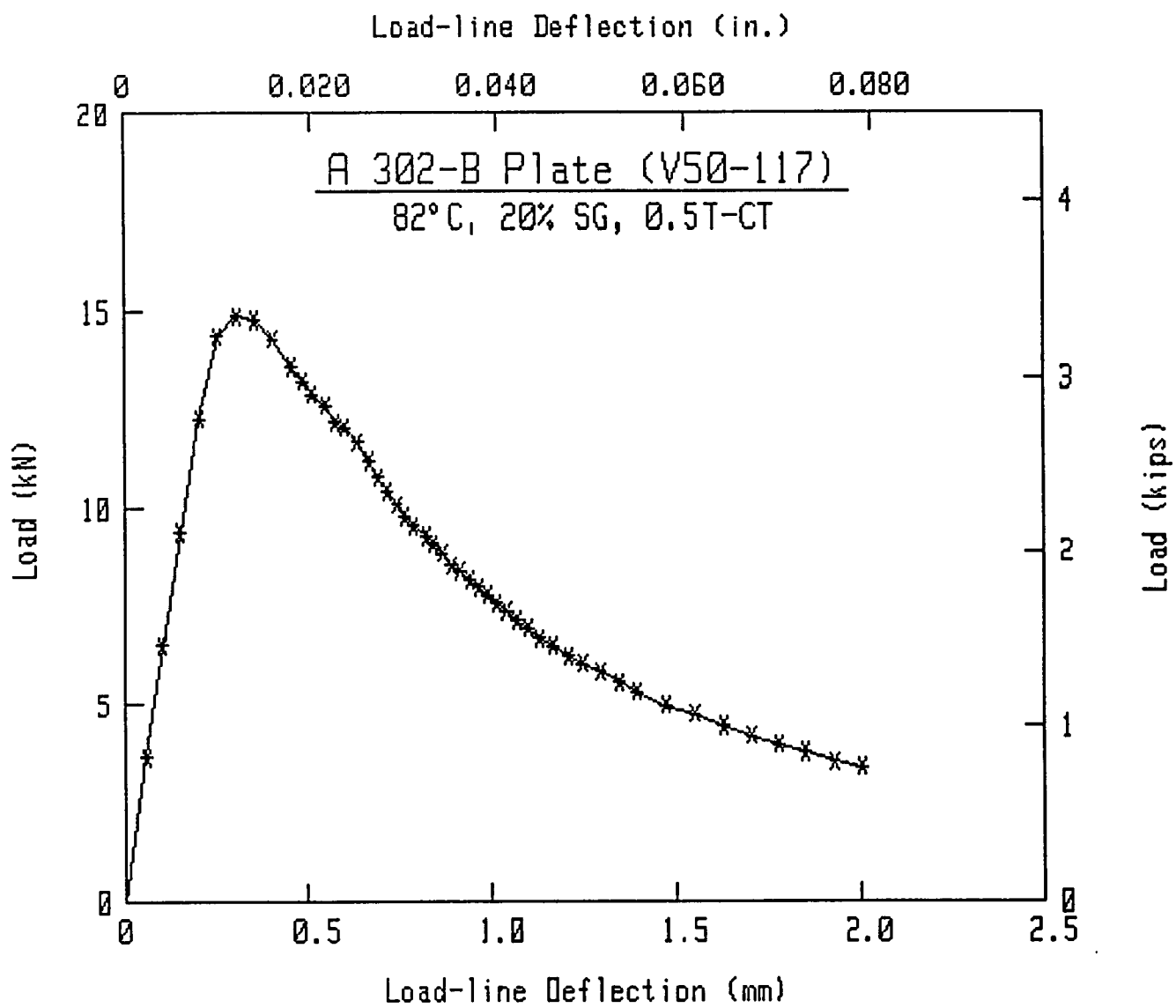
Material Type : A302-B PLATE
Side Groove : 20%
Thickness : .5 in.
Temperature : 180°F
Width : 1 in.
Ao : .5095 in.
Af : .7906 in.
Flow Stress : 75700 psi.
Young's Mod : 29372000 psi.
Initial Slope : 2.6732E-6 in./lbs.
Razor Spacing : .06 in.
Hold-Load Dis : .375 in.
Razor-LL Dis : 0 in.

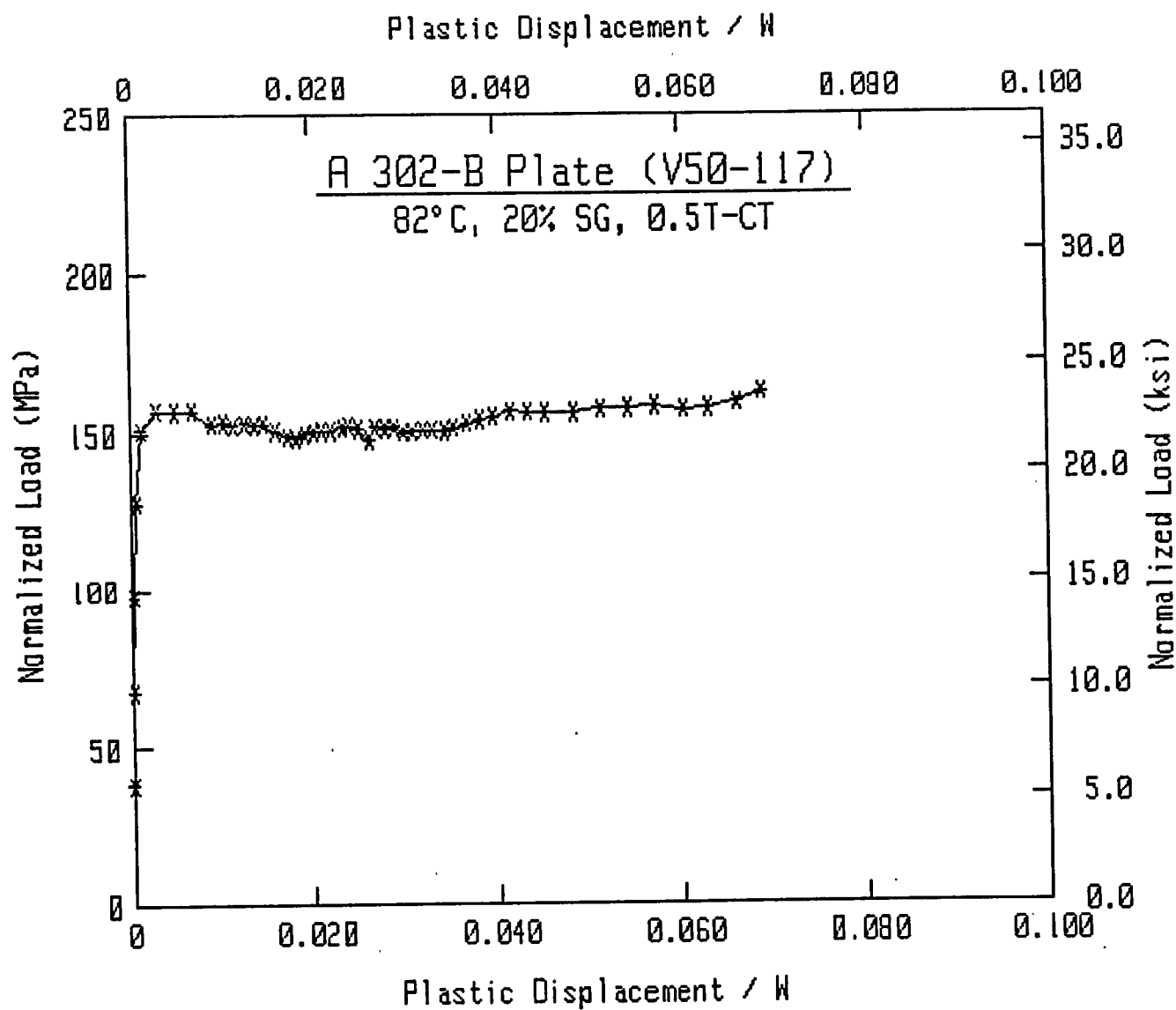
Load (lbs)	Defl. (in.)	Area (in.-lbs)	Slope (in./lbs)	Post-a (in.)	Delta-a (in.)	Jmc	Jd	Jm	Jd*	Jm*	Je
825.6	0.0023	.9	2.67774E-06	0.5100	0.0005	10.6	10.6	10.6	10.8	10.8	10.8
1461.6	0.0041	3.0	2.67358E-06	0.5098	0.0003	34.3	34.3	34.3	34.4	34.4	34.4
2108.4	0.0060	6.4	2.68032E-06	0.5105	0.0010	73.9	73.7	73.7	73.6	73.6	73.6
2762.8	0.0080	11.4	2.67049E-06	0.5099	0.0004	131.0	131.0	131.0	130.2	130.2	130.2
3232.8	0.0100	17.3	2.69508E-06	0.5119	0.0024	199.4	198.3	198.5	197.0	197.2	197.0
3342.8	0.0120	24.1	2.70915E-06	0.5131	0.0036	277.8	275.9	276.4	273.8	274.3	273.9
3321.6	0.0140	30.5	2.72489E-06	0.5143	0.0048	351.1	348.3	349.4	348.7	349.8	348.8
3215.6	0.0160	37.1	2.82418E-06	0.5215	0.0120	427.7	416.9	423.3	416.6	423.0	417.0
3060.8	0.0180	43.2	2.89257E-06	0.5263	0.0168	497.0	481.7	492.3	478.2	488.6	478.7
2978.4	0.0193	46.9	2.98613E-06	0.5325	0.0230	539.8	516.4	533.3	514.4	531.2	515.1
2902.0	0.0203	49.8	3.05121E-06	0.5367	0.0272	573.3	544.6	566.3	542.4	564.0	543.2
2838.0	0.0216	53.3	3.14256E-06	0.5423	0.0328	613.7	577.3	605.9	577.6	606.2	578.6
2744.0	0.0227	56.3	3.24055E-06	0.5482	0.0387	648.0	603.2	639.7	603.2	639.6	604.4
2714.0	0.0236	58.8	3.28666E-06	0.5509	0.0414	677.7	629.9	670.3	630.1	670.3	631.3
2630.8	0.0249	62.0	3.34404E-06	0.5542	0.0447	713.6	662.2	707.7	664.8	710.2	666.2
2522.0	0.0261	65.1	3.45882E-06	0.5605	0.0510	749.4	687.8	743.7	690.2	746.1	691.8
2428.4	0.0271	67.5	3.58301E-06	0.5670	0.0575	777.7	704.7	771.9	706.8	774.0	708.6
2346.0	0.0281	69.9	3.74812E-06	0.5752	0.0657	805.5	717.3	799.2	718.8	800.7	721.0
2264.4	0.0291	72.2	3.91267E-06	0.5828	0.0733	831.8	729.2	825.5	731.5	827.8	734.0
2195.2	0.0300	74.2	4.05743E-06	0.5892	0.0797	855.2	741.0	849.6	742.9	851.6	745.7
2142.0	0.0310	76.3	4.15666E-06	0.5935	0.0840	879.0	758.4	875.6	760.1	877.5	763.0
2080.8	0.0320	79.1	4.32052E-06	0.6002	0.0907	910.7	778.7	910.0	782.4	913.9	785.6
2040.0	0.0331	80.5	4.42417E-06	0.6043	0.0948	927.8	788.6	928.6	792.0	932.4	795.3
1984.0	0.0341	82.6	4.52621E-06	0.6082	0.0987	951.2	806.5	955.3	809.8	959.0	813.3
1913.6	0.0350	84.3	4.58969E-06	0.6105	0.1010	971.1	824.2	978.7	829.6	984.4	833.0
1881.6	0.0360	86.1	4.80408E-06	0.6181	0.1086	992.1	828.5	1000.9	833.0	1005.9	836.8
1830.4	0.0370	88.1	4.92802E-06	0.6223	0.1128	1014.5	844.3	1027.1	848.8	1032.1	852.7
1789.2	0.0380	89.8	5.06440E-06	0.6268	0.1173	1034.0	855.7	1049.7	859.9	1054.6	864.0
1745.6	0.0390	91.5	5.13622E-06	0.6291	0.1196	1054.2	874.5	1074.5	878.8	1079.5	882.9
1701.2	0.0400	93.2	5.28640E-06	0.6337	0.1242	1073.8	885.3	1097.8	889.5	1102.7	893.7
1656.8	0.0410	95.0	5.44696E-06	0.6385	0.1290	1093.9	896.2	1121.8	901.0	1127.4	905.5
1606.8	0.0420	96.6	5.63255E-06	0.6437	0.1342	1112.5	903.6	1143.9	908.3	1149.5	912.9
1557.2	0.0433	98.5	5.80498E-06	0.6484	0.1389	1134.8	917.7	1171.6	922.3	1177.2	927.2
1503.6	0.0444	100.3	6.05847E-06	0.6550	0.1455	1155.3	923.2	1196.3	927.6	1201.8	932.7
1459.6	0.0460	102.5	6.30961E-06	0.6611	0.1516	1180.9	936.8	1228.6	942.4	1235.3	947.9
1403.2	0.0475	104.7	6.62776E-06	0.6683	0.1588	1205.6	945.1	1259.6	950.4	1266.2	956.4
1356.8	0.0491	106.9	6.90778E-06	0.6743	0.1648	1231.0	958.9	1292.8	964.1	1299.4	970.4
1311.6	0.0510	109.4	7.23218E-06	0.6809	0.1714	1260.0	975.6	1331.5	981.6	1339.1	988.4
1249.6	0.0530	112.0	7.59681E-06	0.6878	0.1783	1289.8	992.3	1372.2	998.3	1379.9	1005.6
1194.0	0.0550	114.3	7.95001E-06	0.6940	0.1845	1316.9	1007.4	1409.8	1013.5	1417.8	1021.2
1121.9	0.0580	117.9	8.48490E-06	0.7028	0.1933	1357.7	1032.2	1467.8	1038.5	1476.1	1047.2
1071.6	0.0610	121.1	8.95827E-06	0.7100	0.2005	1395.2	1059.1	1523.1	1066.1	1532.5	1075.5
1005.3	0.0640	124.2	9.60403E-06	0.7188	0.2093	1430.7	1074.4	1575.2	1081.4	1584.9	1091.9
946.8	0.0669	127.1	1.02596E-05	0.7270	0.2175	1463.8	1089.3	1625.6	1096.9	1636.1	1108.4
895.8	0.0700	129.9	1.07809E-05	0.7331	0.2236	1496.0	1113.7	1677.5	1121.5	1688.4	1133.5
851.8	0.0728	132.3	1.13981E-05	0.7397	0.2302	1524.2	1128.0	1722.9	1135.9	1734.2	1148.5
800.6	0.0760	135.0	1.23083E-05	0.7485	0.2390	1554.6	1134.0	1771.8	1141.7	1783.1	1155.6

Specimen V50-117

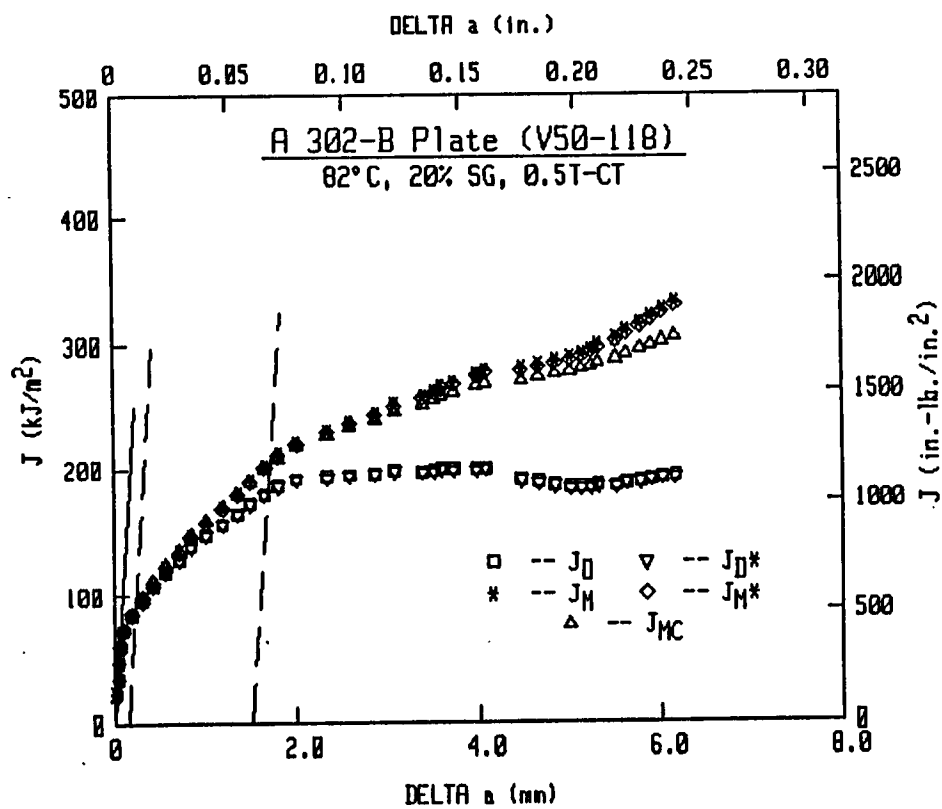
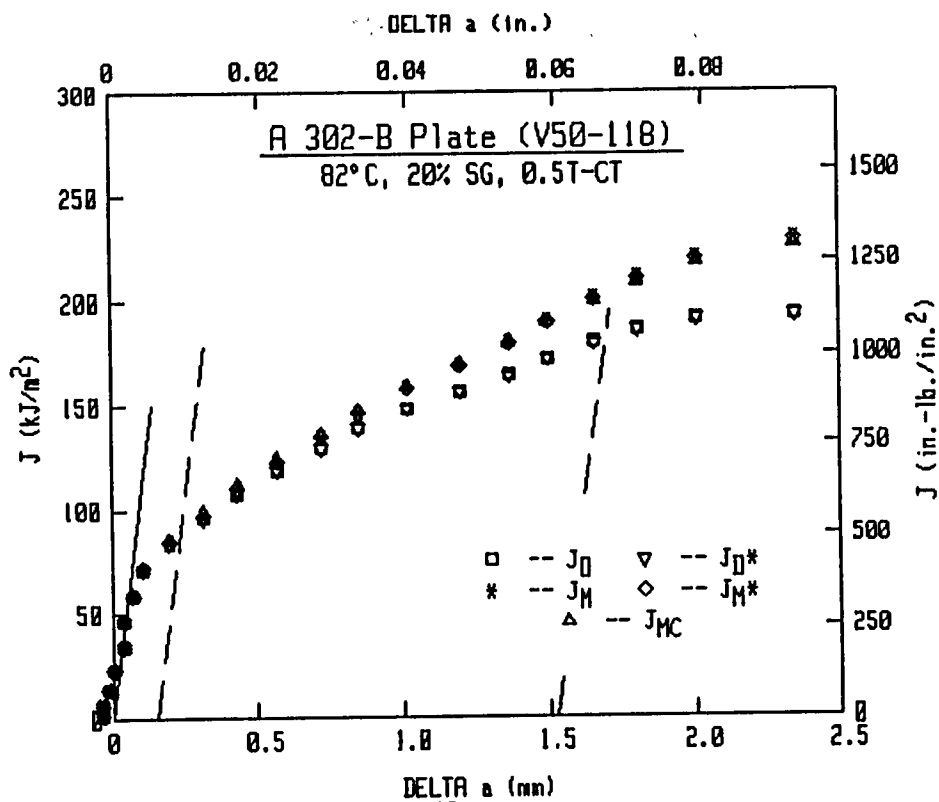
Material Type : A302-B PLATE
Side Groove : 20%
Thickness : .5 in.
Temperature : 180°F
Width : 1 in.
Ao : .5095 in.
Af : .7906 in.
Flow Stress : 75700 psi.
Young's Mod : 29372000 psi.
Initial Slope : 2.6732E-6 in./lbs.
Razor Spacing : .06 in.
Hold-Load Dis : .375 in.
Razor-LL Dis : 0 in.

Load (lbs)	Defl. (in.)	Area (in.-lbs)	Slope (in./lbs)	Post-a (in.)	Delta-a (in.)	Jmc : < - - - - -	Jd - - - - -	Jm (in.-lbs/in. ²)	Jd* - - - - -	Jm* - - - - -	Je - - - - - > :
768.1	0.0790	137.3	1.31259E-05	0.7557	0.2462	1581.8	1143.7	1817.4	1151.1	1828.7	1166.0





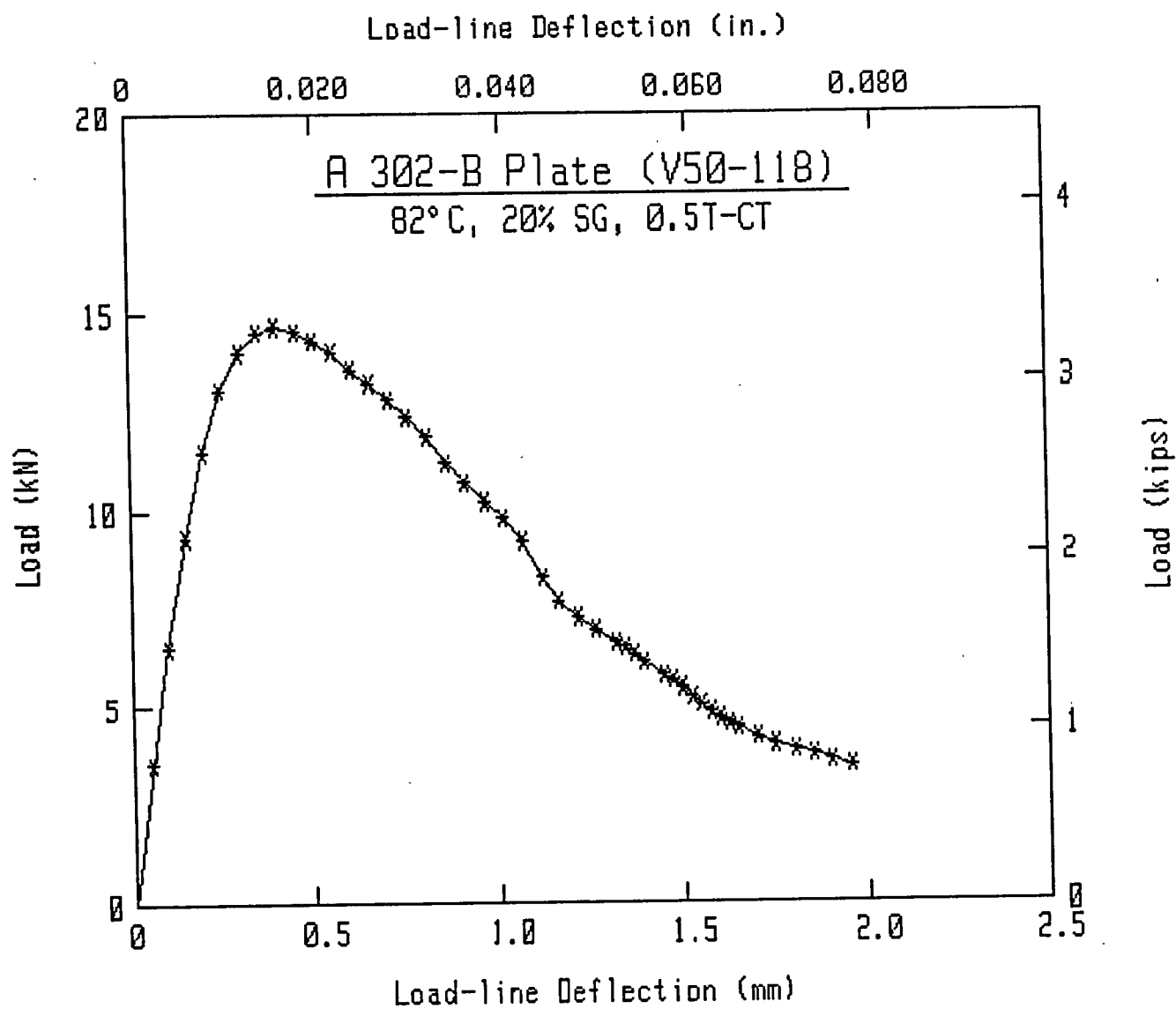
V50-118 (0.5T-CT)

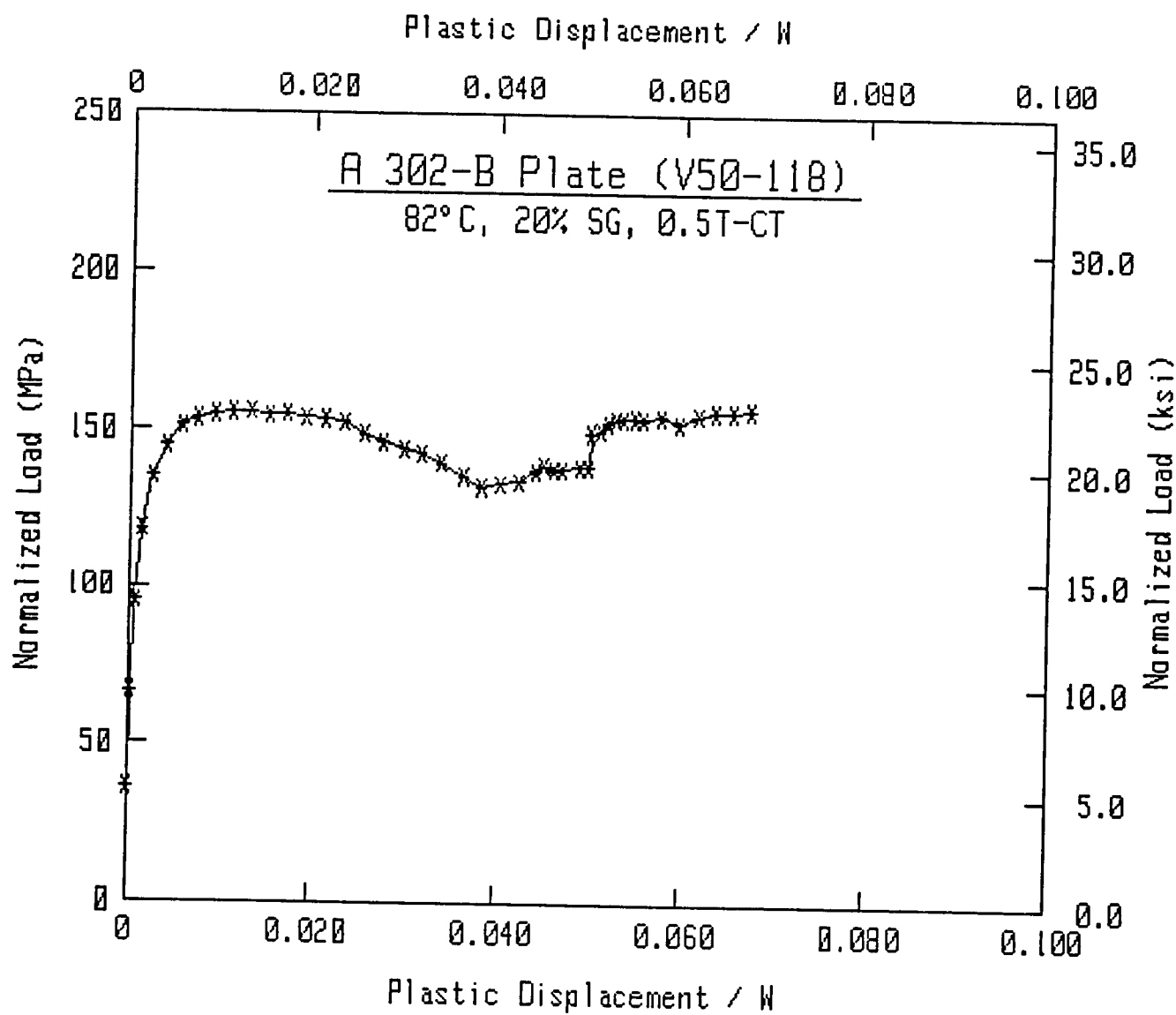


Specimen V50-118

Material Type : A302-B PLATE
 Side Groove : 20%
 Thickness : .5 in.
 Temperature : 180°F
 Width : 1 in.
 Ao : .5069 in.
 Af : .7852 in.
 Flow Stress : 75700 psi.
 Young's Mod : 29372000 psi.
 Initial Slope : 2.5989E-6 in./lbs.
 Razor Spacing : .062 in.
 Hold-Load Dis : .375 in.
 Razor-LL Dis : 0 in.

Load (lbs)	Defl. (in.)	Area (in.-lbs)	Slope (in./lbs)	Post-a (in.)	Delta-a (in.)	Jmc	Jd	Jm	Jd*	Jm*	Je
						<- - - - -	- - - - -	(in.-lbs/in.)	- - - - -	- - - - -	- - - - -
800.9	0.0021	.9	2.57875E-06	0.5055	-0.0014	10.0	10.0	10.0	9.8	9.8	9.8
1464.0	0.0040	3.0	2.57704E-06	0.5055	-0.0014	34.5	34.4	34.4	34.3	34.3	34.3
2094.8	0.0060	6.7	2.58644E-06	0.5064	-0.0005	76.2	75.7	75.8	76.0	76.0	76.0
2584.8	0.0080	11.3	2.59352E-06	0.5071	0.0002	129.2	128.3	128.4	128.9	128.9	128.9
2939.6	0.0100	16.9	2.60802E-06	0.5084	0.0015	193.9	192.3	192.6	192.9	193.2	192.9
3148.0	0.0121	23.2	2.60586E-06	0.5084	0.0015	265.5	264.0	264.2	264.5	264.8	264.5
3265.2	0.0140	29.4	2.62105E-06	0.5097	0.0028	337.5	334.8	335.8	335.3	336.2	335.4
3296.8	0.0160	35.9	2.63763E-06	0.5111	0.0042	411.7	407.6	409.5	408.0	409.9	408.2
3269.2	0.0180	42.5	2.68521E-06	0.5147	0.0078	487.7	479.1	484.2	479.2	484.2	479.4
3216.4	0.0200	49.0	2.74591E-06	0.5193	0.0124	562.2	547.5	557.3	547.2	557.1	547.7
3149.6	0.0220	55.3	2.81070E-06	0.5239	0.0170	634.4	612.9	628.7	612.4	628.2	613.1
3049.2	0.0240	61.6	2.88703E-06	0.5293	0.0224	705.7	675.9	699.5	674.9	698.5	675.8
2972.4	0.0260	67.7	2.97700E-06	0.5353	0.0284	775.6	735.6	769.2	734.4	767.9	735.7
2879.2	0.0280	73.4	3.05434E-06	0.5403	0.0334	841.6	793.3	836.2	791.9	834.7	793.4
2778.8	0.0300	79.3	3.16081E-06	0.5469	0.0400	909.3	848.4	904.9	846.8	903.1	848.7
2666.4	0.0320	84.7	3.28166E-06	0.5540	0.0471	971.3	895.8	968.1	893.8	966.0	896.3
2514.8	0.0340	89.9	3.39958E-06	0.5607	0.0538	1030.4	941.2	1029.5	939.2	1027.4	942.1
2405.6	0.0360	94.7	3.49607E-06	0.5659	0.0590	1085.8	986.6	1088.5	984.5	1086.3	987.7
2296.0	0.0381	99.8	3.61698E-06	0.5722	0.0653	1143.6	1031.0	1150.5	1029.0	1148.2	1032.6
2204.8	0.0400	104.0	3.73632E-06	0.5781	0.0712	1192.0	1065.9	1202.7	1063.8	1200.3	1067.7
2070.0	0.0420	108.3	3.90443E-06	0.5860	0.0791	1242.0	1095.5	1256.6	1093.1	1253.9	1097.6
1864.0	0.0442	112.7	4.21323E-06	0.5993	0.0924	1291.7	1105.0	1308.4	1102.3	1305.3	1108.5
1721.6	0.0460	115.8	4.46141E-06	0.6090	0.1021	1328.0	1112.2	1348.0	1109.6	1344.9	1116.6
1629.6	0.0480	119.2	4.76501E-06	0.6200	0.1131	1367.0	1117.9	1391.1	1115.0	1387.6	1123.2
1561.6	0.0500	122.4	5.01464E-06	0.6283	0.1214	1403.8	1131.2	1434.0	1128.3	1430.4	1137.2
1490.0	0.0520	125.5	5.41279E-06	0.6405	0.1336	1438.6	1126.7	1473.0	1123.3	1468.8	1133.6
1462.4	0.0530	127.0	5.59120E-06	0.6456	0.1387	1455.7	1128.8	1493.7	1125.3	1489.3	1135.7
1421.6	0.0540	128.5	5.70098E-06	0.6486	0.1417	1472.7	1139.2	1515.5	1135.8	1511.2	1146.2
1377.2	0.0550	129.8	5.90162E-06	0.6539	0.1470	1488.4	1138.3	1534.6	1134.8	1530.1	1145.4
1299.6	0.0570	132.5	6.30845E-06	0.6639	0.1570	1519.4	1137.9	1572.7	1134.3	1567.9	1145.9
1269.2	0.0580	133.8	6.46449E-06	0.6675	0.1606	1533.8	1142.6	1591.6	1138.9	1586.7	1150.6
1230.4	0.0590	135.0	7.22121E-06	0.6832	0.1763	1547.7	1093.5	1601.9	1087.6	1594.4	1101.8
1176.0	0.0600	136.3	7.62425E-06	0.6907	0.1838	1562.4	1082.8	1620.3	1076.6	1612.4	1091.2
1134.7	0.0610	137.4	8.03680E-06	0.6978	0.1909	1574.8	1070.3	1635.6	1063.9	1627.3	1078.8
1090.6	0.0620	138.5	8.43977E-06	0.7043	0.1974	1587.6	1061.6	1652.5	1055.1	1644.0	1070.3
1054.5	0.0630	139.5	8.76435E-06	0.7092	0.2023	1599.3	1058.2	1668.9	1051.8	1660.2	1067.0
1023.6	0.0640	140.6	9.05733E-06	0.7134	0.2065	1612.0	1059.6	1687.5	1053.2	1678.8	1068.5
998.4	0.0650	141.6	9.26141E-06	0.7162	0.2093	1623.3	1065.0	1704.7	1058.7	1696.0	1073.9
944.9	0.0670	143.6	9.87127E-06	0.7242	0.2173	1645.8	1064.6	1737.7	1058.5	1729.0	1074.3
902.8	0.0690	145.4	1.02175E-05	0.7284	0.2215	1666.6	1079.3	1771.1	1073.6	1762.6	1089.5
873.3	0.0711	147.2	1.07441E-05	0.7345	0.2276	1688.0	1086.2	1804.9	1080.5	1796.4	1096.7
847.8	0.0730	148.8	1.11674E-05	0.7391	0.2322	1706.5	1095.4	1835.2	1089.9	1826.7	1106.2
813.1	0.0750	150.5	1.16727E-05	0.7442	0.2373	1725.8	1103.2	1867.2	1097.8	1858.6	1114.3
780.3	0.0770	152.1	1.22338E-05	0.7496	0.2427	1744.3	1108.4	1898.1	1103.2	1889.7	1120.0

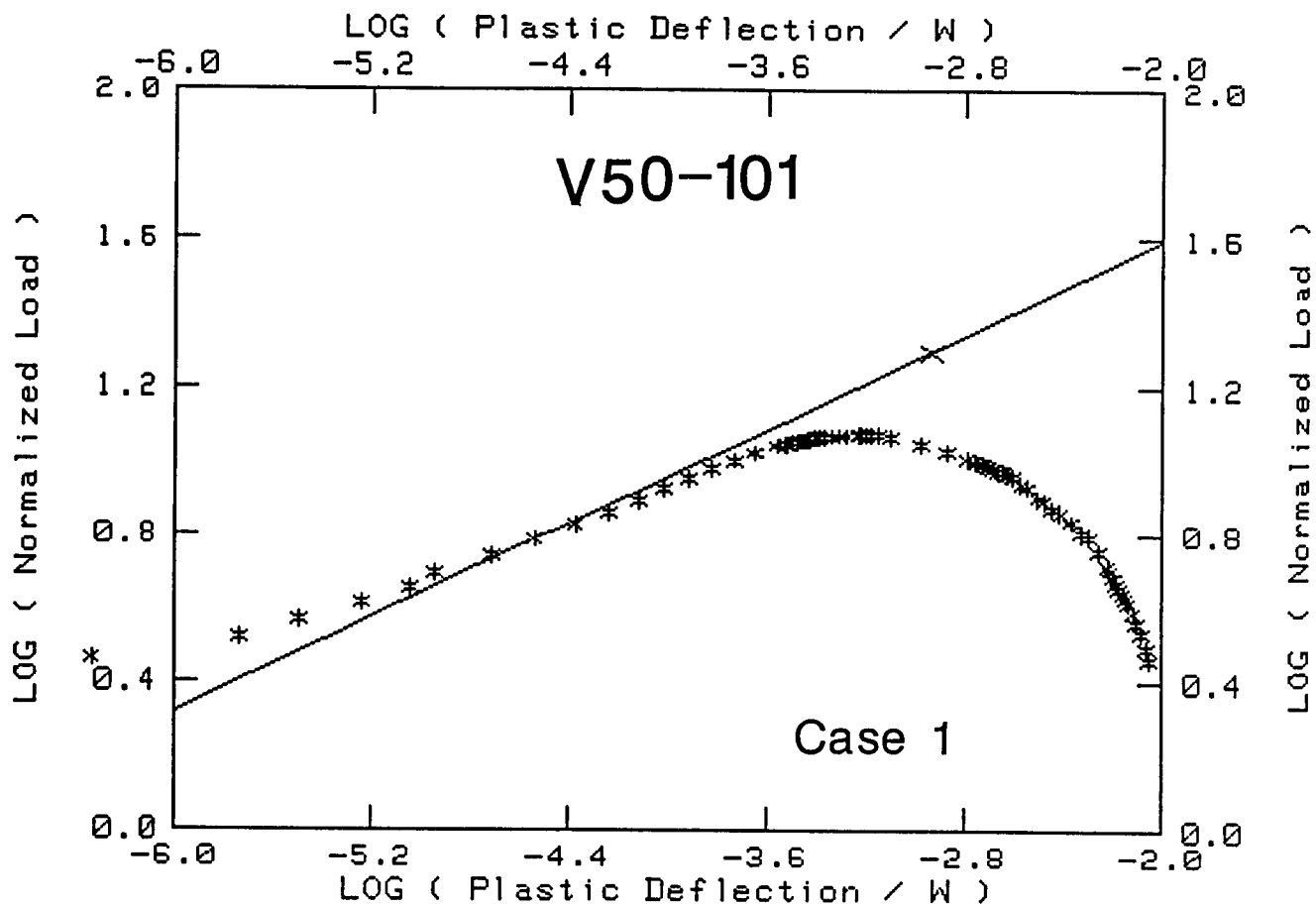




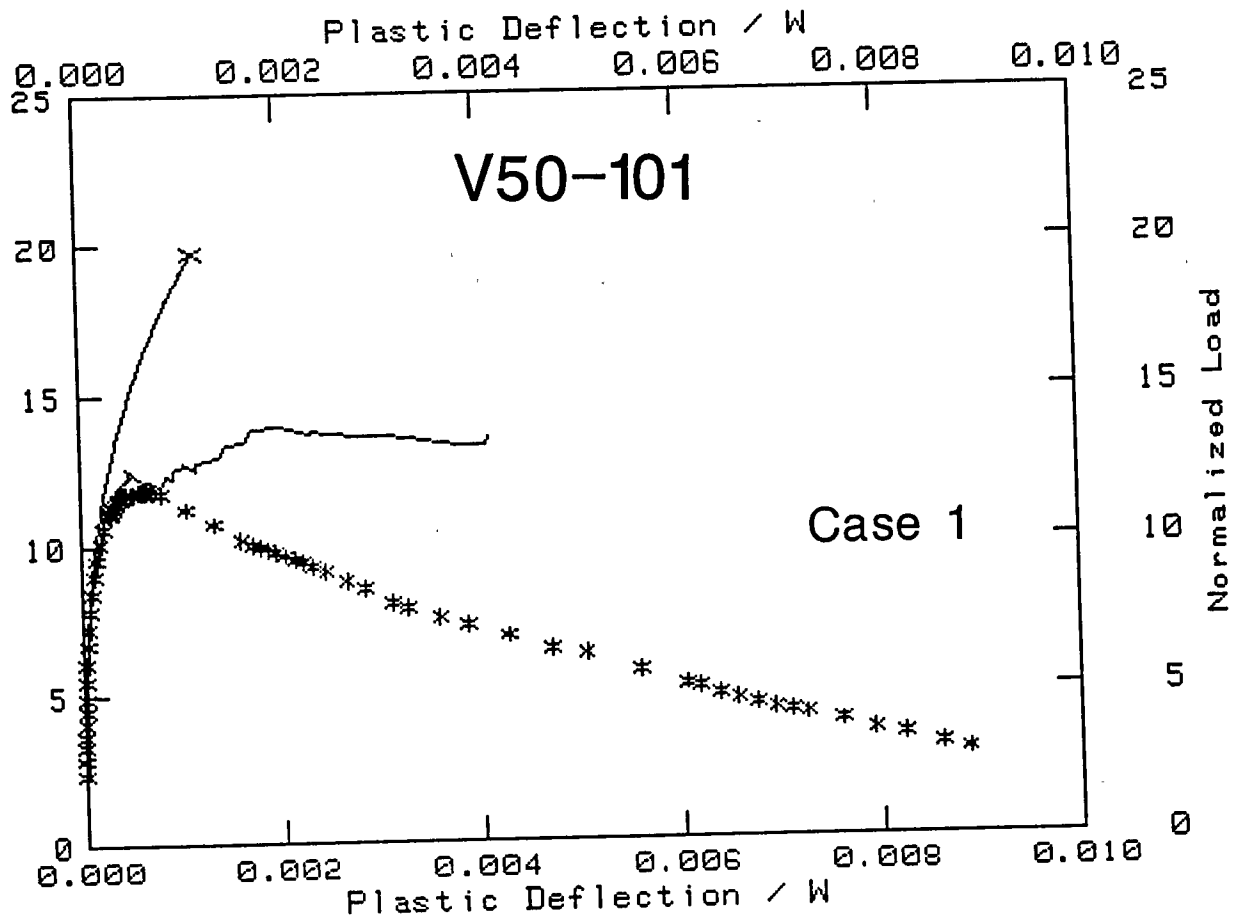
APPENDIX D

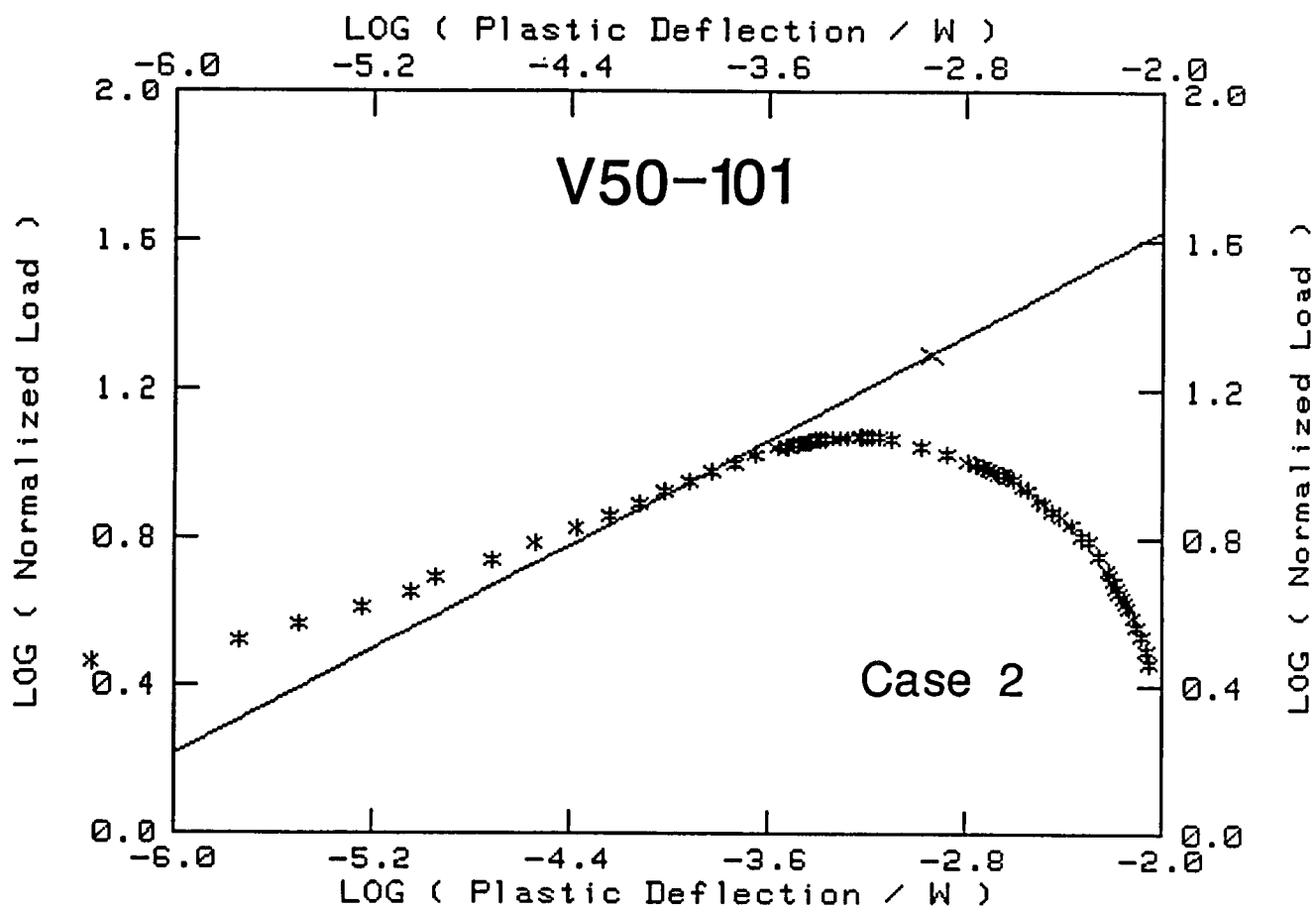
RESULTS FROM NORMALIZATION METHOD ANALYSIS

V50-101 (6T-CT)

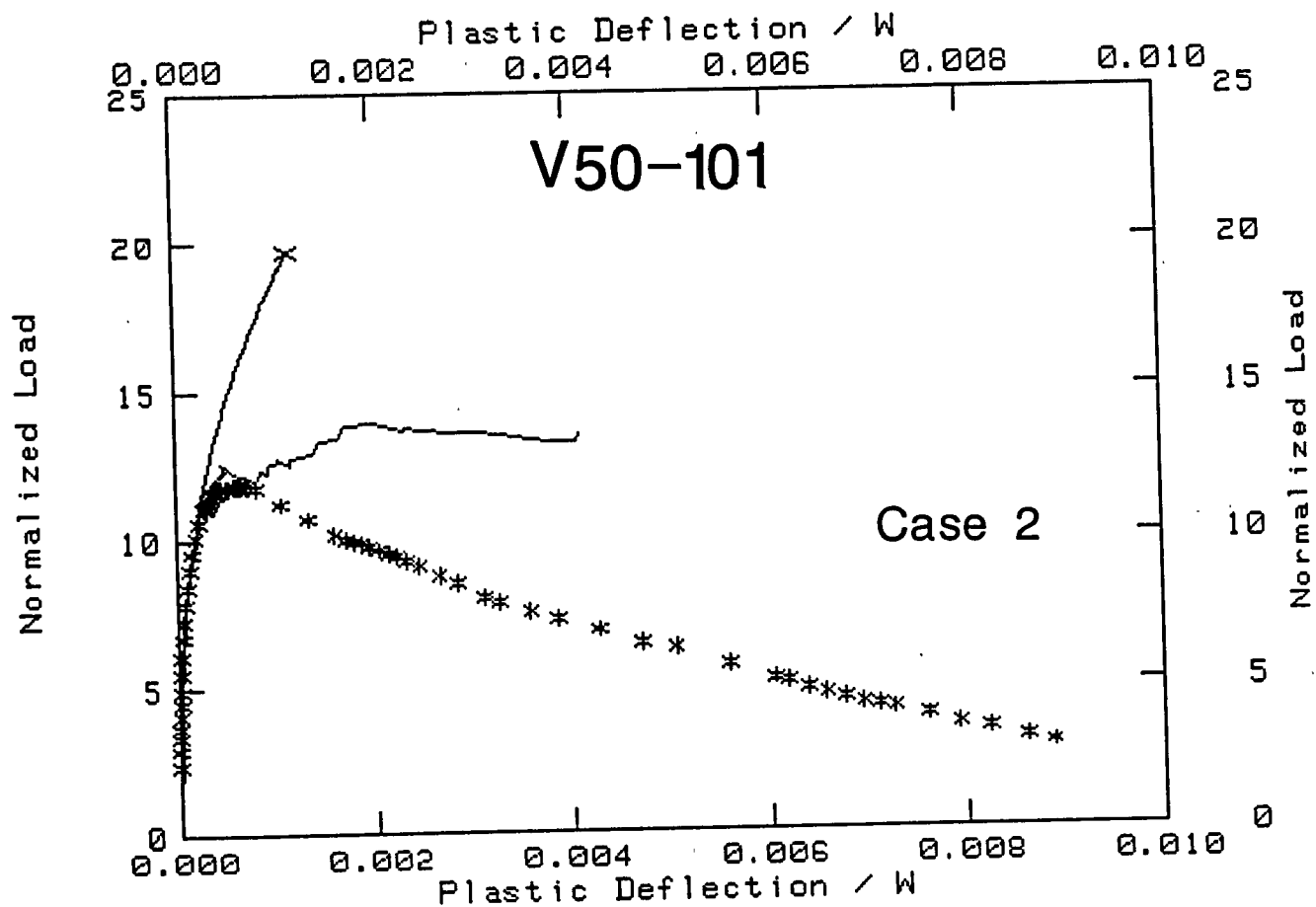


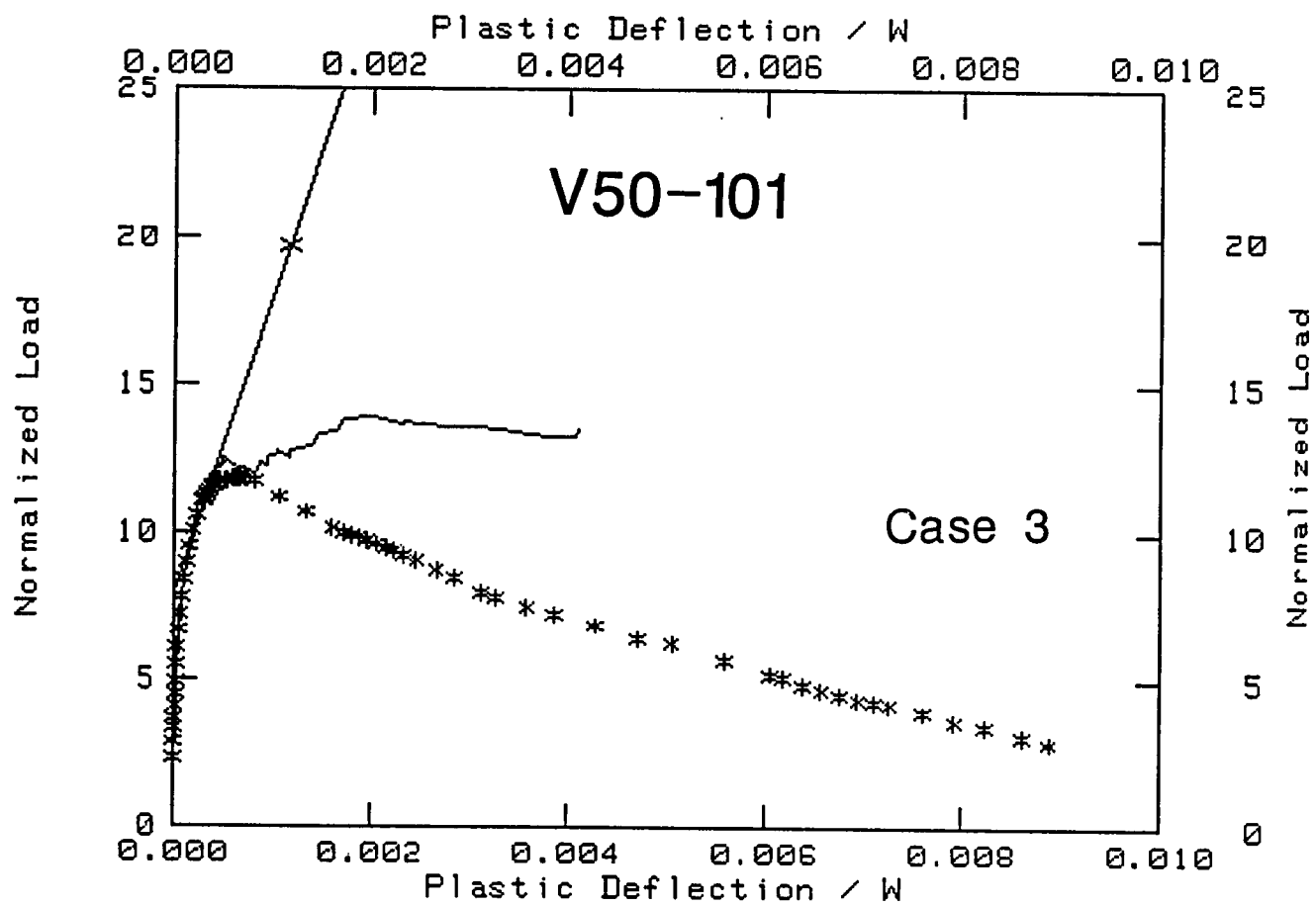
Exponent = .3179
 Coefficient = 169.252 (2.228)

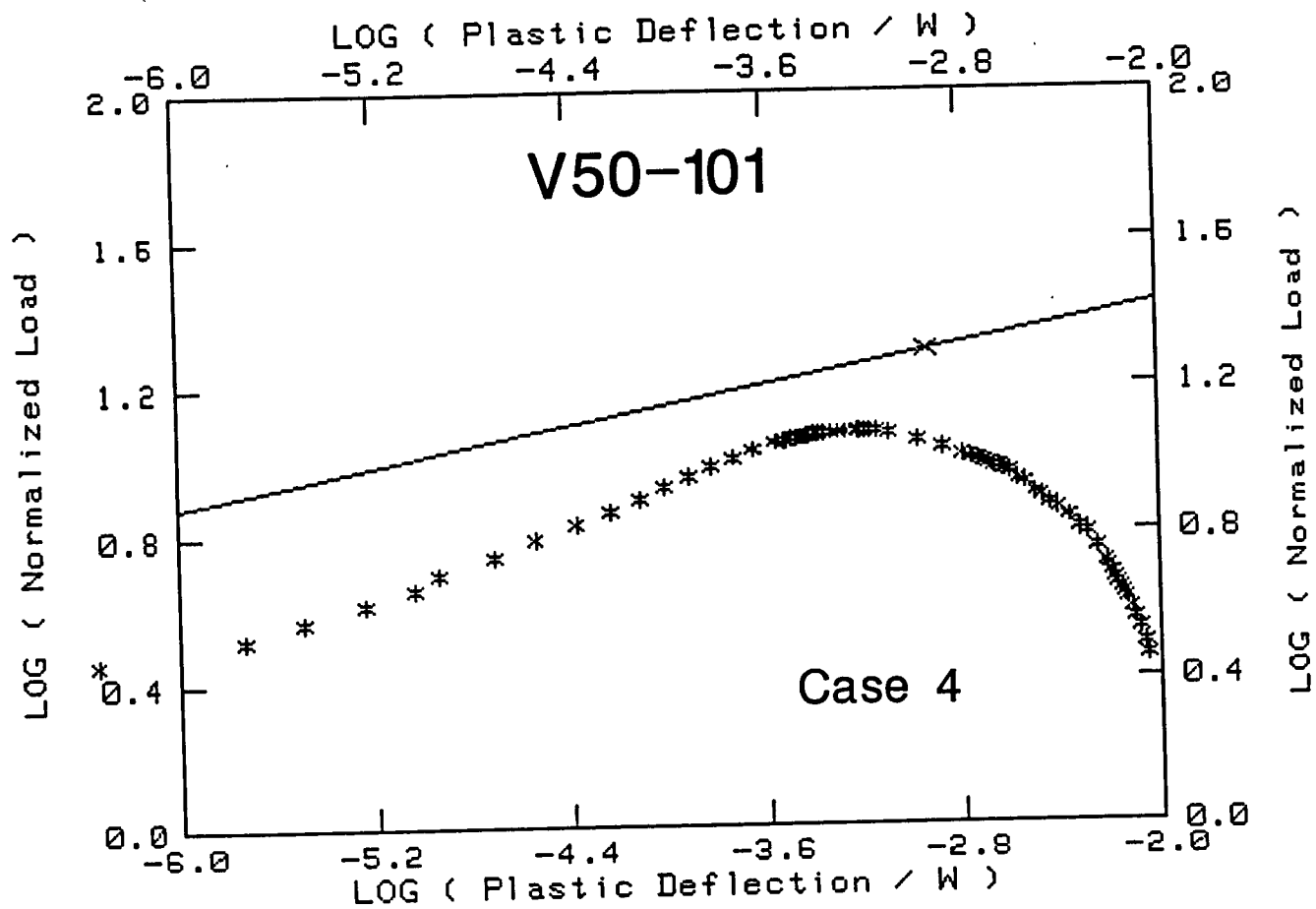




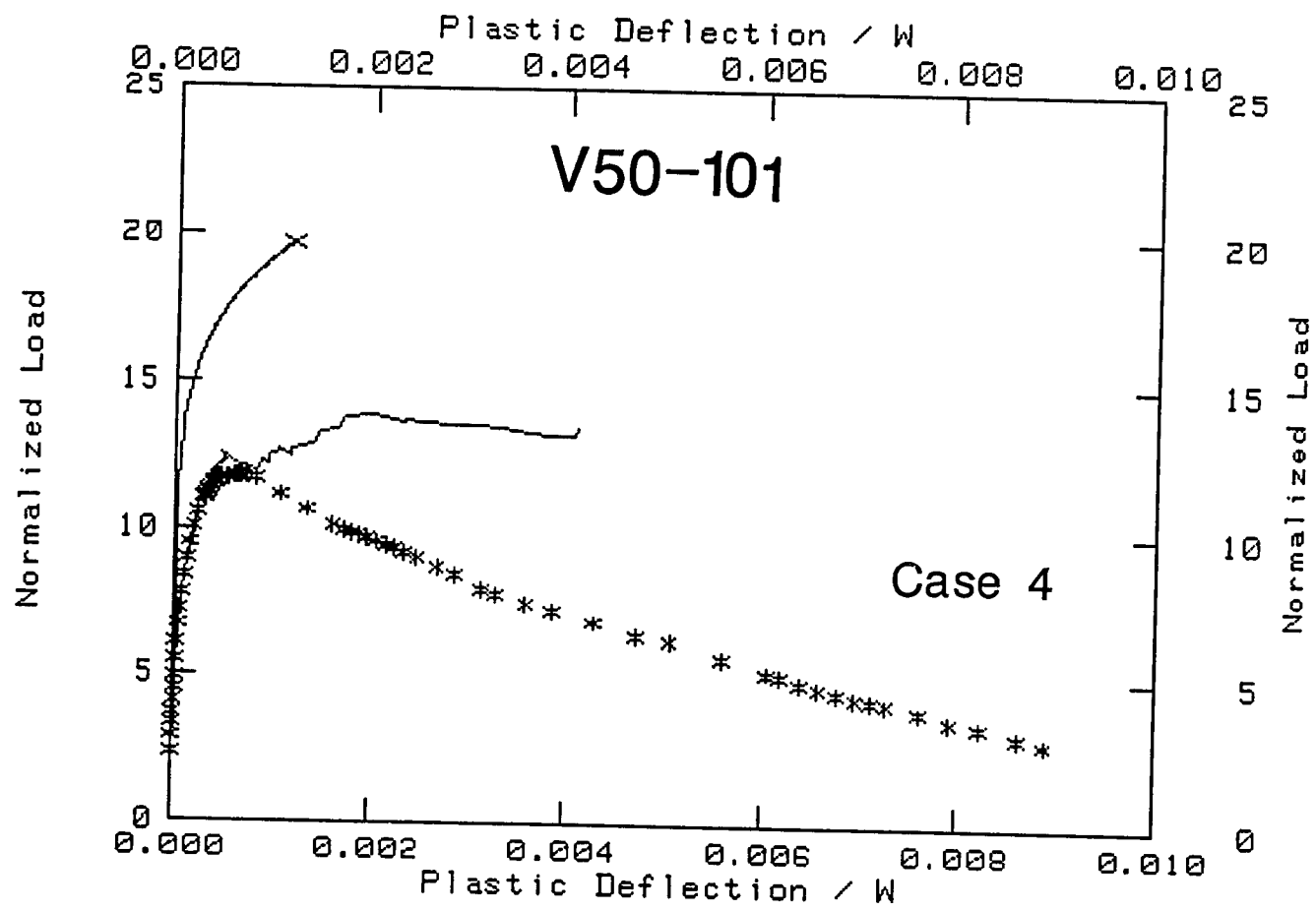
Exponent = .35355
 Coefficient = 215.393 (2.333)

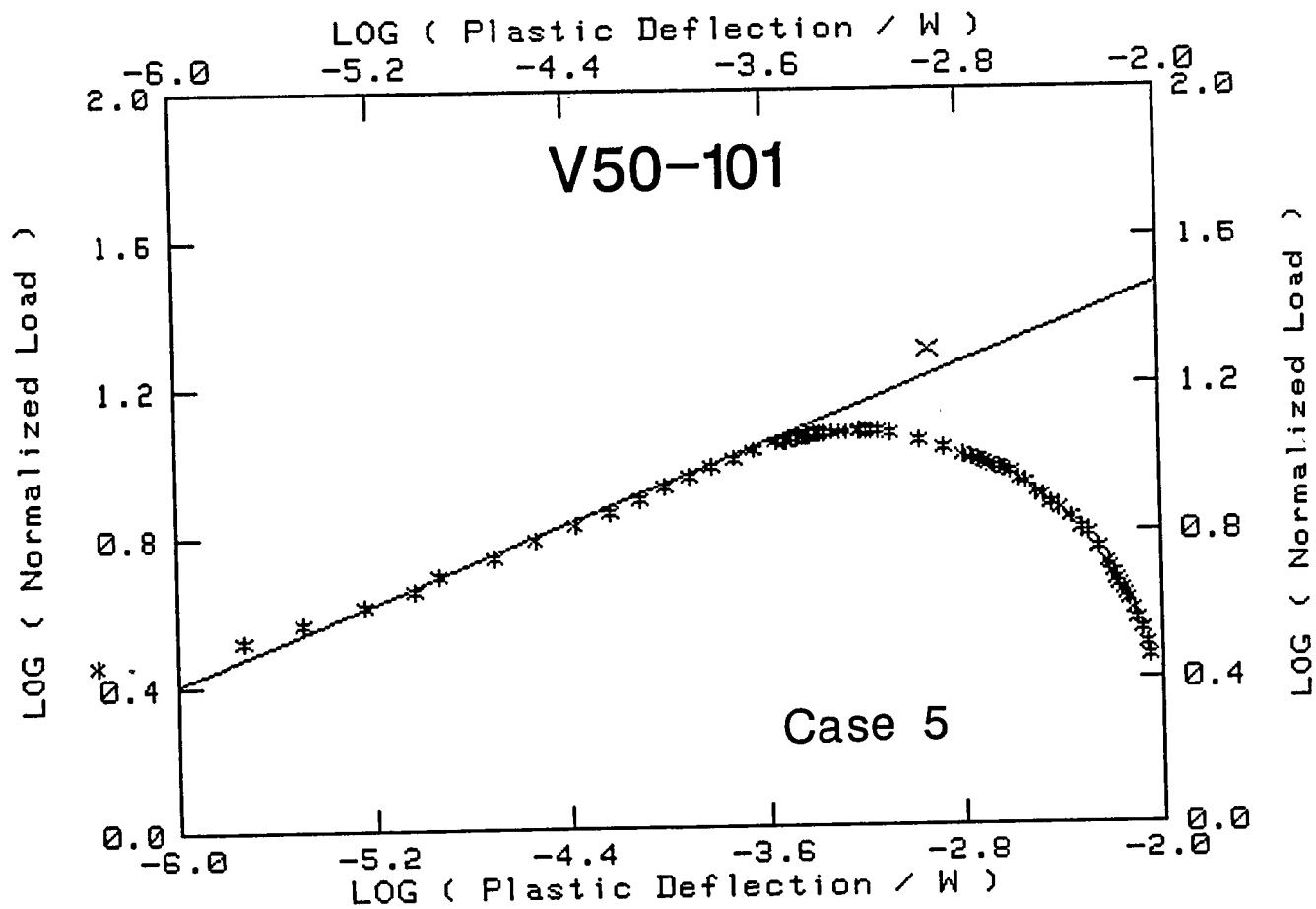




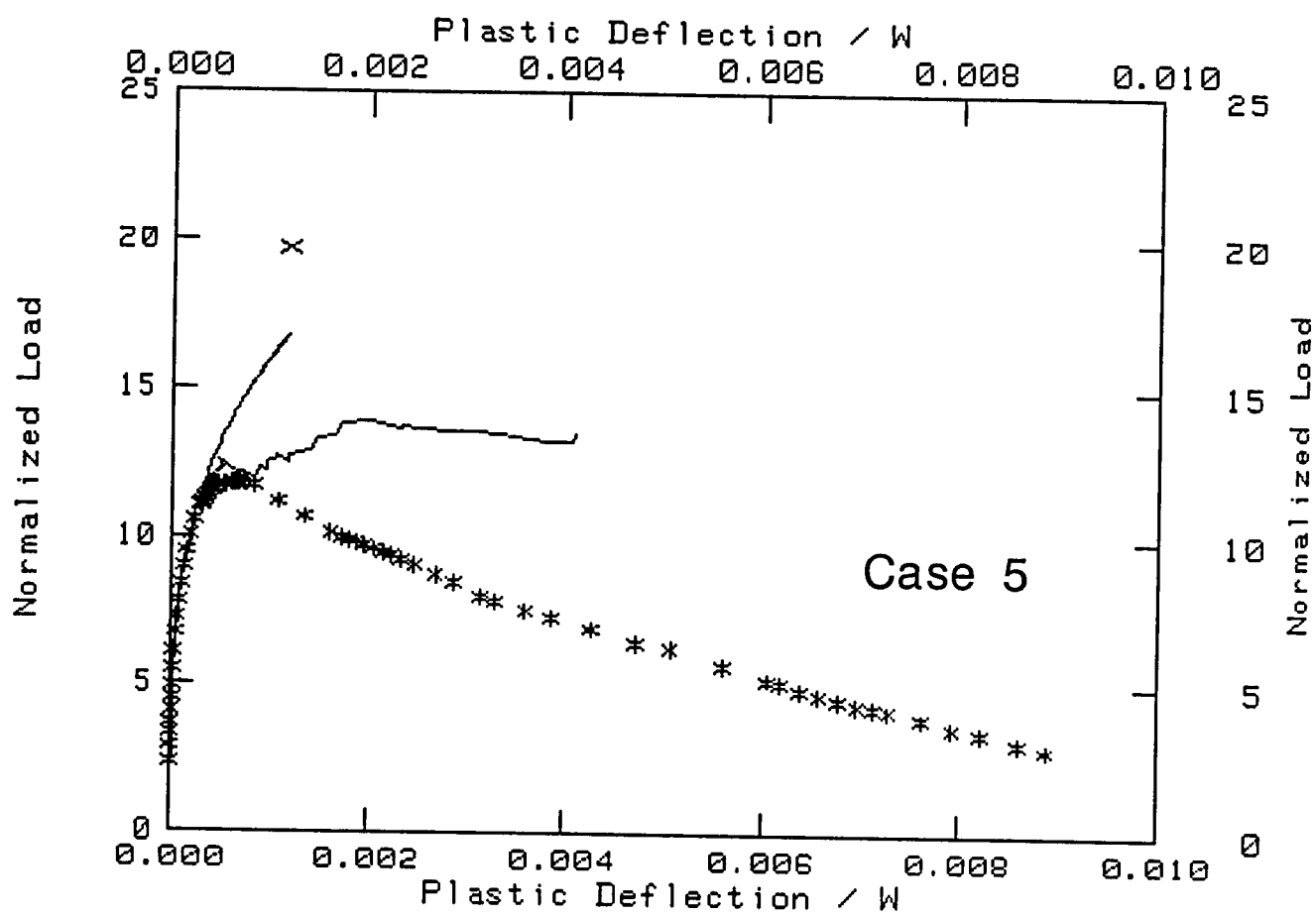


Exponent = .13601
 Coefficient = 49.489 (1.694)

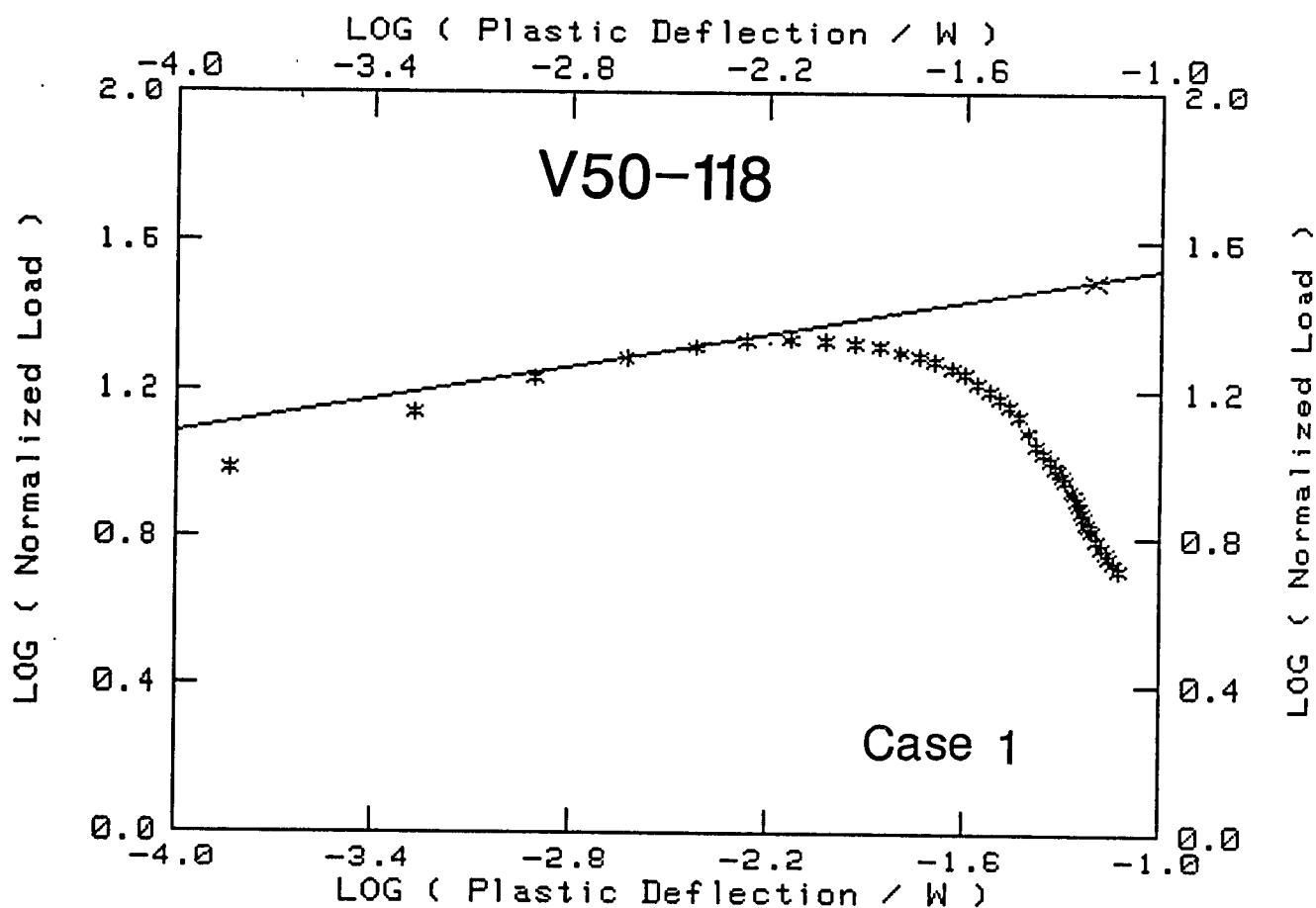




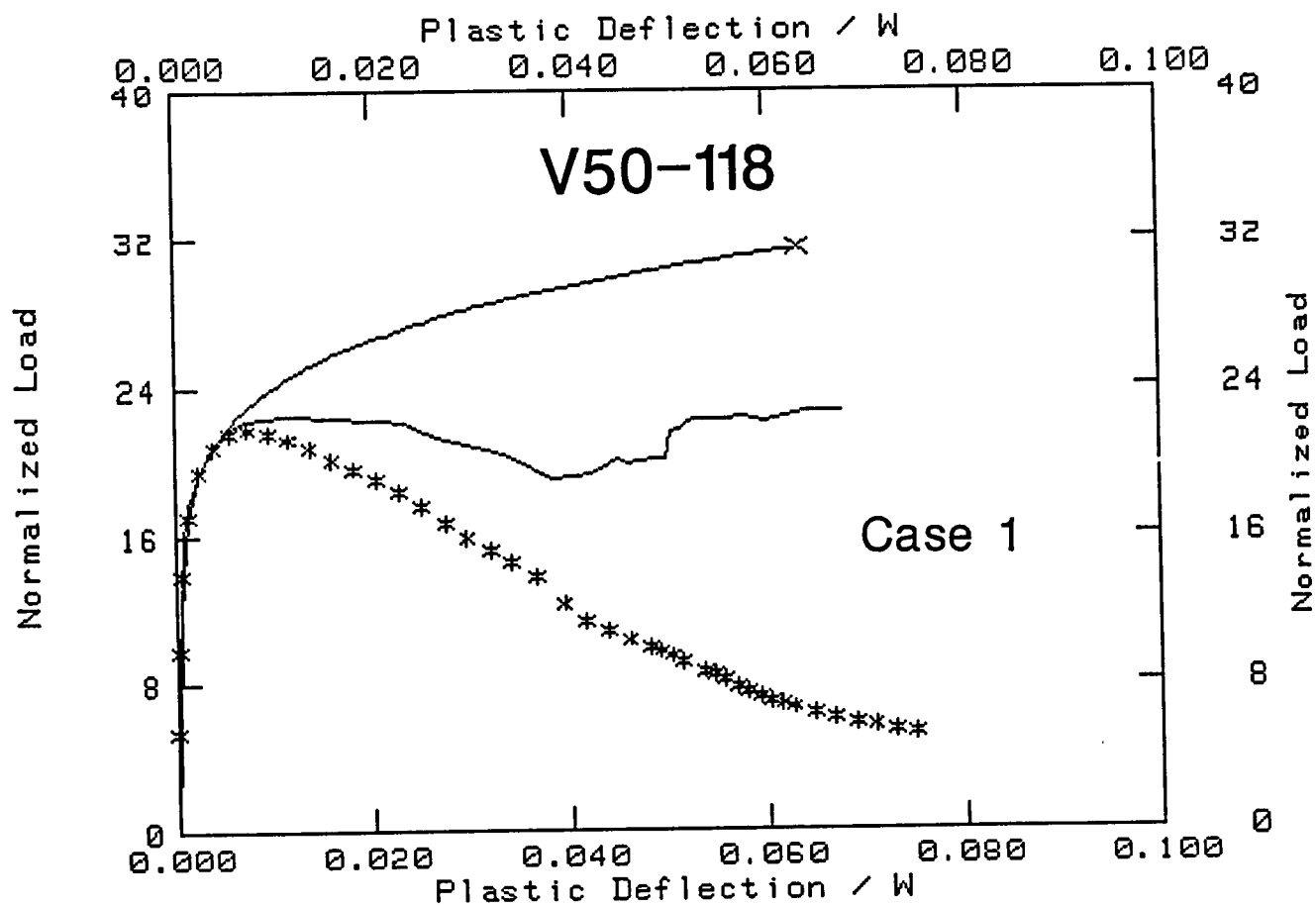
Exponent = .26748
 Coefficient = 102.464 (2.01)

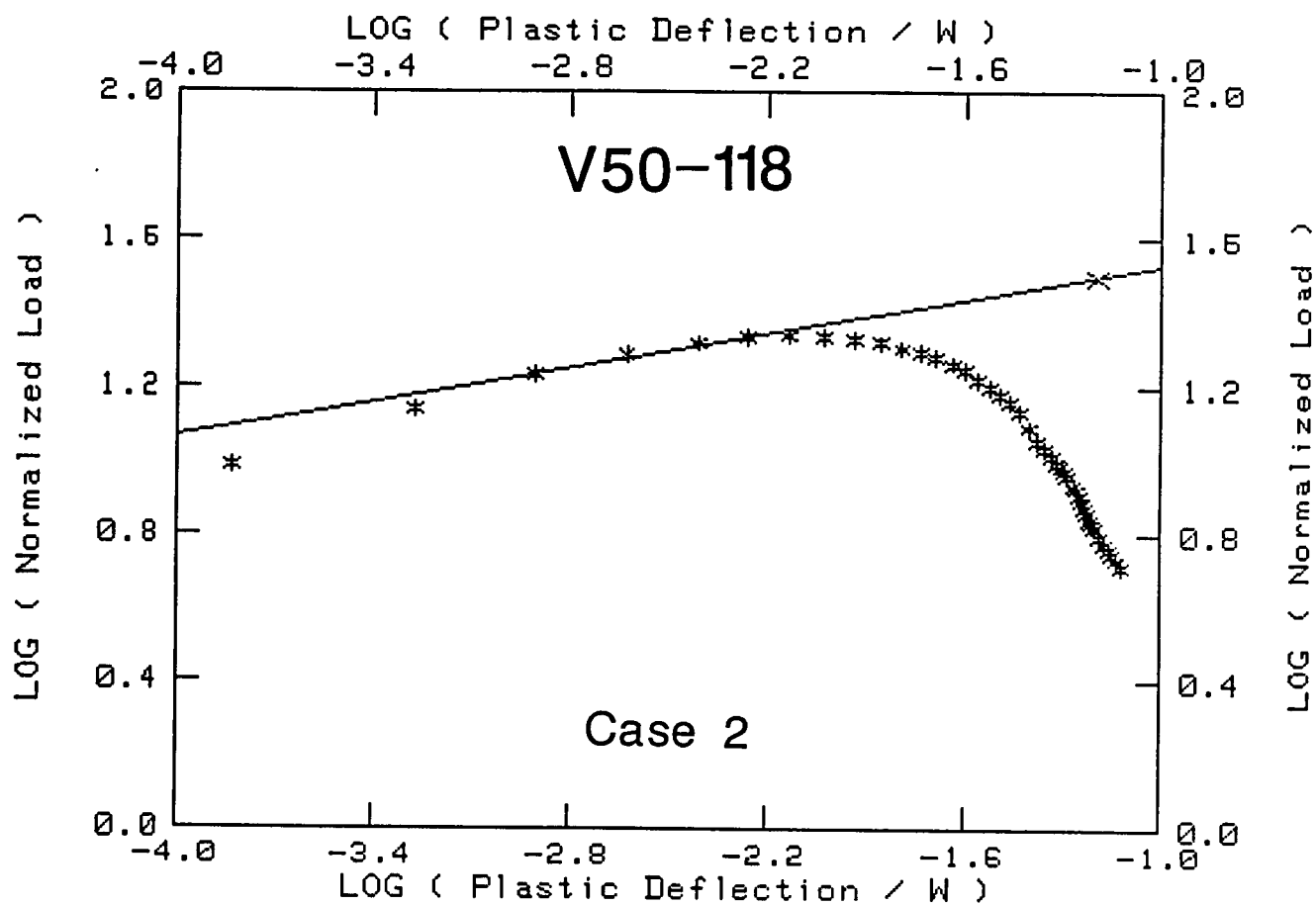


V50-118 (0.5T-CT)

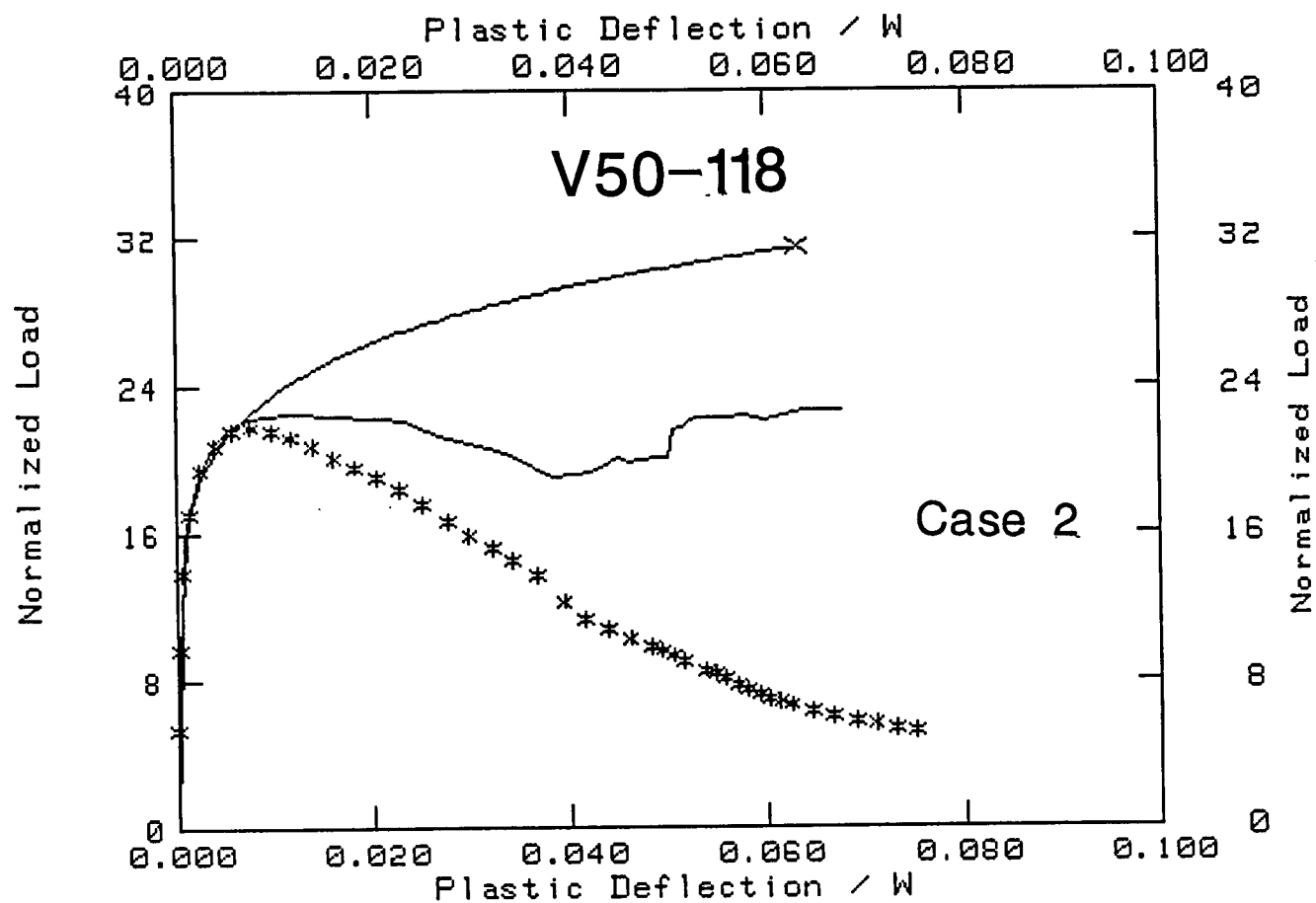


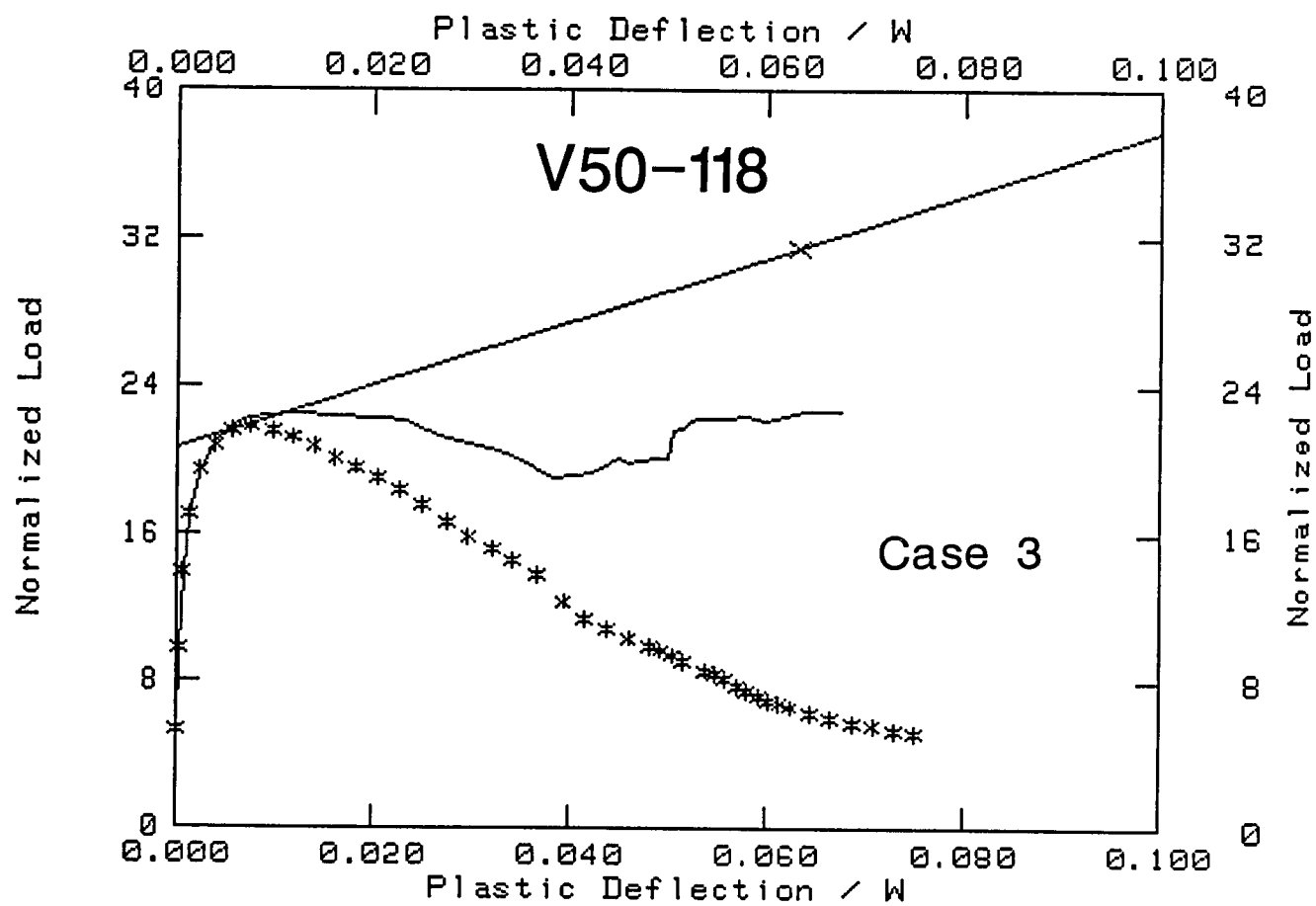
Exponent = .14595
 Coefficient = 47.133 (1.673)

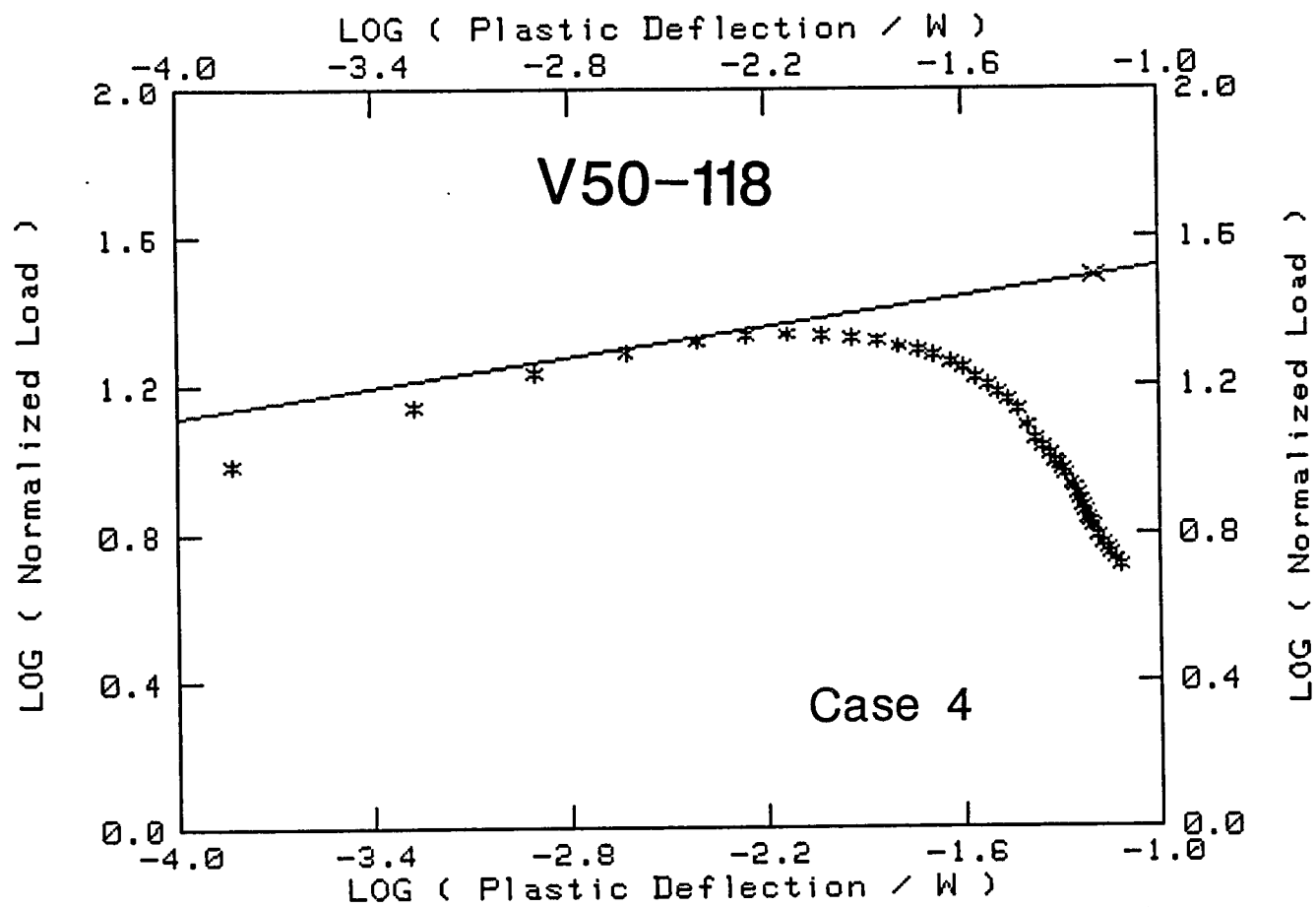




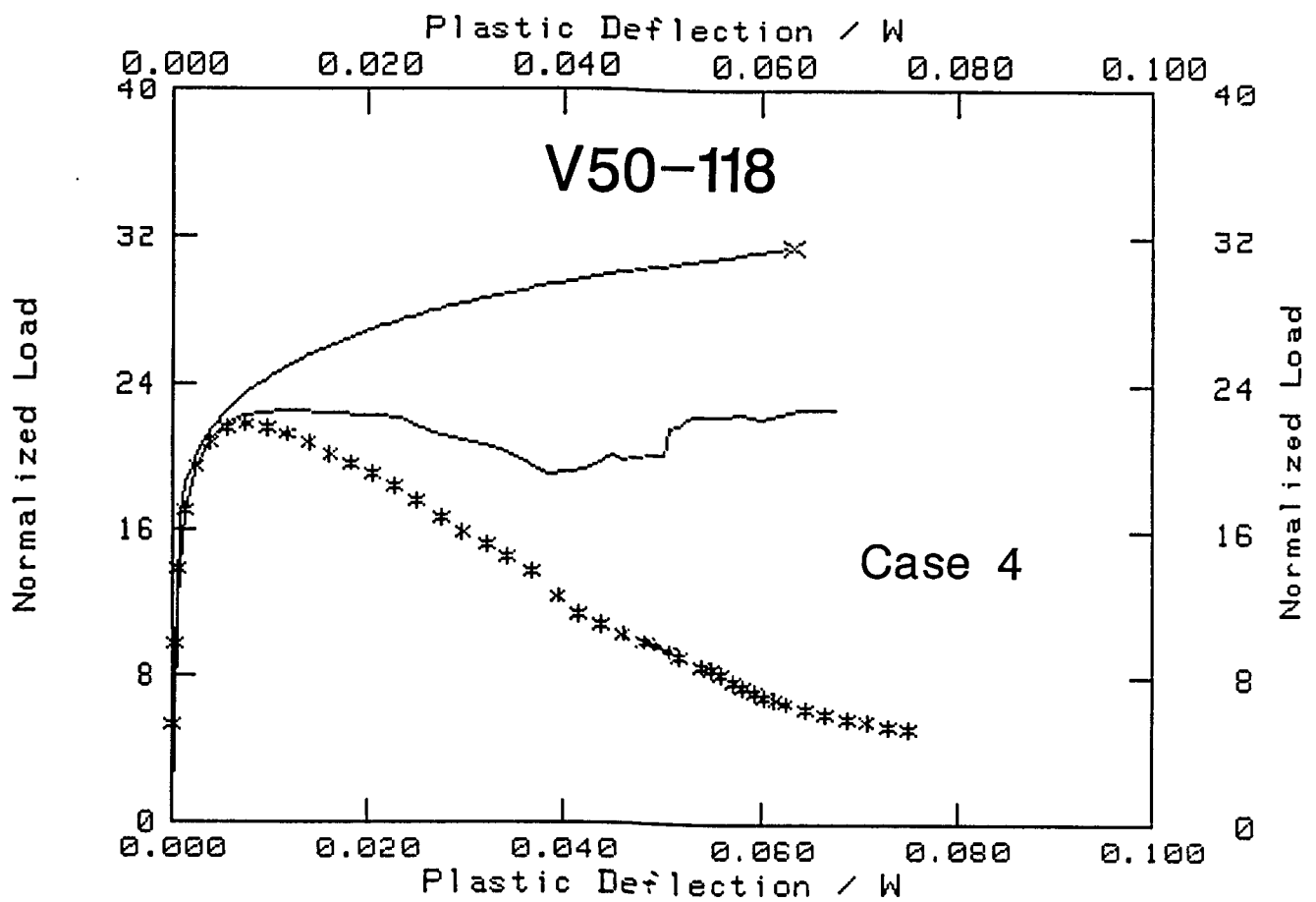
Exponent = .15393
 Coefficient = 48.182 (1.682)

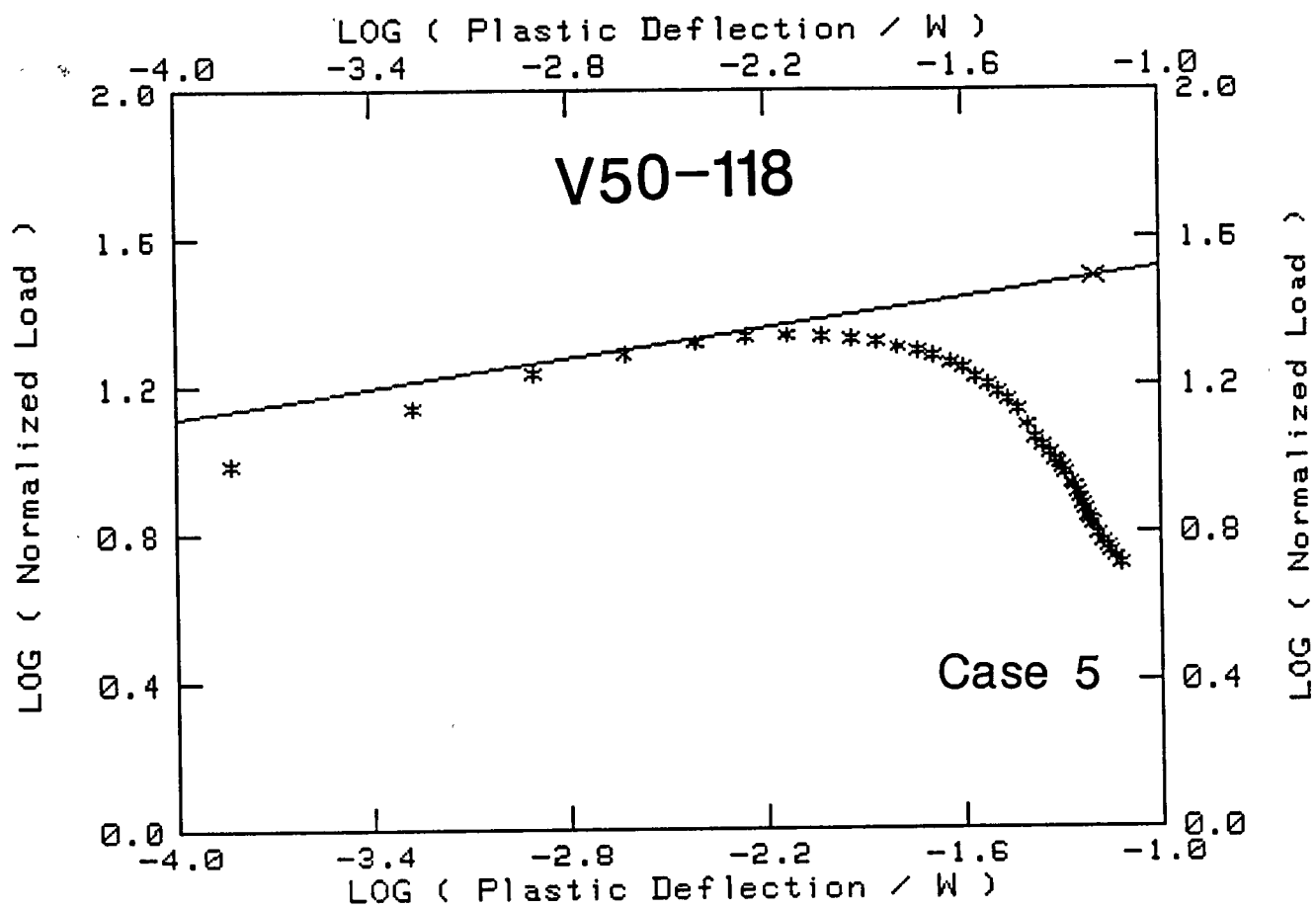




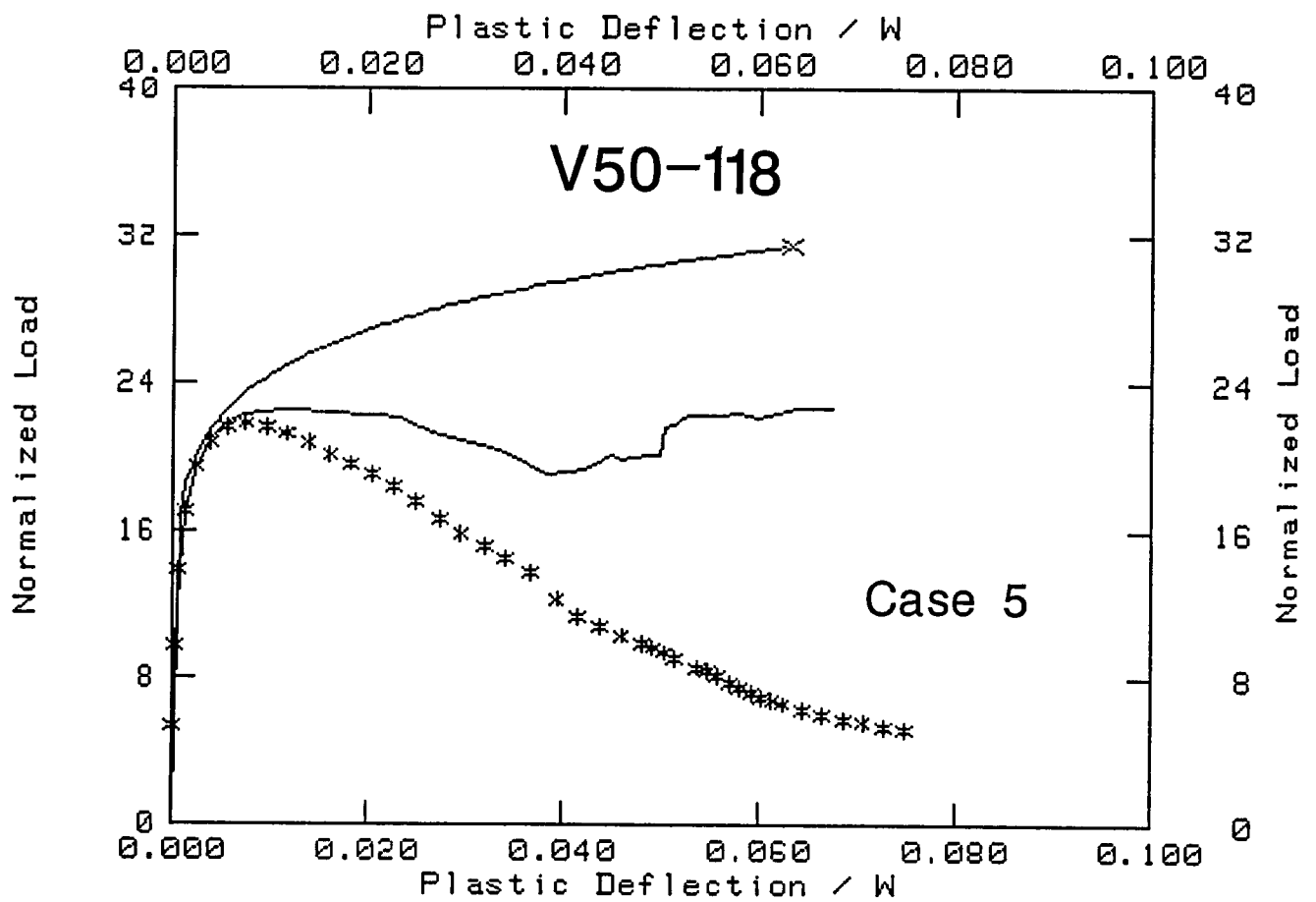


Exponent = .13601
Coefficient = 45.857 (1.661)





Exponent = .13601
 Coefficient = 45.857 (1.661)



NRC FORM 335 (11-81)		U.S. NUCLEAR REGULATORY COMMISSION BIBLIOGRAPHIC DATA SHEET		1. REPORT NUMBER (Assigned by DDC) NUREG/CR-5265 MEA-2320	
4. TITLE AND SUBTITLE (Add Volume No., if appropriate) Size Effects on J-R Curves for A 302-B Plate				2. (Leave blank)	
				3. RECIPIENT'S ACCESSION NO.	
7. AUTHOR(S) A. L. Hiser and J. B. Terrell				5. DATE REPORT COMPLETED MONTH: November YEAR: 1988	
9. PERFORMING ORGANIZATION NAME AND MAILING ADDRESS (Include Zip Code) Materials Engineering Associates, Inc. 9700 Martin Luther King, Jr. Highway Lanham, MD 20706-1837				DATE REPORT ISSUED MONTH: January YEAR: 1989	
				6. (Leave blank)	
				8. (Leave blank)	
12. SPONSORING ORGANIZATION NAME AND MAILING ADDRESS (Include Zip Code) Division of Engineering Office of Nuclear Regulatory Research U. S. Nuclear Regulatory Commission Washington, D. C. 20555				10. PROJECT/TASK/WORK UNIT NO.	
				11. FIN NO. B8900	
13. TYPE OF REPORT Technical Report		PERIOD COVERED (Inclusive dates)			
15. SUPPLEMENTARY NOTES				14. (Leave blank)	
16. ABSTRACT (200 words or less) <p>This study was conceived to determine J-R curves from various sizes of specimens to investigate data extrapolation from small size specimens. This study resulted in the finding of a significant size effect or dependence for the low toughness A 302-B plate investigated. The magnitude of this size dependence is unprecedented for reactor pressure vessel steels. The observed size dependence results in vastly reduced J-R curve toughness levels with increased specimen size, for compact specimens ranging in thickness from 12.7 to 152.4 mm, with all specimens proportional in terms of dimensions.</p> <p>The plate used in this study was specially made to duplicate early production A 302-B plates, which typically exhibit low Charpy-V upper shelf energy levels. The minimal cross-rolling applied to the plate and the high sulfur content result in a high proportion of manganese-sulfide inclusions. The resultant microstructure is one possible explanation for the unexpected results for this plate. Other causes and ideas for future work are also described.</p> <p>An additional observation is that initial crack length-to-width ratio (a/W) did have an influence on the J-R curves for this plate. Specifically, a long crack length (a/W ~ 0.6) can give somewhat higher J-R curve levels than a short crack length (a/W ~ 0.5), for large Δa levels. This finding has a direct impact on the applicability of J_D and J_M, and data extrapolation.</p>					
17. KEY WORDS AND DOCUMENT ANALYSIS			17a. DESCRIPTORS		
RPV steel, J-R curves, Elastic-plastic fracture, A 302-B plate, Size effect, low C_v upper shelf, fracture mechanics					
17b. IDENTIFIERS/OPEN-ENDED TERMS					
18. AVAILABILITY STATEMENT Unlimited			19. SECURITY CLASS (This report) Unclassified		21. NO. OF PAGES
			20. SECURITY CLASS (This page) Unclassified		22. PRICE \$

**UNITED STATES
NUCLEAR REGULATORY COMMISSION
WASHINGTON, D.C. 20555**

**OFFICIAL BUSINESS
PENALTY FOR PRIVATE USE, \$300**

**SPECIAL FOURTH-CLASS RATE
POSTAGE & FEES PAID
USNRC
PERMIT No. G-67**